OptiSystem Lite

Technical Descriptions

Optical Communication System Design Software

Version 1.0
For Windows® 98/Me/2000 and Windows NT™

OptiSystem Lite

Technical Descriptions

Optical Communication System Design Software

Disclaimer

Optiwave Corporation makes no representation or warranty with respect to the adequacy of this documentation or the programs which it describes for any particular purpose or with respect to its adequacy to produce any particular result. In no event shall Optiwave Corporation, its employees, its contractors, or the authors of this documentation, be liable for special, direct, indirect, or consequential damages, losses, costs, charges, claims, demands, or claim for lost profits, fees, or expenses of any nature or kind.

TABLE OF CONTENTS

Chapter 1 – Introduction

Example: Modulation Formats 1-1

Modulation_formats.**osd**

Example: Lightwave System Components 1-4

Lightwave_system_components.**osd**

Chapter 2 – Optical Fibers

Example: Limitations on the Bit Rate 2-1

Limitations on the bit rate.**osd**

Example: Chirped Gaussian Pulse 2-8

Chirped Gaussian pulses.**osd**

Chirped Gaussian pulses_dispersion compensation.**osd**

Example: Attenuation Coefficient 2-21

Attenuation coefficient.**osd**

Example: Material Absorption 2-21

Material absorption of SMF.**osd**

Example: Stimulated Light Scattering 2-22

Raman and GV mismatch.**osd**

Raman spectra.**osd**

Example: Nonlinear Refraction 2-23

SPM.**osd**

XPM and GV mismatch.**osd**

Example: Four-Wave Mixing 2-25

FWM.**osd**

Chapter 3 – Optical Transmitters

Example: Spectral Distribution 3-1

LED spectral distribution**.osd**

Example: LED Modulation Response 3-3

LED modulation response.**osd**

Example: Light-Current Characteristics 3-7

Semiconductor laser L-I curve**.osd**

Example: Semiconductor Laser Modulation Response 3-10

Semiconductor laser large signal modulation**.osd**

Example: Laser Noise 3-11

Laser intensity noise**.osd**

Chapter 4 – Optical Receivers

Example: Front End 4-1

Receiver design**.osd**

Example: *p-I-n* Receivers 4-5

Receiver shot and thermal noise**.osd**

Example: APD Receivers 4-7

Receiver PIN x APD**.osd**

Example: Bit-Error Rate 4-10

Receiver BER - Q factor**.osd**

Example: Minimum Received Power 4-13

Receiver_min. received power**.osd**

Example: Extinction Ratio 4-15

Sensitivity degradation - ER**.osd**

Chapter 5 – Lightwave Systems

Example: Power Budget 5-1

System design_power budget**.osd**

Example: Power Budgeting for Ring Networks 5-2
Optical power level management in metro networks_no amplifier.osd
Gain variation of EDFA depending on input power**.osd**
Optical power level management in metro networks_lumped amplification**.osd**
Optical power level management in metro networks_unity gain**.osd**
Example: Dispersion Broadening 5-18
Dispersions vs power**.osd**

Chapter 6 – Optical Amplifiers

Example: EDFA Basic Concepts 6-1
EDFA basic concepts**.osd**
Example: Booster Amplifier 6-12
Booster amplifier**.osd**
Example: In-Line Amplifier 6-15
In-line amplifier**.osd**
Example: Preamplifier 6-19
Preamplifier**.osd**
Example: Semiconductor Laser Amplifiers Cascaded In-Line Amplifiers: Soliton Pattern Effect at 10 Gb/s in SMF 6-21
SLA cascaded in-line amplifiers soliton pattern effect 10 Gbps in SMF**.osd**
Example: SLA Gain Recovery 6-32
SLA gain recovery**.osd**
Example: SLA Gain Saturation of Chirped and Super Gaussian Pulses 6-54
SLA gain saturation of chirped and super- Gaussian pulses**.osd**
Example: SLA Gain Saturation of Gaussian Pulses 6-69
SLA gain saturation of Gaussian pulses**.osd**
Example: Raman Gain and Bandwidth 6-86
Forw_backward Raman amplification**.osd**
Example: Gain Saturation 6-87
Forw_backward Raman gain saturation**.osd**

Example: Amplifier Performance 6-87

Broadband flat gain Raman amplifer**.osd**

Example: Pumping Requirements 6-88

Pumping requirements**.osd**

Example: Gain Characteristics 6-91

Gain characteristics**.osd**

Example: Amplifier Noise 6-93

Amplifier noise**.osd**

Example: Multichannel Amplification 6-97

Multichannel amplification**.osd**

Example: Optical Preamplifiers 6-99

Preamplifier_system**.osd**

Example: Power Boosters 6-101

Booster_system**.osd**

Example: Local-Area-Network-Amplifiers 6-104

Metro EDFA**.osd**

Example: Cascaded In-Line Amplifiers 6-109

Inline cascaded**.osd**

Example: Non-ideal characteristics of EDFAs in Metro Networks and Effect of Gain Flattening and Controlling 6-110

Considering nonideal gain characteristics of EDFA_nonideal**.osd**

Considering nonideal gain characteristics of EDFA_ideal**.osd**

Example: Cascaded in-line Amplifiers-10 Gbps in SMF 6-116

System applications 10 Gbps in SMF NRZ**.osd**

System applications 10 Gbps in SMF RZ**.osd**

Example: Hybrid 6-124

Hybrid**.osd**

Example: EDFA Dynamic 6-127

EDFA dynamic**.osd**

Chapter 7- Dispersion Management

Example: Dispersion Compensation Techniques 7-1

Dispersion compensation_post.**osd**
Dispersion compensation_pre.**osd**
Dispersion compensation_symmetrical.**osd**

Example: Precompensation Technique using SOA 7-6

Amplifier- induced chirp SLA compression.**osd**

Examples: 40 Gbps 7-19

High-dispersion fibers 40 Gbps in SMF NRZ.**osd**
High-dispersion fibers 40 Gbps in SMF RZ pre.**osd**
High-dispersion fibers 40 Gbps in SMF RZ.**osd**

Example: Uniform-Period Gratings 7-29

Dispersion compensation_post with FBG.**osd**

Example: Fiber Nonlinearities and Dispersion 7-30

Fiber nonlinearities and dispersion_single channel.**osd**
Fiber nonlinearities and dispersion_multi channel.**osd**
Fiber nonlinearities and dispersion_multi channel Tagal.**osd**

Example: Negative Dispersion Fiber and Applications for Metro Networks 7-36

Negative dispersion fiber and applications for metro networks.**osd**

Example: Migrating to 10 Gb/s Metro System and Dispersion Limited Transmission 7-39

Migrating to 10 Gb/s_no dispersion compensation.**osd**
Migrating to 10 Gb/s_dispersion compensation at each node.**osd**
Migrating to 10 Gb/s_lumped dispersion compensation.**osd**

Chapter 8 - Multichannel Systems

Example: WDM Ring Network 8-1

WDM ring with WISE_directly modulated source_RZ.**osd**
WDM ring with WISE_directly modulated source_NRZ.**osd**
WDM ring with WISE_externally modulated source_RZ.**osd**

WDM ring with WISE_externally modulated source_NRZ.**osd**
Example: Dual Fiber Protected Ring Architecture 8-10
Dual fiber protected ring architecture.**osd**
Example: Fabry-Perot Filter 8-13
Fabry-Perot filter.**osd**
Example: Uniform FBG Filter 8-15
FBG filter transmission.**osd**
Example: AWG Demultiplexer 8-16
AWG demultiplexer.**osd**
Example: Star Coupler 8-19
Star couplers.**osd**
Example: 8 by 8 Star Coupler 8-21
8 by 8 Star coupler.**osd**
Example: Optical Cross-Connects 8-21
OXC project.**osd**
Example: Wavelength Converters-SLA and FWM 8-23
Wavelength converters SLA and FWM.**osd**
Example: Wavelength Converters-SLA and XGM 8-33
Wavelength converters SLA and XGM.**osd**
Example: Channel Multiplexing 8-45
OTDM multiplexer.**osd**
Example: Channel Demultiplexing 8-48
DeMUX by FWM.**osd**
Example: Linear Crosstalk 8-49
Interchannel crosstalk at ADM in a ring network.**osd**
Example: Subcarrier Multiplexing 8-53
Subcarrier multiplexing.**osd**

Chapter 9 – Soliton Systems

Example: Fundamental and Higher-Order Solitons 9-1

Fundamental and higher-order solitons**.osd**

Example: Dark Solitons 9-4

Dark solitons**.osd**

Example: Information Transmission with Solitons 9-4

Interaction of a pair of fundamental solitons**.osd**

Example: Average Soliton Regime 9-5

Average-soliton regime**.osd**

Example: Soliton Collisions 9-14

Interaction of multicolor solitons**.osd**

Chapter 1 – Introduction

Example: Modulation Formats

Modulation_formats.**osd**

There are two typical choices for the modulation format of the signal. These are shown in the project file "Modulation_formats**.osd**" (Fig.1) and are known as the return-to-zero (RZ) and nonreturn-to-zero (NRZ).

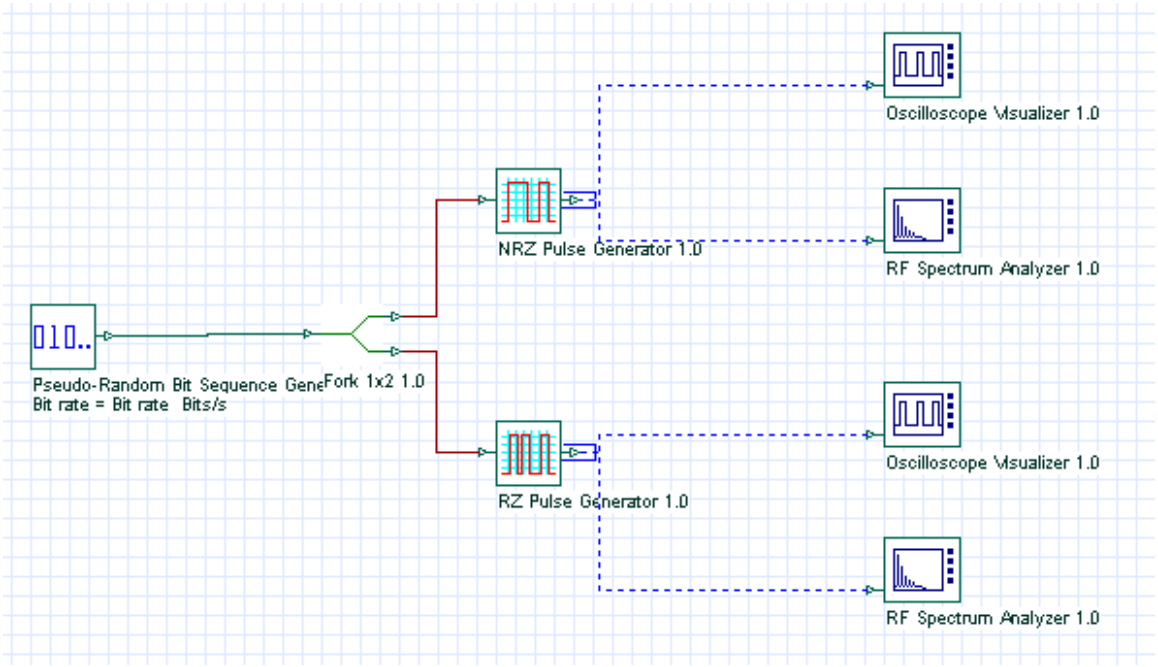

Fig.1: Layout: Modulation formats

In the RZ format (Fig.2), each pulse that represents bit 1 is shorter than the bit slot, and its amplitude returns to zero before the bit duration is over. In the NRZ format (Fig.3), the pulse remains on throughout the bit slot and its amplitude does not drop to zero between two or more successive bits. As a result, pulse width varies depending on the bit pattern, whereas it remains the same in the case of RZ format.

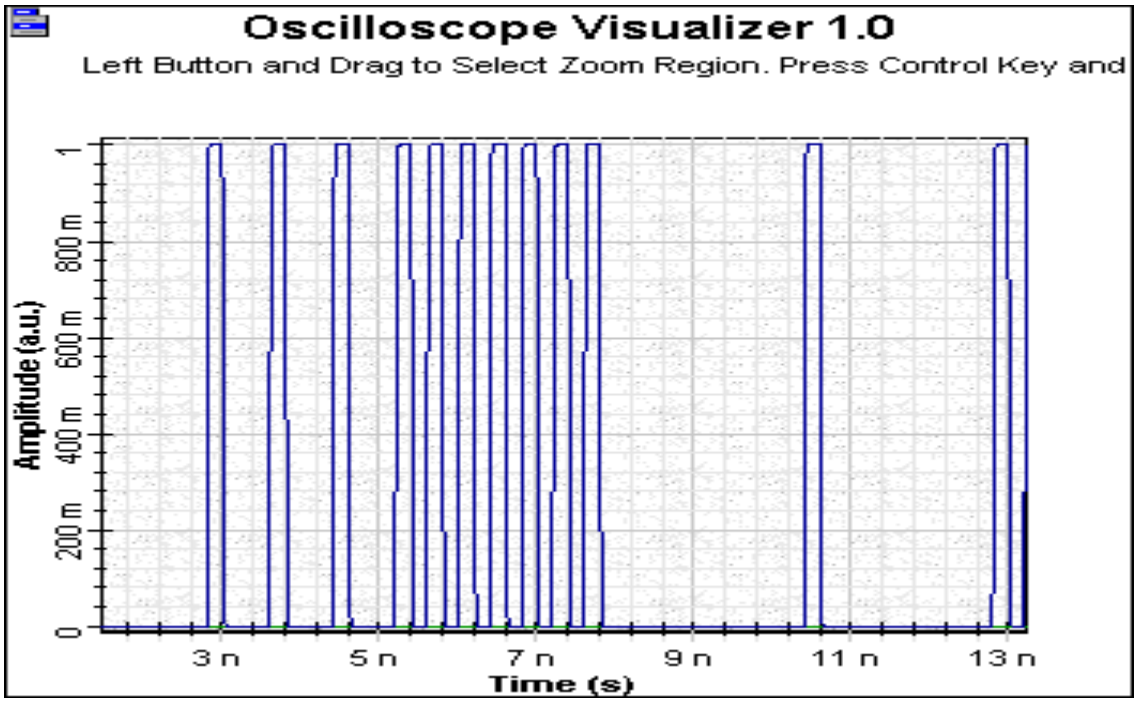

Fig.2: RZ (Amplitude – Time)

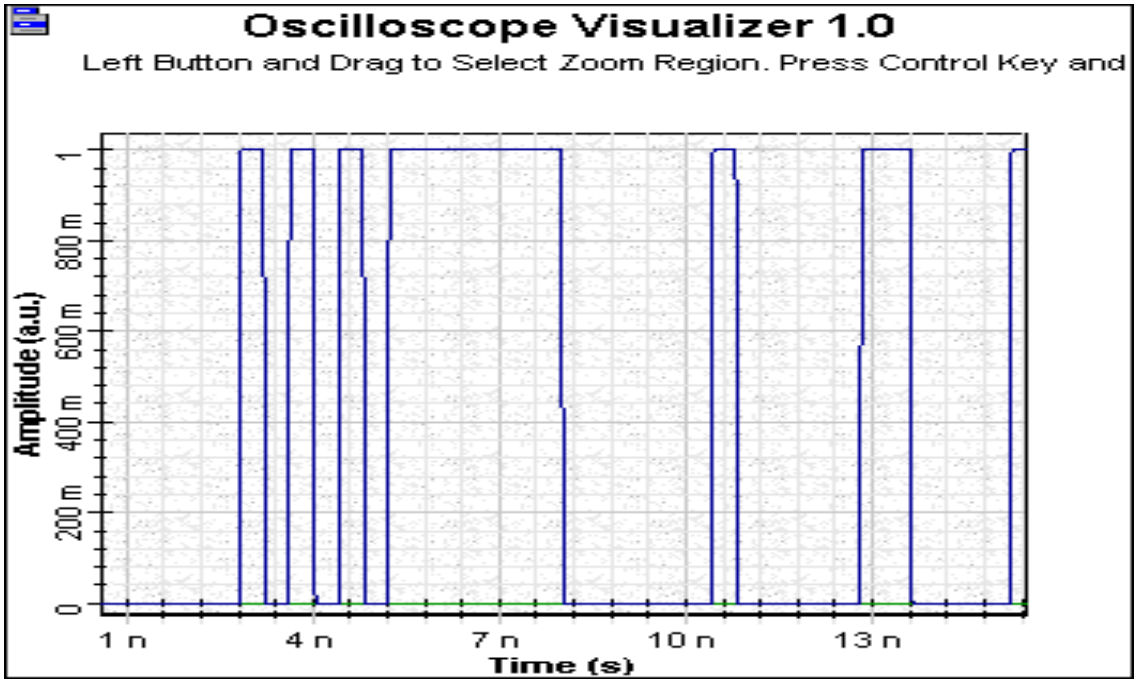

Fig.3: NRZ (Amplitude – Time)

An advantage of the NRZ format is that the bandwidth associated with the bit stream is smaller than that of the RZ format by about a factor of 2 simply because on-off transitions occur fewer times **(Figs. 4 and 5).**

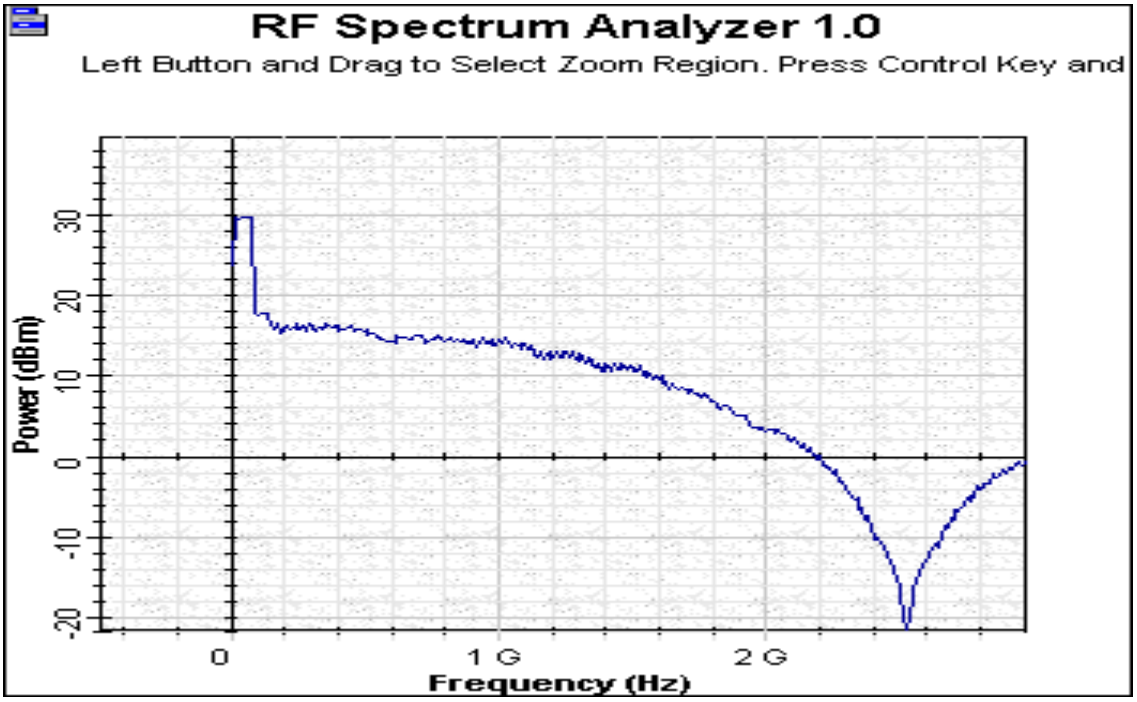

Fig.4: NRZ (Power- Frequency)

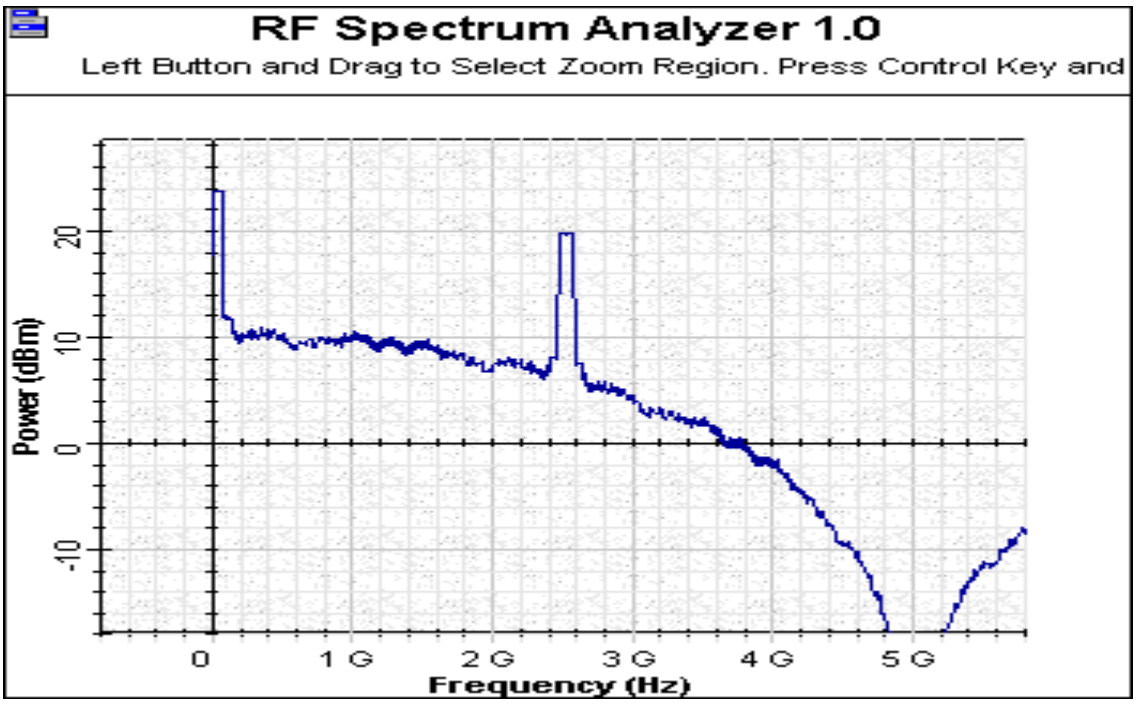

Fig.5: RZ (Power- Frequency)

Example: Lightwave System Components

Lightwave_system_components.**osd**

Project "Lightwave_system_components.**osd**" (Fig. 6) shows a generic block diagram of an optical communication system. It consists of a communication channel with a transmitter in the front and a receiver at the back.

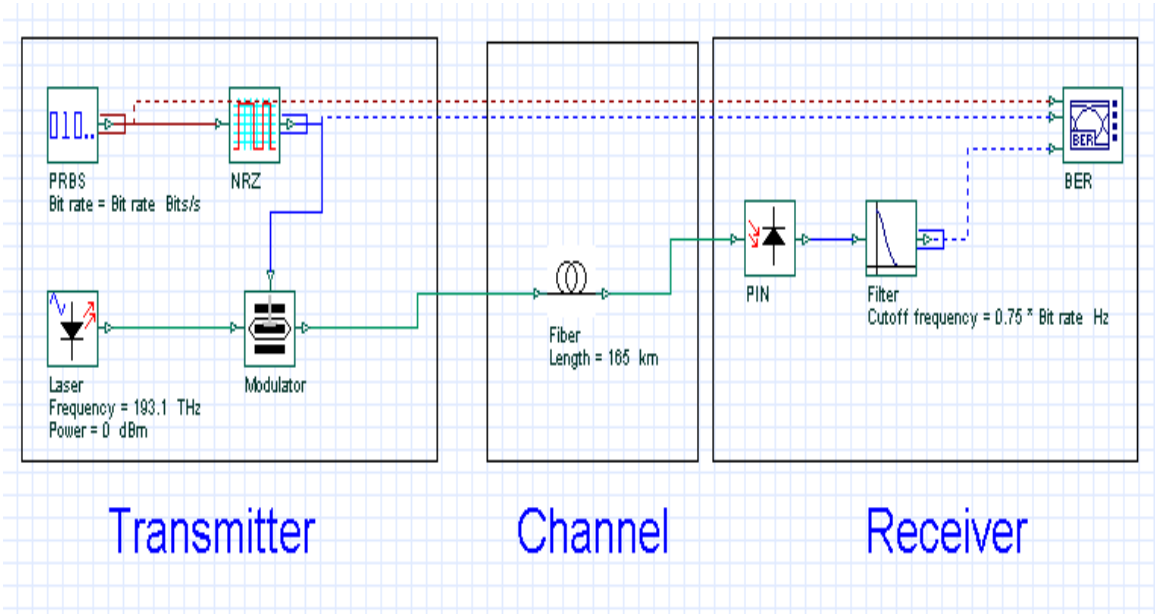

Fig.6: Layout: Lightwave system components

(a) Communication Channel

The role of the communication channel is to transport the optical signal from transmitter to receiver without distorting it. Most lightwave communication systems use optical fibers as the communication channel because fibers can transmit light with a relatively small amount of power loss.

Fiber loss is, of course, an important design issue, as it determines directly the repeater spacing of a long-haul lightwave system. Another important design issue is fiber dispersion, which leads to broadening of individual pulses inside the fiber.

In order to observe the effects of loss and dispersion in the optical signal the user can change the values of fiber length and visualize the degradation of the signal at the receiver stage (Figs. 7,8 & 9).

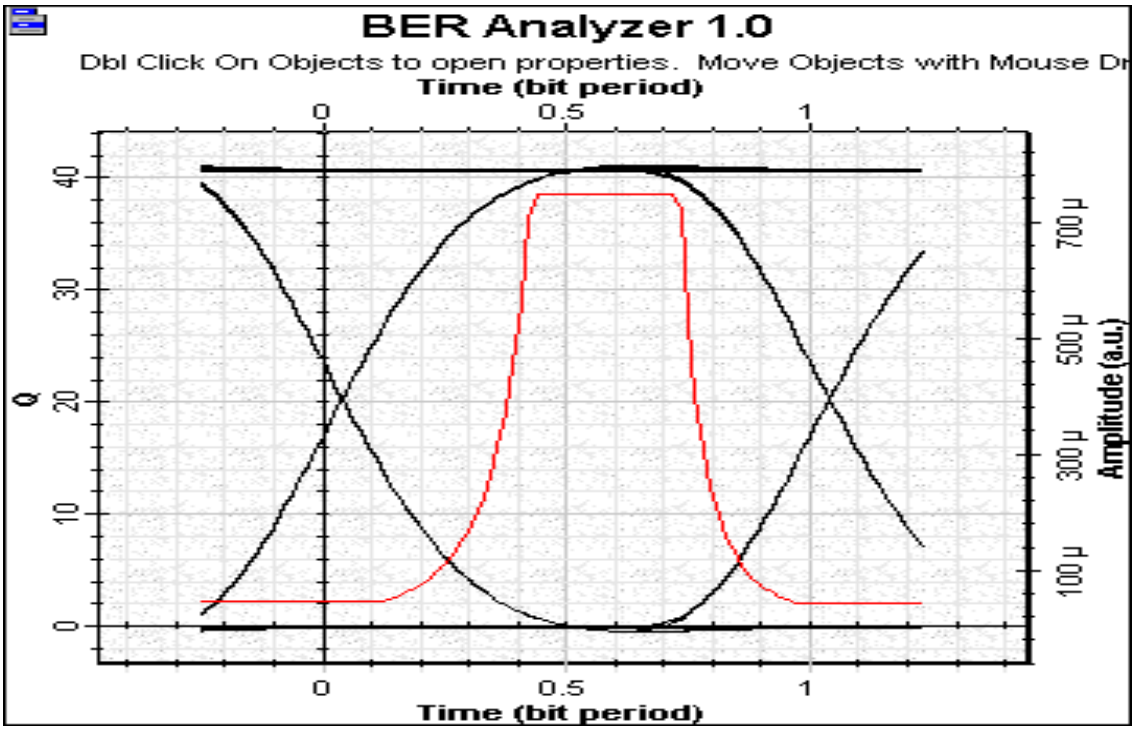

Fig.7: Fiber 0 km

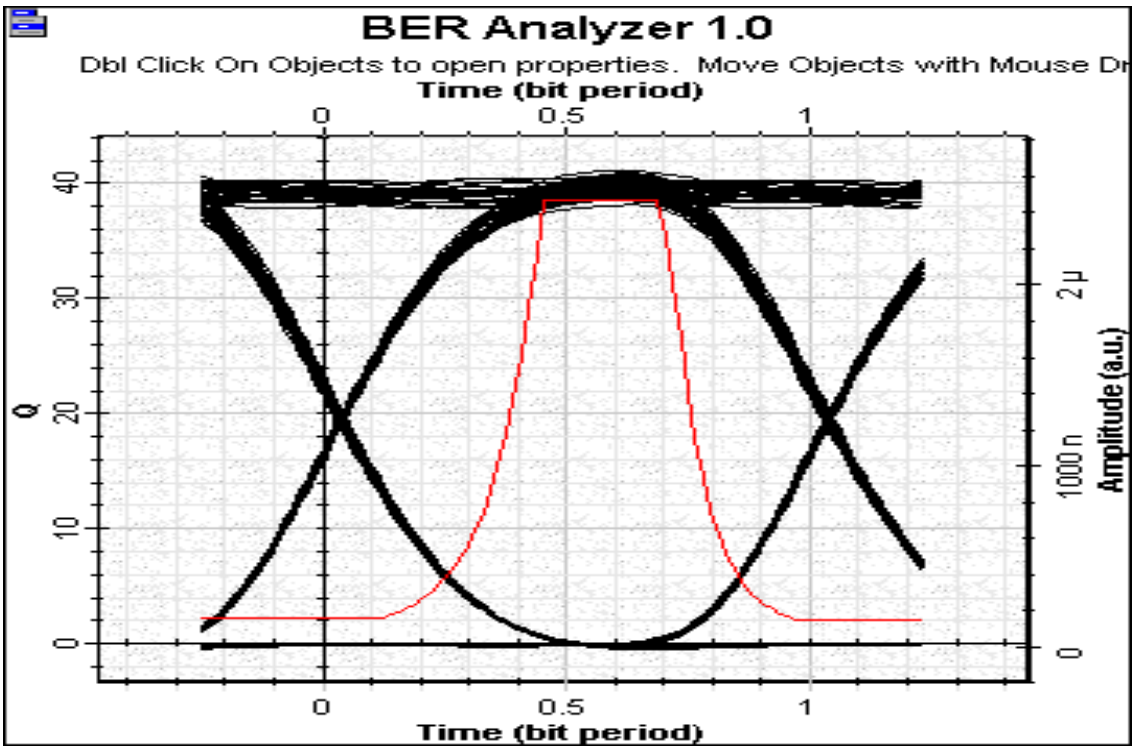

Fig.8: Fiber 100 km

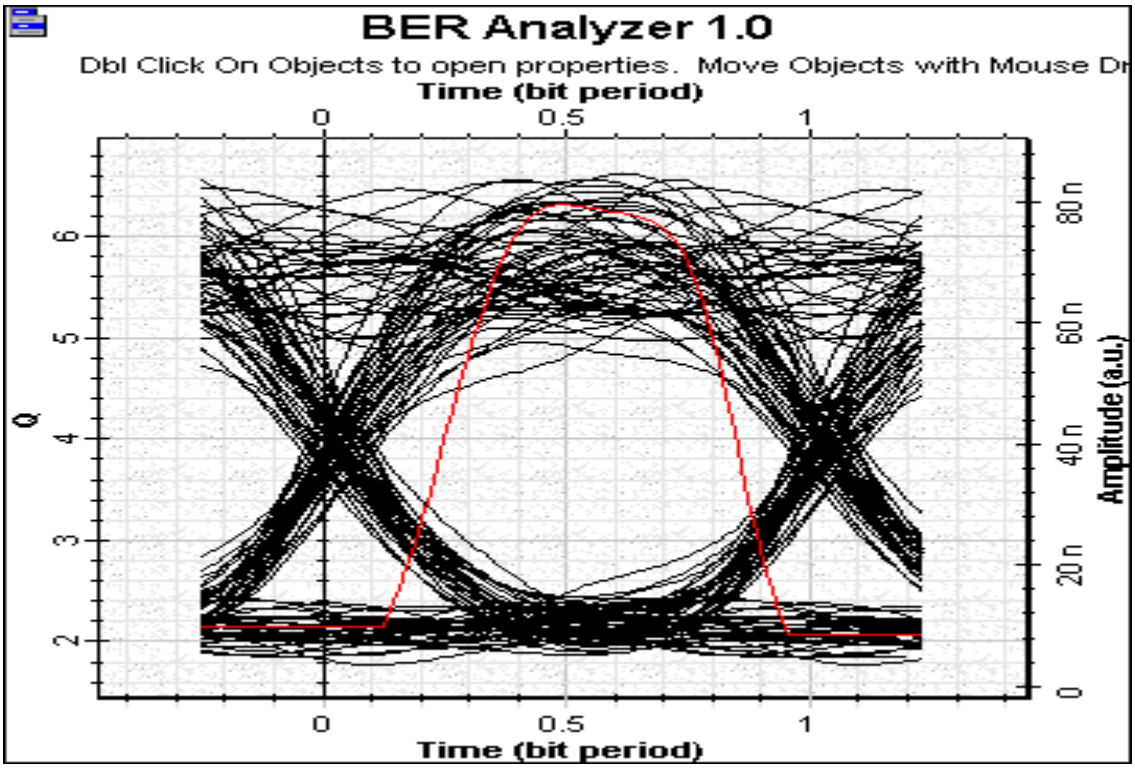

Fig.9: Fiber 165 km

(b) Optical Transmitters

The role of the optical transmitter is to convert the electrical signal into optical form and to launch the resulting optical signal into the optical fiber. It consists of an optical source, an electrical pulse generator and an optical modulator.

The launched power is an important design parameter, as it indicates how much fiber loss can be tolerated. It is often expressed in units of dBm with 1 mW as the reference level. Table 1 shows the laser power units.

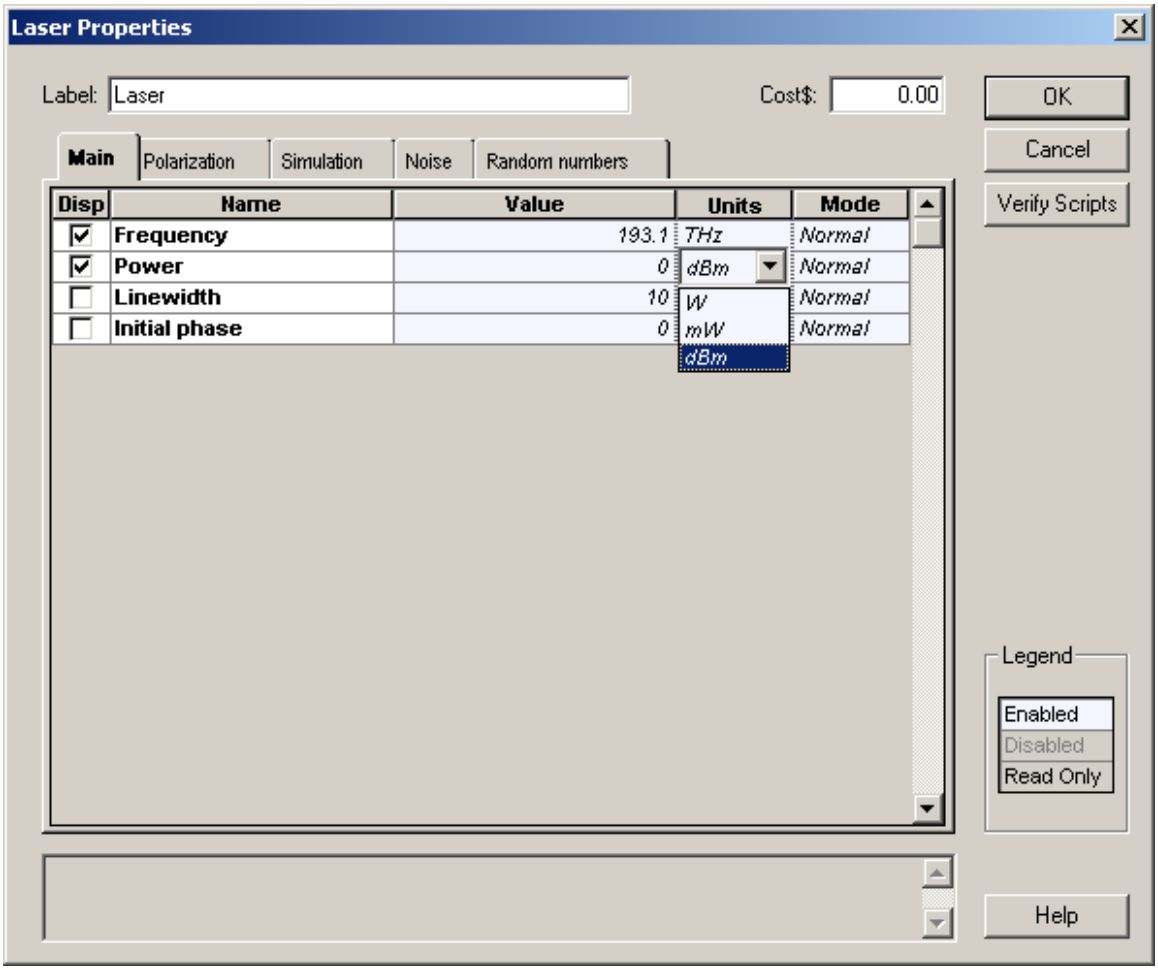

Table 1: Laser power units

(c) Optical Receivers

An optical receiver converts the optical signal received at the output end of the optical fiber back into the original electrical signal. It consists of a photodetector, filter and a demodulator. Often the received signal is in the form of optical pulses representing 1 and 0 bits and it is converted directly into an electrical current. Such a scheme is referred to as intensity modulation with direct detection (IM/DD). Demodulation is done by a decision circuit that identifies bits as 1 or 0, depending on the amplitude of the electrical current.

The performance of a digital lightwave system is characterized through the bit-error rate (BER). It is customary to define the BER as the average probability

with incorrect bit identification. Most lightwave systems specify a BER of 10^{-9} as the operating requirement.

For this project file a laser output power of 0 dBm with 167 km of fiber length will have a BER of 10^{-9} **(Fig.10).**

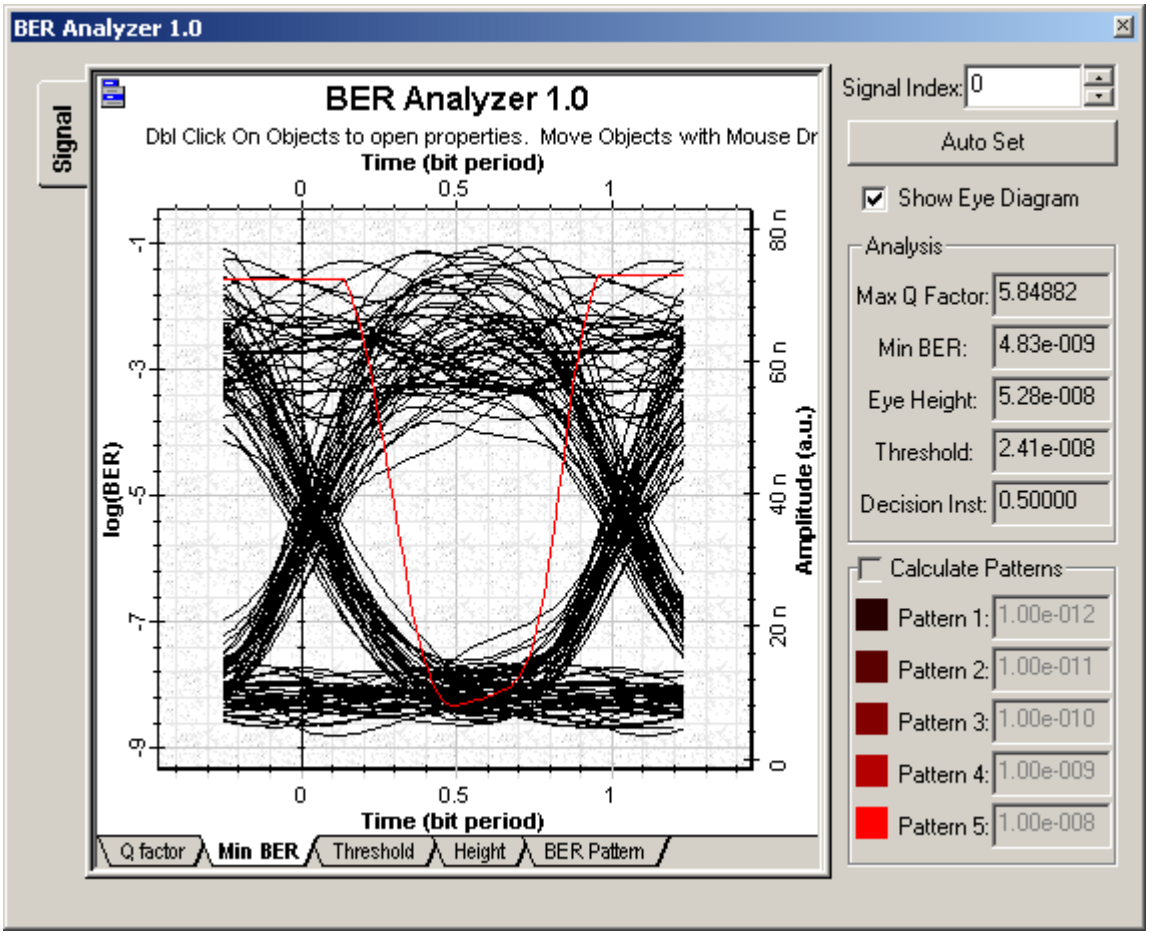

Fig.10: BER for 167 km of fiber length

Chapter 2 – Optical Fibers

Example: Limitations on the Bit Rate

Limitations on the bit rate**.osd**

In this example we demonstrate the influence of the group velocity dispersion in SMF at 1.55 μm using externally and directly modulated optical sources. We consider the unchirped pulse and neglect the influence of the initial pulse.

Case A: Optical source with a small spectral width

Externally modulated laser is used as an optical source with a small spectral width. We consider a 10 Gb/s transmission with the layout as shown in Fig.1.

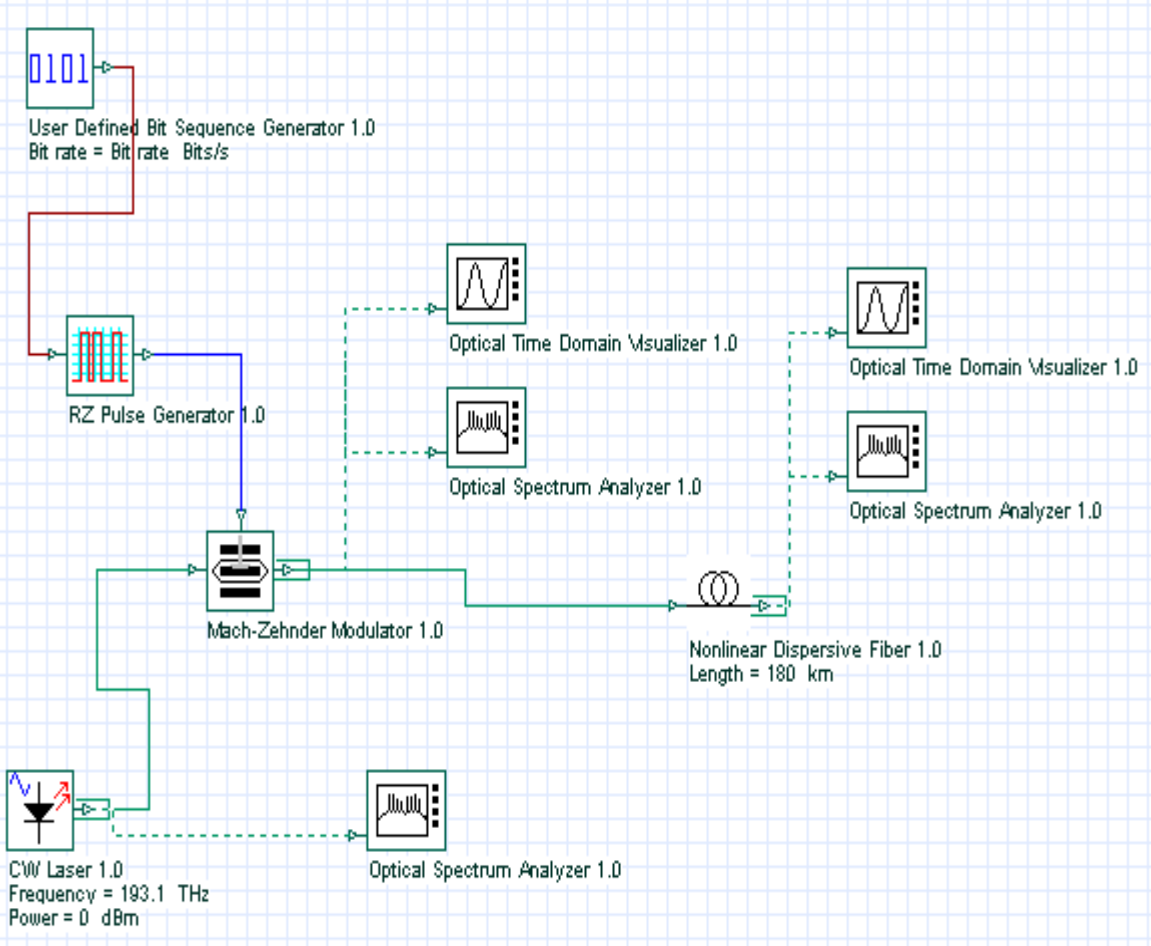

Fig.1: Layout: Optical source with a small spectral width

For simulation, we consider duty cycle = 0.5 and T_{FWHM} = 50 ps $\Rightarrow$ T_0 = 30 ps $\Rightarrow$ L_D = 45 km$\Rightarrow$ $\Delta\omega$ = 33 GHz, giving σ_w ~ $2\pi \times 10$ MHz. Fig.2 shows the generated spectrum of the CW laser. Since $\sigma_w / \Delta\omega << 1$, for the spread of the pulse width, we can expect the validity of the following formula:

$$\frac{\sigma^2}{\sigma_0^2} = 1 + \left(\frac{\beta_2 z}{2\sigma_0^2}\right)^2 = 1 + \left(\frac{z}{L_D}\right)^2 \qquad (1)$$

Equation (1) shows that to get 4 times increase of the pulse width a distance of approximately 4 L_D (~ 180 km) is needed.

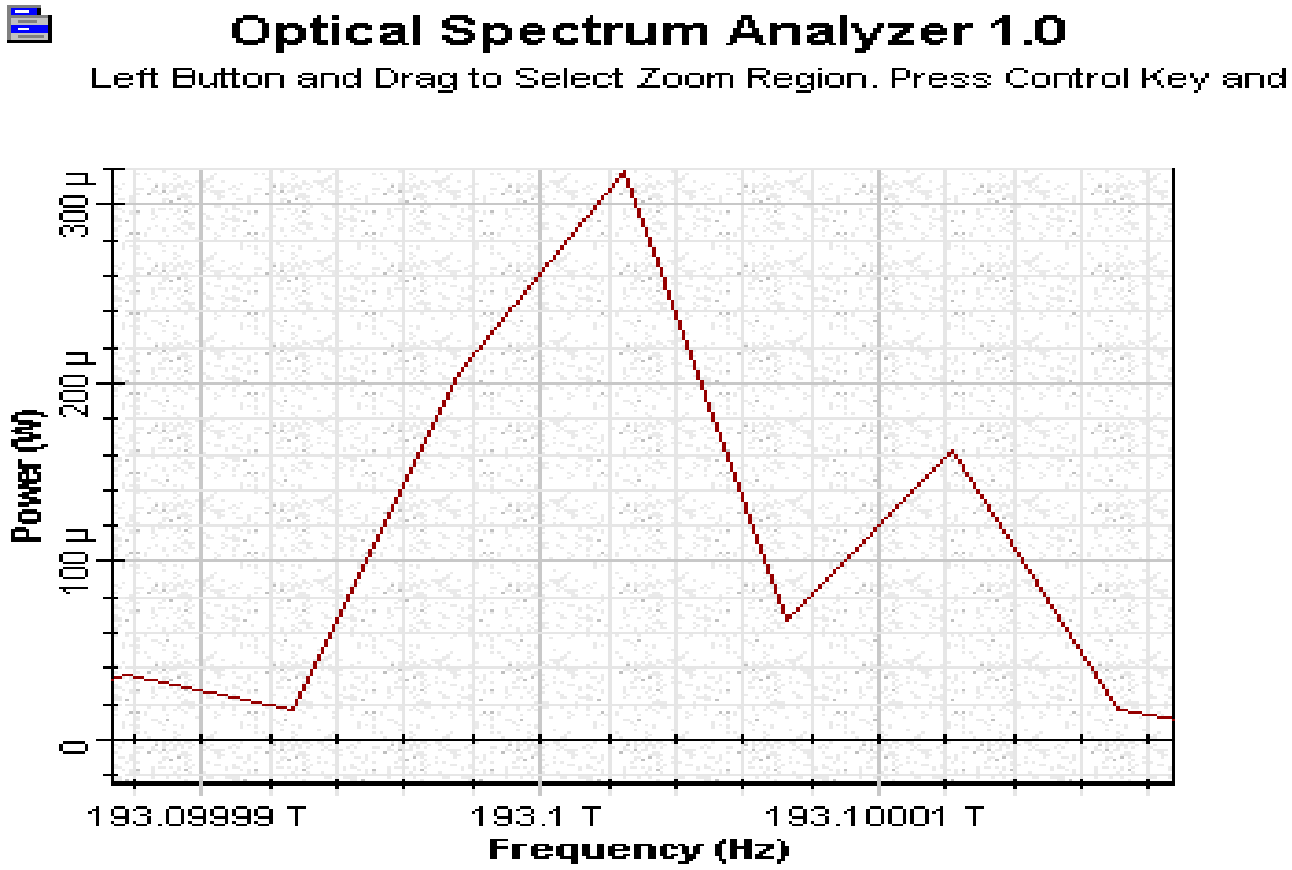

Fig.2: Part of the spectrum of the CW laser

(Note that to get enough spectral resolution a very large time window was used with sequence length 2048 bits and 64 samples per bit).

Obtained results after simulations, are presented in Figs. 3,4 and 5.

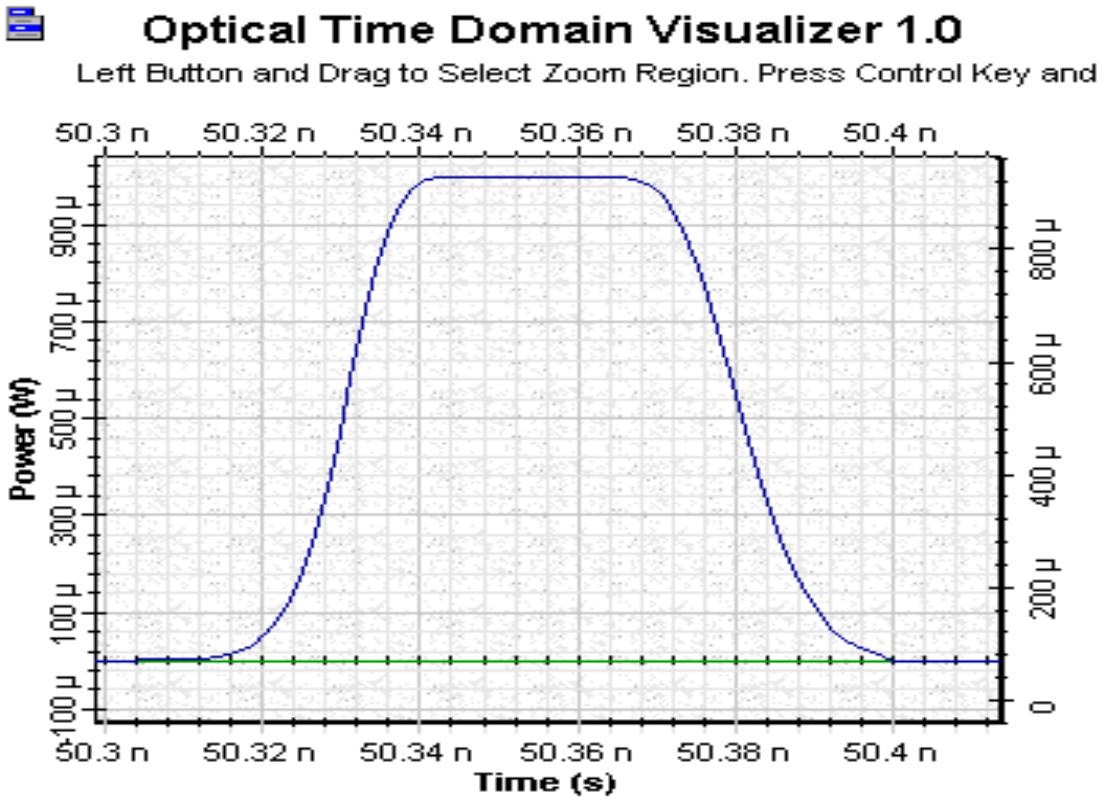

Fig.3: Pulse shape after modulator

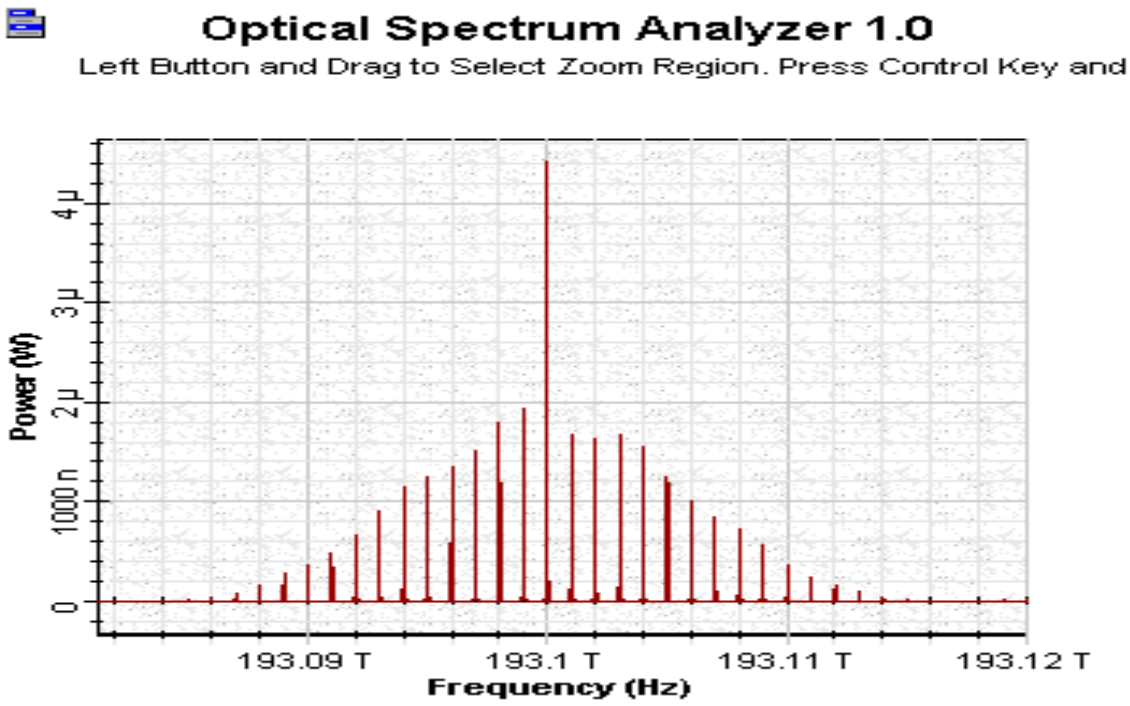

Fig.4: Pulse spectrum after modulator

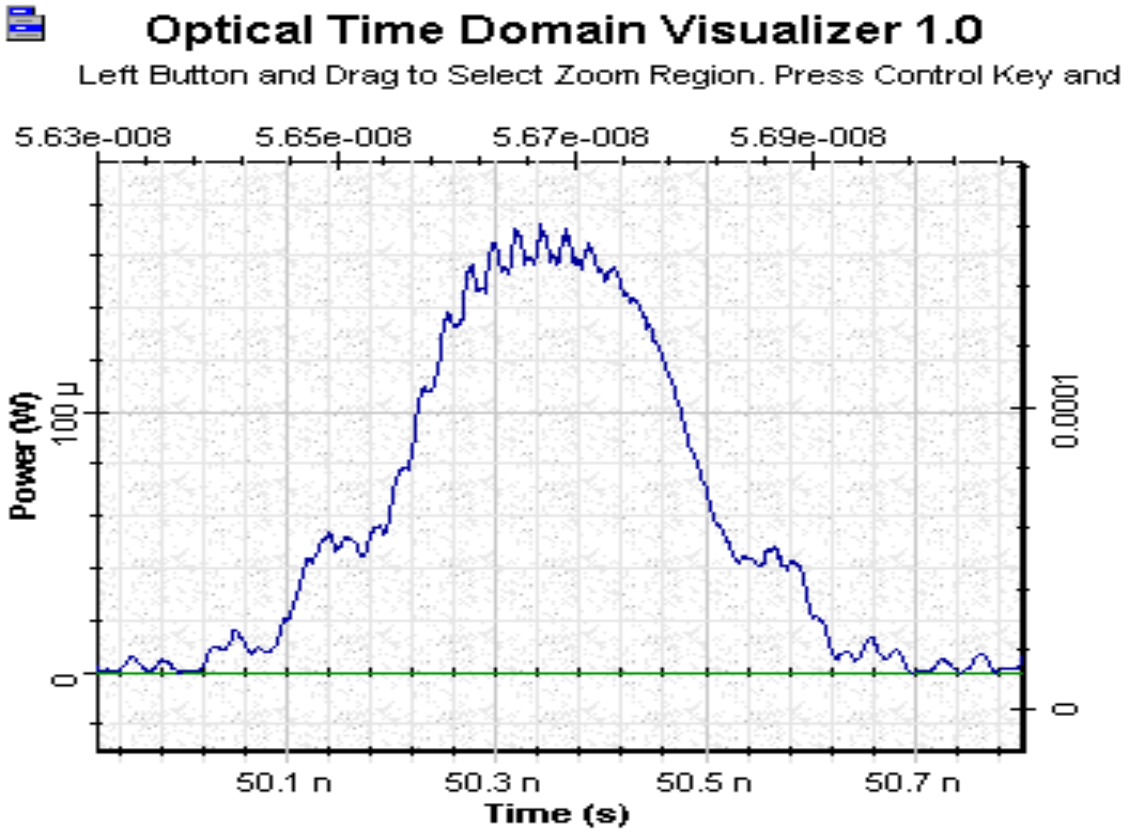

Fig.5: Pulse shape after 180 km transmission in SMF

As can be seen that the pulse width increases of approximately 5 times (cf. Equation (1)).

Case B: Optical source with a large spectral width

Directly modulated laser is used as optical source with a large spectral width. A 2.5 Gb/s transmission is considered. The corresponding layout is shown in Fig.6.

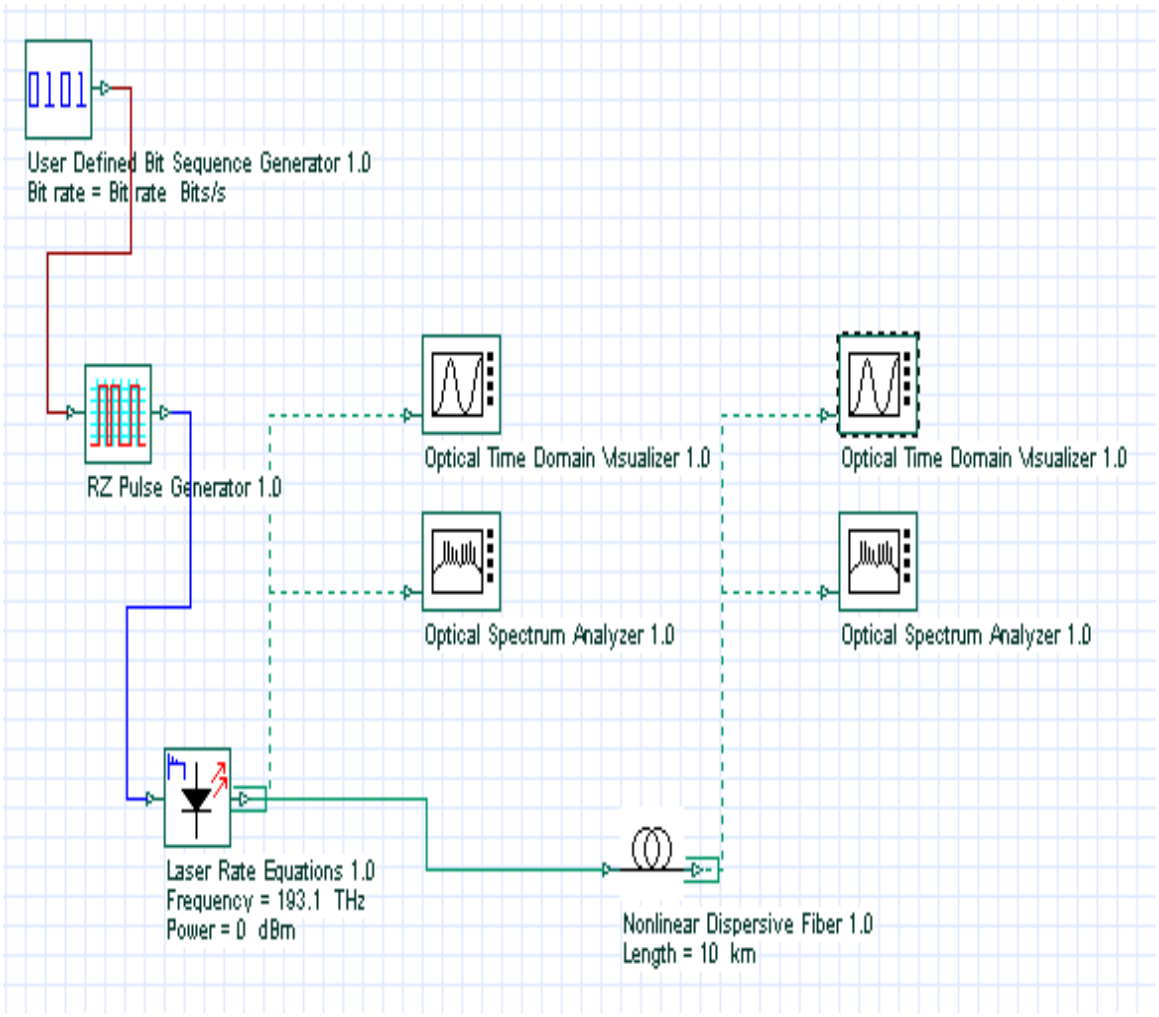

Fig.6: Lay out : Optical source with a large spectral width

Laser is described by Laser rate equations model. **Figs. 7 and 8** show the shape and spectral characteristics produced by the laser source pulses.

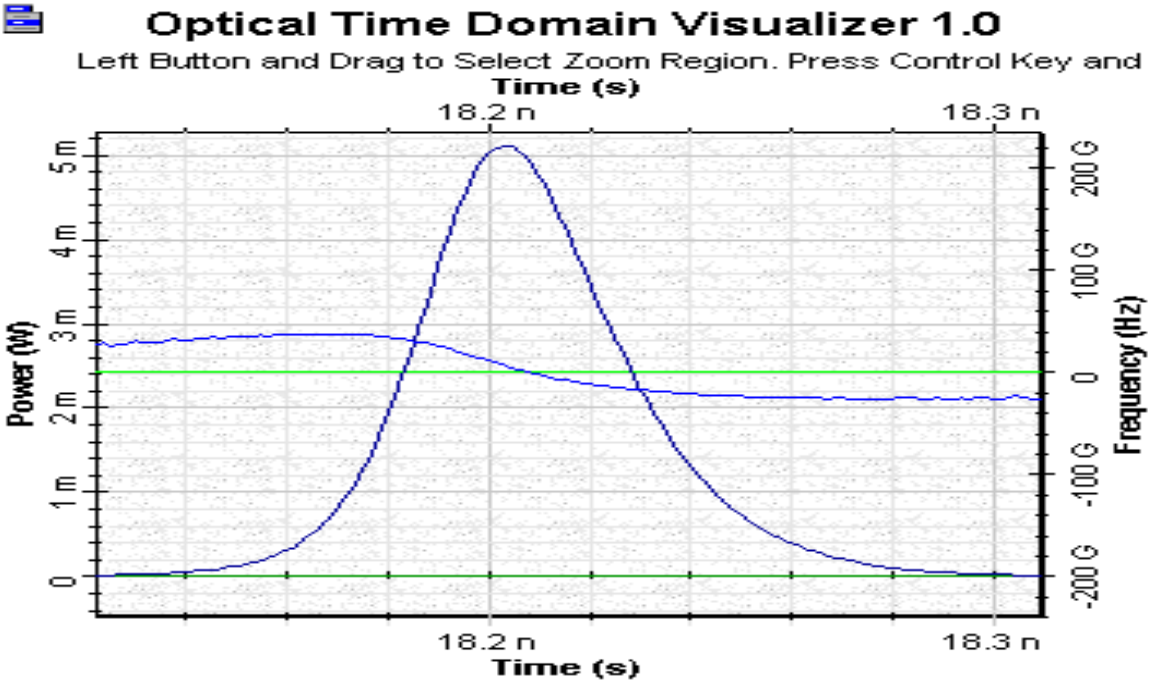

Fig.7: Initial pulse shape

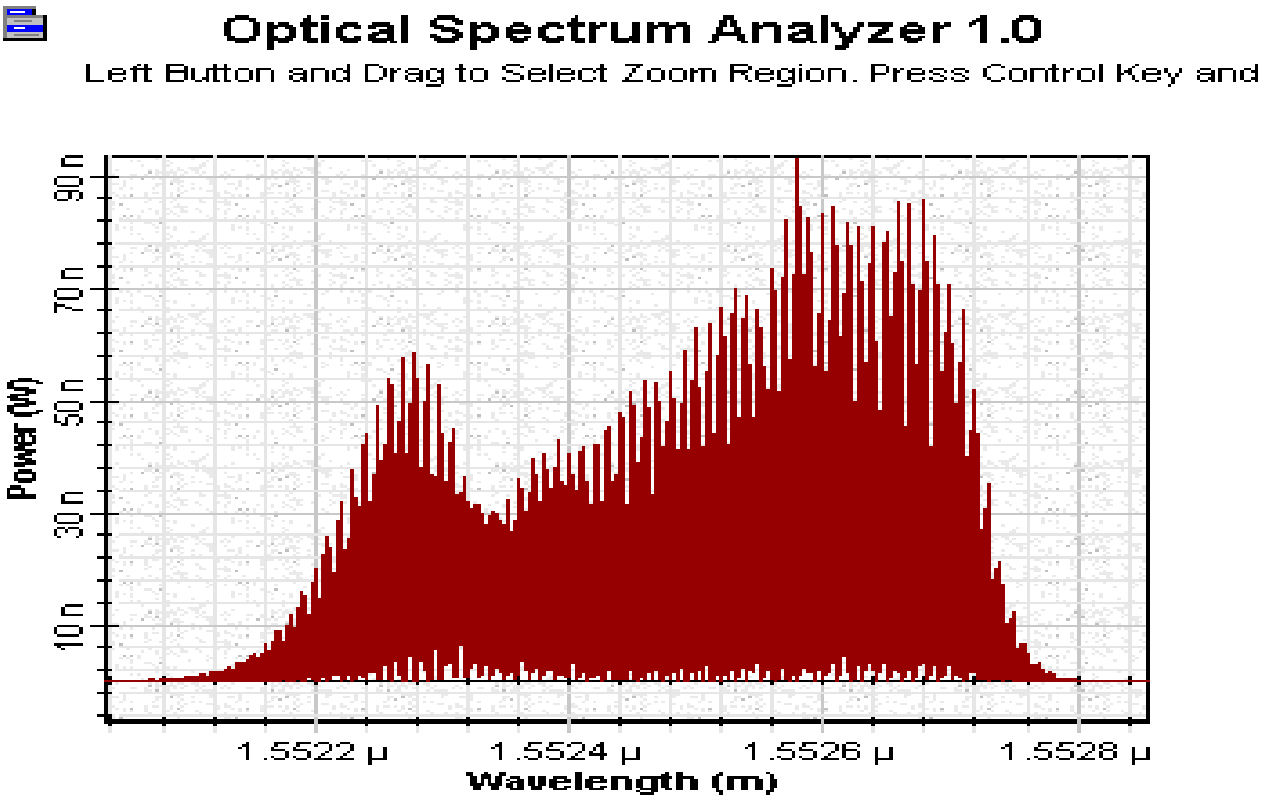

Fig.8: Initial source spectrum

We considered an initial pulse with T_{FWHM} ~ 40 ps $\Rightarrow T_0$ = 24 ps $\Rightarrow L_D$ = 29 km$\Rightarrow \Delta\omega = 2\pi \times 40$ GHz. The negative initial chirp of the pulse can also be seen in Fig.7. It's contribution in calculation of $\Delta\omega$ has been neglected. The spectral width from Fig. 8 is σ_λ ~ 0.5 nm ($\sigma_w \sim 2\pi \times 62$ GHz) $\Rightarrow \sigma_w / \Delta\omega$ ~ 2. For $\sigma_w / \Delta\omega$ >> 1 (neglecting the influence of the initial chirp) the following approximate equation can be found:

$$\frac{\sigma^2}{\sigma_0^2} = 1 + \left(\frac{\beta_2 z \sigma_w}{\sigma_0} \right)^2 \qquad (2)$$

In accordance with this equation to get ~ 4 times increase in pulse width ~ 10 km propagation in SMF is required. Results from calculations of such transmission are shown in Fig.9.

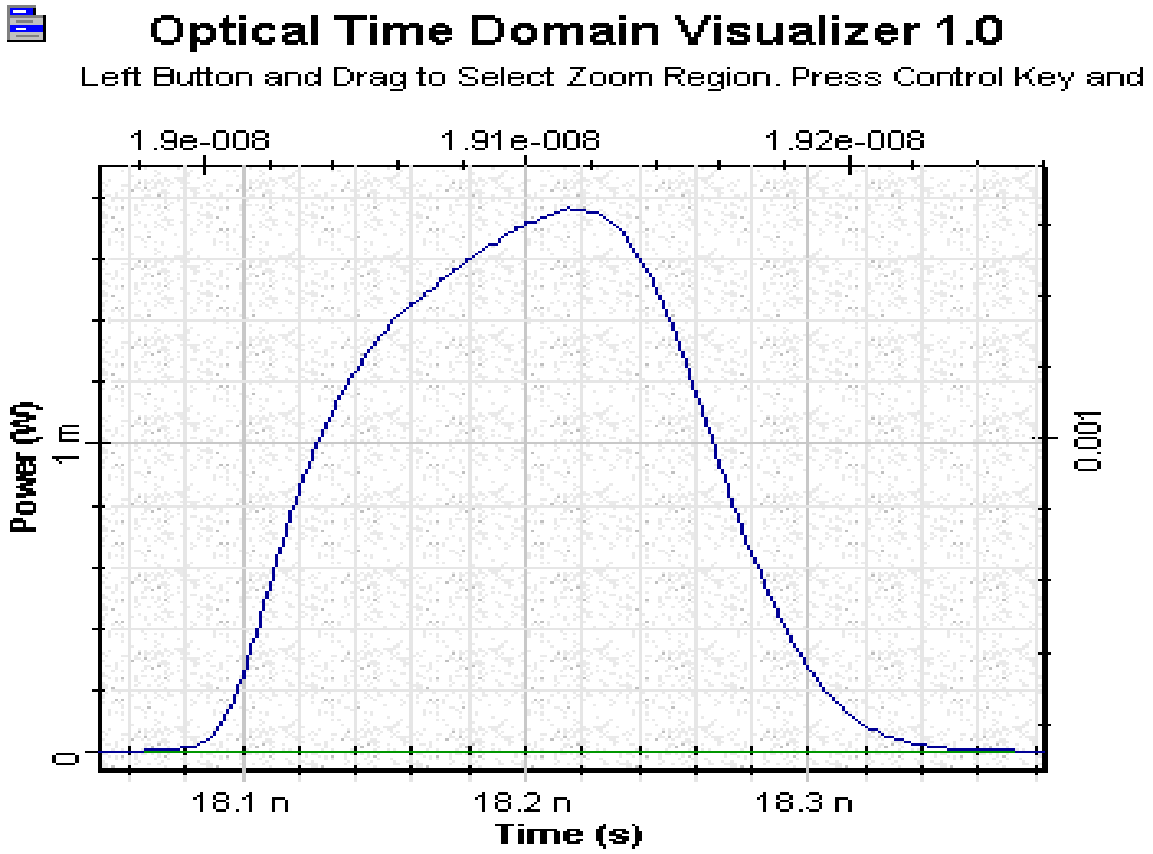

Fig.9: Pulse shape after 10 km transmission in SMF

As can be seen that the pulse width increases approximately 3.5 times (cf. Equation (2)).

Reference:

G.P.Agrawal, "Nonlinear Fiber optics", third edition, Academic Press, 2001.

Example: Chirped Gaussian Pulse

Chirped Gaussian pulses.**osd**
Chirped Gaussian pulses_dispersion compensation.**osd**

Chirped Gaussian Pulses

In this example we show the influence of the GVD on the spatial evolution of the pulse width of initially chirped Gaussian pulse.The general expression for the spatial evolution of pulse width in dispersive media is given by:

$$\frac{\sigma^2}{\sigma_0^2} = \left(1 + \frac{C\,\beta_2\,z}{2\sigma_0^2}\right)^2 + \left(1 + V_\omega^2\right)\left(\frac{\beta_2\,z}{2\sigma_0^2}\right)^2 \qquad (1)$$

where: C is the initial chirp of the pulse,

σ is the root mean square (RMS) width of the pulse,

$V_w = 2\sigma_w\sigma_0 = \sqrt{2}\ \sigma_w / \Delta\omega$ is the parameter describing the relative contribution of spectral width of the source and of the pulse

$\sigma_0 = T_0 / \sqrt{2}$, where T_0 is the initial pulse width,

$\beta_2 = -2\pi c / \lambda^2 D$.

$\Delta\omega = 1/ T_0$, is the spectral width of the unchirped Gaussian pulse

The typical value of $\beta_2 = -20$ ps^2/ km at 1.55 μm for SMF leads to D = 16 ps/(nm . km).

For the considered optical source (source with small spectral width) the limiting transmission distances are determined from pulse width and the GVD. For such sources the dispersive action of the media is described by the dispersion length $L_D = T_0^2 / |\beta_2|$, which characterizes the pulse spreading in dispersive media. In this case (cf. Eq.(1)), initially unchirped pulse can be simplified to:

$$\Rightarrow \qquad \frac{\sigma^2}{\sigma_0^2} = 1 + \left(\frac{\beta_2\,z}{2\sigma_0^2}\right)^2 = 1 + \left(\frac{z}{L_D}\right)^2 \qquad (2)$$

If for a Gaussian pulse we assume duty cycle = 0.5, then

B = 2.5 Gb/s $\Rightarrow$ T_B = 400 ps $\Rightarrow$ T_{FWHM} = 200 ps $\Rightarrow$ T_0 = 120 ps $\Rightarrow$ L_D = 720 km$\Rightarrow$ $\Delta\omega$ = 8.3 GHz $\Rightarrow$ $\sigma_w / \Delta\omega << 1$

B = 10 Gb/s $\Rightarrow$ T_B = 100 ps $\Rightarrow$ T_{FWHM} = 50 ps $\Rightarrow$ T_0 = 30 ps $\Rightarrow$ L_D = 45 km$\Rightarrow$ $\Delta\omega$ = 33 GHz $\Rightarrow$ $\sigma_w / \Delta\omega << 1$

B = 40 Gb/s $\Rightarrow$ T_B = 25 ps $\Rightarrow$ T_{FWHM} =12.5 ps $\Rightarrow$ T_0 = 7.5 ps $\Rightarrow$ L_D = 2.8 km$\Rightarrow$ $\Delta\omega$ = 133 GHz $\Rightarrow$ $\sigma_w / \Delta\omega << 1$

Let us consider B= 40 Gb/s. In accordance with Eq.(2) at 4 L_D the width of the initially unchirped pulse will increase approximately 4 times. This can be demonstrated with chirped Gaussian pulses**.osd** which has the following layout **(Fig.10):**

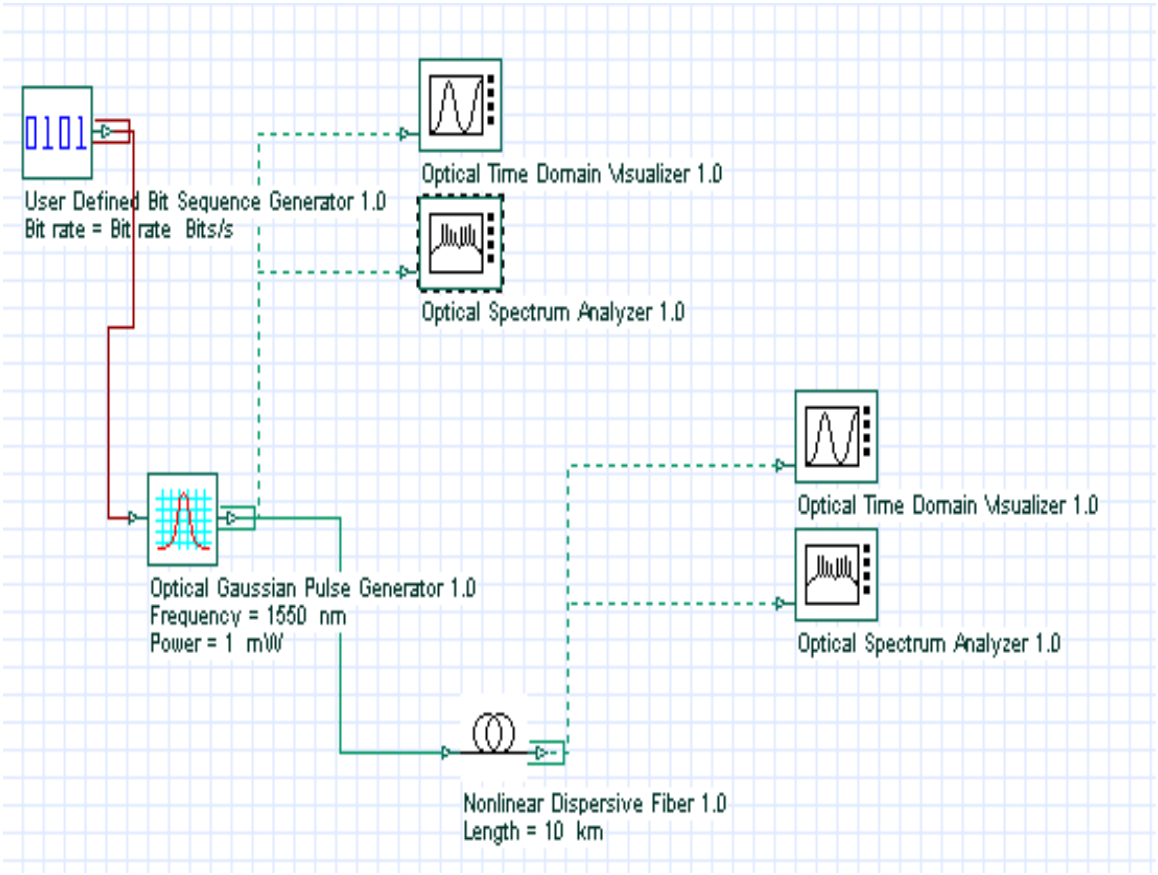

Fig.10: Lay out: Chirped Gaussian pulses

The obtained results for 40 Gb/s transmission, duty cycle = 0.5 and for SMF with D = 16 ps/(nm . km) or β_2 = - 20 ps^2/ km at 1.55 μm are shown in the Figs.11(a),11(b),11(c) and 11(d), respectively.

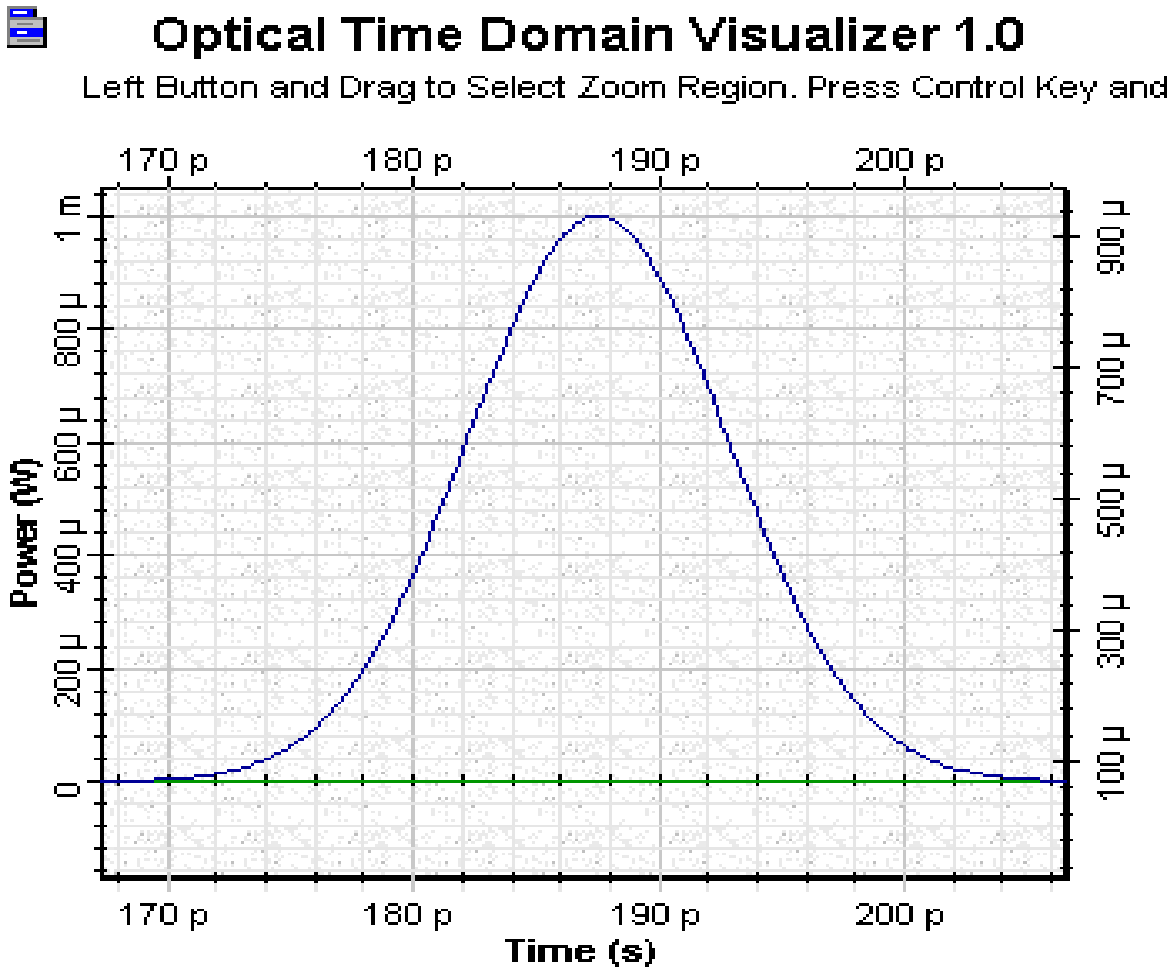

Fig.11(a): Initial pulse shape

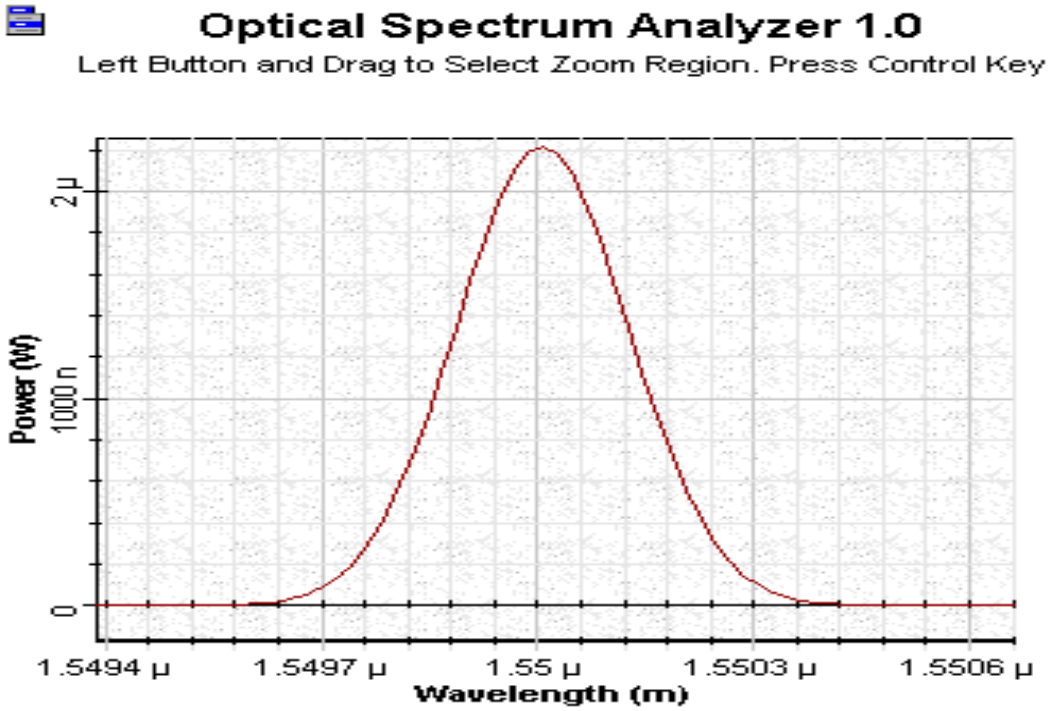

Fig.11(b): Initial pulse spectrum

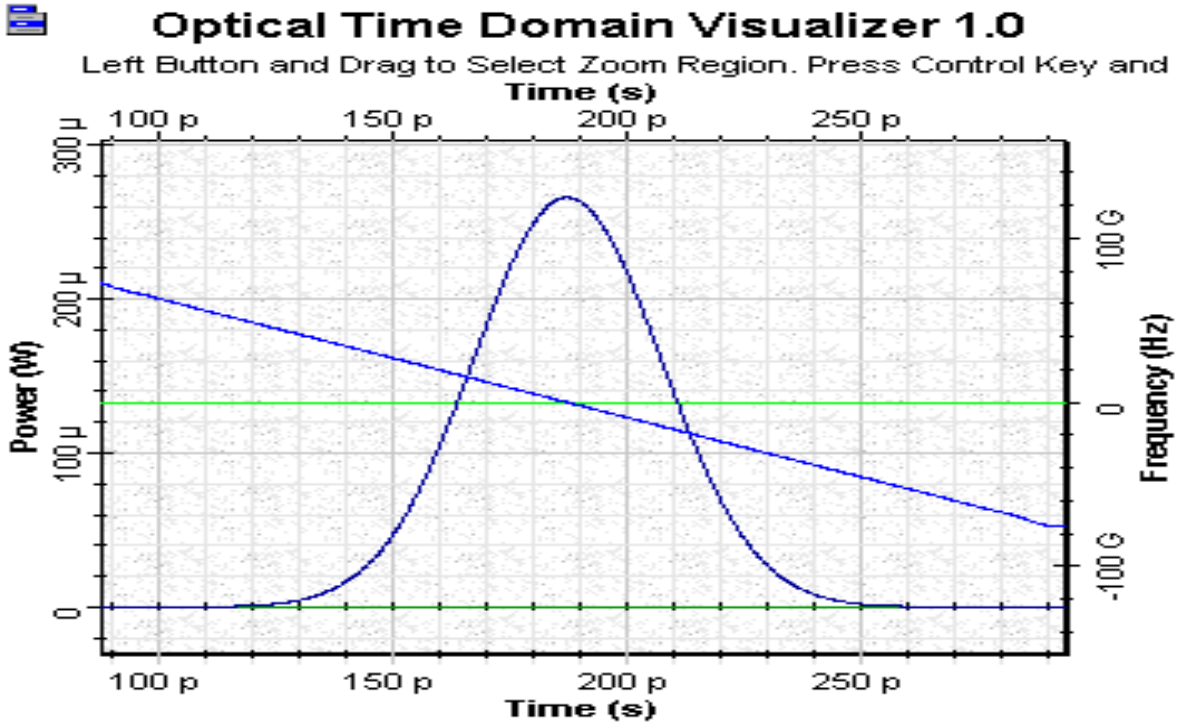

Fig.11(c): Pulse shape after 10 km transmission in SMF

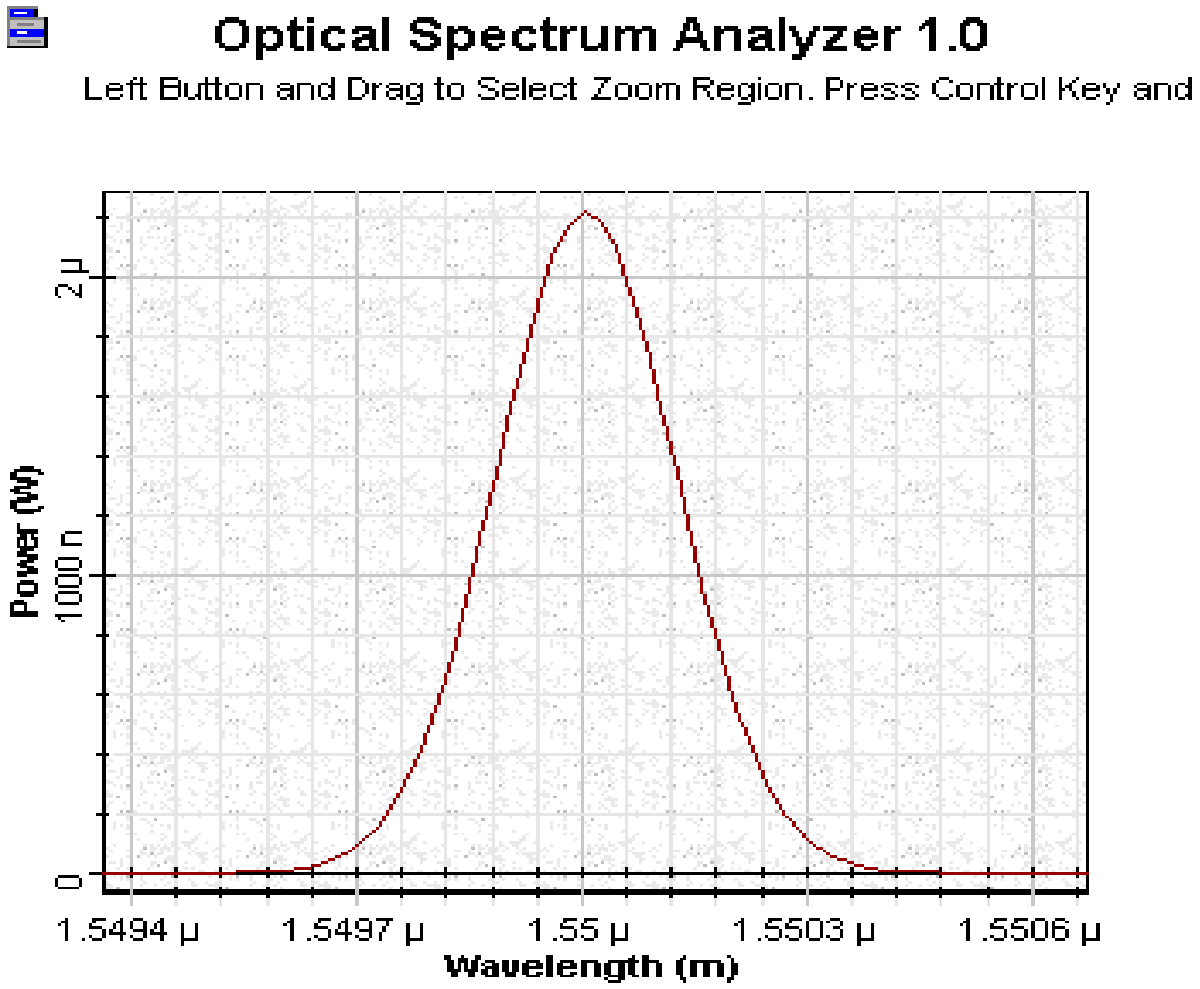

Fig.11(d): Pulse spectrum after 10 km transmission in SMF

As expected (cf. Eq. (2)), an increase of the initially unchirped pulse width by approximately 4 times can be clearly seen. Note the appearance of the negative chirp of the pulse after 10 km transmission in anomalous group velocity dispersion region (Fig.11(c)). Because the GVD is the only included effect in the calculation, no changes in the spectrum after transmission can be observed.

General view of the behavior of the pulse shape during propagation in fiber can also be seen in Fig.12.

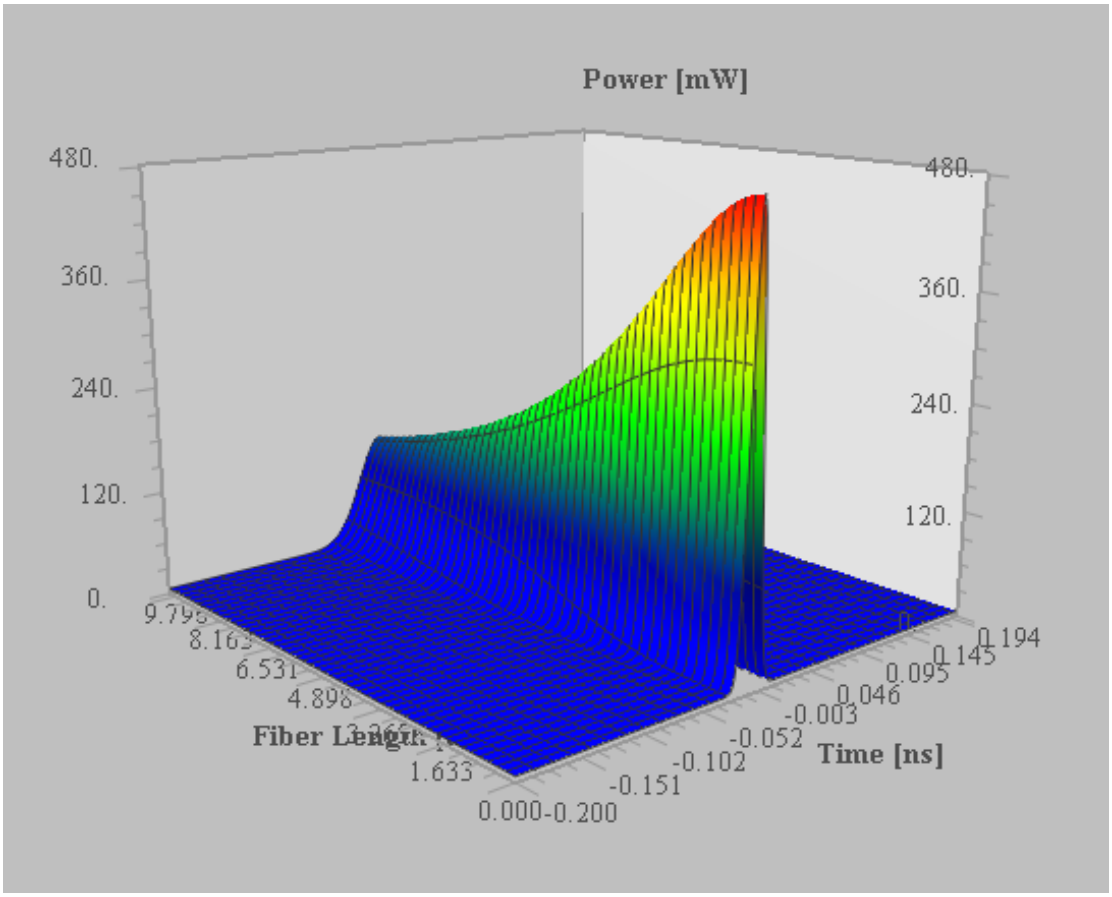

Fig.12: Evolution of the pulse shape up to 10 km

Now, we consider the pulse evolution of the initially chirped pulse (Version Chirped C = -2) for transmission distance of 8 km. From Eq.(2) we see that when $C\beta_2$ > 0 the dispersion of the pulse is increased with comparison to unchirped initial pulse. Results are shown in **Figs.13 and 14.**

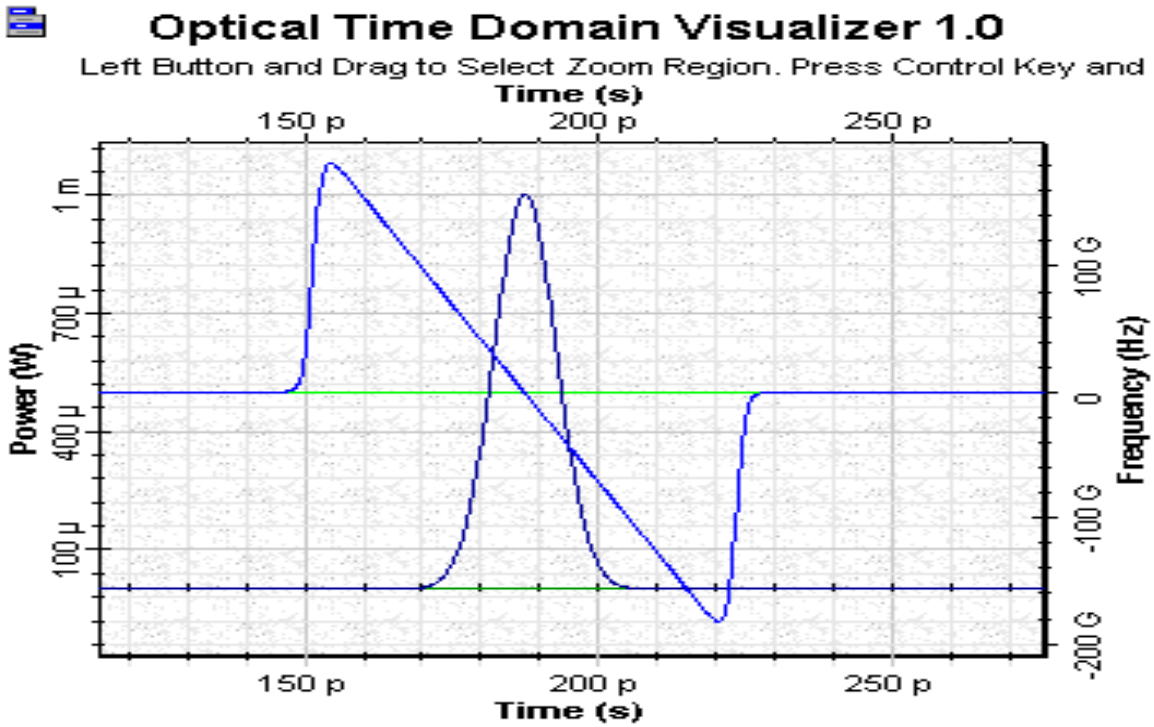

Fig.13:Initial chirped pulse shape (C = - 2). Note the negative initial chirp shown in the figure.

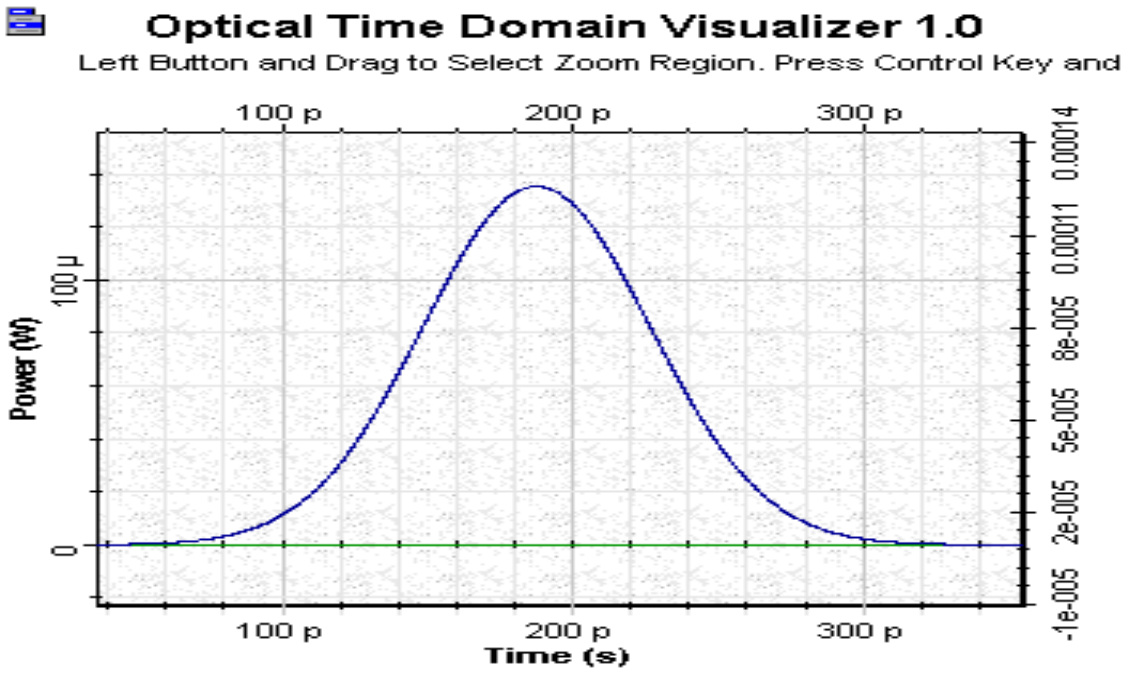

Fig.14: Increase of pulse dispersion after 5 km transmission in SMF

As we see from Fig.14, after only 8 km the pulse width increases approximately 7 times or much more as compared to the case of initially unchirped pulse.

However, if we substitute $C\beta_2$ < 0 in Eq.(1), the pulse compression could be expected. To demonstrate this type of behavior (Version Chirped C = 2), we consider the transmission distance of 0.8 km.

Results are shown in Figs. 15 and 16.

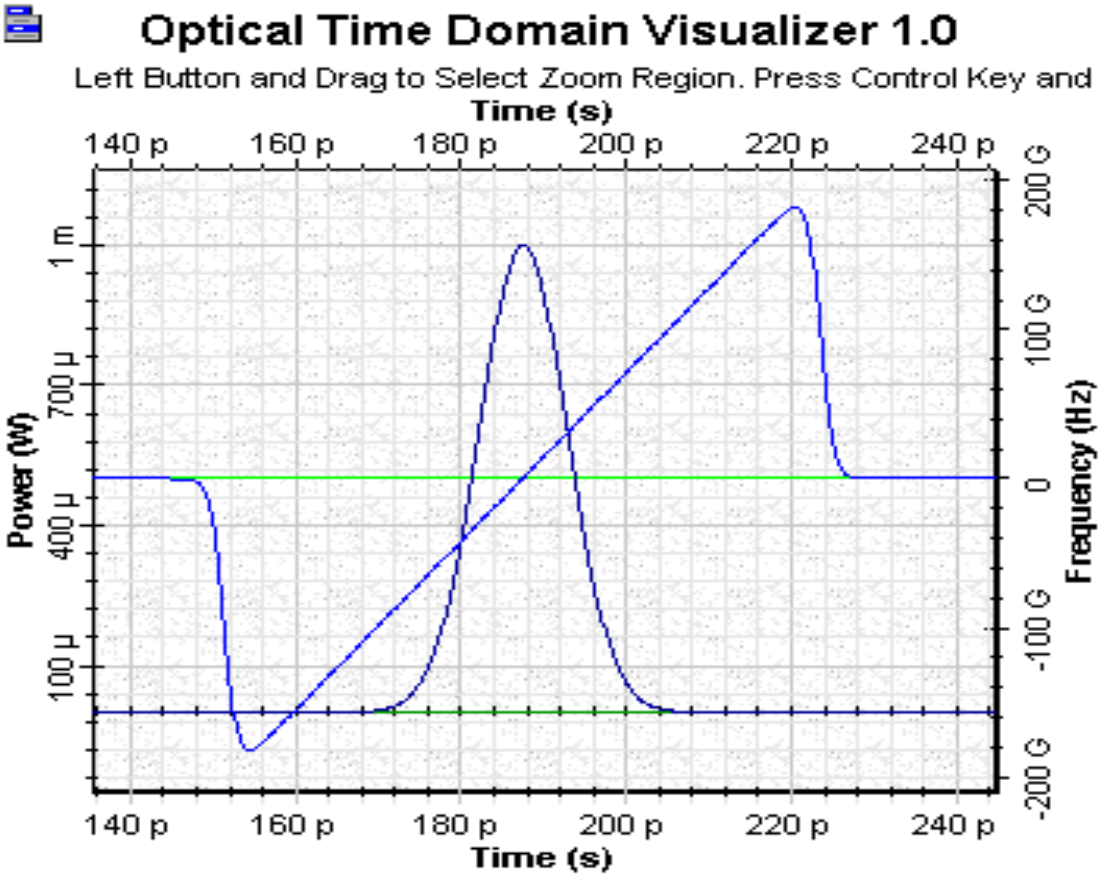

Fig.15: Initial chirped pulse shape (C = 2). Note the positive initial chirp shown in the figure.

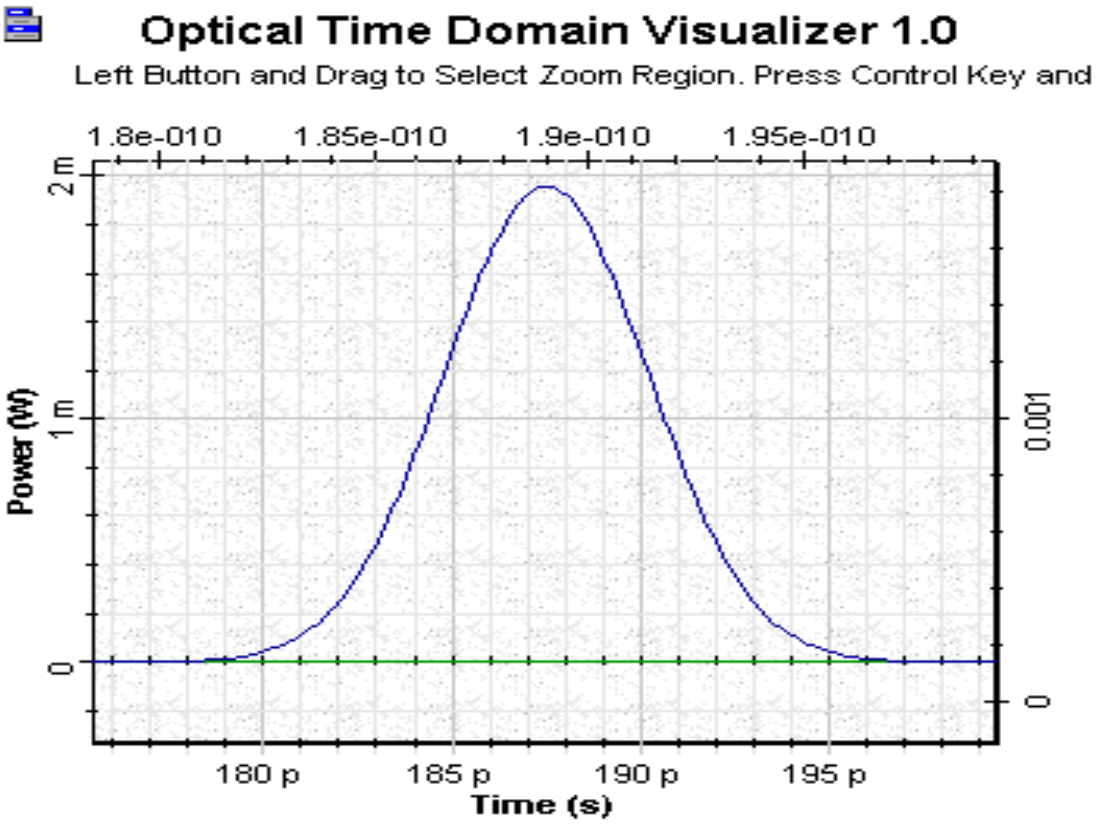

Fig.16: Pulse compression after 0.8 km transmission in SMF

As we see pulse gets reduced approximately two times as compared to its initial width after 0.8 km propagation in SMF.

Chirped Gaussian pulses_dispersion compensation

Now, we will pay the attention of the cancellation of the chirps in both fibers. The project has the following layout (Fig.17):

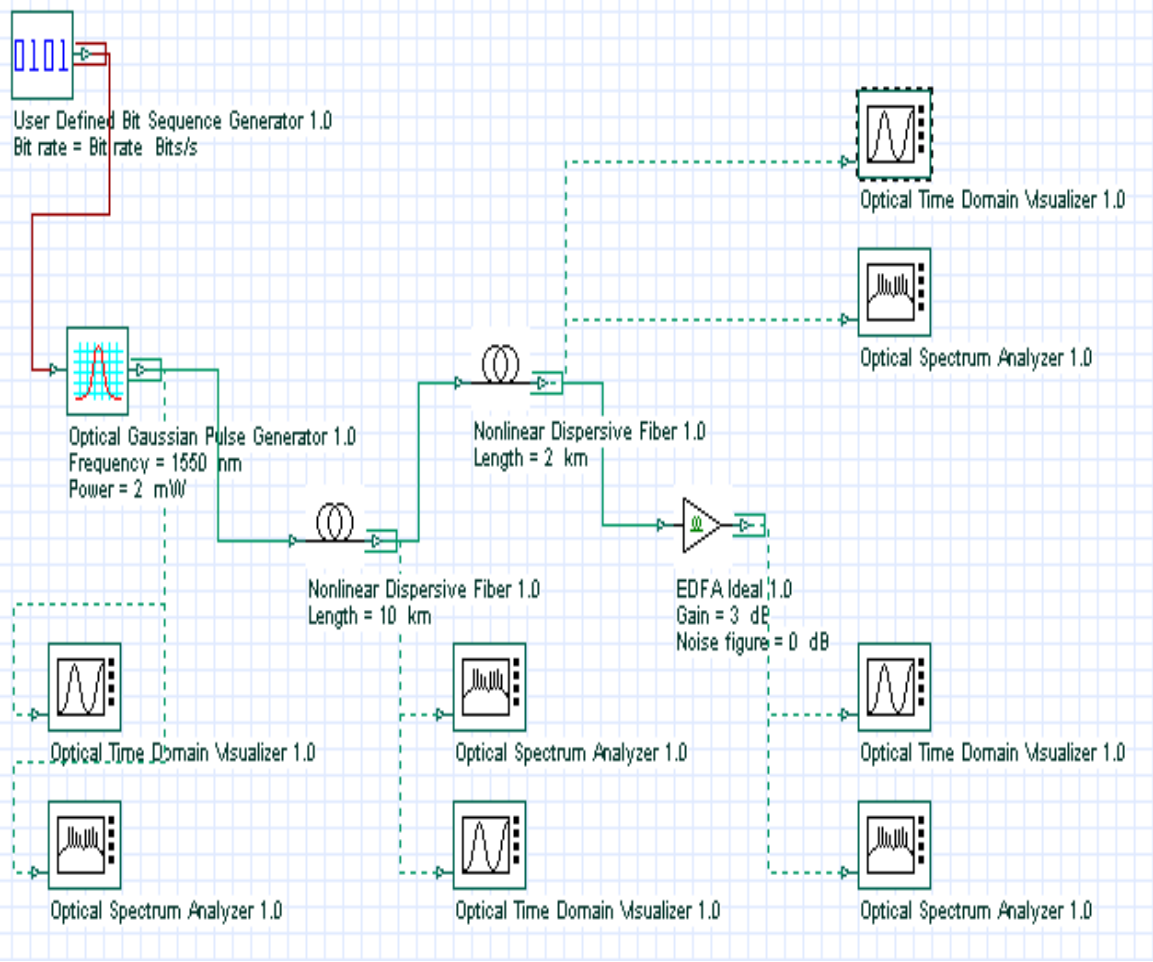

Fig.17: Layout: Chirped Gaussian pulses_dispersion compensation

We choose the following parameters for standard single mode fiber:

D_{SMF} = 17 (ps/nm. km), $\partial D_{SMF} / \partial \lambda$ = 0.08 (ps/nm^2 .km), γ_{SMF} = 1.31 (1 / km. W), α_{SMF} = 0.2 (dB / km) and L_{SMF} = 10 km.

And the following parameters for dispersion compensation fiber:

D_{DCF} = -80 (ps/nm. km), $\partial D_{DCF} / \partial \lambda$ = 0.08 (ps/nm^2 .km), γ_{DCF} = 5.24 (1 / km. W), α_{DCF} = 0.5 (dB / km) and L_{DCF} = 2 km.

The results are shown in Figs.18 and 19.

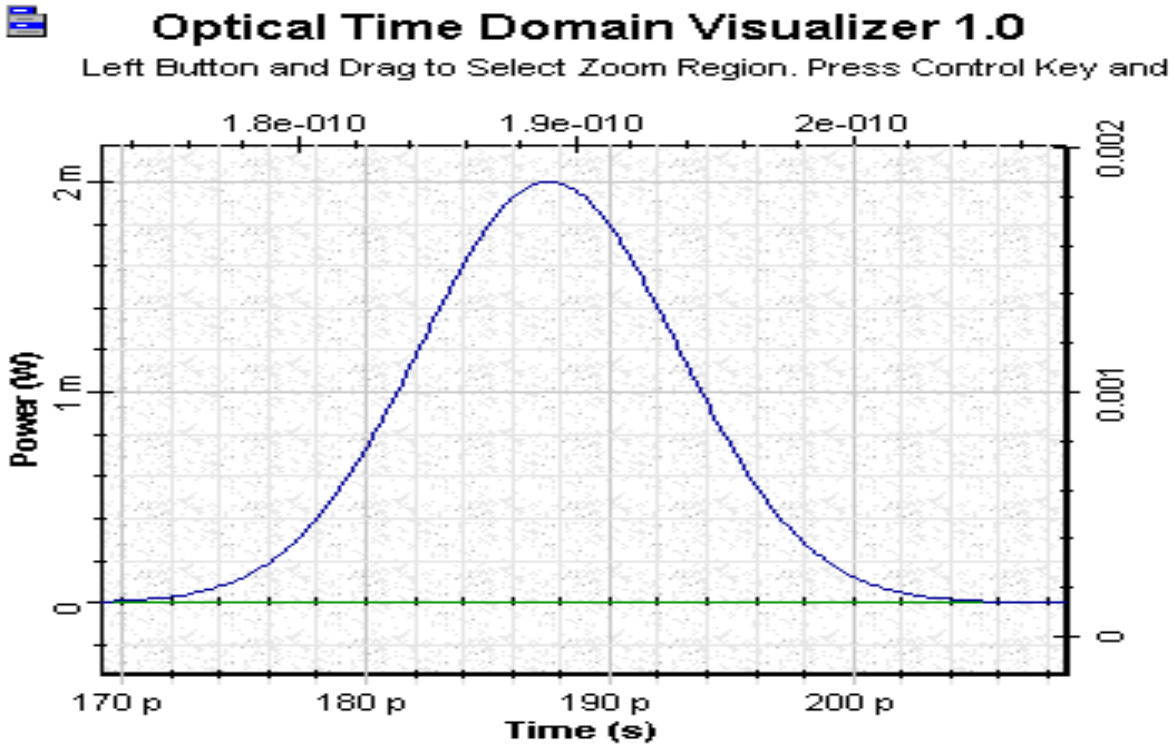

Fig.18: Initial Gaussian pulse (2 mW)

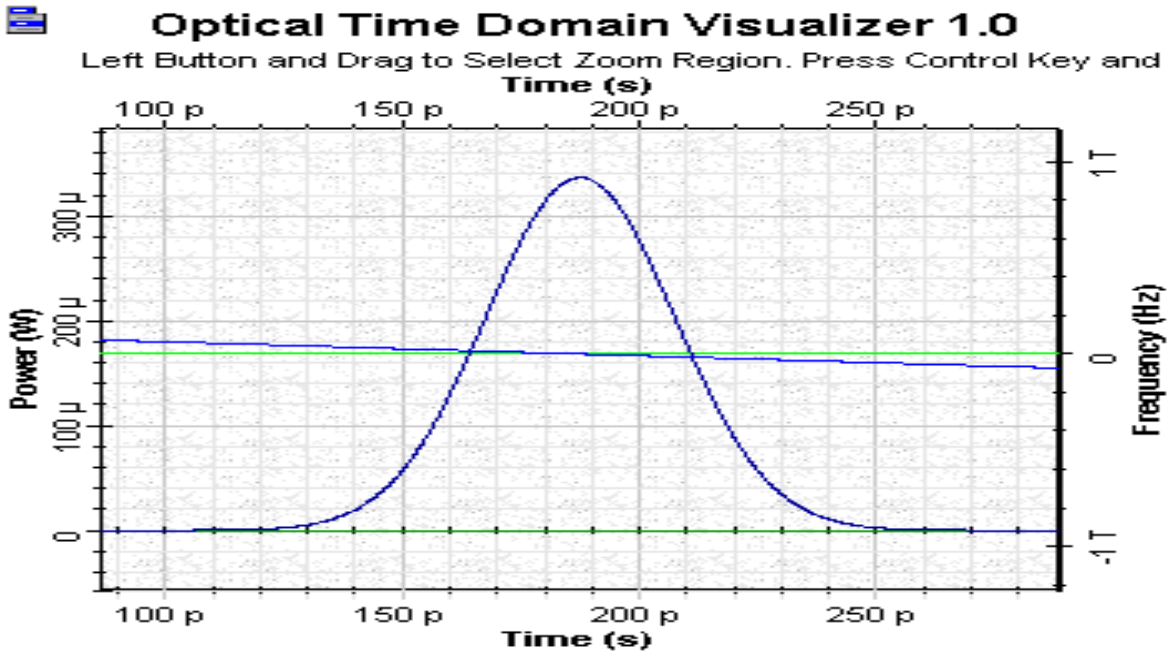

Fig.19: Pulse after 10 km in SMF

Note the negative chirp appears after 10 km propagation in SMF (Fig.19). The shape and the obtained chirp of the pulse, after 2 km propagation in DCF are shown in Fig. 20.

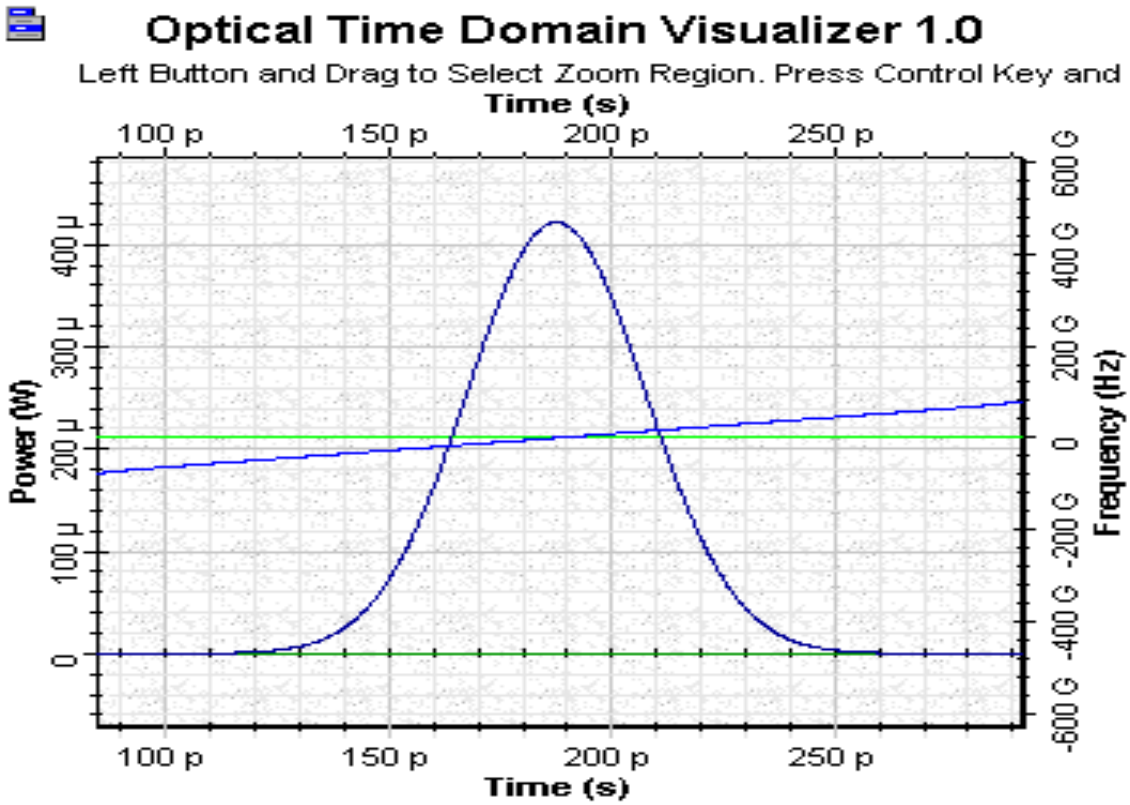

Fig.20: Shape and the obtained chirp of the pulse after 2 km propagation in DCF

Note that the obtained chirp in DCF is positive one. Just the fact that the chirp obtained in DCF is with opposite sign as compared to SMF, it leads to the complete compensation of dispersion of the SMF as shown in Figs. 21 and 22. After dispersion compensation no chirp is observed and hence the complete recovery of the pulse can be seen.

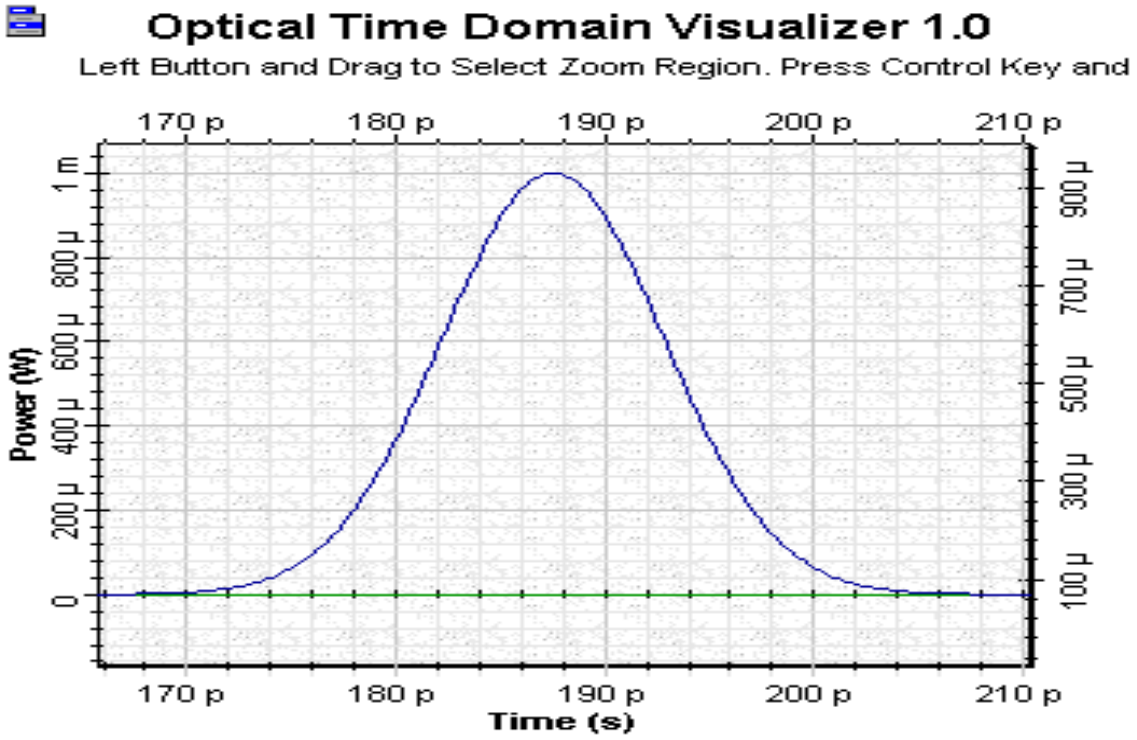

Fig.21: Pulse after 10 km in SMF and 2 km in DCF

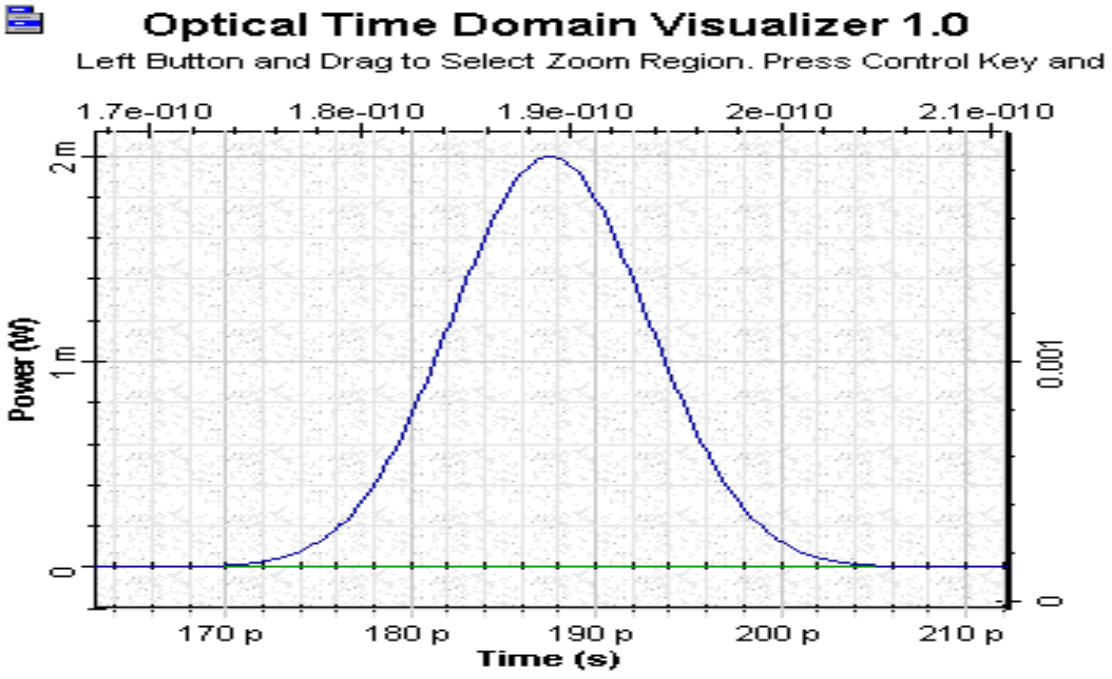

Fig.22: Pulse after amplification

References:

G.P.Agrawal, "Nonlinear Fiber optics", third edition, Academic Press, 2001.
G.P.Agrawal, Fiber optics communication Systems", John Wiley&Sons, INC, 1997.

Example: Attenuation Coefficient

Attenuation coefficient**.osd**

Project file "Attenuation coefficient**.osd**" shows power loss in the fiber. In this example a basic 50 km fiber link is designed. The system works in 1.3 μm window and the loss of fiber at this wavelength is 0.5 dB/km. Fiber is spliced after every 5 km and has two connectors of 1-dB loss at both ends. Splice loss is 0.2 dB. You can calculate the required minimum launch power to get at least 0.3 mW at the receiver. It is 10*log(0.3) dBm+50*0.5 dB+2*1 dB-9*0.2 dB = 23.57 dBm. You can see the received signal power by double clicking on power meter after you run the simulation with 24 dBm launch power.

You can change the connecter attenuation to see that the received power is also changing. As an additional work, change the attenuation constant of the fibers and repeat your calculation with this new parameter. Check the validity of your calculation by running a new simulation with this new attenuation constant.

Example: Material Absorption

Material absorption of SMF**.osd**

Project file "Material absorption of SMF**.osd**" shows the spectral dependence of SMF-28 fiber losses in the second (1.3 μm) and third (1.5 μm) telecom windows. As is well known that the loss of the fiber depends on wavelength. A broadband source is used to cover second and third windows. Optical spectrum analyzer just after the source shows a flat power profile across these two windows whereas it reshaped according to loss curve of the fiber after propagating in the fiber. You will notice the dip in the profile around 1.4 μm which is due to water peak at this wavelength. You can calculate the minimum and maximum losses per km by comparing the power spectrums of two different fiber lengths. You can see that the max loss is about 0.5 dB/km.

Example: Stimulated Light Scattering

Raman and GV mismatch**.osd**

Raman spectra**.osd**

Raman and GV mismatch

Project file "Raman and GV mismatch**.osd**" illustrates pulsed SRS amplification in the time domain. Fiber acts as a Raman amplifier such that long wavelength channels are amplified by the short wavelength channels. This effect depends on the bit pattern; it occurs only when 1 bits are present in both channels simultaneously. This example shows how SRS causes a cross-talk between channels and how group-velocity mismatch can eliminate this cross-talk. To do so, two single pulses at two different frequencies multiplexed and sent to fiber. The fiber model includes either a constant or wavelength dependent group delay. In the first two versions we have used a fiber model with wavelength dependent group delay. In the first version, both pulses overlap at input. They experience different amount of delays and walk-off from each other in the fiber, because group delay is wavelength dependent. Therefore there is a very small power transfer from the pulse at shorter wavelength channel to the pulse at longer wavelength channel. This small power transfer is due to the fact that they overlap at the beginning and walk off from each other during propagation. You can see this by looking at the OSA at the end of the fiber. In the second version, pulses do not overlap at beginning, instead they are separated. Due to different group delays for two different channels, their positions in time is swept after propagating in fiber. There is almost no cross talk between the channels since they overlap for very short time when they pass through each other. You can change the wavelengths of the sources and see how it affects the amount of cross talk by comparing the powers of each channel. In last version, the group delay is set to a constant value and the pulses overlap at the input of fiber. Therefore, they will stay overlapped in the fiber during propagation. This is the worst-case scenario for SRS cross talk. This increases the power transfer between channels. Interestingly enough, power spectrum and time domain visualizers show that almost all power of lower wavelength channel is transferred to higher wavelength channel. You can easily see how middle part of the pump pulse is "eaten up" by stokes pulse by looking at the optical time domain visualizer (Output pump pulse).

Raman spectra

Project file "Raman spectra**.osd**" shows SRS in spectral domain for two different cases. A broad band source is used for this purpose. In the first version, a signal at 1450 nm (pump) is multiplexed with the broad band source signal. You can see how the spectrum of the signal from broadband source is affected. Fiber acts

as a Raman amplifier such that longer wavelengths are amplified by the shorter ones. In this example, some power is transferred from the pump to other broad band spectrum components. As can be seen from the spectrum, the gain is a function of wavelength. In the second version, we have used two pump signals and swept the separation between them. You can see how the gain spectrum is changed depending on the separation of the pumps. Note also that the power of the second pump increases as its wavelength increases, because it sees more and more gain according to the gain spectrum.

Example: Nonlinear Refraction

SPM**.osd**

XPM and GV mismatch**.osd**

Self Phase Modulation (SPM)

Project file "SPM**.osd**" shows how SPM affects the spectral shape of a Gaussian pulse. In this example, we set only the SPM on our fiber modal; all other effects are set to off. You can see the spectral shape of the pulse depending on its power on OSA at the fiber end. The nonlinear phase shift depends on input pulse power and nonlinear parameter. Changing the effective area of the fiber changes the nonlinear parameter. You can rerun the simulation with different effective areas and see how the results are changed. Since dispersion effect set to off, you will not see any change on the pulse intensity shape. In fact, nonlinear phase shifts with time, resulting in frequency chirp, which in turn affects the pulse shape through group velocity dispersion (GVD). You can see this by setting the GVD effect on and re-running the simulation. In that case, you will see that pulse goes through a contraction phase when the dispersion parameter D is positive ($\beta_2 < 0$, anomalous-GVD). With correct parameters you can even get a "soliton". As an extra work, try to see what happens when the dispersion is negative ($D < 0$, $\beta_2 > 0$).

Cross Phase Modulation (XPM) and GV mismatch

Project file "XPM and GV mismatch**.osd**" demonstrates that XPM induced distortions can be canceled out, if the dispersion is sufficiently high. As in the case of SPM, there is no impact of spectral broadening introduced by XPM if there is no GVD to transform this spectral broadening to pulse broadening. On the other hand, walk off between the channels because of GVD also tends to lessen the impact of XPM. In this example, we consider two isolated pulses in different channels propagating in a lossless fiber. As shown in Fig.23, the leading edge of the interfering pulse is superimposed on the center of the second pulse. In this case, the signal pulse receives a red shift due to rising intensity of the interfering pulse.

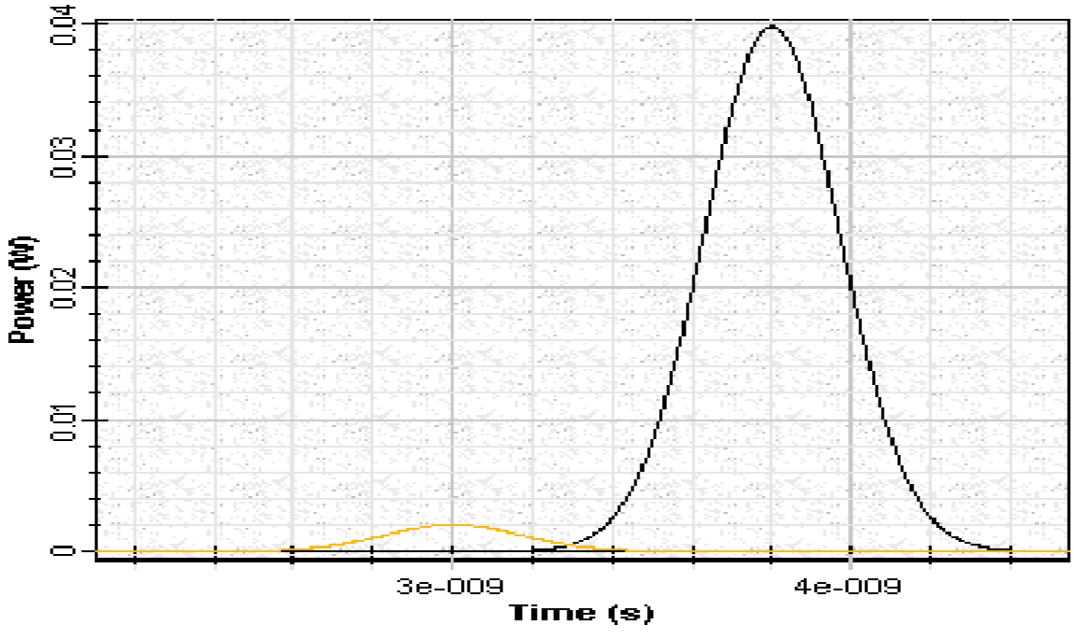

Fig.23: Superimposed pulses at the input of fiber

As the pulses walk through each other, and trailing edge of the interfering pulse is superimposed, the signal pulse receives a blue shift. In fact, the net frequency shift experienced by a particular part of the signal pulse is proportional to the integral of the derivative of the intensity of the interfering pulse. Therefore, when the pulses have completely walked through each other, there is no residual effect. Here we have considered two 400 ps pulses with 800 ps center-to-center separation. The channels are separated by 1 nm. Dispersion of the standard single mode fiber is taken to be 16 ps/km/nm. The signal pulse has a lower power than the interfering pulse. The pulses begin to overlap at 25 km, are perfectly superimposed at 50 km, and are separated again at 100 km. Since power of the signal pulse is low, SPM is negligible. However, XPM should be large because the power of interfering pulse is high. You can see that the spectrum broadening of the signal due to XPM is smaller than the spectrum broadening of the interfering pulse arising from SPM by looking at the spectrum at 50 km. Note that, pulses are completely overlapped at this distance. You can also see the new spectrum components generated by FWM. At 100 km, the pulses are separated and effects of XPM have completely vanished, while the effect of SPM on the interfering pulse remains. Fig.24 shows the evaluation of power spectrum. This shows that dispersion can reduce the effects of XPM. Our simulation results are in perfect agreement with the results presented in [1].

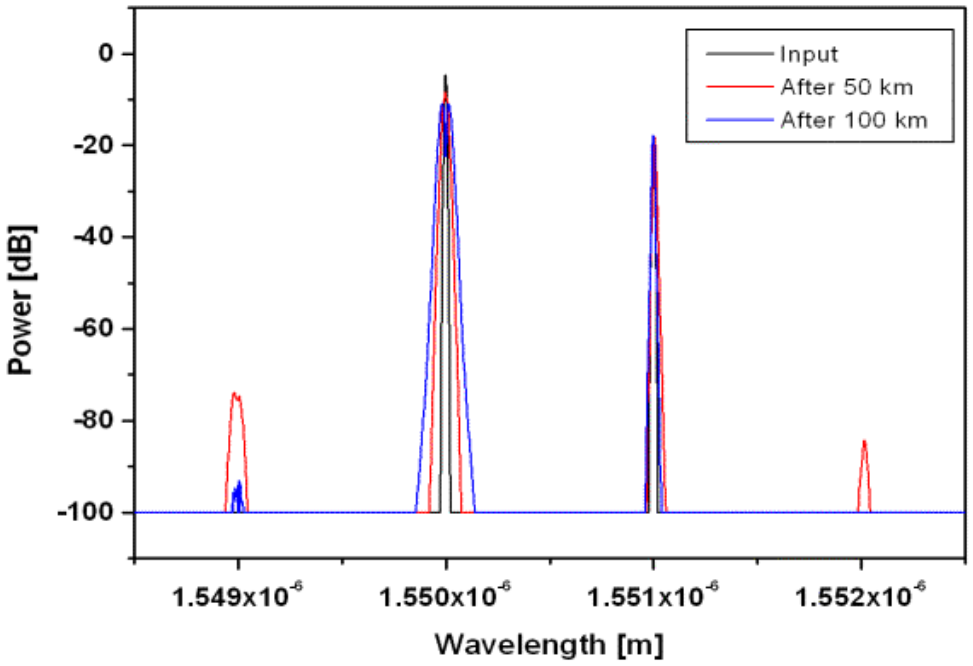

Fig.24: Power spectrums at input of fiber and after 50 km and 100 km of propagation

Reference:

"Optical Fiber Telecommunications IIIa", ed. by I. Kaminov and T. Koch, chapter "Fiber Nonlinearities and their Impact on Transmission Systems" by F. Forghieri, R. Tkach and A. Chraplyvy

Example: Four-Wave Mixing

FWM**.osd**

Project file "FWM**.osd**" demonstrates FWM effect. When three optical fields with carrier frequencies f_1, f_2, and f_3 co-propagate inside the optical fiber simultaneously, nonlinear effect generates a fourth field whose frequency f_4 is related to other frequencies by a relation $f_4 = f_1 \pm f_2 \pm f_3$. In principle, several frequencies corresponding to different plus and minus signs combinations are possible. In practice, the frequency combinations of the form $f_4 = f_1 + f_2 - f_3$ are most troublesome. For an *N* channel system, $M = \frac{1}{2}\left(N^3 - N^2\right)$ mixing products

are generated. In this example, we have two versions of the same project; one with equidistant channel spacings and one with non-equidistance channel spacings. In the first version, some of the generated fields by FWM overlap with existing channels. Therefore, you will not be able to see all the mixing products in the spectrum for this case. In the second version, on the other hand, you can see all the mixing products in the spectrum. You can also see that the above given formula is satisfied and the number of generated mixing product is 9. You can change the separation between channels to see how the spectrum is affected. You can also add new channels and verify that this formula is valid. Try to see what happens when you only have two channels. Why?

Chapter 3 – Optical Transmitters

Example: Spectral Distribution

LED spectral distribution**.osd**

The spectral distribution of light sources affects the performance of optical communication systems through fiber dispersion. The spectral distribution is governed by the spectrum of spontaneous emission and typically follows a Gaussian shape. Fig.1 shows the layout for LED Spectral Distribution. It generates the output spectrum of a typical 1300 nm LED with 50 nm of spectral width (Figs.2 and 3).

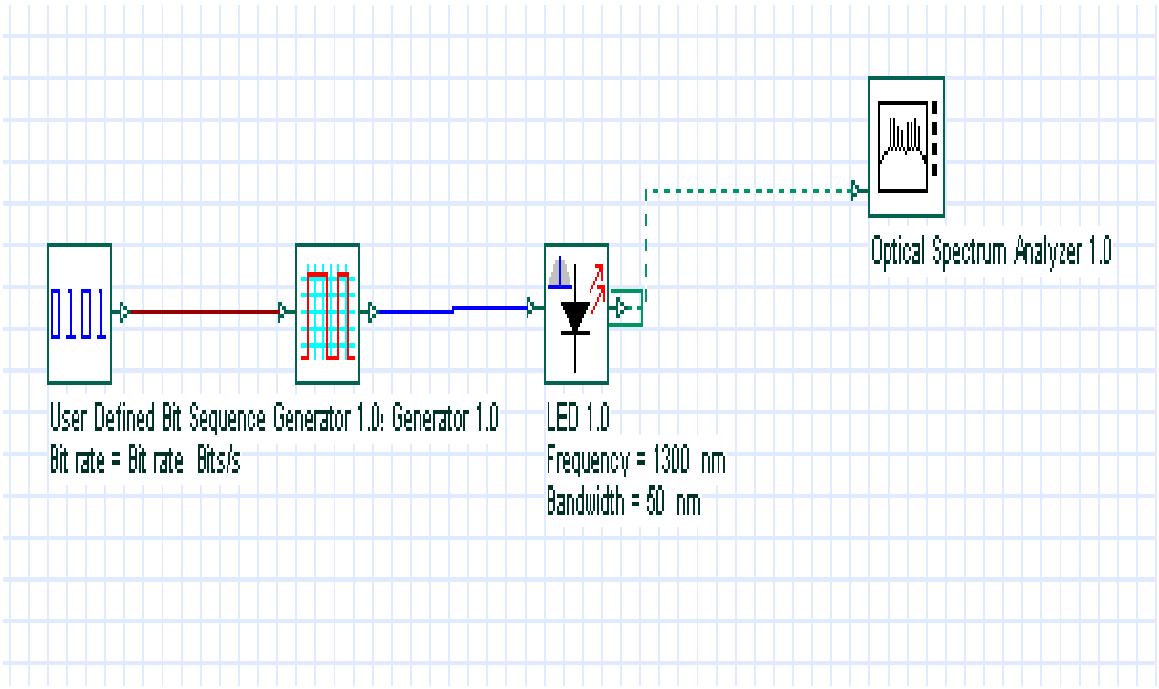

Fig.1: Layout: LED spectral distribution

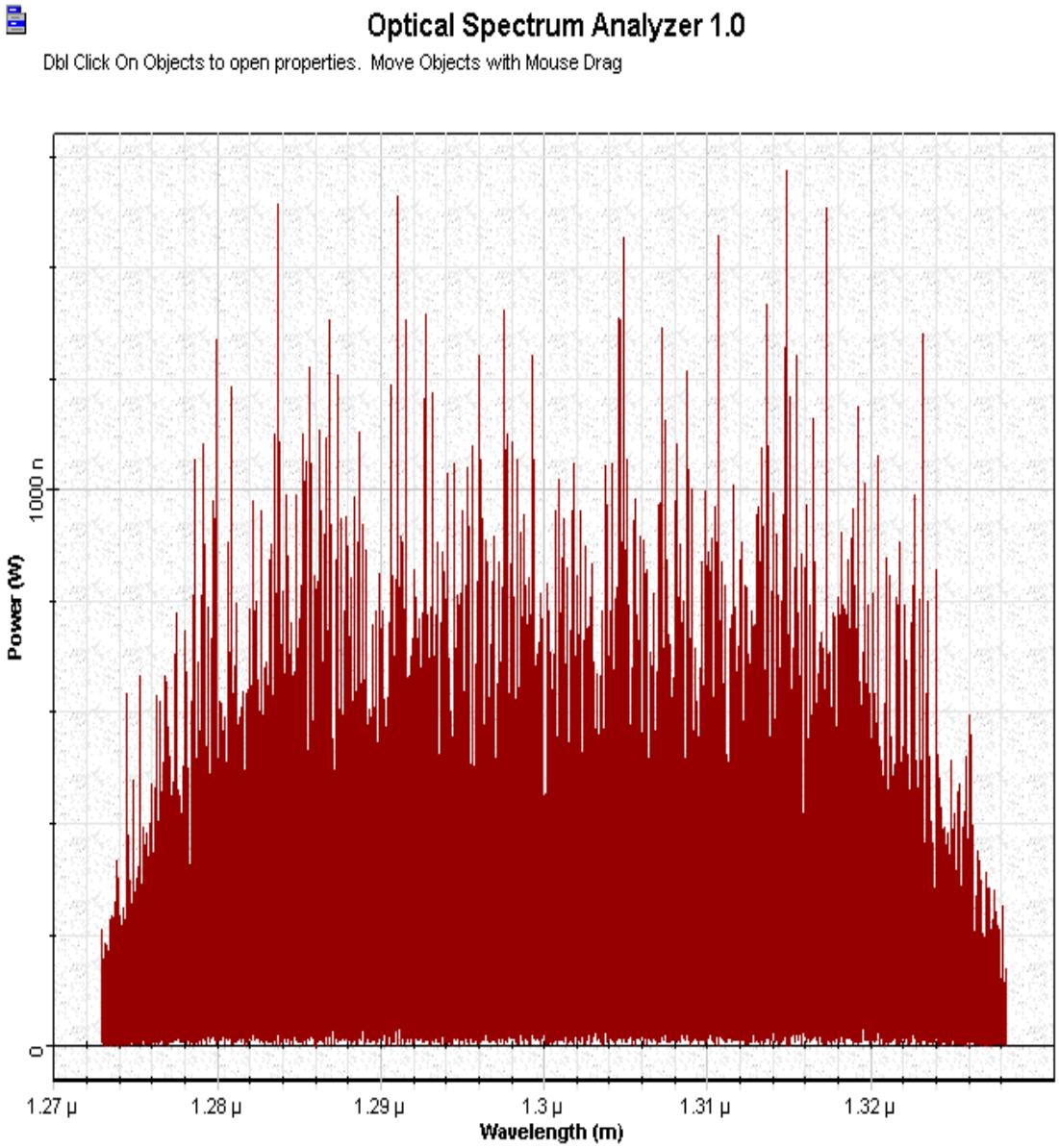

Fig.2: Output spectrum of LED

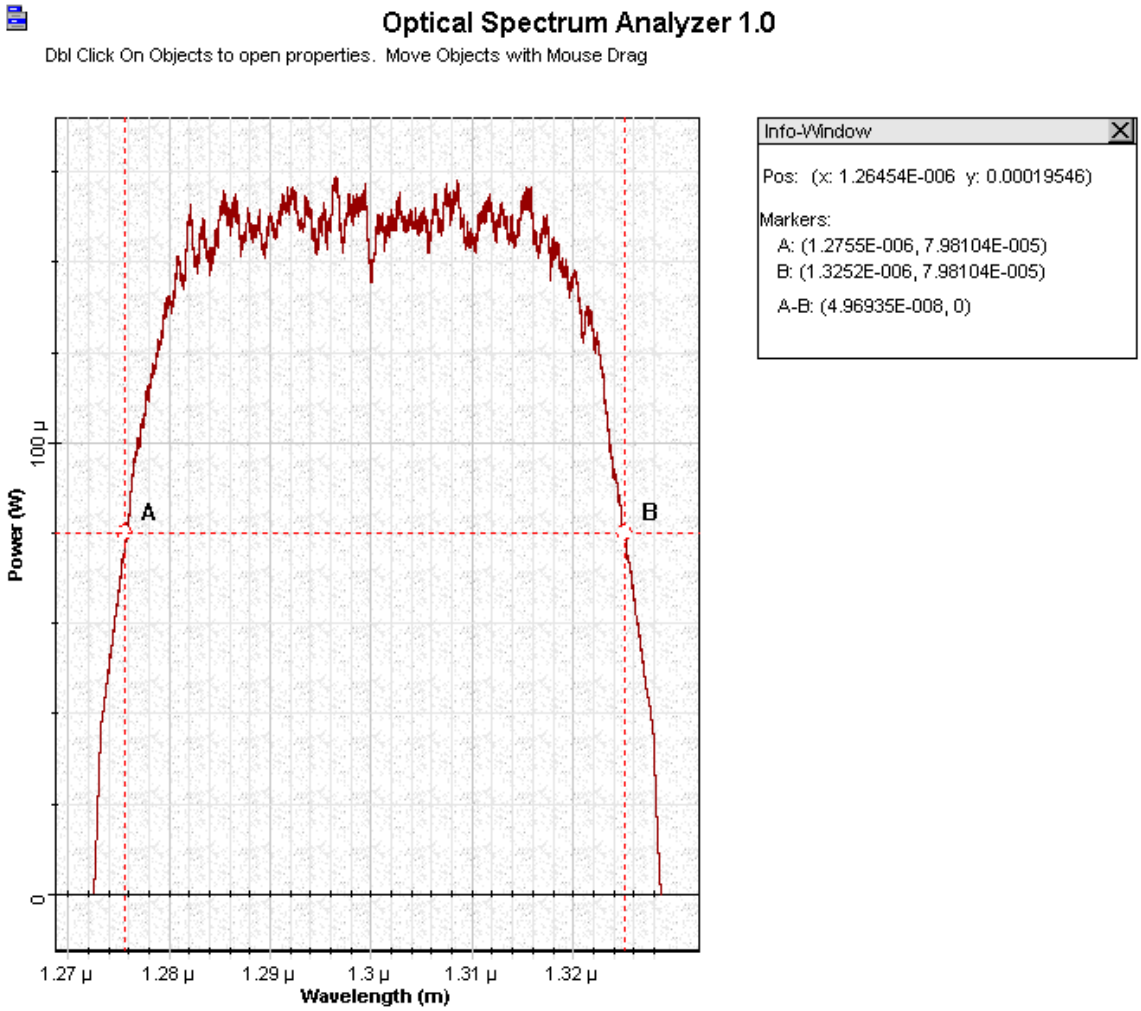

Fig.3: Output spectrum of LED 1 nm resolution (Markers were used in order to measure the spectral width).

Example: LED Modulation Response

LED modulation response**.osd**

The modulation response of LEDs depends on carrier dynamics and is limited by the carrier lifetime. The LED 3-dB modulation bandwidth is defined as the modulation frequency at which the LED transfer function is reduced by 3 dB or by a factor of 2. Fig.4 shows the lay out for LED Modulation Response.

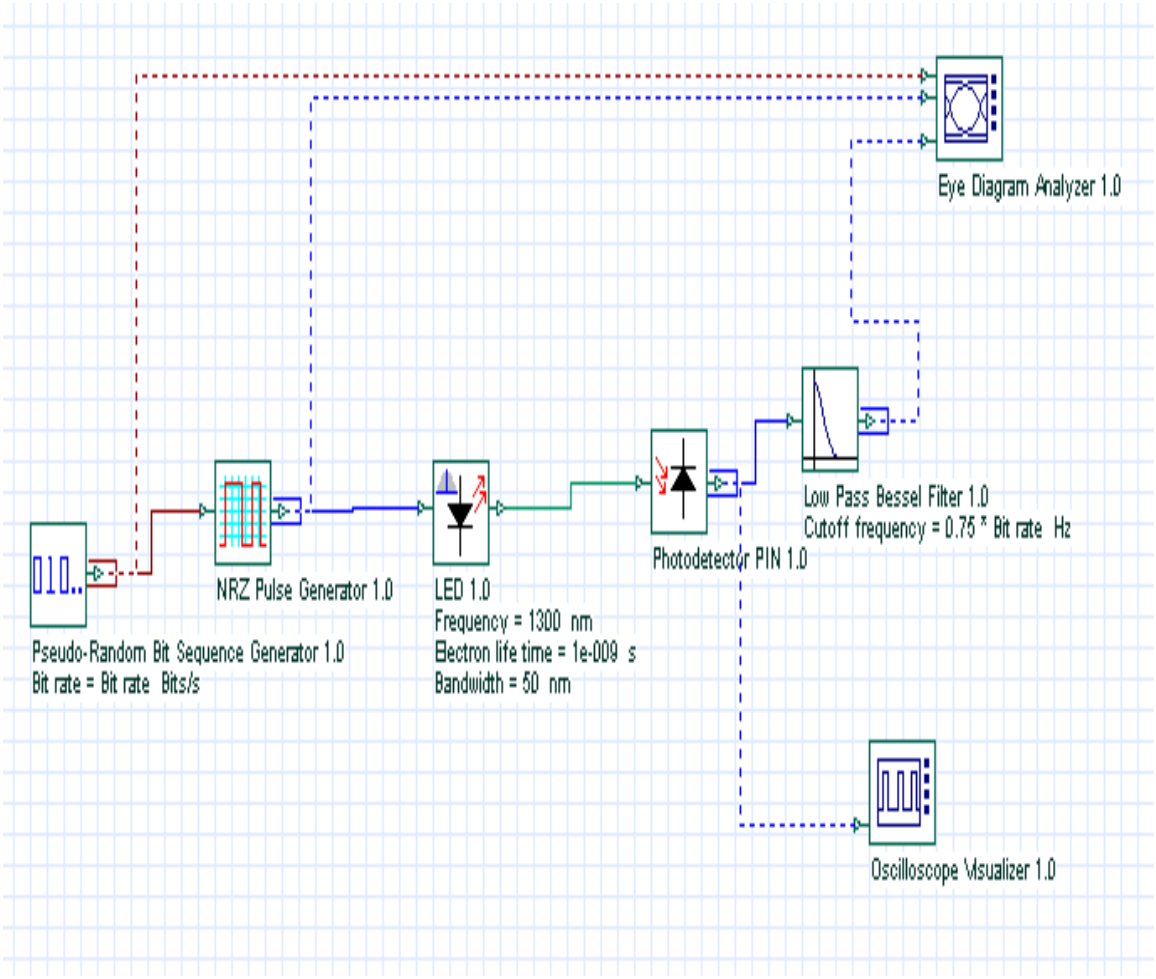

Fig.4: Layout: LED modulation response

The project "LED modulation response**.osd**" shows the closure of the eye diagram when the modulation bit rate increases from 100 MB/s to 400 MB/s **(Figs. 5,6,7 and 8).** This effect occurs because of the LED modulation response. Reducing the carrier lifetime value will increase the LED modulation response.

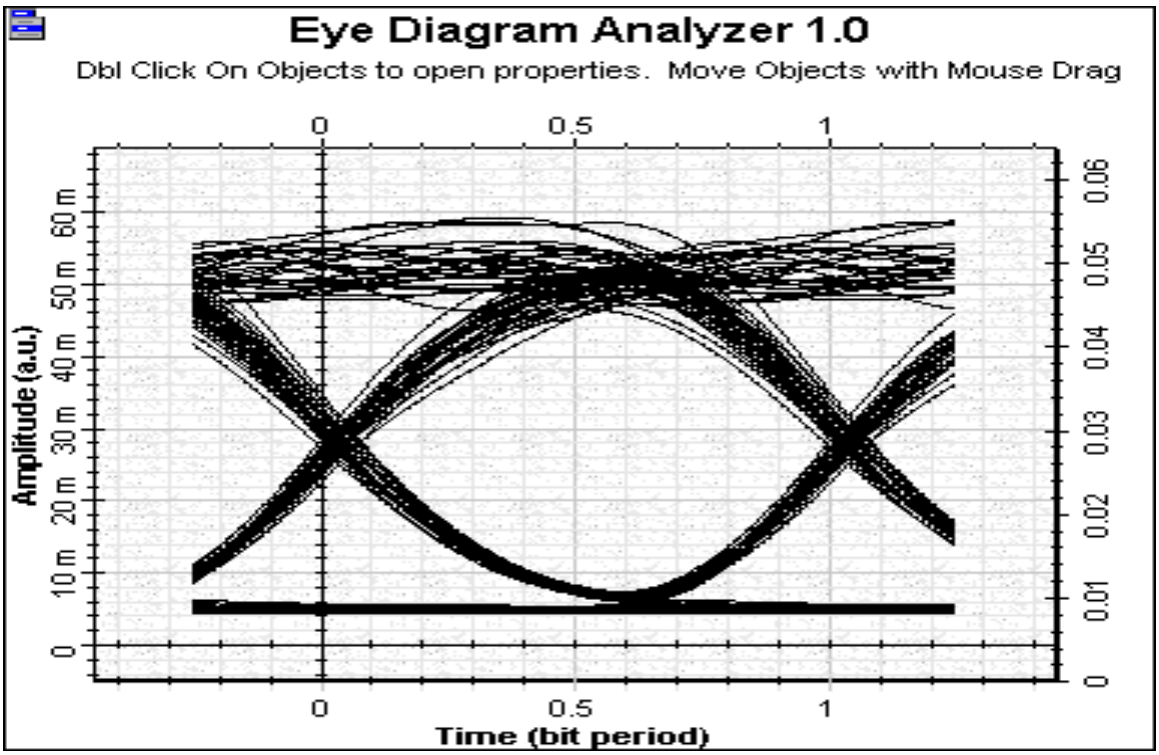

Fig.5: LED modulation 100 MB/s

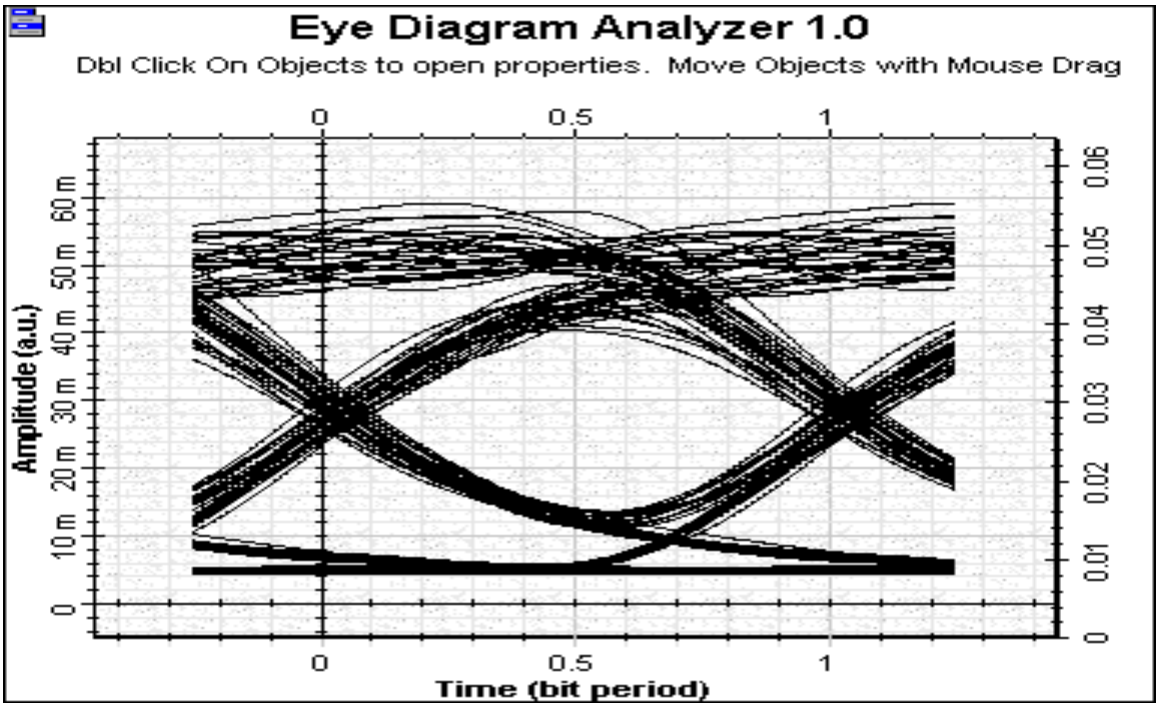

Fig.6: LED modulation 200 MB/s

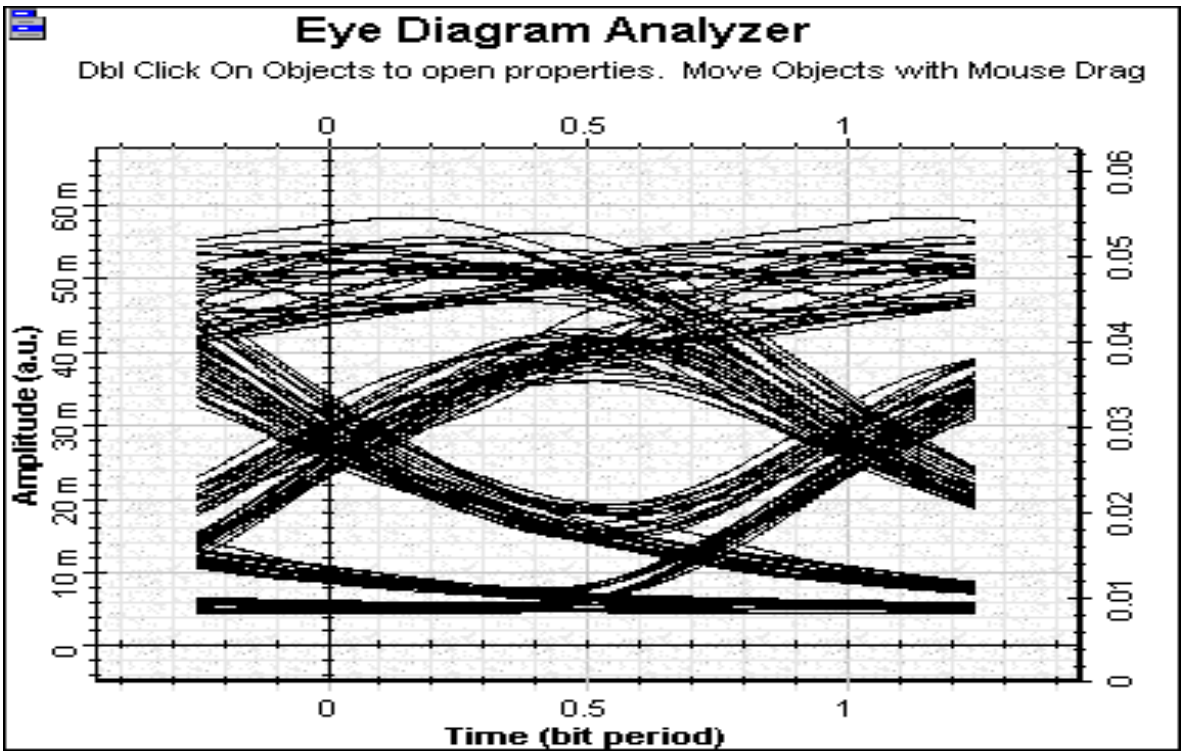

Fig.7: LED modulation 300 MB/s

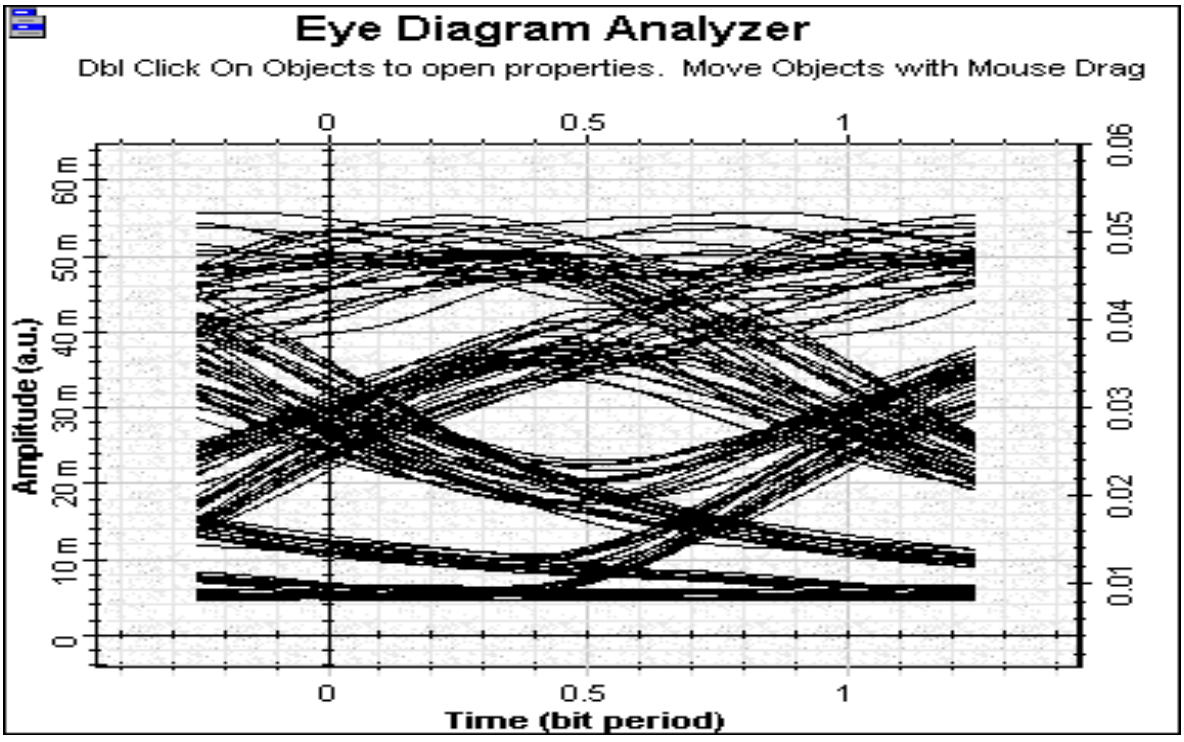

Fig.8: LED modulation 400 MB/s

Fig.9 shows the electrical signal at the photodetector before the electrical filter.

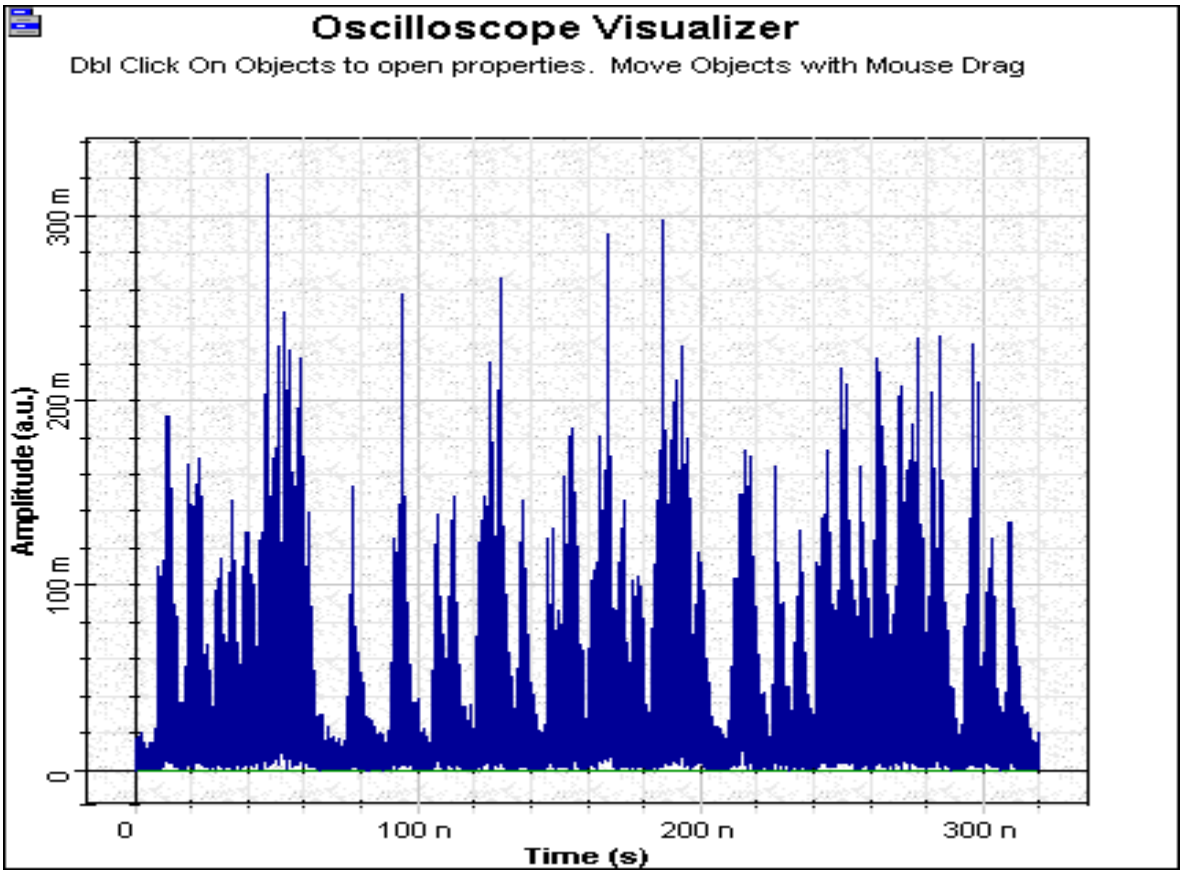

Fig.9: Electrical signal_LED modulation 400 MBs

Example: Light-Current Characteristics

Semiconductor laser L-I curve**.osd**

The Light-Current (L-I) curve characterizes the emission properties of a semiconductor laser, as it indicates not only the threshold level but also the current that needs to be applied to obtain a certain amount of power. Project "Semiconductor laser L-I curve**.osd**" (Fig.10) generates the L-I curve of a laser.

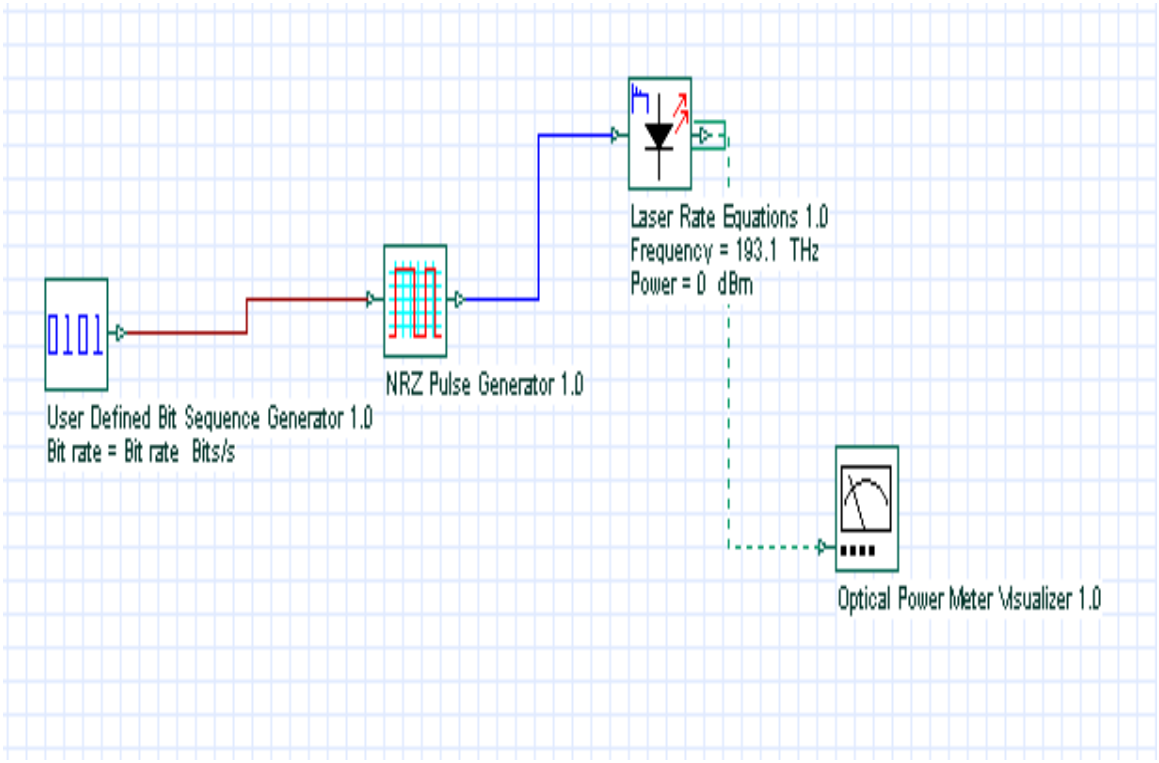

Fig.10: Layout: Semiconductor laser L- I curve

The L-I curve is generated after sweeping the parameter modulation peak current from 1 to 100 mA. The Bias current is 25 mA. After running the simulation we obtain the following curve **(Fig.11)**.

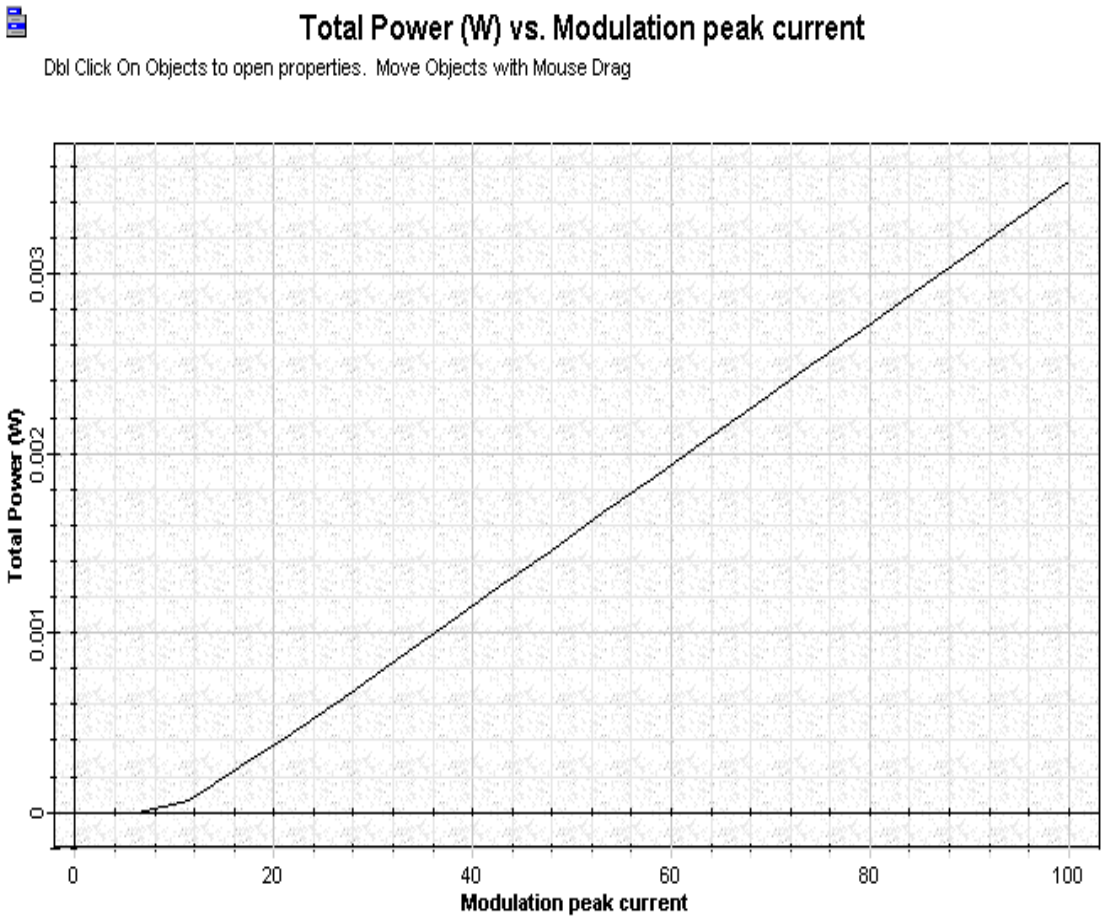

Fig.11: Laser L-I curve

Example: Semiconductor Laser Modulation Response

Semiconductor laser large signal modulation**.osd**

Amplitude modulation in semiconductor lasers is accompanied by phase modulation. A time-varying phase is equivalent to transient changes in the mode frequency from its steady-state value. Such a pulse is called chirped. The project "Semiconductor laser large signal modulation**.osd**" (Fig.12) generates the amplitude and signal chirp for a directly modulated semiconductor laser**.** Fig.13 shows the amplitude and signal chirp for directly modulated semiconductor laser

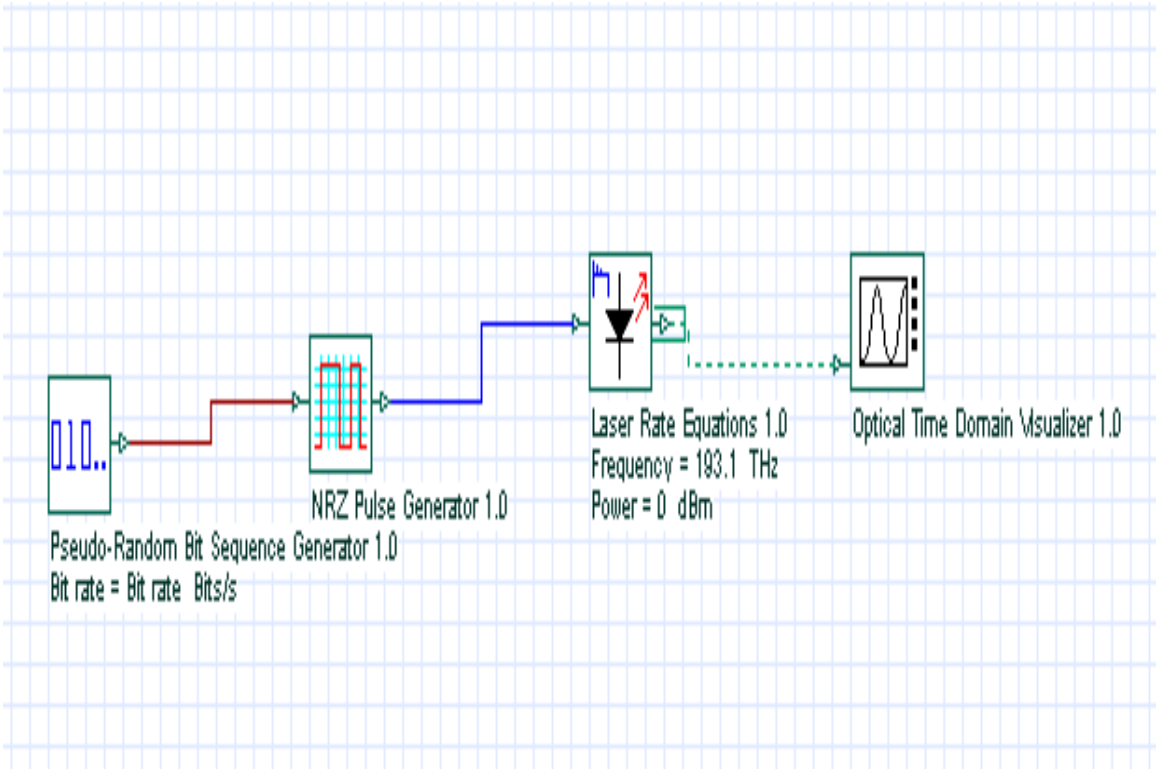

Fig.12: Layout: Semiconductor laser large signal modulation

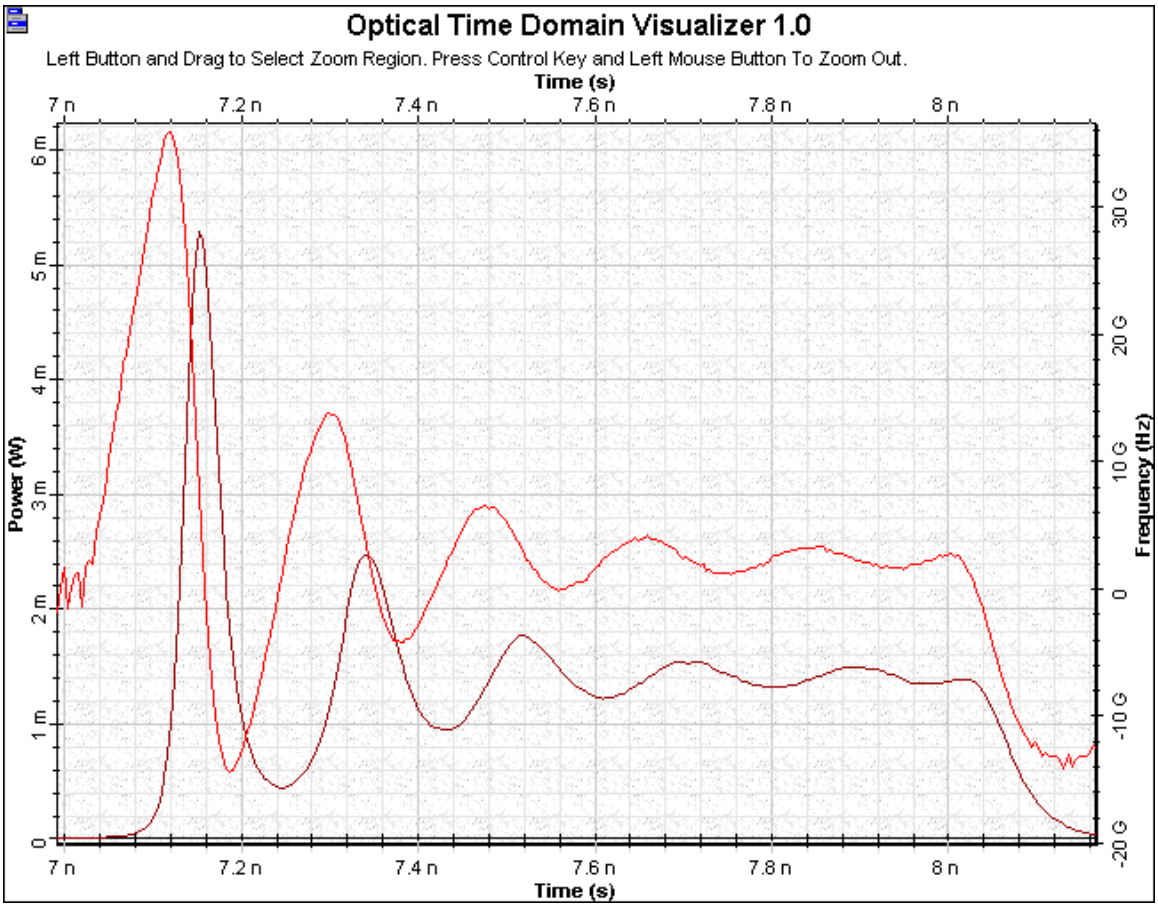

Fig.13: Amplitude and signal chirp for directly modulated semiconductor laser

Example: Laser Noise

Laser intensity noise**.osd**

Project "Laser intensity noise**.osd**" (Fig.14) shows the laser spectral in CW operation at several power levels.

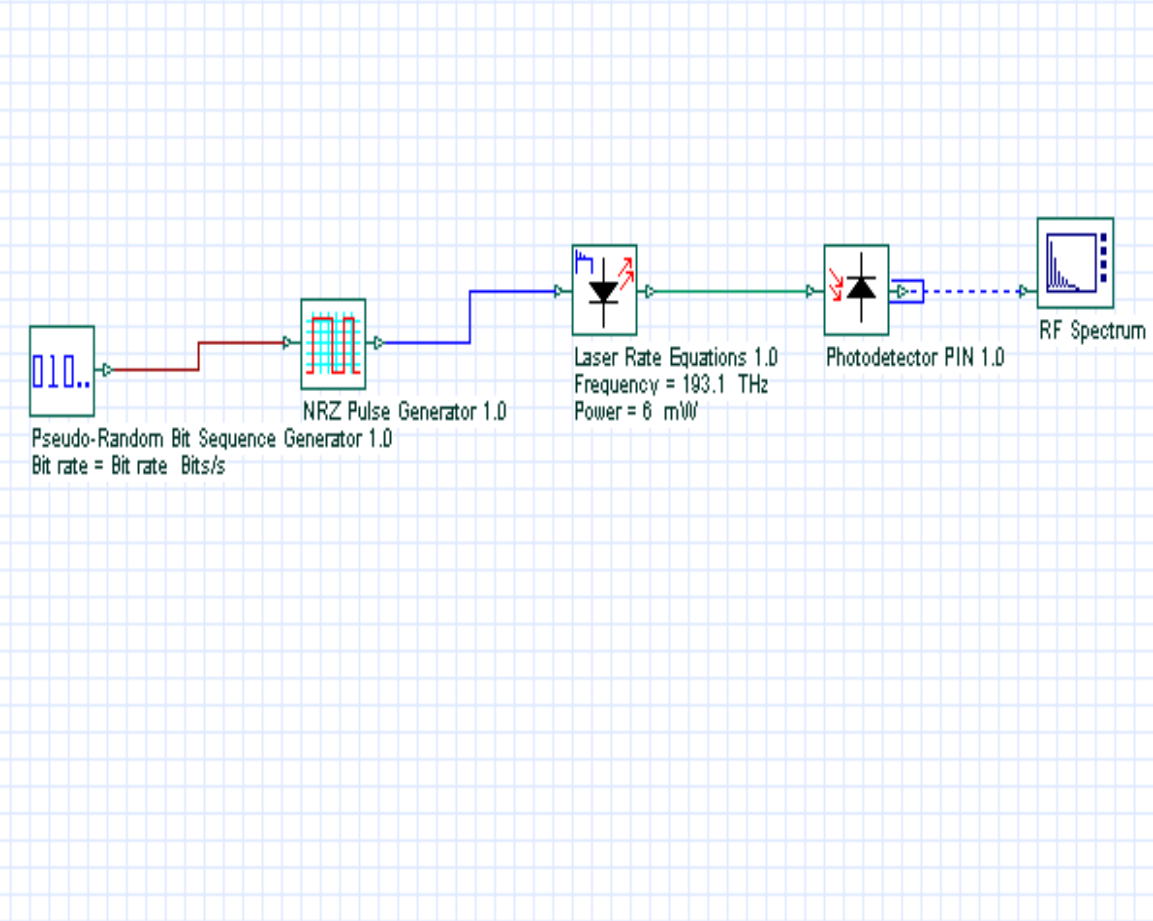

Fig.14: Layout: Laser intensity noise

The laser exhibits fluctuations in its intensity, phase and frequency even when the laser is biased at a constant current with negligible current fluctuations **(Fig.15)**.

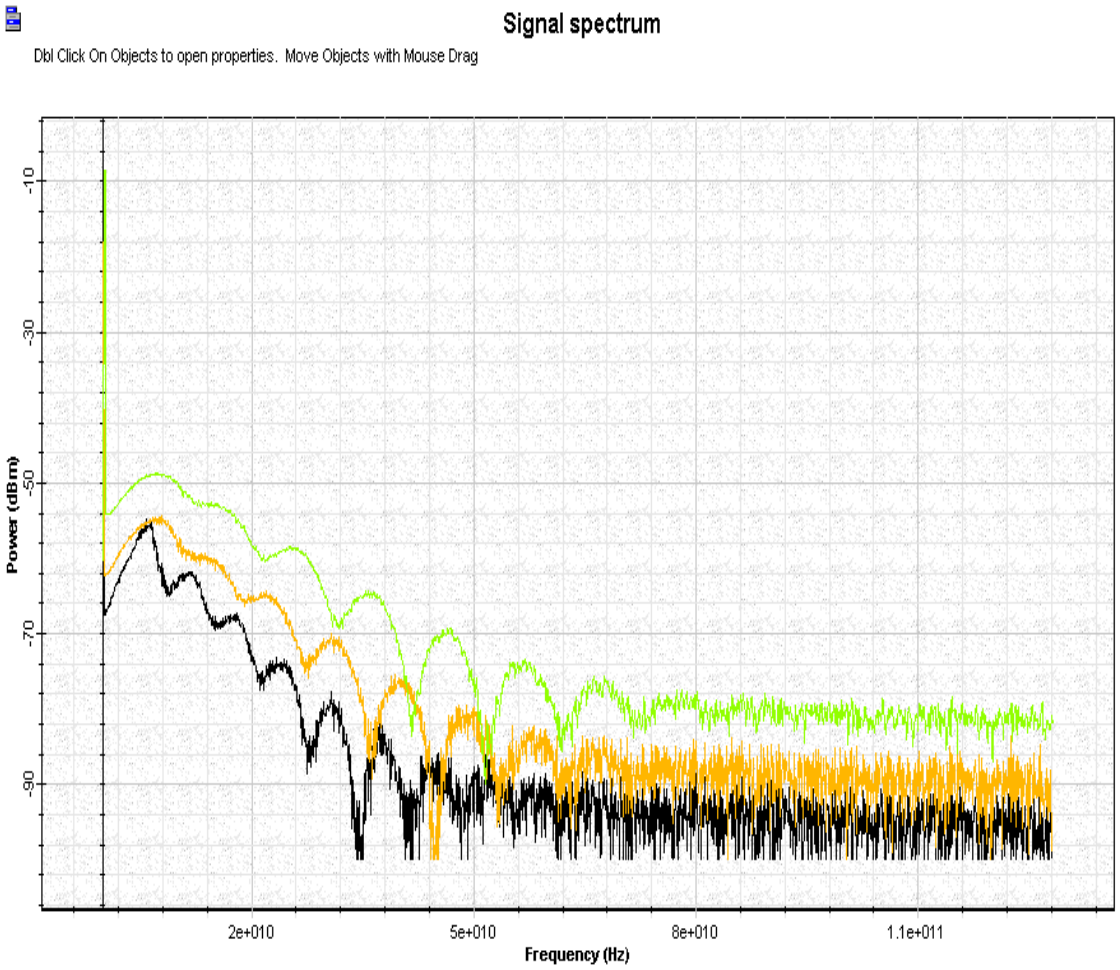

Fig.15: Laser intensity noise

Chapter 4 – Optical Receivers

Example: Front End

Receiver design**.osd**

The design of an optical receiver depends largely on the modulation format used by the transmitter. Project "Receiver design**.osd**" (Fig.1) shows a digital receiver design. Its components can be arranged into three groups, the front end, the linear channel and the data-recovery section.

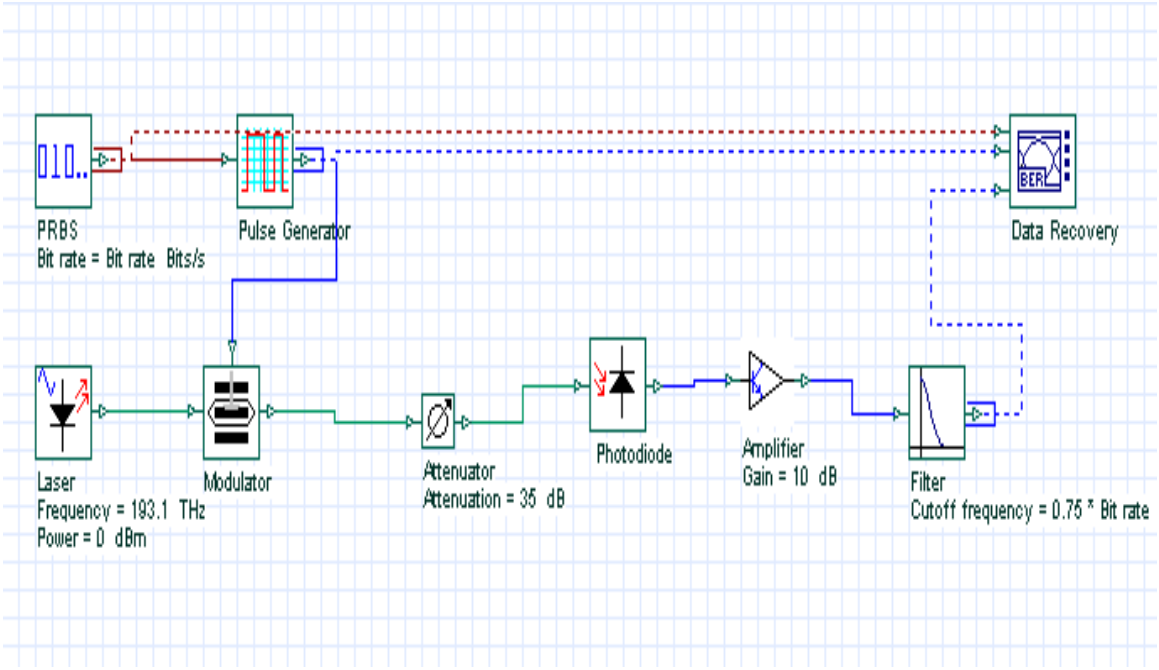

Fig.1: Layout: Receiver design

The front-end of a receiver consists of a photodiode with a built in preamplifier, the linear channel consists of a high-gain amplifier and an low-pass filter and the data recovery is done by the BER Analyzer with a built in clock recovery and decision circuit.

The linear channel has a low pass filter that shapes the pulse. The receiver noise is proportional to the receiver bandwidth and can be reduced by using a low-pass filter whose bandwidth is smaller than the bit rate. The pulse spreads beyond the

time slot. Such spreading can interfere with the detection of neighboring bits, the phenomenon referred to as intersymbol interference (ISI).

By setting the attenuator to 0 dB, you can observe the ideal eye diagram **(Fig.2)**.

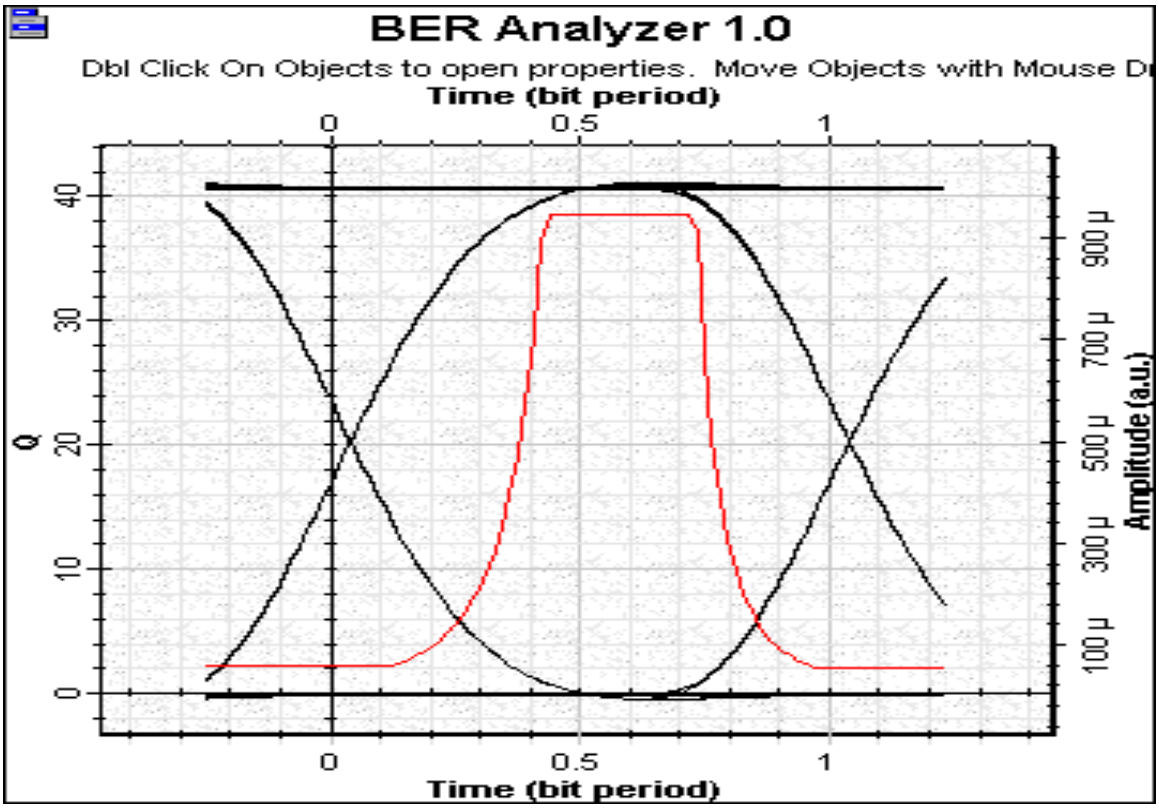

Fig.2: Receiver EYE (ideal)

By setting the attenuator to 35 dB, you can observe the degraded eye diagram **(Fig.3)**.

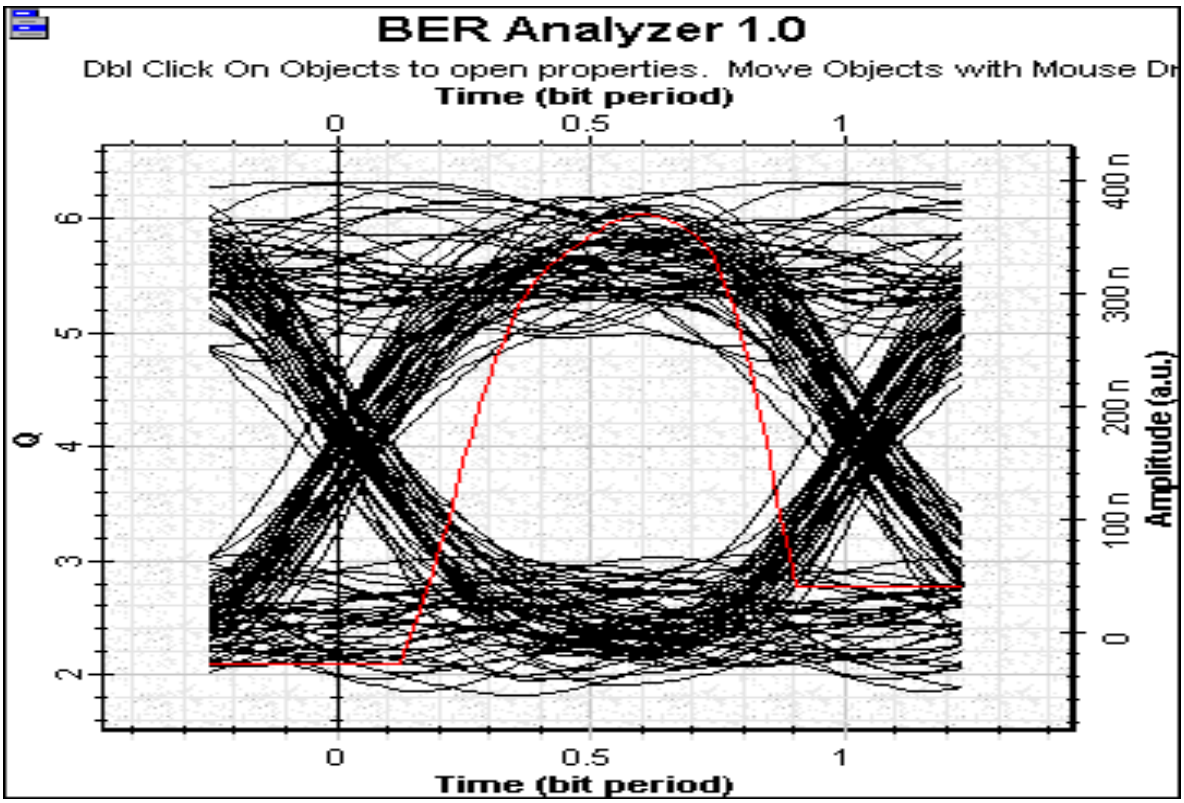

Fig.3: Receiver EYE (degraded)

The decision circuit compares the output from the linear channel to a threshold, at a decision instant determined by the clock recovery circuit, and decided whether the signal corresponds to bit 1 or bit 0. The optimum threshold level is calculated for each decision instant in order to minimize the BER (Fig. 4).

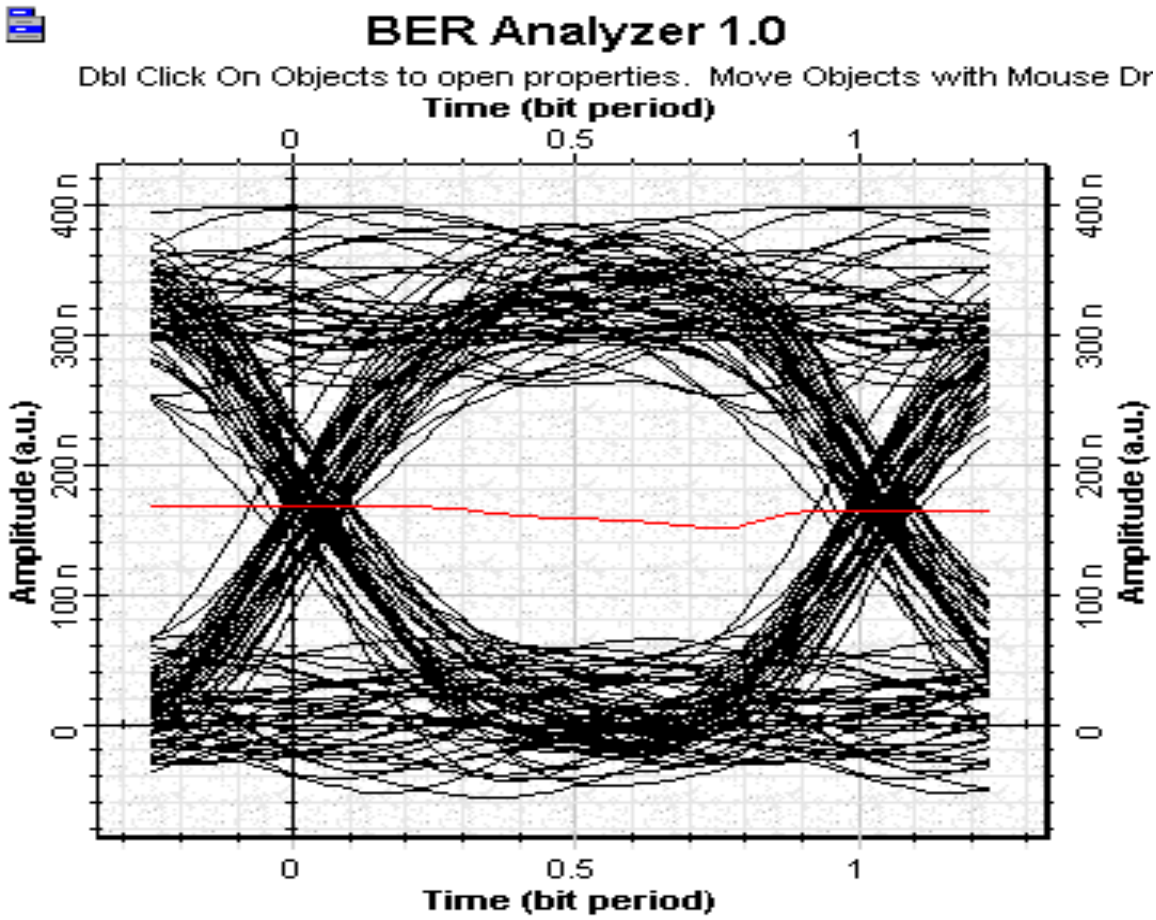

Fig.4: Receiver EYE (threshold)

Example: *p-I-n* Receivers

Receiver shot and thermal noise**.osd**

There are two fundamental noise mechanisms in a photodetector : shot noise and thermal noise. The project "Receiver shot and thermal noise**.osd**" (Fig. 5) shows the signal degraded by thermal and shot noise in the PIN photodetector. The low-pass filter has cutoff frequency with the same value as the bit rate.

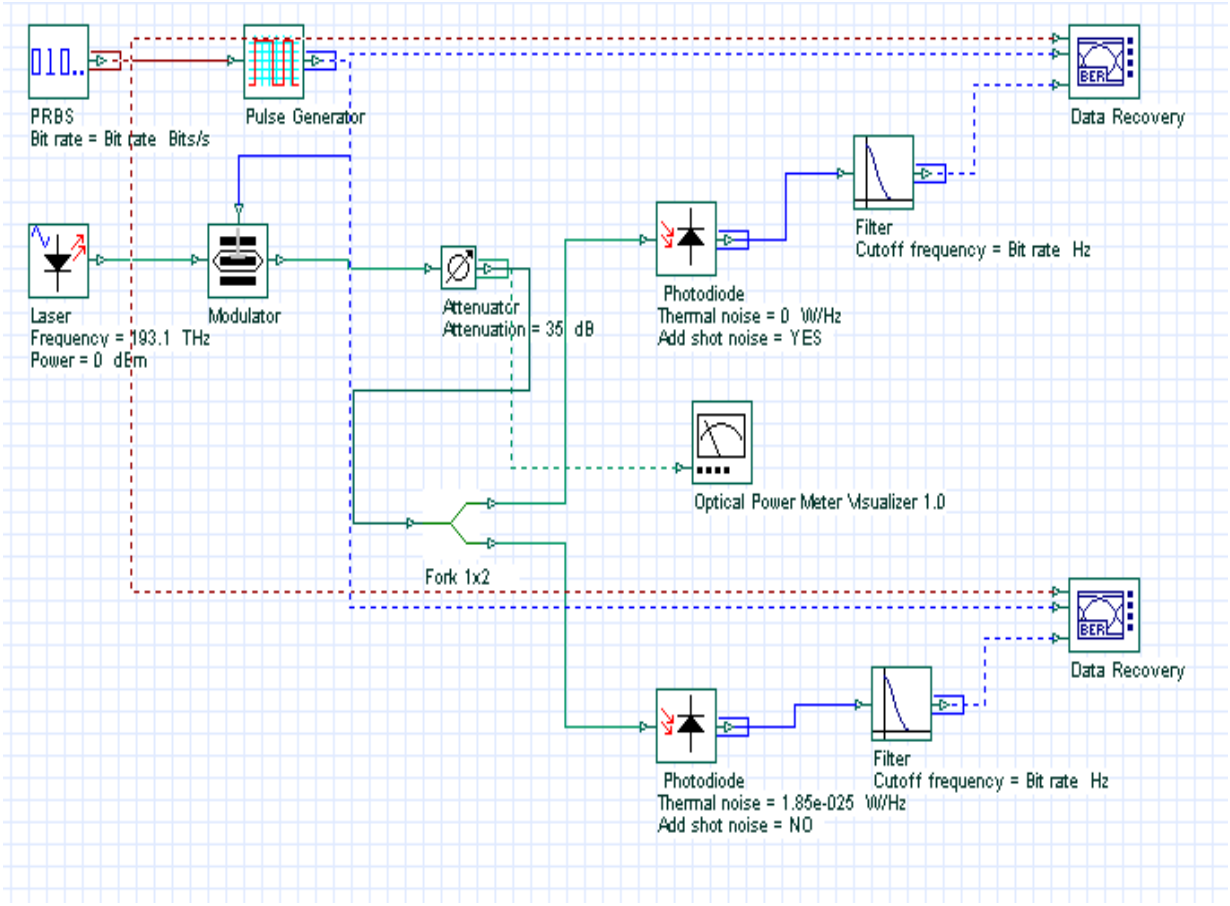

Fig.5: Layout: Receiver shot and thermal noise

The upper system has the photodetector without thermal noise; the only noise generated at the output is the shot noise. You can observe that the shot noise is signal amplitude dependent (Fig.6).

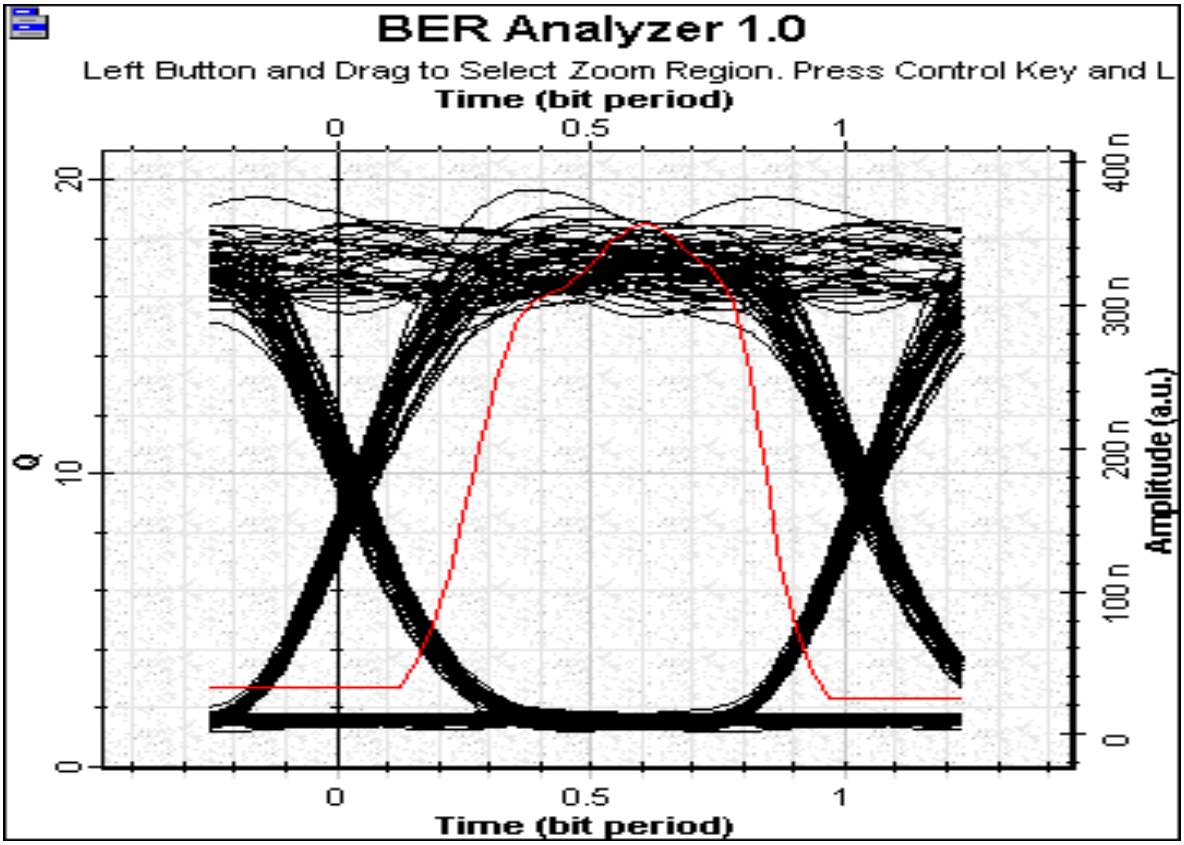

Fig.6: Receiver shot noise

The lower system has the photodetector with shot noise; the only noise generated at the output is the thermal noise. You can observe the thermal noise is signal amplitude independent (Fig.7).

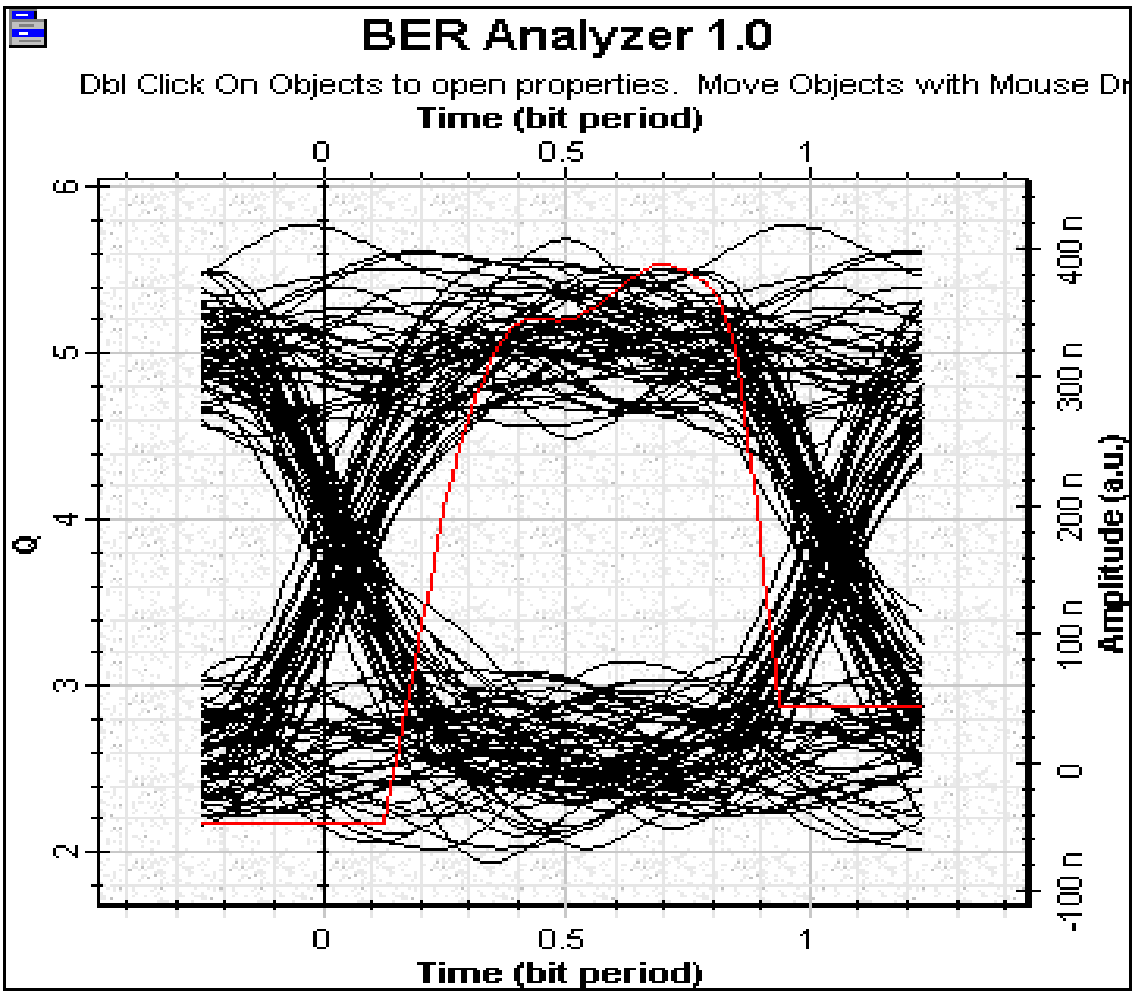

Fig.7: Receiver (thermal noise)

Example: APD Receivers

Receiver PIN x APD**.osd**

Optical receivers with APD generally provide a higher SNR for the same incident optical power. The improvement is due to the internal gain that increases the photocurrent by the multiplication factor M. The project "Receiver PIN x APD**.osd**" (Fig.8) shows a comparison with two systems using PIN and APD.

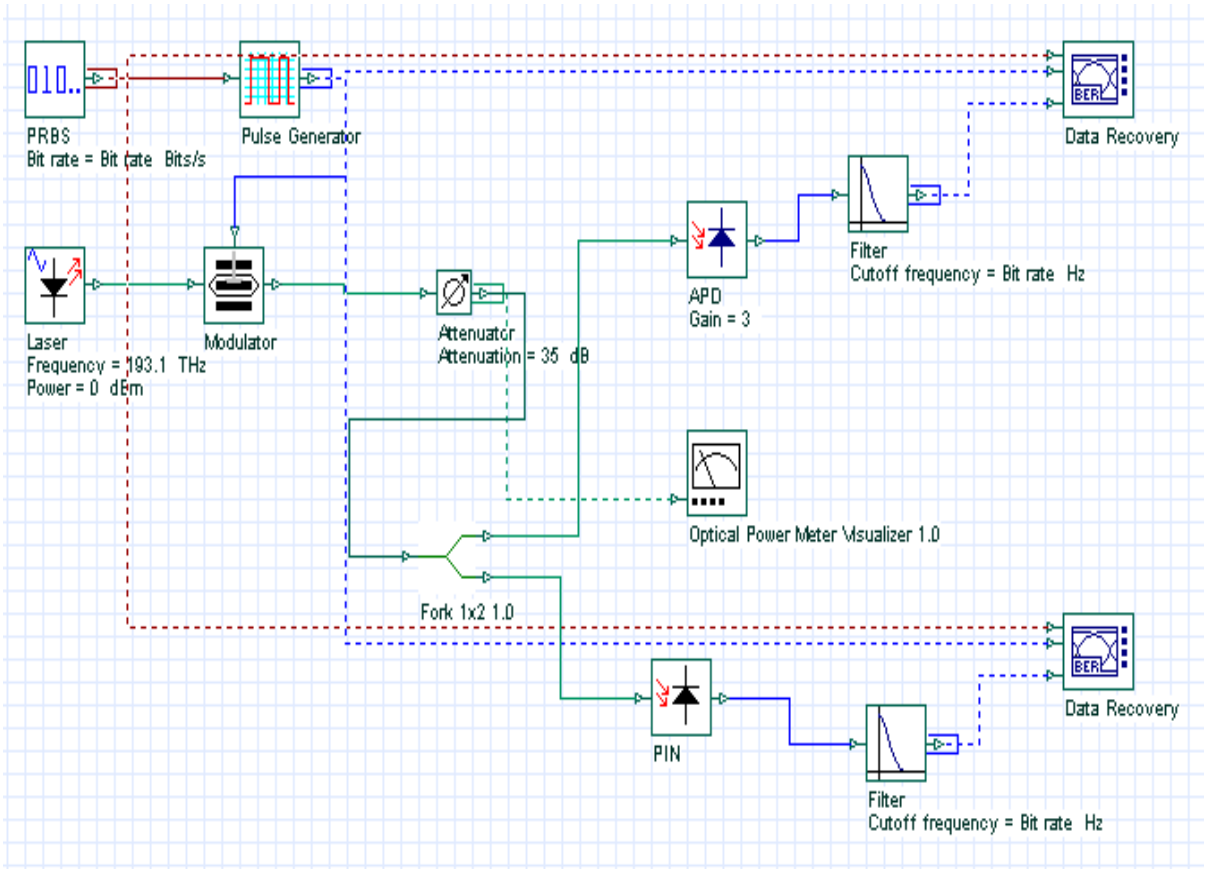

Fig.8: Layout: Receiver PIN x APD

The APD photodetector system has a Q factor higher (Fig. 9) than the PIN photodetector by a multiplication factor of 3 (Fig. 10).

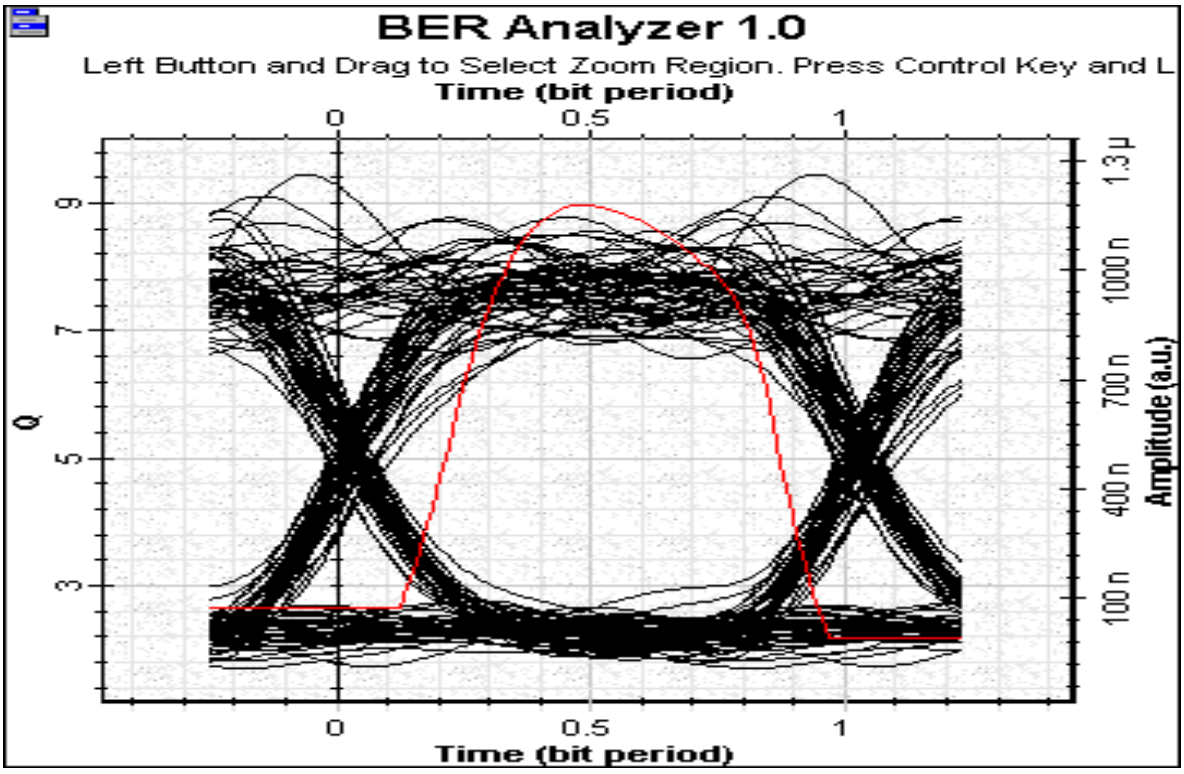

Fig.9: APD Q factor

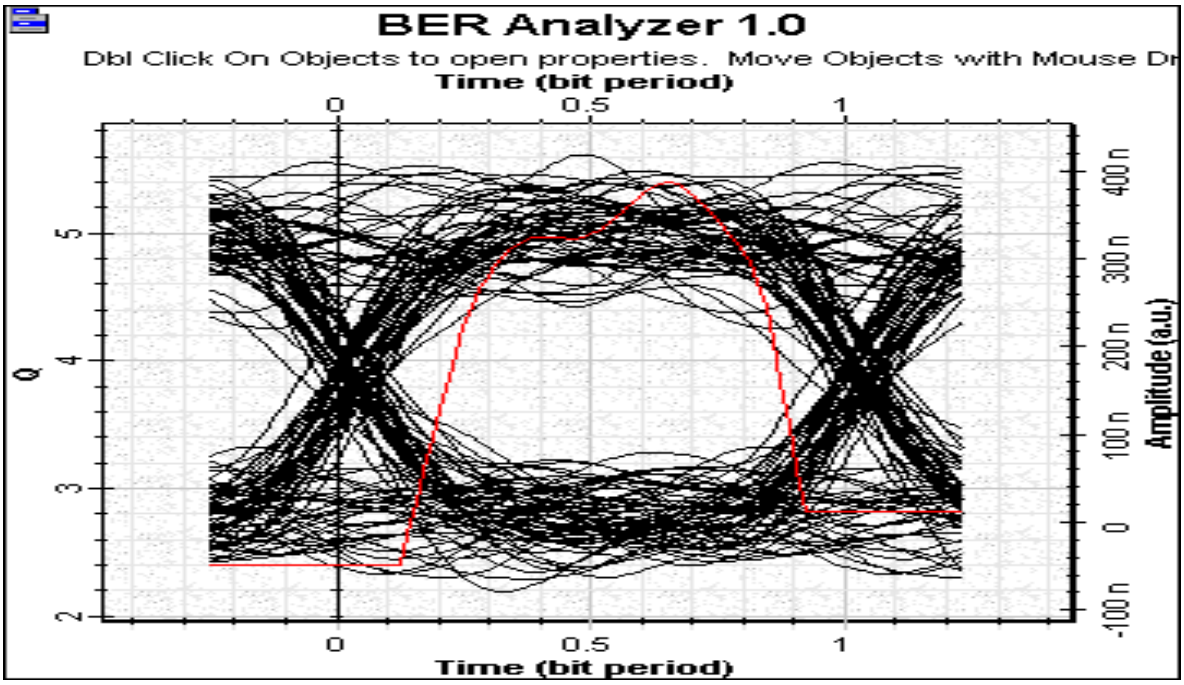

Fig.10: PIN Q factor

If we increase the multiplication factor then there is a limit where the shot noise will degrade the system performance, therefore it's important to find the optimum APD gain.

If we run the same simulation varying the value of the multiplication factor we can observe the evolution of the Q factor (Fig.11).

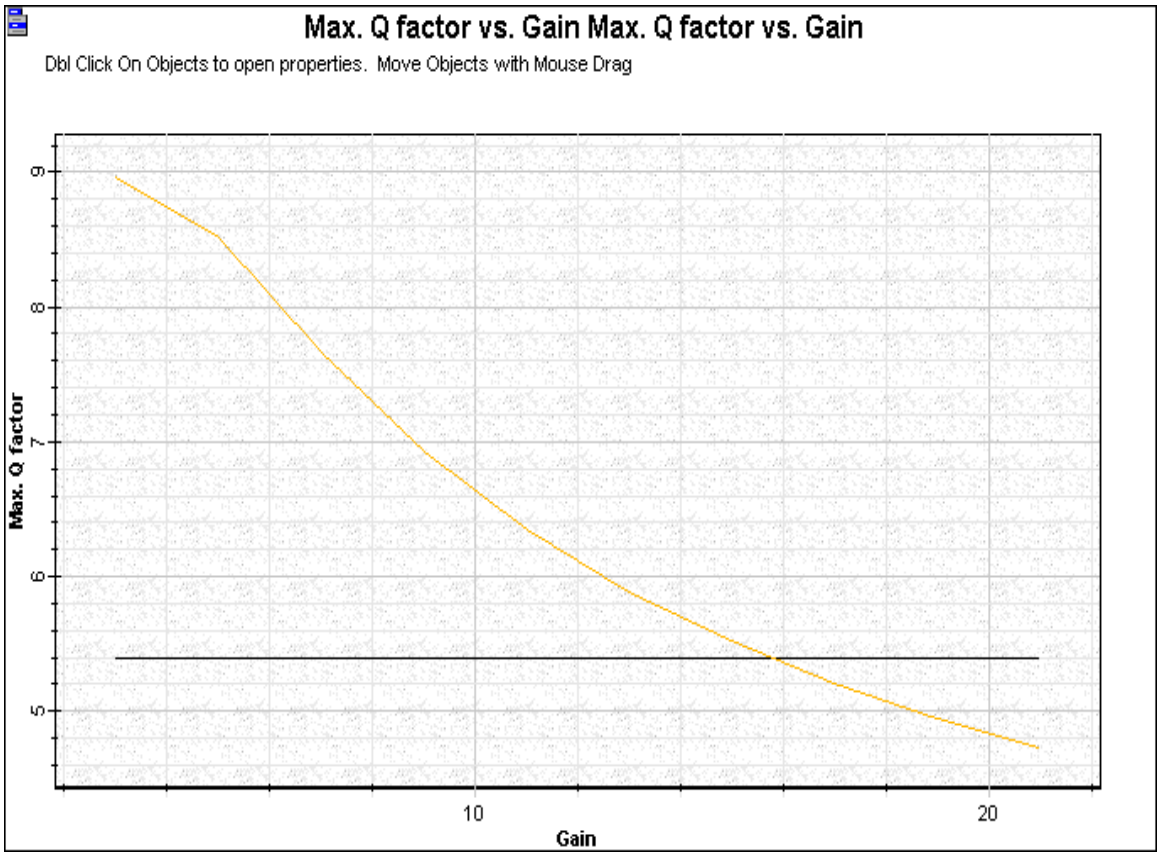

Fig.11: Q factor – APD gain

In this case for a gain higher of 16 there is no advantage of using the APD, since it will not improve the receiver sensitivity.

Example: Bit-Error Rate

Receiver BER - Q factor**.osd**

The performance criteria for digital receivers, if governed by the bit-error-rate (BER), defined as the probability of incorrect identification of a bit by the decision circuit of the receiver. The project "Receiver BER - Q factor**.osd**" generates the BER and Q factor at the data recovery stage for different values of input power:

In the project, by changing the signal input power we can calculate not only Q-Factor versus attenuation (Fig.12) and BER versus attenuation (Fig.13), but also the BER versus Q factor (Fig.14).

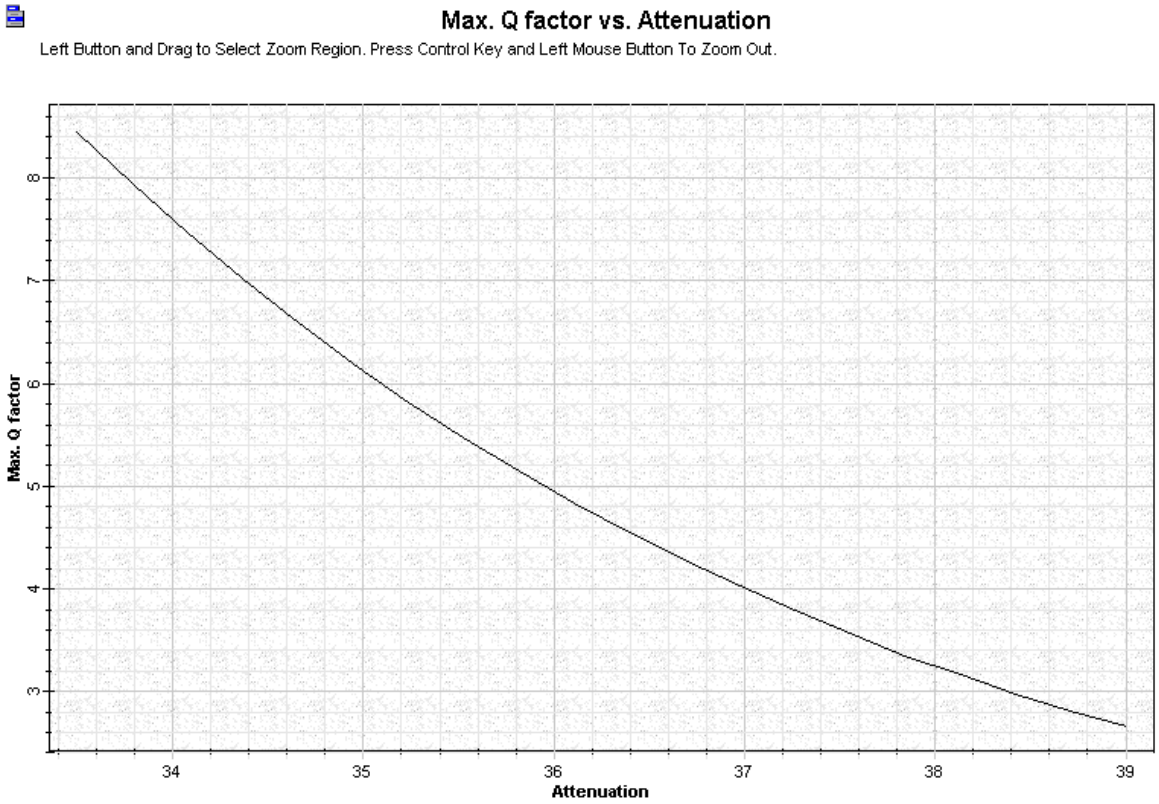

Fig.12: Q factor vs. Attenuation

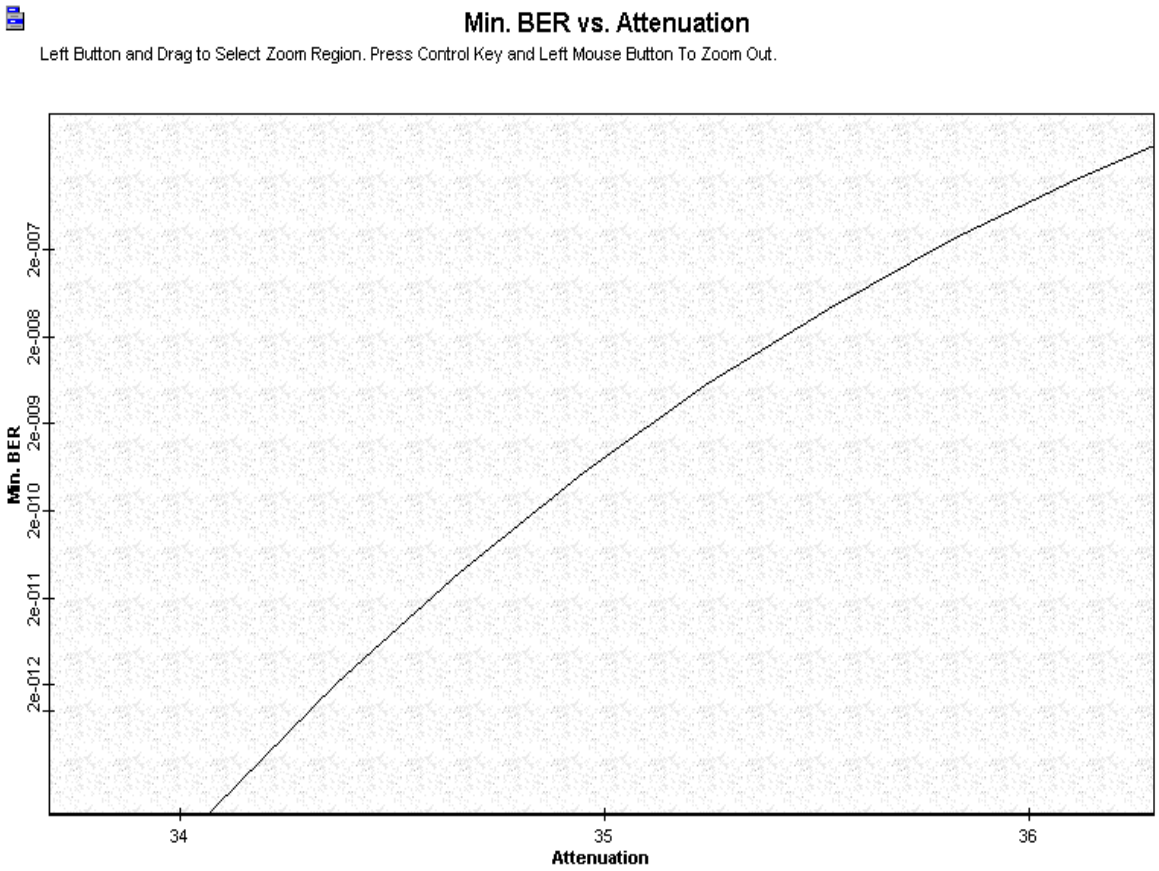

Fig.13: BER vs. Attenuation

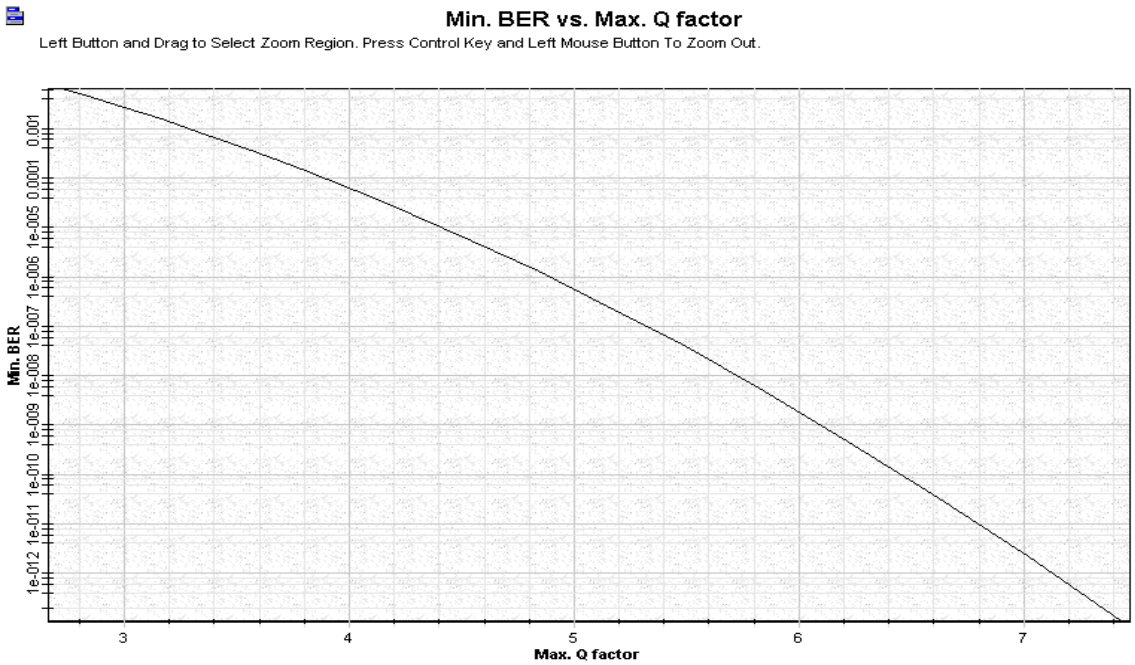

Fig.14: BER vs. Q factor

Example: Minimum Received Power

Receiver_min. received power**.osd**

The project "Receiver_min. received power**.osd**" (Fig.15) shows the minimum optical power that a receiver needs to operate reliably with a BER below a specific value. In this example we calculate this input power by targeting a BER of 10^{-9} means Q factor equal to 6 for a PIN photodetector and an APD.

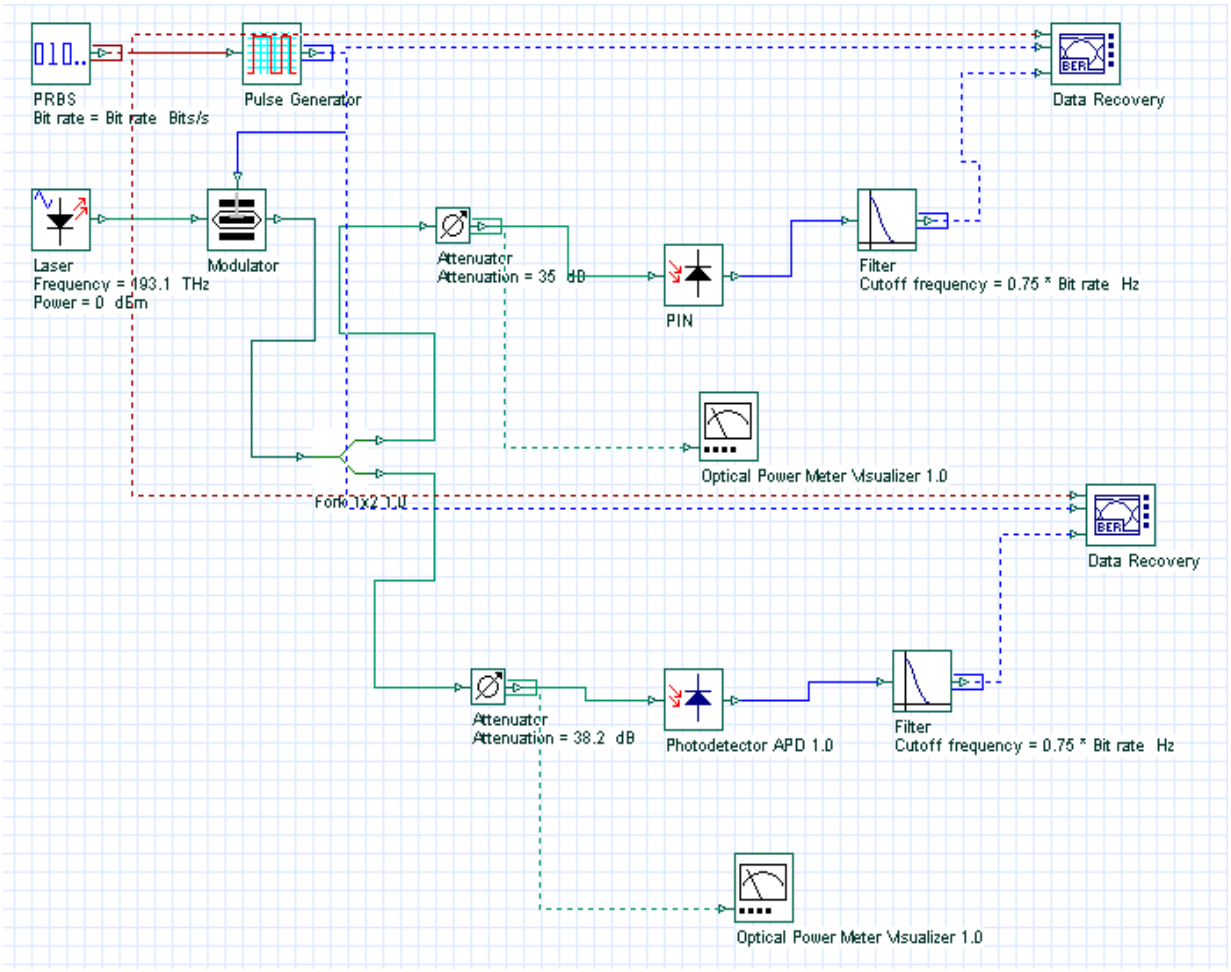

Fig.15: Layout: Receiver_min. received power

This example shows that the receiver sensitivity by using the PIN is –32.8 dBm (Fig. 16). When using the APD with gain equal to 3 the sensitivity increases to – 41.4 dBm (Fig.17). Figs. 18 and 19**,** show corresponding EYE pattern for PIN and APD receivers.

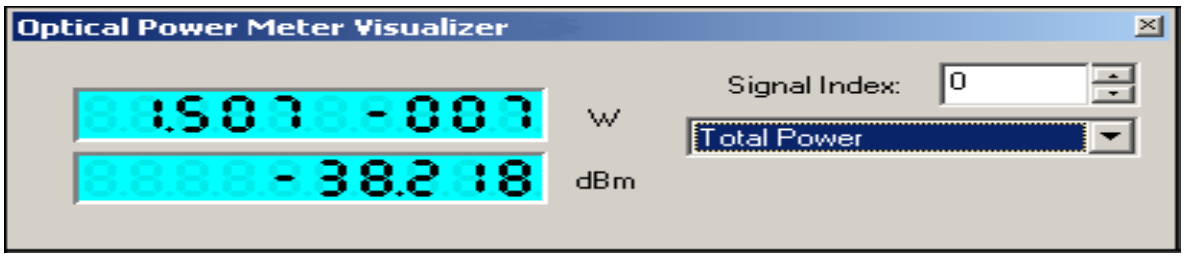

Fig.16: Optical power PIN

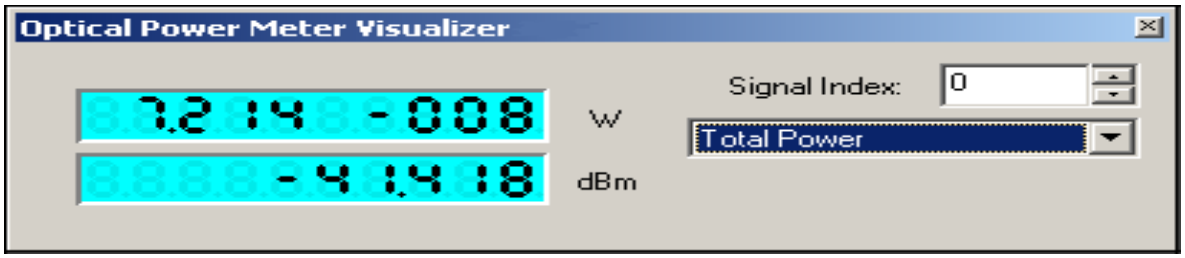

Fig.17: Optical power APD

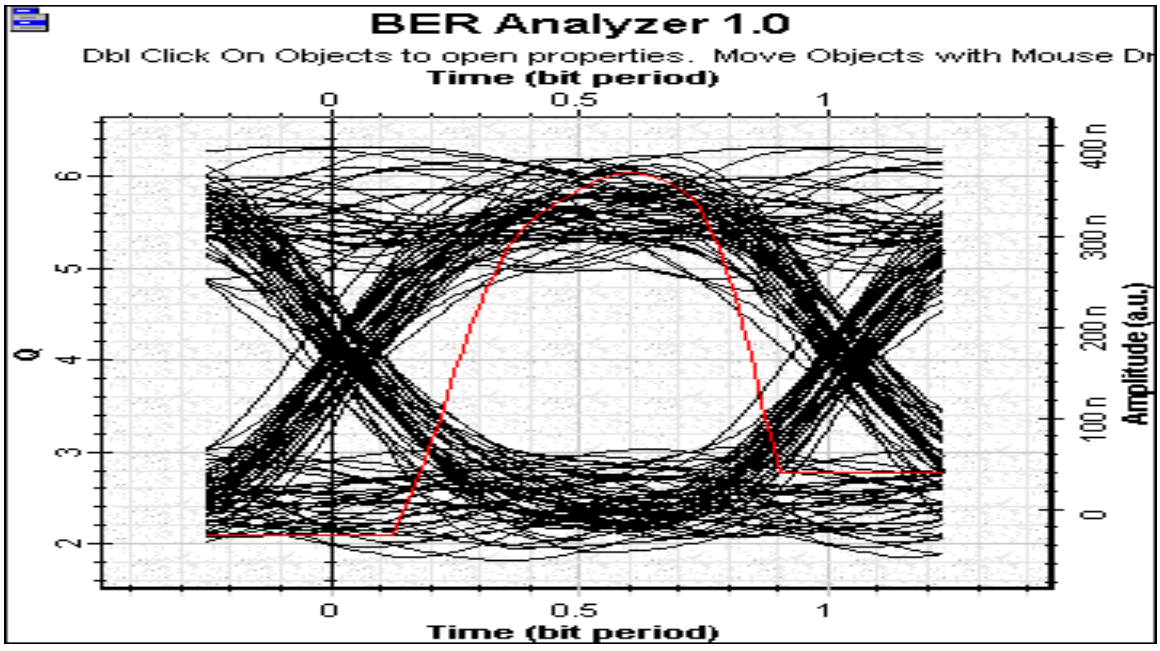

Fig.18: EYE pattern - PIN receiver

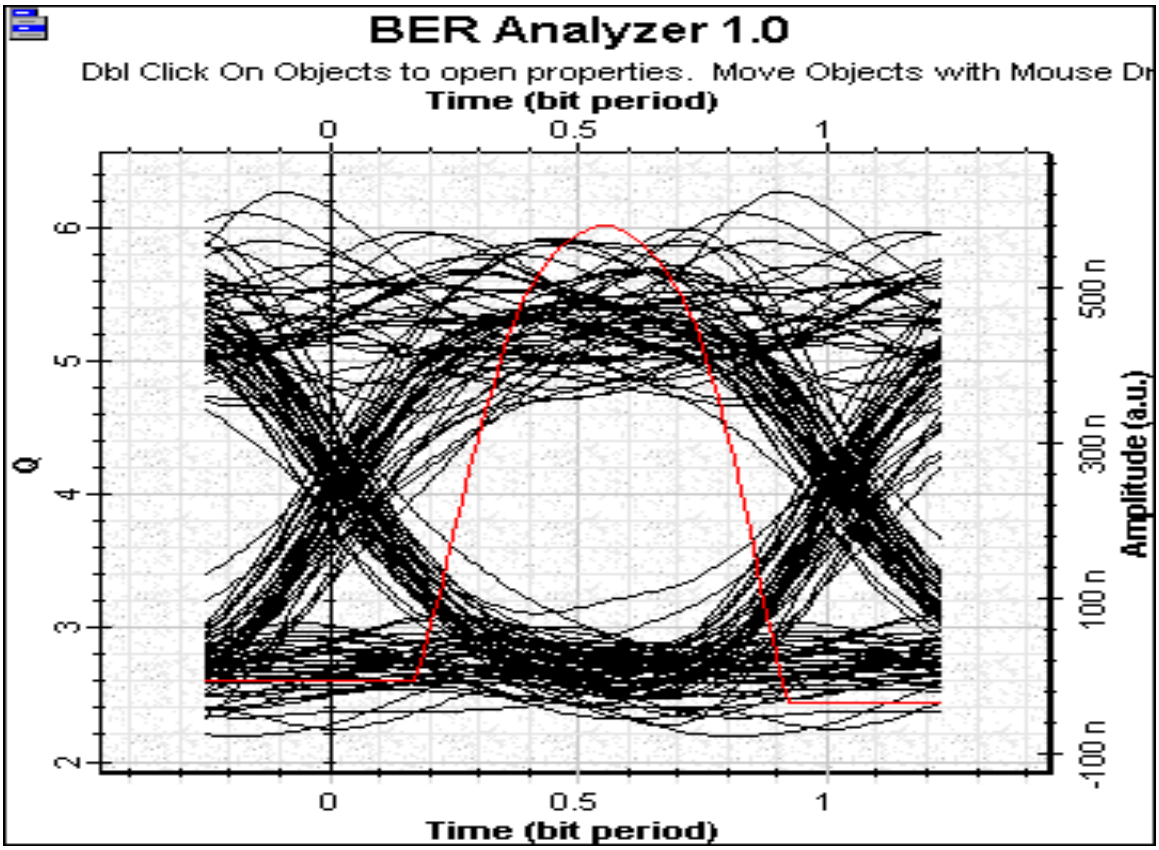

Fig.19: EYE pattern – APD receiver

Example: Extinction Ratio

Sensitivity degradation - ER**.osd**

A simple source of power penalty is related to the energy carried by 0 bits. Some power is emitted by transmitters even in the off-state. In the project "Sensitivity degradation - ER**.osd**" (Fig.20), we have an external modulated laser where you can specify the extinction ratio (ER) at the modulator.

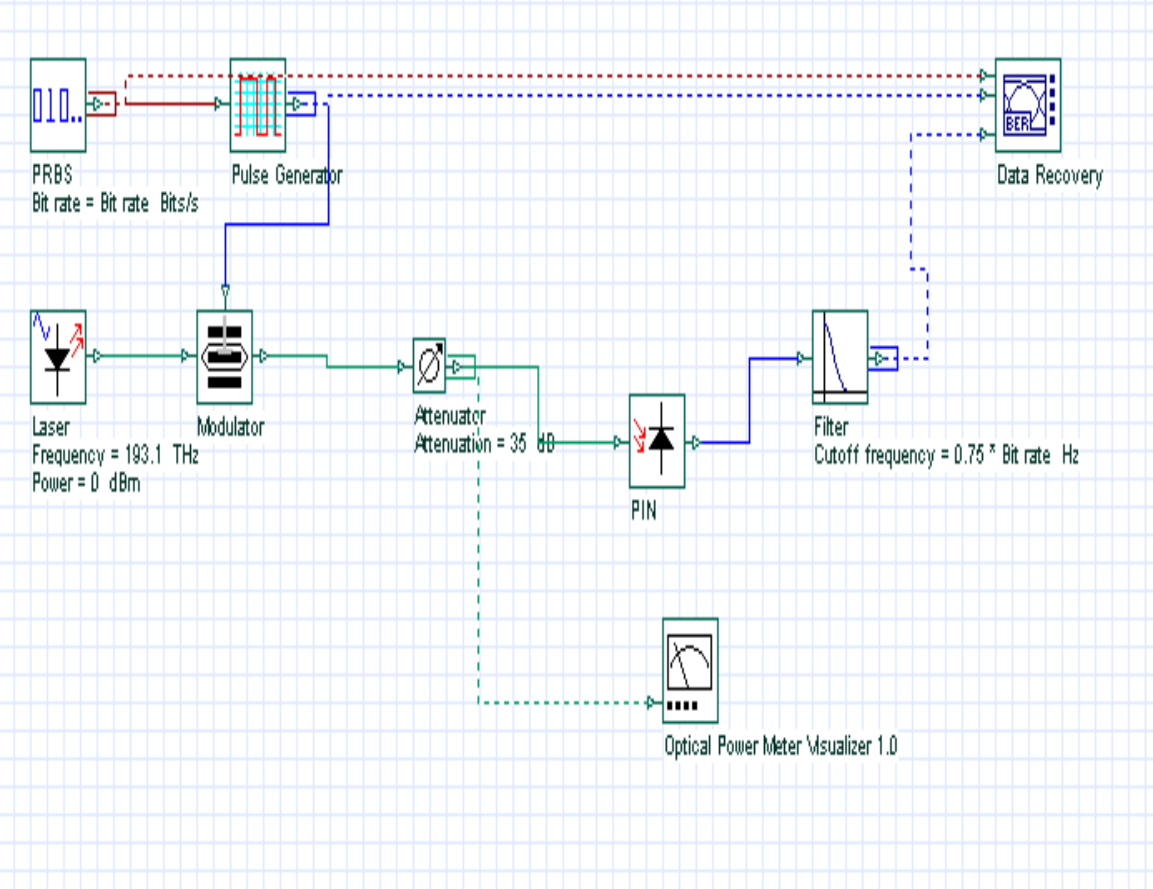

Fig.20: Sensitivity degradation - ER

In this project we vary the value of the ER and we calculate the Q factor at the receiver. Variation of Q factor with extinction ratio has been shown in **Fig.21**.

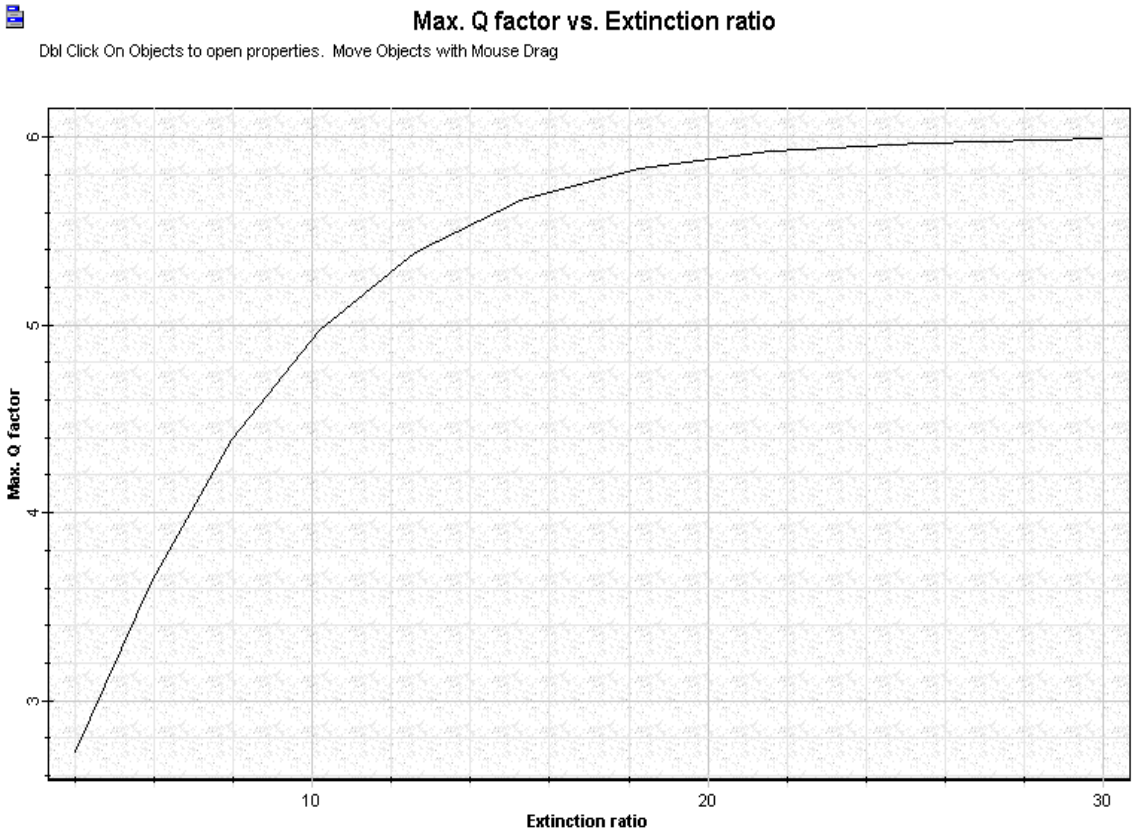

Fig.21: Q factor vs. Extinction ratio

Chapter 5 – Lightwave Systems

Example: Power Budget

System design_ power budget**.osd**

The purpose of power budget is to ensure that enough power will reach the receiver to maintain reliable performance during the entire system lifetime. The minimum average power required by the receiver is the receiver sensitivity. The average launch power is generally specified for each transmitter with optical powers expressed in dBm.

In order to estimate the maximum fiber length we should specify the output power of the transmitter and the receiver sensitivity. We can also specify a system margin. The purpose of the system margin is to allocate a certain amount of power to additional sources of power penalty that may develop during the system lifetime.

The project "System design_power budget**.osd**" shows (Fig.1) a system design using a receiver with –38 dBm sensitivity and external modulated transmitter with output power of –3 dBm.

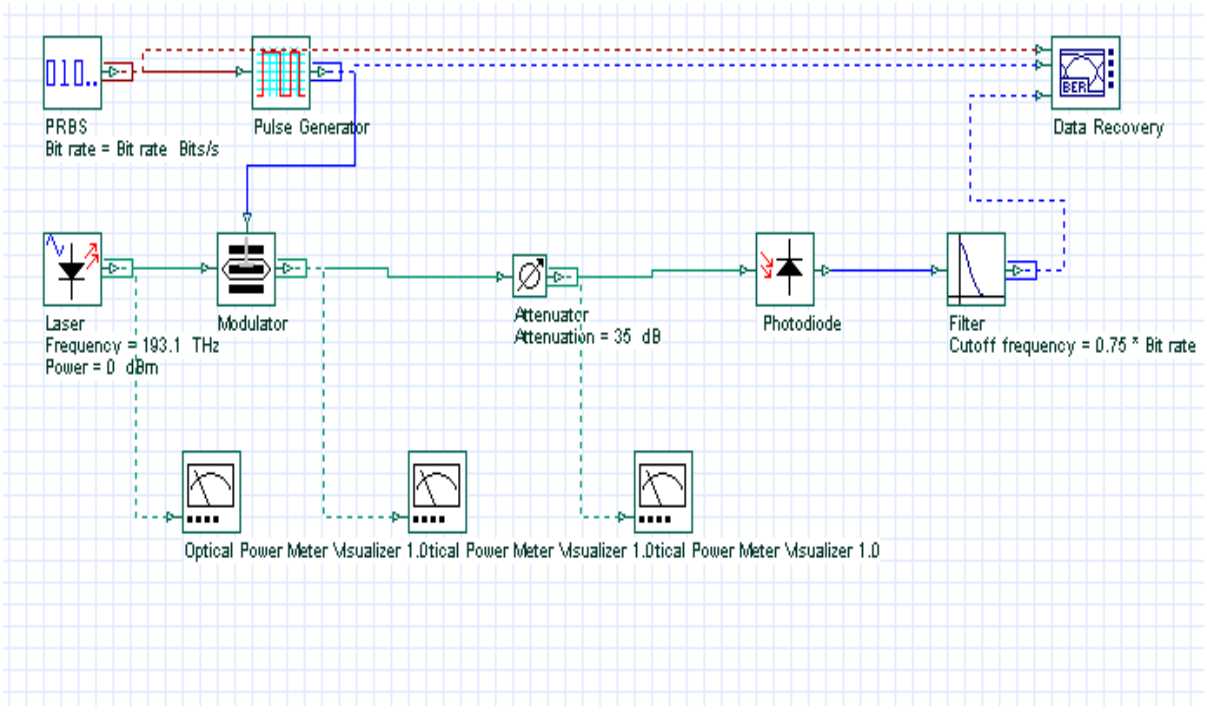

Fig.1: Layout: System design_ power budget

Using a system margin of 0 dB the total loss allocated for the channel will be:

Channel Loss = System Margin + Receiver Sensitivity + Transmitter power
Therefore, Channel Loss = 38 – 3 = 35 dB.

For a typical fiber attenuation of 0.25 dB/km, the maximum distance through which light can propagate in this system is 140 km. In this case we are not including dispersion effects that will limit the system performance.

Example: Power Budgeting for Ring Networks

Optical power level management in metro networks_no amplifier**.osd**
Gain variation of EDFA depending on input power**.osd**
Optical power level management in metro networks_lumped amplification**.osd**
Optical power level management in metro networks_unity gain**.osd**

Project files "Optical power level management in metro networks_no amplifier**.osd**", "Gain variation of EDFA depending on input power**.osd**", "Optical power level management in metro networks_lumped amplification**.osd**", and "Optical power level management in metro networks_unity gain**.osd**" consider the power budgeting for metro networks. They show alternative amplifier placements in the network and its effect to system performance. It also gives the details of calculations.

Case I: No amplifier option

Optical power level management in metro networks_no amplifier**.osd**

In this example, our goal is to design a basic ring network without amplification and discover the power related issues.

Metro networks using ring topology are expected to have more dynamic traffic pattern compared to most long-haul networks. In addition to this, they are expected to have optically transparent nodes with minimum number of regenerators being used. Therefore, we need to consider all the optical power variations. These variations may result from the wavelength dependent loss in fibers, wavelength dependent gain in amplifiers, and channel to channel insertion loss variation in the multiplexers/demultiplexers etc. These optical degradations accumulate along the links until the optical termination. Due to dynamic nature of the network, only proper dynamic power level management can reduce them. Let us consider first the loss elements.

Optical Add/Drop Multiplexers (OADMs) introduce insertion loss. It contains two parts: deterministic and random.

In fact, loss varies with the wavelength. The loss of fiber depends on fiber type and wavelength. Variation of optical switch types and different path lengths in the network will result in a random loss, which is difficult to predict.

There are several limiting factors in terms of power in the network. These are nonlinear effects, receiver sensitivity, and losses in the fiber, OADMs, OXCs etc.

Typical loss, transmitter power, and receiver sensitivity values are given in **Tables 1 and 2** [1].

Symbol	Description	Loss value
L_{mon}	Tap loss for monitoring	0.2 dB
L_{conn}	Loss of a connector	0.25 dB
L_{splice}	Loss of a splice	0.15 dB
L_{span}	Loss of the fiber span	0.25 dB/km
L_{mux}	Loss of a multiplexer	4 dB
L_{demux}	Loss of a demultoplexer	4 dB
L_{foadm}	Loss of a fixed OADM	2 dB
L_{roadm}	Loss of a re-configurable OADM	10 dB

Table 1: Typical losses for components used in metro links.

Symbol	Description	Optical Power/Receiver Sensitivity
$P_{T-DM@2.5}$	2.5 Gbps/DM output power	3 dBm
$P_{T-EM@10}$	10 Gbps/EM output power	0 dBm
$P_{R-sen@2.5}$	2.5 Gbps pin diode receiver sensitivity	-23 dBm
$P_{R-sen@10}$	10 Gbps pin diode receiver sensitivity	-16 dBm

Table 2: Typical values for transmitter and receiver

Total allowable loss depends on the transmitted power and receiver sensitivity. As shown in **Table 2**, receiver sensitivity is also a function of bit rate. The allowable loss is given by $L_{allowable} = P_T - P_{R-sens}$. Assuming two splices and six connectors total loss at each node is given by $L_{node} = 2L_{splice} + 6L_{conn} + L_{foadm}$.

Let us consider a typical WDM metro ring at 2.5 Gbps with 200 km in circumference with four intermediate fixed OADMs as shown in **Fig. 2**. In this network, node 1 and 4 communicate on channel 1 whereas node 2 and 3 communicate on channel 2. Design project is given in Optical power level management in metro networks_no amplifier**.osd** file.

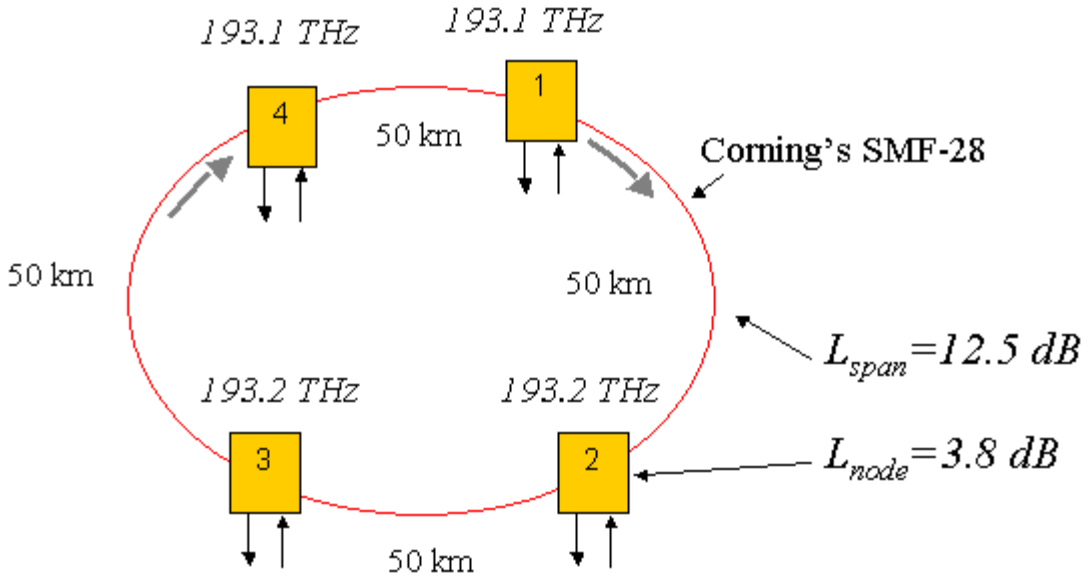

Fig. 2: A basic optical ring network with four nodes and two channels

Without any inline amplification, the allowable loss by using direct modulated source is $L_{allowable} = 3-(-23) = 26\ dB$. Node (including two splices and six connectors) and span losses are $L_{node} = 2\times 0.15 + 6\times 0.25 + 2 = 3.8\ dB$ and $L_{span50km} = 50\times 0.25 = 12.5\ dB$, respectively. Therefore total loss will be $12.5\times 4 + 3.8\times 4 = 65.2\ dB$.

Comparing the allowable loss and total loss in the network shows that it is not a good idea to make a design without amplification. Of course, increasing power is another option, but nonlinear effects may become important impairments at high powers. In this case, the required launch power will be *65.2-23-3=39.2 dBm/channel*. Let us now discuss these affects [2,3].

Self-Phase Modulation

The effect of SPM is to chirp the pulse and broaden its spectrum. As a rough design guideline SPM effects are negligible when $P_0 < \alpha/\gamma$ where $\gamma = {n_2\omega_0}/{cA_{eff}}$ [1/(Wkm)] is non-linearity coefficient, P_0 is the peak power and α is the loss parameter. For the fiber we used $\gamma \approx 1.5\, W^{-1}km^{-1}$. Therefore, SPM effects can be negligible when the peak power is below 166 mW or 18 dBm average power.

Cross-Phase Modulation

When two or more pulses of different wavelengths propagate simultaneously inside fibers, their optical phases are affected not only by SPM but also by XPM. Fiber dispersion converts phase variations into amplitude fluctuations. XPM induced phase shift should not affect the system performance if the GVD effects are negligible. As a rough estimate, the channel power is restricted with $P_{ch} < \alpha/\left[\gamma(2N_{ch}-1)\right]$ where N_{ch} is the number of channels.

For a two channel system, limiting power is around 56 mW (17.5 dBm). Separation between channels also effects the XPM. Increase in the separation will decrease the penalty which originates from XPM.

Four-Wave Mixing

FWM is the major source of nonlinear cross-talk for WDM communication systems. It can be understood from the fact that beating between two signals generates harmonics at difference frequencies. If the channels are equally spaced new frequencies coincide with the existing channel frequencies. This may lead to nonlinear cross-talk between channels. When the channels are not equally spaced, most FWM components fall in between the channels and add to overall noise. FWM efficiency depends on signal power, channel spacing, and dispersion. If the GVD of the fiber is relatively high $|\beta_2| > 5\ ps^2/km$, FWM efficiency factor almost vanishes for a typical channel spacing of *50 GHz* or more. If the channel is close to zero dispersion wavelength of the fiber, considerably high power can be transferred to FWM components. To reduce the effect of FWM to the system performance, one can use either uneven channel spacing or use dispersion-management technique.

Stimulated Raman Scattering

Because of SRS, short wavelength channels act as pump for longer wavelength channels. In a WDM system, the SRS will impair the system performance such that energy is transferred from the short-wavelength to the long-wavelength channels. The Raman threshold for a single channel system is given by :

$$P_{th} \approx {}^{16 A_{eff}} \Big/ g_R L_{eff}$$

where

$$L_{eff} = \frac{1-\exp(-\alpha L)}{\alpha}$$

and it is approximately equal to $1/\alpha$ for long fibers. In fact, it is a function of the number of the channels and channel power. For a single channel system it is around 500 mW near 1.55 micrometer if $g_R = 1\times10^{-13}\ m/W$. For a 20 channel system P_{th} exceeds 10 mW whereas it is around 1 mW for a 70 channel system. It has little impact on system performance.

Stimulated Brillouin Scattering

It results from the interaction of light with acoustic wave in fiber and scatters power backward. Back scattered light is downshifted in frequency from the original signal frequency. Threshold level depends on effective core area and effective fiber length as given below:

$$P_{th} \approx {}^{21 A_{eff}} \Big/ g_B L_{eff}$$

Typical value for g_B is around $5\times10^{-11}\ m/W$. The threshold value also depends on modulation format, source line width and duration of pulse. Some values for threshold power are given below:

(1) 9 dBm for CW light
(2) 12 dBm for externally modulated transmitter
(3) >18 dBm for externally modulated transmitter with source wavelength dither.

Generally speaking, SBS has little effect on system performance.

Fig. 3 shows the Q factor for channel 1 at the receiver end verses launch power, when no amplifier is used. When the launch power is around *23 dBm*, the power received by the receiver is around *–26 dBm* which is below the receiver sensitivity. Moreover, this figure shows that after about *18 dBm* launch power (as predicted) nonlinearity becomes an issue and Q factor starts to decay.

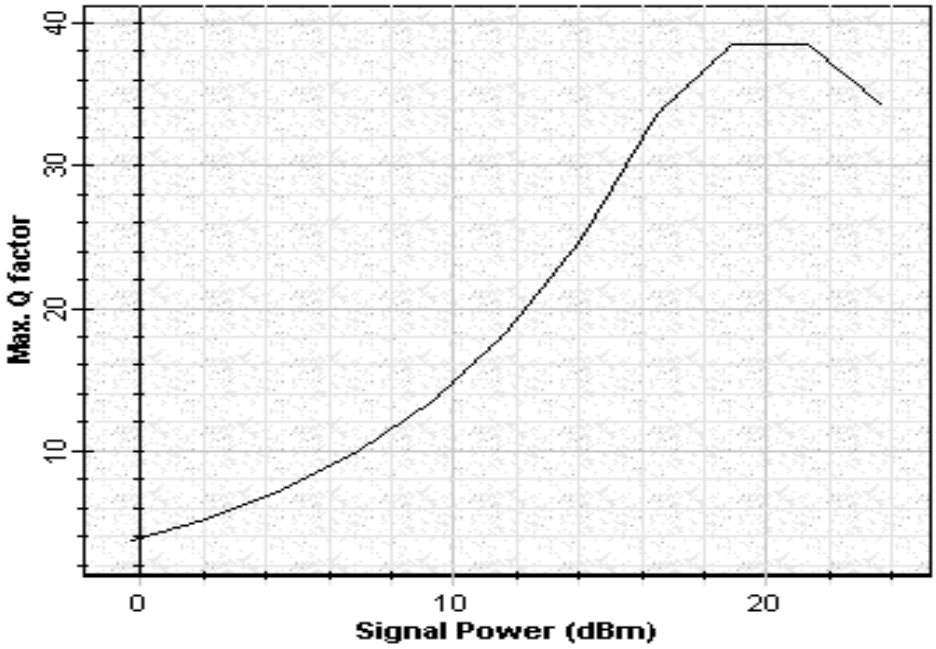

Fig. 3: Q factor verses launch power at node 4 when no amplifier is used

Fig. 4 shows *OSNR* at the receiver with respect to launch power. Figs. 5 and 6 show the eye diagram for the launch power of 3 dBm/channel and 27 dBm/channel; respectively. From these figures we can conclude that, limiting factor below *18 dBm* region is mainly *OSNR* whereas above this value, it is non-linearity. This example shows that non-linearity may become an issue in no-amplifier ring networks.

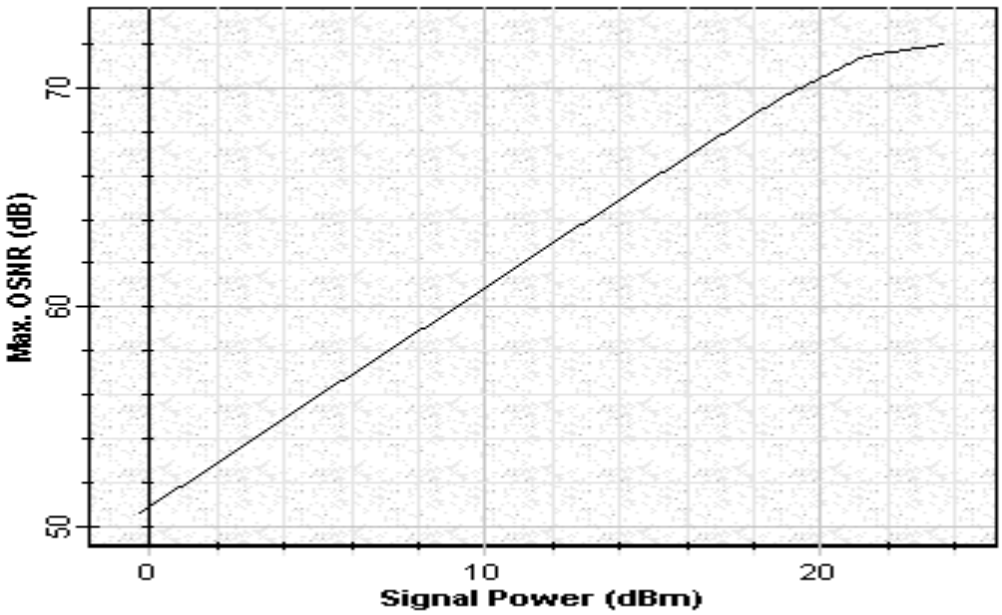

Fig. 4: OSNR verses launch power at node 4 when no amplifier is used

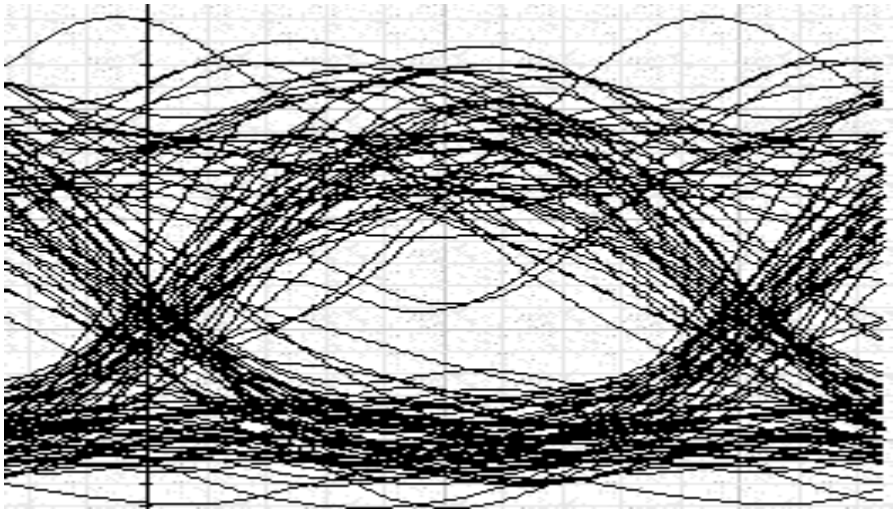

Fig. 5: Eye diagram at the receiver when the launch power is 3 dBm

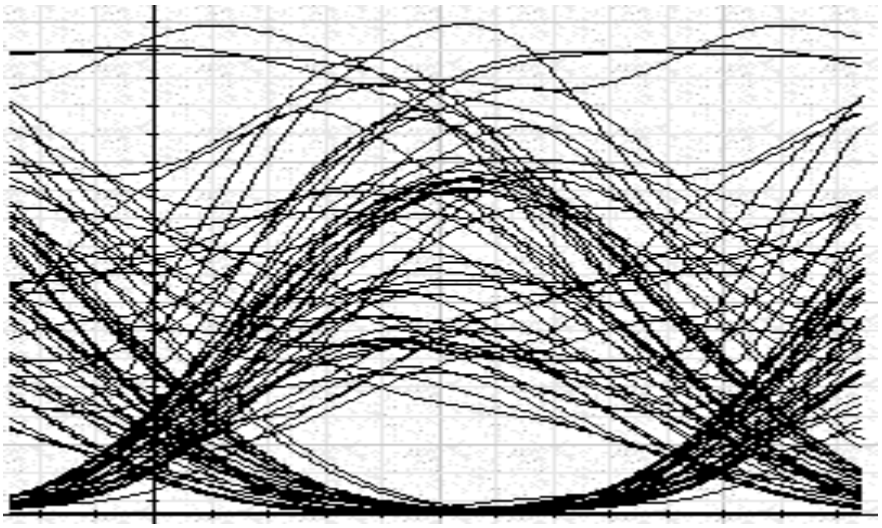

Fig. 6: Eye diagram at the receiver when the launch power is 27 dBm

References:

1. Sidney Shiba et. al., “Optical Power Level Management in Metro Networks”, NFOEC’01, 2001.
2. Bigo et. al., “Investigation of Cross-Phase Modulation Limitation over Various Types of Fiber Infrastructures”, IEEE Photon. Tech. Lett. 11, pp. 605, 1999.
3. Tarek S. El-Bawab et. al., “Design Considerations for Transmission Systems in Optical Metropolitan Networks”, Opt. Fib. Tech. 63, pp. 213, 2000.

Case II: Lumped amplification

Gain variation of EDFA depending on input power**.osd**

Optical power level management in metro networks_lumped amplification**.osd**

Metro ring networks have more dynamic traffic pattern compared to most long-haul networks. In this configuration we need to consider all the optical power variations resulting from the wavelength dependent loss in the fiber, wavelength dependent gain in the amplifires, channel to channel insertion loss variation in the multiplexers/demultiplexers etc. These optical degradations accumulate along the links and may grow very fast depending on the path followed by the wavelength. Due to dynamic nature of the network, only proper *dynamic power level management* can reduce them. Typical values for the loss elements are given in the **Table 1.**

In this example we consider compensation of the loss in fibers and ADMs using amplifiers. To do so, let's first investigate the amplifier gain characteristics.

Optical Amplifier

Gain variation of EDFA depending on input power**.osd**

Optical power level management in metro networks_lumped amplification**.osd**

The gain and the gain tilt of the optical amplifier changes with the input power [1]. This is shown below **(Fig. 7)** for EDFA (length of the fiber 5 m, pump power at 980 nm is 100 mW). The project file is Gain variation of EDFA depending on input power**.osd**. When the span losses of different spans in the ring are different, the input power of different amplifier will be different. Therefore, depending on the path of the signal, each communication link between two nodes will experience different amplification. Tilt can accumulate depending on the path followed. To eliminate this effect, pump control, variable attenuator at the input or gain tilt compensating amplifier/filter can be used.

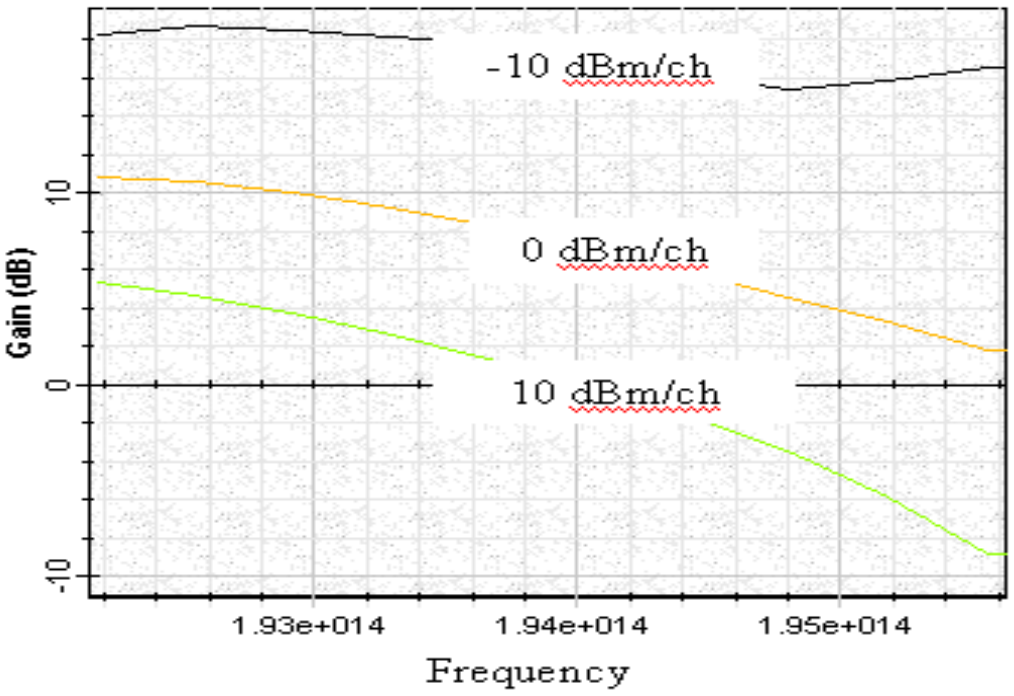

Fig. 7: Value and shape of optical amplification depend on input power

Fig. 8 shows, for example, results of two cascaded EDFA amplifier (length of the fiber 4 m, pump power at 980 nm is 35 mW, input power -13.3 dBm/channel or –133 dBm total power). Here, we consider a 16.4 dB loss between amplifires to model the total span and node loss. It is clear from this figure that tilt is increased. For example, a channel near 193 THz will see a gain of around 17 dB after two node pass, whereas it is around 16 dB for a channel around 194 THz. Therefore, this effect may be an issue for a 100 GHz separated 10 channel system even though each channel passes through same number of amplifiers.

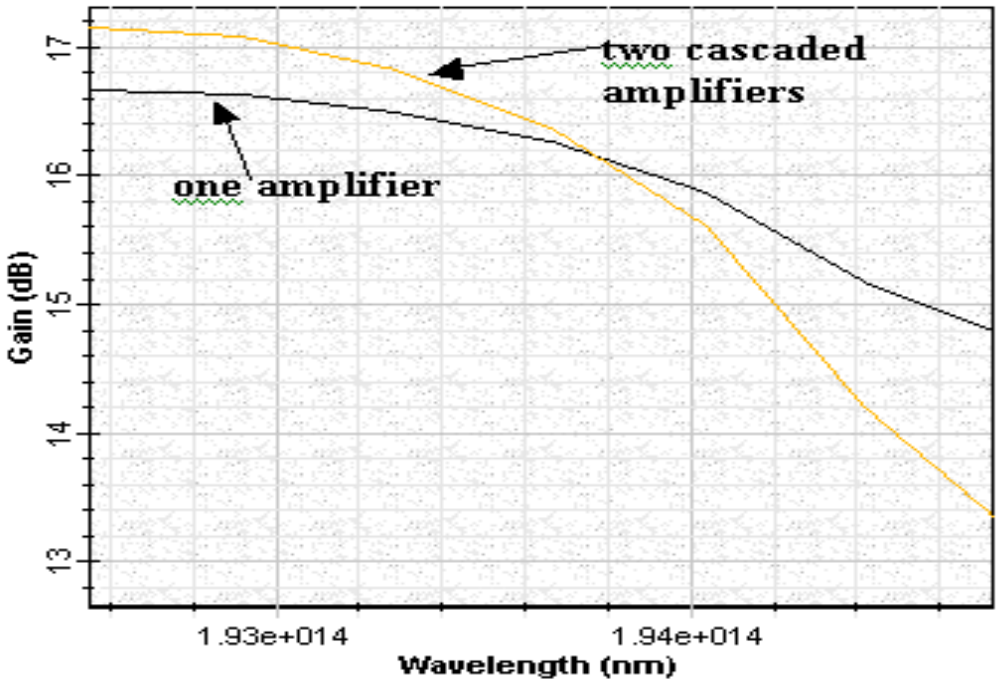

Fig. 8: Gain profile of one and two cascaded amplifiers

Let us now consider a typical WDM metro ring at 2.5 Gbps with 200 km in circumference with four intermediate fixed OADMs as shown in Fig. 9. In this network node 1 and 4 communicate on channel 1 whereas node 2 and 3 communicate on channel 2. Design project is given in Optical power level management in metro networks_lumped amplification**.osd** file

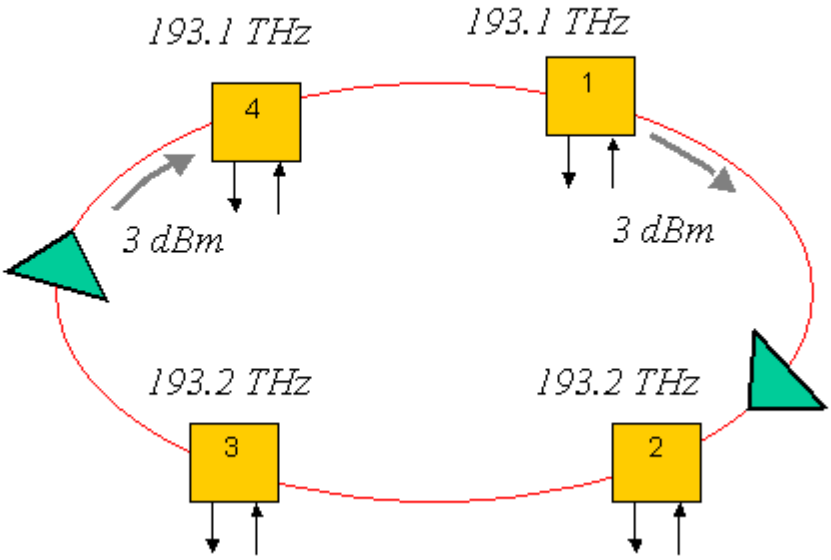

Fig. 9: Ring network layout with two amplifiers

Assuming a launch power of 3 dBm per channel, the amount of amplification needed in the ring is:

$$G_{required} = -\left(3 - 4 \times 0.25 \times 50 - 4 \times 3.8 - (-23) - 3\right) = 42.2\ dB$$

This gain can be obtained by using two high-gain (25 dB), high performance amplifiers as shown in Fig. 9. In this configuration two amplifiers are placed just before node 2 and node 4. Required gain values for amplifiers are higher than the gain target value for metro EDFA (Table 3 [2]) and therefore this configuration is in fact not practical for metro applications. Moreover, it will not allow addition of new node [1,3].

	Metro target
Gain	10 to 20 dB
Power	10 to 15 dBm
Noise Figure	6 dB
Gain Flatness	1 dB

Table 3: Typical values for amplifiers

Measured signal power and OSNR at the receiver is given below (Table 4) when two 15 dB amplifiers are used instead of 25 dB ones. Figure 10 shows the eye diagram for this case. In this case Q factor is 25.

Frequency (THz)	Signal Power (dBm)	Noise Power (dBm)	OSNR (dB)
193.1	-19.169929	-40.899899	21.72997
193.2	-92.554518	-100	7.4454824

Table 4: Measured signal power and OSNR at the receiver

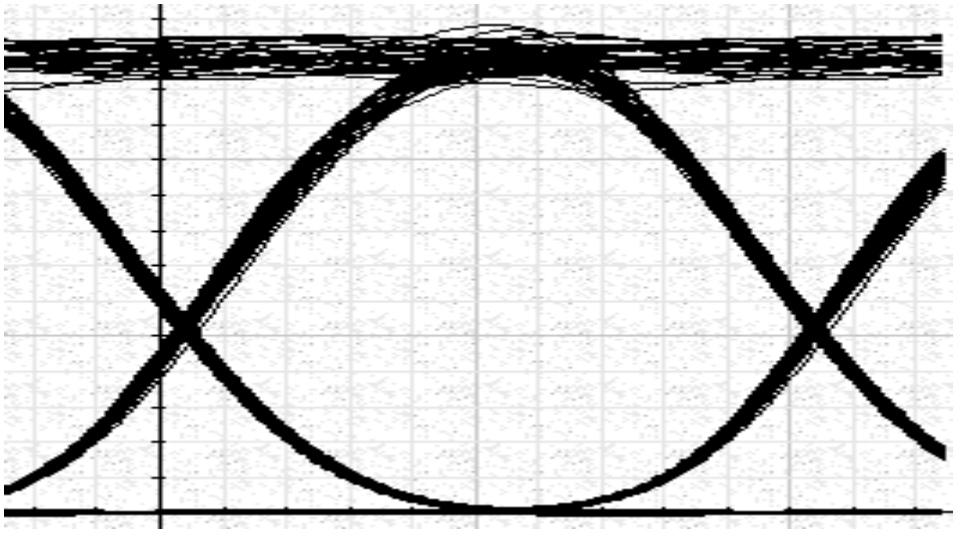

Fig. 10: Eye diagram at node 4 when two amplifiers with 15 dB gain each are inserted before node 4 and node 2

Figure 11 on the other hand shows the eye diagram when the gain of the two amplifiers is 25 dB each. In this case, Q factor is 38 and OSNR is about 31 dB as shown below (Table 5):

Frequency (THz)	Signal Power (dBm)	Noise Power (dBm)	OSNR (dB)
193.1	0.82416429	-30.229305	31.053469
193.2	-82.554598	-100	17.445402

Table 5: OSNR value when the gain of the two amplifiers is 25 dB each

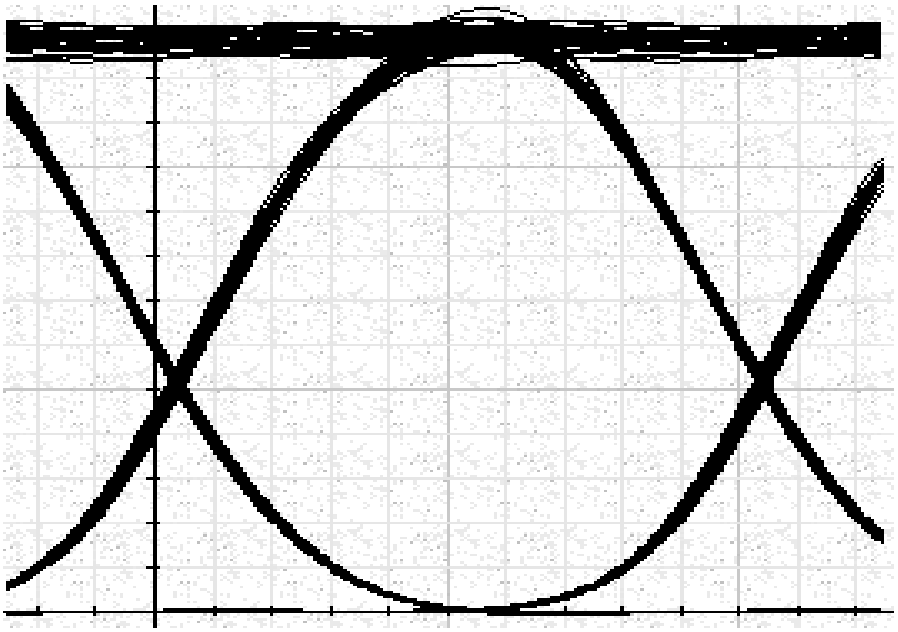

Fig. 11: Eye diagram at node 4 when two amplifiers with 25 dB gain each are inserted before node 4 and node 2

Even though this configuration will do the job for a static configuration, it will not allow addition of new node or complex wavelength routing schemes where one signal may follow different paths depending on the routing.

References:

1. R. Ramaswami and K. N. Sivarajan, Optical Networks: A Pactical Perspective, Morgan Kaufmann, 1998.
2. Sidney Shiba et. al., “Optical Power Level Management in Metro Networks”, NFOEC’01, 2001.
3. Tarek S. El-Bawab et. al., “Design Considerations for Transmission Systems in Optical Metropolitan Networks”, Opt. Fib. Tech. 63, pp. 213, 2000.

Case III: Unity gain approach

Optical power level management in metro networks_unity gain**.osd**

In optical ring topology, we need to consider all the optical power variations resulting from the wavelength dependent loss in the fiber, wavelength dependent gain in amplifiers, and channel to channel insertion loss variation in the multiplexers/demultiplexers etc. These optical degradations accumulate along the links and may grow very fast depending on the path followed by the wavelength. Due to dynamic nature of the network, only proper *dynamic power level management* can reduce them. Typical values for the loss elements are

given in the section “Optical power level management in metro networks, no amplifier option”. We have also discussed the characteristics of optical amplifiers and replacement of amplifiers at certain points in network in section “Optical power level management in metro networks, lumped amplification”. In these two sections we have seen that no amplifier option is not a good choice for loss compensation since required high power may trigger fiber nonlinearity. Even though lumped loss compensation seems to do the job in terms of good eye diagram, it is not the best considering the dynamic nature of metropolitan networks.

In this example we will show an alternative approach, so called unity gain approach. In this approach, each amplifier matches the loss of one.

The span loss will be node ($L_{node} = 2 \times 0.15 + 6 \times 0.25 + 2 = 3.8\, dB$) and span preceding it ($L_{span50km} = 50 \times 0.25 = 12.5\, dB$). For this approach, an amplifier with modest gain of 16.3 dB at every node can be used. This approach is only economically feasible with a low cost-compact optical amplifier yet the best one considering dynamic routing in the network.

Let us now consider a typical WDM metro ring at 2.5 Gbps with 200 km in circumference with four intermediate fixed OADMs as shown in Fig. 12. In this network node 1 and 4 communicate on channel 1 whereas node 2 and 3 communicate on channel 2. Loss of each span and node is compensated at the node following the span. Gain of each amplifier is 16.3 dB. Design project is given in Optical power level management in metro networks_unity gain**.osd** file. This configuration is scalable. Moreover, regardless of path followed by a certain wavelength, the power is always balanced [1-3].

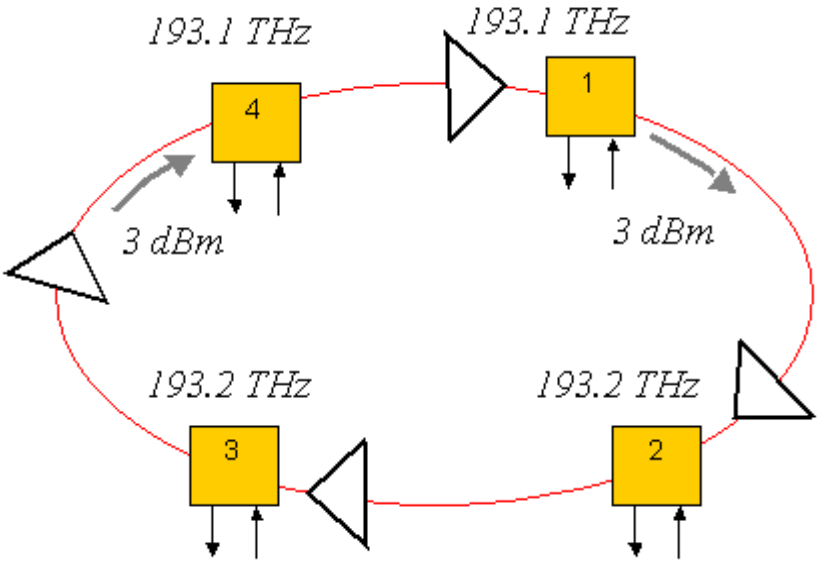

Fig. 12: Ring network layout with amplifier at each node

Eye diagrams of channel 1 at node 4 are shown in Fig.13, when transmitter power is 3 dBm. Fig.14, on the other hand shows the eye diagram at node 4 when the transmitter power is –27 dBm. Fig.15 shows Q factor verses transmitter signal power.

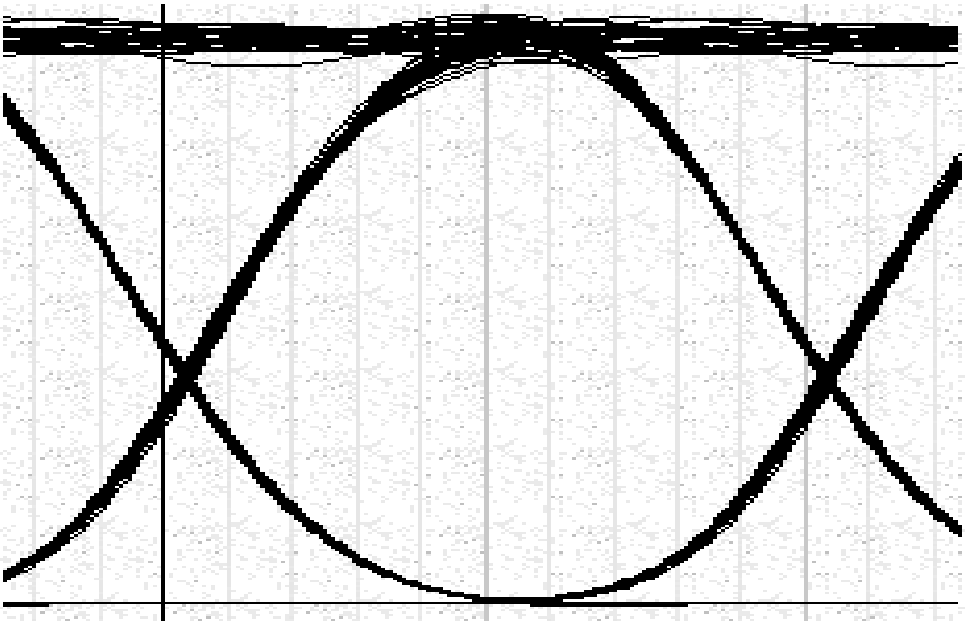

Fig. 13: Eye diagram of channel 1 at node 4 when transmitter power is 3 dBm and bit rate is 2.5 Gbps

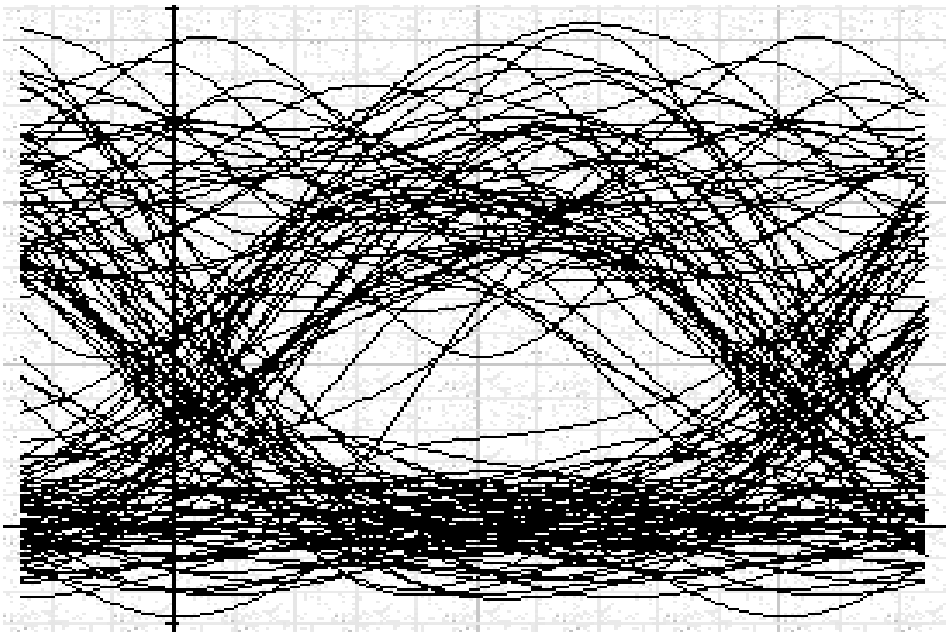

Fig. 14: Eye diagram of channel 1 at node 4 when transmitter power is -27 dBm and bit rate is 2.5 Gbps

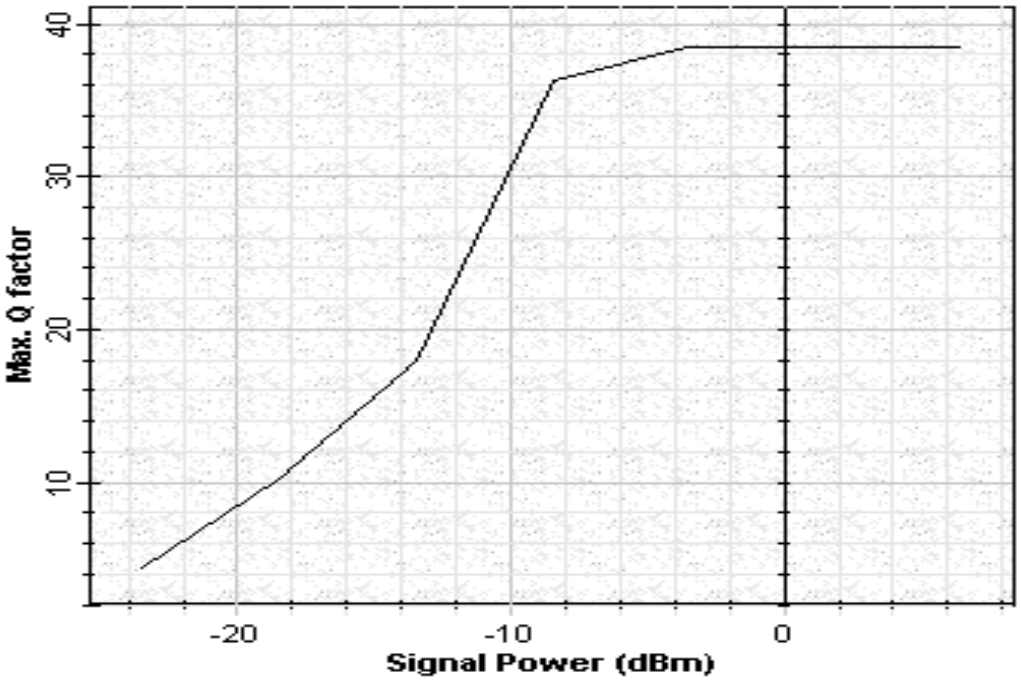

Fig. 15: Q factor verses transmitter power at node 4 when bit rate is 2.5 Gbps

References:

1. R. Ramaswami and K. N. Sivarajan, Optical Networks: A practical Perspective, Morgan Kaufmann, 1998.
2. Sidney Shiba et. al., "Optical Power Level Management in Metro Networks", NFOEC'01, 2001.
3. Tarek S. El-Bawab et. al., "Design Considerations for Transmission Systems in Optical Metropolitan Networks", Opt. Fib. Tech. 63, pp. 213, 2000.

Example: Dispersion Broadening

Dispersions vs power**.osd**

Project file "Dispersions vs power**.osd**" shows that the dispersion broadening penalty of the system using un-chirped NRZ input pulses is lower when the dispersion is positive. In this example, a 10 Gb/s NRZ signal is transmitted through two nominally identical 150 km long fibers with opposite signs of dispersion. For the first case, fiber has –2.27 ps/nm/km dispersion and for the second case it is +2.27 ps/nm/km. Power is swept from 2 dBm to 20 dBm for these two cases. You can compare these cases by looking at the eye diagrams. This simulation shows that system penalty when a negative dispersion fiber is used is larger than when a positive dispersion fiber is used. The penalty in the negative dispersion fiber arises from the pulse broadening due to SPM. However, in the case of positive dispersion, nonlinear pulse compression interacts with dispersion resulting with negative power penalties. Up to about 15 dBm input power, Q factor increases with the increase of power when the dispersion is positive **(Fig. 16)**. This figure also shows that the positive dispersion fiber provides superior performance for all input powers, even exhibiting negative penalties (taking 14 dB as a reference Q) over a power range between 7 dBm and 15 dBm.

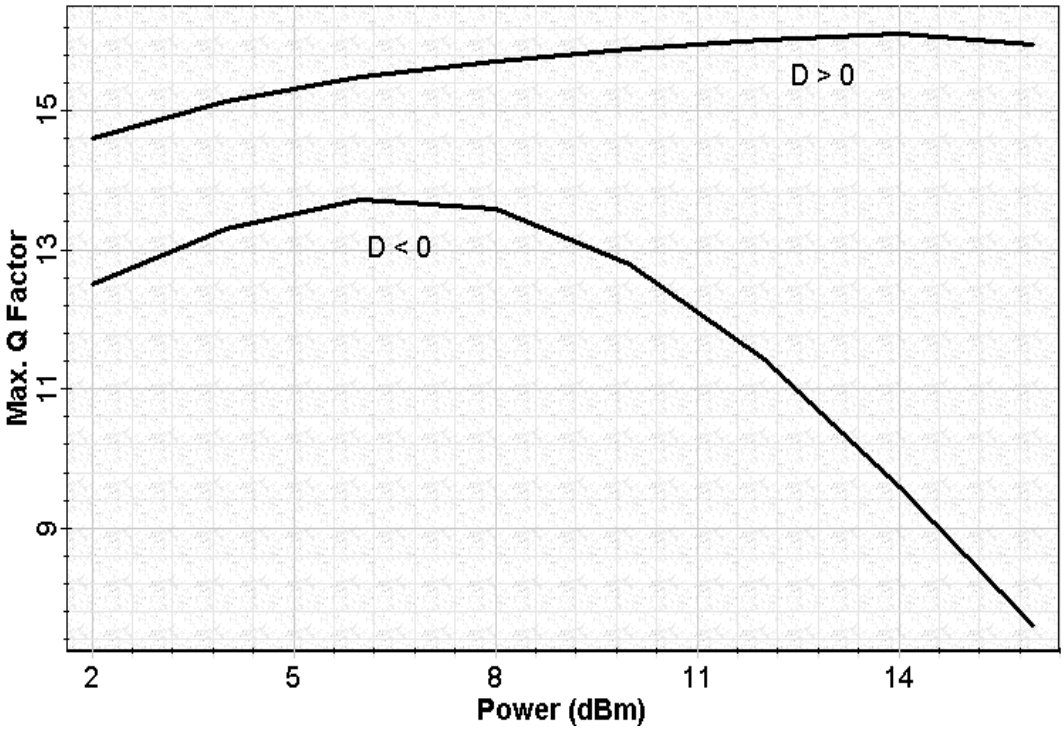

Fig. 16: Q factor verses input power for negative and positive dispersions

Fig. 17 compares negative and positive dispersion cases when the input power is 14.5 dBm. These results are in perfect agreement with the results shown in [1].

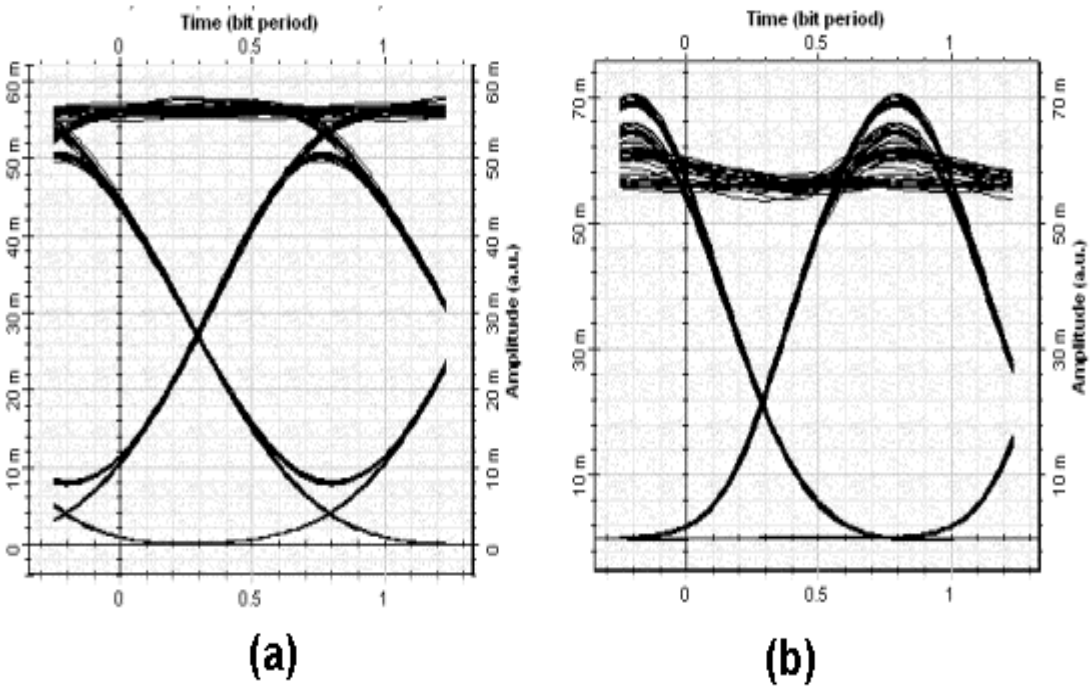

Fig. 17: Eye diagrams (a) through 150 km of negative dispersion fiber, (b) through 150 km positive dispersion fiber.

Reference:

1. Optical Fiber Telecommunications IIIa, Eds: I. Kaminov and T. Koch, chapter "Fiber Nonlinearities and their Impact on Transmission Systems" by F. Forghieri, R. Tkach and A. Chraplyvy.

Chapter 6 – Optical Amplifiers

Example: EDFA Basic Concepts

EDFA basic concepts**.osd**

The sample file "EDFA basic concepts**.osd**" shows the basic characterization of the Erbium doped fiber amplifier. We have considered the three design versions namely, (a) Gain Spectrum_bandwidth (b) Gain Saturation and (c) Amplifier noise. These enable characterizing the gain, noise figure and output power under unsaturated and saturated signal input regime. These versions refer to the topics: Gain Spectrum and Bandwidth, Gain Saturation, and Amplifier Noise, respectively.

In these examples the amplifier performance is characterized by using sweeps for the input parameters of the amplifier. Versions Gain Spectrum_bandwidth and Amplifier Noise, sweep the signal wavelength, while version Gain Saturation sweeps the input power for the cases: small signal input power (-30 dBm) and saturated input signal power (0 dBm).

The three versions created in this project file are shown in Fig.1. The basic layout used in each version considers Erbium-doped fiber stage setup in a co-propagating pump scheme. EDFA 1.0 model was used in this simulation. A single input signal with small and large signal input operating in the C-band wavelength range is set in the laser.

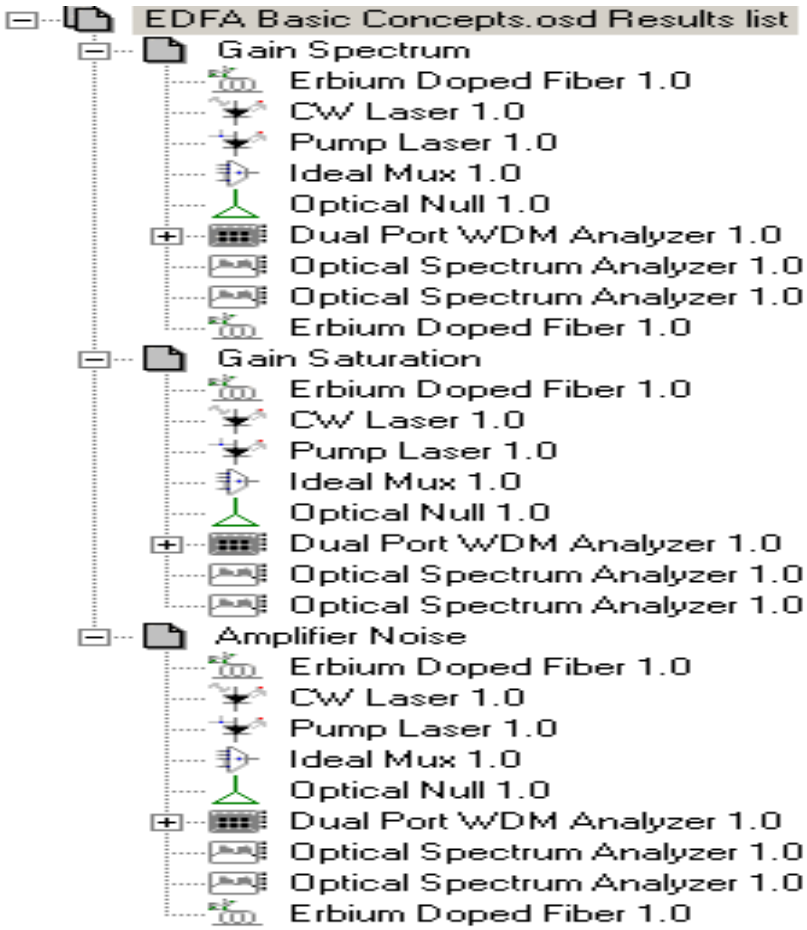

Fig. 1: Three different versions created in this project file

For each design version we have plotted three graphs showing the Output Signal Power, Gain and Noise Figure; as a function of sweep parameter. In the project, the components settings can be modified and the simulations can be repeated in order to analyze the amplifier performance.

The graphs that characterize the amplifier performance such as gain, noise figure and output power as a function of the different sweep parameters are listed on the docker View, as shown in Fig. 2. Some graph facilities such as zoom, tracer, markers, legend etc. can be accessed just right clicking on the graph screen.

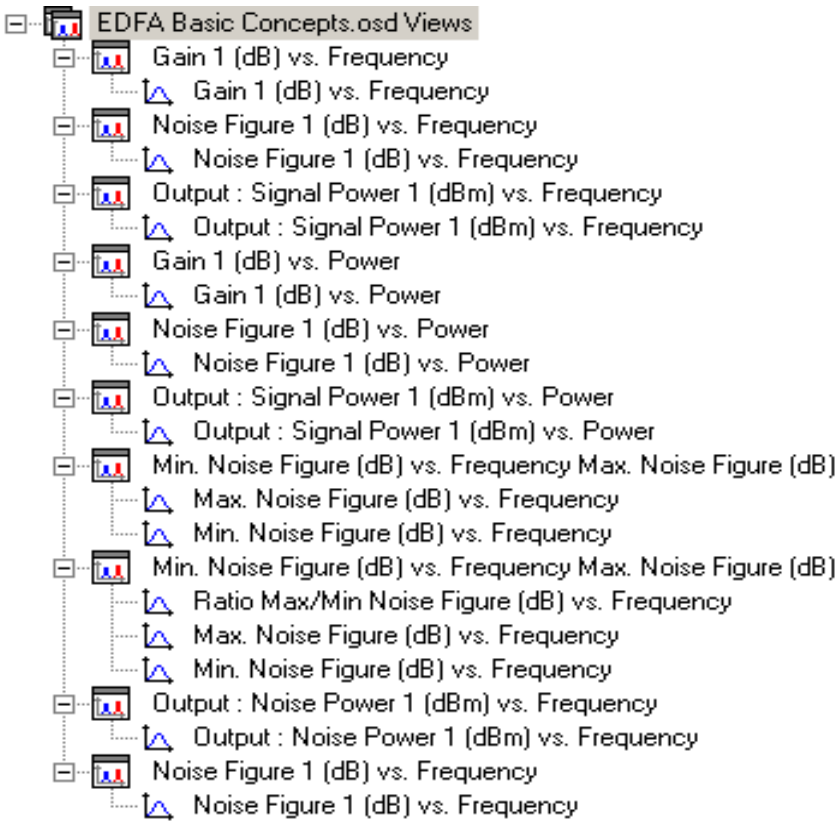

Fig. 2: List with graphs available on docker view

The same graphs visualized on view are also listed in the docker Graphs along with additional graphs as shown in Fig. 3.

The absorption and emission cross section, and the input parameters which are critical in the numerical solution of coupled rate and propagating equations, are displayed in Erbium doped fiber component. The gain and noise figure are calculated using the power results. Fig. 4 shows the cross-section file used in this project.

The cross section input files are characteristic to a specific fiber as well as the fiber dimensions (Table 1). However, it is interesting to change fiber specifications in order to evaluate how it can modify the calculated results.

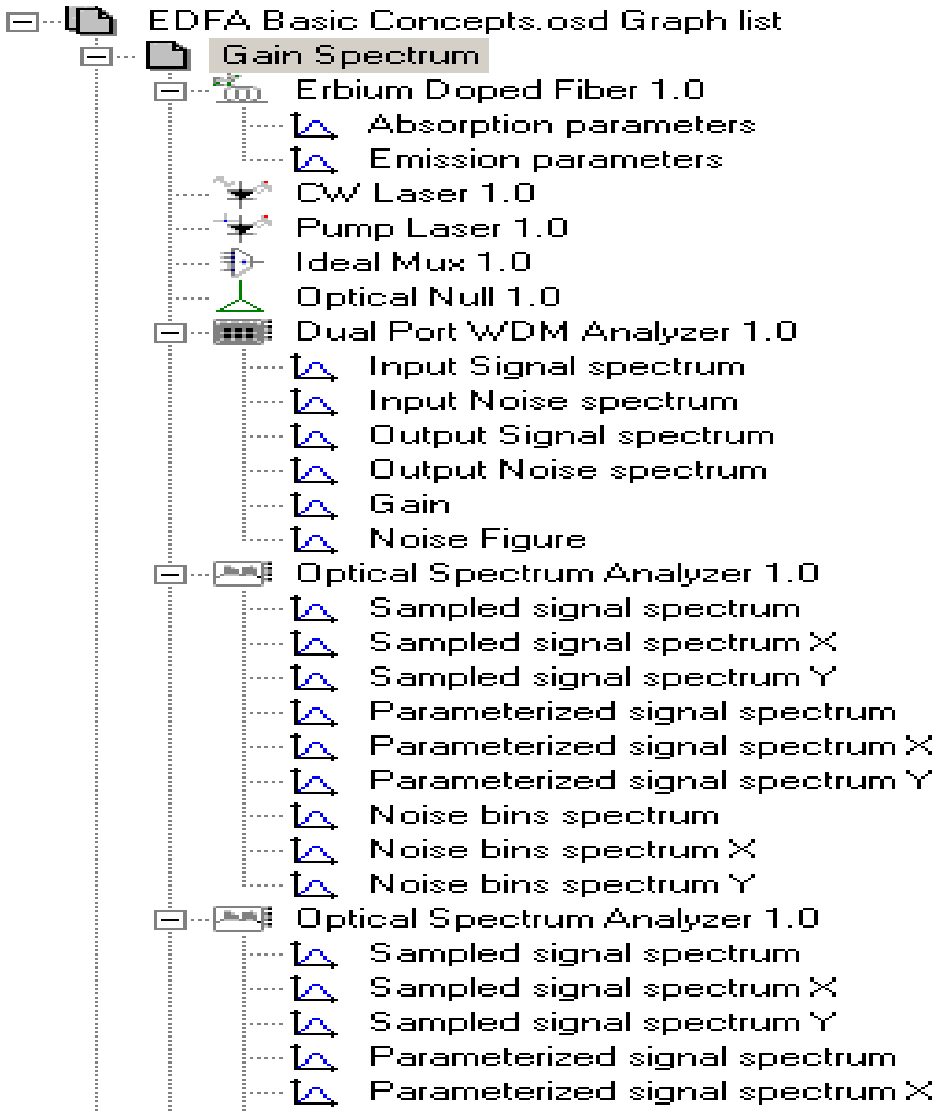

Fig. 3: List with additional graphs showing calculated results that are available on Graphs

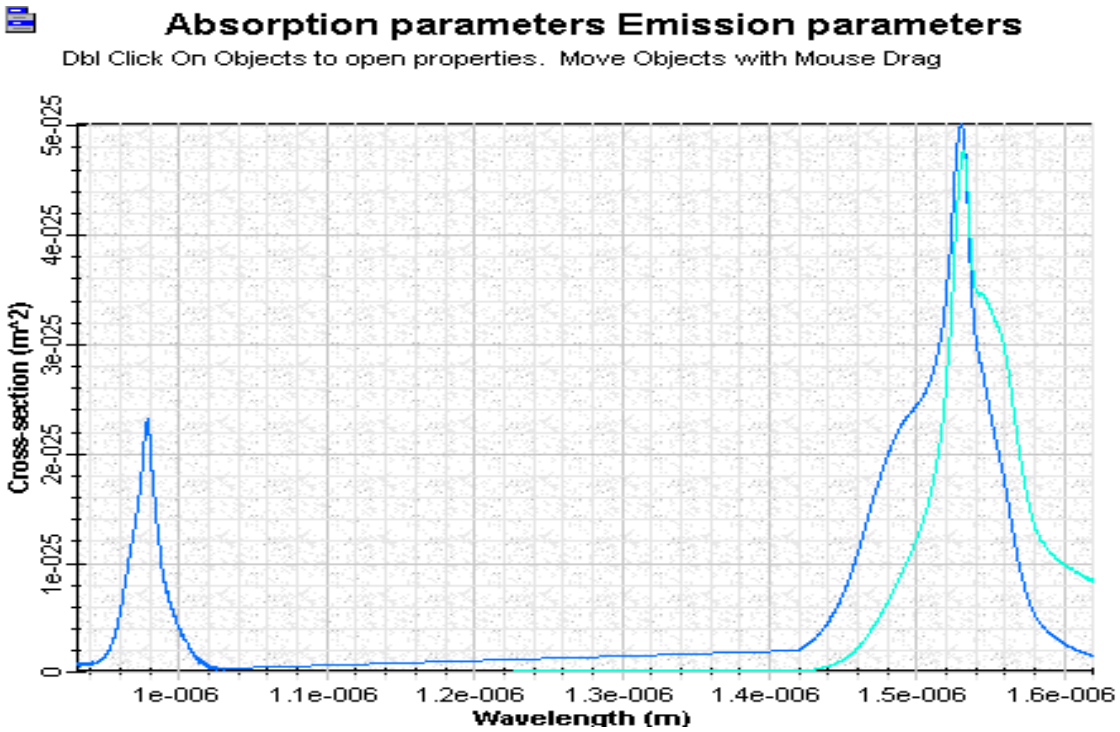

Fig. 4: Cross-section file displayed in the Erbium doped fiber component graphs

Erbium Doped Fiber 1.0 Properties

Label: Erbium Doped Fiber 1.0 Cost$: 0.00 OK Cancel Verify Scripts

Main | Cross-sections | Numerical | Simulation | Noise | Random numbers

Disp	Name	Value	Units	Mode
☐	Core radius	2.2	um	Normal
☐	Er doping radius	2.2	um	Normal
☐	Er metastable lifetime	10	ms	Normal
☐	Numerical aperture	0.24		Normal
☐	Er ion density	1e+025	m^-3	Normal
☐	Loss at 1550 nm	0.1	dB/cm	Normal
☐	Loss at 980 nm	0.15	dB/cm	Normal
☑	Length	10	m	Normal

Table 1: Er doped fiber specifications

The basic layout used in the calculations for each version is shown in Fig. 5.

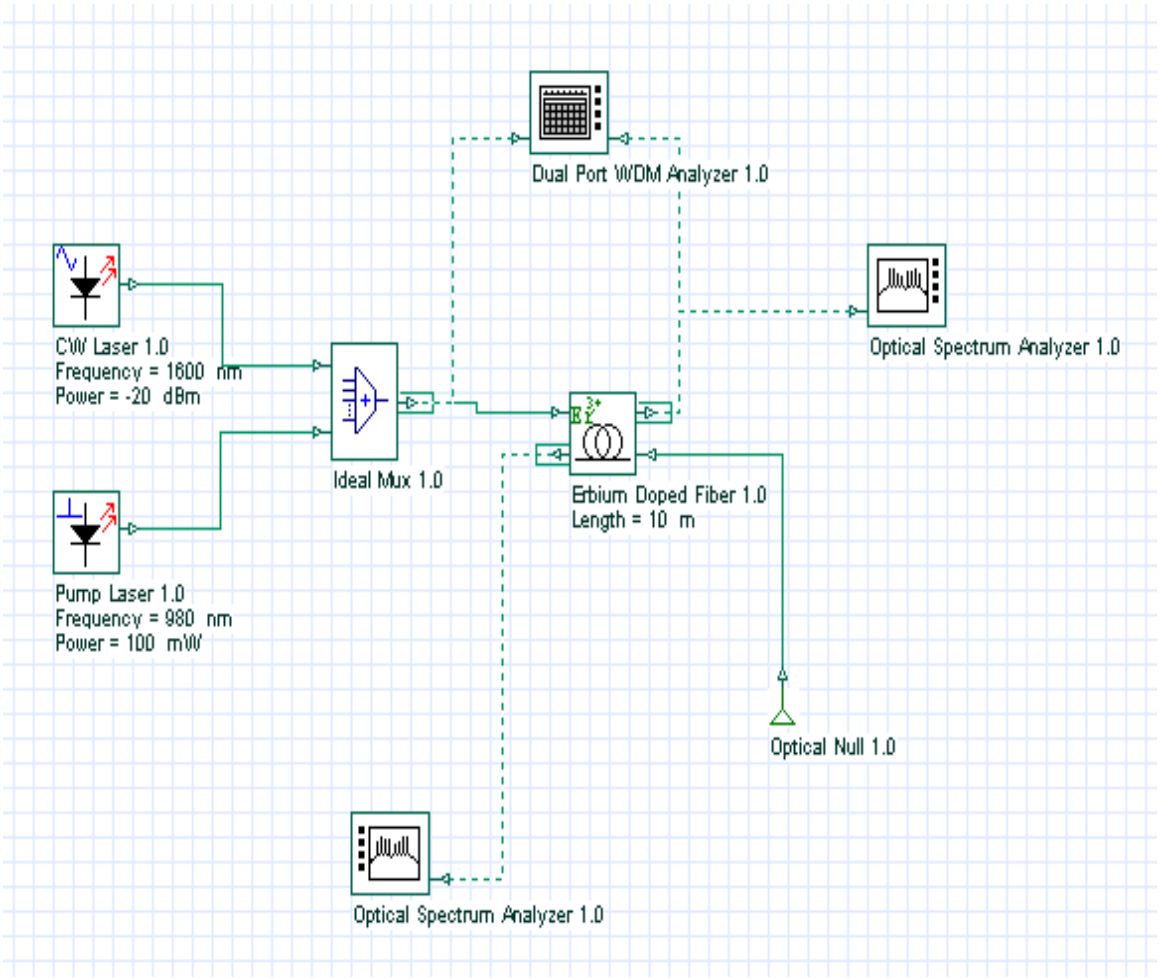

Fig. 5: Layout: EDFA basic concepts

Version Gain Spectrum

In this first version named Gain Spectrum the signal wavelength of the CW laser signal is swept from 1525 nm to 1600 nm which enables evaluating the spectral gain and the bandwidth of the amplifier.

The spectral gain calculated for -20 dBm of input signal power is shown in Fig. 6.

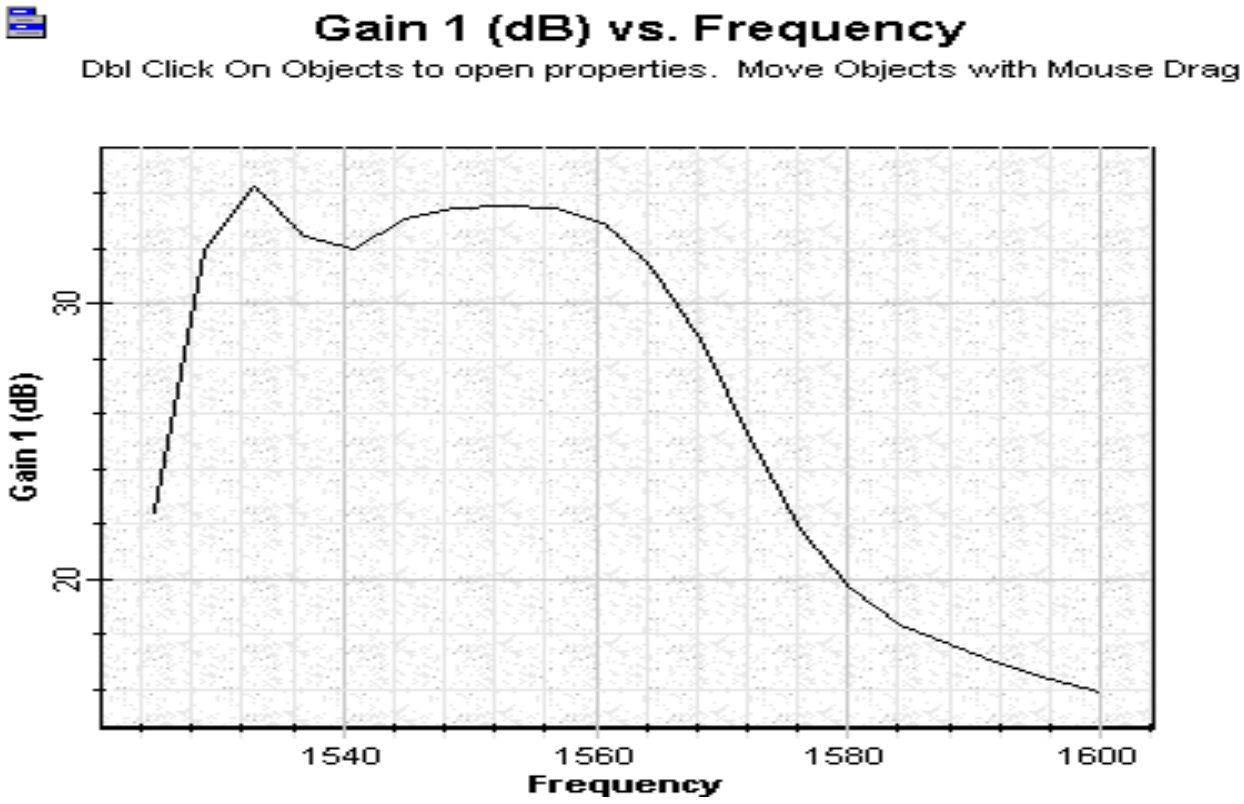

Fig. 6: Gain versus signal wavelength given in [nm] unit considering signal input power equal to - 20 dBm

An additional graph that can be checked in the Gain Spectrum version is the output power versus signal wavelength as shown in Fig. 7.

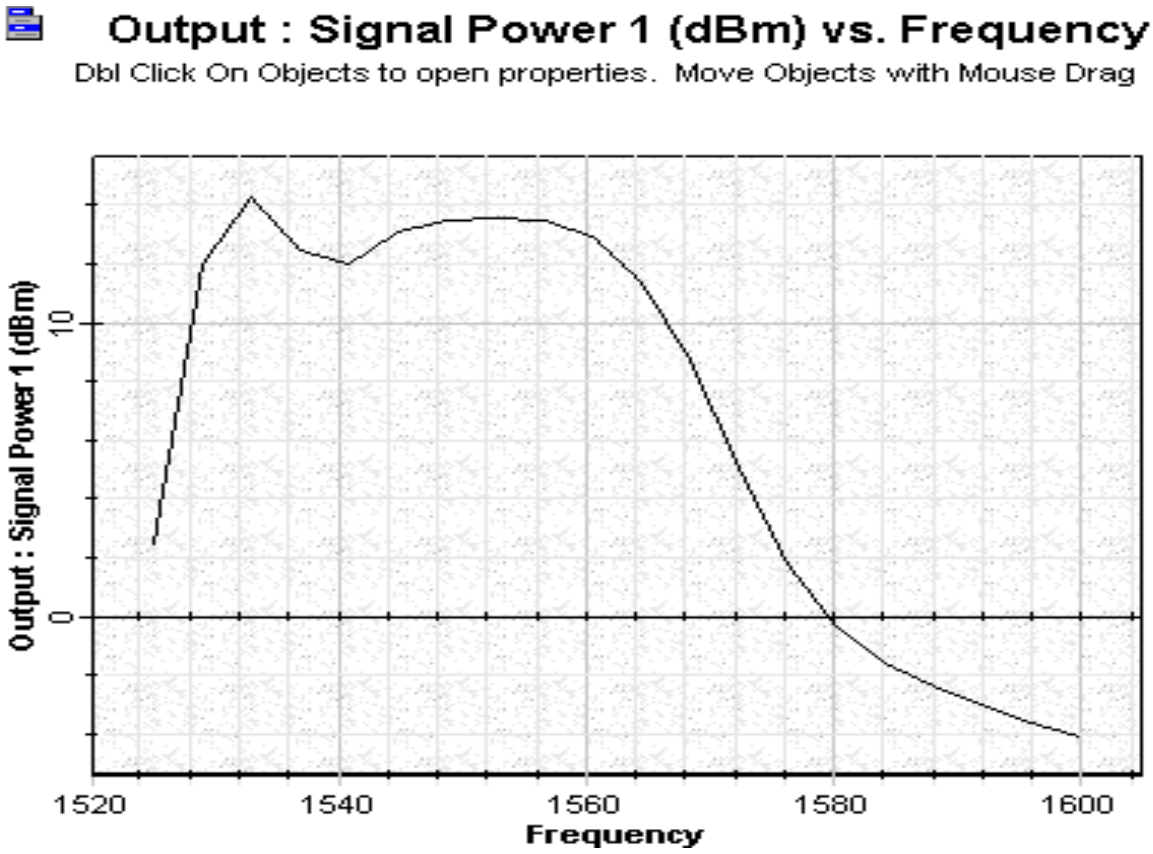

Fig. 7: Signal output power versus signal wavelength given in [nm] unit calculated to a signal input power equal to - 20 dBm

Version Gain Saturation

The version Gain Saturation enables evaluating the amplifier performance as a function of the signal input power. The signal input power is swept from small signal to large signal regime, i.e. - 40 dBm to 0 dBm. The amplifier performance in terms of gain, output power and noise figure are shown in Fig. 8, Fig. 9 and Fig. 10, respectively.

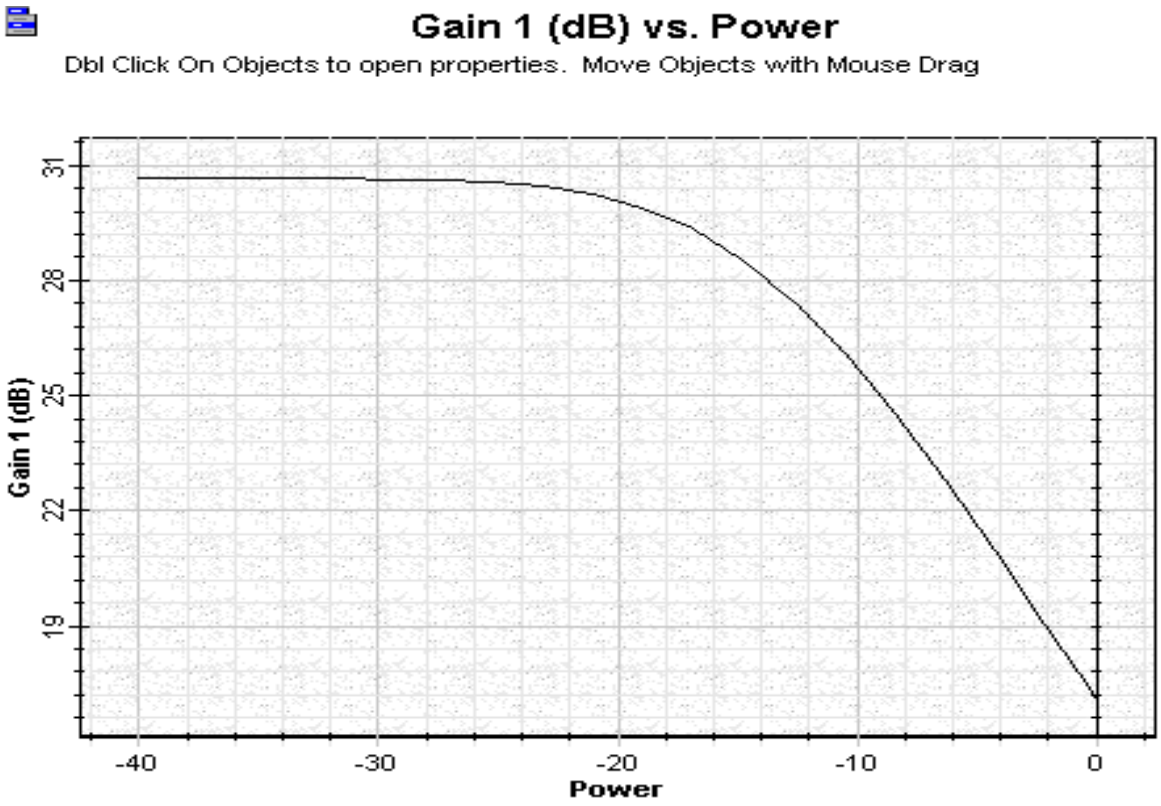

Fig. 8: Gain versus signal input power

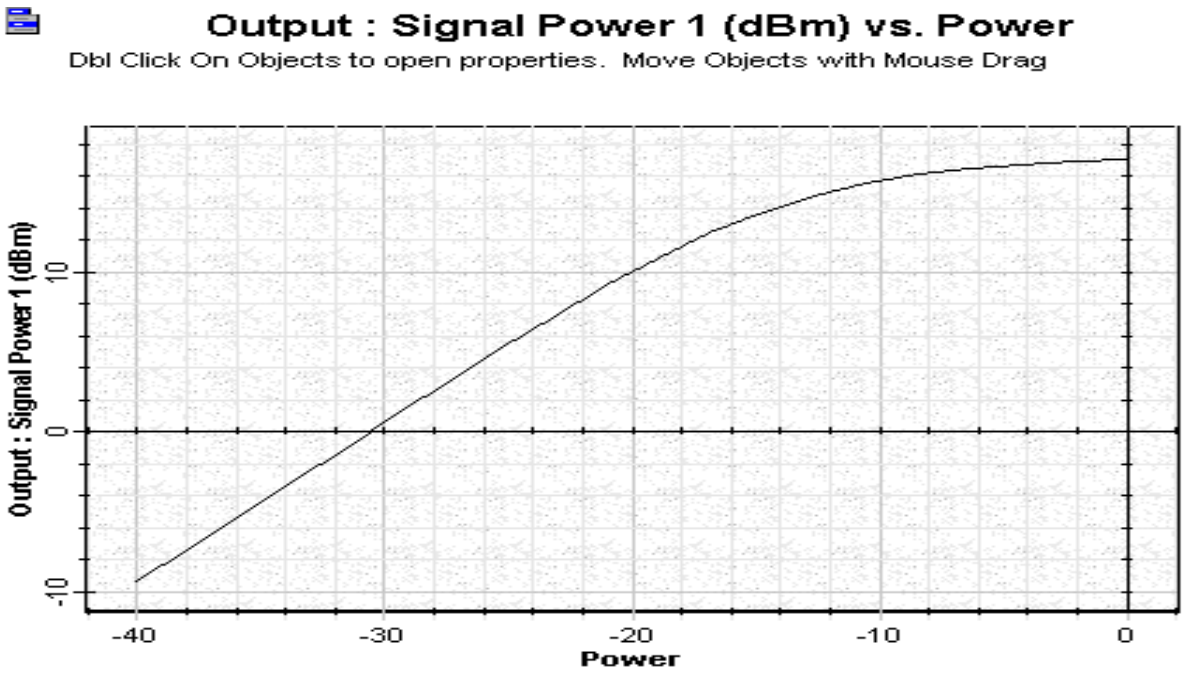

Fig. 9: Amplified signal versus signal input power

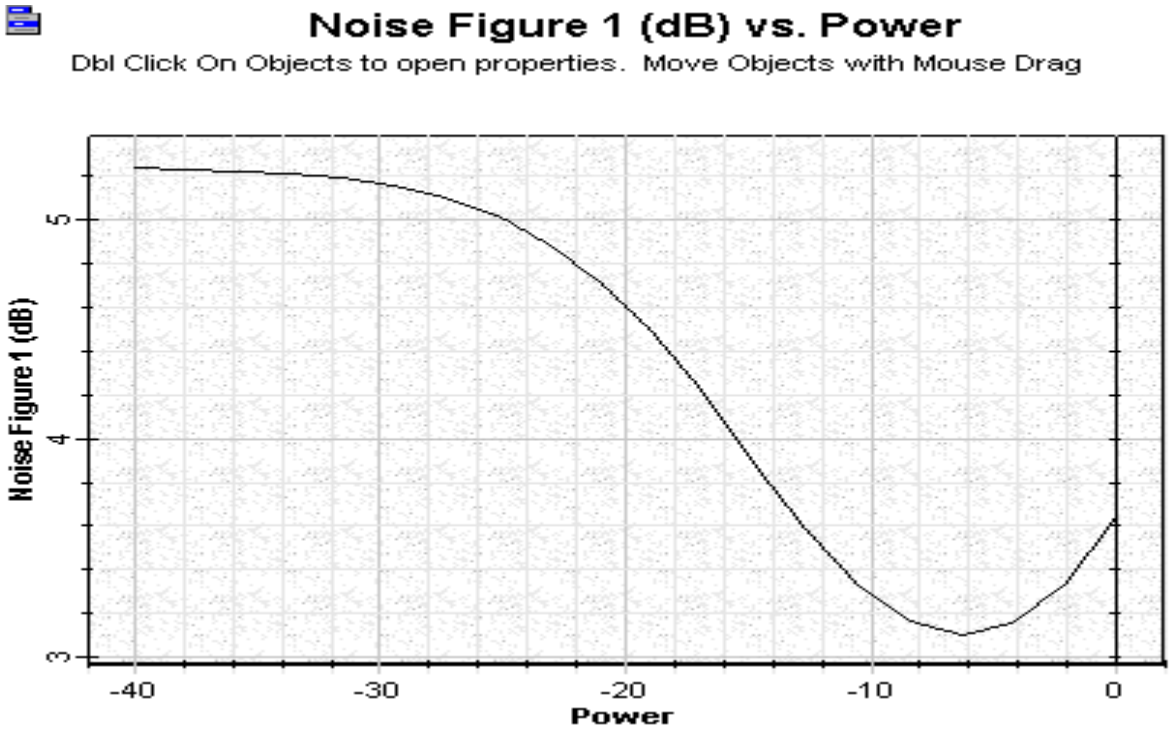

Fig. 10: Noise figure versus signal input power

Version Amplifier Noise

The signal wavelength is the parameter swept in this version, which enables calculating the spectral noise of the amplifier. The noise figure versus signal wavelength grouped in the Splitter View is shown in Fig. 11. Signal and pump wavelength as well as the fiber parameters can be changed for further evaluation of the amplifier performance.

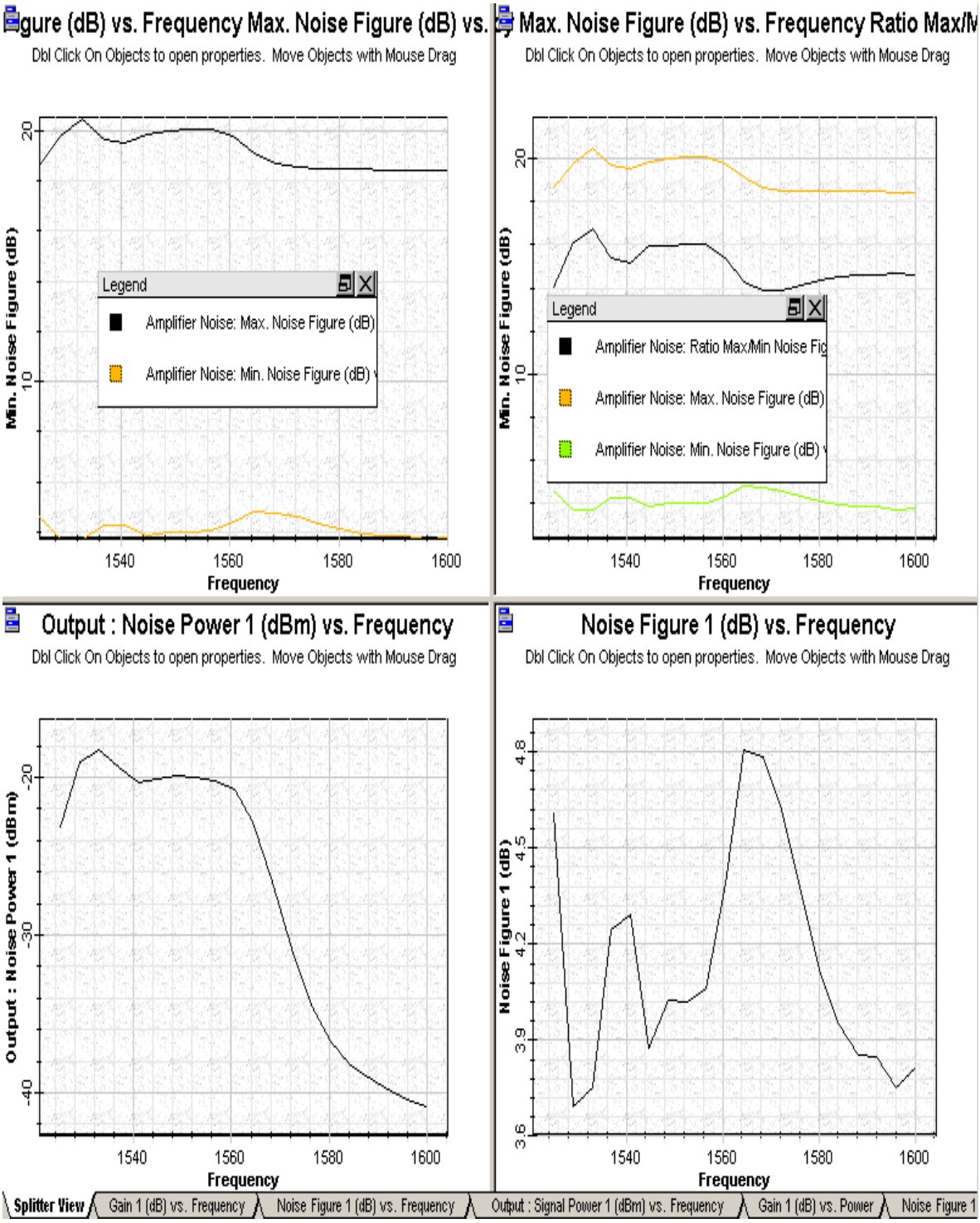

Fig. 11: Amplifier noise characterization presented in splitter view

Fig. 12 shows the ASE spectrum stored after calculating each iteration of the signal wavelength.

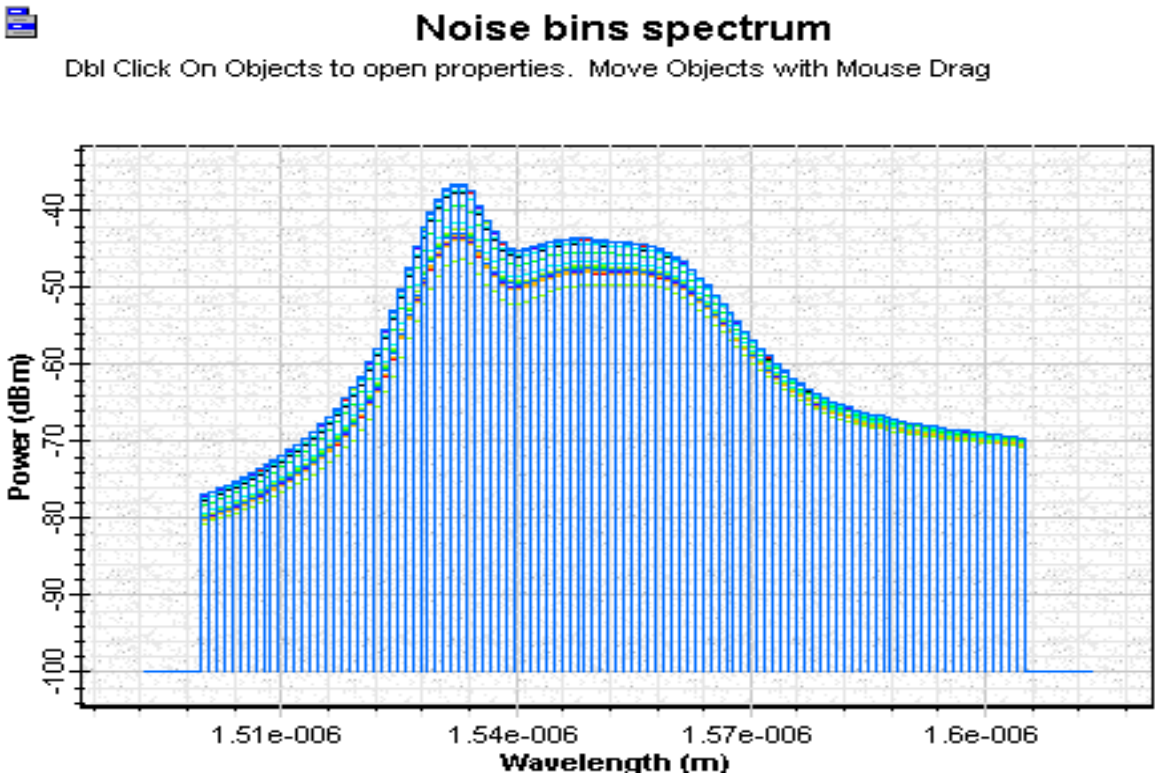

Fig. 12: Noise bins as a function wavelength used in the calculations. Each curve in this graph resulted from the different iterations

Example: Booster Amplifier

Booster amplifier**.osd**

The project file "Booster amplifier**.osd**" shows the characterization of a booster/power amplifier setup in a single heavily doped erbium-doped fiber, bidirectionally pumped by two 980 nm-pump lasers. In this case, large signal input power is considered because large signal input power contributes to obtain high output power, which is a requirement to booster/power amplifiers. As a consequence, moderate gain will be observed in this case. The low noise figure requirement to EDFAs is not so tight here, where an increase in NF can be tolerated. It is important to mention that typical configurations of booster amplifiers include multiple Er-doped fiber stages.

Fig. 13 shows the layout of the booster amplifier. Bidirectional pump was used to produce the typical pump scheme observed in booster amplifiers. The optical spectrum analyzer connected at the output port 1 shows the amplified signal

obtained after running this project file. The component dual port WDM analyzer gives the calculated results performed to all the propagating signals and pump.

The output power, gain and noise figures calculated as a function of signal input power are shown in **Figs. 14,15 and 16**, respectively. It is possible to observe the gain being compressed as a function of the increasing signal input as shown in **Fig. 15**.

The noise figure curve is calculated by sweeping the signal input power to the booster amplifier assuming identical input parameters. There is a region in the curve where NF is minimized as a function of the signal input.

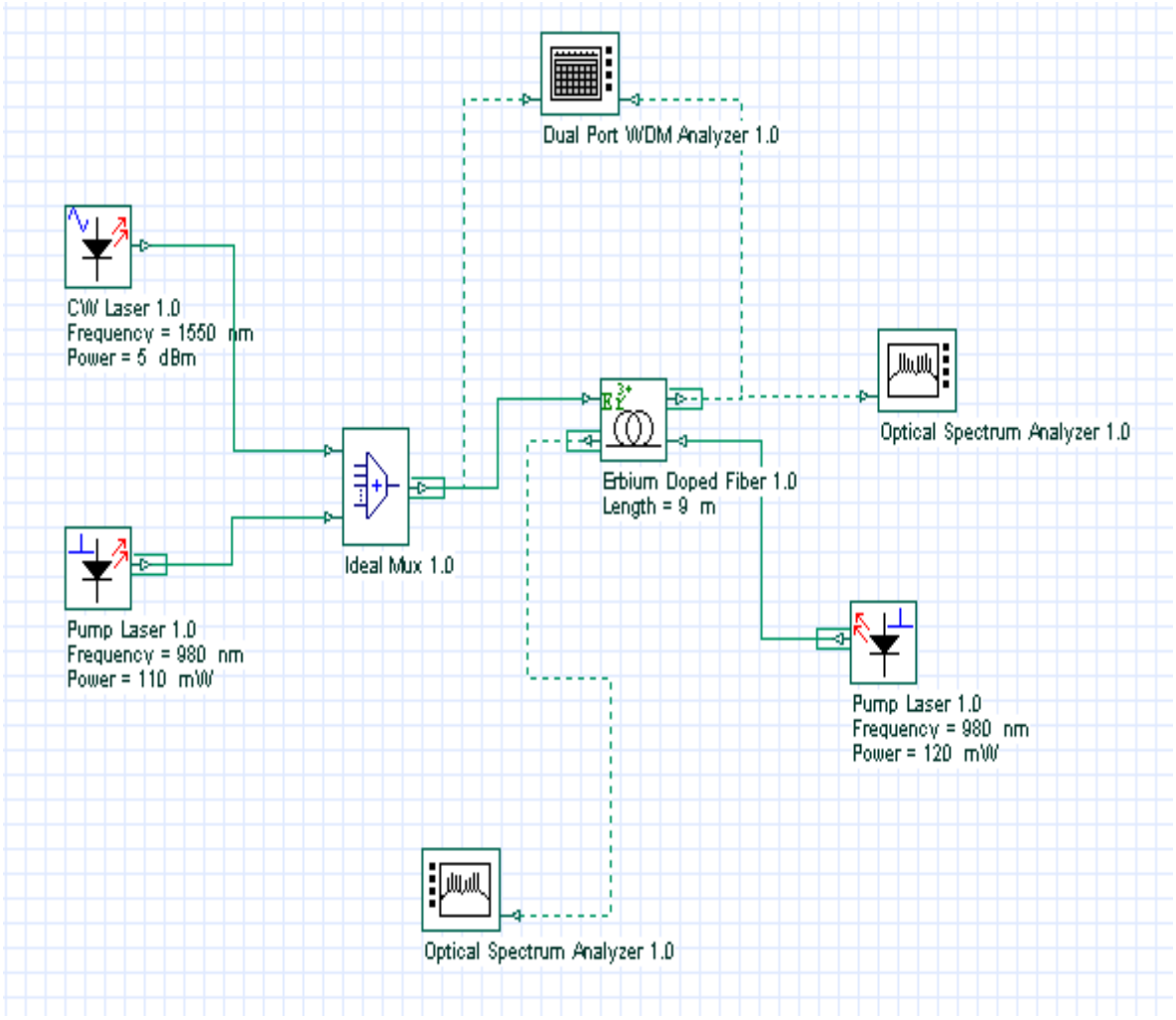

Fig. 13: Layout: Booster amplifier

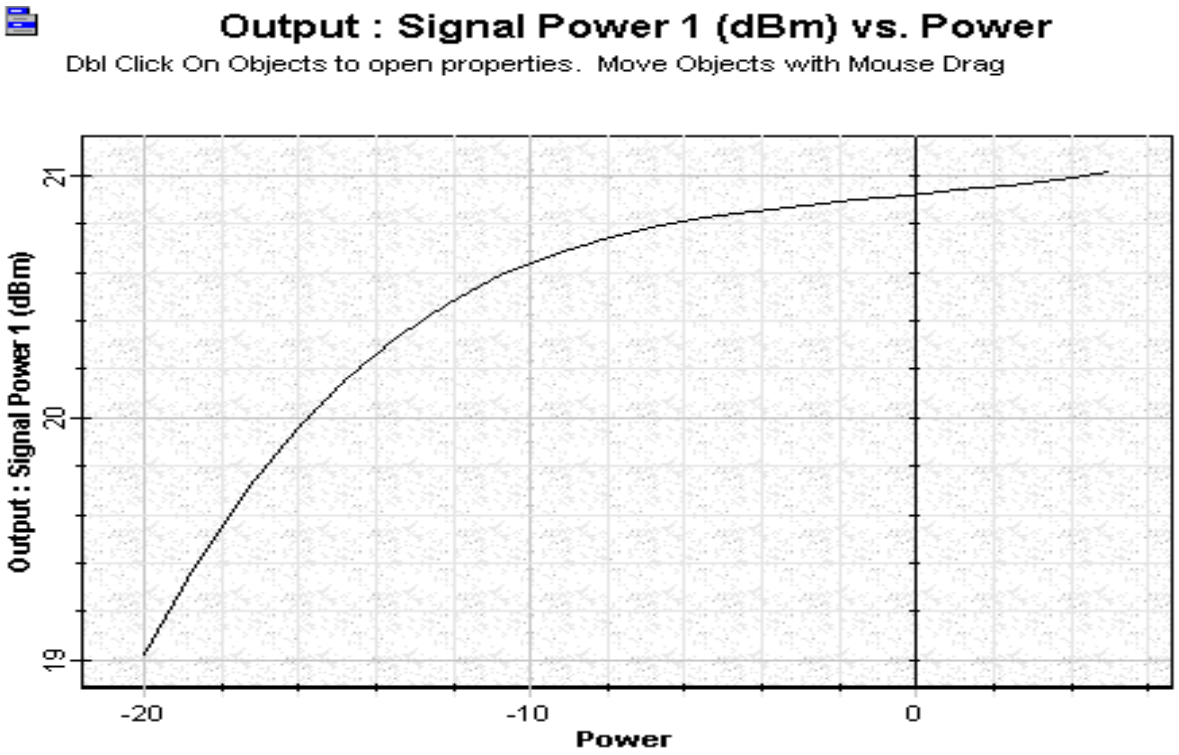

Fig. 14: Signal output power versus signal input power calculated for the booster amplifier

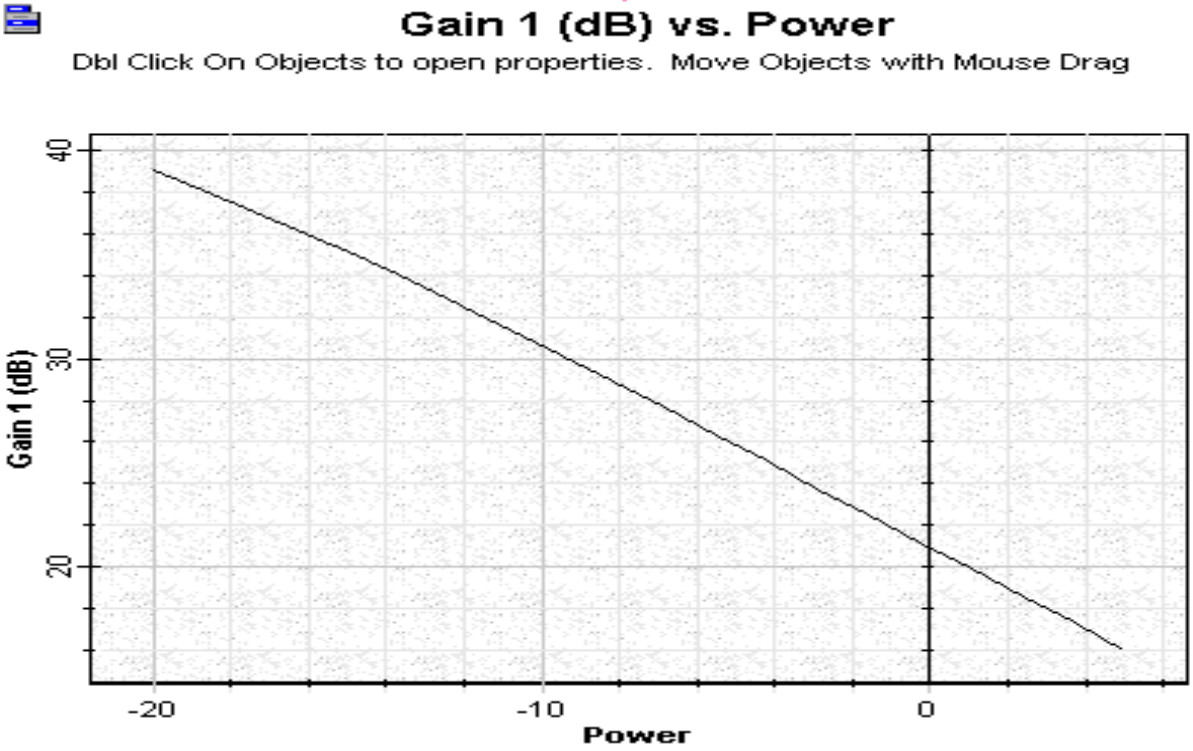

Fig. 15: Gain versus signal input power calculated for the booster amplifier

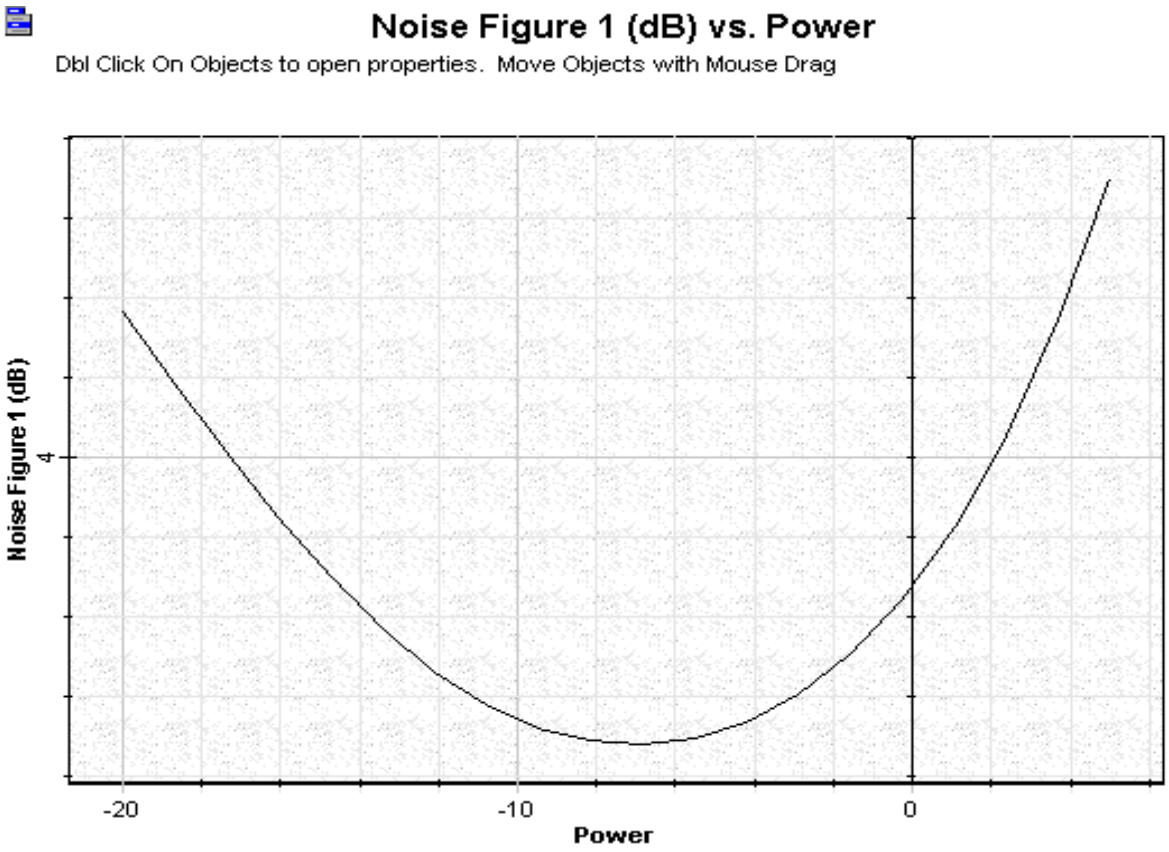

Fig. 16: Noise figure versus signal input power calculated for the booster amplifier

The power of both pump lasers, co- and counter-propagating as well as the Er-doped fiber length can be modified. Fiber specifications can also be modified and the results can be compared with the previous case.

Example: In-Line Amplifier

In-line amplifier**.osd**

The project file "In-line amplifier**.osd**" shows the characterization of an in-line amplifier setup in a single erbium-doped fiber stage, pumped by one 980 nm-pump laser.

In this case, small signal input power is considered to obtain high gain and small noise figure values. The signal input power is swept from - 40 dBm to -20 dBm

that enables checking the gain, noise figure, output power and OSNR as a function of signal input power.

After sweeping iterations over the signal input power, the amplifier performance can be checked in the graphs displayed on View, as shown in Fig. 17.

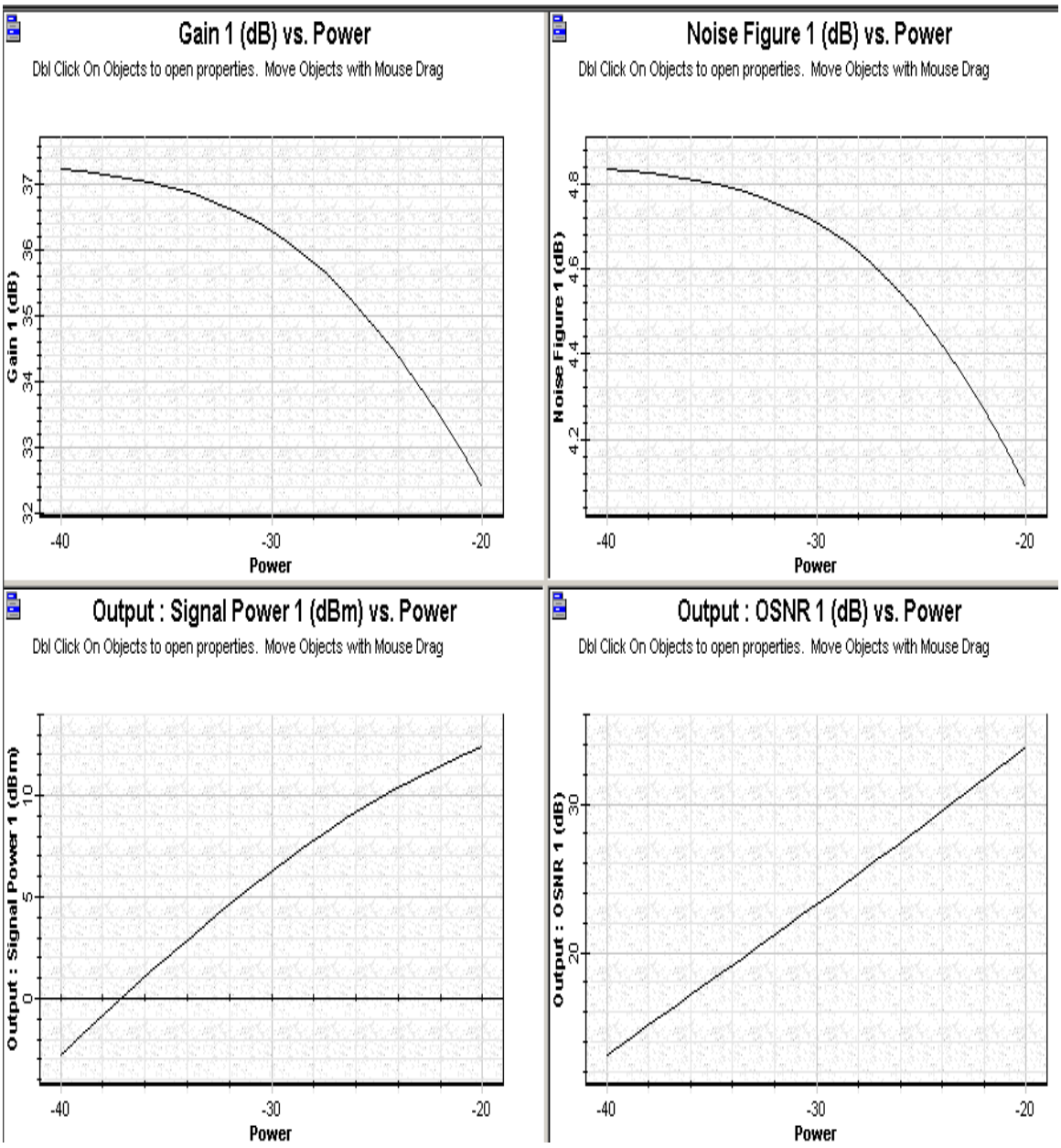

Fig. 17: Graphs presenting the inline amplifier performance setup in a co-propagating pump scheme

Two different pump schemes that consider co- and counter-propagating pump are available in “Co-pump power” and “Counter-pump power” versions for which layouts are shown in Fig. 18 and Fig. 19, respectively. The performance of the inline amplifier related to the co- and counter-propagating pump schemes can be seen in the graphs of gain, noise figure and output power displayed in “Views”.

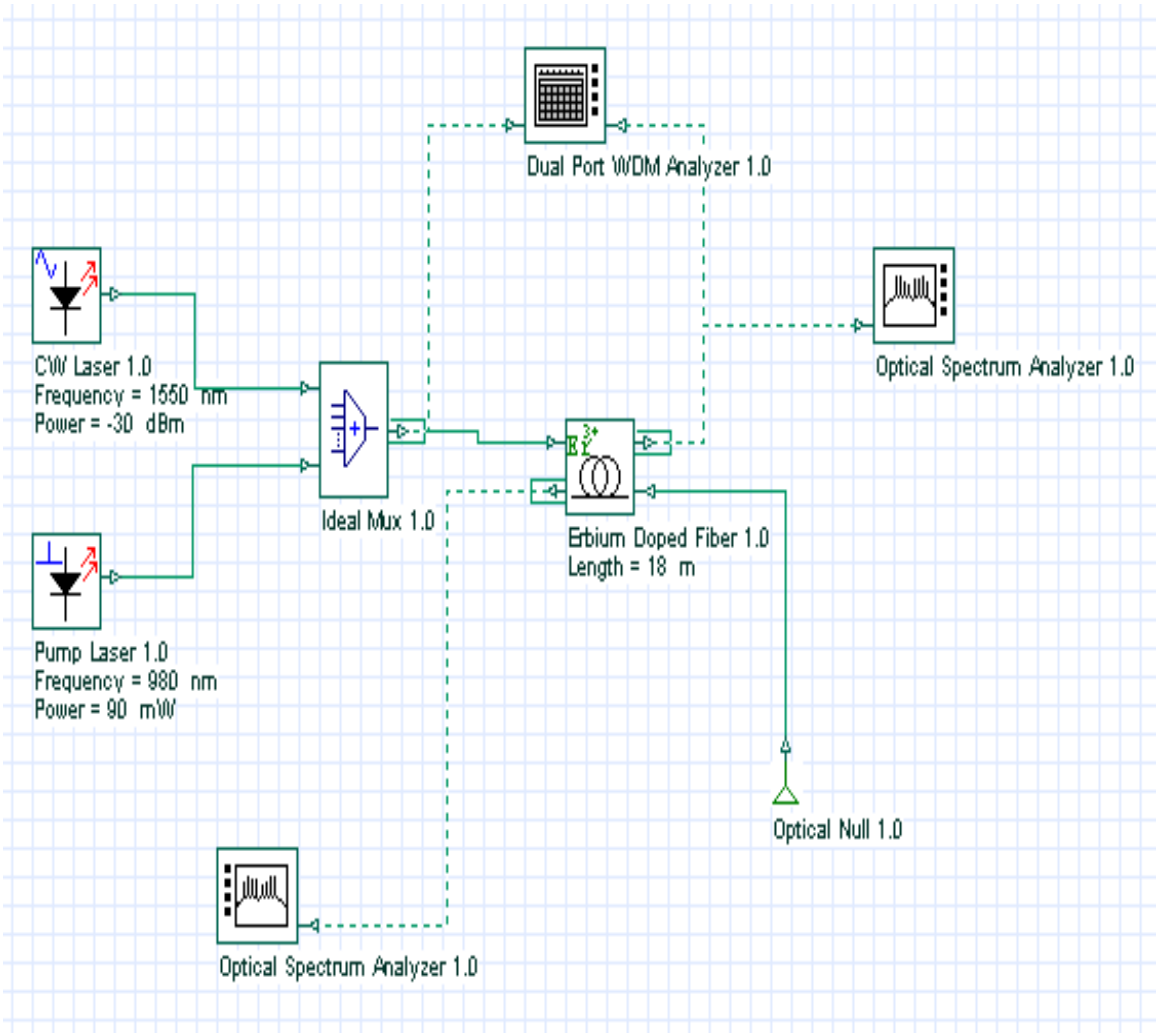

Fig. 18: Layout: In-line amplifier: Co-propagating pump scheme

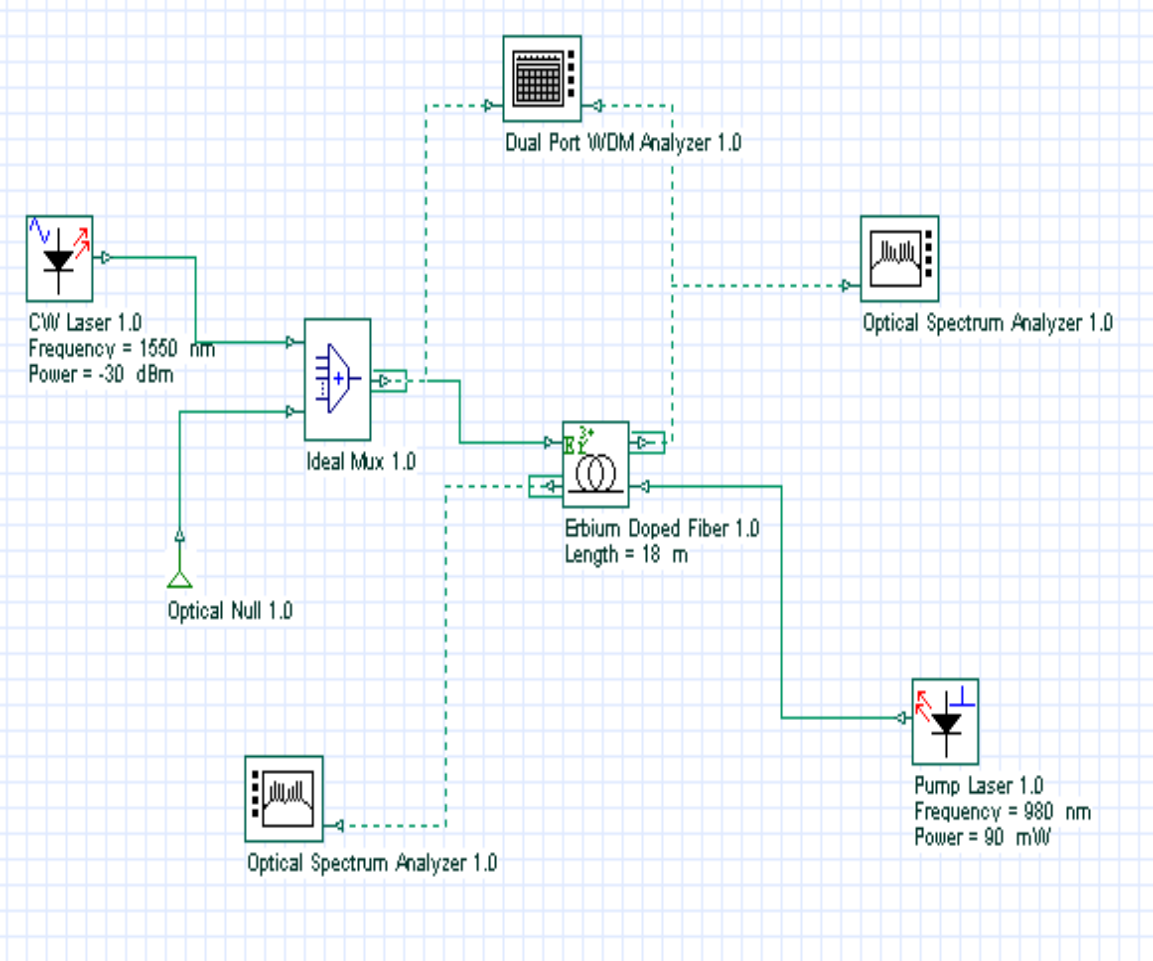

Fig. 19: Layout: In-line amplifier: Counter-propagating pump scheme

The amplifier performance in case of co- and counter-propagating pump schemes can be compared through graphs available on Views. Pump wavelength equal to 980 nm was considered in both cases. The gain versus pump power is shown in **Fig. 20** considering the co- and counter-pump schemes that enable evaluating the most efficient pump scheme to the EDFAs.

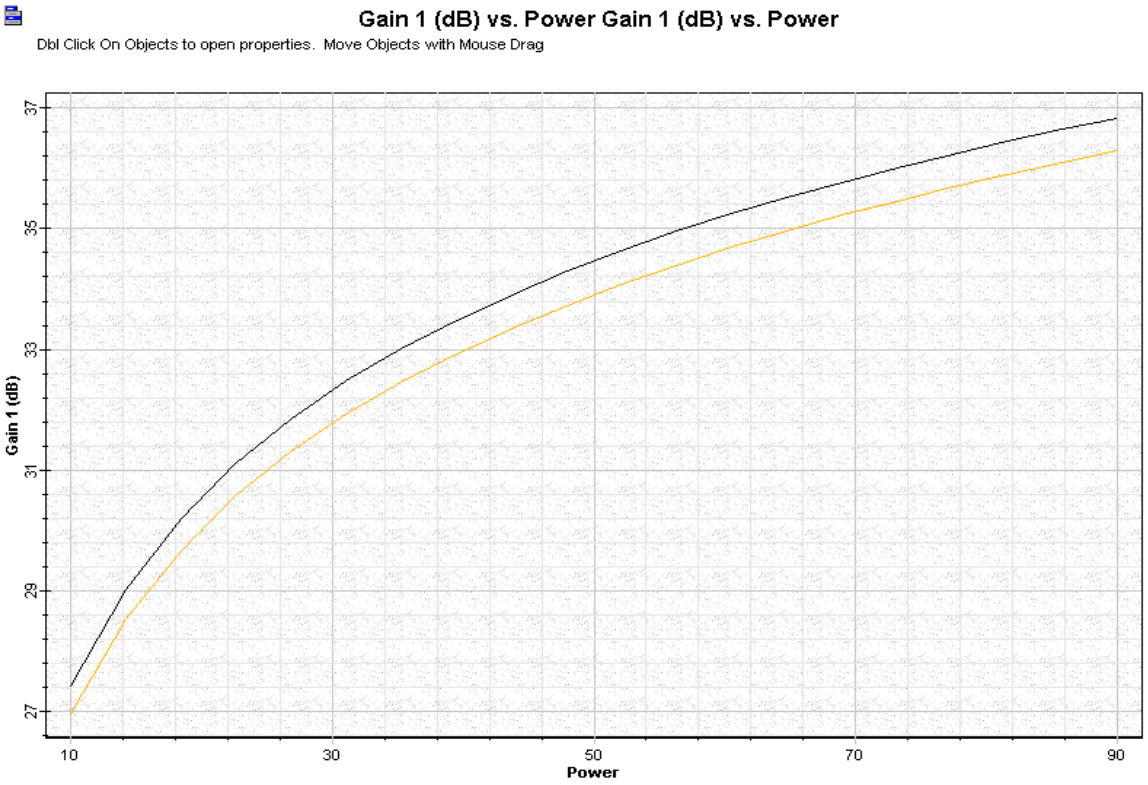

Fig. 20: Comparing gain performance of an EDFA setup in a co- and counter-propagating pump scheme

The wavelength pump power equal to 980 nm considered in the three different version included in this project file can be substituted by 1480 nm. Different pump power, signal wavelength, and fiber parameters can be considered to perform additional simulations.

Example: Preamplifier

Preamplifier**.osd**

The project file "Preamplifier**.osd**" shows the characterization of an in-line amplifier setup in a single erbium-doped fiber stage, pumped by one 980 nm-pump laser in a co-pump scheme.

In this case, small signal input power is considered to obtain high gain and small noise figure values. The erbium doped fiber length is swept from 6 m to 15 m that enables checking the gain, noise figure, output power and OSNR as a function of

fiber length. The pump wavelength considered in versions “Pump 980 nm” and “Pump 1480 nm” is 980 nm and 1480 nm, respectively.

In the two different versions, “Pump 980 nm” and “Pump 1480 nm”, signal input power is -35 dBm at 1550 nm, respectively. The performance of the preamplifier for the pump wavelength can be seen in the graphs of gain, noise figure and output power displayed in “Views”.

The basic layout used in this preamplifier example is shown in Fig. 21, where just the pump wavelength is changed from 980 nm to 1480 nm in the component Pump Laser 1.0.

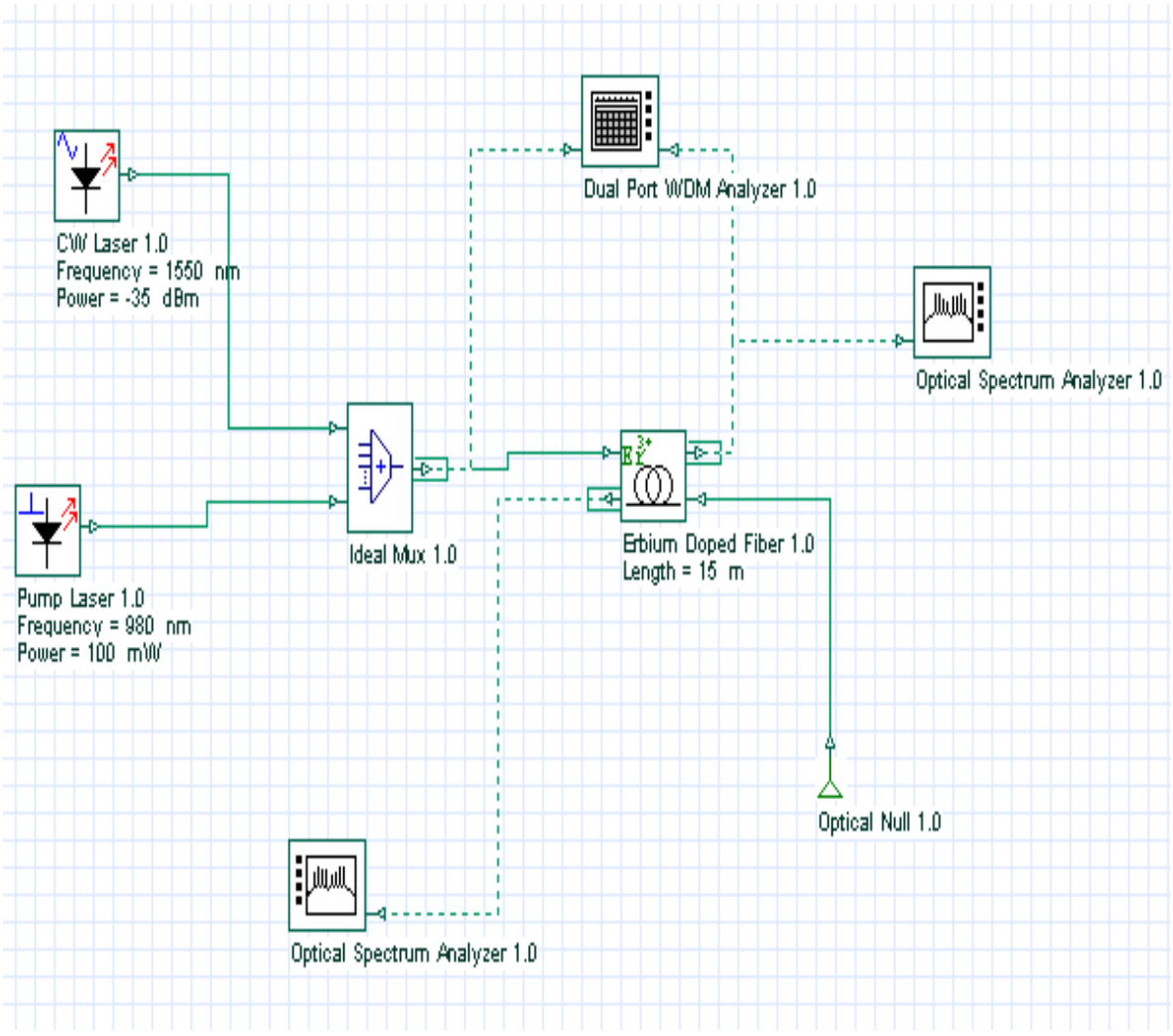

Fig. 21: Layout: Preamplifier

The gain for the preamplifier is shown in Fig. 22. Different pump power, signal wavelength, and fiber parameters can be considered to perform additional simulations.

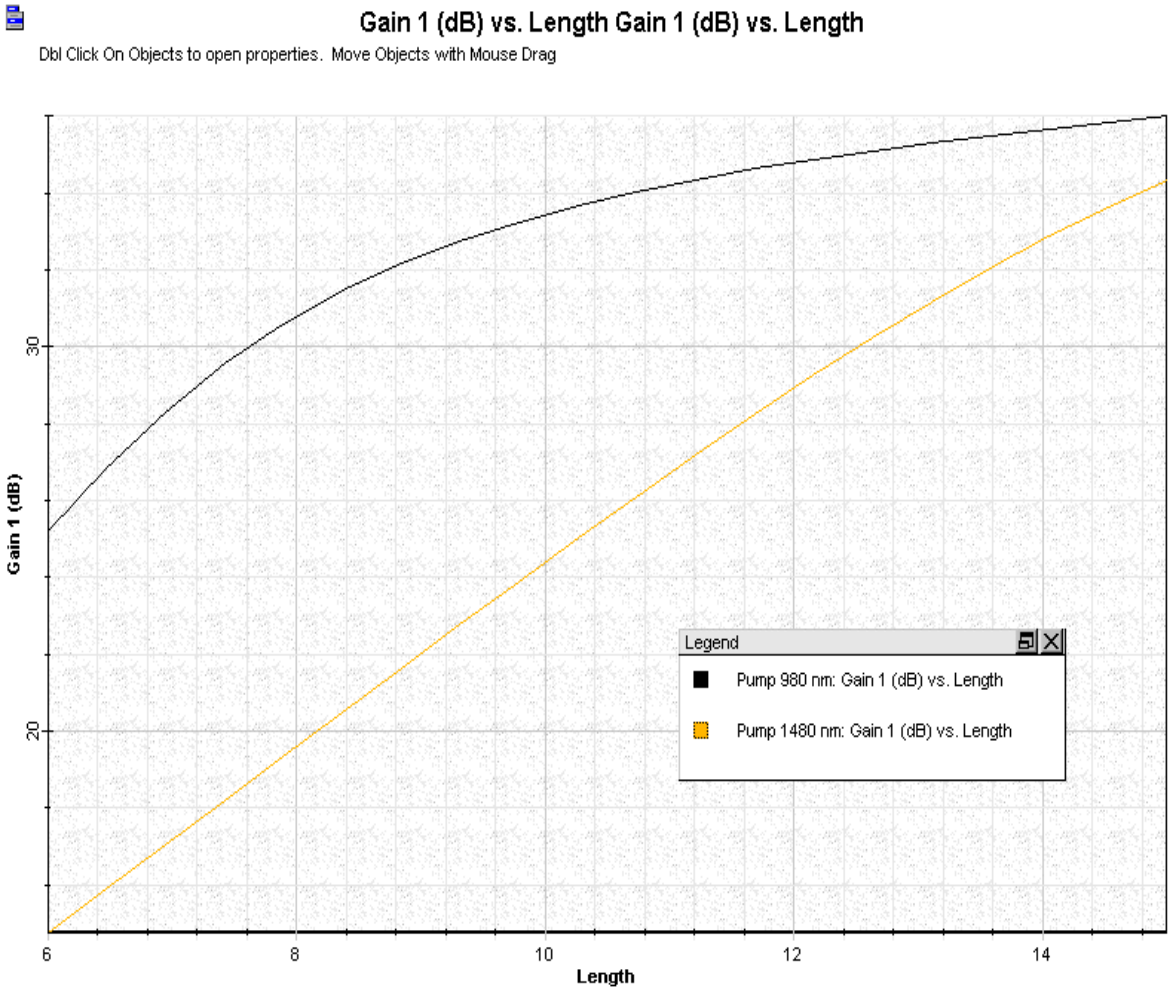

Fig. 22: Gain versus erbium doped fiber length considering 980 nm and 1480 nm as pump wavelength

Example: Semiconductor Laser Amplifiers Cascaded in-line Amplifiers: Soliton Pattern Effect at 10 Gb/s in SMF

SLA cascaded in-line amplifiers soliton pattern effect 10 Gb/s in SMF**.osd**

One of the possibilities to upgrade existing network of already installed standard single mode optical fibers operating at 1.3 μm is the use of SOA, where the zero dispersion of these fibers exists. The advantages of using SOA are the low dispersion of the SMF at this carrier wavelength and attractive features of semiconductor optical amplifiers. However, there are two major negative factors in the utilization of SOA as in-line optical amplifiers: (a) gain-saturation effects, which lead to non-equal amplification of pulses in the pattern (so called pattern effect) and (b) the chirp that pulse acquires after amplification.

The aim of this project is to demonstrate the pattern effect at 10 Gb/s transmission over a 500 km optical link consisting of SMF and in-line SOA's [1]. We consider the parameters similar to those in [1].

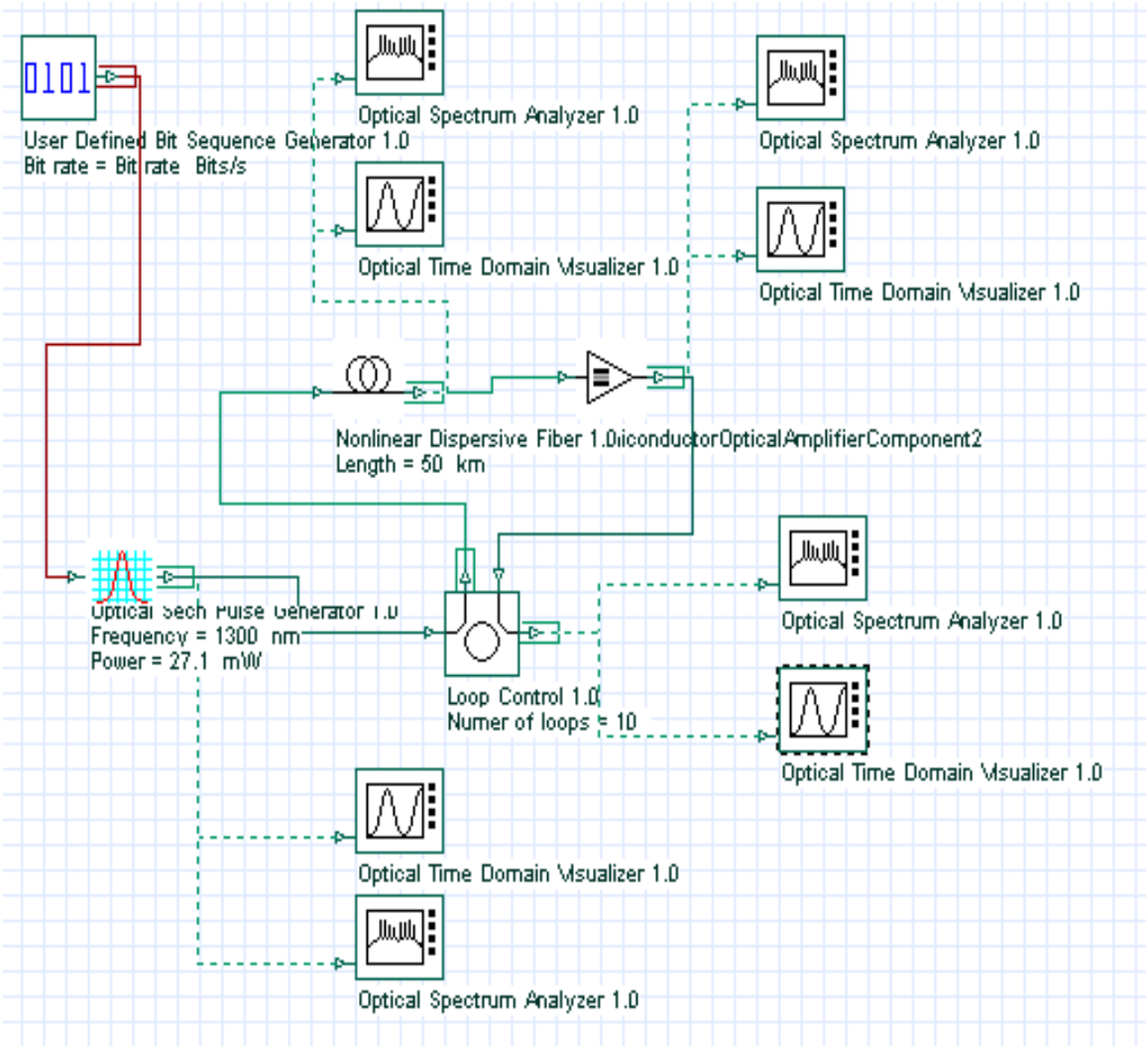

Fig.23: Layout: SLA cascaded in-line amplifiers: Soliton pattern effect at 10 Gb/s in SMF

Table 2 and Table 3 show the global and pulse parameters to get transmission at 10 Gb/s.

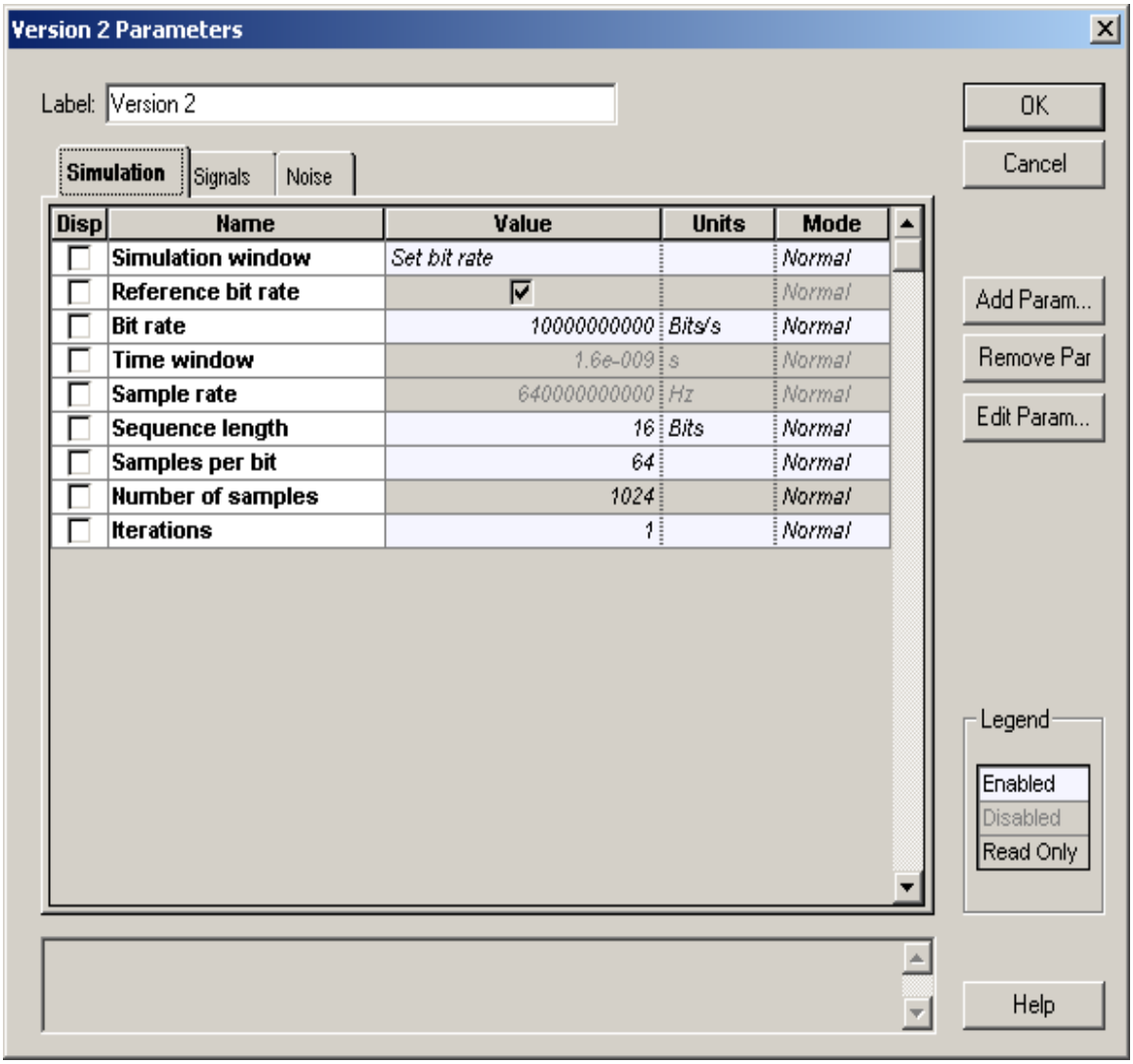

Disp	Name	Value	Units	Mode
☐	Simulation window	Set bit rate		Normal
☐	Reference bit rate	☑		Normal
☐	Bit rate	10000000000	Bits/s	Normal
☐	Time window	1.6e-009	s	Normal
☐	Sample rate	640000000000	Hz	Normal
☐	Sequence length	16	Bits	Normal
☐	Samples per bit	64		Normal
☐	Number of samples	1024		Normal
☐	Iterations	1		Normal

Table 2: Global parameters

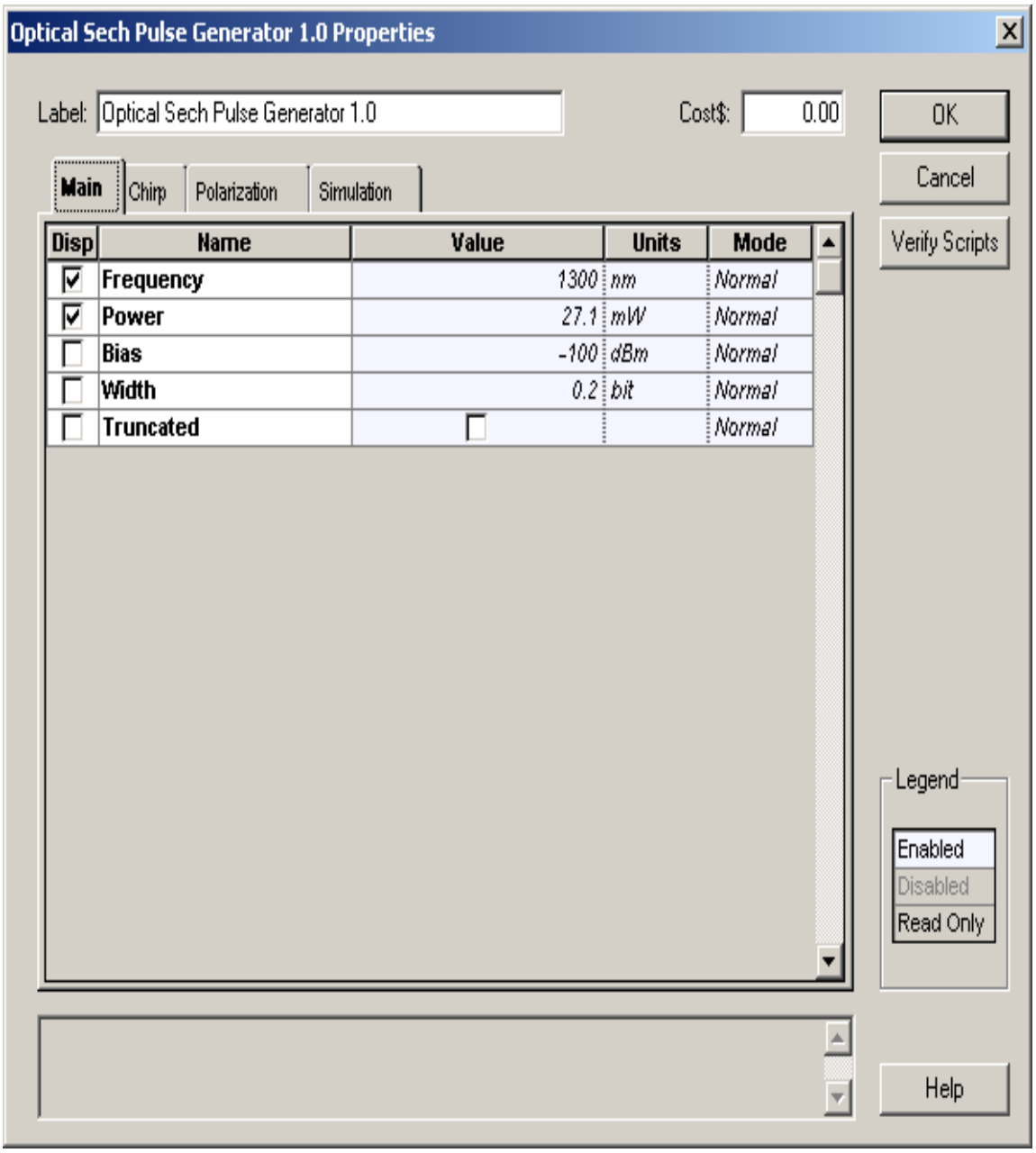

Table 3: Optical Sech pulse generator parameters (main)

We fix B= 10 Gb/s $\Rightarrow$ T_B = 100 ps. The sequence length is 16 bit. The carrier wavelength of the pulse is λ ~1300 nm. The T_{FWHM} = 20 ps $\Rightarrow$ $T_0 = 0.567\ T_{FWHM}$ ~ 11.34 ps. The input peak power is 21.7 mW. Let us now fix fiber parameters **(Table 4 and Table 5).**

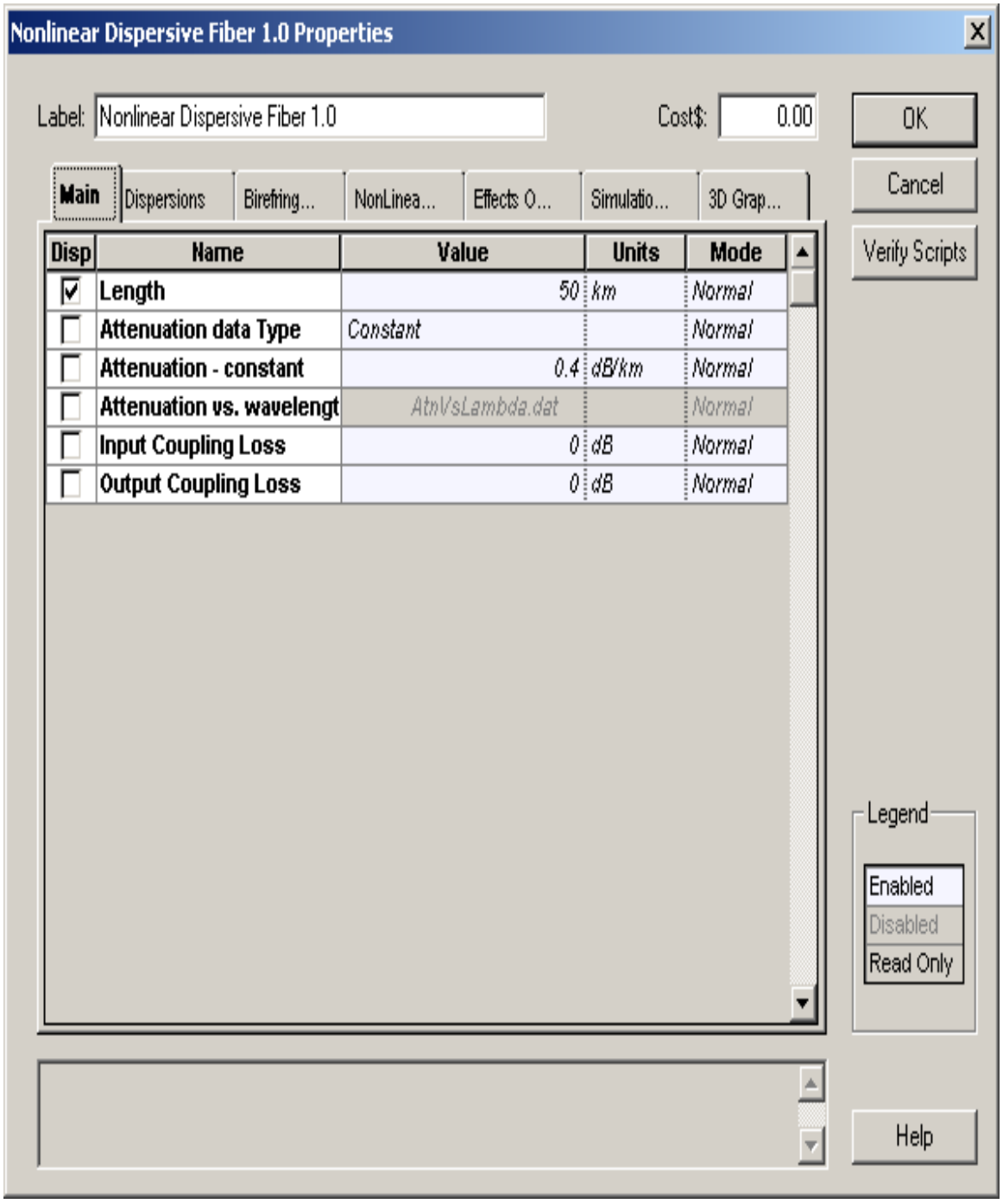

Table 4: Fiber parameters (main)

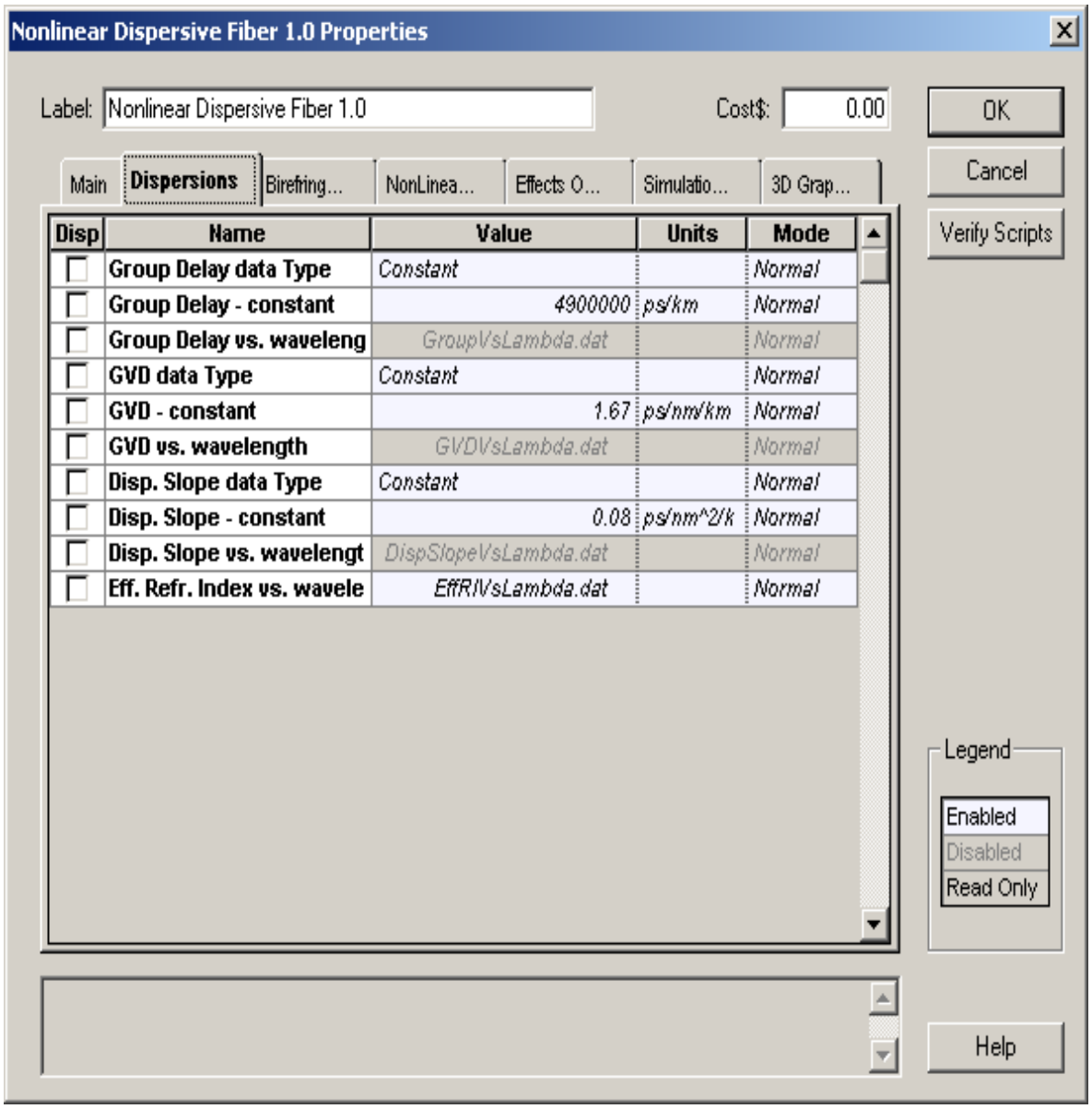

Table 5: Fiber parameters (dispersion)

We will consider SMF with length 50 km and losses 0.4 dB/km. The parameter k_2 (= - $\lambda^2 D/(2\pi c)$) ~ -1.5 (ps^2/km) $\Rightarrow$ D ~1.67 (ps/nm.km)$\Rightarrow$ L_D (= $T_0^2/|k_2|$) ~ 85 km. (The effects of group delay and third order dispersion are not taken into account). After each fiber the signal will be amplified with SOA, therefore L_A ~ 50 km. Note that the condition $L_A < L_D$ is satisfied.

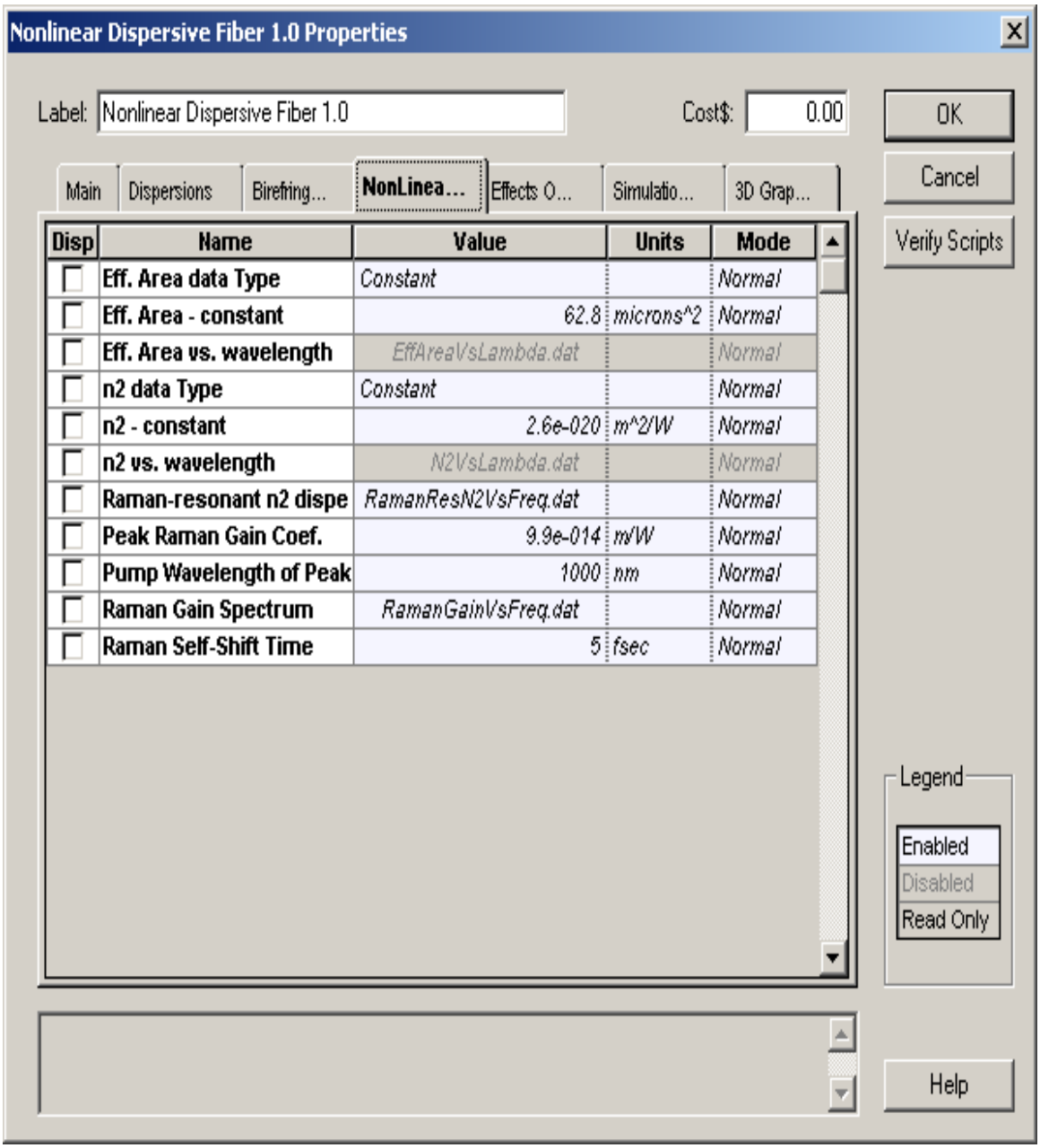

Table 6: Fiber parameters (nonlinear)

The Kerr nonlinearity coefficient γ is equal to $n_2\ \omega_0 / c\ A_{eff.}$ For the fixed values of nonlinear refractive index $n_2 = 2.6\ 10^{-20}$ [m^2/W], $\omega_0 / c = 2\ \pi / \lambda = 2\ \pi /1.3\ 10^{-6}$ [m^{-1}], $A_{eff} = 62.8$ [μm^2], γ will be equal to 2 [1/km.W] **(Table 6).**

The linear loss for 50 km SMF is 20 dB. This requires an unsaturated single pass gain from SOA. To get such gain following parameters have been used **(Table 7 and Table 8)**.

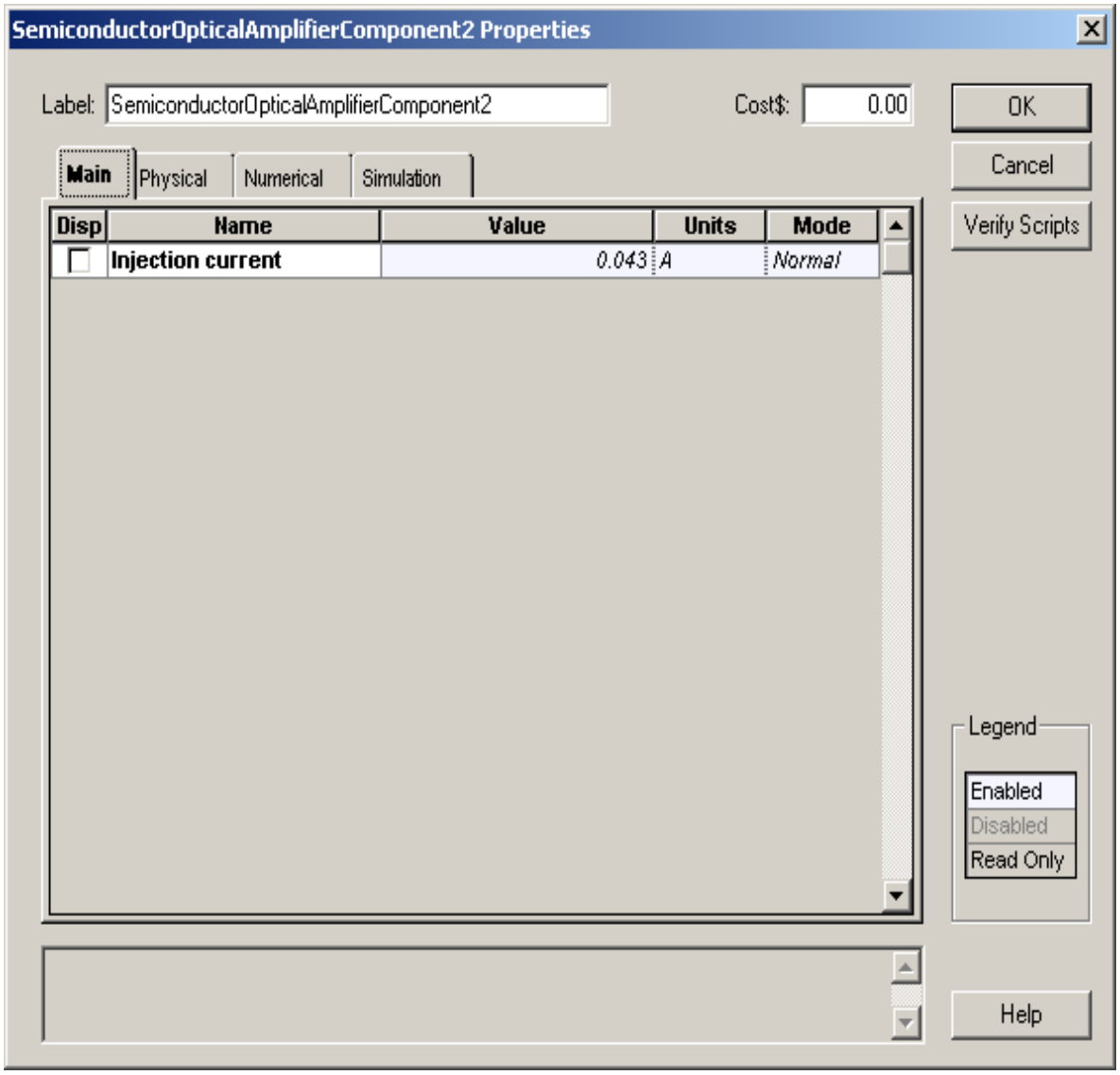

Table 7: Semiconductor optical amplifier parameters (main)

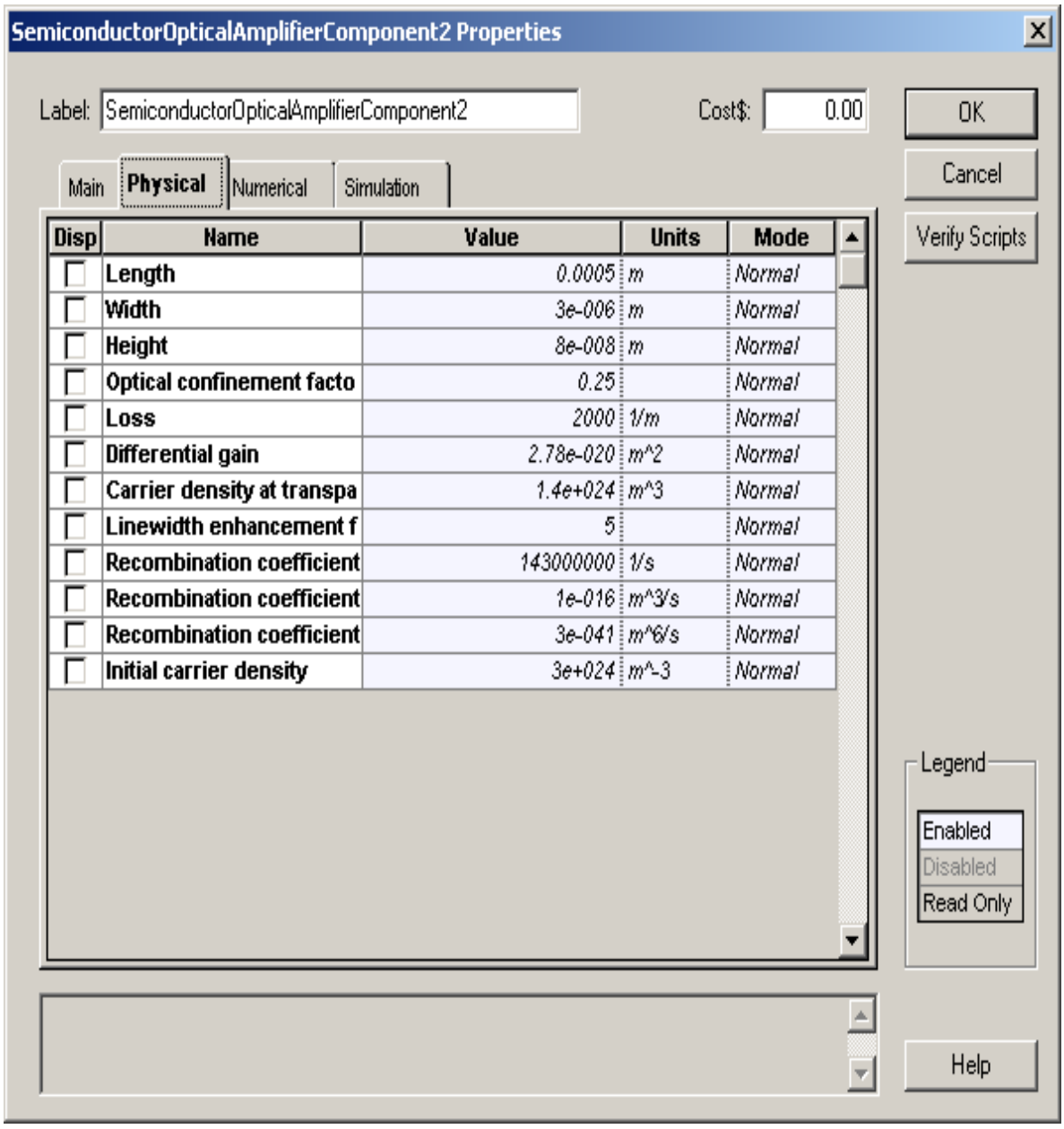

Table 8: Semiconductor optical amplifier parameters (physical)

Note that the inner losses are 2000 [m^{-1}] and the linewidth enhancement factor is equal to 5. Also, note that P_{sat} ~ 30 mW and carrier lifetime τ_C = 200 ps in [1] therefore E_{sat} ~6 pJ. For default values of SOA component, Γ =0.25 $\Rightarrow$ E_{sat} ~ 5.2 pJ.

Figs. 24, 25, 26 and 27, show the initial pattern of pulses, and the same pattern of pulses after 200, 350 and 500 km transmission in SMF with periodic amplification at every 50 km using SOA.

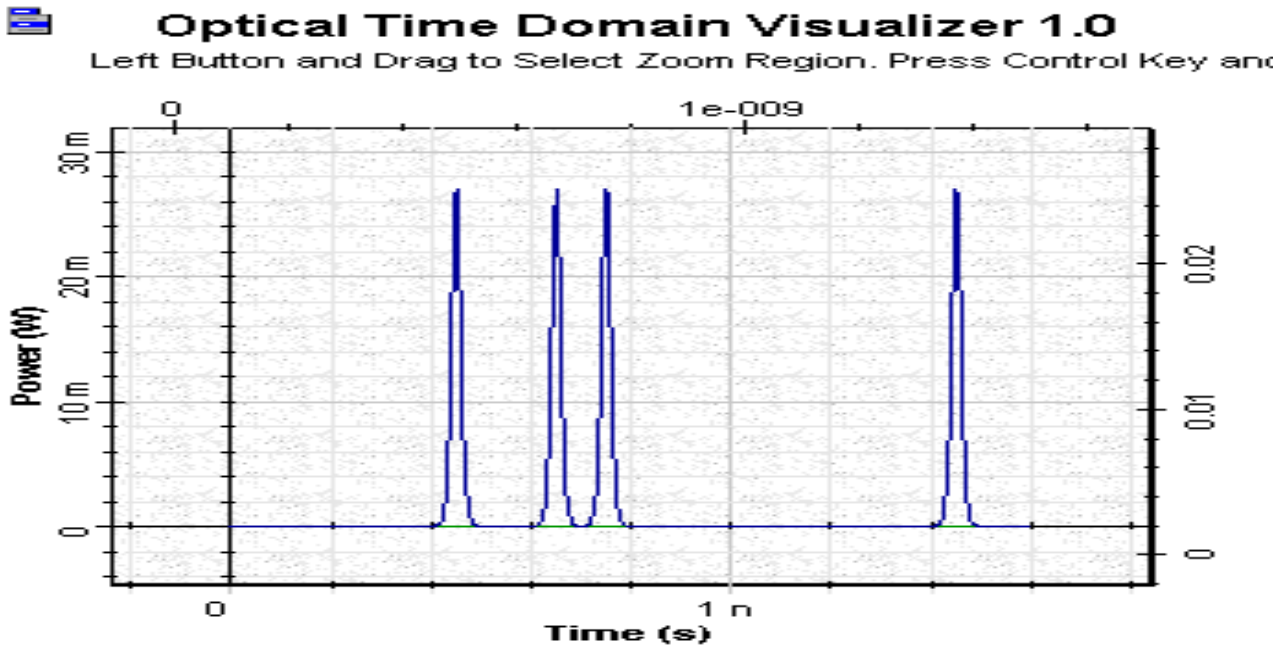

Fig.24: Initial pattern of pulses

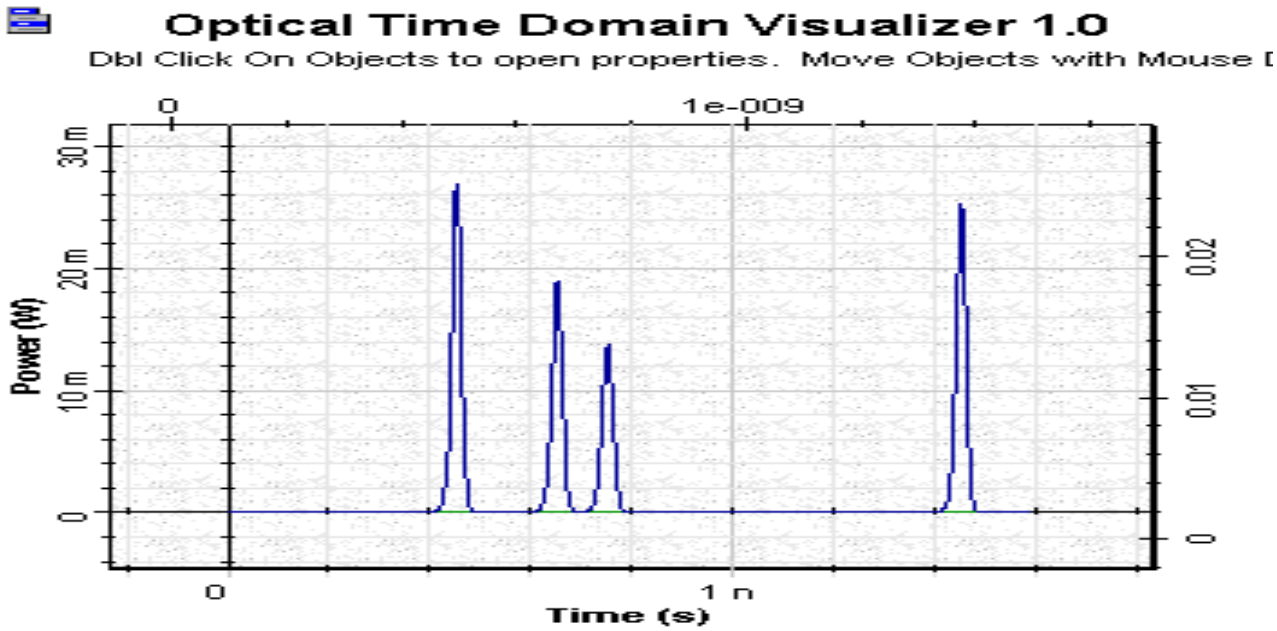

Fig.25: Pulses after 200 km transmission in SMF with periodic amplification using SOA at every 50 km

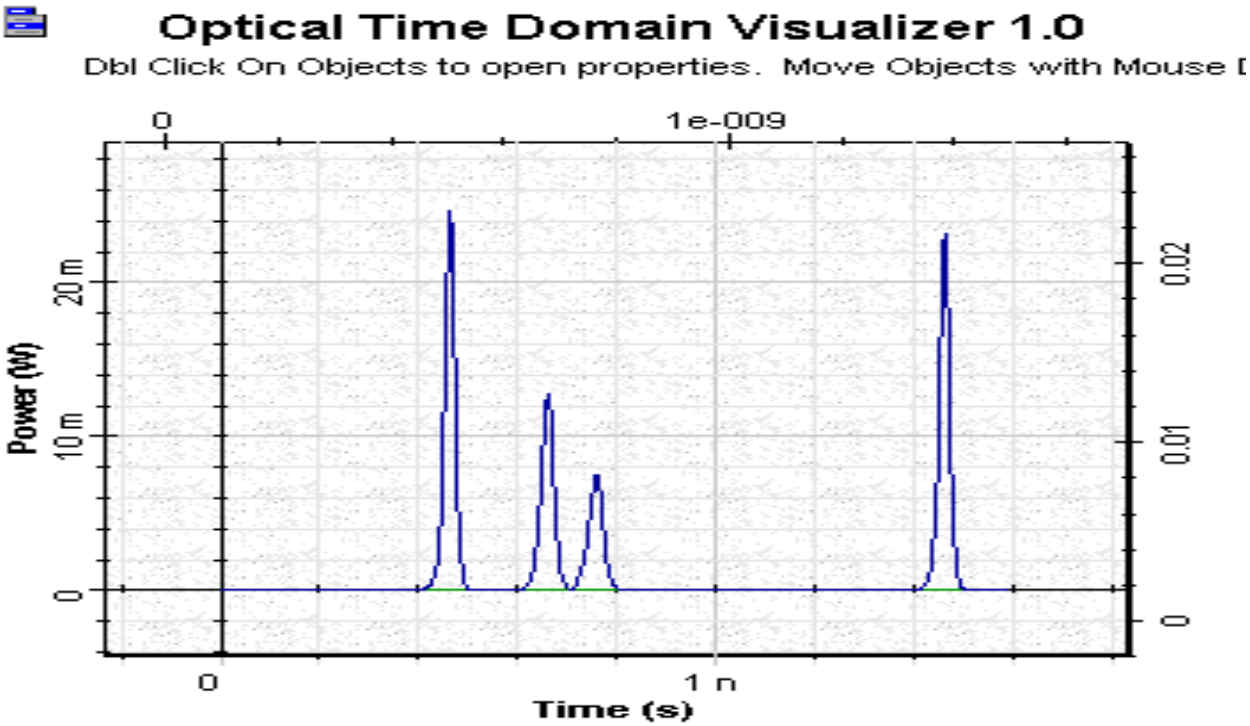

Fig.26: Pulses after 350 km transmission in SMF with periodic amplification using SOA at every 50 km

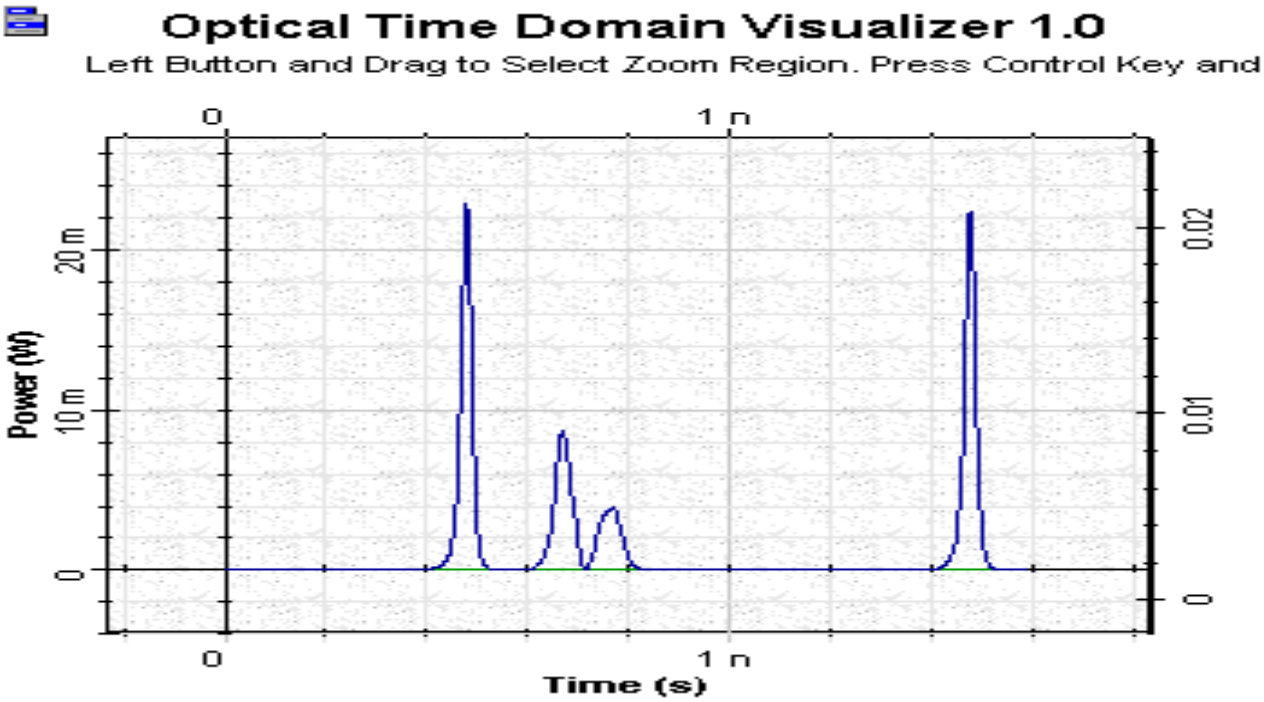

Fig.27: Pulses after 500 km transmission in SMF with periodic amplification using SOA at every 50 km

What we can see form these figures is the pattern effect, which leads to reduction in the gain of the pulses after the first one in the first group. As for our default parameters the carrier lifetime is approximately 1.4 ns even for the last pulse, which is at a distance of approximately 1 nm from the first one.

References:

[1] M. Settembre, F. Matera, V. Hagele, I. Gabitov, A. W. Mattheus, and S. Turitsyn, "Cascaded optical communication systems with in-line semiconductor optical amplifiers", Journal of Lightwave Technology, vol.15, pp. 962-967, 1997.

[2] F. Matera and M. Settembre, "Study of 1.3 μm transmission systems on standard step-index fibers with semiconductor optical amplifiers", Optics communications, vol. 133, pp.463-470, 1997.

[3] G.P. Agrawal, "Fiber Optic Communication Systems", second edition, John Wiley @ Sons, Inc., 1997.

Example: SLA Gain Recovery

SLA gain recovery**.osd**

When the pulse width becomes comparable to the carrier lifetime, the saturated gain has time to recover during the pulse. The recovery effect influences the shape and spectrum of the amplified pulse.

The aim of this project is to study this influence. Three subtopics will be considered:

a) Partial gain recovery;
b) Complete gain recovery
c) Appearance of gain-saturation induced self-phase modulation.

SOA parameters considered are : carrier lifetime τ_C ~ 1.4 ns, Γ = 0.22 and E_{sat} = 5 pJ. **Table 9** shows the physical parameters of SOA. The unsaturated single pass amplifier gain ~30 dB and Inner loss=0 are used to make the comparison with [1].

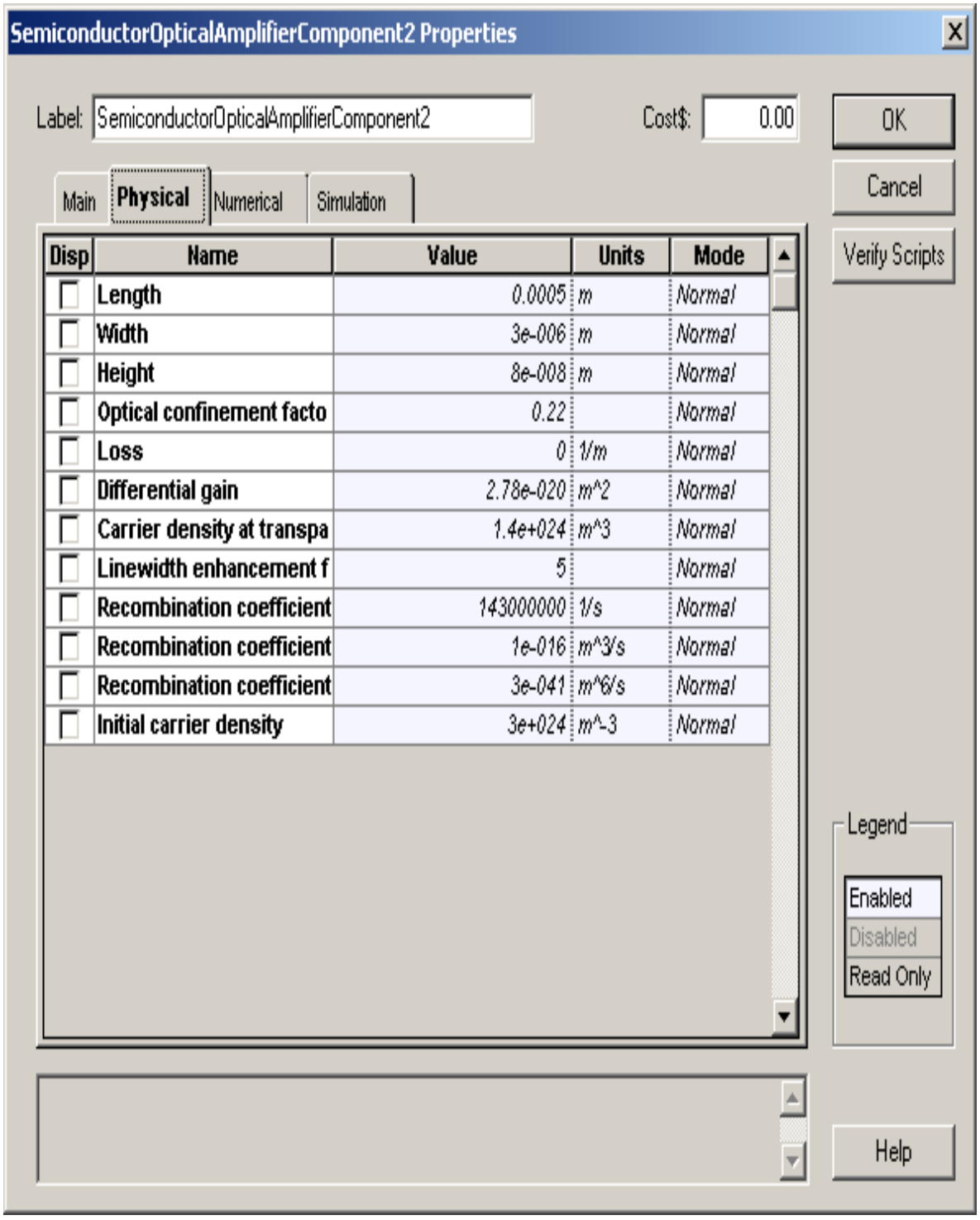

Table 9: Semiconductor optical amplifier parameters (physical)

Fig. 28 shows the layout of the project.

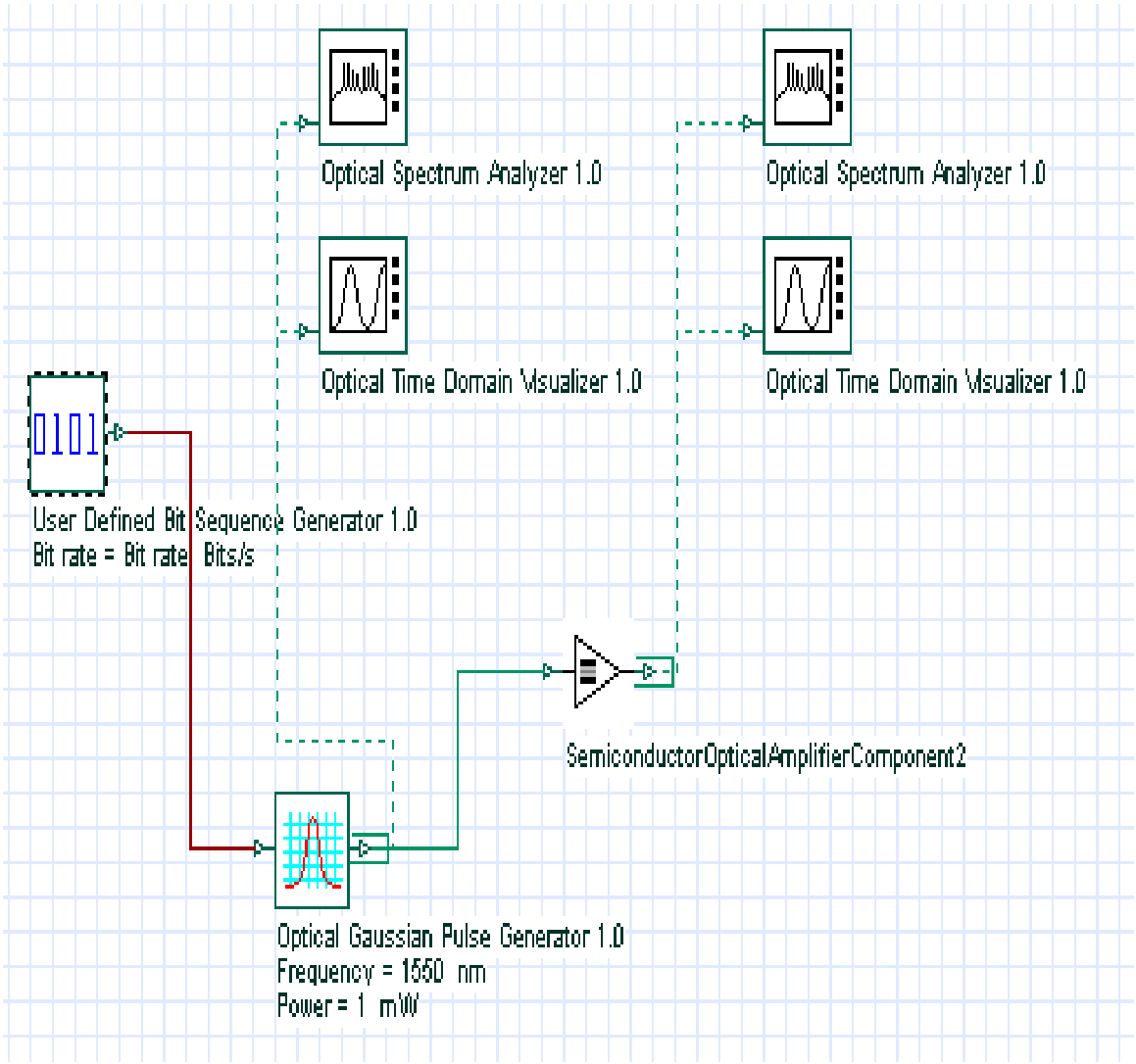

Fig. 28: Layout: SLA gain recovery

a) Partial gain recovery

As the carrier lifetime of SOA is: τ_C ~ 1.4 ns, we will consider here pulses with widths smaller than 1.4 ns. Keeping the ratio E_{in} / E_{sat} = 0.1, we will investigate the influence of the increase of the pulse duration which will approach the carrier lifetime but will remain smaller than it.

We consider the parameters as shown in Table 10. The bit rate B= 1 GHz implies T_B = 1ns.

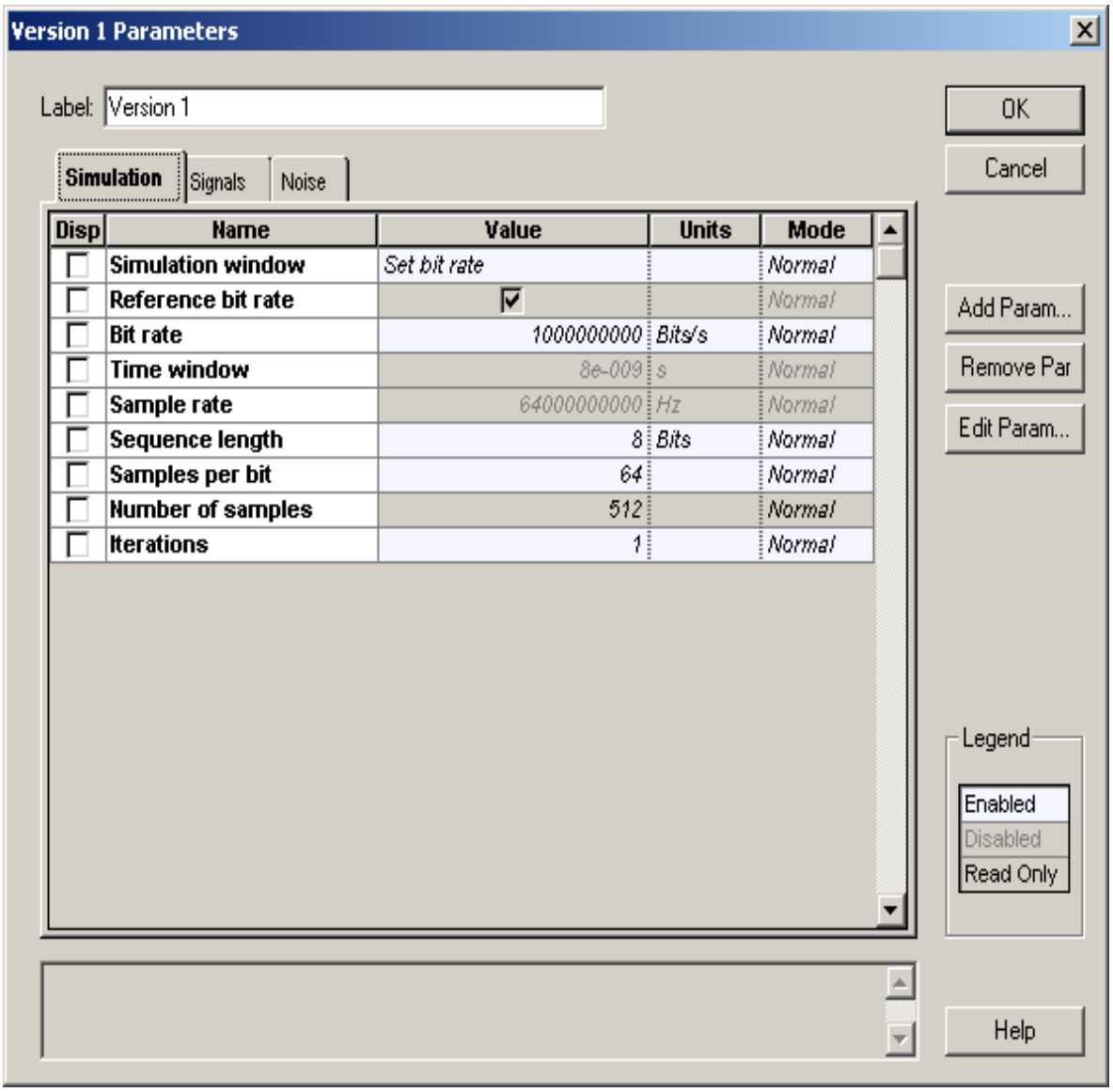

Disp	Name	Value	Units	Mode
☐	Simulation window	Set bit rate		Normal
☐	Reference bit rate	☑		Normal
☐	Bit rate	1000000000	Bits/s	Normal
☐	Time window	8e-009	s	Normal
☐	Sample rate	64000000000	Hz	Normal
☐	Sequence length	8	Bits	Normal
☐	Samples per bit	64		Normal
☐	Number of samples	512		Normal
☐	Iterations	1		Normal

Table 10: Global parameters

We will consider three pulses (pulse 1,2 and 3) with widths 0.25ns, 0.5 ns and 1 ns. In all the three cases, the ratio E_{in} / E_{sat} = 0.1 will be kept constant.

The parameters for pulse 1 are: duty cycle = 0.25, T_{FWHM} ~ 0.25 ns $\Rightarrow$ T_0 ~ 0.14 ns and P_{in} =3.5 mW. Therefore, T_0/τ_C ~ 0.1.

Figs. 29, 30, 31 and 32 show the shape and spectra of the initial and amplified pulse 1.

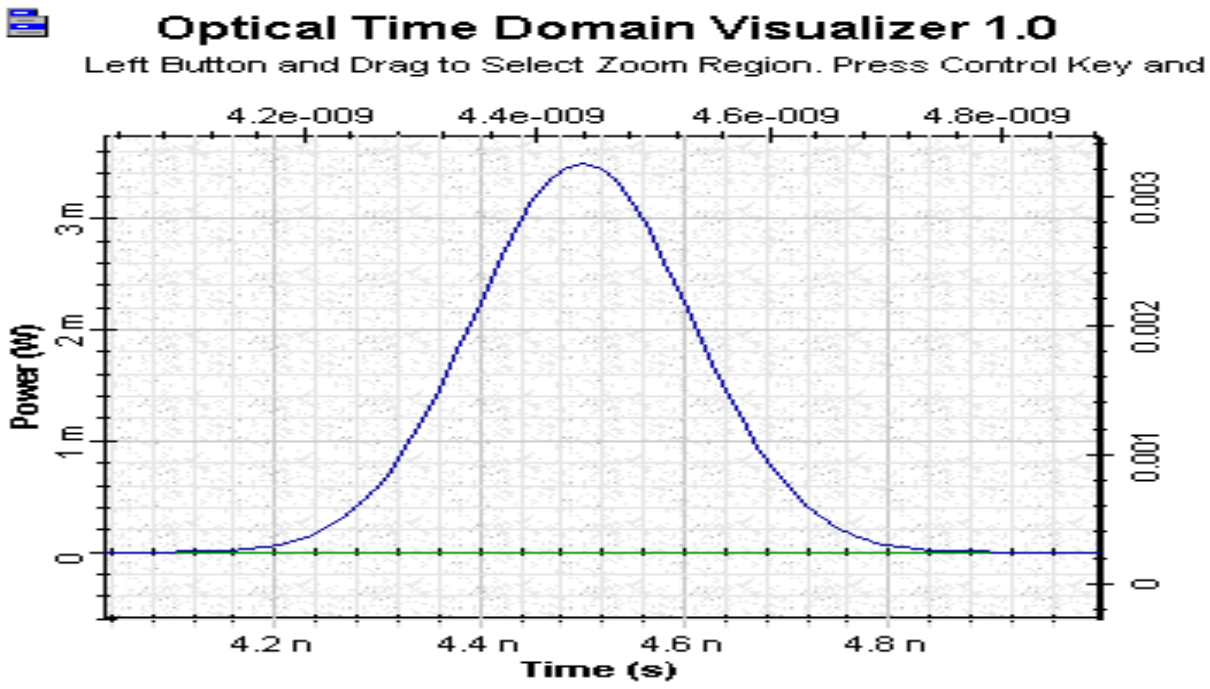

Fig.29: Shape of the initial pulse 1

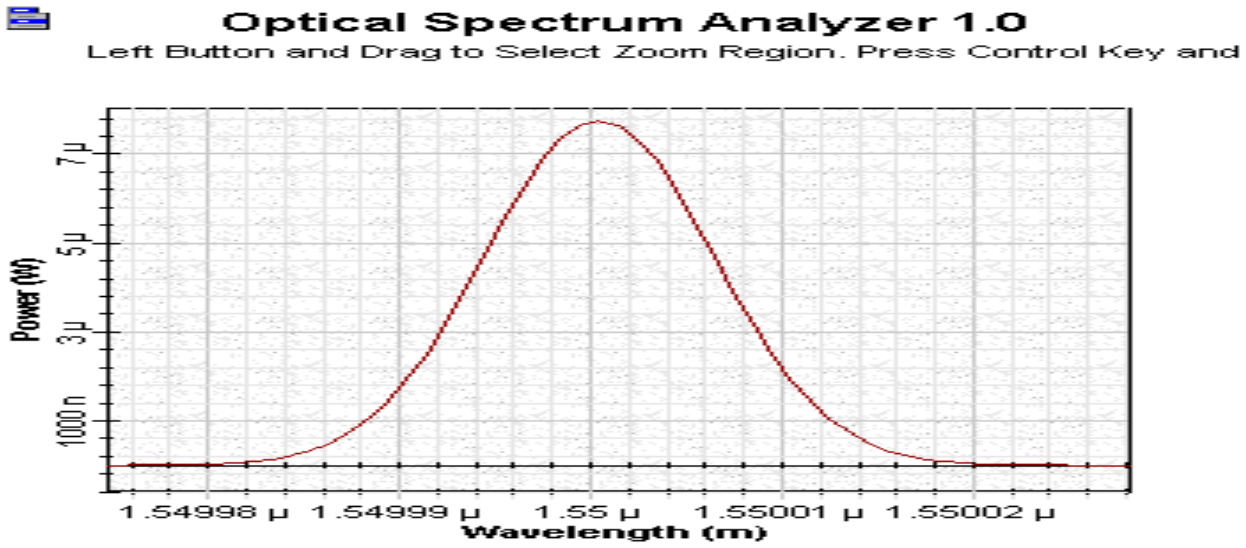

Fig.30: Spectra of the initial pulse 1

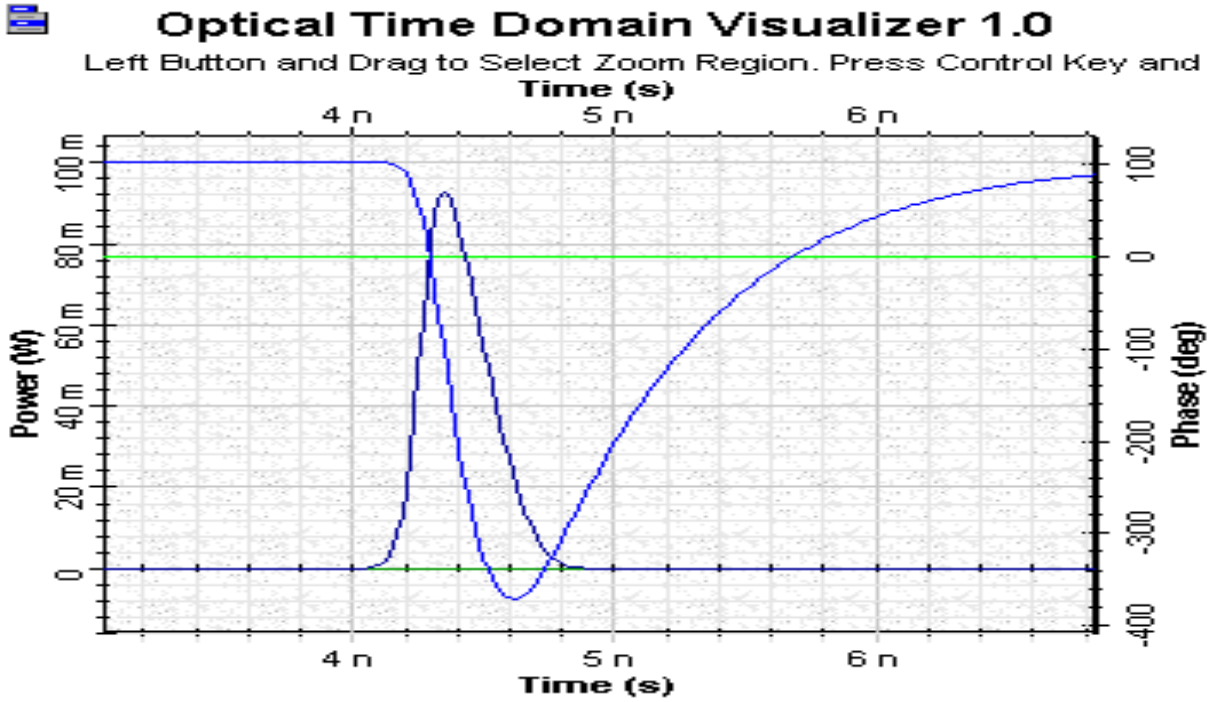

Fig.31: Shape of amplified pulse 1

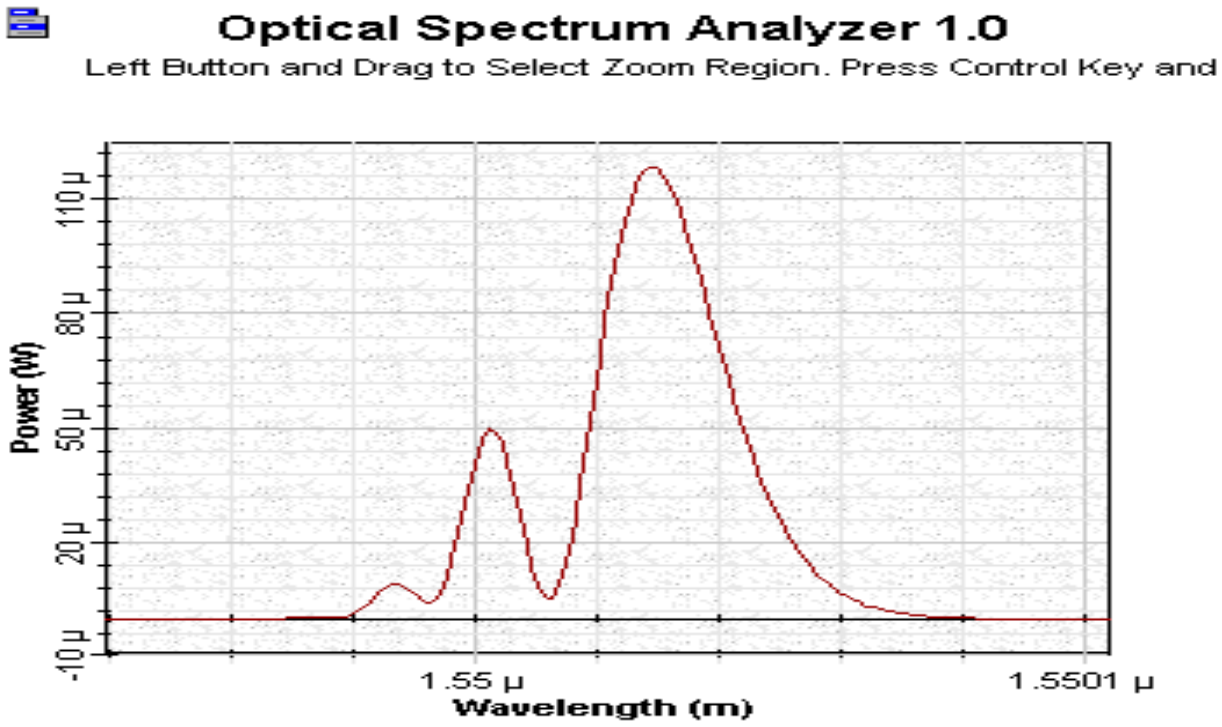

Fig.32: Spectra of amplified pulse 1

The parameters for pulse 2 are: duty cycle = 0.5, T_{FWHM} ~ 0.5 ns $\Rightarrow$ T_0 ~ 0.28 ns and P_{in} = 1.75 mW. Therefore, T_0/τ_C ~ 0.2.

Figs. 33, 34, 35 and 36 show the shape and spectra of the initial and amplified pulse 2.

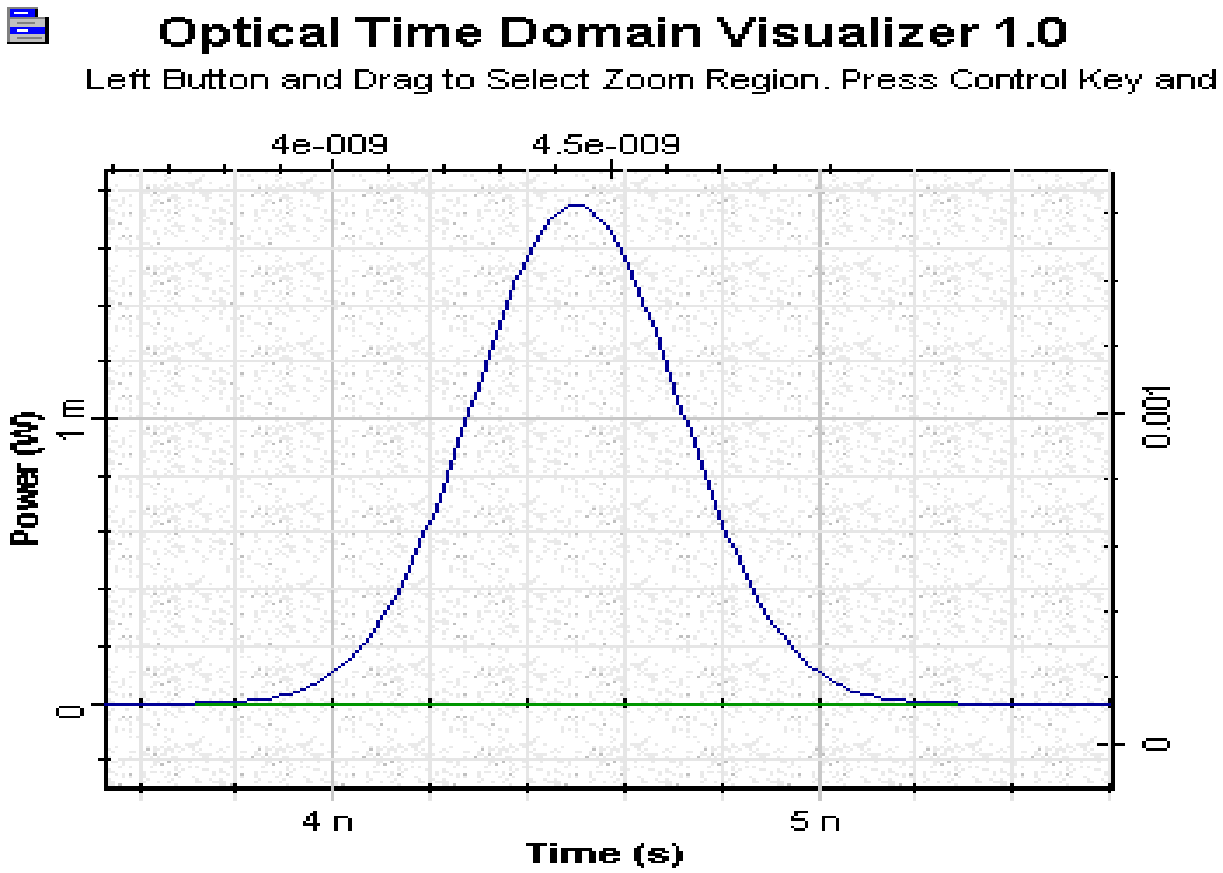

Fig.33: Shape of the initial pulse 2

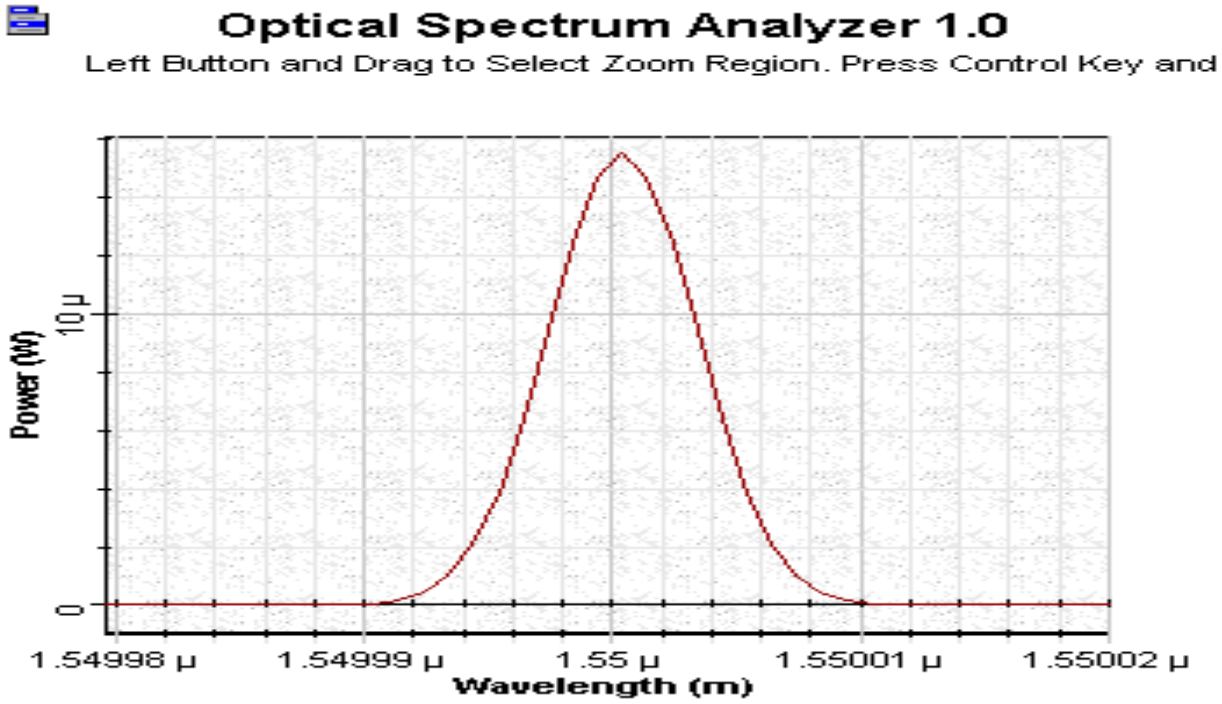

Fig.34: Spectra of the initial pulse 2

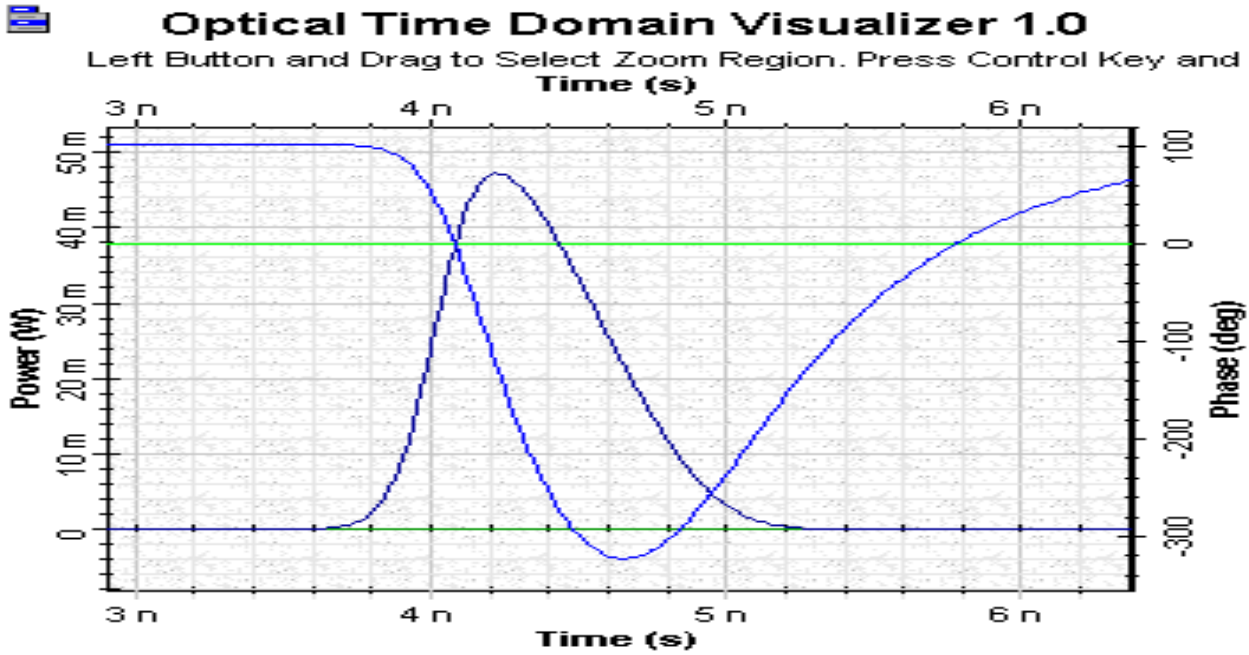

Fig.35: Shape of amplified pulse 2

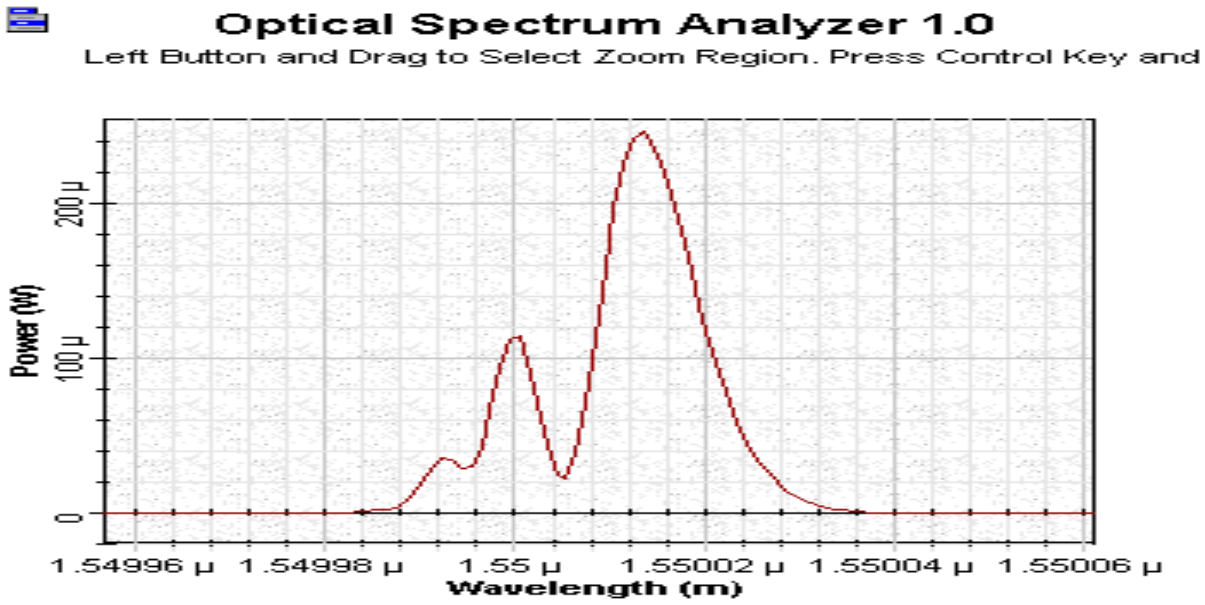

Fig.36: Spectra of amplified pulse 2

The parameters for pulse 3 are: duty cycle = 1, T_{FWHM} ~ 1 ns $\Rightarrow$ T_0 ~ 0.567 ns and P_{in} = 0.875 mW. Therefore, T_0/τ_C ~ 0.4.

Figs. 37, 38, 39 and 40 show the shape and spectra of the initial and amplified pulse 3.

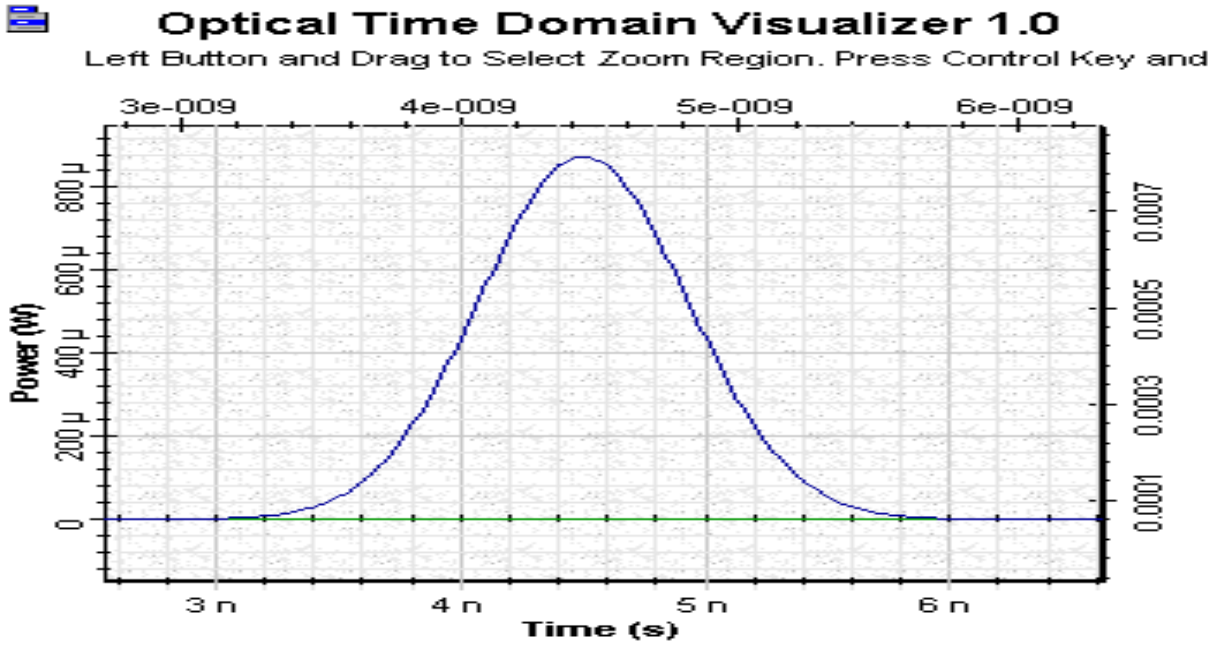

Fig.37: Shape of the initial pulse 3

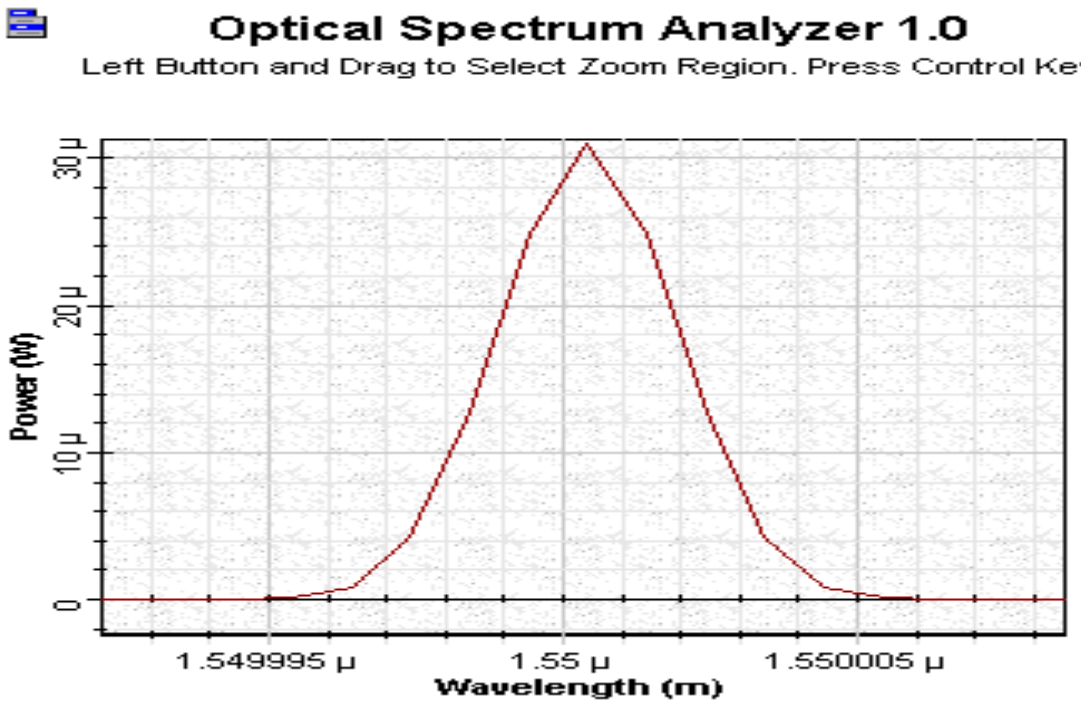

Fig.38: Spectra of the initial pulse 3

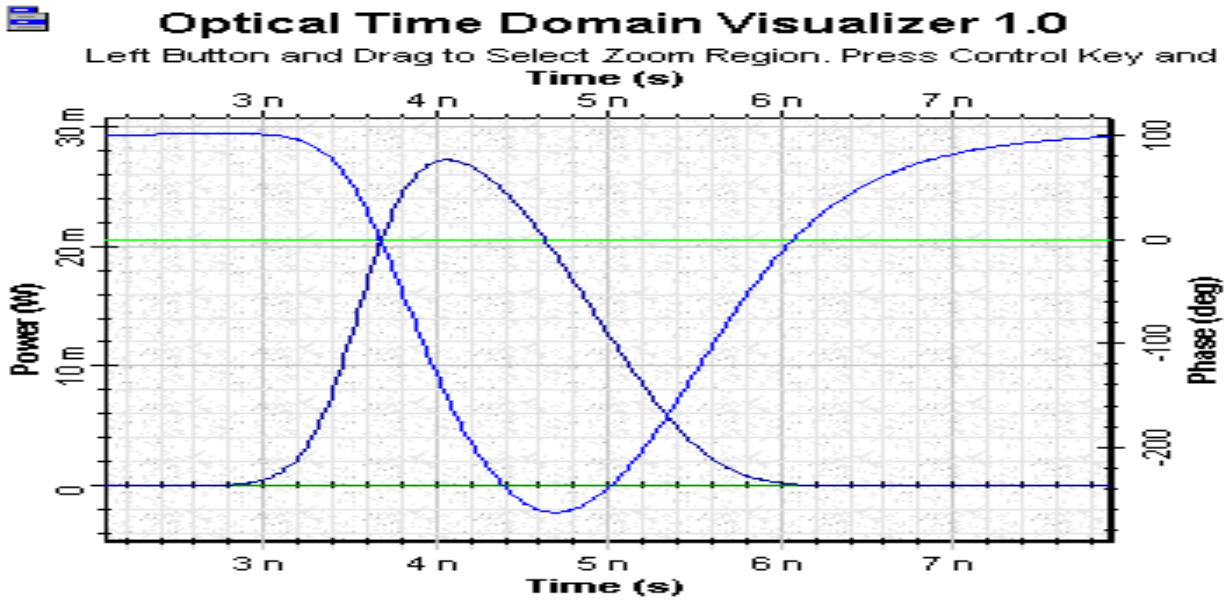

Fig. 39: Shape of amplified pulse 3

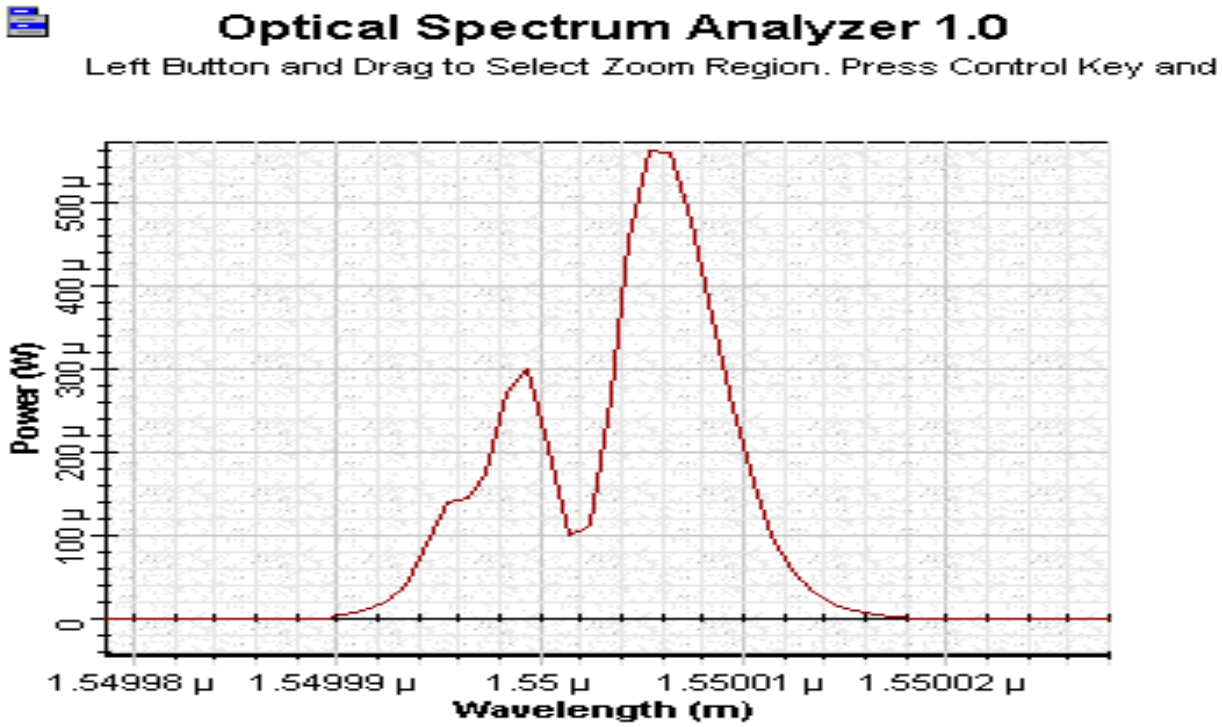

Fig.40: Spectra of amplified pulse 3

Following properties of the three amplified pulses considered above can be observed. First, we see that increasing the pulse width, keeping the ratio $\Rightarrow$ E_{in} / E_{sat} = 0.1, the pulse shape becomes less asymmetrical and broader than the input pulse. At the same time increasing the pulse width, the spectrum becomes less asymmetrical and the spectral shift reduces. Note the behavior of the phase that is shown in the figures of the shapes of amplified pulses. As the phase of amplified pulse gives the information for the gain we can see that for such pulses the gain has not enough time to recover completely.

b) Complete gain recovery (the quasi CW operation)

As the carrier lifetime of SOA is: τ_C ~ 1.4 ns, we will consider pulses with widths larger than 1.4 ns. We consider the parameters as shown in **Table 11**. The bit rate B= 100 MHz GHz implies T_B = 10ns.

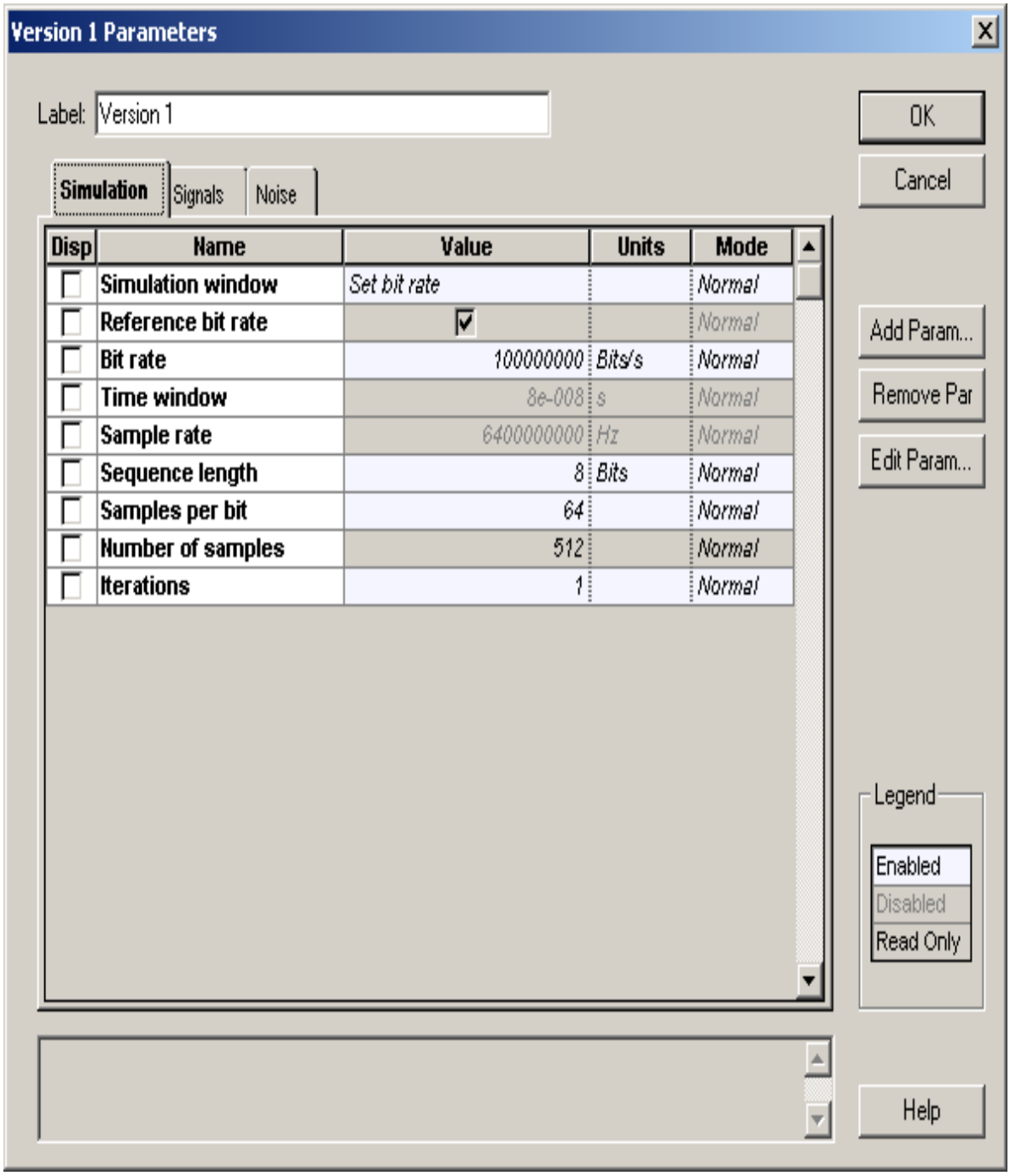

Table 11: Global parameters

We will consider three pulses (pulse 4, 5 and 6) with widths 2.5ns, 5 ns and 10 ns. In all the three cases the ratio E_{in} / E_{sat} = 0.1 will be kept constant.

The parameters for pulse 4 are: duty cycle = 0.25, T_{FWHM} ~ 2.5 ns $\Rightarrow$ T_0 ~ 1.42 ns and P_{in} = 0.15 mW. Therefore, T_0/τ_C ~ 1.8 and P_{in} / P_{sat} = 0.04.

Figs. 41, 42, 43 and 44 show the shape and spectra of the initial and amplified pulse 4.

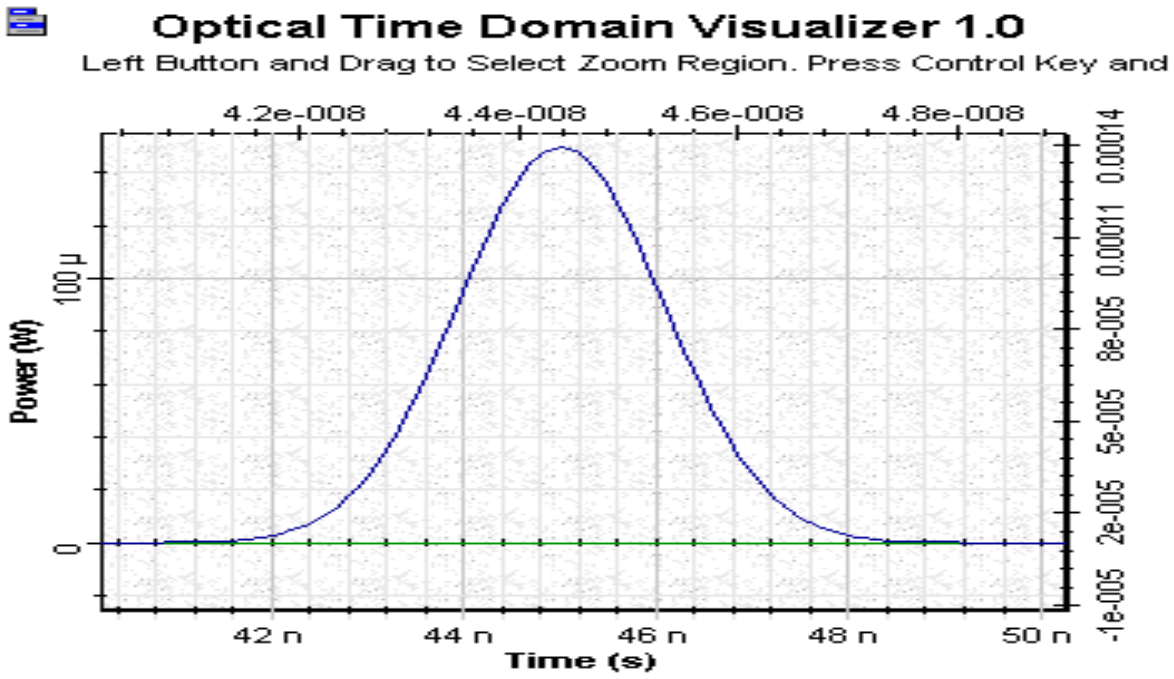

Fig.41: Shape of the initial pulse 4

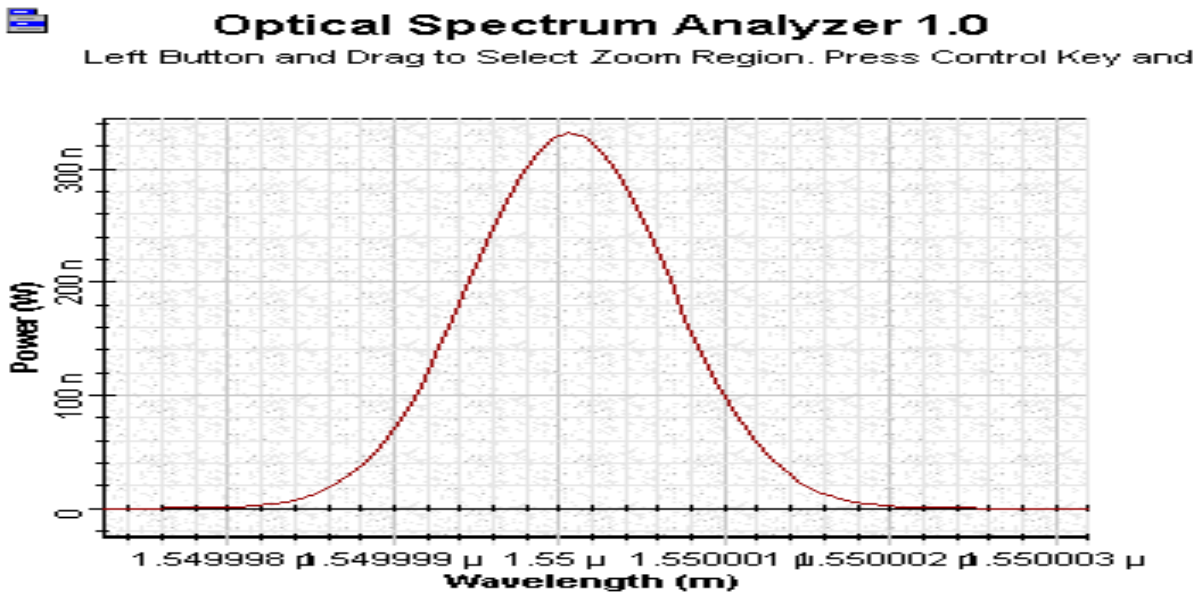

Fig.42: Spectra of the initial pulse 4

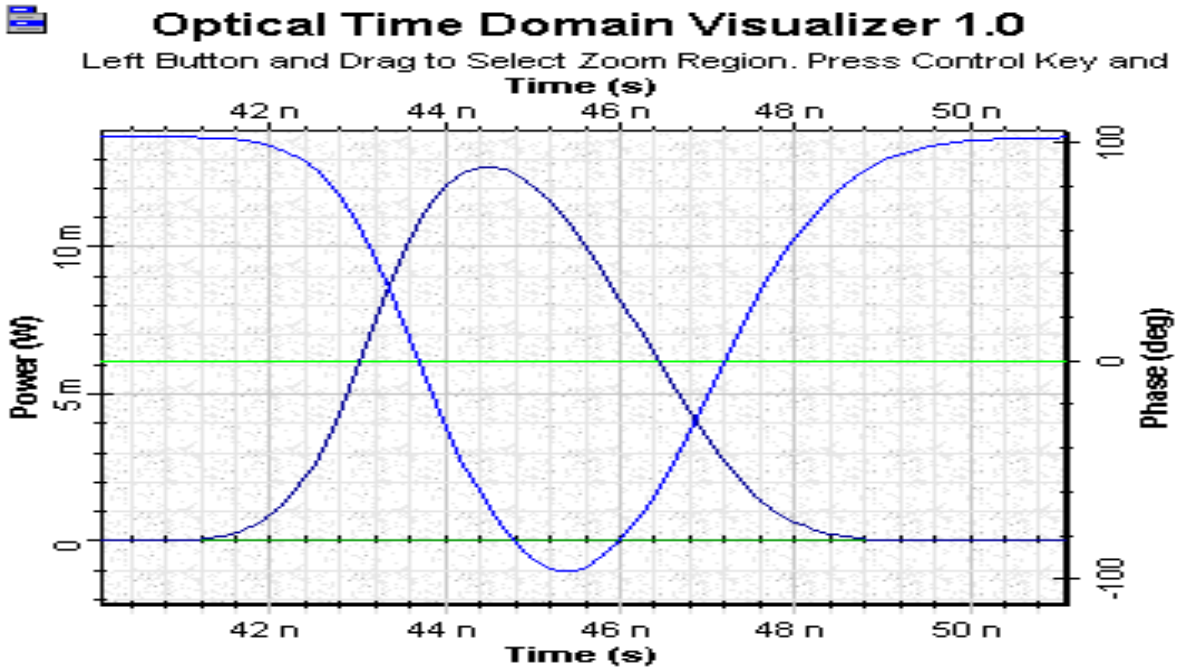

Fig.43: Shape of amplified pulse 4

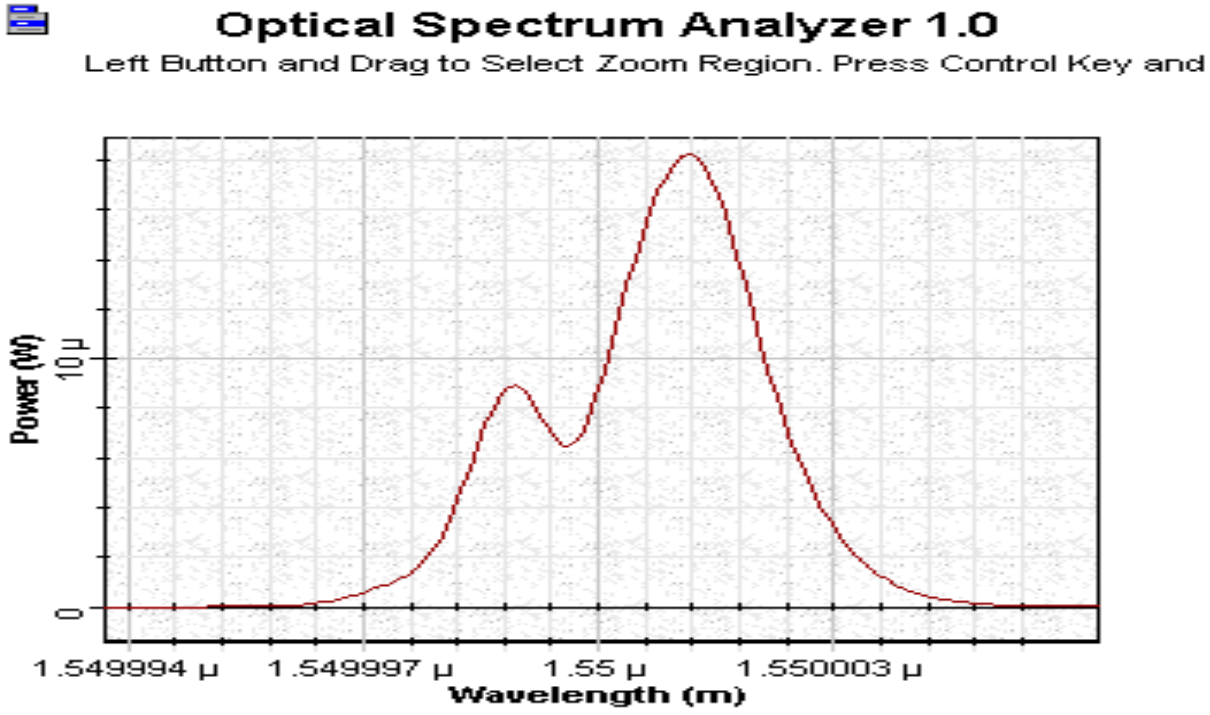

Fig.44: Spectra of amplified pulse 4

The parameters for pulse 5 are: duty cycle = 0.5, T_{FWHM} ~ 5 ns $\Rightarrow$ T_0 ~ 2.83 ns and P_{in} = 0.28 mW. Therefore, T_0/τ_C ~ 3.6 and P_{in}/P_{sat} = 0.08.

Figs. 45, 46, 47 and 48 show the shape and spectra of the initial and amplified pulse 5.

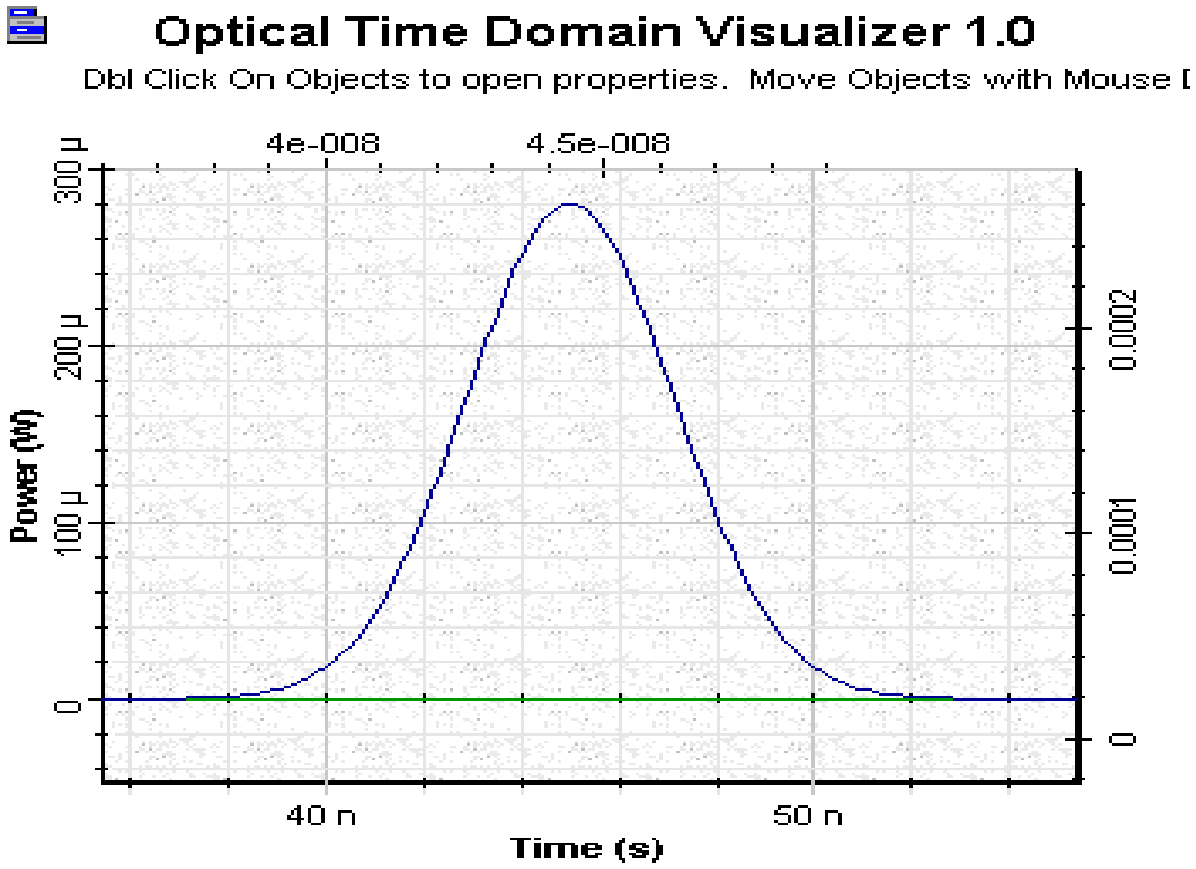

Fig.45: Shape of the initial pulse 5

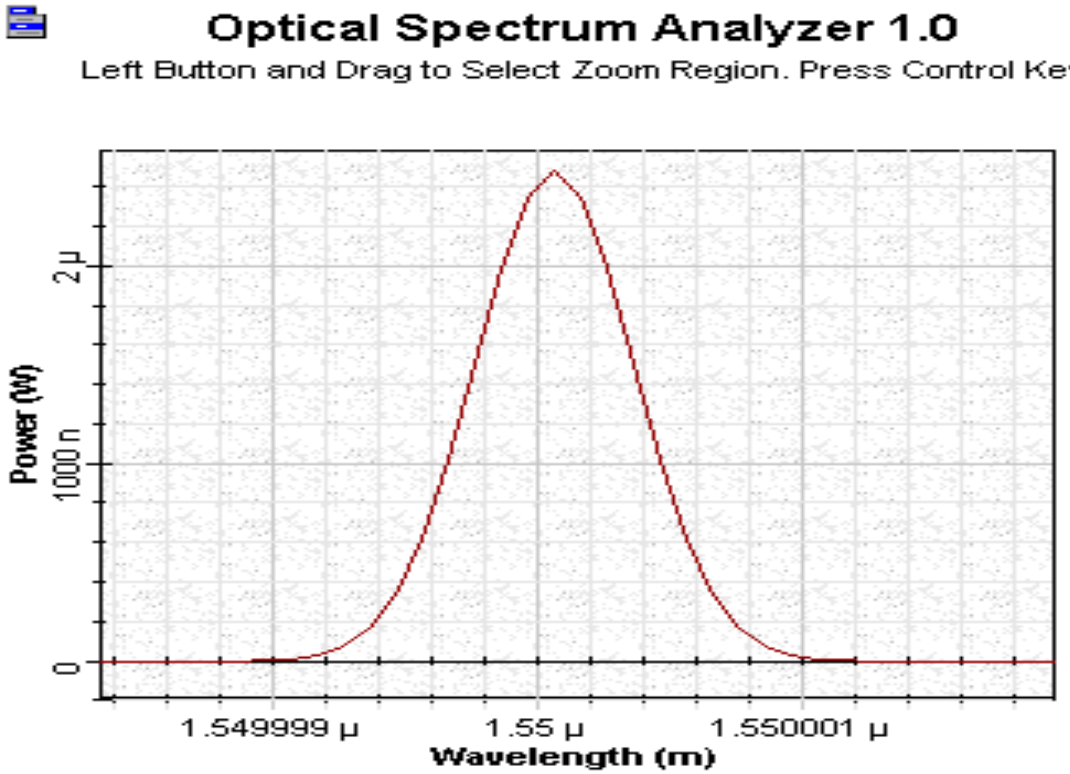

Fig.46: Spectra of the initial pulse 5

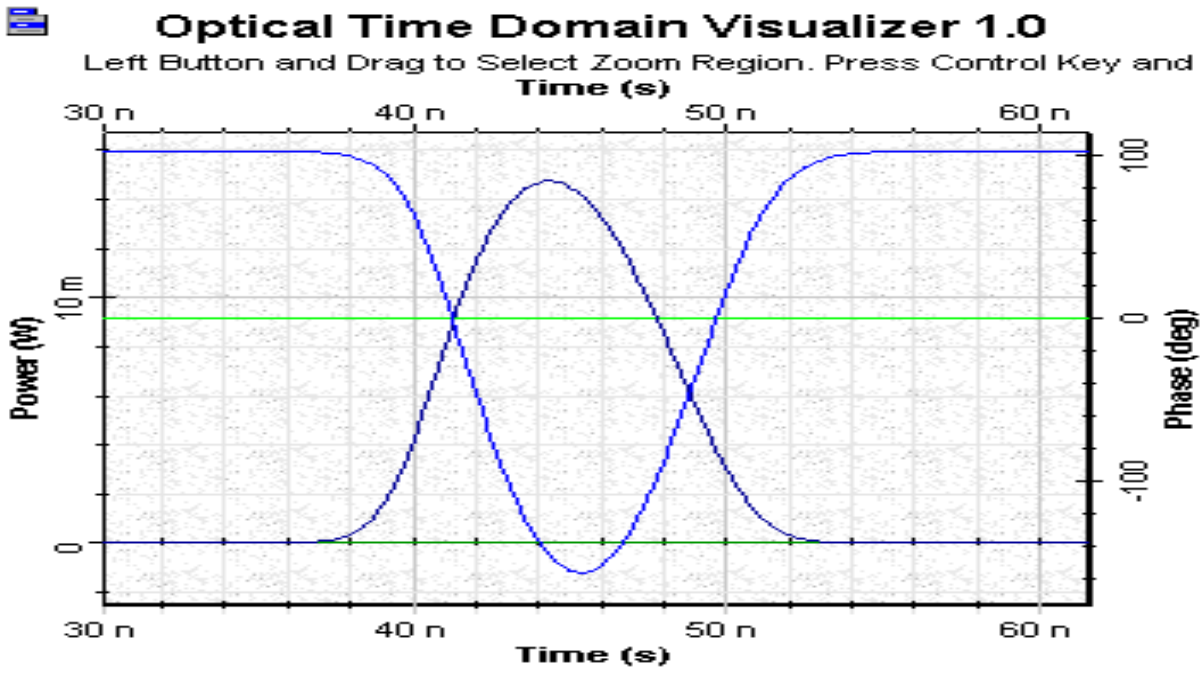

Fig.47: Shape of amplified pulse 5

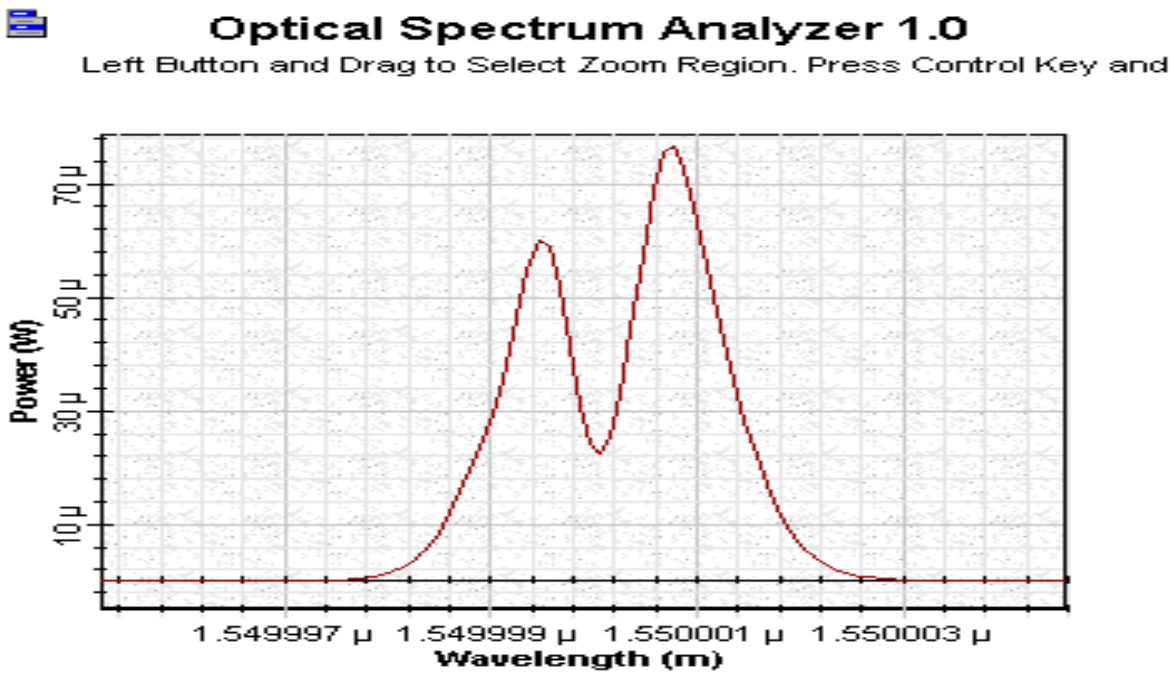

Fig.48: Spectra of amplified pulse 5

The parameters for pulse 6 are: duty cycle 1, T_{FWHM} ~ 10 ns $\Rightarrow$ T_0 ~ 5.67 ns and P_{in} = 0.736 mW. Therefore, T_0/τ_C ~ 7.1 and P_{in}/P_{sat} = 0.2.

Figs. 49, 50, 51 and 52 show the shape and spectra of the initial and amplified pulse 6.

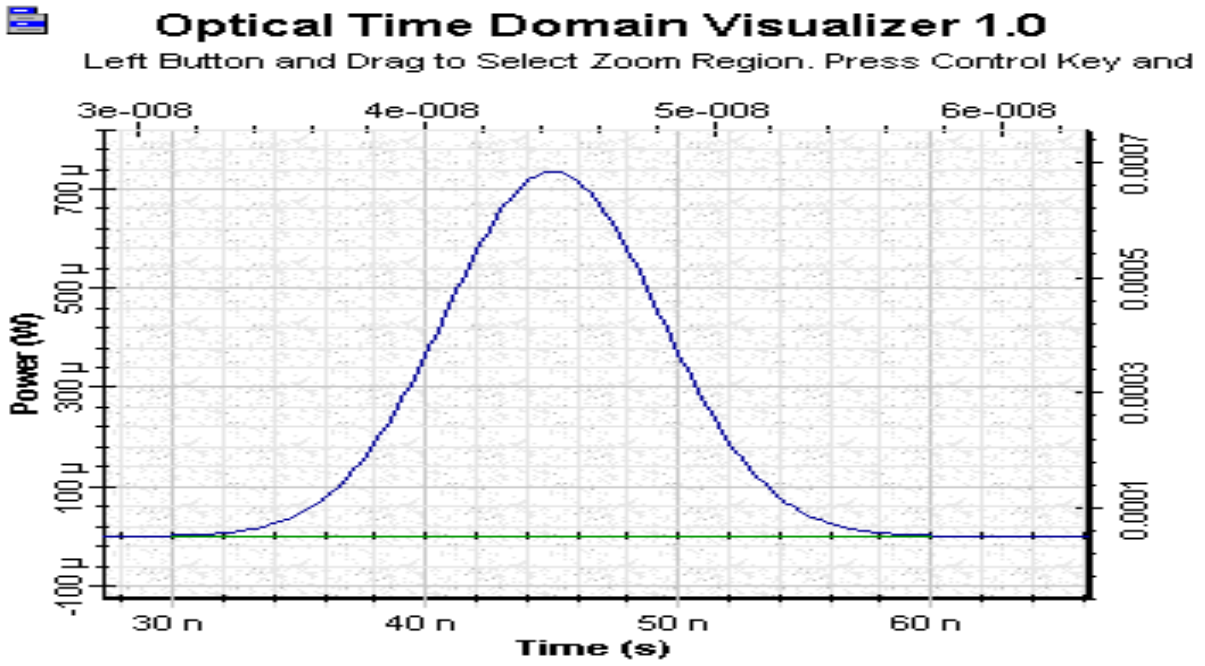

Fig.49: Shape of the initial pulse 6

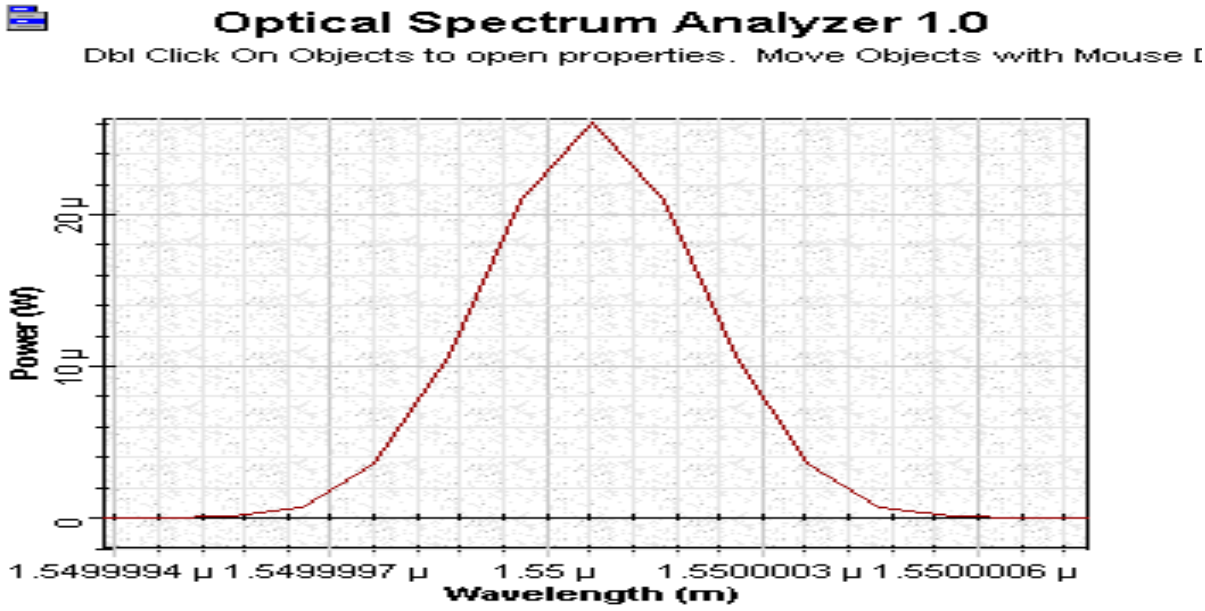

Fig.50: Spectra of the initial pulse 6

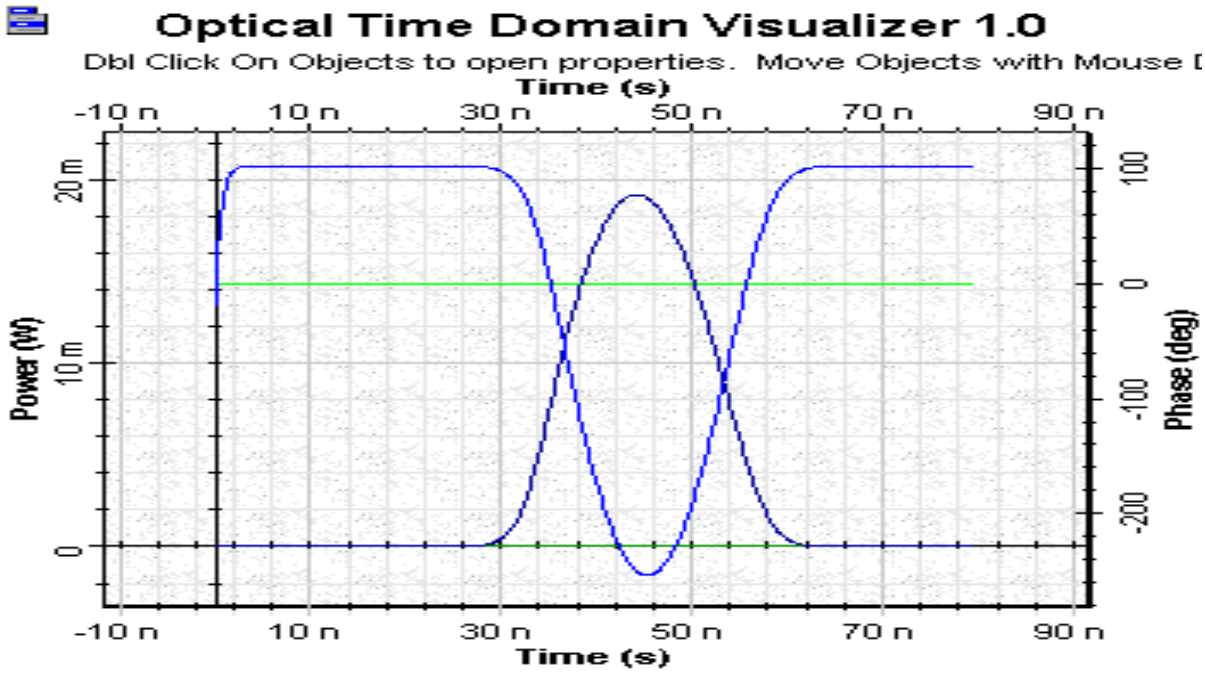

Fig.51: Shape of amplified pulse 6

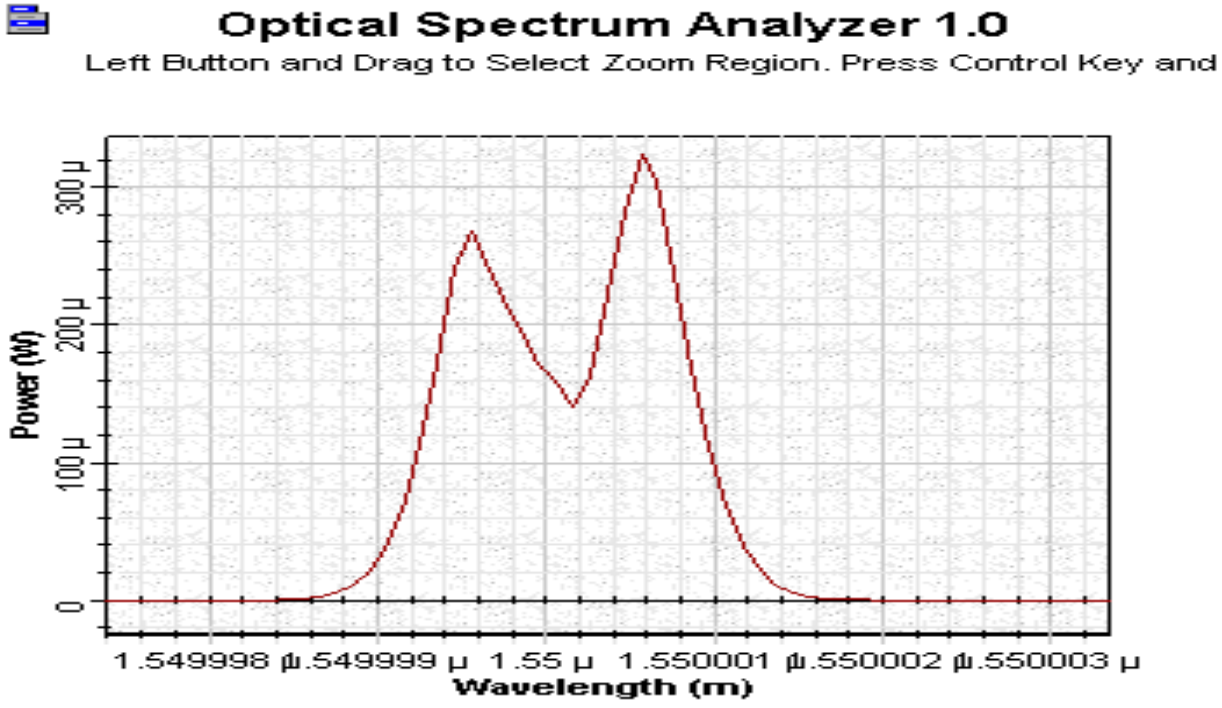

Fig.52: Spectra of amplified pulse 6

We see from the properties of the last three amplified pulses that increasing the pulse width well above the carrier lifetime leads to much more symmetrical shapes of the amplified pulses. They become also much broader than the shapes of the corresponding initial pulses. At the same time increasing the pulse width the spectrum of the amplified pulses become less asymmetrical and the red shift continuously reduce. The phase is shown in the figures of the shapes of amplified pulses. We see now that for such pulses the gain has enough time to recover completely.

c) Appearance of gain-saturation induced self- phase modulation

Now we will compare the obtained results for the pulse 6 (for which P_{in} / P_{sat} = 0.2) with that of P_{in} / P_{sat} = 0.4. To make this we will increase the initial power 10 times. The compared Results for the shapes and spectra of the amplified pulses are shown in Figs. 53 and 54, respectively.

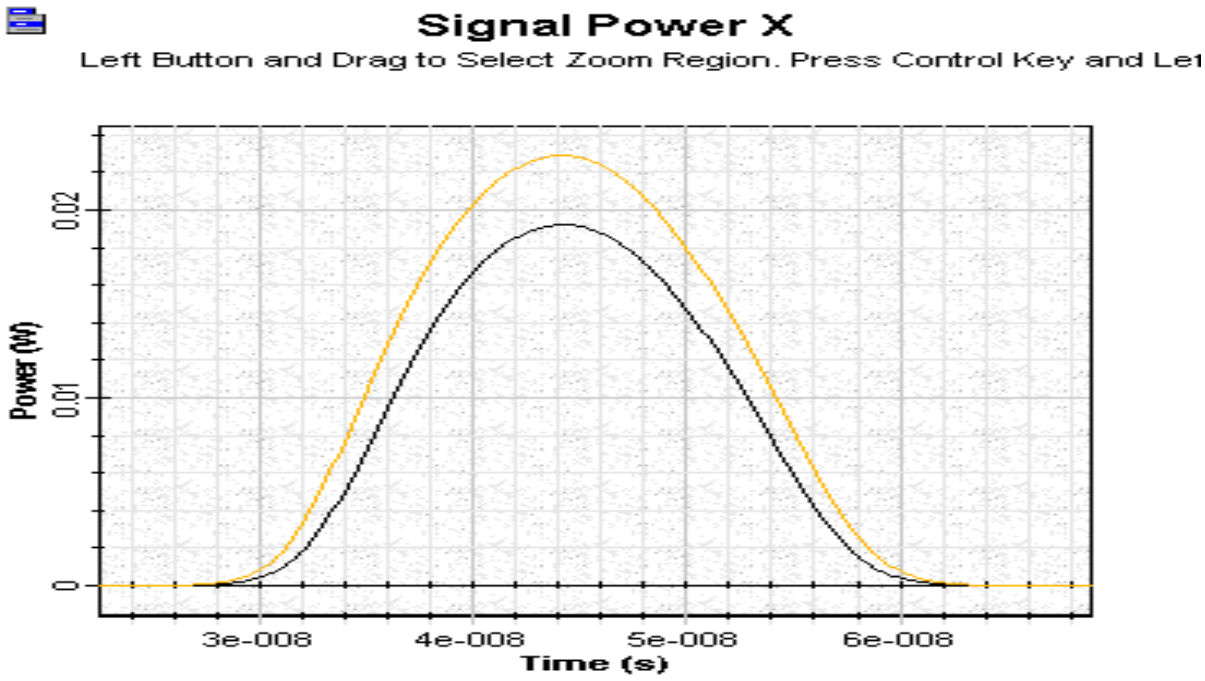

Fig.53: Comparison of results for the shapes of the amplified pulses

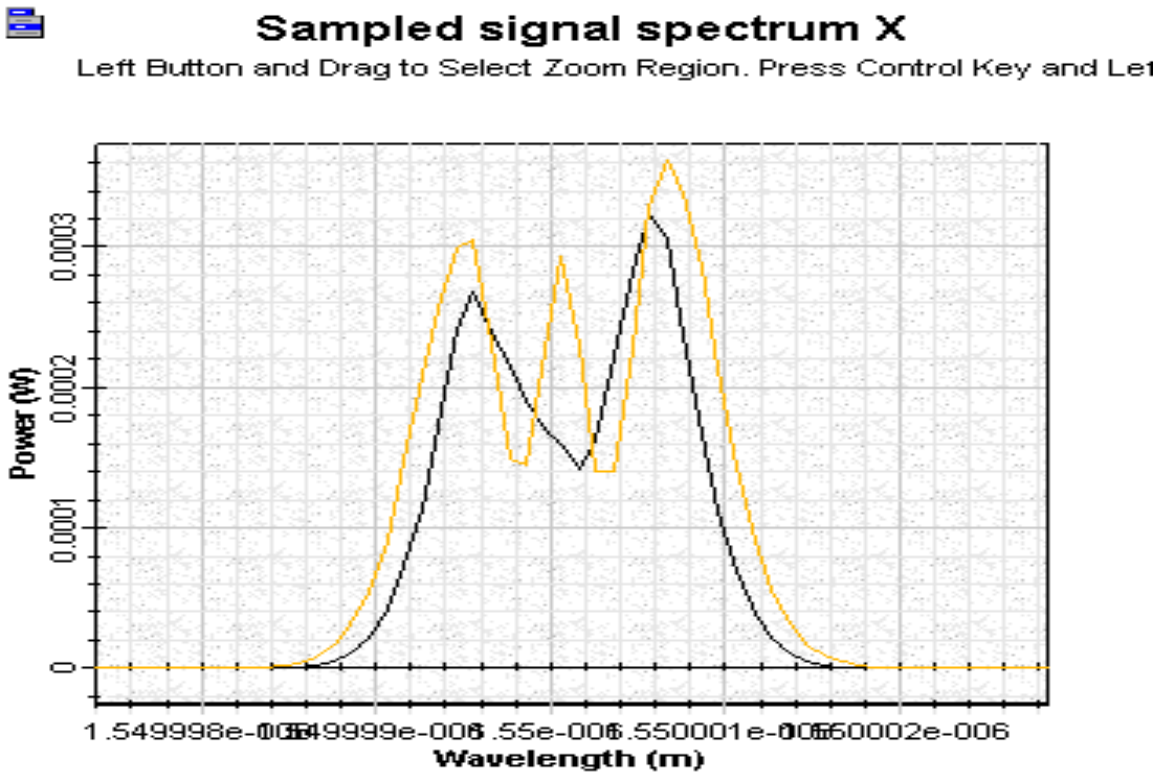

Fig.54: Comparison of results for the spectra of the amplified pulses

Obtained spectra for the complete gain recovery example exhibits the shape that is very similar to the case of pulse propagation in a medium with Kerr nonlinearity [2]. These spectra show the concept of gain saturation induced self-phase modulation [1]. Note that such kinds of spectra are possible only in the case of pulses longer than the carrier lifetime.

References:

[1]G.P. Agrawal and N.A. Olsson, “Self_phase modulation and spectral broadening of optical pulses in semiconductor laser amplifiers”, IEEE Journal of Quantum electronics, vol. 25, pp.2297-2306, 1989.

[2]G.P.Agrawal, “Nonlinear Fiber optics”, third edition, Academic Press, 2001.

Example: SLA Gain Saturation of Chirped and Super Gaussian Pulses

SLA gain saturation of chirped and super- Gaussian pulses**.osd**

In this project we will study the effect of gain saturation induced self-phase modulation for the amplification of optical pulses. However, we will concentrate on the pulses with different shape and initial frequency shift. The chirped Gaussian input pulses are the pulses that are usually produced from directly modulated semiconductor laser.

We will consider the pulses with pulse width much shorter than the carrier lifetime. The carrier wavelength of the Gaussian pulse is 1.55 μm.

In the first part of this project we will consider chirped Gaussian pulses, and in the second part, the super Gaussian pulses.

Saturation of amplification of chirped Gaussian pulse

Table 12 shows the SOA parameters used in the project.

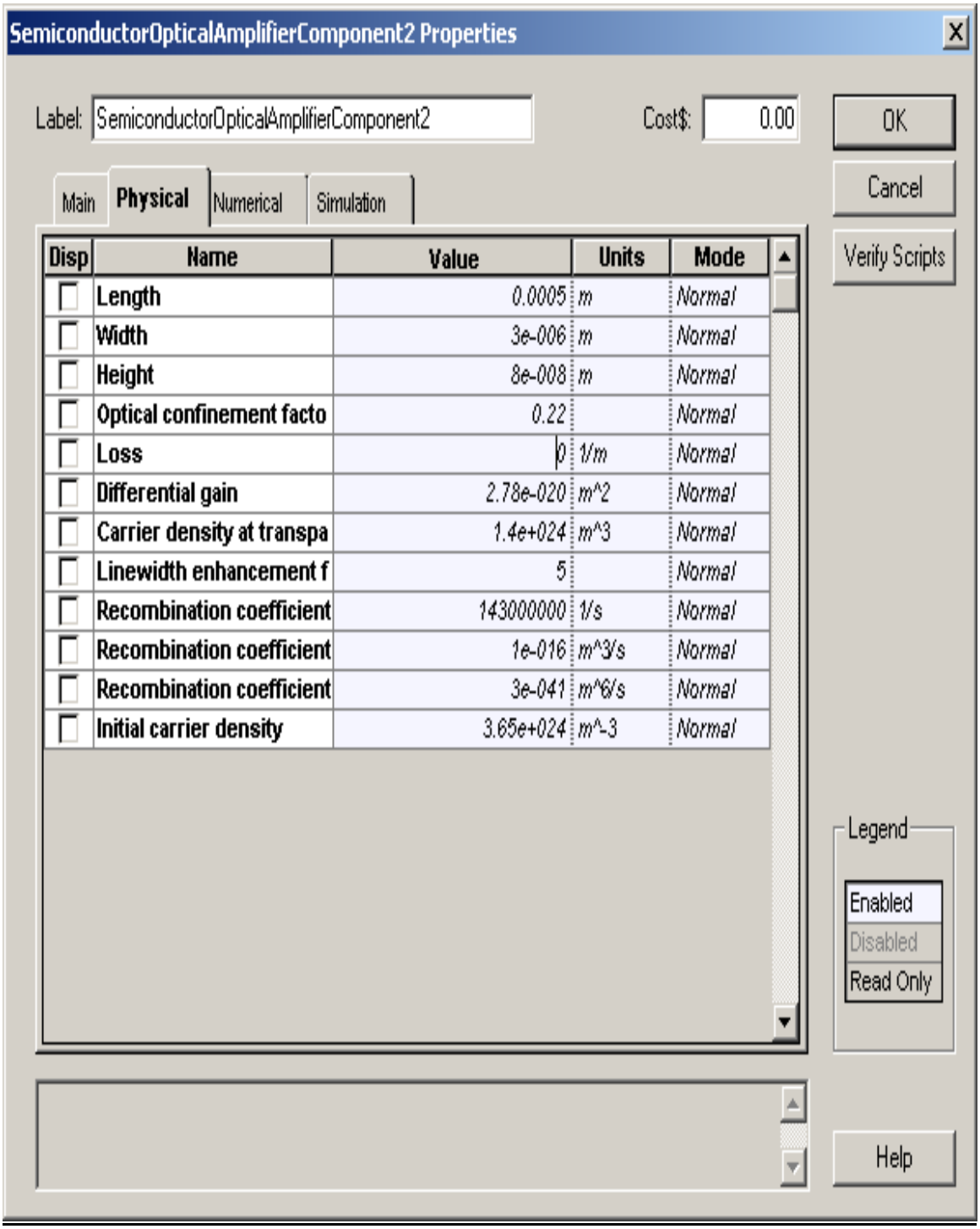

Table 12: Semiconductor optical amplifier parameters (physical)

For the default values of physical parameters of SOA we obtain the following values of the parameters:

Carrier lifetime τ_C ~ 1.4 ns
Saturation energy E_{sat} ~ 3.7 pJ

Amplification factor G_0 =29 dB.

Note that as a typical value of the linewidth enhancement factor, α = 5 is chosen.

Gaussian pulse with the parameters: Energy E_0 ~ 0.73 pJ, T_{FWHM} = 14 ps $\Rightarrow$ P~ 50 mW and the Chirp – linewidth enhancement factor 5 is considered.

To get the required carrier wavelength and power the parameters of the chirped and super optical Gaussian pulse generators have been fixed **(Tables 13 and 14).**

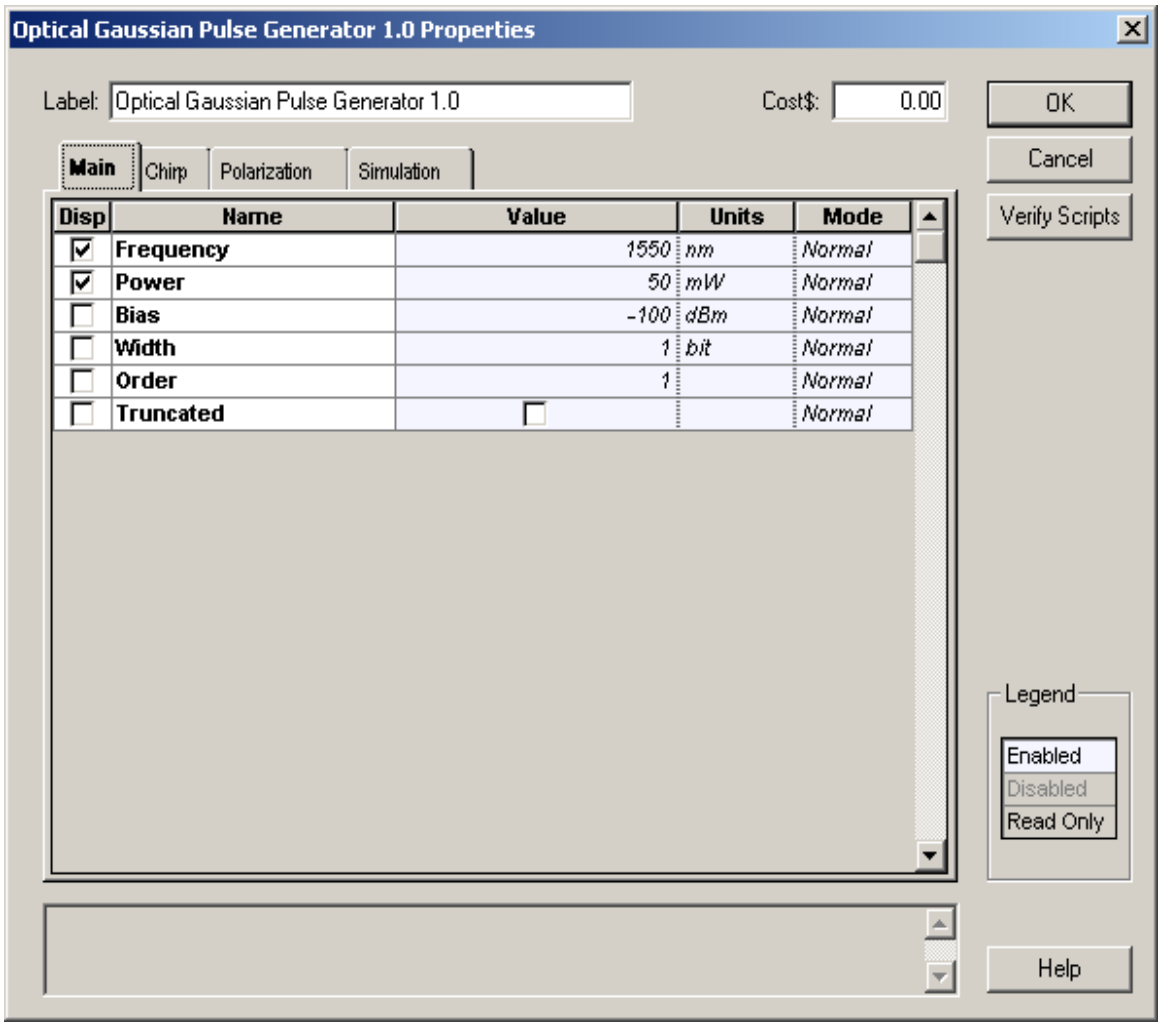

Table 13: Optical Gaussian pulse generator (main)

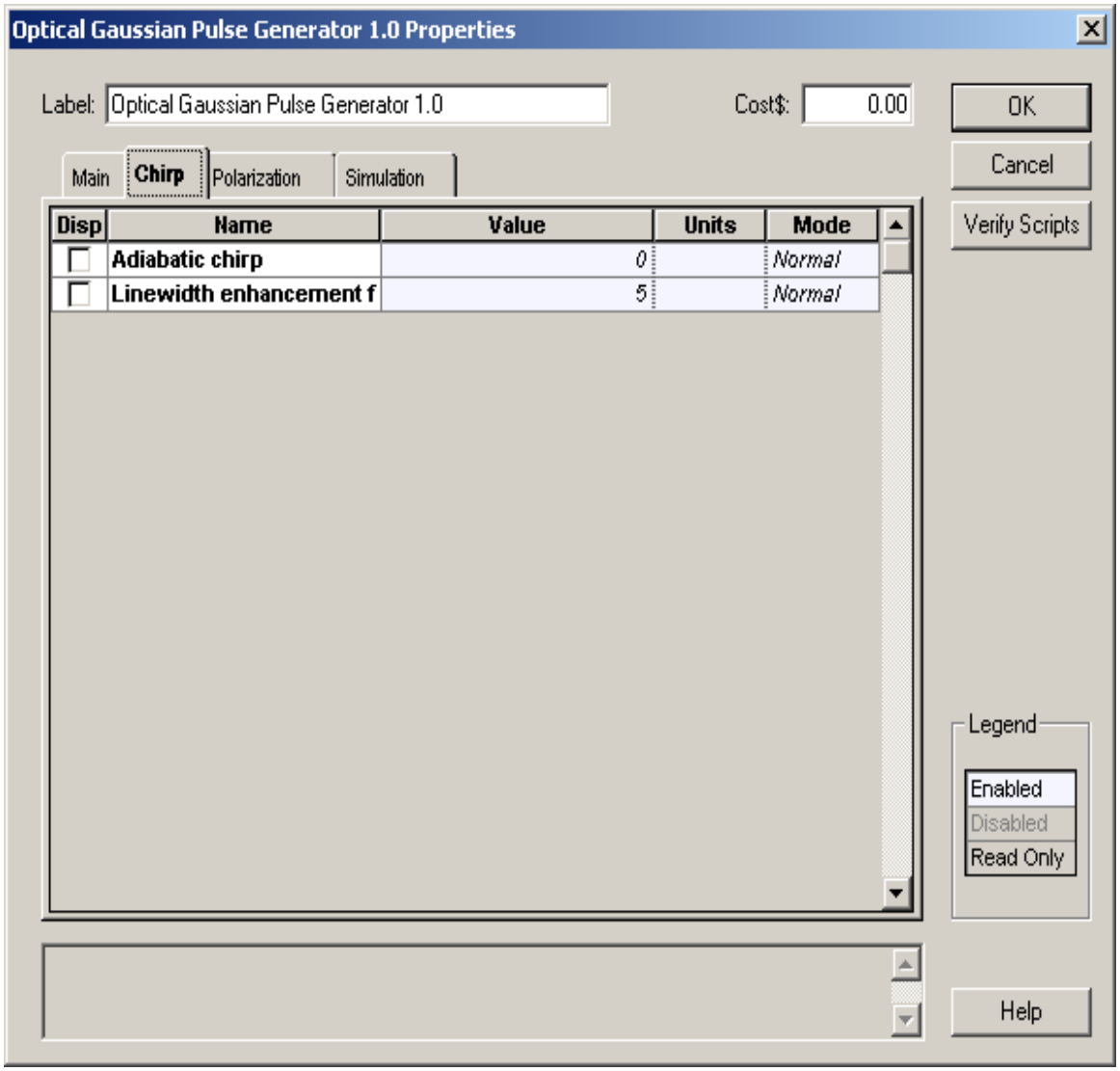

Table 14: Optical Gaussian pulse generator parameters (chirp)

To get chirped and super Gaussian pulse with desired T_{FWHM} = 14 ps, the global parameters have been chosen as shown in **Table 15**.

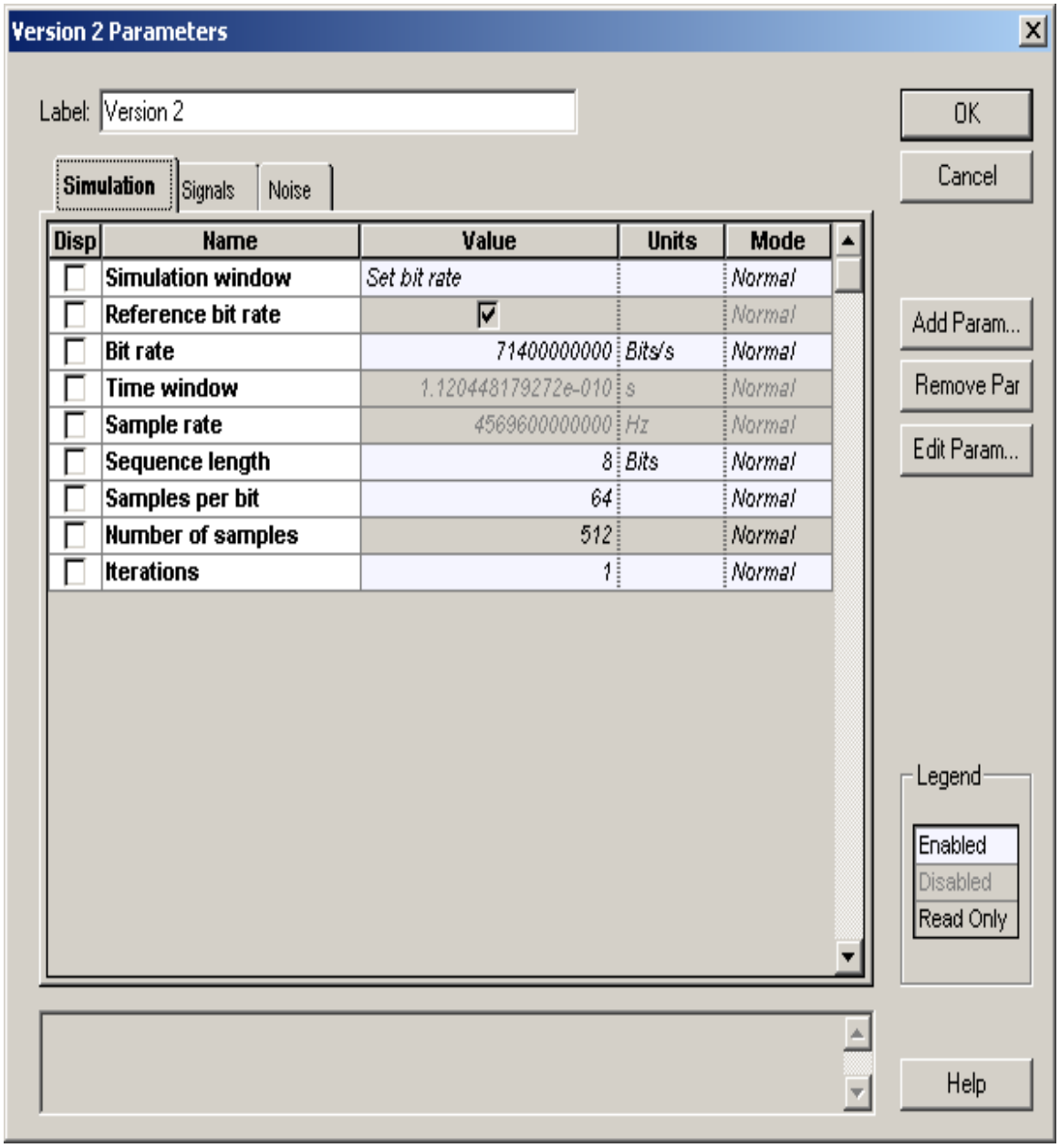

Table 15:Global parameters

As a result, we get, T_0 / τ_C ~ 0.006 and E_0 / E_{sat} ~0.2. According to the first ratio the input pulse width is much smaller than the carrier lifetime. The meaning of the second one is that pulse energy is comparable with the SOA saturation energy.

The project in the framework of which the amplification of the Gaussian pulse with SOA will be analyzed is shown in Fig. 55.

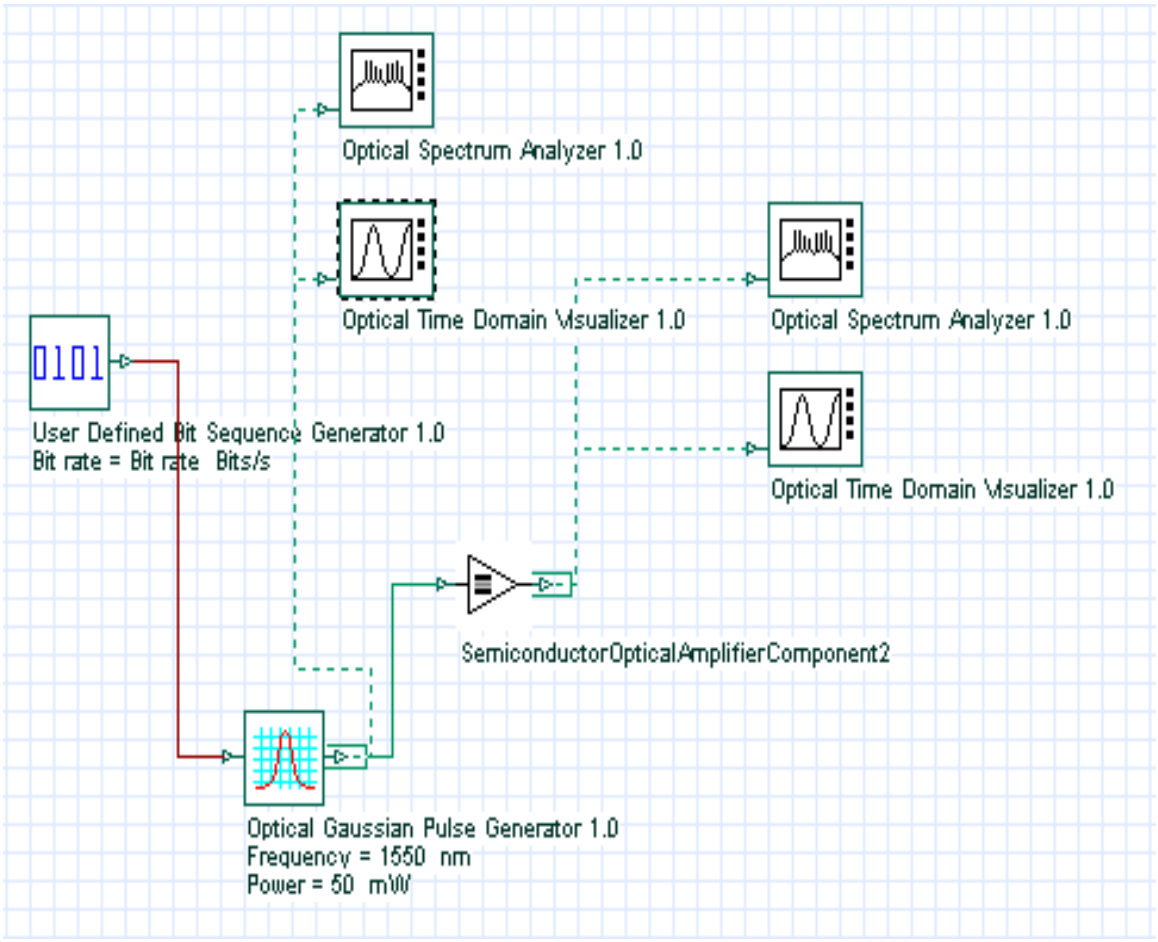

Fig. 55: Layout: SLA gain saturation of chirped and super- Gaussian pulses

The shape and spectrum of the initial chirped Gaussian pulse are shown in **Figs. 56** and **57**. Note that the initial negative chirp is also shown in **Fig. 56**.

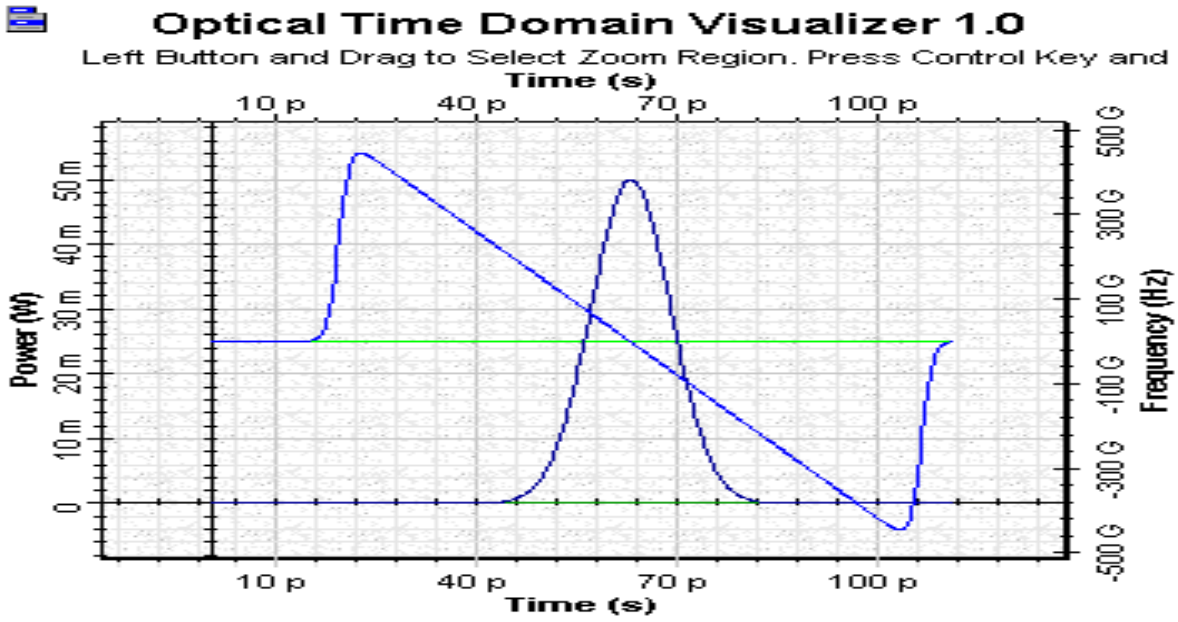

Fig. 56: Shape of the initial chirped Gaussian pulse

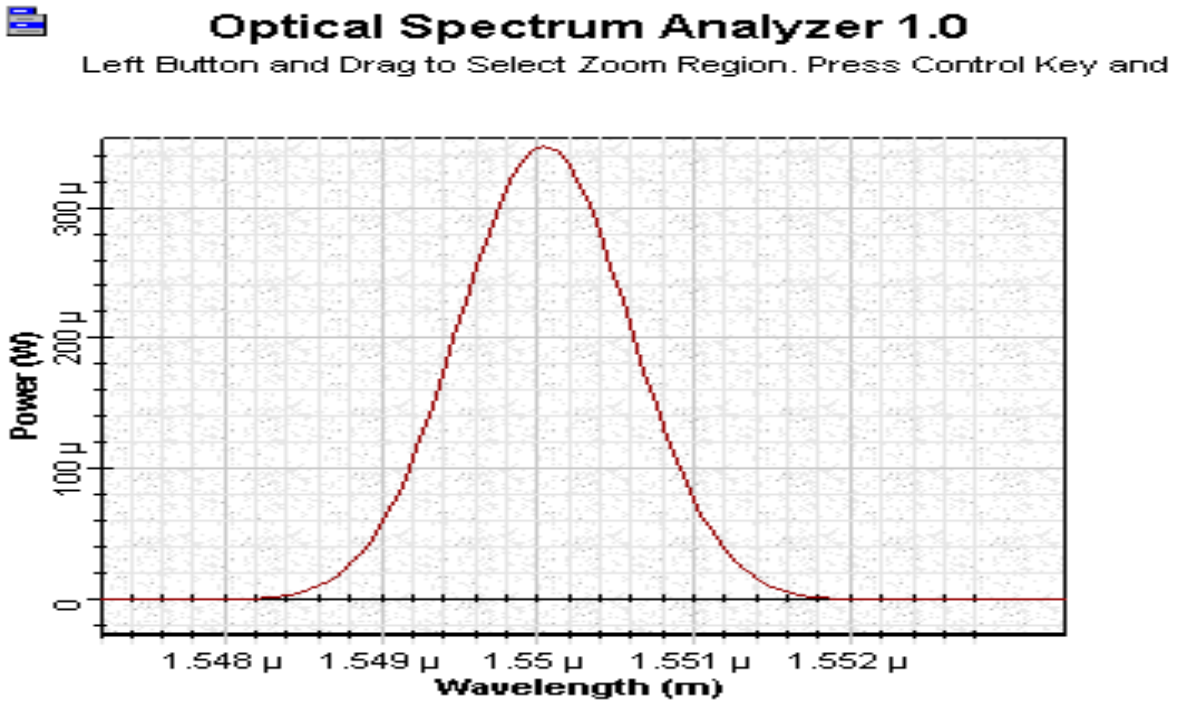

Fig.57: Spectra of the initial chirped Gaussian pulse

Note that the frequency in the Fig. 56 decreases with time across the pulse that is usually referred to as negative chirp.

Figs. 58 and 59 show the shape and spectrum of the amplified chirped pulse.

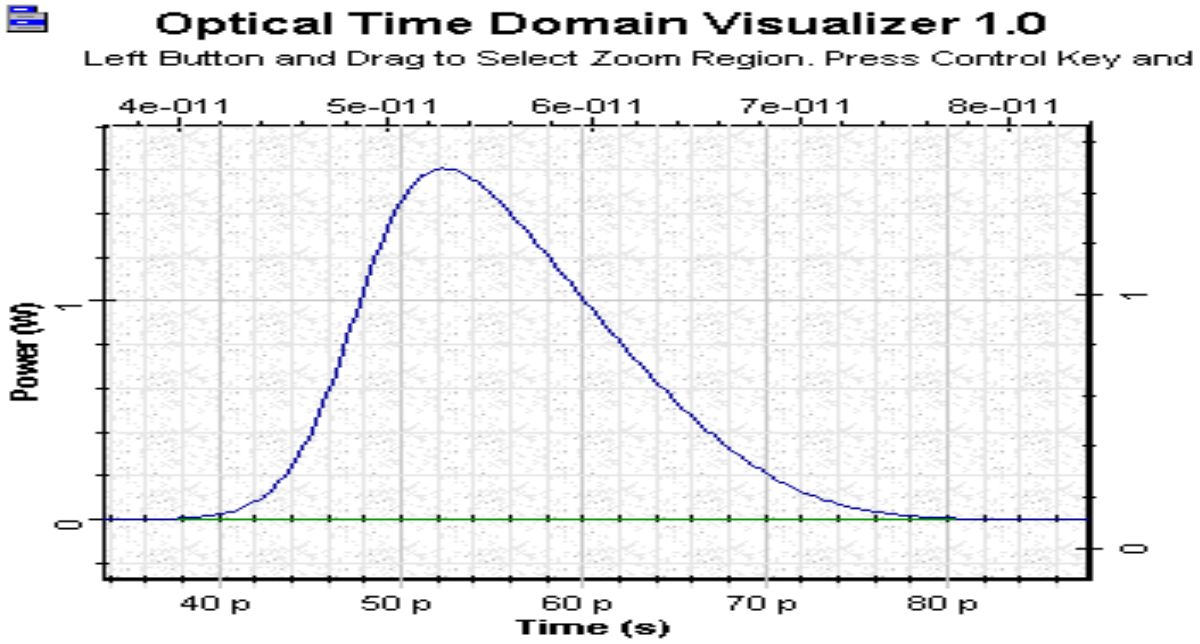

Fig.58: Shape of the amplified chirped pulse

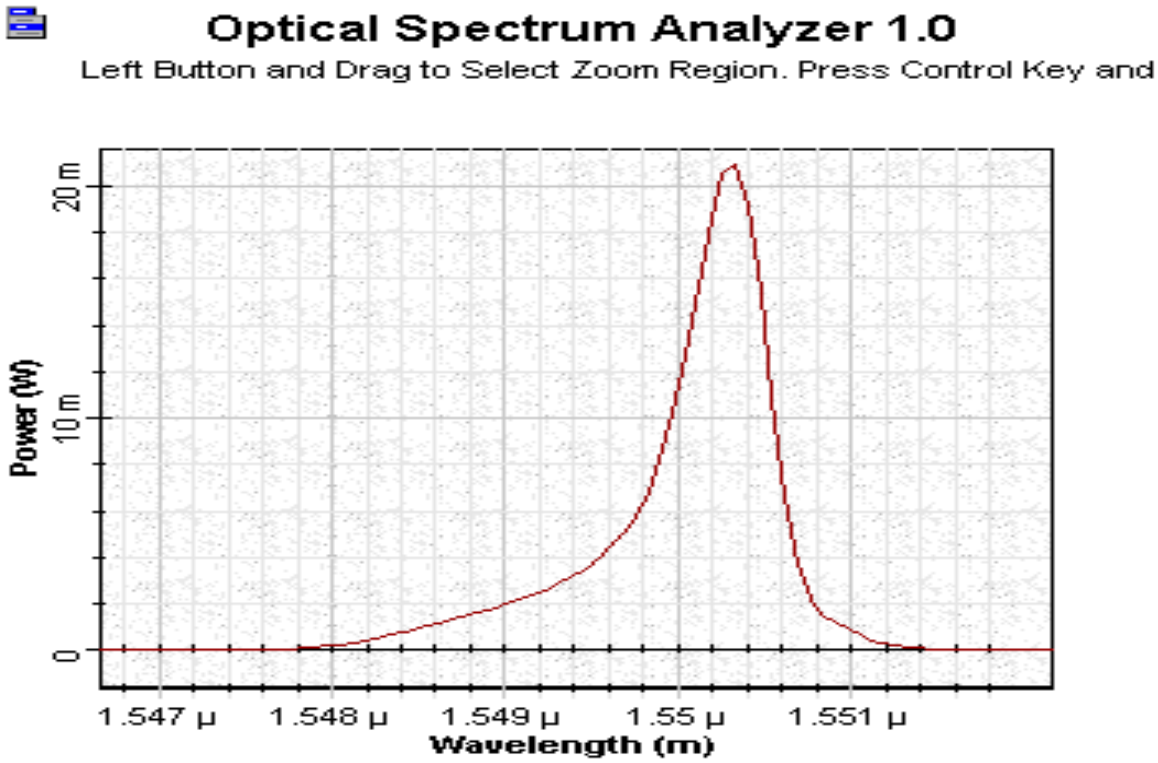

Fig. 59: Spectrum of the amplified chirped pulse

Fig. 58 reveals already expected sharpening of the leading edge. Note the different form of the output pulse spectrum and the reduced red shift in comparison with the amplified Gaussian pulse.

In Fig. 60, phase of the pulse with the gain saturation induced chirp across the pulse is shown together with its shape. In Fig. 61 the deformation of the initial negative chirp after amplification can be easily seen.

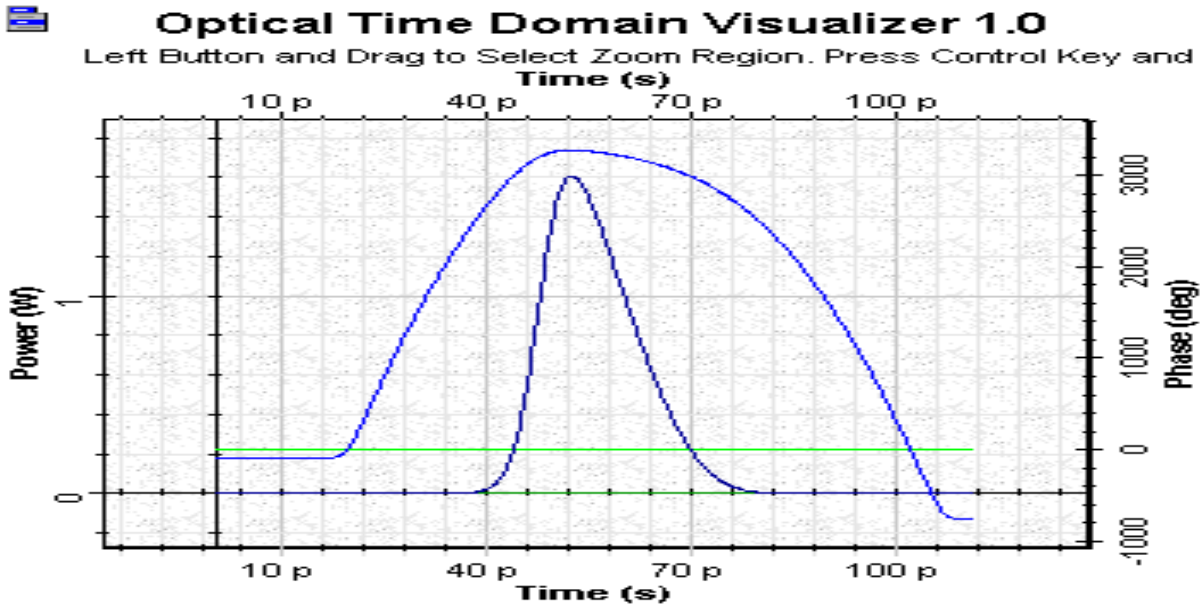

Fig.60: Shape and phase of the pulse with the gain saturation induced chirp across the pulse

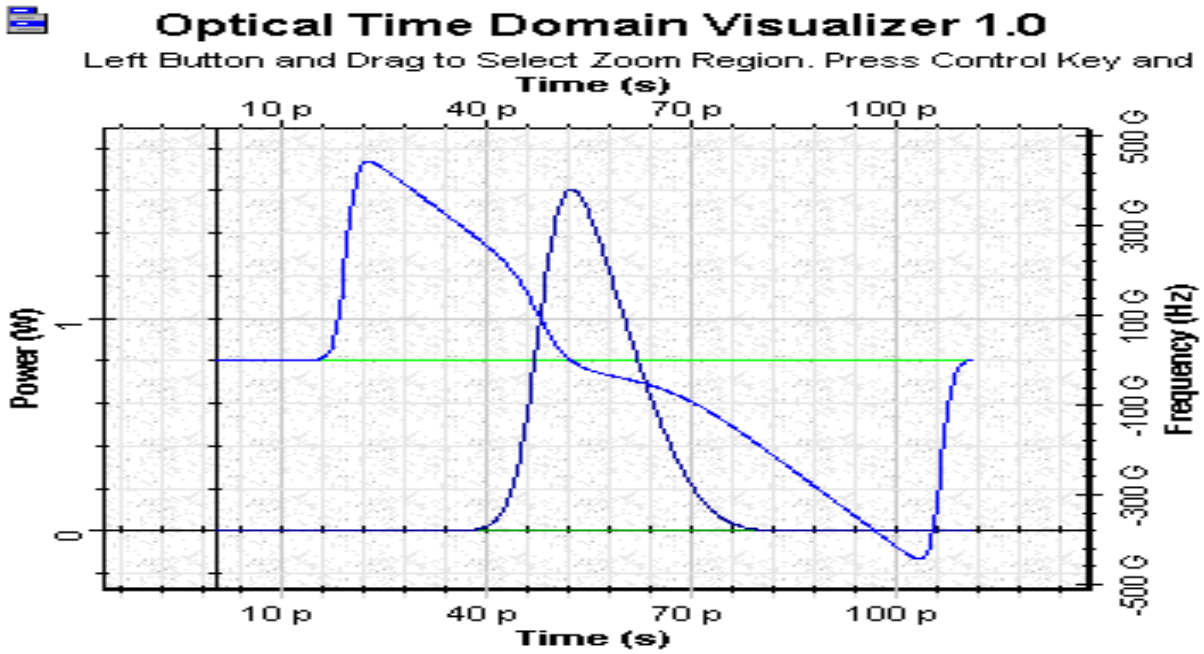

Fig.61: Deformation of the initial negative chirp after amplification

For negative initial chirp the gain saturation induced red shift reduces. For the opposite sign of initial chirp the spectrum shifts even more to the red side than for the case of zero initial chirp.

Saturation of amplification of super - Gaussian pulse

The additional pulse parameter which is considered for the super Gaussian pulse is m = 3 (Note that the pulse now will be without initial chirp).

To get the additional order parameter following change in the optical Gaussian pulse generator has been done **(Table 16).**

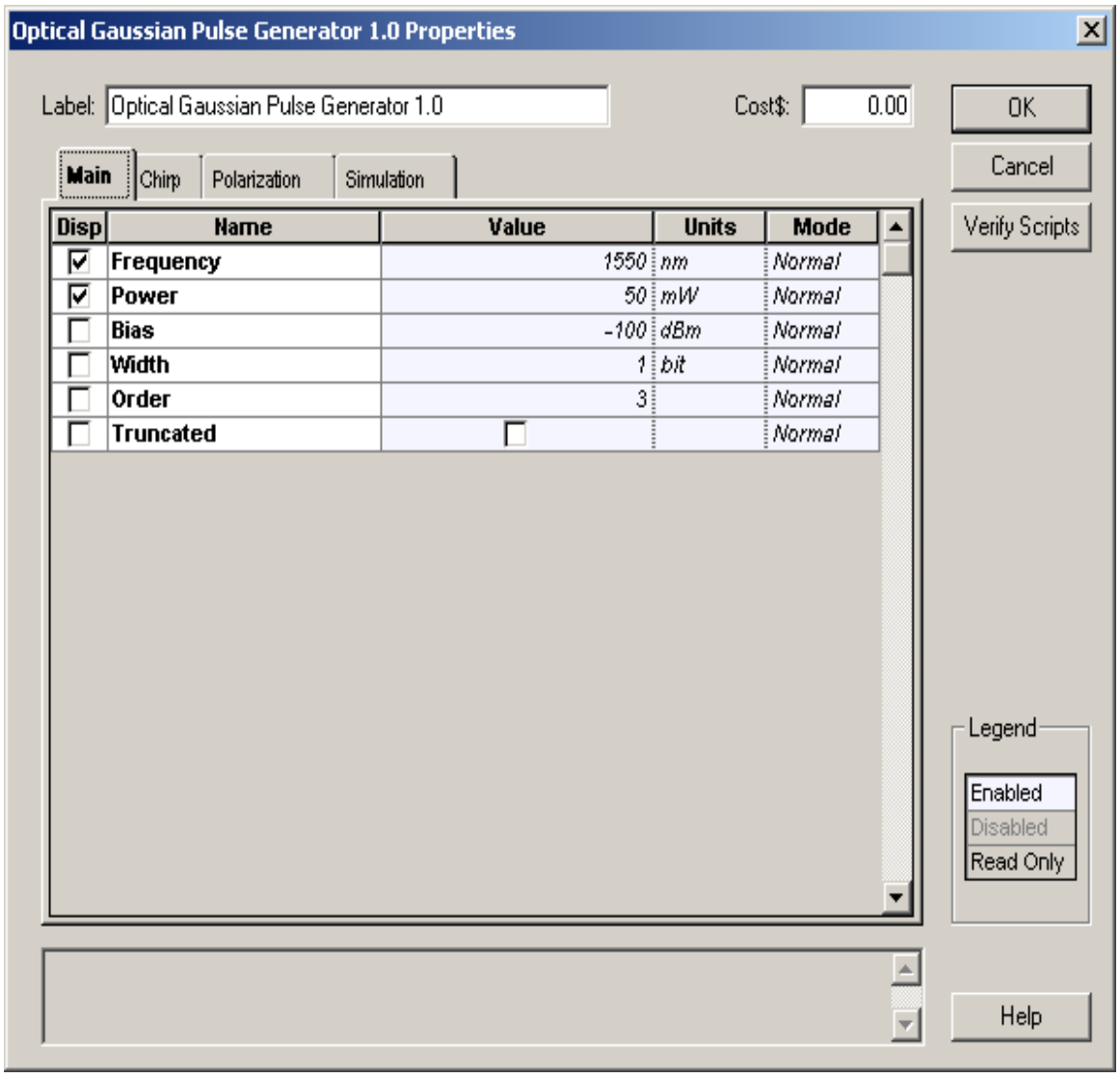

Table 16: Optical Gaussian pulse generator parameters (main)

The shape and spectrum of the initial super Gaussian pulse are shown in Figs. 62 and 63.

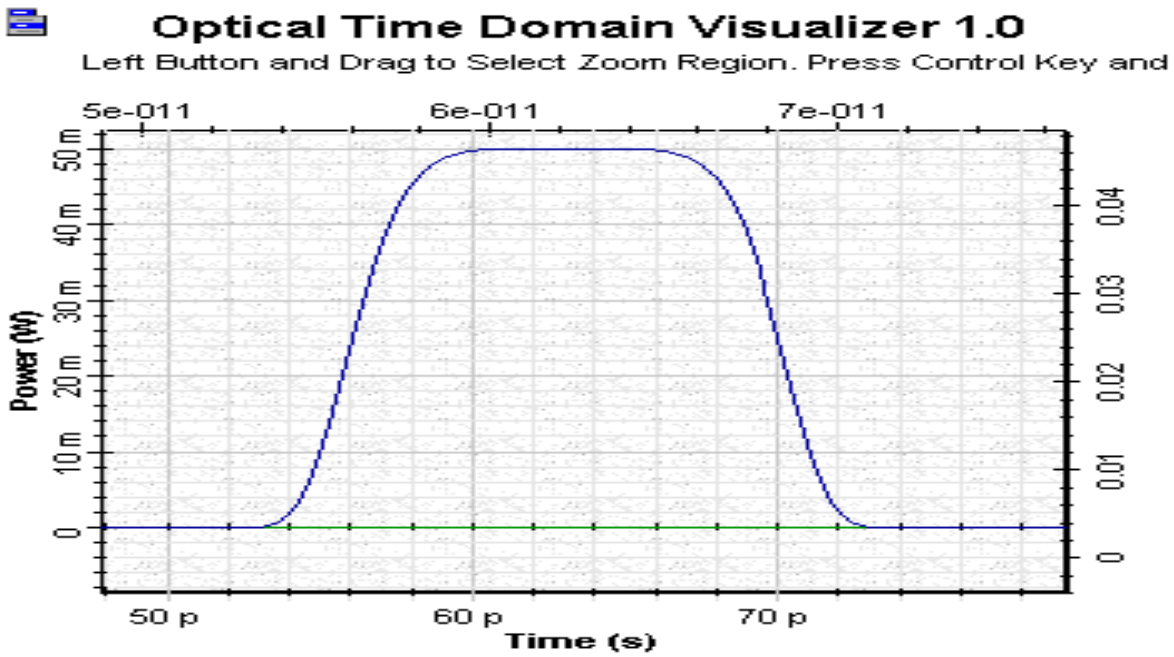

Fig.62: Shape of the initial super Gaussian pulse

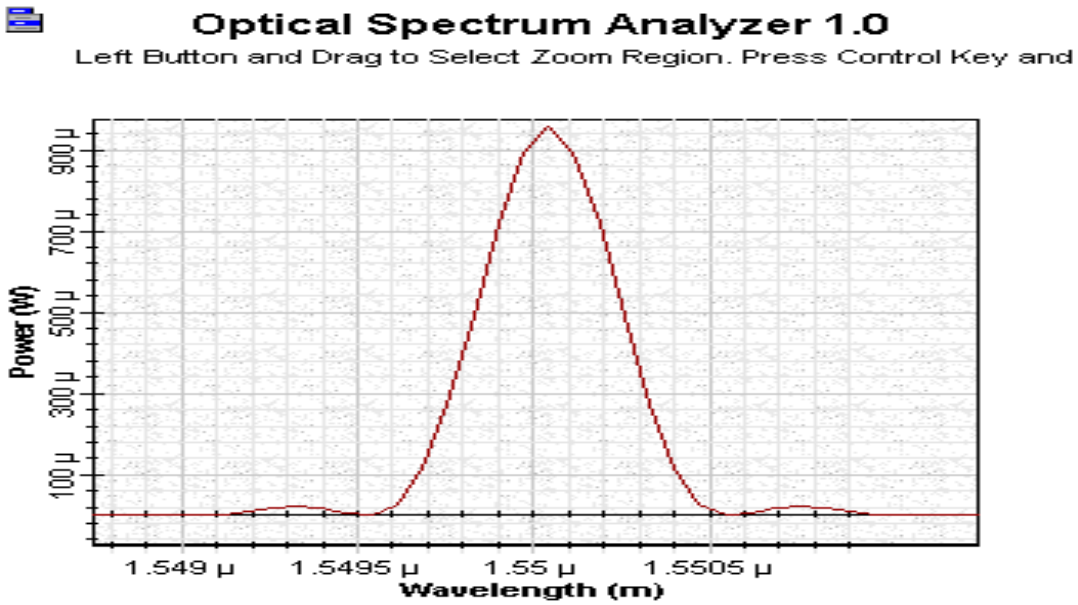

Fig.63: Spectrum of the initial super Gaussian pulse

Figs. 64 and 65 show the shape and spectrum of the amplified super Gaussian pulse.

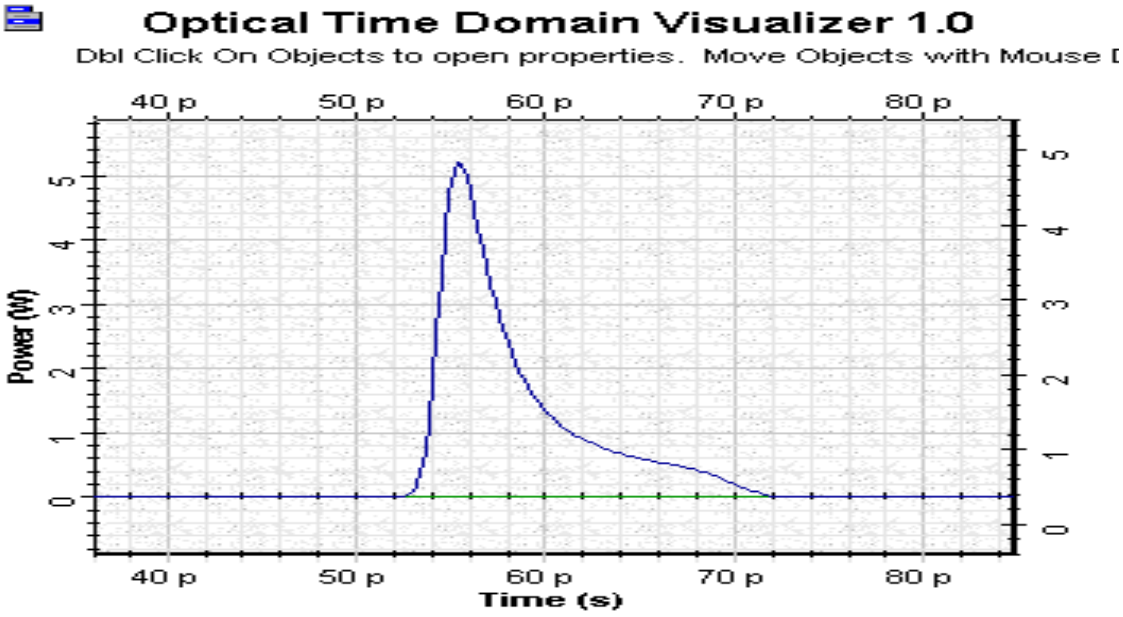

Fig.64: Shape of the amplified super Gaussian pulse

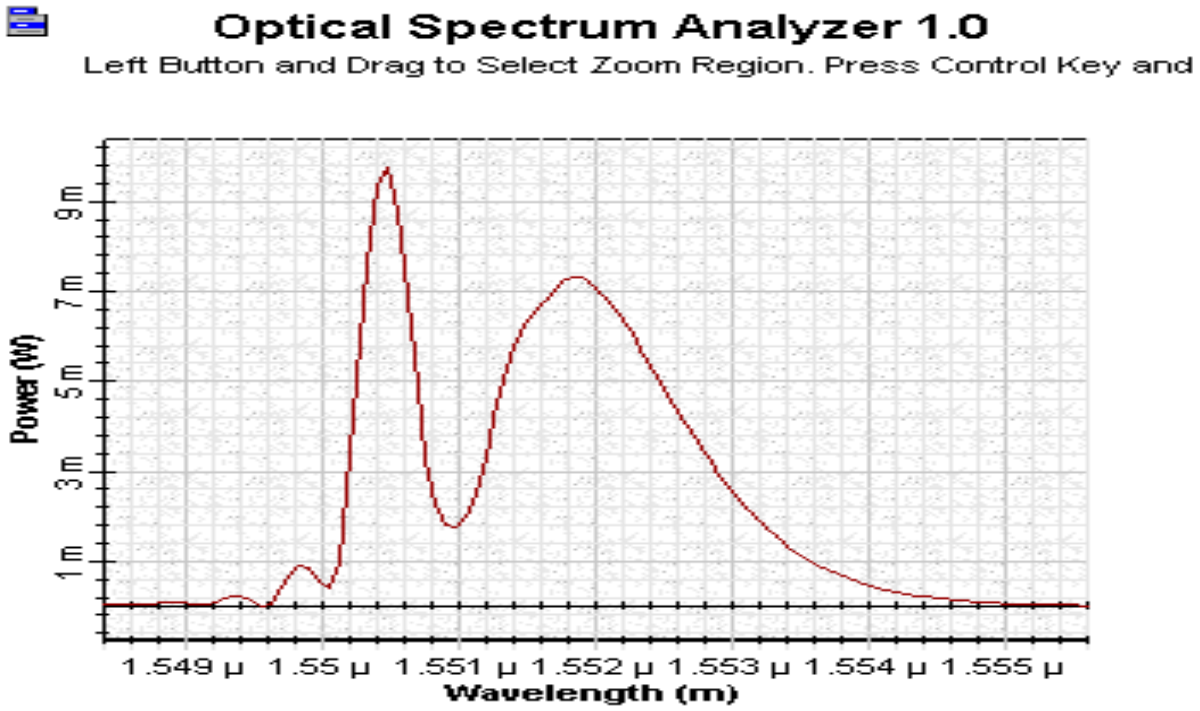

Fig.65: Spectrum of the amplified super Gaussian pulse

The output pulse has a long tail on the trailing edge and appears to be narrower than the input pulse. The situation is very different from the case of amplification of Gaussian pulse where the T_{FWHM} of the output pulse was larger than the input one.

The spectrum of the output spectrum has a multi-peak structure and very well expressed red shift. Comparision of this spectrum with the one of the amplified Gaussian pulse show a clear difference. Therefore the form of the spectrum and amount of the red shift strongly depends on the initial pulse shape.

In Fig. 66, phase of the pulse with the gain saturation induced chirp across the pulse is shown together with its shape. In Fig. 67 the deformation of the initial negative chirp after amplification can be easily seen.

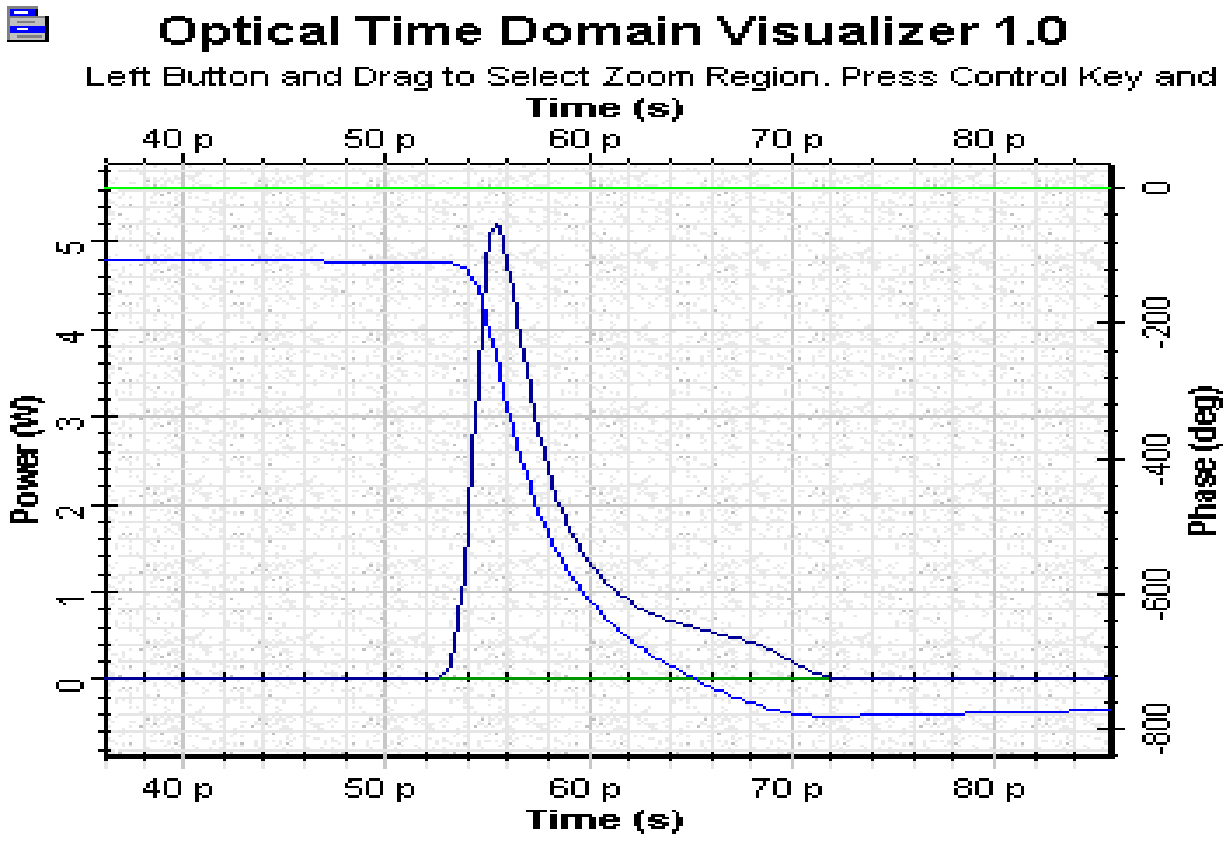

Fig.66: Shape and phase of the pulse with the gain saturation induced chirp across the pulse

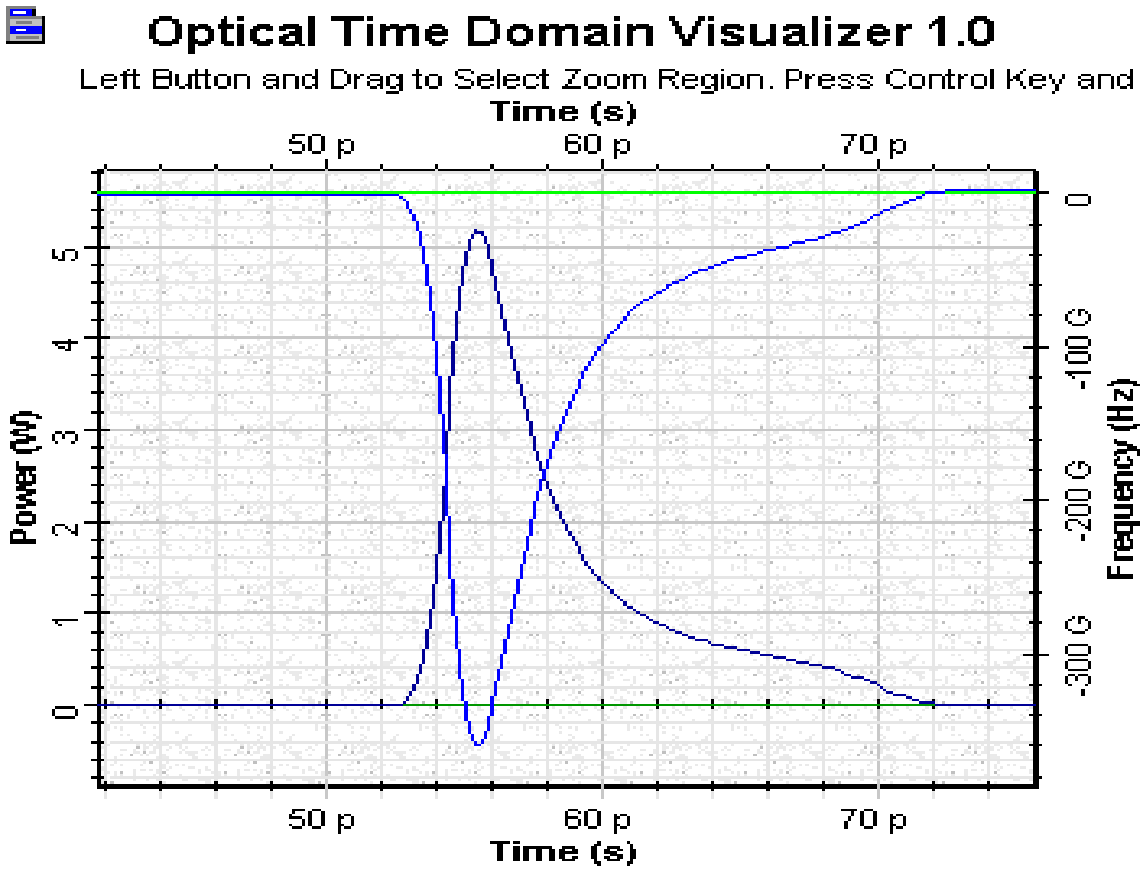

Fig.67: Deformation of the initial negative chirp after amplification

In this project we described the basic properties of the chirped and super Gaussian pulse amplification with SOA component of OptiSys software. We have shown that the shape and spectrum pulse distortions with the amplification of SOA strongly depends on the shape and initial frequency modulation of the pulse. These properties can be very important in the case when pulses produced by directly modulated semiconductor lasers are amplified.

The obtained results are in complete agreement with results published in [1] and [2]:

References:

[1]G.P. Agrawal and N.A. Olsson, “Self_phase modulation and spectral broadening of optical pulses in semiconductor laser amplifiers”, IEEE Journal of Quantum electronics, vol. 25, pp.2297-2306, 1989.
[2]G.P. Agrawal, “Fiber-Optic Communication Systems”, second edition, John Wiley &Sons, INC., 1997.

Example: SLA Gain Saturation of Gaussian Pulses

SLA gain saturation of Gaussian pulses**.osd**

Amplification of ultra-short optical pulses in SOA produces considerable spectral broadening and distortion due to the non-linear phenomenon of self-phase modulation. The physical mechanism behind SPM is gain saturation, which leads to intensity dependent changes of refractive index in response to variations in carrier density. Signal-gain saturation in SOA is caused by a reduction of the population inversion in the active layer due to an increase in stimulated emission. Gain saturation characteristics are especially important in optical repeaters and multi-channel amplifiers which require high-power operation.

In this project the effect of gain saturation induced self-phase modulation on the amplification of Gaussian pulse will be considered. We will consider the pulses with pulse width much shorter than the carrier lifetime. The carrier wavelength of the Gaussian pulse is 1.55 μm.

Table 17 shows the SOA parameters used in the project.

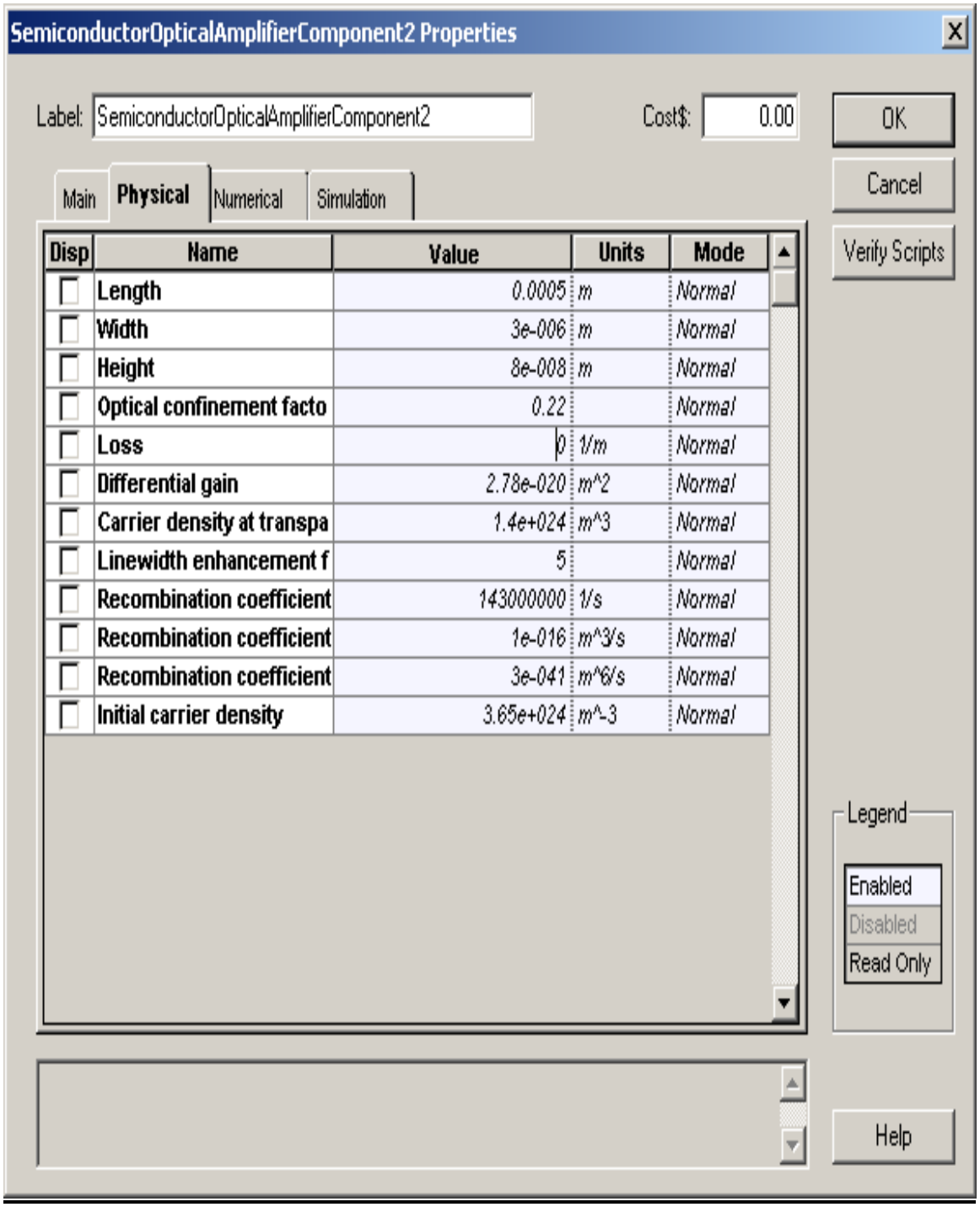

Table 17: Semiconductor optical amplifier parameters (physical)

For these default values of physical parameters of SOA we obtain the following values of parameters:

The carrier lifetime τ_C ~ 1.4 ns

The saturation energy E_{sat} ~ 3.7 pJ

The amplification factor G_0 =29 dB.

As a typical value of the linewidth enhancement factor, α = 5 is chosen. Note that we have chosen the internal losses to be zero. Such choice allows a comparison to be done with existing analytical solution (see the referred paper at the end of this section). We will also analyze the influence of the internal losses.

Gaussian pulse with following parameters is considered: Energy E_0 ~ 0.73 pJ and T_{FWHM} = 14 ps $\Rightarrow$ P~ 50 mW. Note the large value of the pulse initial power. It allows in a best way to demonstrate the basic qualitative features of gain-saturation induced properties of the pulse amplification. The influence of the value of the pulse initial power will be considered later in this section.

To get the required carrier wavelength and power the parameters of the optical Gaussian pulse generator have been fixed as given in the **Table 18**.

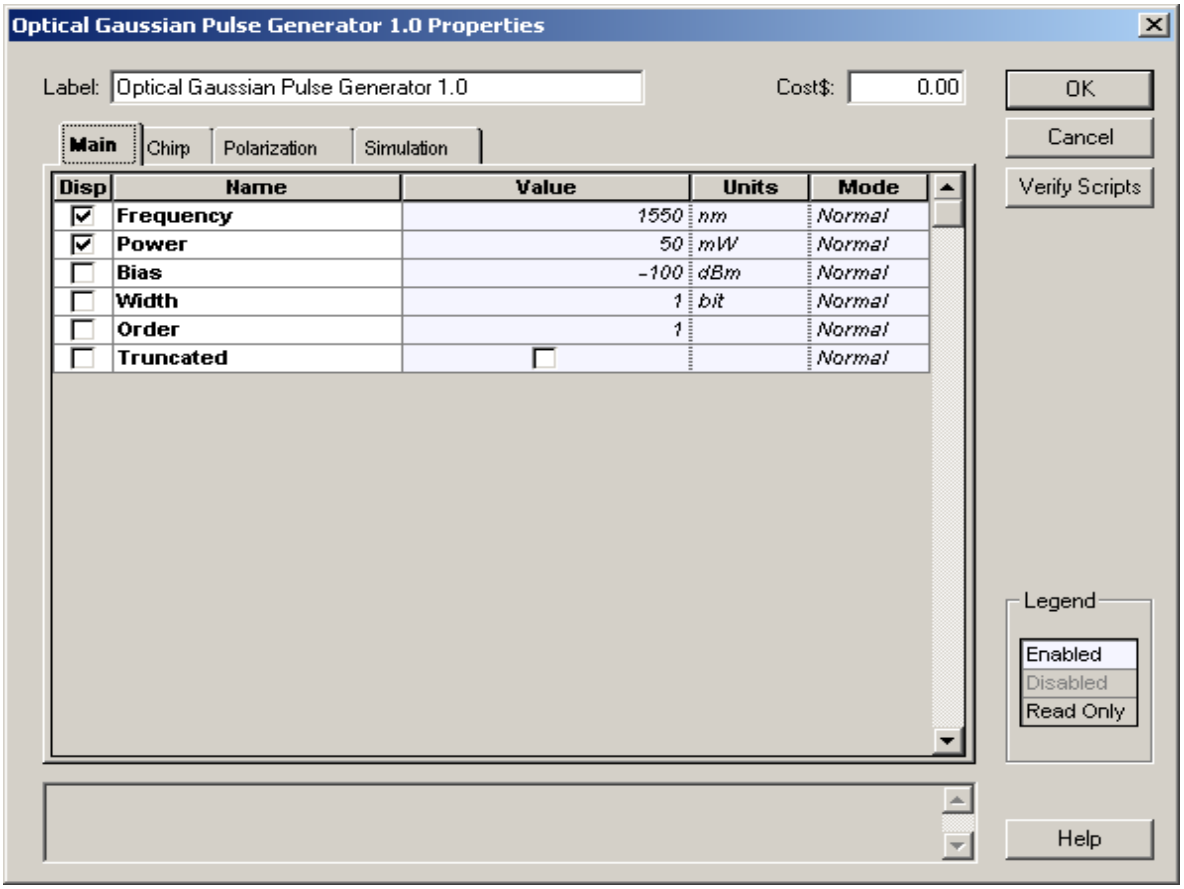

Table 18:Optical Gaussian pulse generator parameters (main)

To get Gaussian pulse with desired T_{FWHM} = 14 ps, the global parameters have been chosen as given in **Table 19.**

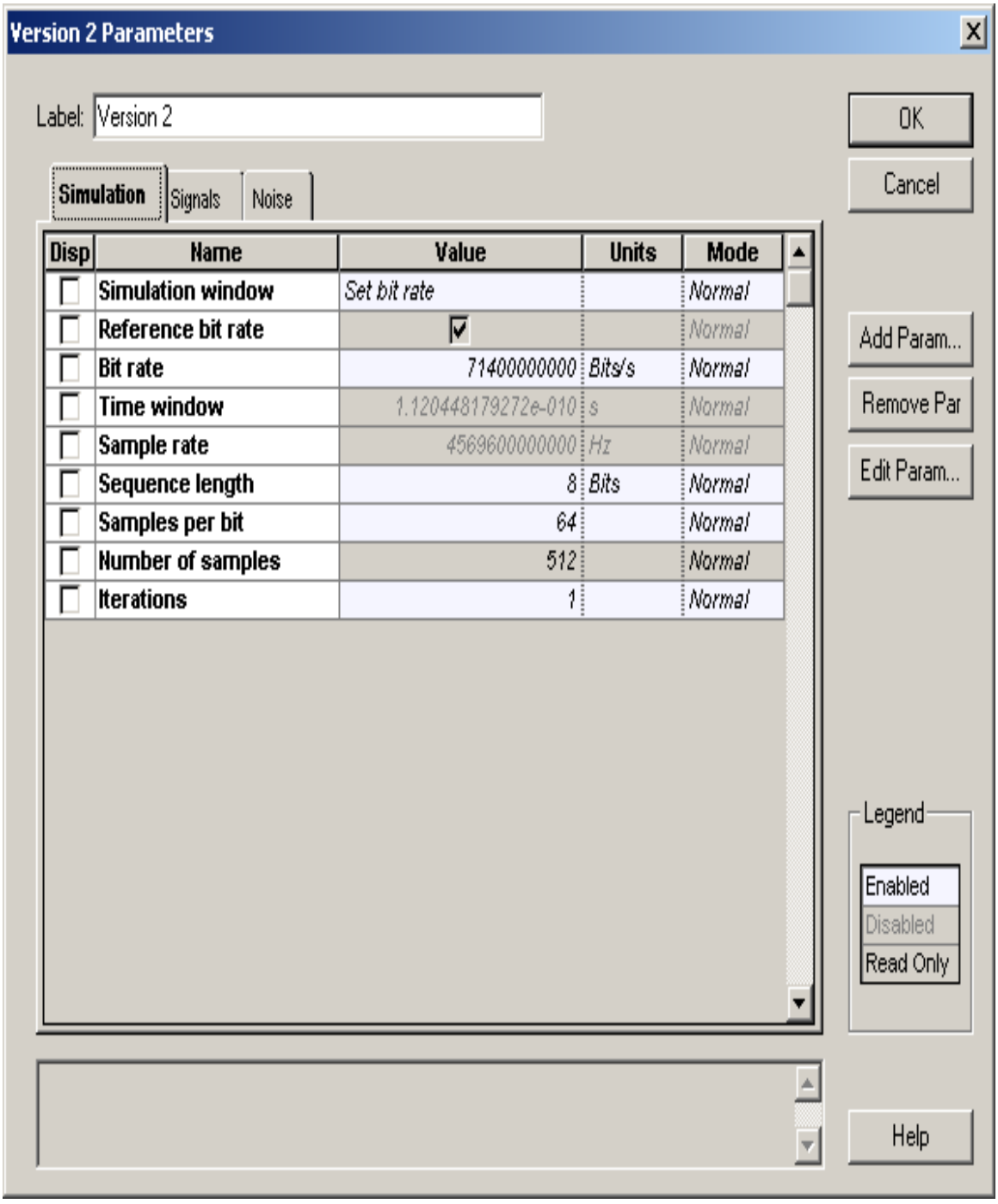

Disp	Name	Value	Units	Mode
☐	Simulation window	Set bit rate		Normal
☐	Reference bit rate	☑		Normal
☐	Bit rate	71400000000	Bits/s	Normal
☐	Time window	1.120448179272e-010	s	Normal
☐	Sample rate	4569600000000	Hz	Normal
☐	Sequence length	8	Bits	Normal
☐	Samples per bit	64		Normal
☐	Number of samples	512		Normal
☐	Iterations	1		Normal

Table 19: Global parameters

As a result we get T_0/τ_C ~ 0.006 and E_0 / E_{sat} ~0.2.

According to the first ratio the input pulse width is much smaller than the carrier lifetime. The meaning of the second one is that pulse energy is comparable with the SOA saturation energy.

The project layout for amplification of the Gaussian pulse with SOA is shown in Fig. 68.

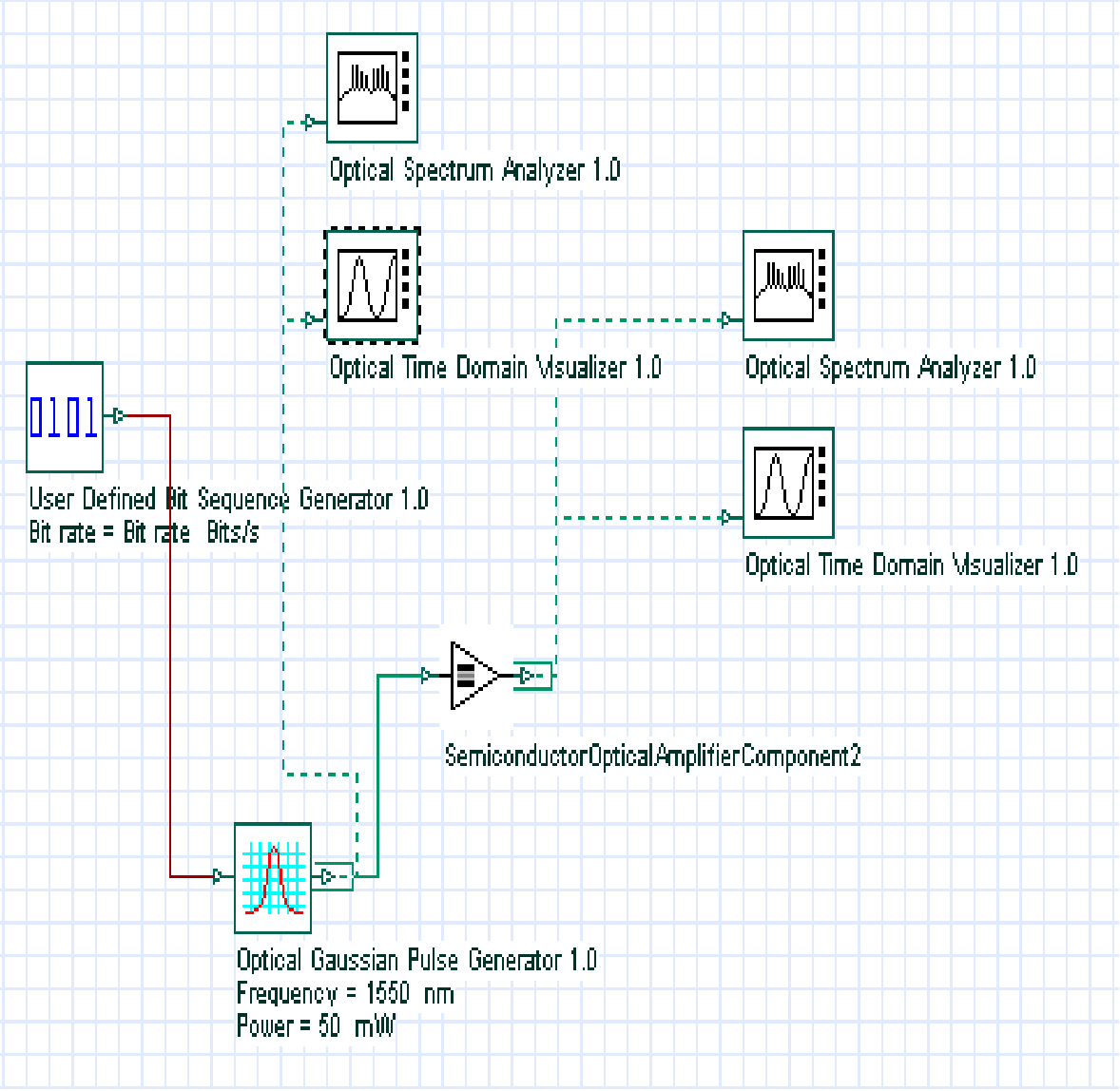

Fig. 68: Layout: SLA gain saturation of Gaussian pulses

To illustrate the appearance of the gain saturation induced effects first we will show the amplification of very weak pulse. The shape and spectrum of the weak Gaussian pulse are shown in Figs. 69 and 70.

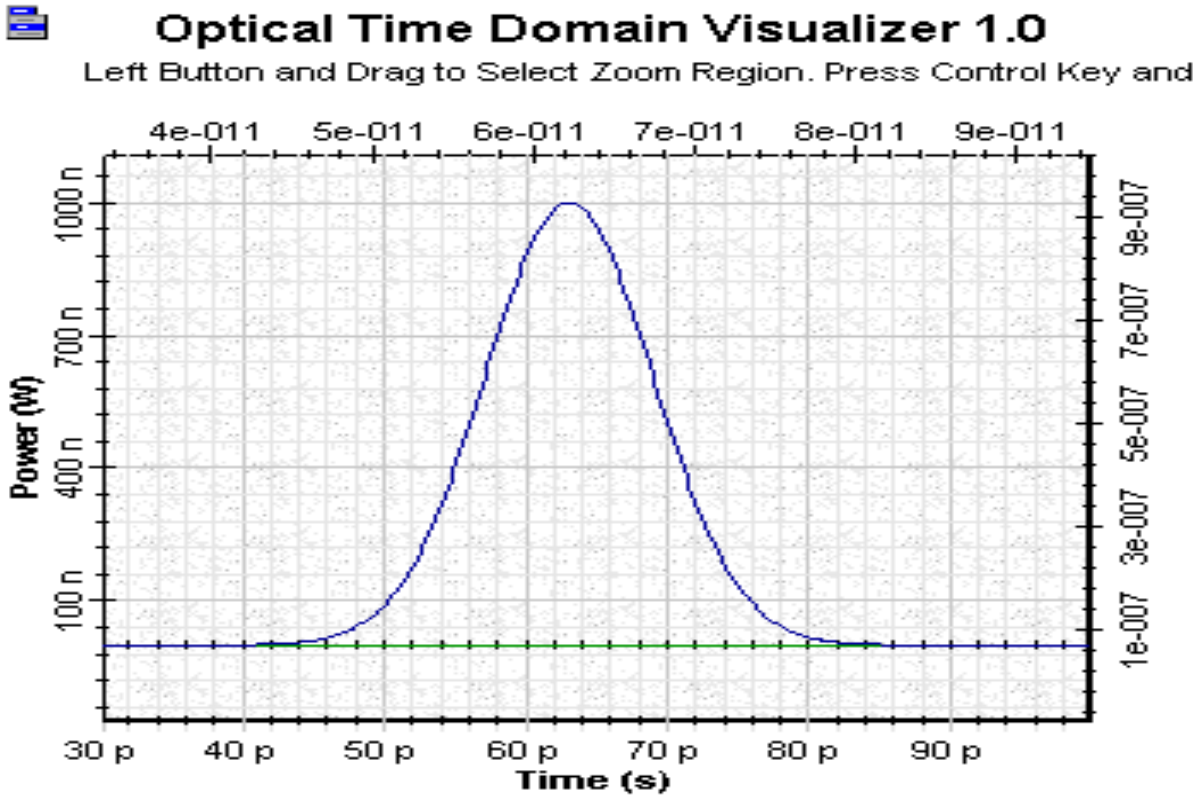

Fig. 69: Shape of the weak Gaussian pulse

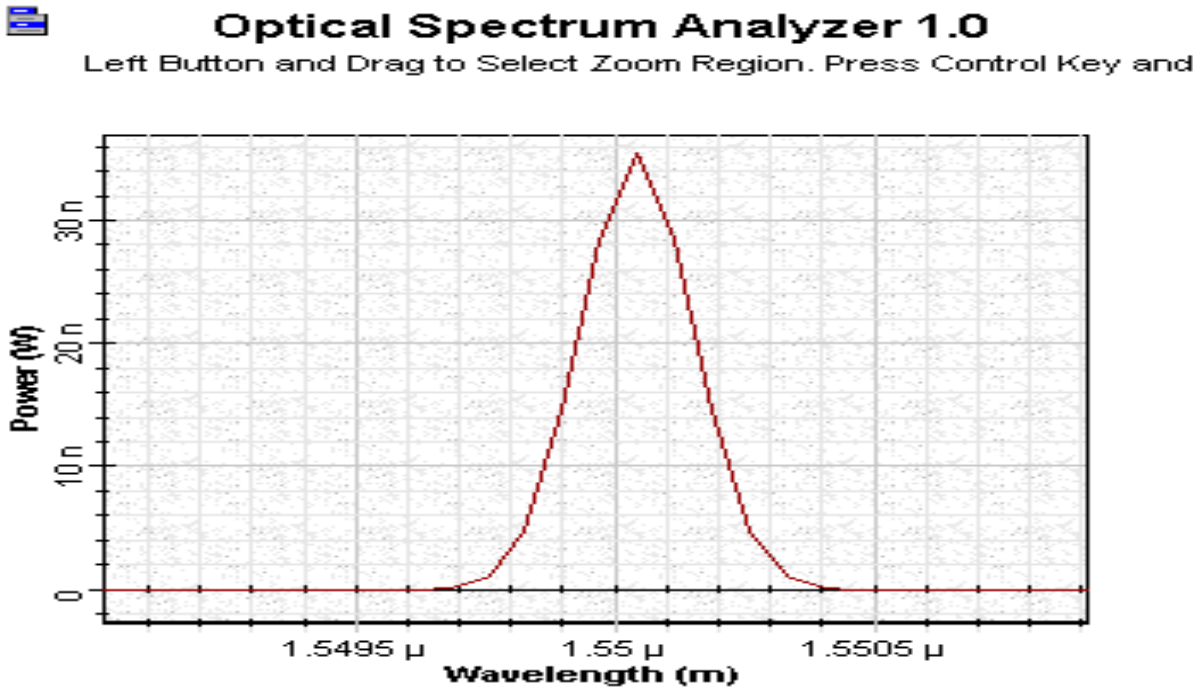

Fig.70: Spectrum of the weak Gaussian pulse

Figs. 71 and 72 show the shape and spectrum of the amplified weak pulse.

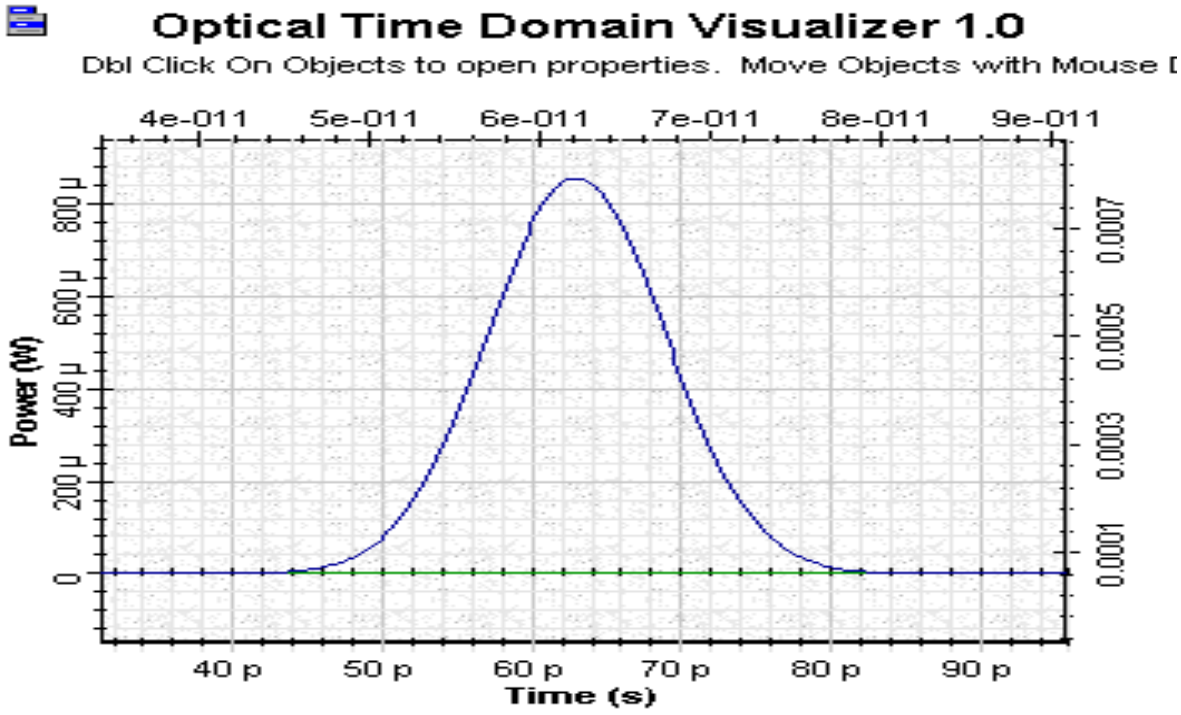

Fig.71: Shape of the amplified weak pulse

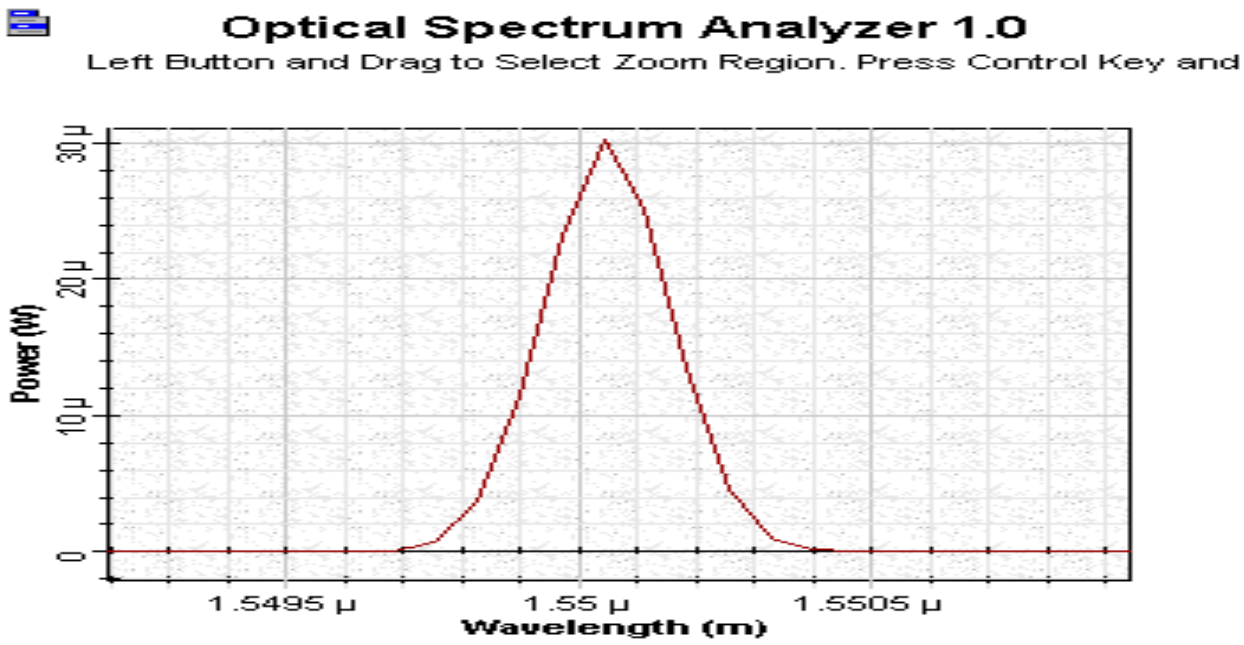

Fig.72: Spectrum of the amplified weak pulse

Comparison of the above figures shows that the pulse is amplified in unsaturated region. No qualitative changes in the spectra of the amplified pulse could be observed.

Figs. 73 and 74 show the shape and spectrum of the initial Gaussian pulse, which will be amplified in saturation region.

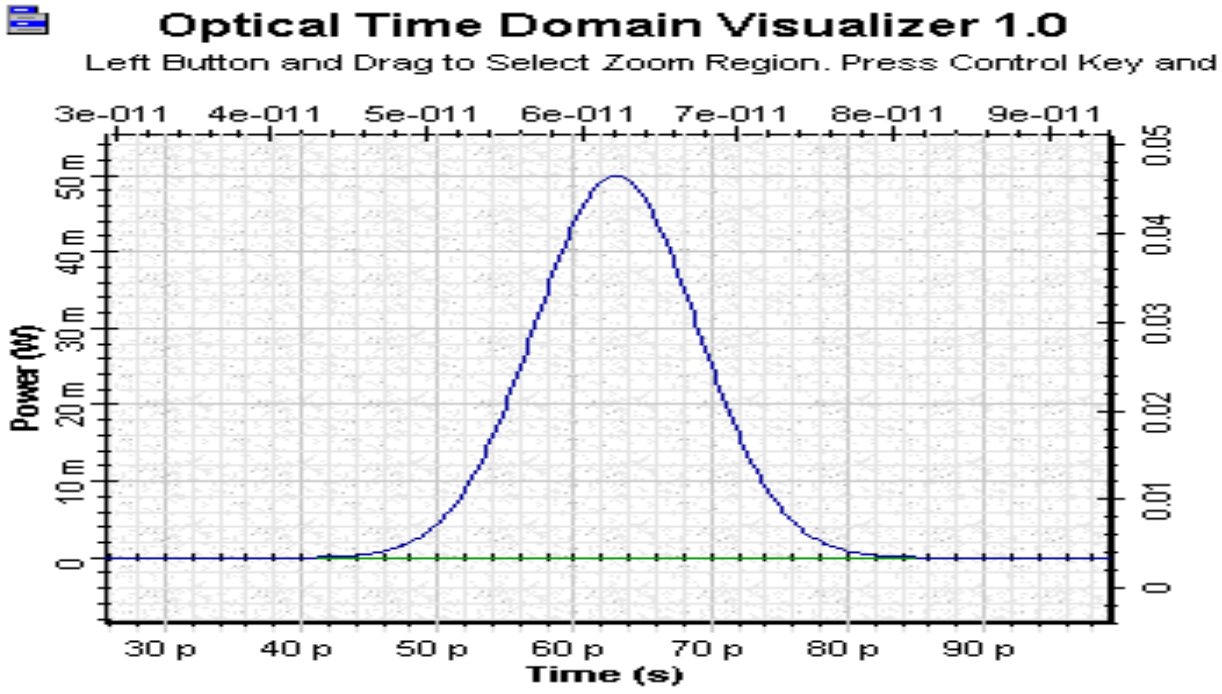

Fig.73: Shape of the initial Gaussian pulse

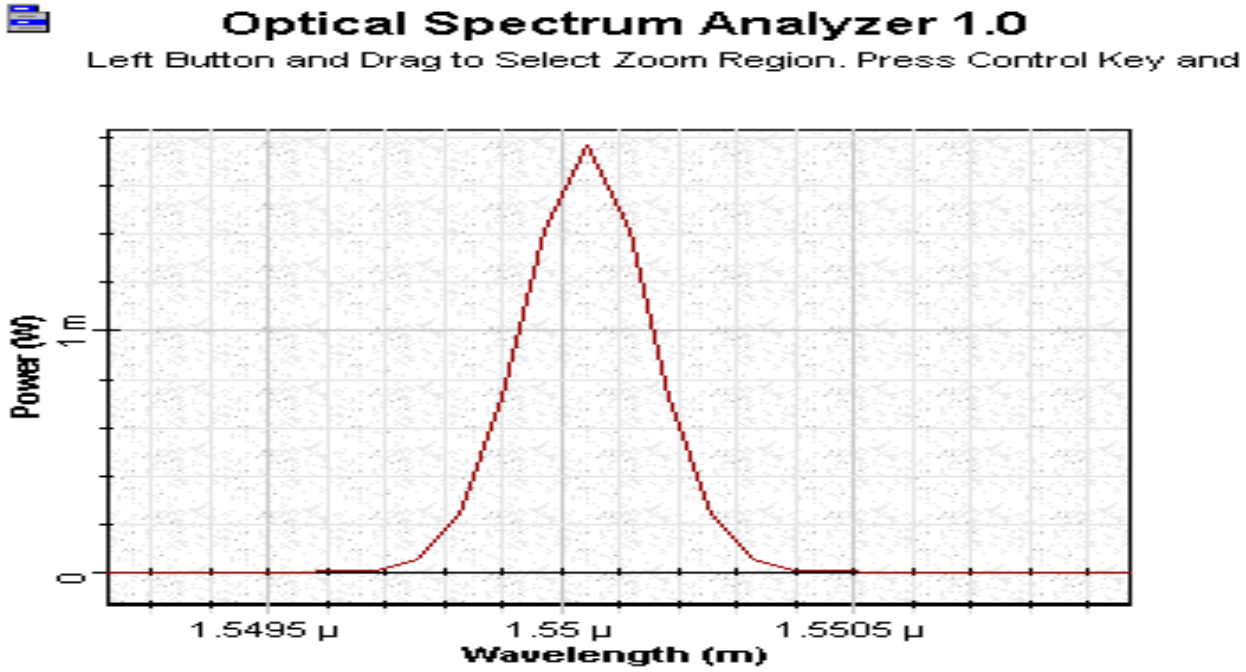

Fig.74: Spectrum of the initial Gaussian pulse

Figs. 75 and 76 show the shape and spectrum of the amplified pulse.

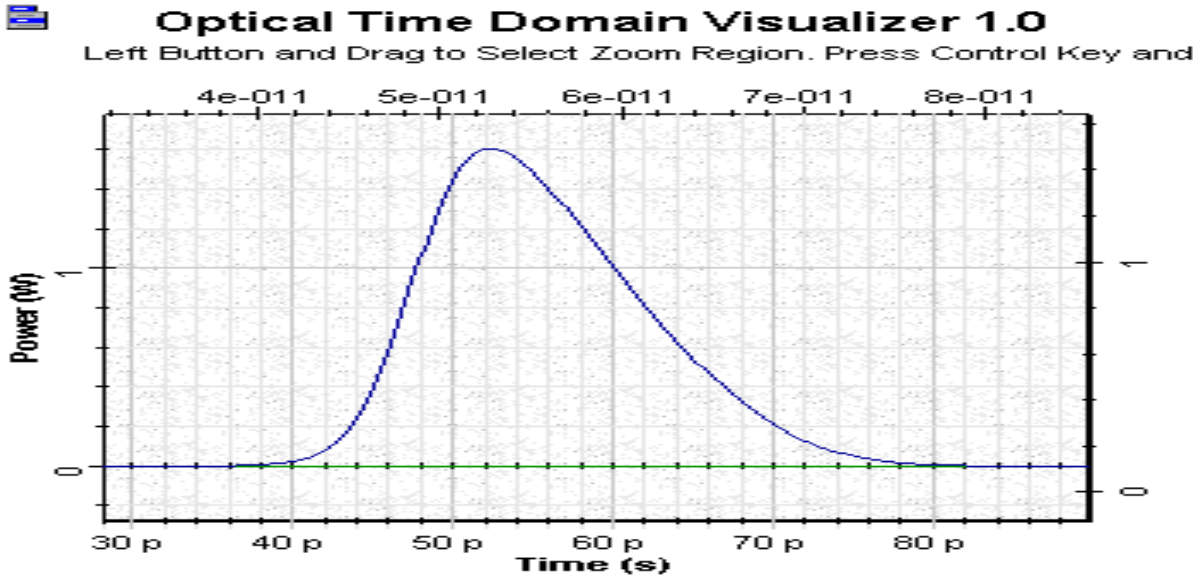

Fig.75: Shape of the amplified pulse

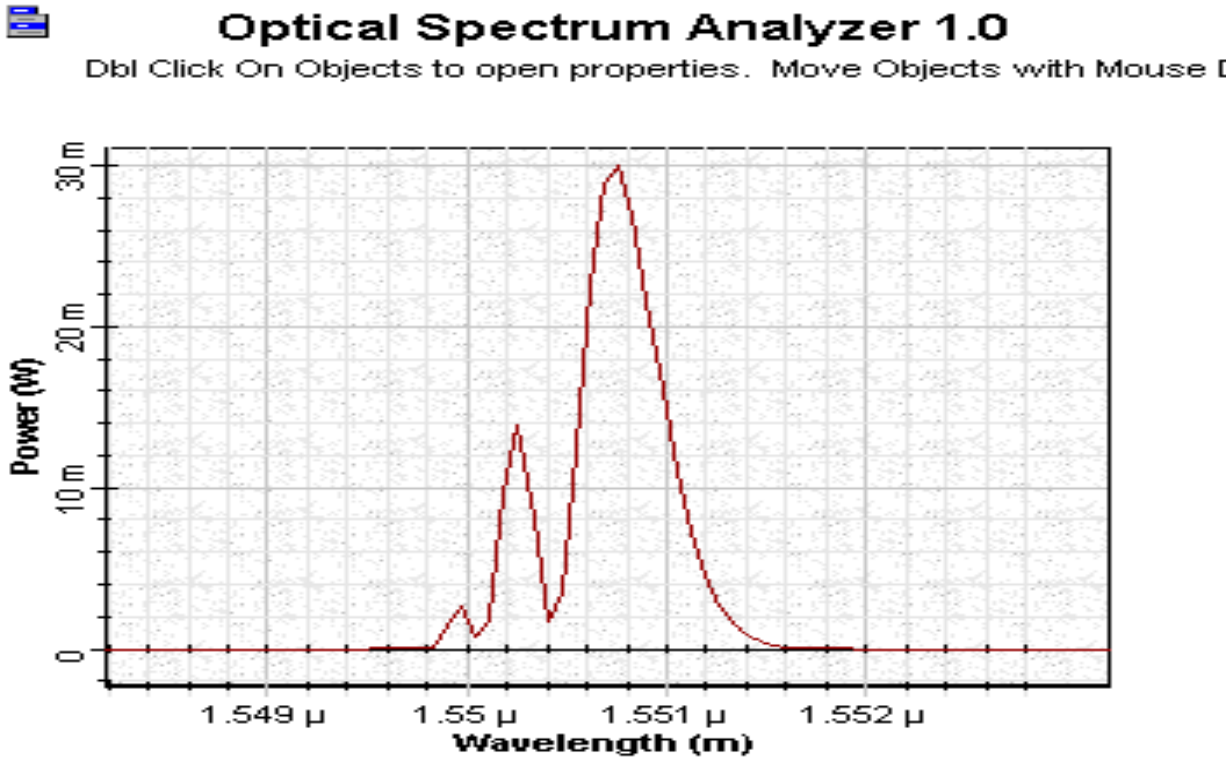

Fig.76: Spectrum of the amplified pulse

Fig. 75 reveals that the amplified pulse becomes asymmetric so that its leading part is sharper compared with the trailing edge. Note that sharpening of the leading edge is a common feature of all amplifiers.

The pulse spectrum of the amplified pulse however, reveals features that are particular for the SOA.

The spectrum develops a multi-peak structure and the dominant peaks shift toward longer (red) wavelengths. This red shift increases with the increase of the amplification factor. The red shift observed from this figure is ~ 0.001 μm ~ 120 GHz.

In Fig. 77 a phase of the pulse is shown together with its shape. The important circumstance that has to be mentioned is that the phase follows the time evolution of the gain. We see that for such short pulse, gain has no time to recover (remember T_0/τ_C ~ 0.006).

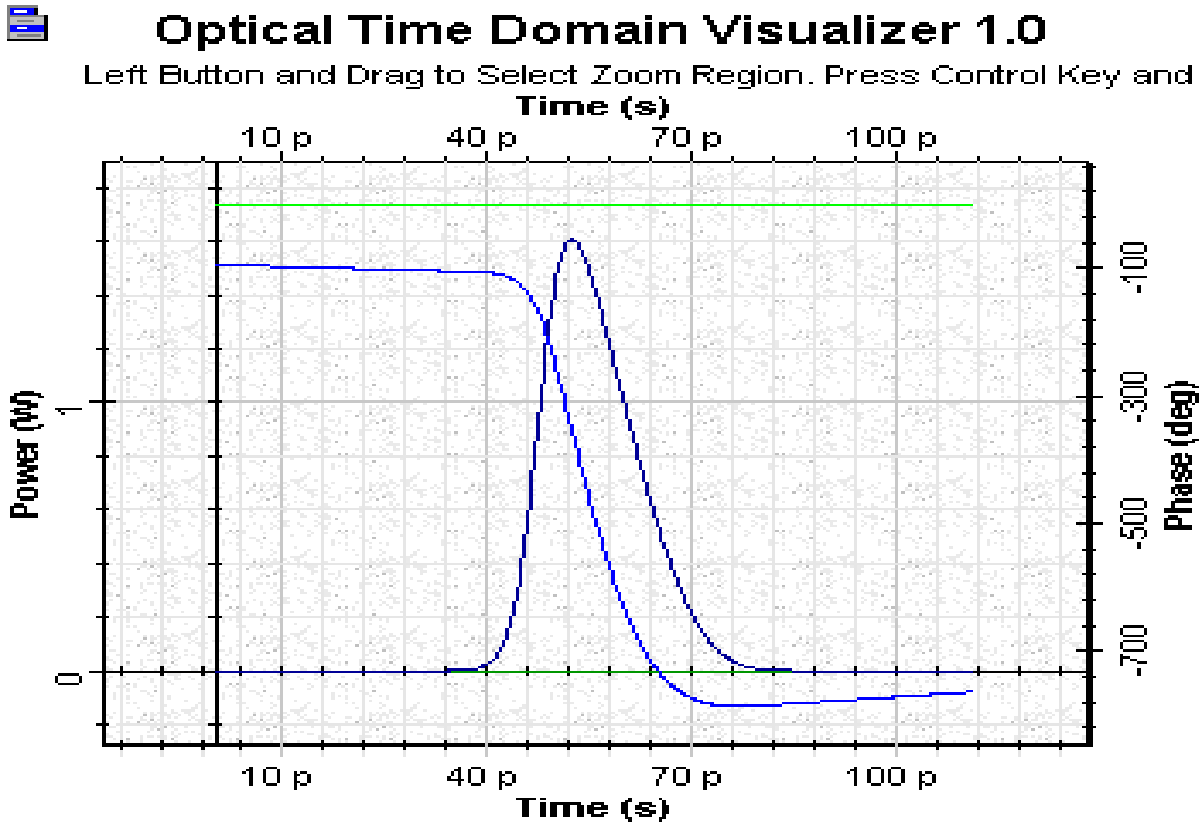

Fig.77: Phase and shape of the pulse

In Fig. 78, the gain saturation induced chirp across the pulse is shown together with its shape. Note that the initial Gaussian pulse was unchirped.

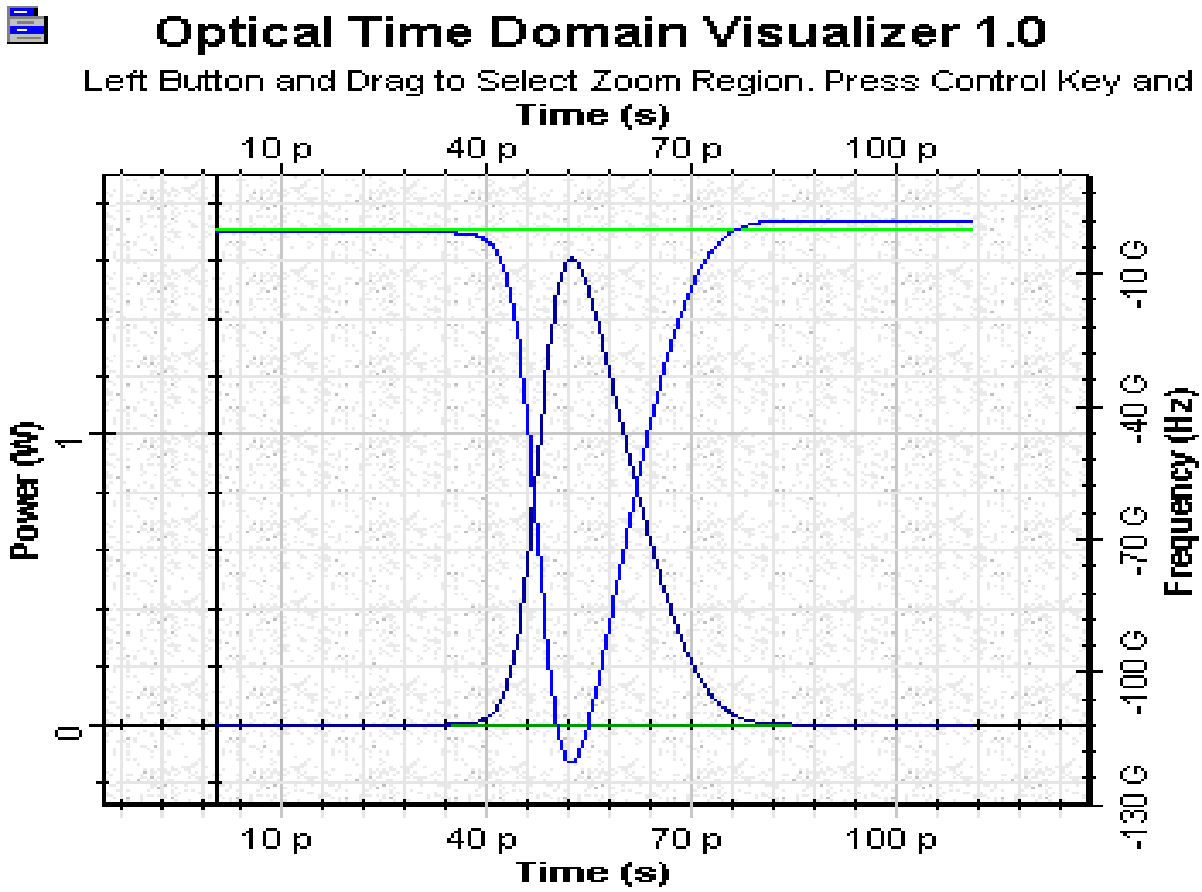

Fig.78: Gain saturation induced chirp across the pulse

The gain saturation induced chirp is negative across the entire pulse, therefore the instantaneous frequency is down shifted (the red shift) from the incident frequency. Nevertheless because of the fact that induced chirp increases towards the trailing part of the pulse, such chirp is known as positive one. From the theory of propagation of phase modulated pulses in the medium with group velocity dispersion [3] it follows that appearance of positive chirp can be used for pulse compression in the medium with anomalous group velocity dispersion. Let us now consistently analyze the influence of the initial power, optical confinement factor and inner losses on the observed properties. Note that in model used in [1], [2] the inner losses have been neglected.

First we will see how the shape and spectrum of the amplified Gaussian pulse (for the same pulse and SOA parameters as above) change as a function of the initial pulse power. The values of the initial power considered are P = 5, 10,20,30, 50 mW. In the first case we consider $E_0 / E_{sat} \sim 0.02$.

To get these results, mode sweep can be used **(Table 20).**

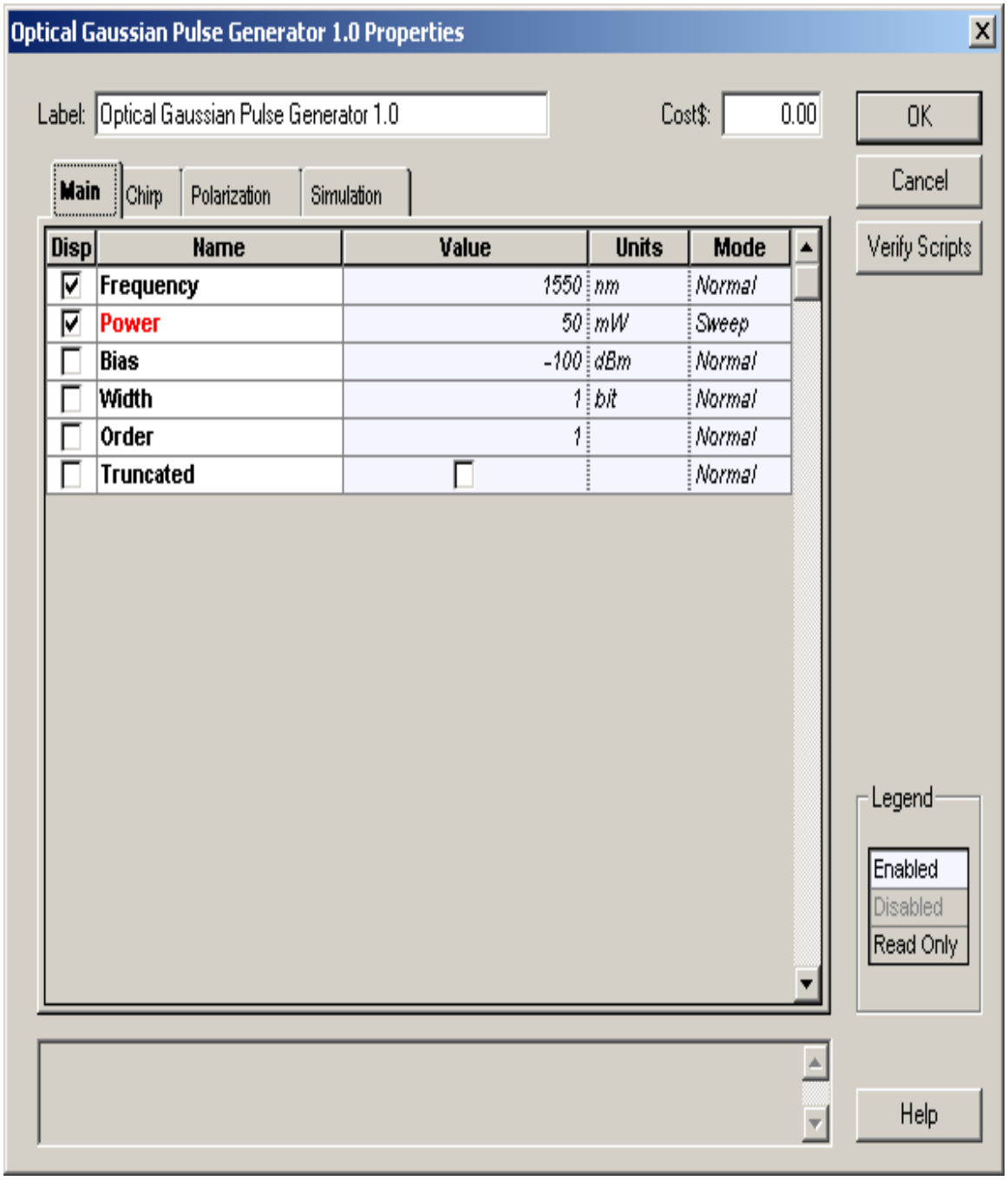

Table 20: Optical Gaussian pulse generator parameters (main)

In Figs. 79 and 80, the shape and spectrum of the amplified Gaussian pulse are shown for different initial powers.

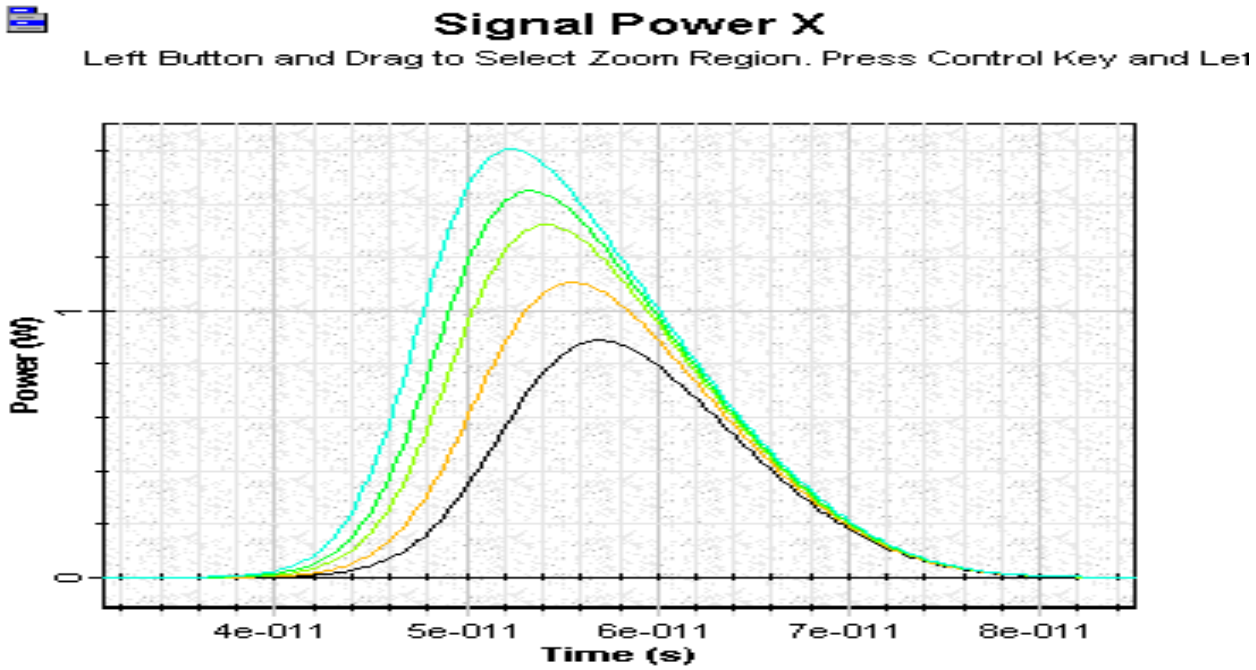

Fig.79: Shape of the amplified Gaussian pulse for different initial powers

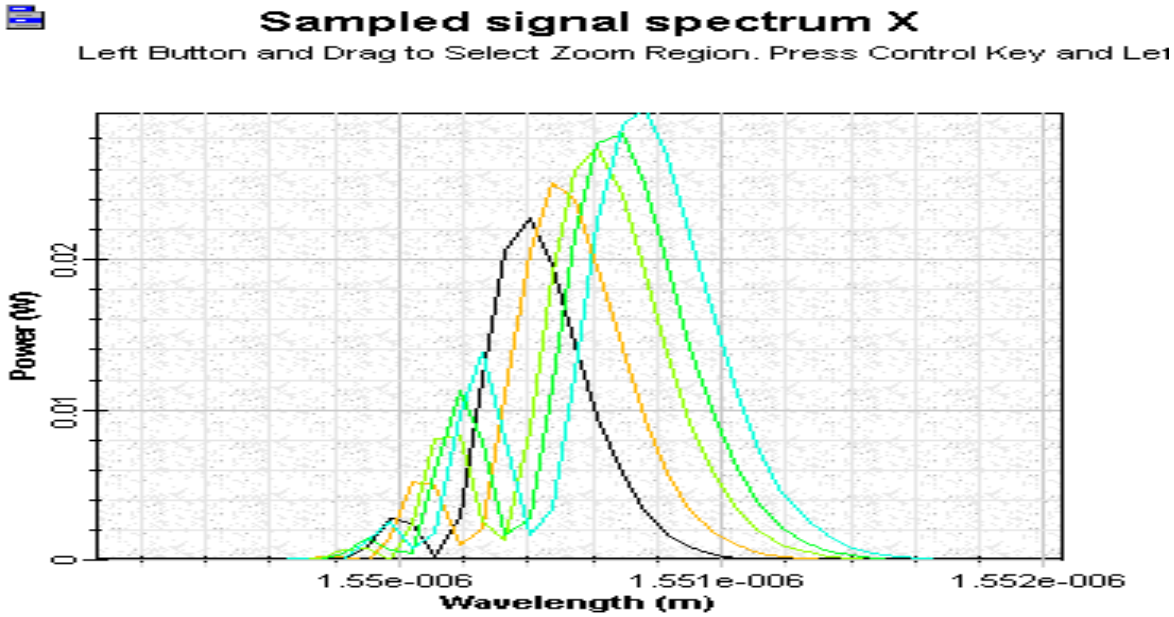

Fig.80: Spectrum of the amplified Gaussian pulse for different initial powers

As we could expect increasing the ratio E_0 / E_{sat} (for fixed pulse width) leads to increase in the number of the peaks in the spectrum alongwith the increase of the red shift.

In Figs. 81 and 82, the shape and spectrum of the amplified Gaussian pulse (for the same pulse and SOA parameters as above) are shown as a function of the optical confinement factor. The values of optical confinement factor considered are Γ = 0.1, 0.2,0.3,0.4 and 0.5.

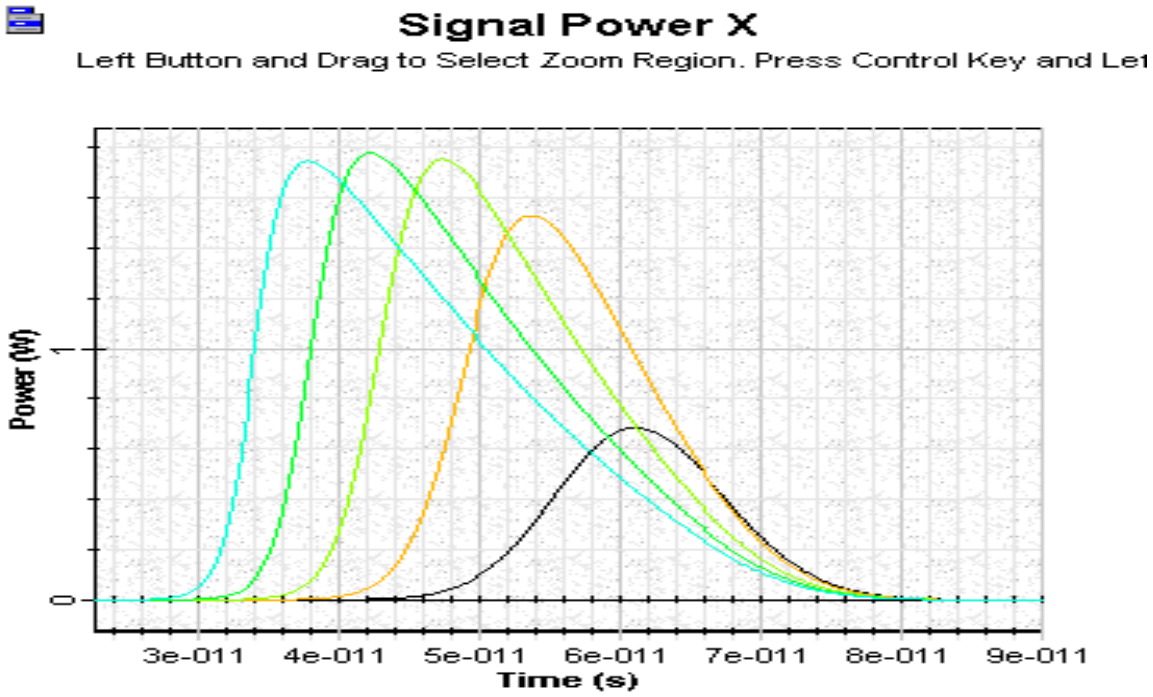

Fig. 81: Shape of the amplified Gaussian pulse (for the same pulse and SOA parameters as above) as a function of the optical confinement factor

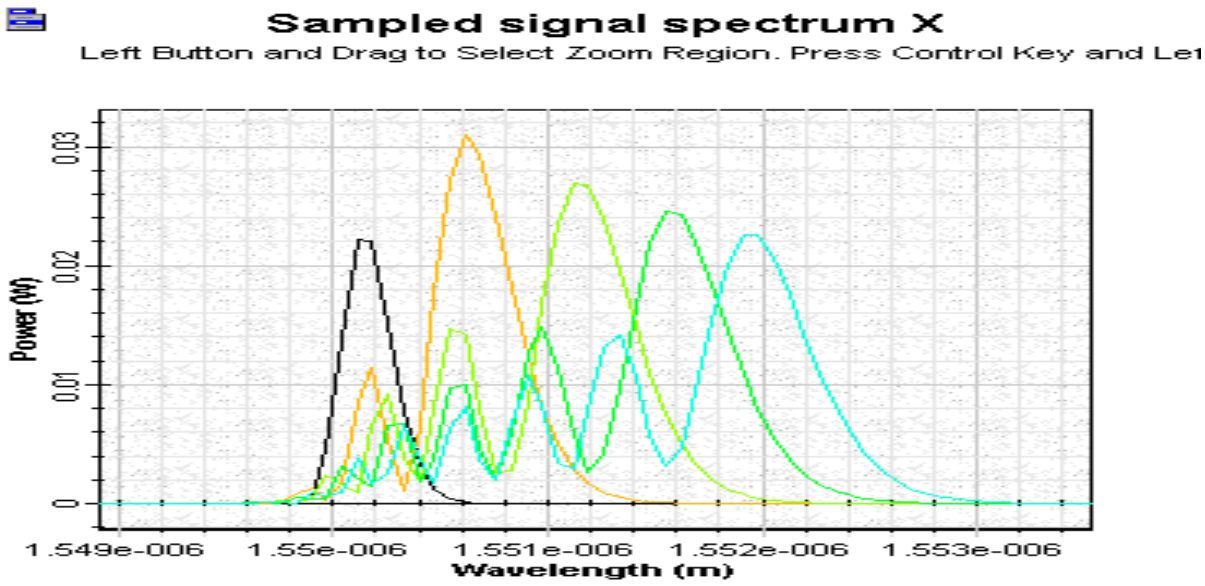

Fig. 82: Spectrum of the amplified Gaussian pulse (for the same pulse and SOA parameters as above) as a function of the optical confinement factor

As we see the optical confinement factor influences the pulse spectrum and shape.

Figs. 83 and 84 show the shape and spectrum of the amplified Gaussian pulse (for the same pulse and SOA parameters as above) as a function of the internal losses. The values of internal losses considered are α_{int} = 0, 1000,2000,3000 and 4000 (1/m).

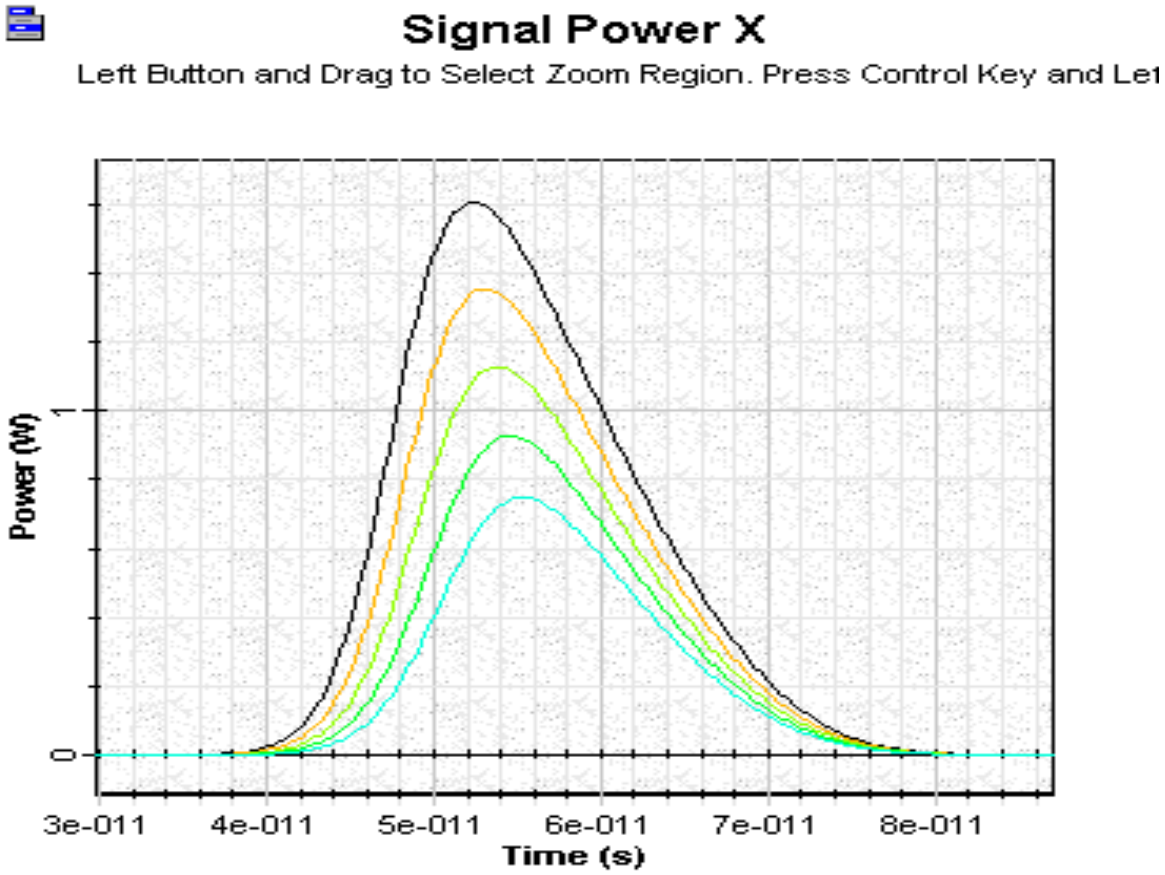

Fig.83: Shape of the amplified Gaussian pulse (for the same pulse and SOA parameters as above) as a function of the internal losses

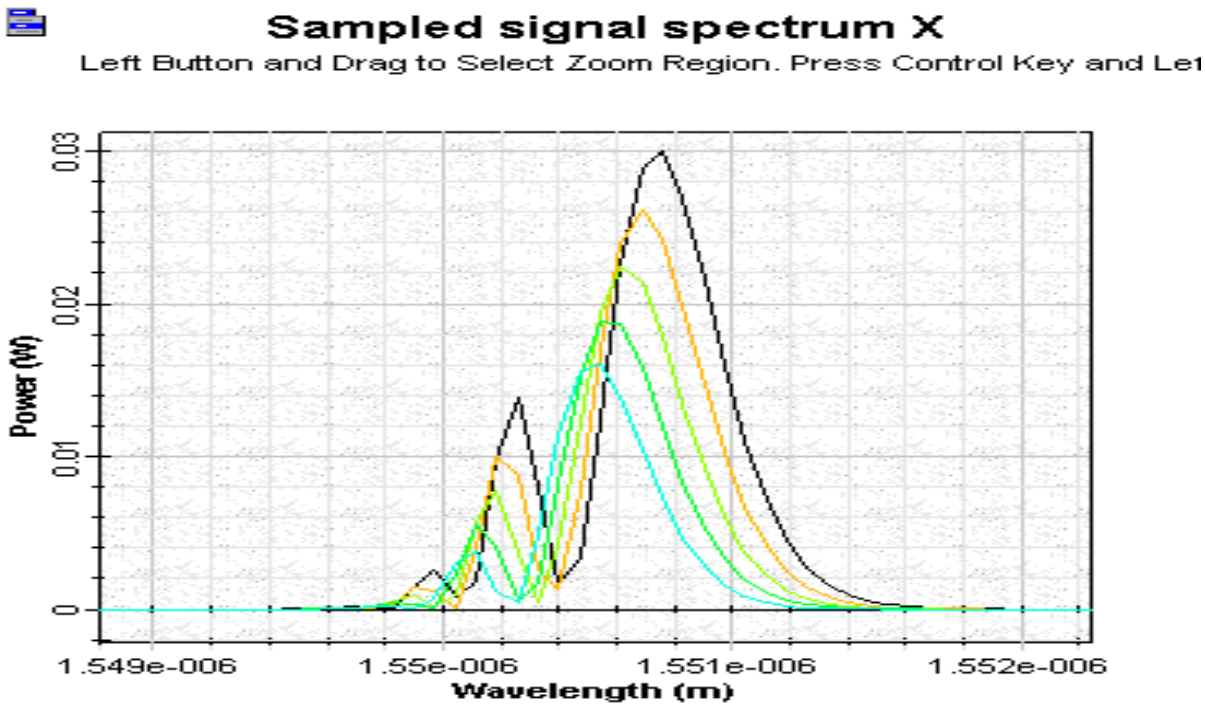

Fig. 84: Spectrum of the amplified Gaussian pulse (for the same pulse and SOA parameters as above) as a function of the internal losses

As we see in contrast to the optical confinement factor, the internal losses do not influence the pulse spectrum and shape.

References:

[1] G.P. Agrawal and N.A. Olsson, "Self_phase modulation and spectral broadening of optical pulses in semiconductor laser amplifiers", IEEE Journal of Quantum electronics, vol. 25, pp.2297-2306, 1989.
[2] G.P. Agrawal, "Fiber-Optic Communication Systems", second edition, John Wiley &Sons, INC., 1997.
[3] G.P. Agrawal, "Nonlinear Fiber Optics", third edition, Academic Press, 2001.

Example: Raman Gain and Bandwidth

Forw_backward Raman amplification**.osd**

Project file "Forw_backward Raman amplification**.osd**" demonstrates forward and backward Raman amplification in a 16-channel WDM system. This project file includes two versions of the same project; one with forward pump and one with backward pump. 16 channels in 191-195.5 THz band, separated with 3 GHz are multiplexed and sent to Raman amplifier. The frequency difference between stokes and pump beam (Stokes shift) is important in SRS process. The Raman

gain coefficient scales linearly with pump frequency. Maximum gain is obtained when the Stokes shift is about 13.2 THz. This example shows that, a relatively flat and high gain can be obtained when the frequency of the pump signal is about 206.75 THz, in which case the Stokes shift is about 13.3 THz for the center channel. In fact, signal frequency can differ from pump frequency up to 20 THz. You can experiment how the value of Stokes shift affects the gain by changing the frequency of the pump signal. Overall optical gain is a function of signal frequency and pump intensity (pump power divided by effective area of the fiber). To test this, you can change the effective area of the fiber or the pump signal power.

Example: Gain Saturation

Forw_backward Raman gain saturation**.osd**

Project file "Forw_backward Raman gain saturation**.osd**" demonstrates the gain saturation due to pump depletion in forward and backward pumped Raman amplifier in a 4-channel WDM system. In Raman amplifier, since the pump supplies energy for signal amplification, it begins to deplete as the signal power increases. A decrease in the pump power reduces the optical gain. This reduction in the gain is referred to as gain saturation. In this example, we see how the gain saturation differs depending on forward or backward pump configuration. You can see this by clicking on results table for both cases and comparing them. Can you explain whey they differ?

Example: Amplifier Performance

Broadband flat gain Raman amplifer**.osd**

The specifics of the stimulated Raman scattering effect allow for an interesting new technique for gain flattening of broadband Raman amplifiers. Project file "Broadband flat gain Raman amplifier**.osd**" demonstrates that multi-pump can be used to flatten the Raman amplifier gain in a broad band. In this example, several pumps are arranged in 90 nm broad spectral range and they are used to pump in 100 km SMF-28 in backward direction. This gain flattening technique requires only a suitable multiple-pump configuration and does not rely on any passive gain equalizing optics.The key feature of this technique is the proper choice of number of pumps, pump wavelengths, and pump powers. You can experiment by altering the power distribution and wavelengths of the pumps. Try to understand how this type of configuration works. Hint: See the gain spectrums when you disable all pumps but leave one pump. Do this for all seven pumps. If you add up gain spectrums from each individual pump in dB scale, what you get?

Example: Pumping Requirements

Pumping requirements**.osd**

The amplifier performance characterized by the signal output power, gain and noise figure depends on the pump wavelength. The project file "Pumping requirements**.osd**" (Fig. 85) shows two different versions, "Pump power 980 nm" and "Pump power 1480 nm". The 980 nm and 1480 nm pump wavelengths are the most important to be used in EDFAs. Fig. 85 shows the layout setup in a co-propagating pump scheme in both versions considering 980 nm and 1480 nm as pump wavelengths.

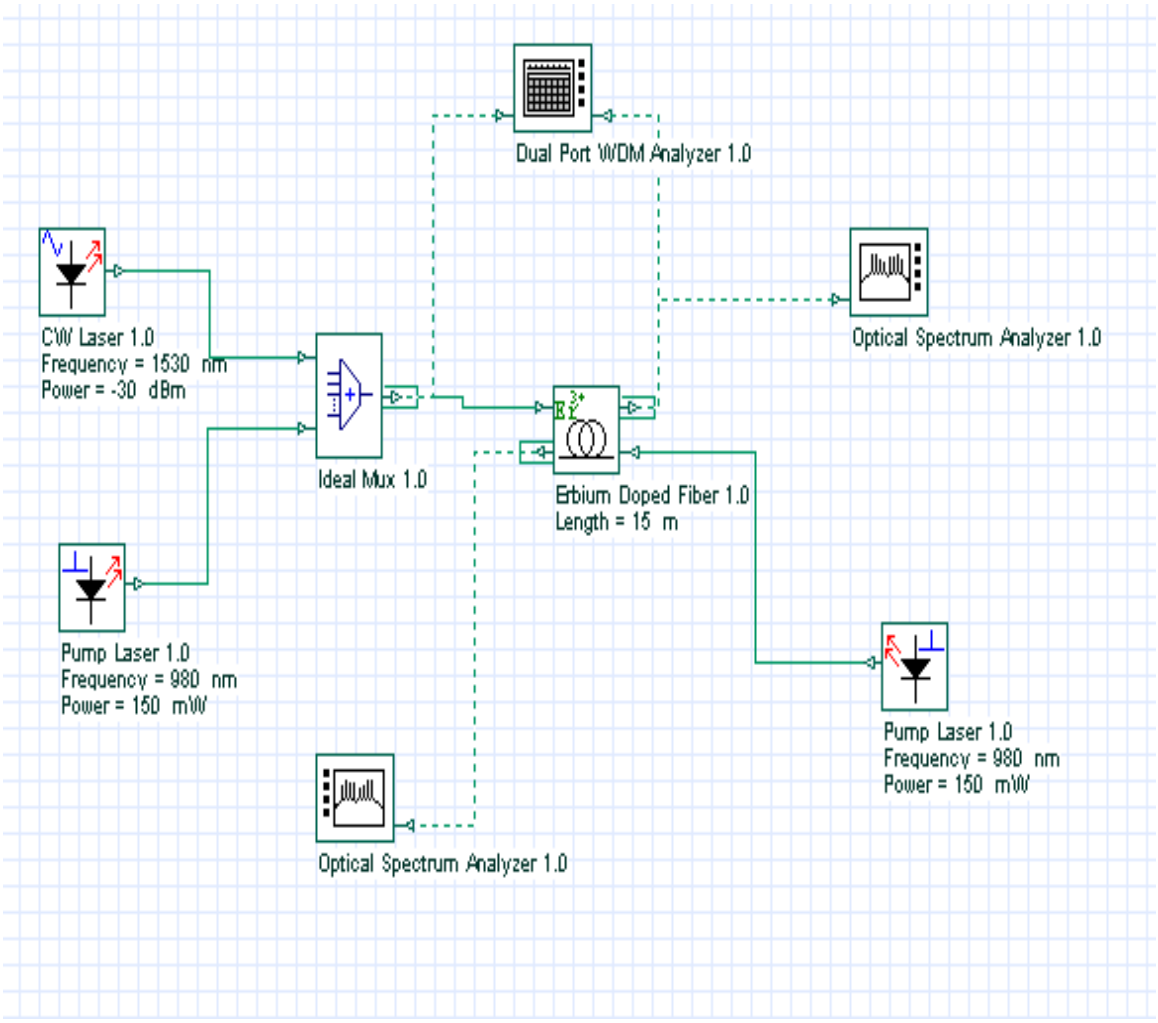

Fig. 85: Layout: Pumping requirements: Co-propagating

High amplifier gains in the range 30-40 dB can be obtained in this project file by sweeping the pump power from 10 mW to 200 mW. The signal input power considered in this case is -20 dBm. The calculated output power is in the range of 6 - 17 dBm, while the noise figure varied between 3 – 5 dB. Results obtained with these versions are shown in Fig. 86.

EDFAs can be designed to operate in such a way that the pump and signal beams propagate in opposite directions, a configuration referred to as backward pumping to distinguish it from forward-pumping configuration in which both beams propagate along the same direction. Backward or counter-propagating pump scheme is exemplified in the version “Backward pump @ 980 nm”. The pump power is swept from 10 to 150 mW with the signal input power kept equal to -20 dBm.

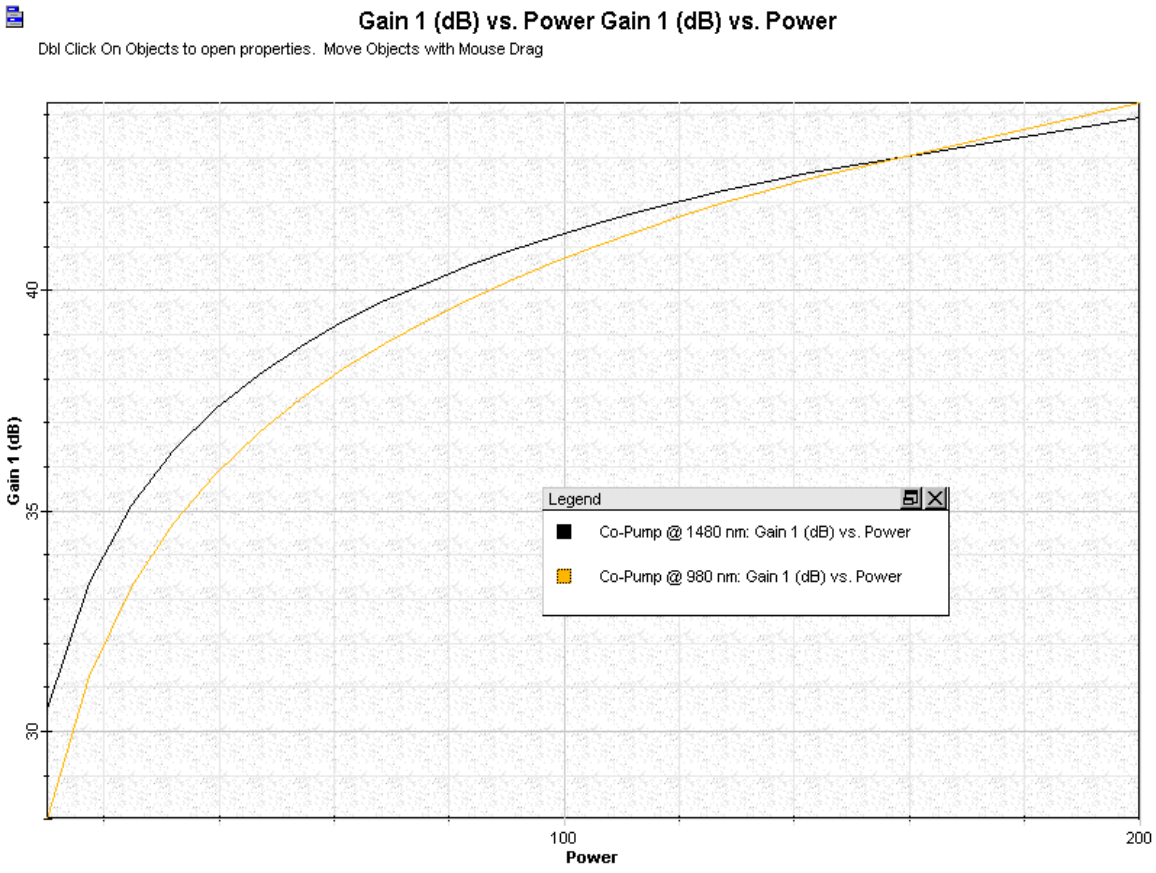

Fig. 86: Gain versus pump power considering a co-propagating pump schemes @ 980 nm and @ 1480 nm pump wavelength

The layout considering backward or counter-propagating pump scheme is shown in Fig. 87. Fig. 88 shows the gain versus pump power when 980 nm and 1480 nm are considered as pump wavelength. The influence of the selected pump

scheme in the amplifier performance can be seen by considering unsaturated or saturated regime by just changing the signal input power range.

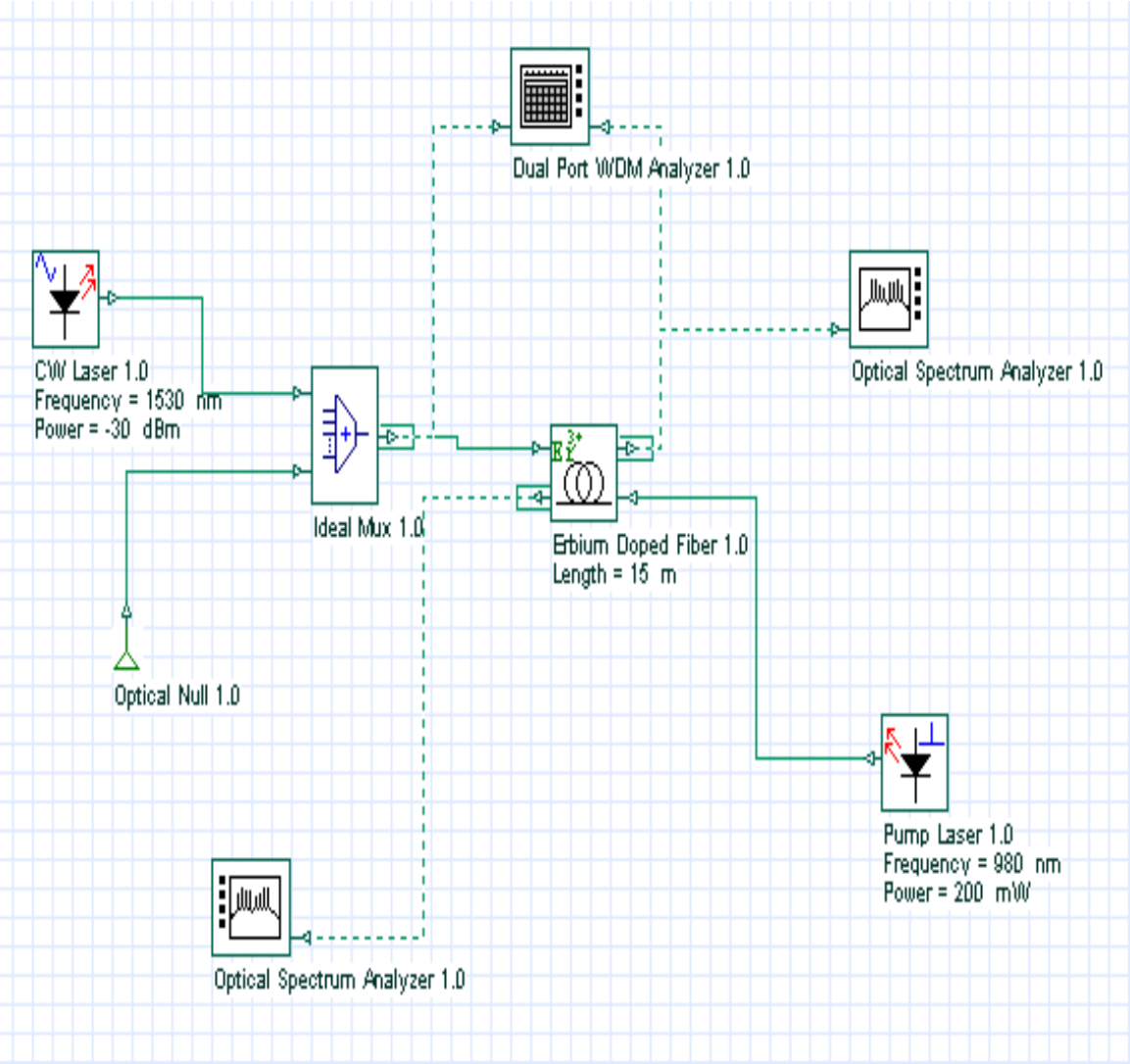

Fig. 87: Layout: Pumping requirements: Counter-propagating

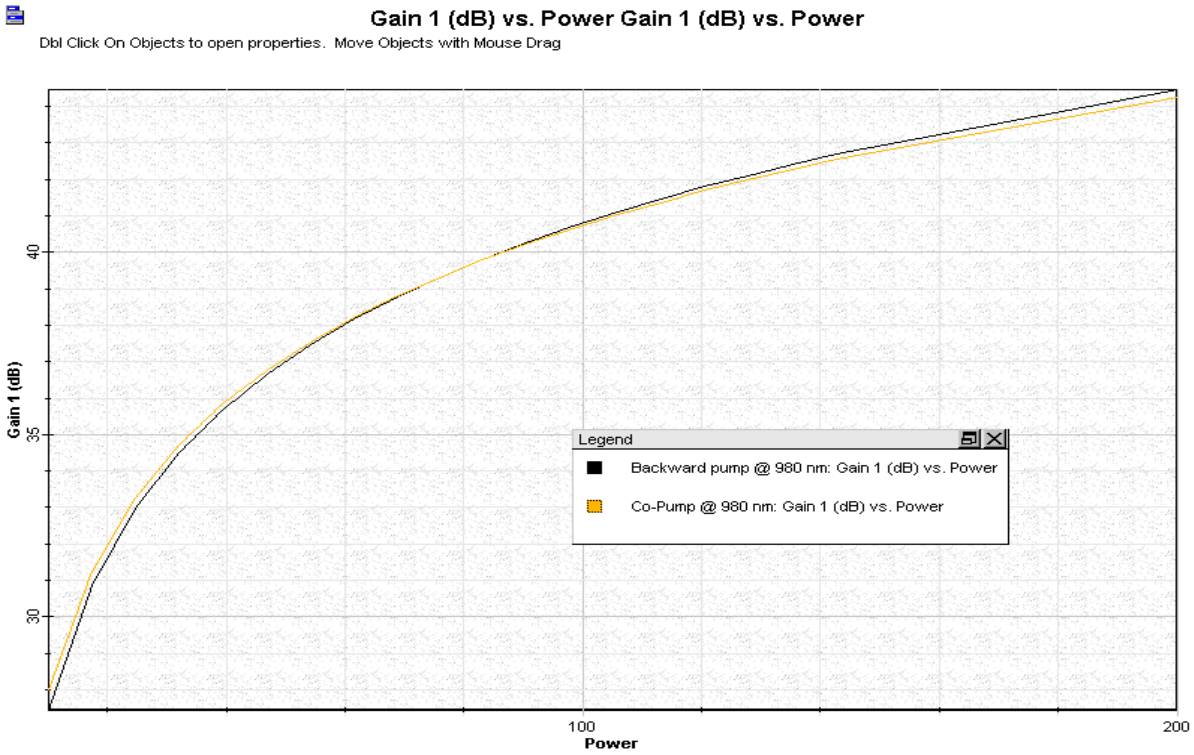

Fig. 88: Gain versus pump power considering a counter-propagating pump schemes @ 980 nm and @ 1480 nm pump wavelength

The version "Bidirectional pump @ 980 nm" added to this project file considers the bidirectional pumping configuration, where the amplifier is pumped in both directions simultaneously by using semiconductor pump lasers located at the two fiber ends. The advantage of this pump scheme can be checked setting small-signal or large signal input and observing the amplifier performance given by the gain, output power and noise figure graphs displayed in Views.

Example: Gain Characteristics

Gain characteristics**.osd**

The gain of EDFA depends on a large number of device parameters such as erbium ion concentration, amplifier length, core radius, Er doping radius, and pump power. The gain spectrum is affected considerably by the codopants contained in the core such as germanium and aluminum.

The same erbium doped fiber is considered in the three different versions of the project file "Gain characteristics**.osd**" (Fig. 89) where sweep iterations are performed over signal wavelengths, pump powers and fiber lengths. Spectral

gain characterization, gain characterized as a function of pump power, and gain calculated as a function of fiber length, are shown in this example.

The basic amplifier layout used in the versions “Signal Wavelength”, “Pump Power” and “Amplifier Length” is shown in Fig. 89.

Some results that can be observed in this sample are shown in Fig. 90. Gain characteristics are shown as a function of signal wavelength, pump power, and erbium-doped fiber length.

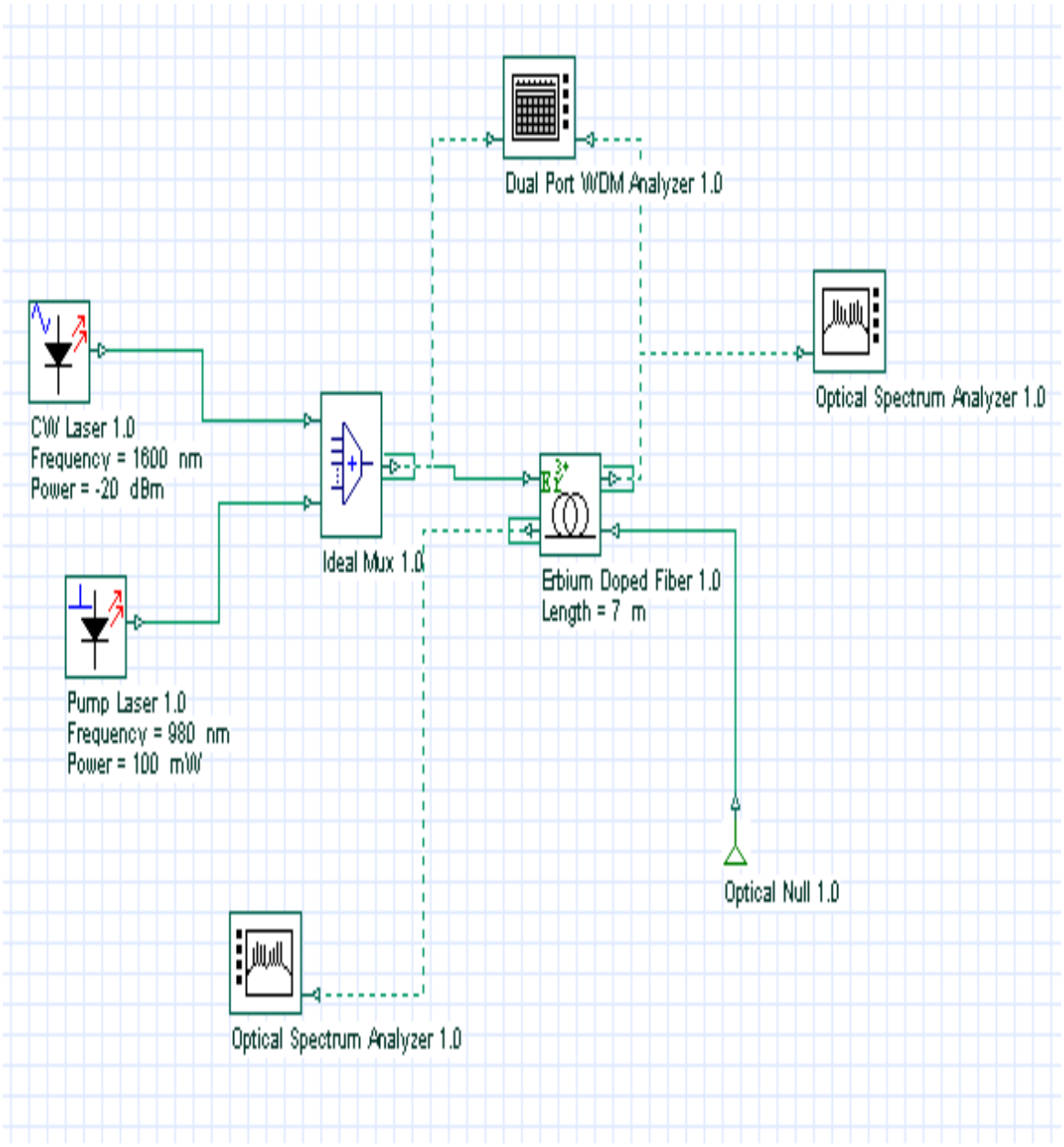

Fig. 89: Layout: Gain characteristics

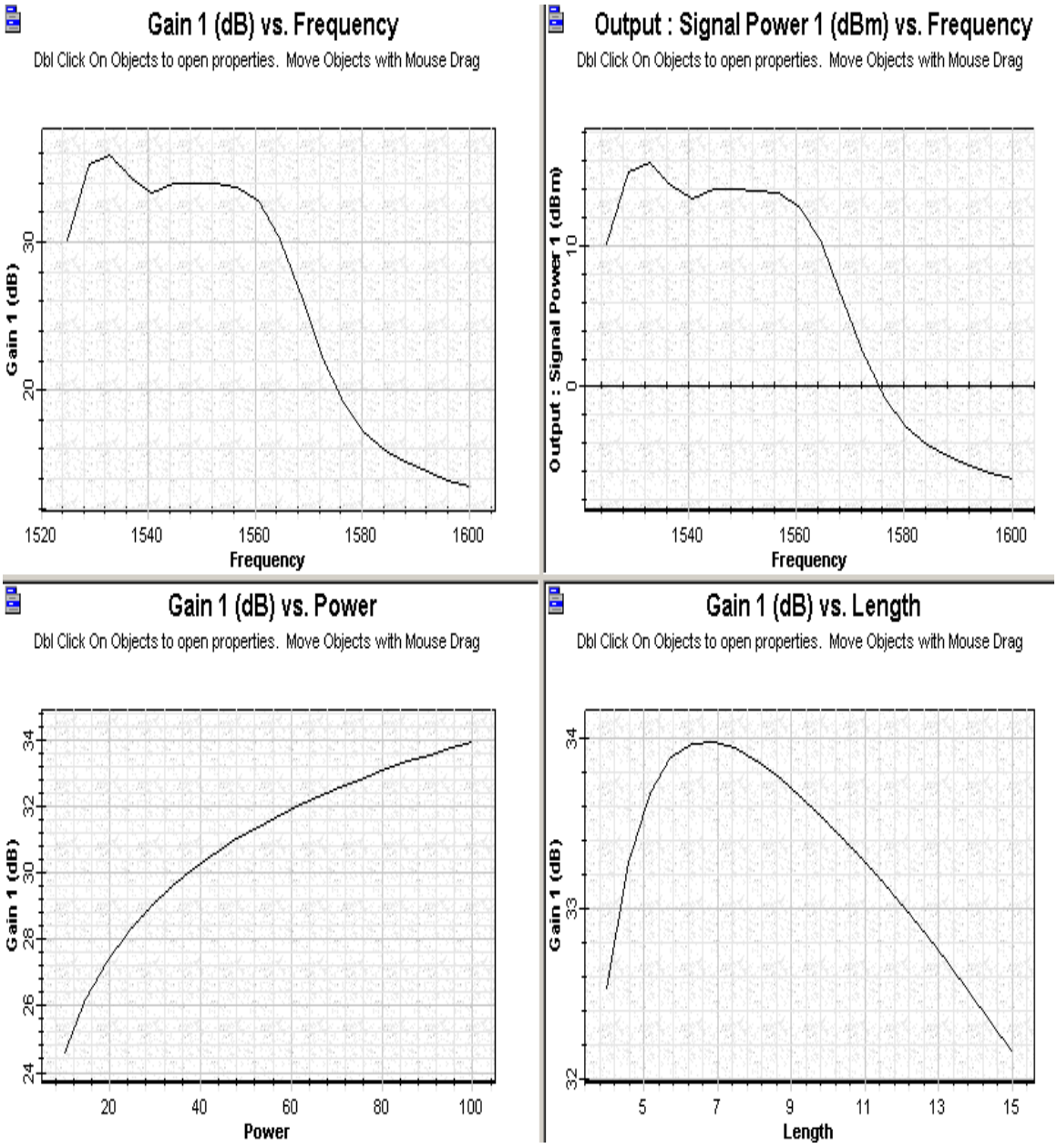

Fig. 90: Gain characteristics calculated as a function of signal wavelength, pump power and Er-doped fiber length

Example: Amplifier Noise

Amplifier noise**.osd**

The amplifier performance is evaluated by sweeping iterations over signal wavelength and fiber length. The spectral evaluation of noise in the amplifier is

done for 980 nm and 1480 nm wavelengths at different pump powers. Different versions in the project file "Amplifier noise**.osd**" (Fig. 91) enable the evaluation of gain, output power and noise figure for different input conditions.

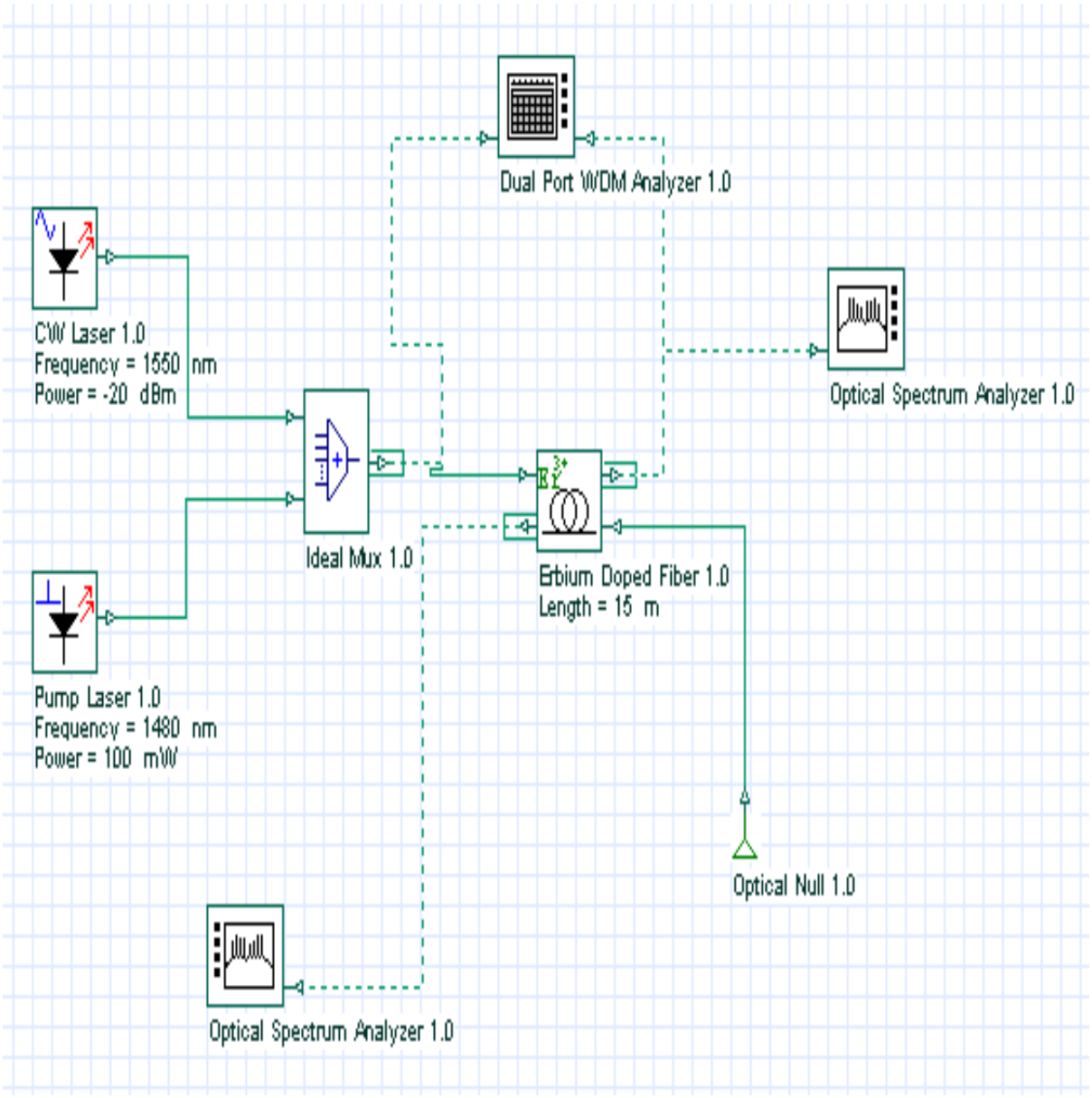

Fig. 91: Layout: Amplifier noise

The spectral noise characterization for this setup with a co-propagating pump scheme is shown in Fig. 92.

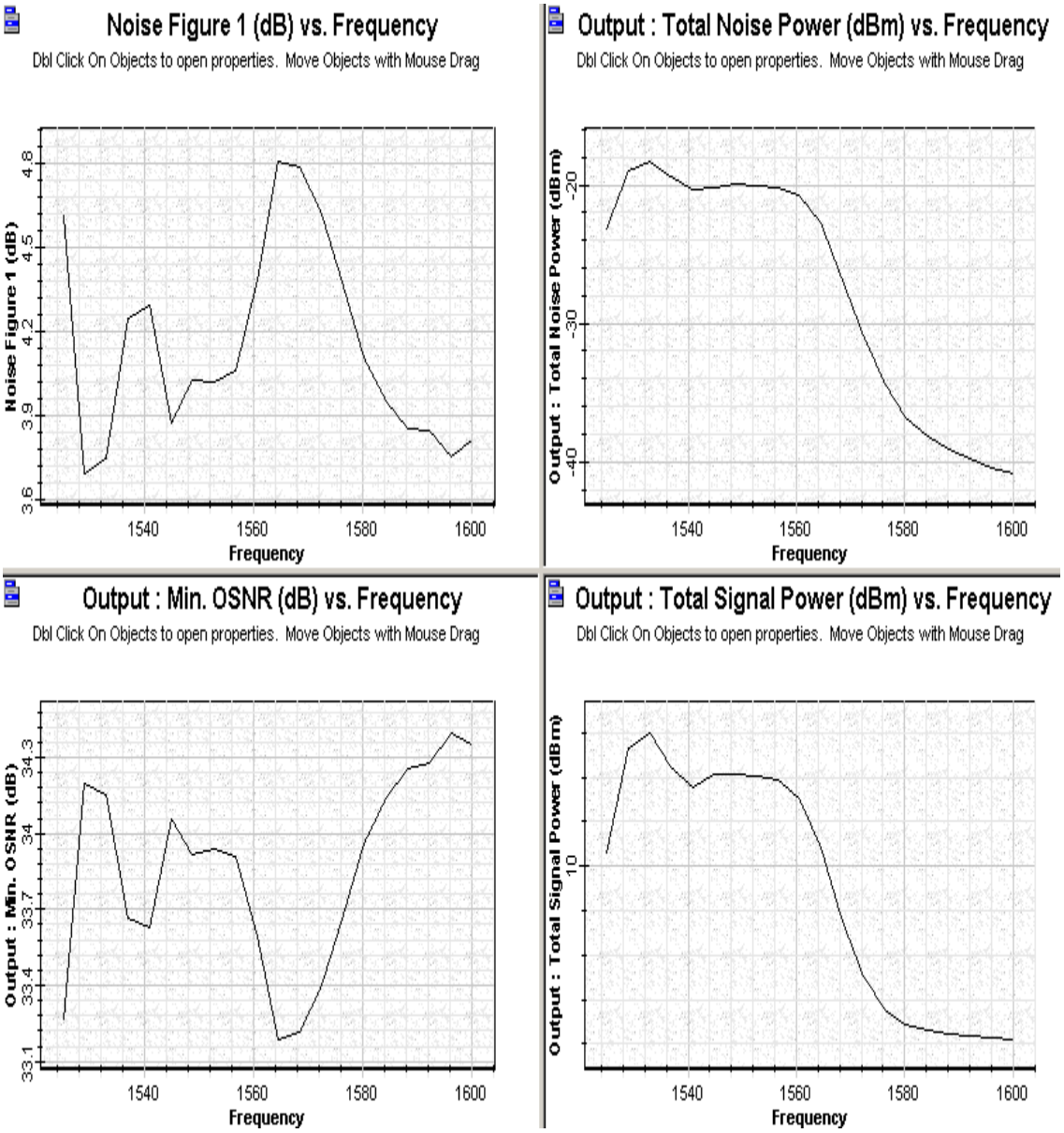

Fig. 92: Spectral noise characterization

Noise figure versus fiber length is shown in Fig. 93 where three different pump powers 50 mW, 70 mW, and 100 mW are considered.

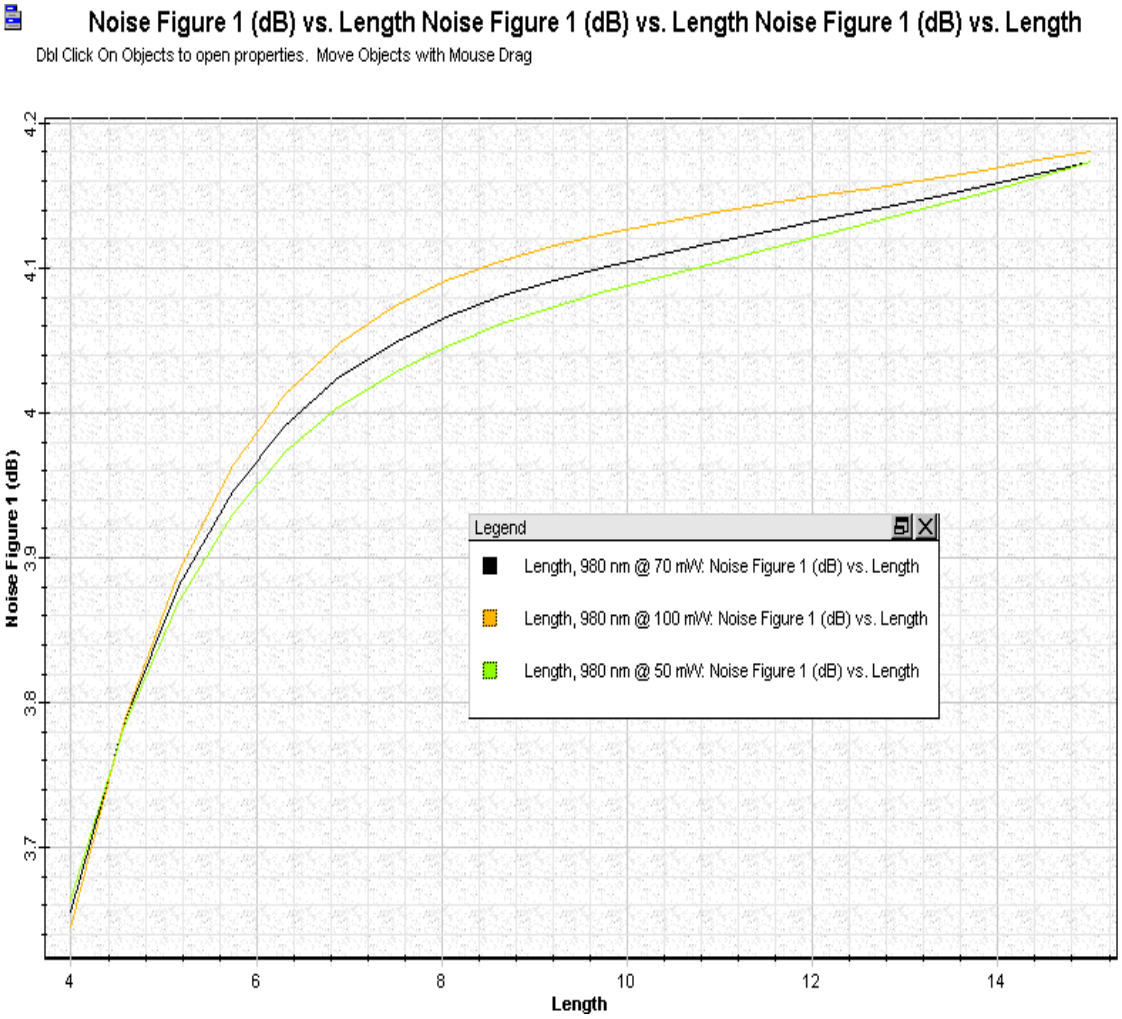

Fig. 93: Noise figure versus Er-doped fiber length calculated to 50 mW, 70 mW and 100 mW of pump power

The noise figure calculated by coupling 100 mW of pump power to the Er-doped fiber at 980 nm and at 1480 nm has been compared in Fig. 94.

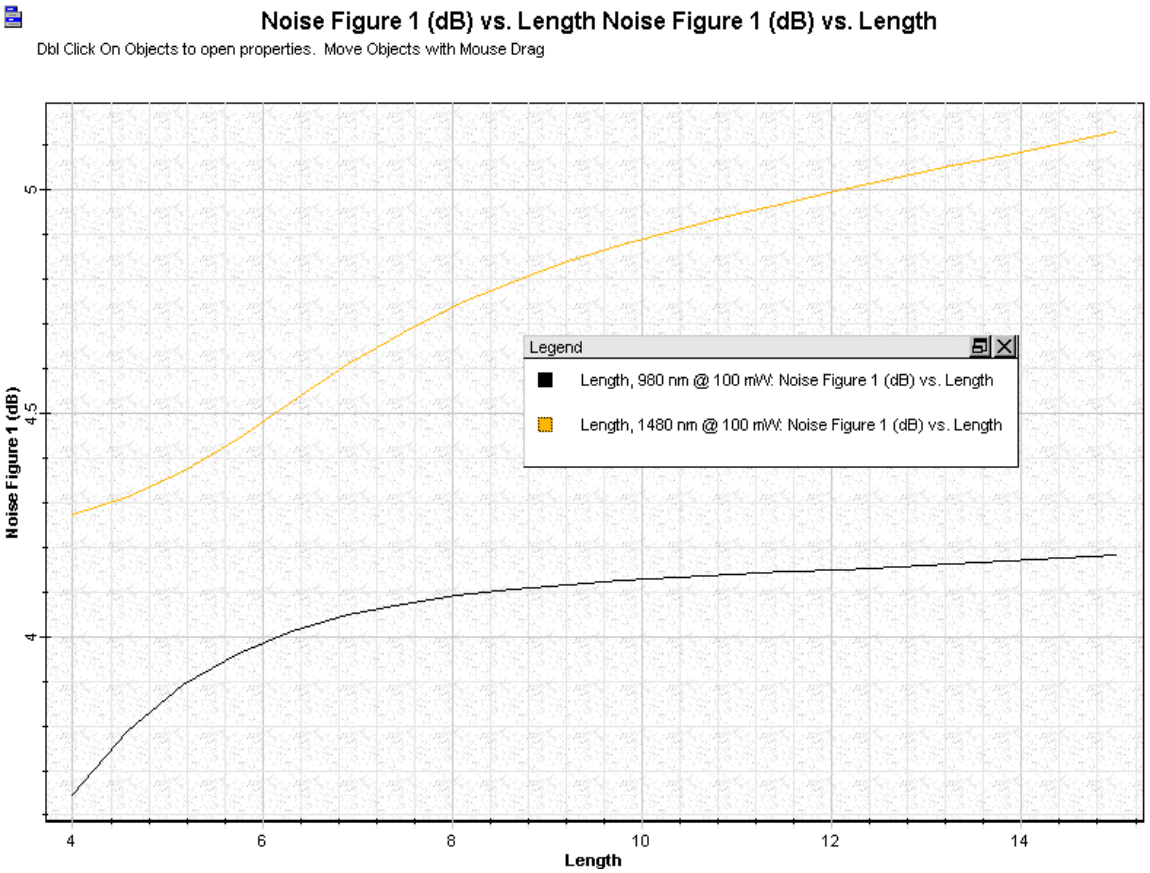

Fig. 94: Noise figure versus fiber length considering 100 mW of pump power at 980 nm and at 1480 nm as pump wavelength

Example: Multichannel Amplification

Multichannel amplification**.osd**

EDFA performance is evaluated considering multiple signal input. The amplifier is setup in a copropagating pump scheme, as shown in Fig. 95, and the amplified signal referring to the signal input can be checked by fiber output connected to the optical spectrum analyzer. The project file that enables calculating the amplifier performance considering multiple signal input is "Multichannel amplification**.osd**" (Fig. 95).

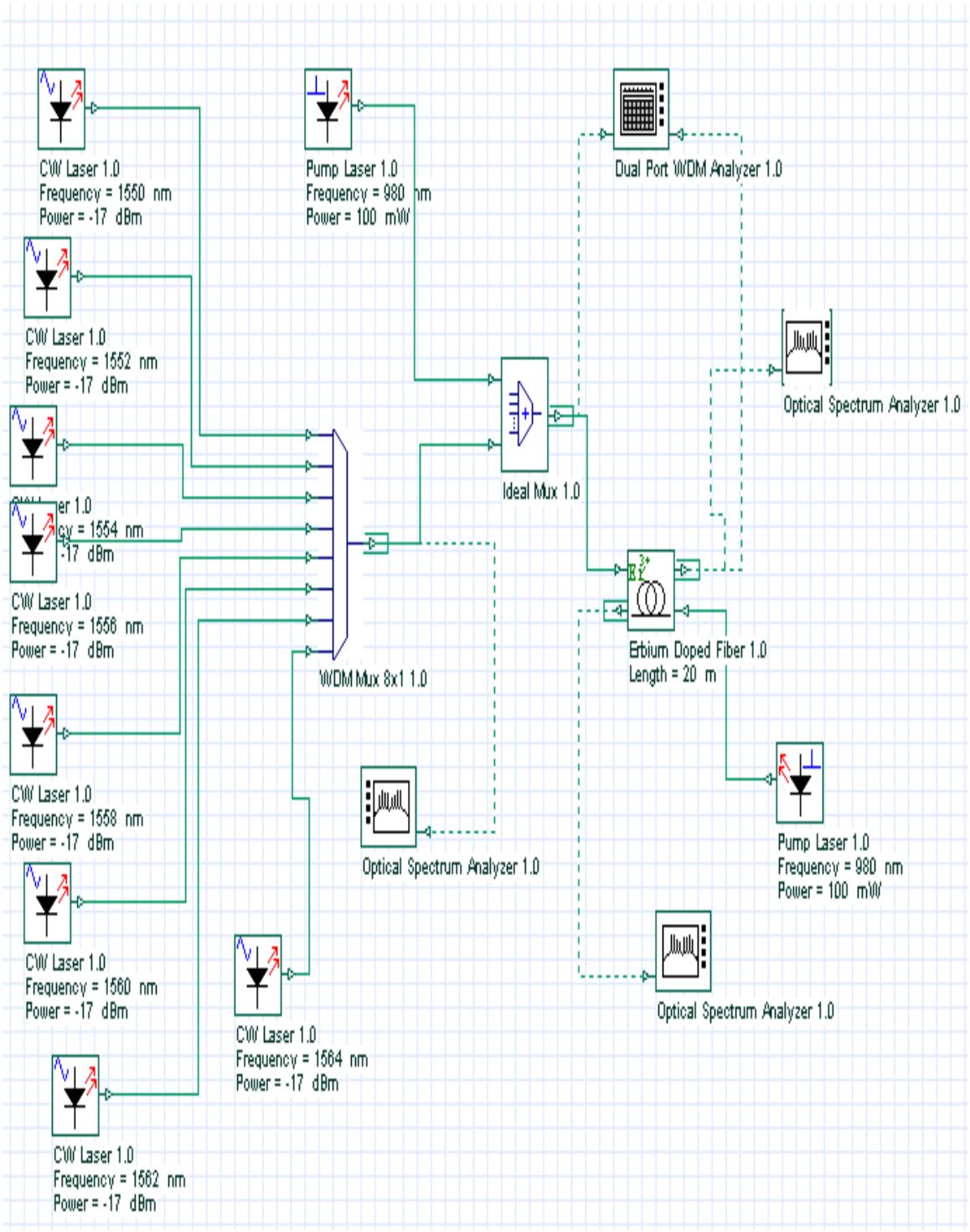

Fig. 95: Layout: Multichannel amplification

In the project, the amplifier is setup in a bidirectional pump scheme that enables extending the analysis to co-propagating or counter-propagating pump schemes.

In this example, flattening gain techniques were not added to the simulations that means that different signal amplitude will be observed at the amplifier output.

Example: Optical Preamplifiers

Preamplifier_system.**osd**

The performance of a preamplifier positioned at the receiver input is evaluated in the project "Preamplifier_system.**osd**" (Fig. 96). Characteristics of noise, gain and the improvement in the sensitivity of the photodetector/receiver can be calculated.

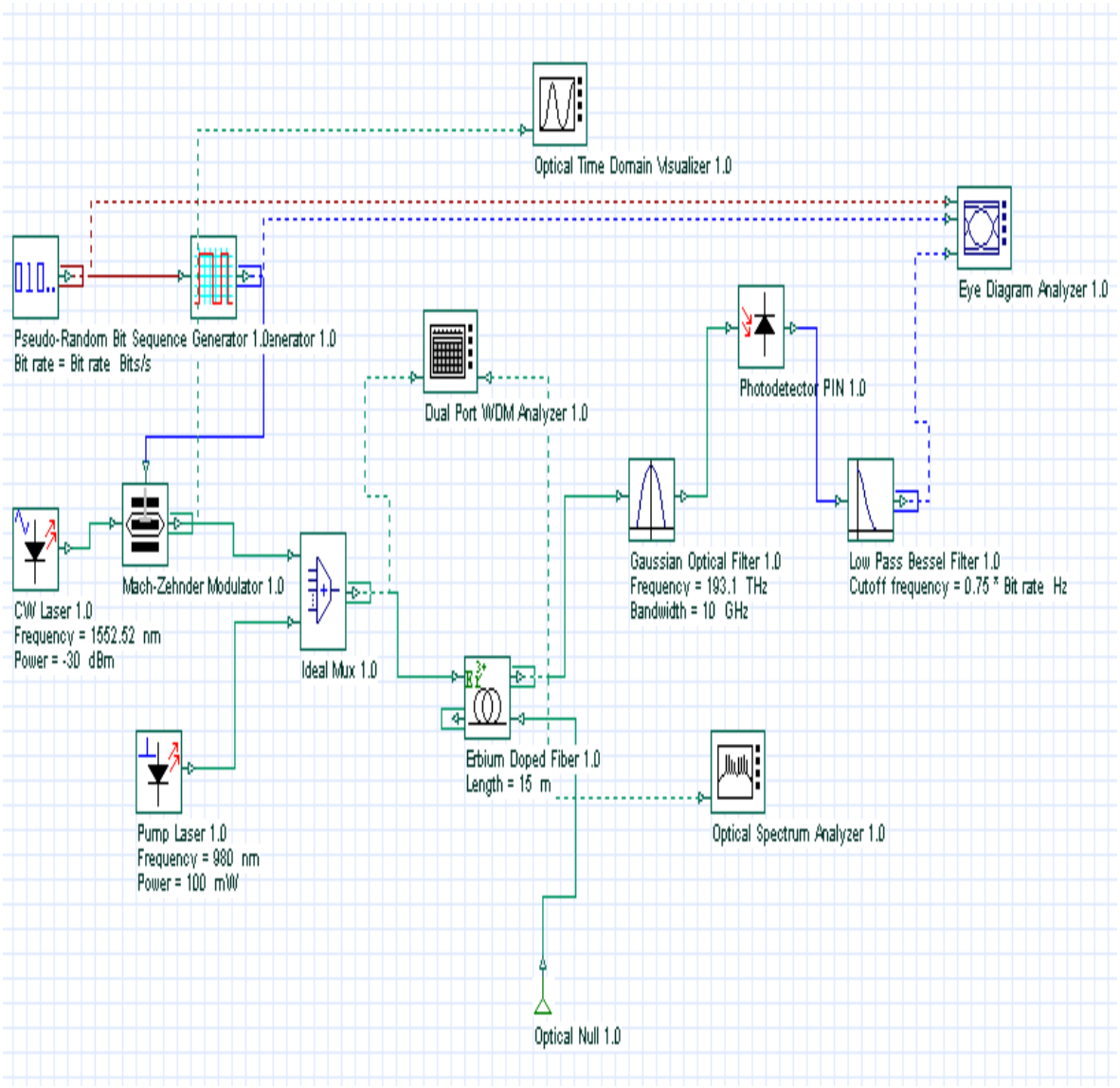

Fig. 96: Layout: Preamplifier_system

A modulated signal is coupled to the EDFA preamplifier and the corresponding characteristics are displayed on Dual Port WDM Analyzer by double clicking on this visualizer or on the permanent graphs available on Graphs.

The direct-detected signal on the receiver is pre- and post- filtered and the BER is evaluated through the Eye Diagram Analyzer 1.0. The eye diagram observed in Fig. 97 considers the parameters set in the photodector and in the filter. Different responsivity or thermal noise values can be set in the photodector so that changes can be observed in the eye diagram.

Changing the parameters in the specified modulation of the signal as well as in the filters will affect the transmission and the detection of signal. Consequently the observed eye diagram will be different.

The amplifier performance will affect the eye diagram observed at the Eye Diagram Analyzer 1.0. Input conditions such as signal and pump wavelength (980 nm or 1480 nm), signal and pump power, fiber specifications when modified will affect the amplifier performance.

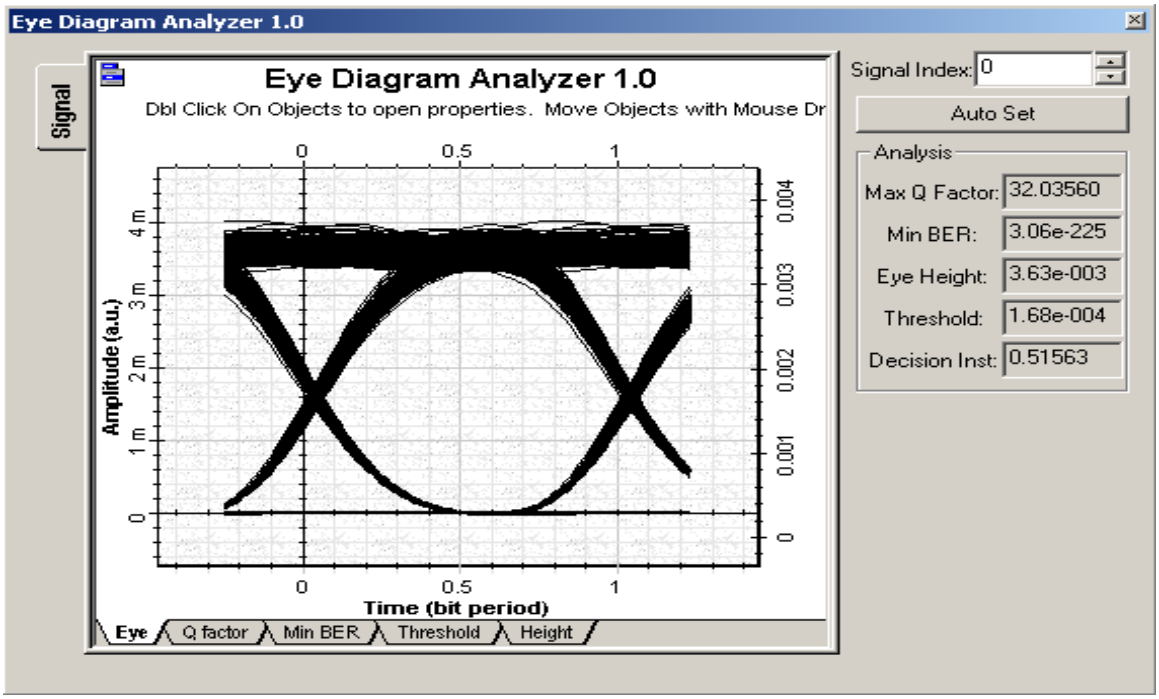

Fig. 97: Eye diagram observed to the specified conditions set in the photodetector

Example: Power Boosters

Booster_system**.osd**

Booster amplifiers are usually positioned at the transmitter output or for amplifying the multiple outputs of nodes in broadcast networks. The project "Booster_system**.osd**" (Fig. 98) presents the characteristics of a booster amplifier positioned at the transmitter output.

Two different types of modulation are considered in this project: direct and external modulation. In the first case, the electrical signal is directly modulated on the signal laser. The other option uses an electroabsorption modulator to modulate the signal source laser. Both schemes can be observed by coupling the modulated signal to the EDFA 1.0 and evaluating the obtained results.

Figs. 99 and 100 show the eye diagram obtained after detecting the signal using direct modulation and external modulation, respectively.

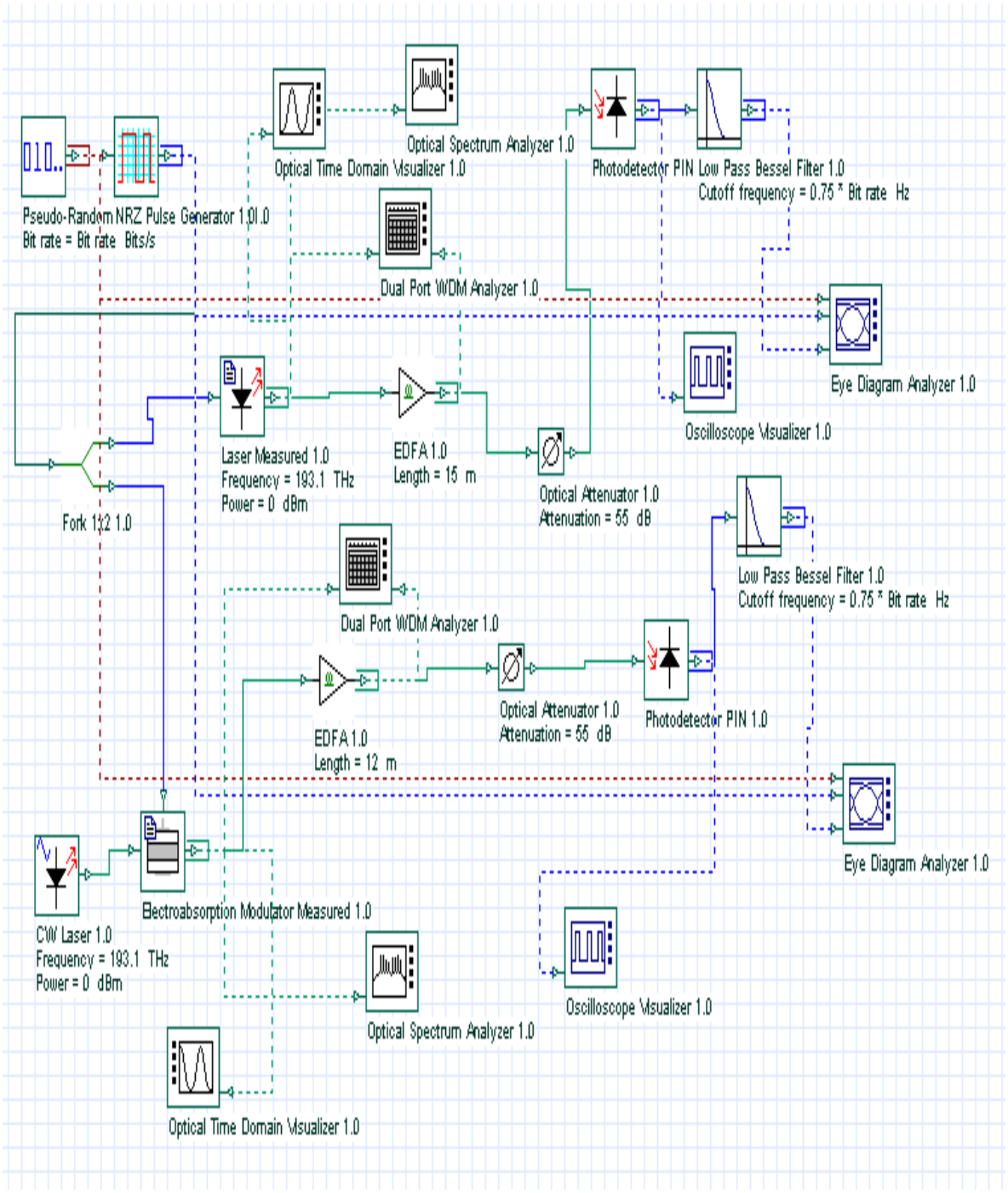

Fig. 98: Layout: Booster_system

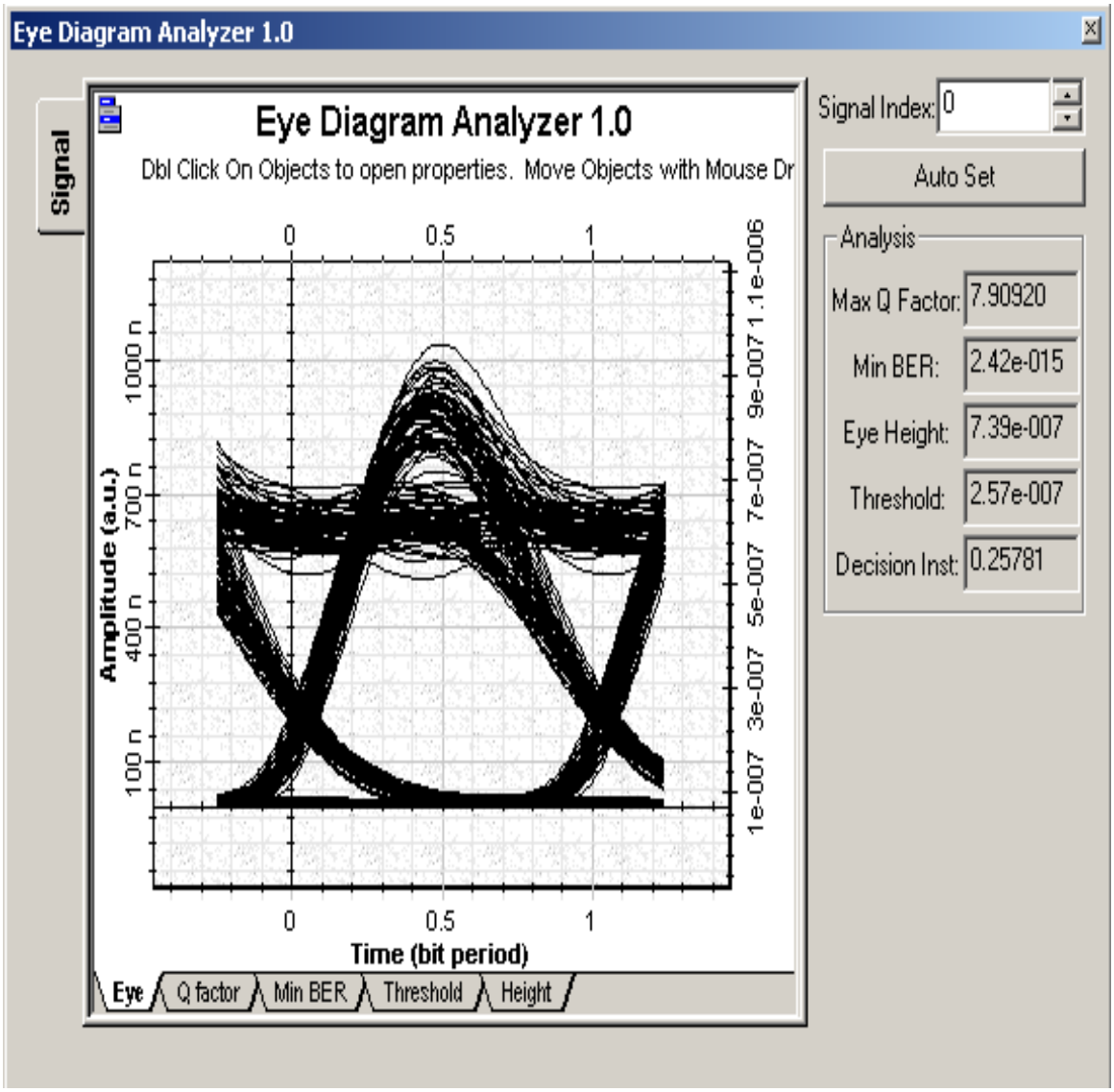

Fig. 99: Eye diagram observed after detecting the signal using direct modulation

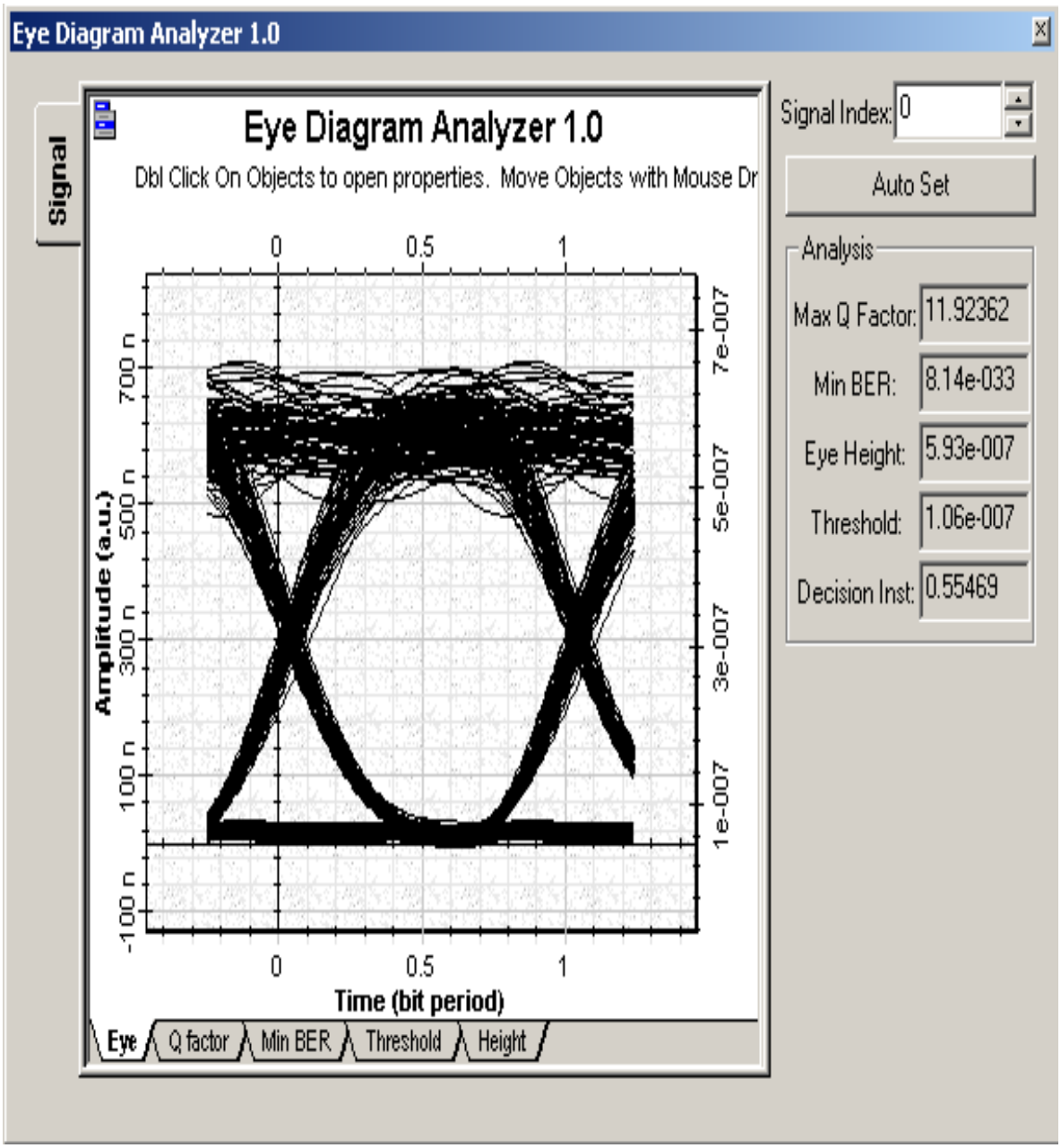

Fig. 100: Eye diagram observed after detecting the signal using external modulation

Example: Local-Area-Network-Amplifiers

Metro EDFA**.osd**

This example "Metro EDFA**.osd**" illustrates EDFAs included in a four nodes network setup in a ring topology where Node 1 communicates with Node 3 at

193.1 THz, and Node 2 communicates with Node 4 at 193.2 THz. Add-drop components enable the selective signal input/output in each node. Ideal amplifiers are included in these simulations. Subsystems like this can be found in metropolitan area networks. Fig. 101 shows the layout used to evaluate the amplifier performance in a metropolitan network.

The component Ring Control 1.0 determines the number of loops considered in the two nodes connected in a ring topology. The signal output and bit error rate are visualized in the Optical Spectrum Analyzer and BER Analyzer for different loops where 0 refers to the first turn in the loop and 1 is related to the second turn in the loop.

The signal going through Node 1 to Node 3 on channel 1 at 193.2 THz as well as the communication between Node 2 and Node 4 at 193.1 THz can be observed using different visualizers inserted in the project file. Some facilities are displayed in these visualizers that can be tried.

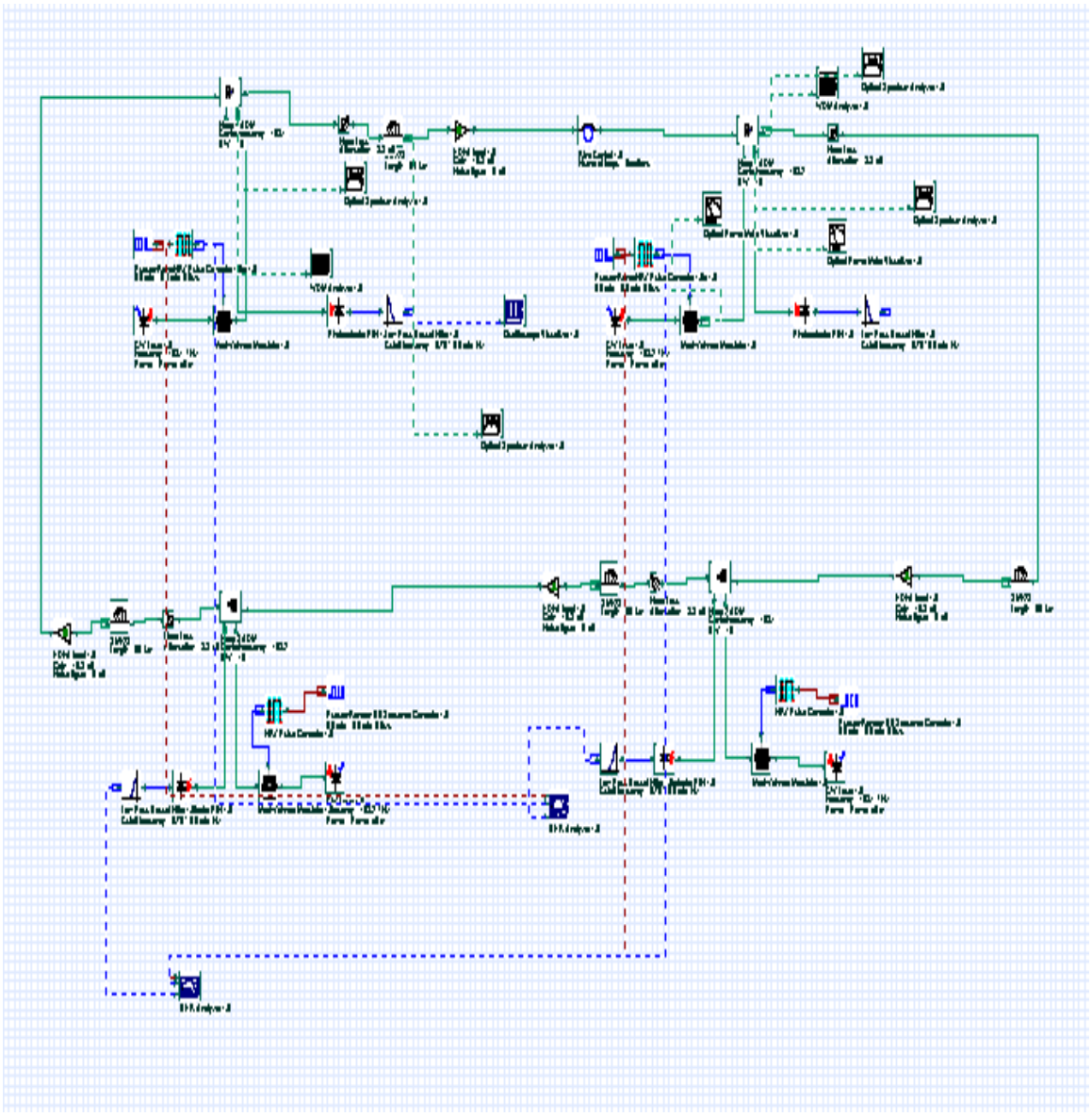

Fig. 101: Metro EDFA: Metro amplifier layout

The amplified signal observed at the Node 3 output is shown in Fig. 102. The eye diagram is shown in Fig. 103.

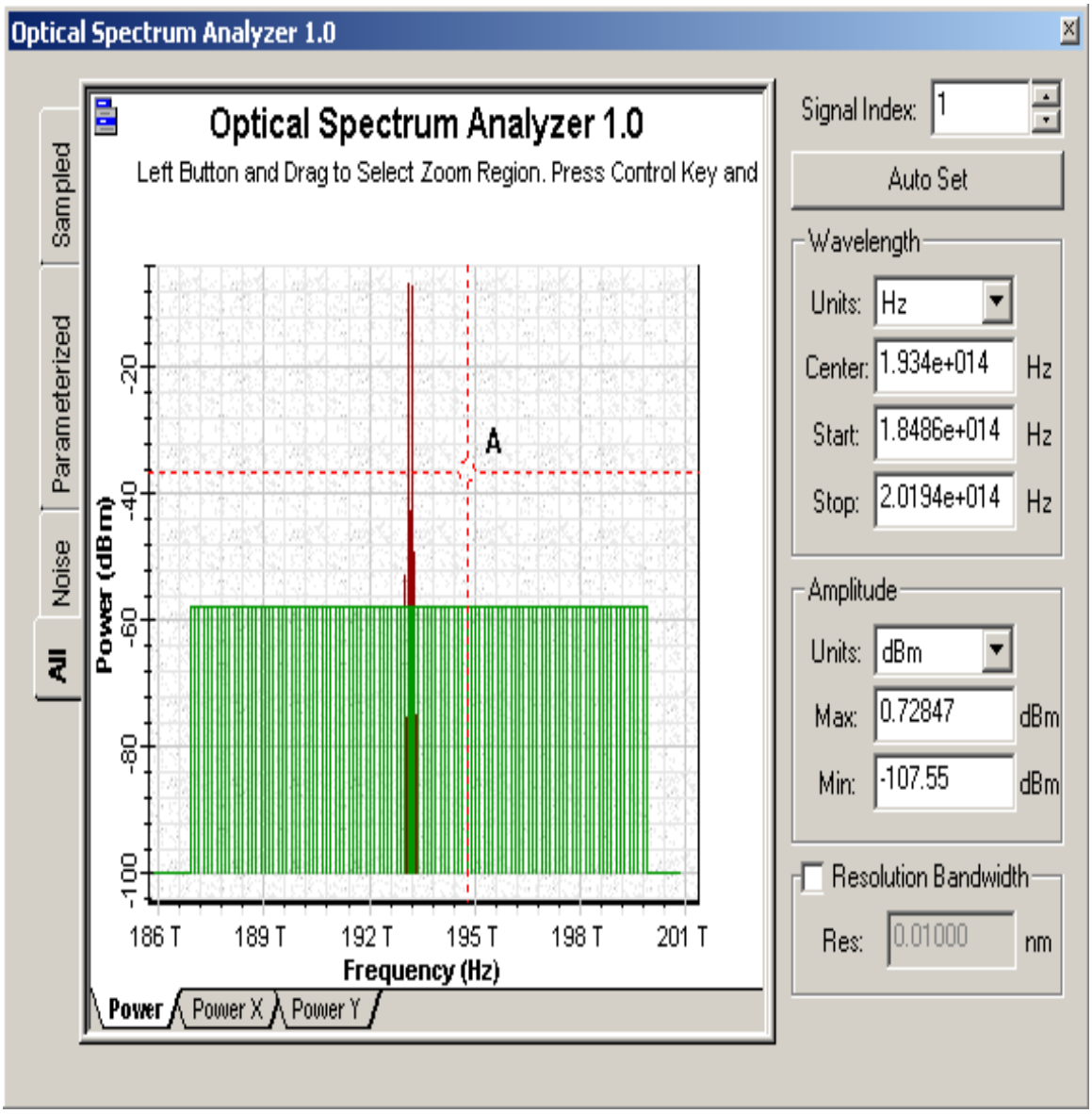

Fig. 102: Spectrum observed at OSA referring to the turn 1 in the loop

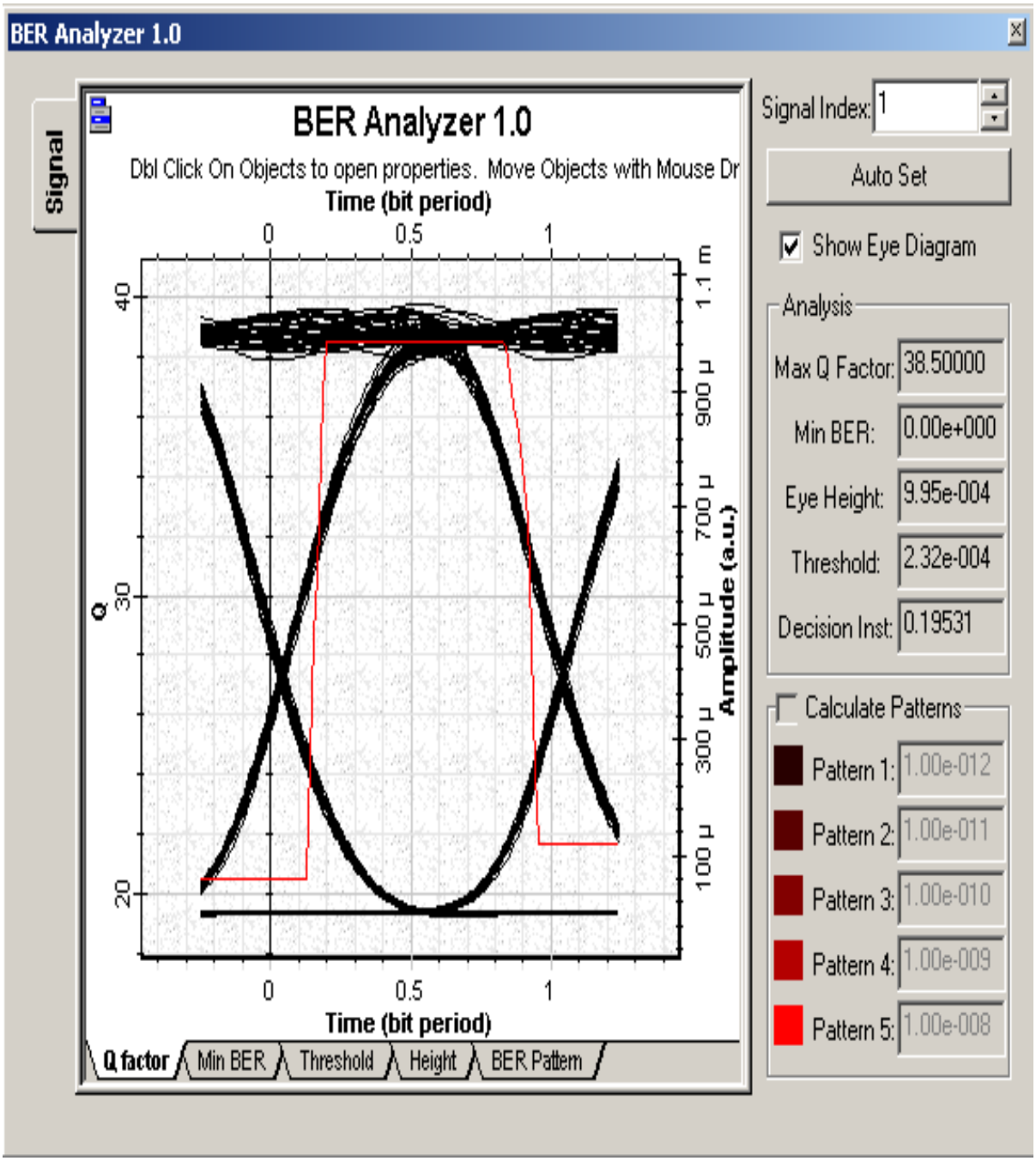

Fig. 103: Spectrum observed at the BER analyzer referring to the turn 1 in the loop

Example: Cascaded In-Line Amplifiers

In-line cascaded**.osd**

In the example In-line cascaded**.osd,** Ideal amplifiers are cascaded simulating the propagating signal along the system. A signal laser source is coupled to the cascaded amplifiers and the noise amplifier performance can be evaluated.

The effective noise figure for this cascaded chain amplifier can be calculated after running the simulations. One can change the input signal power as well as gain and noise figure for each amplifier in the system. Fig. 104 shows three ideal cascaded amplifiers at the output of a signal laser source. The Dual Port WDM Analyzer 1.0 inserted in the layout enables checking the amplifier performance. The effective noise figure for a cascaded chain can be compared considering different amplifier gain and noise figure.

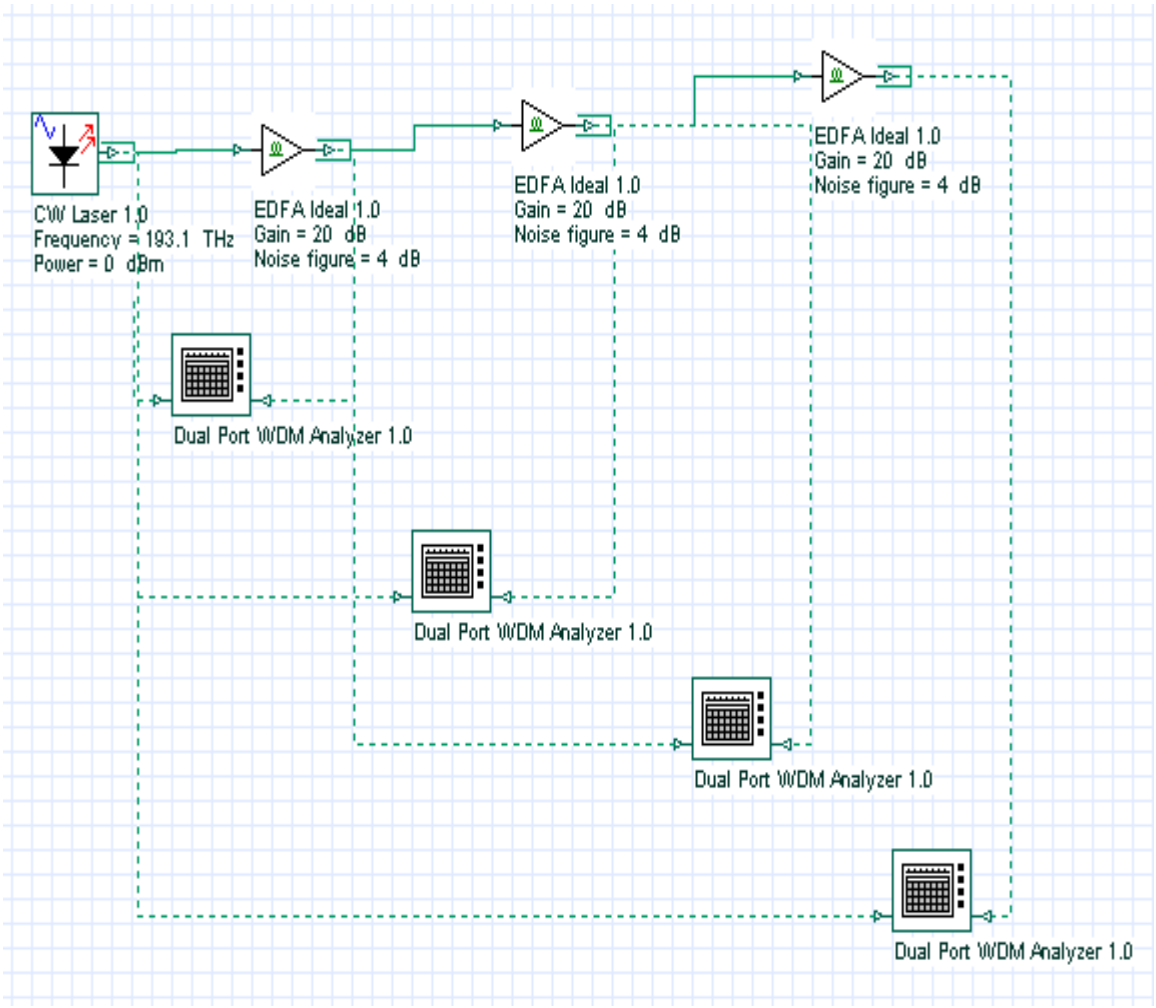

Fig. 104: Layout: In-line cascade

Example: Non-ideal characteristics of EDFAs in Metro Networks and Effect of Gain Flattening and Controlling

Considering nonideal gain characteristics of EDFA_nonideal**.osd**
Considering nonideal gain characteristics of EDFA_ideal**.osd**

Project files "Considering nonideal gain characteristics of EDFA_nonideal**.osd**" and "Considering nonideal gain characteristics of EDFA_ideal**.osd**" generates the design of a two rings network connected with OXCs. It investigates the effects of amplifier gain to network performance. First project file uses non-ideal amplifiers where the gain depends on input power and wavelength. The second one uses ideal amplifiers (to modal the gain flattening and control) with a flat and stable gain. At the end the results are compared.

To show the effect of gain tilt, lets consider a two rings system as shown in Fig. 105. Actual simulation project is given in Considering nonideal gain characteristics of EDFA_nonideal**.osd** file.

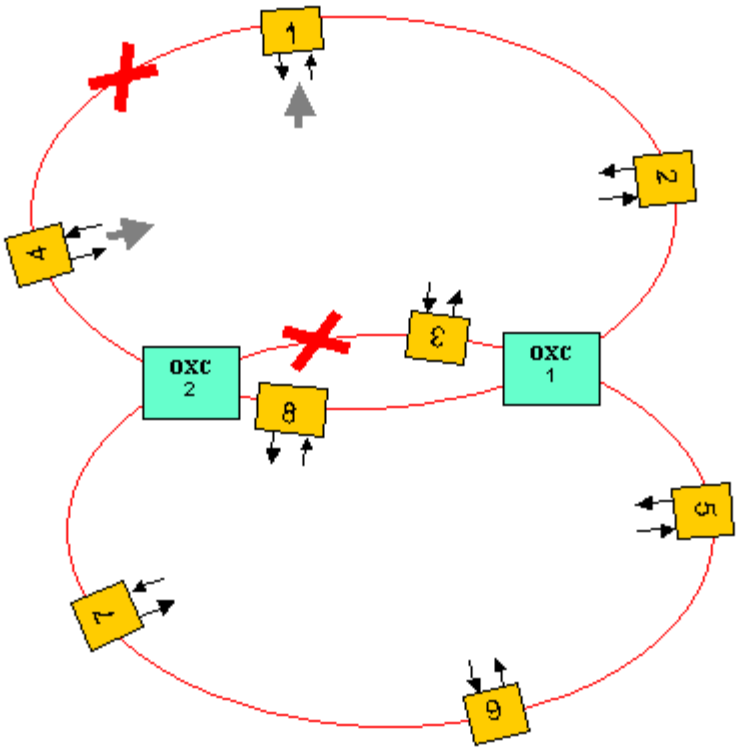

Fig.105: Two interconnected ring network layout

In this system, restoration is done in the optical layer and each ring can be used to restore the other one [1]. OXCs are designed by using subsystems and contains digital optical switches and loop control elements. Functional diagram of OXCs is given in Fig. 106.

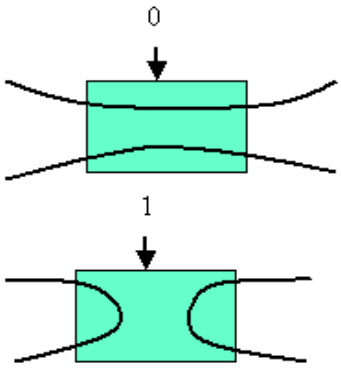

Fig. 106: Functional diagram of OXCs

Each span between nodes is made up by single mode fiber and non-ideal EDFA to compensate the span loss. There is no need to use dispersion compensation fiber since the communication is done at 2.5 Gb/s data rate. In this network node 1 communicates with node 4 on channel 1, node 5 communicates with node 7 on channel 2, node 6 communicates with node 8 on channel 3, and node 2 communicates with node 3 on channel 4. Frequency spectrum of channels is shown in Fig. 107. Node 1 can send data following a path passing through 1, 2, OXC 1, 3, OXC 2, 4. This path will require 4 amplifications.

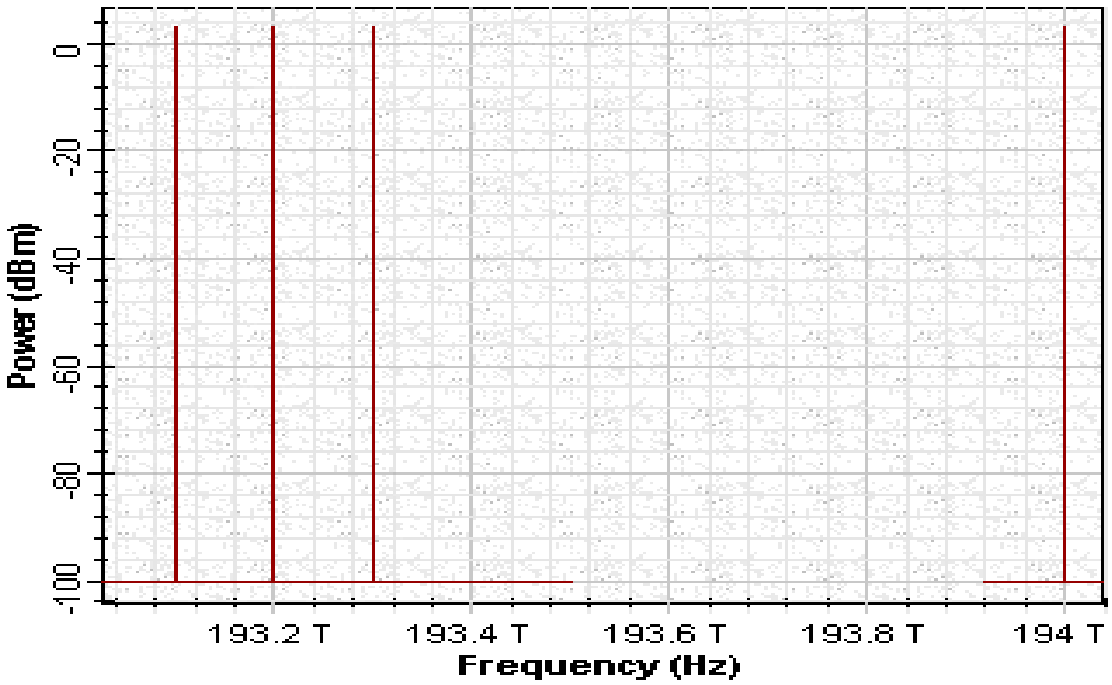

Fig. 107: Power spectrum of the 4 channel 8 node ring network

Lets assume that there is a fiber break between OXC 1 and OCX 2 or a problem at node 3 while node 2 wants to send data to node 1. Fiber break is modeled by using OXC designed as a subsystem before. To see the details, just go to the subsystem, right click on it and select look onside. Depending on the switching on OXC 1 and OXC 2, there is more than one path that the signal on channel 1 can follow. Lets consider the following: Node 1 communicates with node 4 following the path passing through 1, 2, OXC 1, 5, 6, 7, OXC 2, 4 by using the second ring as recovery path. This path will require 6 amplifications.

As stated before, gain of EDFAs depend on the input power. Because of the dynamic nature of the metro network, total power at the input of each amplifier will be different. Moreover, the gain spectrum is not flat but tilted. Therefore, it will require some extra planning to balance the power through the network. This will increase the total cost.

Figs. 108 and 109 show the eye diagram for these two different paths before and after fiber break. Since the power is not balanced, it increases along the path and may trigger the non-linearity of the fibers. For the first path, received signal power is 9.8 dBm and OSNR at the receiver end is 30 dB. The second path requires 6 amplifications whereas the first path requires 4. Received signal power after 6 amplifications is about 15 dBm (SNR is about 40 dB) and brings the nonlinear effects into picture. Because of that, the eye closes.

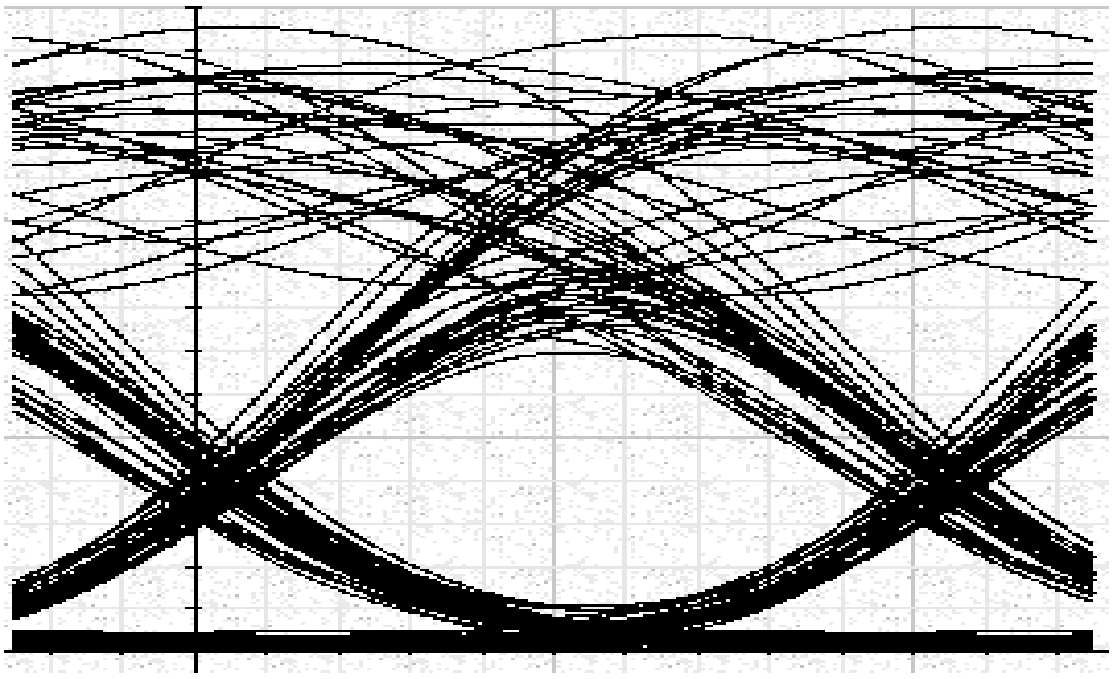

Fig. 108: Eye diagram of the signal at node 4 when the first path (node 1, node 2, OXC 1, node 3, OXC node 2, and node 4) is followed

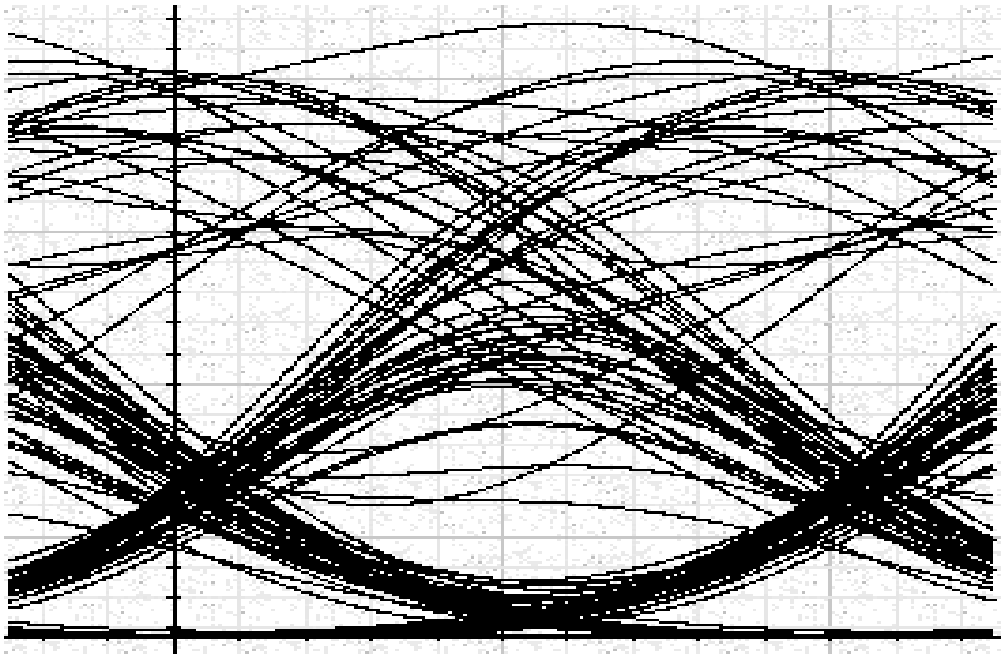

Fig. 109: Eye diagram of the signal at node 4 when the second path (node 1, node 2, OXC 1, node 5, node 6, node 7, OXC node 2, and node 4) after a fiber break is followed

This example shows that due to dynamic nature of metro network, a careful and intelligent power budget planning and control [2] should be done. Moreover, gains of EDFAs should be controlled and flattened. Let us assume that the gains of the EDFAs are flattened and stabilized with respect to input power change. To model this condition we have used ideal optical amplifiers. In this case, we have used an ideal EDFA with 16.3 dB gain after each fiber span. The simulation project is given in Considering nonideal gain characteristics of EDFA_ideal.**osd** file. Simulation results are shown in **Figs. 110** and **111** before and after the fiber break. These results show that gain control of amplifiers is important for metro applications and dynamic routing can be done easily without any problem when unity gain approach is used (Please see Optical power level management in metro networks_unity gain.**osd**).

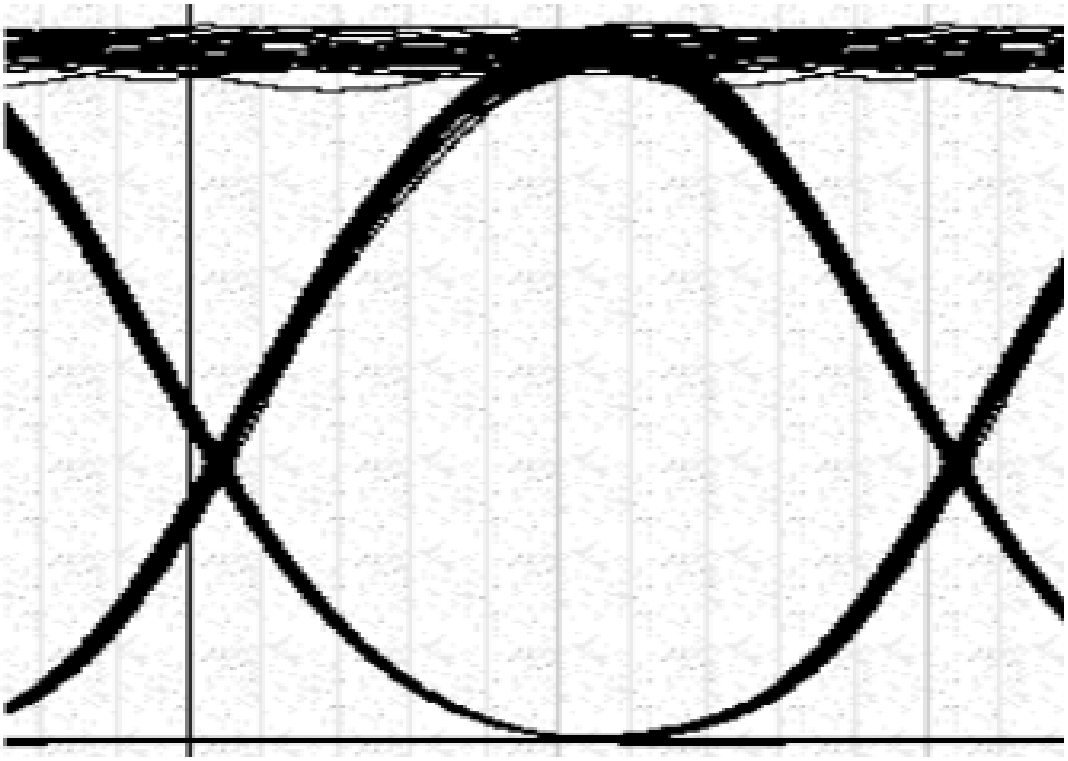

Fig. 110: Eye diagram of the signal at node 4 when the first path (node 1, node 2, OXC 1, node 3, OXC node 2, and node 4) is followed and gain flattened and controlled amplifiers are used

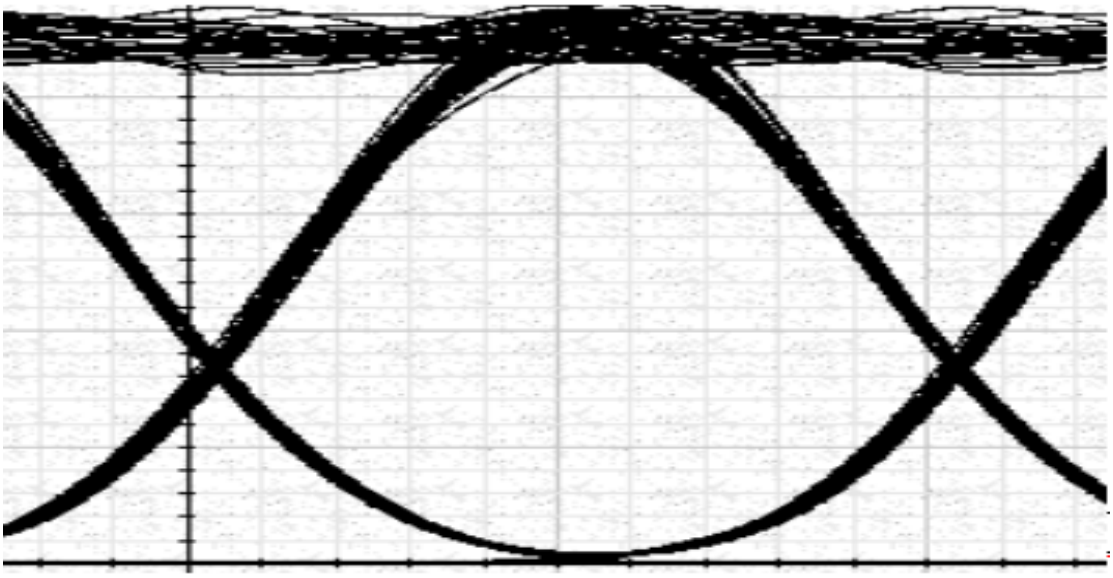

Fig. 111: Eye diagram of the signal at node 4 when the second path (node 1, node 2, OXC 1, node 5, node 6, node 7, OXC node 2, and node 4) after a fiber break is followed and gain flattened and controlled amplifiers are used

References:
1. K. M. Sivalingam and S. Subramaniam, Optical WDM Networks: Prenciples and Practice, Kluwer Academic Publishers, 2001.
2. Sidney Shiba et. al., “Optical Power Level Management in Metro Networks”, NFOEC’01, 2001.

Example: Cascaded in-line Amplifiers 10 Gb/s in SMF

System applications 10 Gb/s in SMF NRZ**.osd**
System applications 10 Gb/s in SMF RZ**.osd**

10 Gb/s single channel transmission in standard mode fibers (SMF)

The fundamental limitation to high- speed communication systems over the embedded standard single mode fiber at 1.55 μm is the linear chromatic dispersion.

Typical value of β_2 = - 20 ps^2/ km at 1.55 μm for SMF leads to D = 16 ps/ (nm . km). For bit rate B = 10 Gb/s the slot duration will be T_B = 100 ps. Considering duty cycle 0.5 $\Rightarrow$ T_{FWHM} = 50 ps $\Rightarrow$ T_0 = 30 ps. Therefore the corresponding dispersion length L_D will be ~ 45 km.

The aim of this example is to compare RZ versus NRZ- modulation format transmission in SMF at 10 Gb/s taking into account: group velocity dispersion, self-phase modulation due to the Kerr nonlinearity, linear losses and periodical amplification with ASE noise.

Two tasks will be considered: first, we will compare RZ and NRZ format transmission for lossless case. Obtained results could be compared with results of [1]. In the second the linear losses and periodical amplification taking into account ASE noise will be investigated.

Figs. 112 and 113 show the layouts used for the investigation of RZ and NRZ modulation formats.

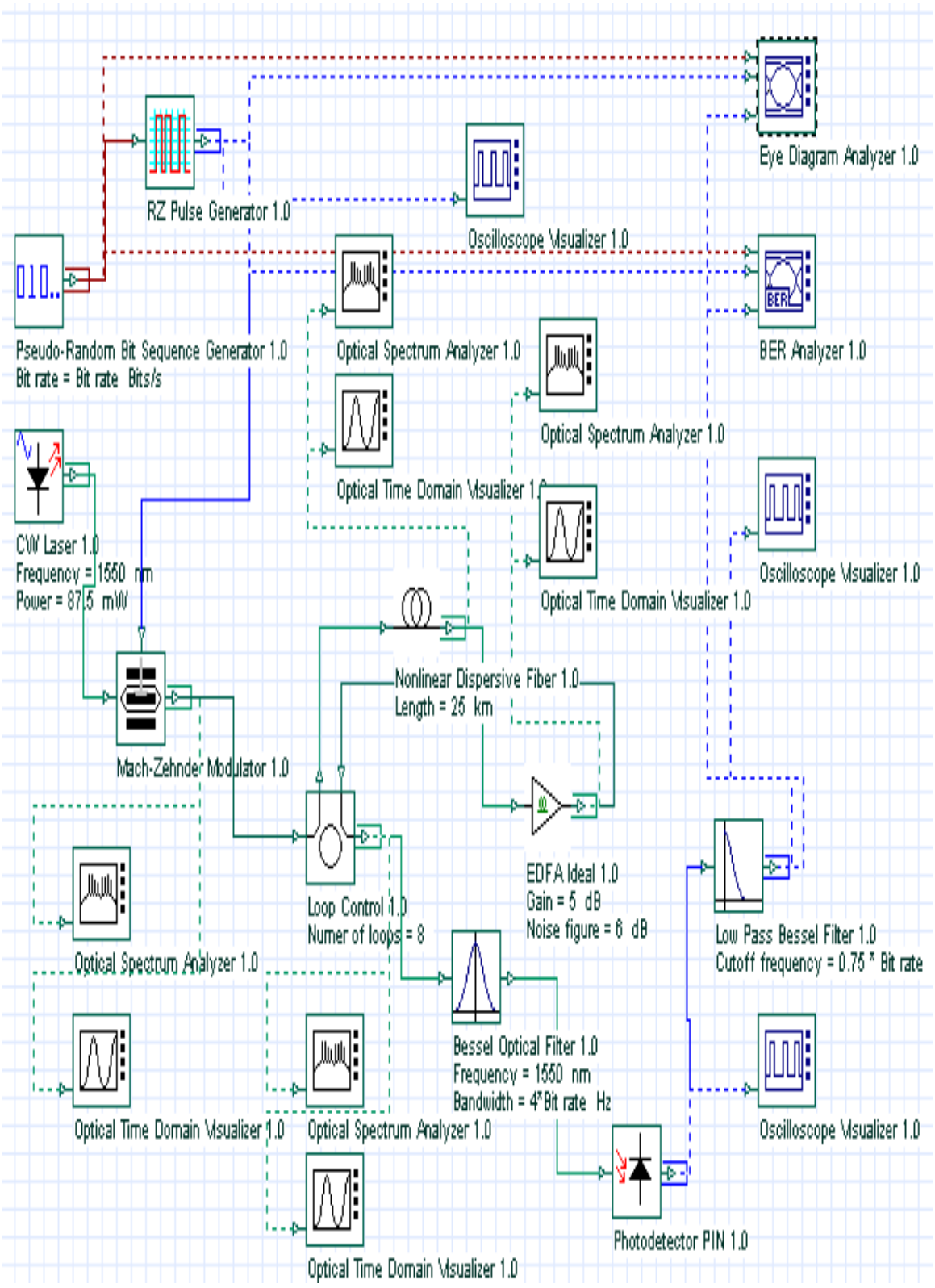

Fig.112: Layout: System applications 10 Gb/s in SMF_RZ

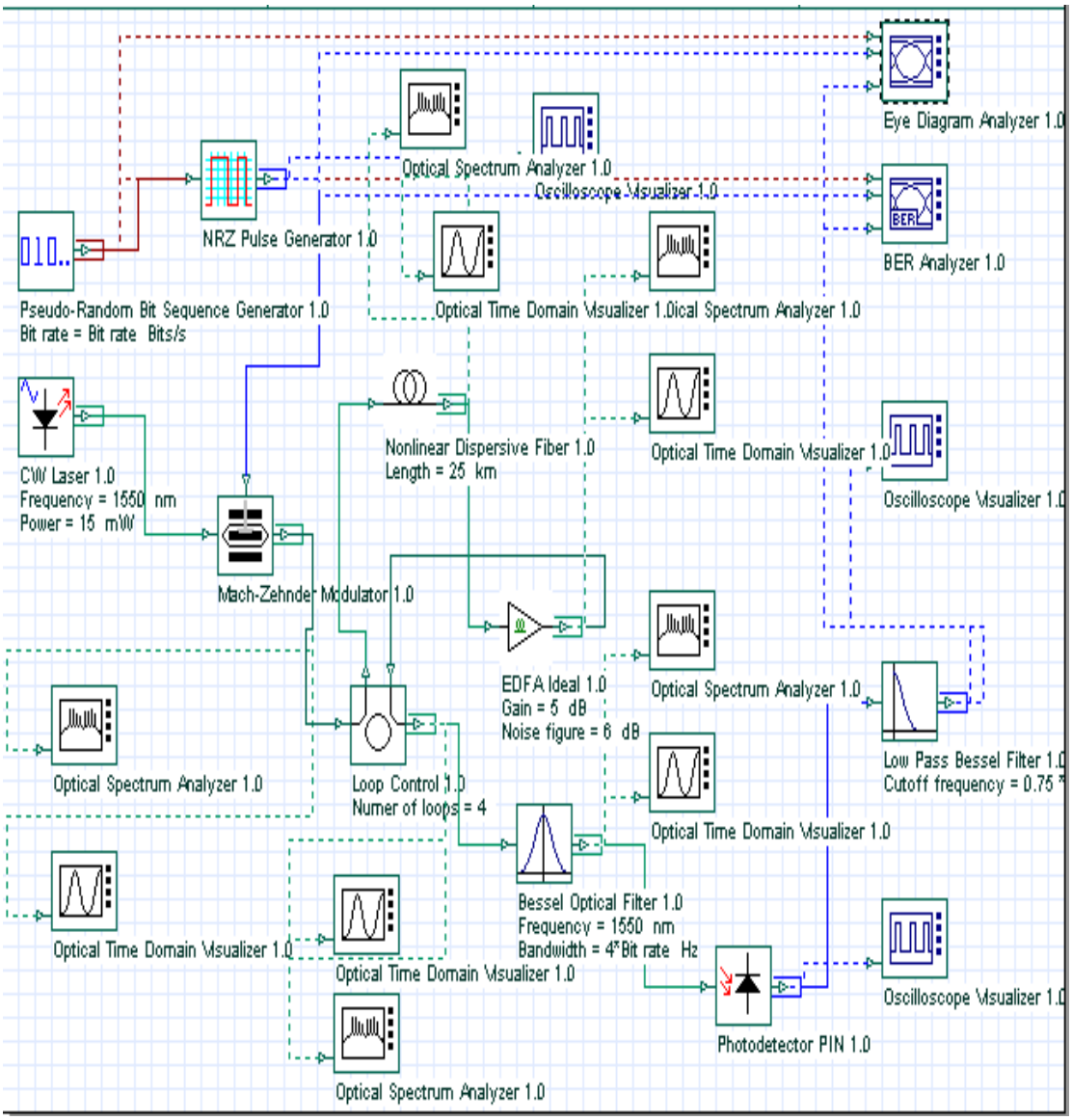

Fig.113: Layout: System applications 10 Gb/s in SMF_NRZ

The global parameters used are: Bit rate = 10 Gb/s, Sequence length = 128 Bits and Samples per bit = 128.

RZ- generator has following properties: rectangle shape: Gaussian; duty cycle= 0.5 bit; rise time= 0.15 bit and fall time = 0.25 bit.

Externally modulated CW Laser with carrier wavelength λ=1550 nm and linewidth = 0.1 MHz was used as optical source.

Standard single mode optical fiber used, has following properties: dispersion coefficient $D=17\left[\frac{ps}{nm.km}\right]$, dispersion slope $\frac{\partial D}{\partial \lambda}=0.08\left[\frac{ps}{nm^2\ km}\right]$, nonlinear coefficient $\gamma=1.31\left[\frac{1}{km\ W}\right]$ and linear loss α = 0.2 dB/ km.

Properties of the Bessel optical filter are: carrier wavelength λ=1550 nm and bandwidth = 4 $\times$ Bit rate.

The cutoff frequency of the low pass Bessel electrical filter is 0.75 $\times$ Bit rate.

Some of above parameters are chosen in accordance with [1], which allows comparison of results.

Let us first compare RZ and NRZ format transmission for lossless case.
Figs. 114 and 115 show eye diagrams for both modulation formats after 100 km transmission at 10 Gb/s in lossless SMF.

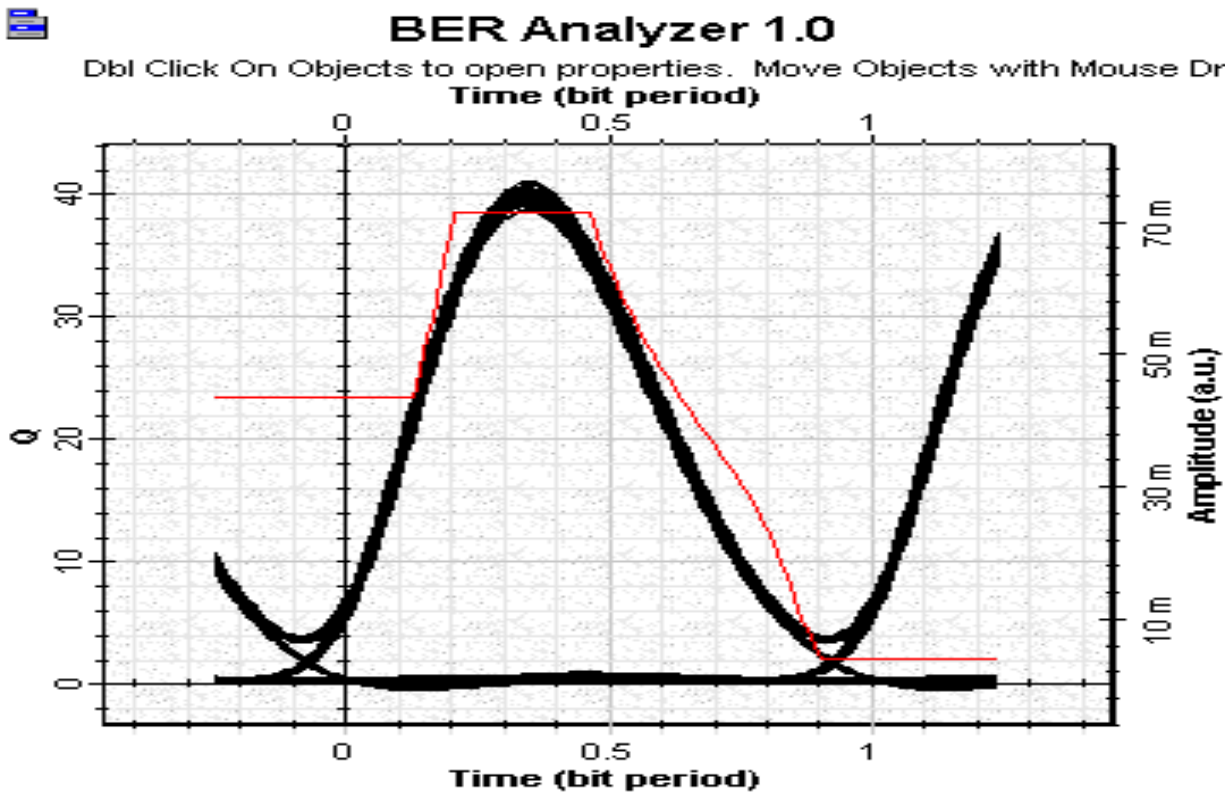

Fig.114: Eye diagram: RZ format

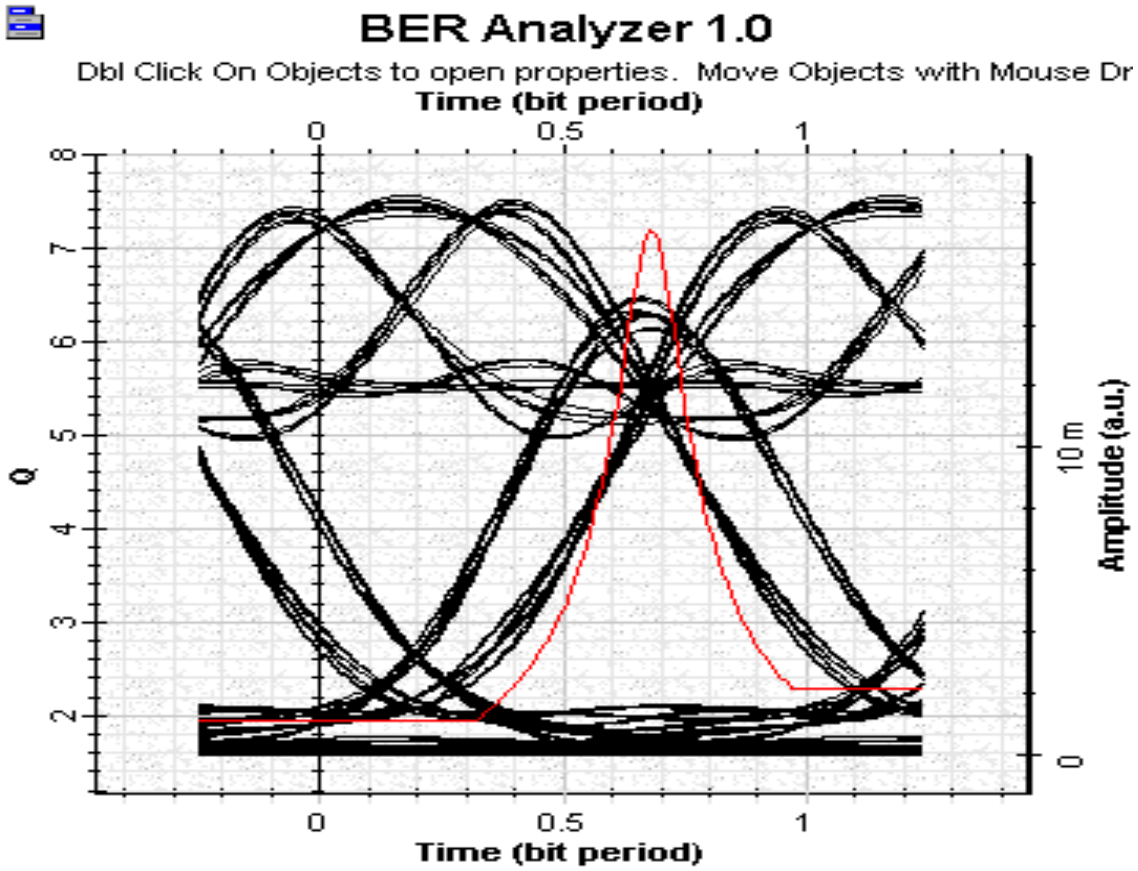

Fig. 115: Eye diagram: NRZ format

Now we analyze a 10 Gb/s transmission over SMF taking into account linear losses and ideal periodical amplification. Ideal periodical amplification is performed with the help of ideal EDFA component of OptiSystem, which also takes ASE noise into account.

Figs. 116 and 117 show the results obtained with system applications 10 Gb/s in SMF RZ**. osd** for 10 Gb/s RZ modulation format transmission (duty ratio = 0.5) over the distance of 200 km in SMF (8 loops × 25 km) and periodical amplification (gain = 5 dB, and noise figure = 6 dBm) after each 25 km. The dependence of the max Q with input power is shown in figures. The Fig. 117 shows the eye diagram for the optimal point of ~ 87.5 mW (cf.Fig. 116)**.**

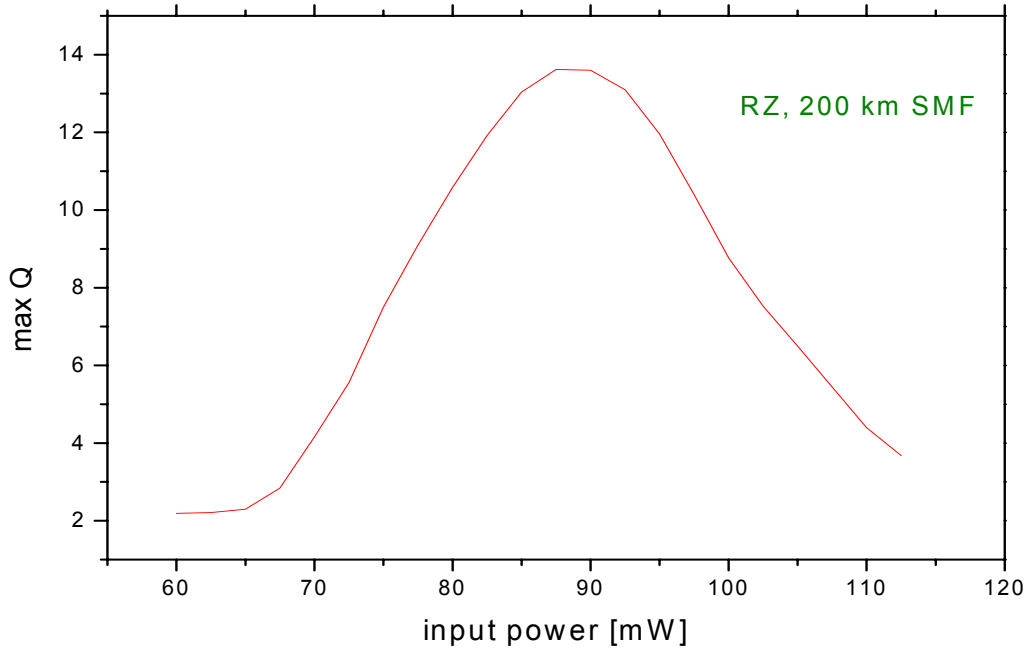

Fig.116: Max. Q vs input power

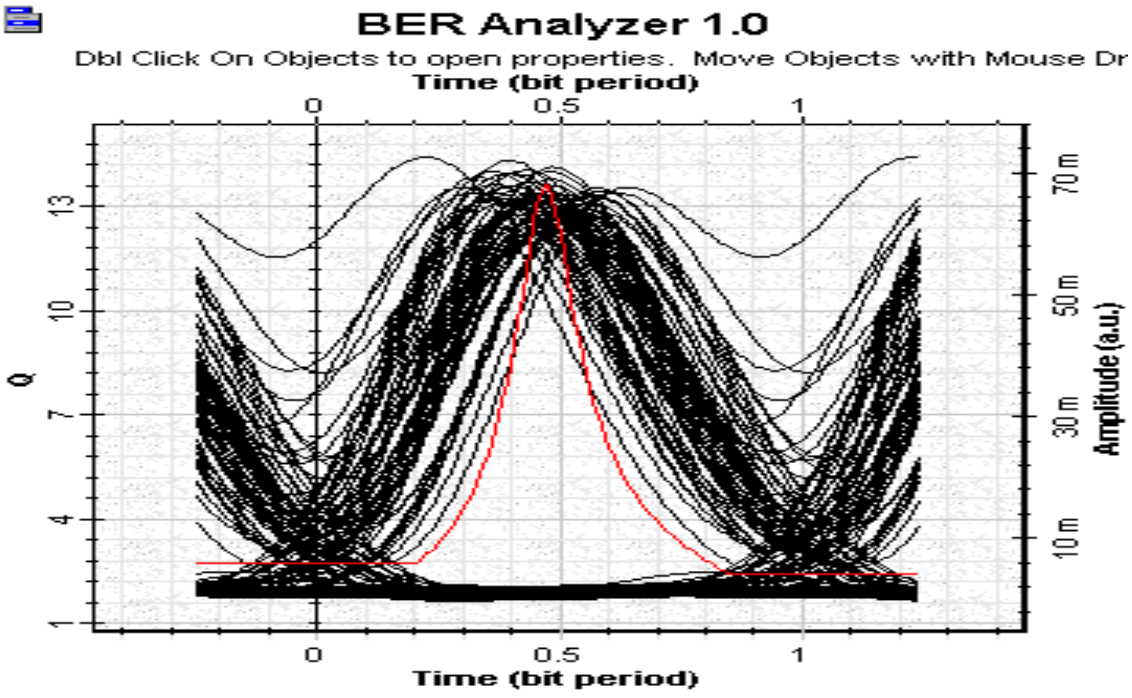

Fig.117: Eye diagram for the optimal point of ~ 87.5 mW (cf. Fig. 116)

Well-defined maxima in Fig. 116 could be identified. (Note that we have not performed any fitting to obtain this curve). As seen from the figure, at distances larger than 200 km max Q becomes smaller than 6, therefore this is the maximum distance with good Q performance.

Figs. 118 and 119 show the results obtained with system applications 10 Gb/s in SMF NRZ. **osd** for 10 Gb/s NRZ modulation format transmission over the distance of 100 km in SMF (4 loops $\times$ 25 km) and periodical amplification (gain = 5 dB, and noise figure = 6 dBm) after each 25 km. The dependence of the max Q with input power is shown in Fig. 118. The Fig. 119 shows the eye diagram for the optimal point of ~ 15 mW (cf. Fig. 118).

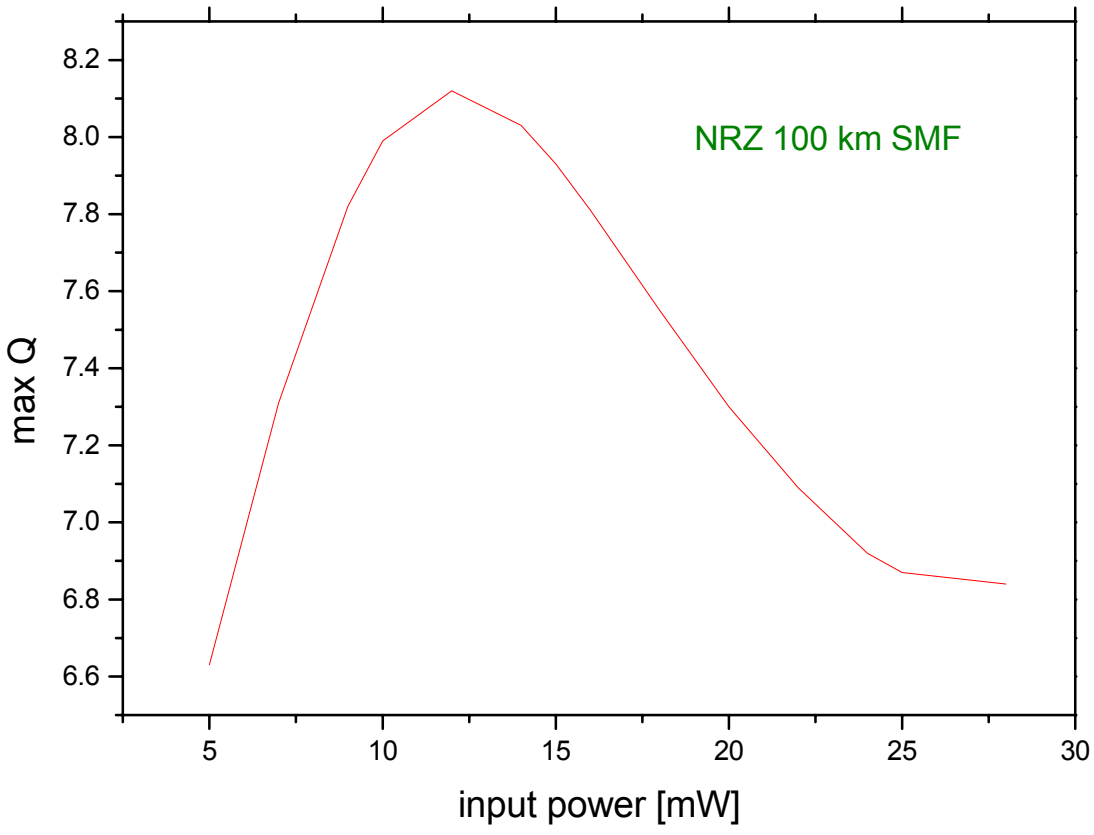

Fig. 118: Max. Q vs input power

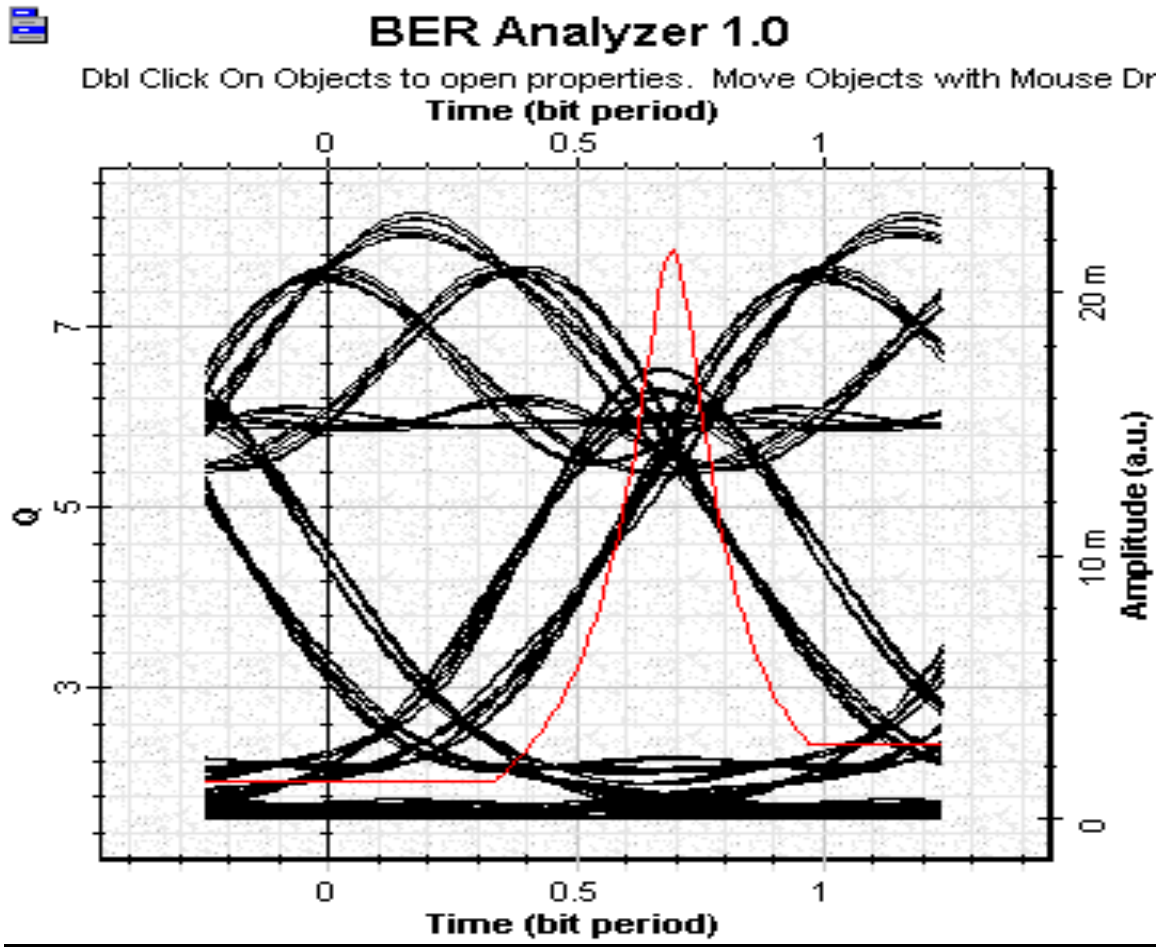

Fig.119: Eye diagram for the optimal point of ~ 15 mW (cf. Fig. 118)

Well-defined maxima in Fig. 118 could be identified. (Note that we have not performed any fitting to obtain this curve). As seen from the figure, at distances larger than 100 km max Q becomes smaller than 6, therefore this is the maximum distance with good Q performance.

Comparing positions of the maxima in both the curves we can clearly see the shift toward larger input powers in the case of RZ format.

References:

[1] K. Ennser and K. Petermann, "Performance of RZ- Versus NRZ-Transmission on Standard Single Mode Fibers", IEEE Photon. Technol. Lett., vol. 8, pp.443-445, 1996.

[2] M.I. Hayee and A.E. Willner, "NRZ Versus RZ in 10-40 Gb/s Dispersion – Managed WDM Transmission systems", IEEE Photon. Technol. Lett., vol. 11, pp.991-993, 1999.

Example: Hybrid

Hybrid**.osd**

A hybrid amplifier setup with two-stage Raman amplifier and one-stage EDFA is considered in the sample "Hybrid**.osd**" (Fig.120)**.** Basic characteristics concerning Raman amplifier design and EDFA design are discussed. Each Raman amplifier is setup in a bidirectional pump scheme, while the EDFA is setup in a co-propagating pump configuration. The flexibility to select the wavelength pump in the Raman amplifier is also illustrated.

The EDFA is pumped by a 1480 nm laser in a co-propagating pump scheme, while each stage of Raman amplifier is bidirectionally pumped by lasers at 1471.5 nm, 1495.1 nm, 1502.5 nm and 1503 nm using different powers.

The multi-line source that enables to couple a WDM signal to the hybrid amplifier can be expanded by selecting the option "Look inside" after right clicking on the Multi-Line source component. Details of the multi-line source will appear on the screen as shown in Fig. 121.

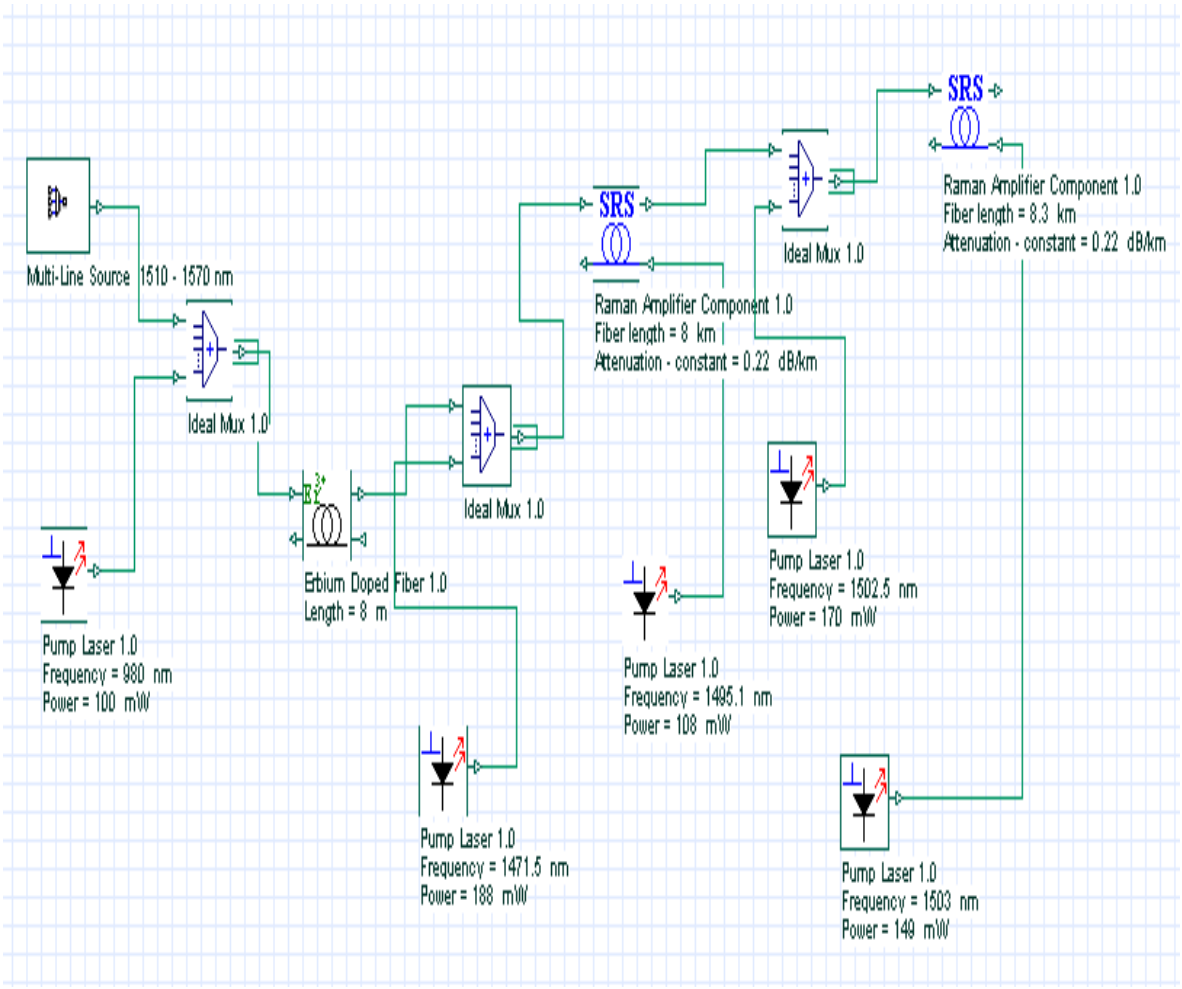

Fig. 120: Layout: Hybrid

The signal wavelength from the multi-line source can be modified clicking on View/Parameter Groups, when a window containing details of the signal opens on the screen. Different signal values can be assigned to one or all the listed wavelength signal by right clicking on “Values” and selecting “Spread” or “Assign Multiple”.

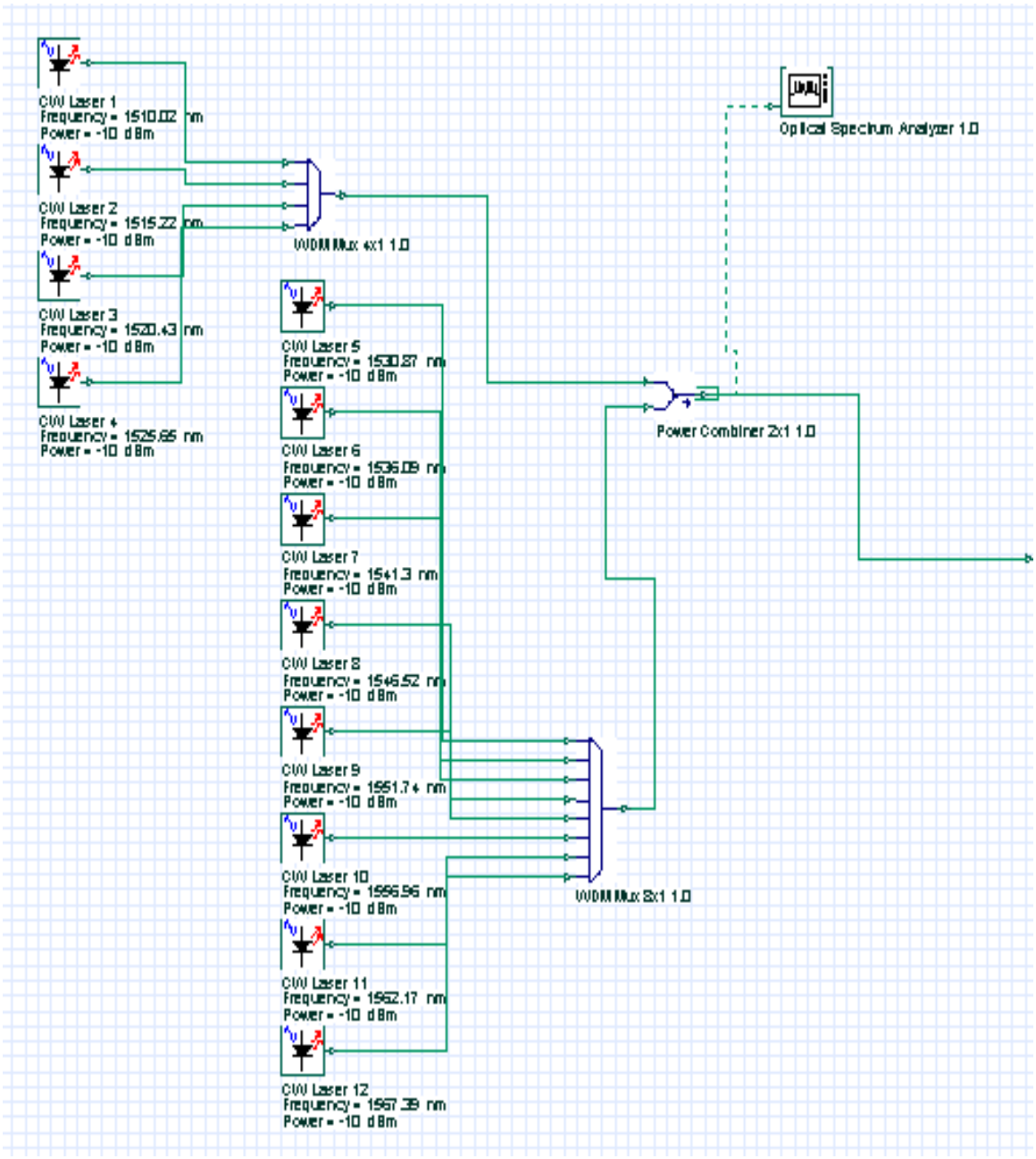

Fig. 121: Layout: Multi-line source viewed in details

The hybrid amplifier performance can be optimized. Techniques that flatten the gain are not included in this example. It is interesting to note that the gain obtained at the hybrid amplifier output gives a contribution of the Raman amplifier gain at longer signal wavelengths.

Example: EDFA Dynamic

EDFA dynamic**.osd**

In the example "EDFA dynamic**.osd**" (Fig.122) we simulate the function response of a C-band EDFA to a step excitation at a signal wavelength. The step function has a period of 1.2 ms, longer enough to enable the amplifier to achieve the steady-state solution. The pump power is constant over the time and is counter-propagating with relation to the signal. Power transients which occur in one amplifier can be studied as a function of the pump power, the signal power, the erbium-doped fiber length or any other parameter.

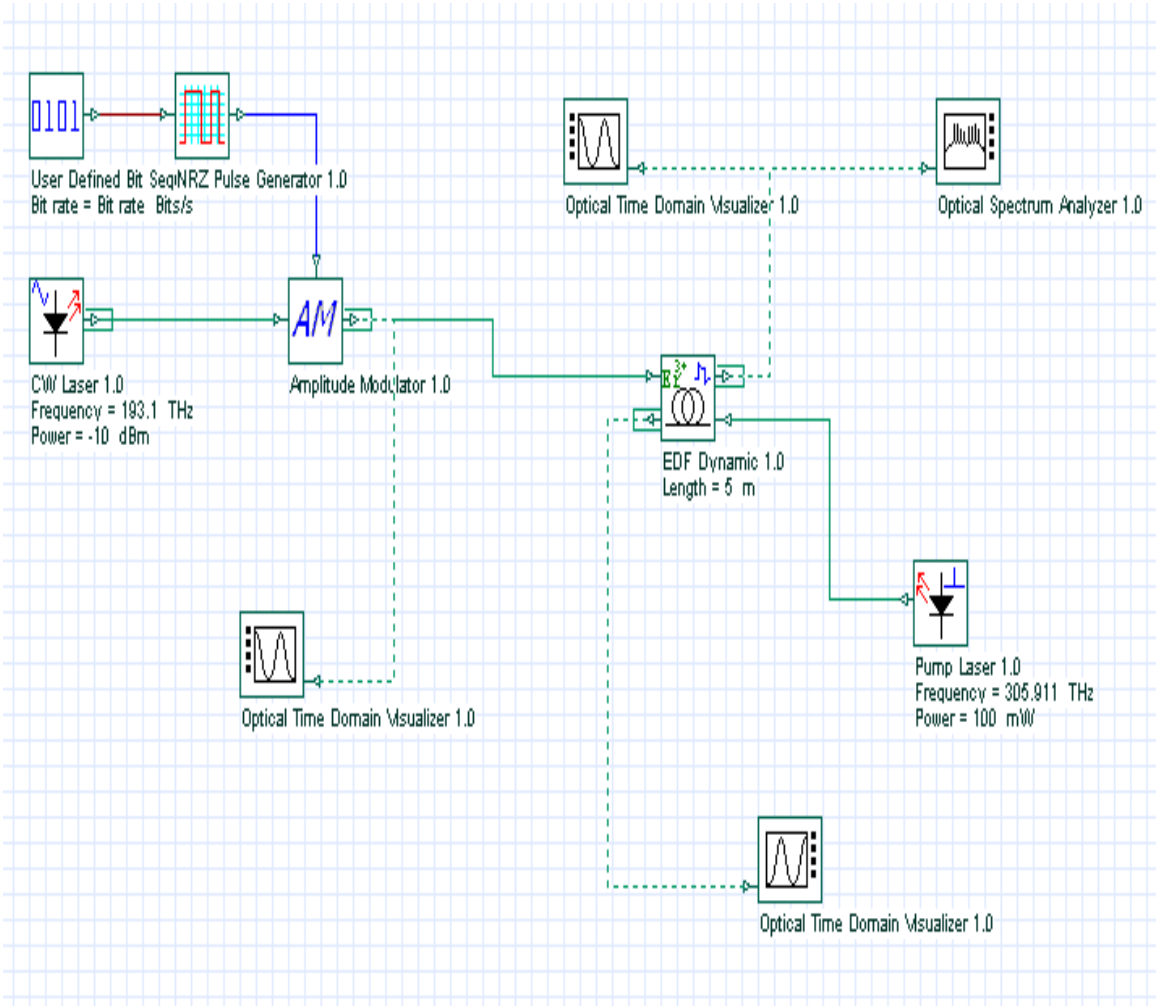

Fig. 122: Layout: EDFA dynamic

The Optical Time Domain Visualizer 1.0 enables to observe the power decay at the amplifier output.

The signal input coupled to the amplifier that enables dynamic analysis is shown in Fig. 123, while the signal output is shown in Fig. 124.

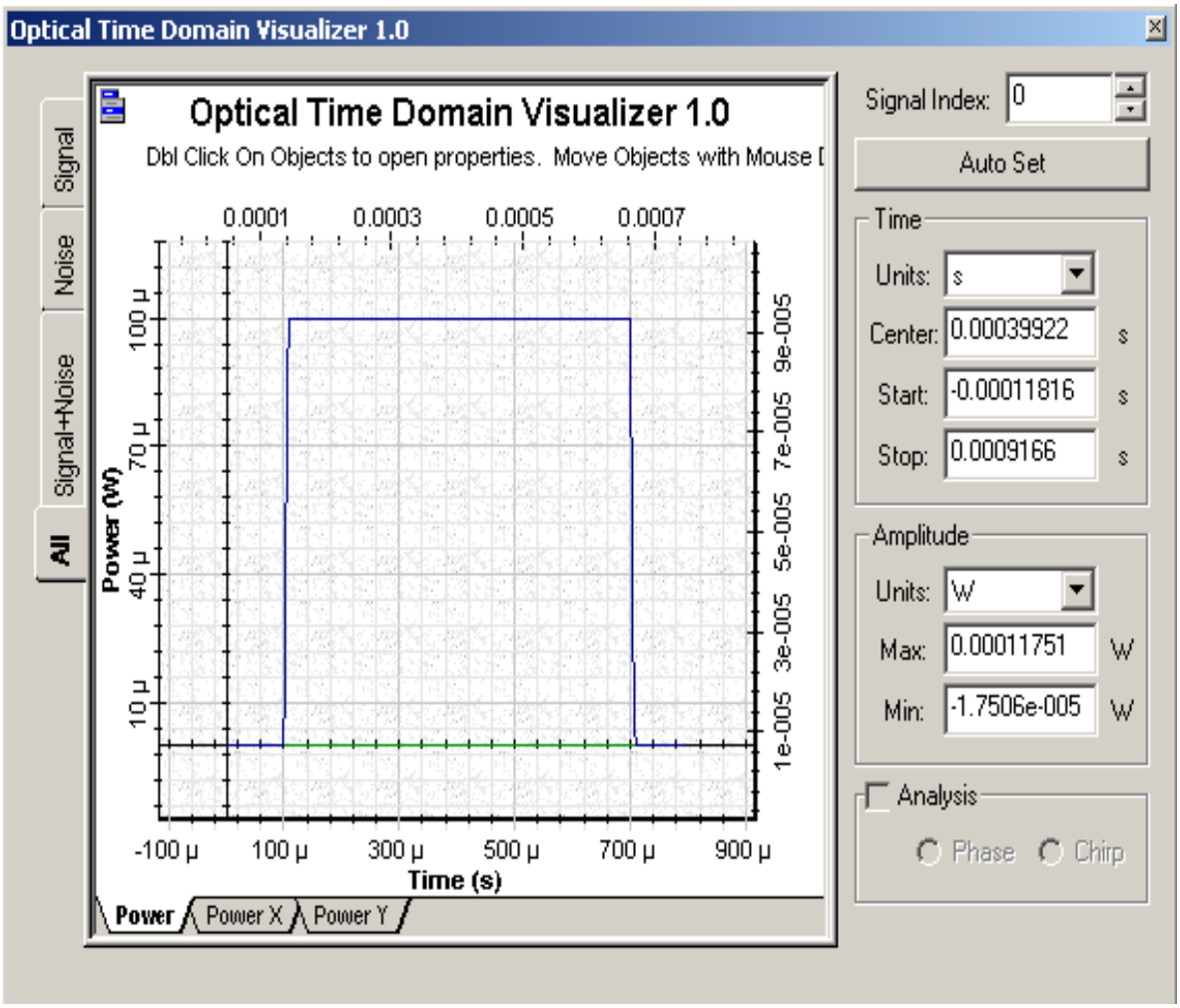

Fig. 123: Input signal observed at the output of the amplitude modulator

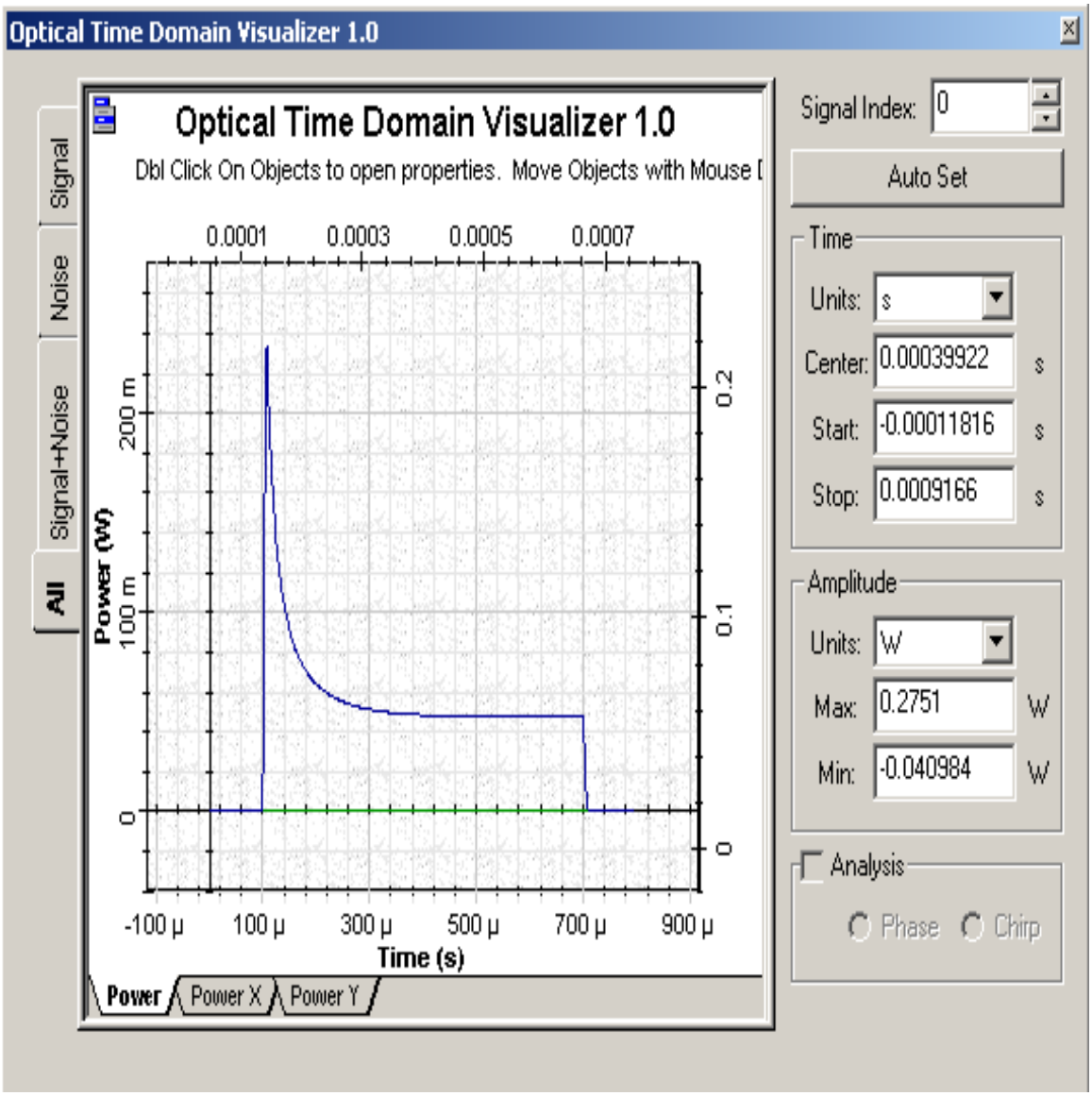

Fig. 124: Power versus time observed at the amplifier output

Chapter 7- Dispersion Management

Example: Dispersion Compensation Techniques

Dispersion compensation_post.**osd**
Dispersion compensation_pre.**osd**
Dispersion compensation_symmetrical.**osd**

Project files "Dispersion compensation_post.**osd**" (Fig.1(a))
"Dispersion compensation_pre.**osd**" (Fig.1(b))
and "Dispersion compensation_symmetrical.**osd**" (Fig.1(c))

compare three different dispersion compensation techniques, namely pre-, post, and symmetrical dispersion compensations by using DCFs. These examples consider just one channel. The bit rates used for the examples are 2.5 Gb/s and 10 Gb/s, respectively.

Although there are several forms of dispersion, the main form of dispersion we are concerned with is chromatic dispersion or group velocity dispersion (GVD). Pulse broadening effect of chromatic dispersion causes the signals in the adjacent bit periods to overlap. This is called inter-symbol interference (ISI). Broadening is a function of distance as well as dispersion parameter D. Dispersion parameter is given in ps/nm/km and changes from fiber to fiber. D is also a function of wavelength and is usually about 17 ps/nm/km in the 1.55 μm wavelength range for a standard single mode fiber (SMF). It is about 3.3 ps/nm/km in the same window for a dispersion-shifted fiber (DSF). Nonzero dispersion shifted fiber (NZDSF) has a chromatic dispersion between 1 and 6 ps/nm/km for (+) NZDSF and –1 and –6 ps/nm/km for (-) NZDSF.

For externally modulated sources, transmission distance limited by chromatic dispersion is given by [1]

$$L < \frac{2\pi c}{16|D|\lambda^2 B^2}$$

Again for example for D=16 ps/(km-nm) and at 2.5 Gb/s $L \approx 500\,km$ whereas it drops to 30 km at 10 Gb/s bit rate.

Several techniques such as dispersion compensating fiber or fiber Bragg grating can be used to compensate the accumulated dispersion in the fiber. In this example we will show three different schemes, namely pre-, post-, and symmetrical compensation, to compensate the fiber dispersion. To do so, we will first use dispersion compensating fibers (DCFs). We will then show how the

amount of accumulated dispersion from the dispersion compensator affects the performance. For this case we will use Fiber Bragg Grating (FBG) as dispersion compensator.

Pre-, post-, and symmetrical compensation configurations are shown in Figs. 1(a), 1(b) and 1(c), respectively. In our simulations we have used optical amplifiers after each fiber to compensate the fiber loss. Dispersion parameter of SMF is 16 ps/nm-km and it is 120 km long. Therefore, total accumulated dispersion is 16×120 = 1920 ps/nm. This much dispersion can be compensated by using a 24 km long DCF with – 80 ps/km-nm dispersion. In post-compensation case, DCF is placed after SMF whereas in pre-compensation case it is inserted before SMF. In symmetrical compensation case, fiber placement follows the sequence of DCF, SMF, SMF, DCF.

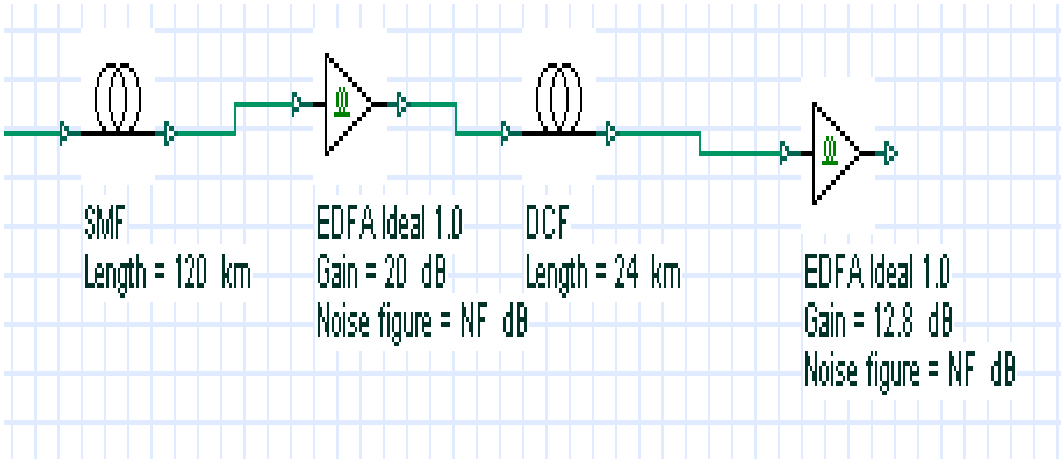

Fig. 1a: Dispersion_post-compensation

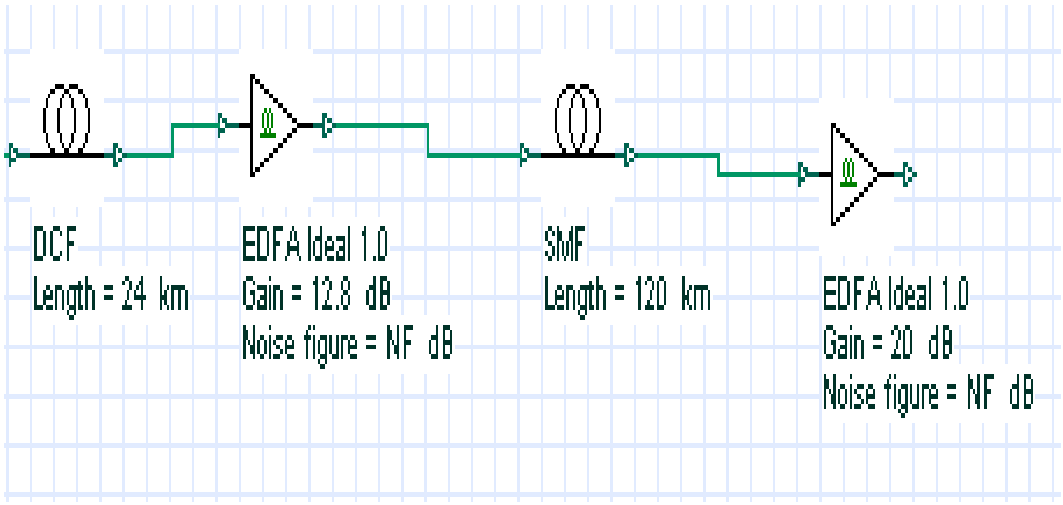

Fig. 1b: Dispersion_pre-compensation

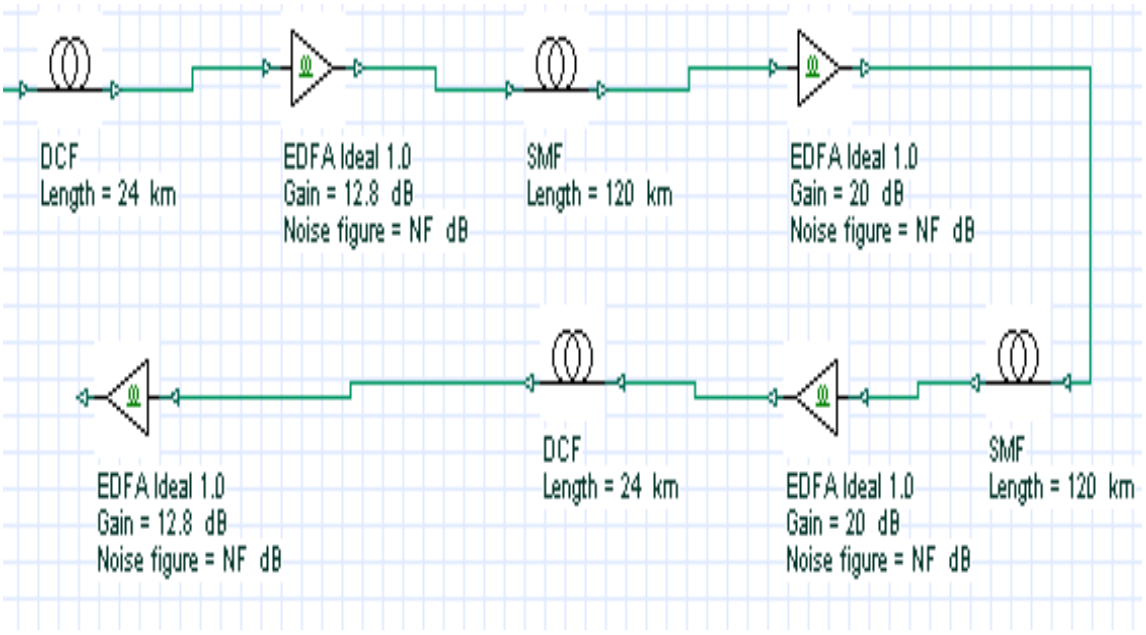

Fig. 1c: Dispersion_symmetrical-compensation

Simulation results are shown in **Figs. 2 and 3**. **Fig. 2** shows *Q* factor of received signal verses transmitted signal power for these three schemes at 2.5 and 10 Gb/s bit rates. These figures are obtained by sweeping the power from –12 dBm to 12 dBm and using the software's Graph Builder. From these figures, we can conclude that the best performance is obtained by using symmetrical dispersion compensation. The worst case is dispersion pre-compensation. Post-compensation gives a result as good as symmetrical compensation [2,3]. This can be seen from the eye diagrams given in **Fig. 3**.

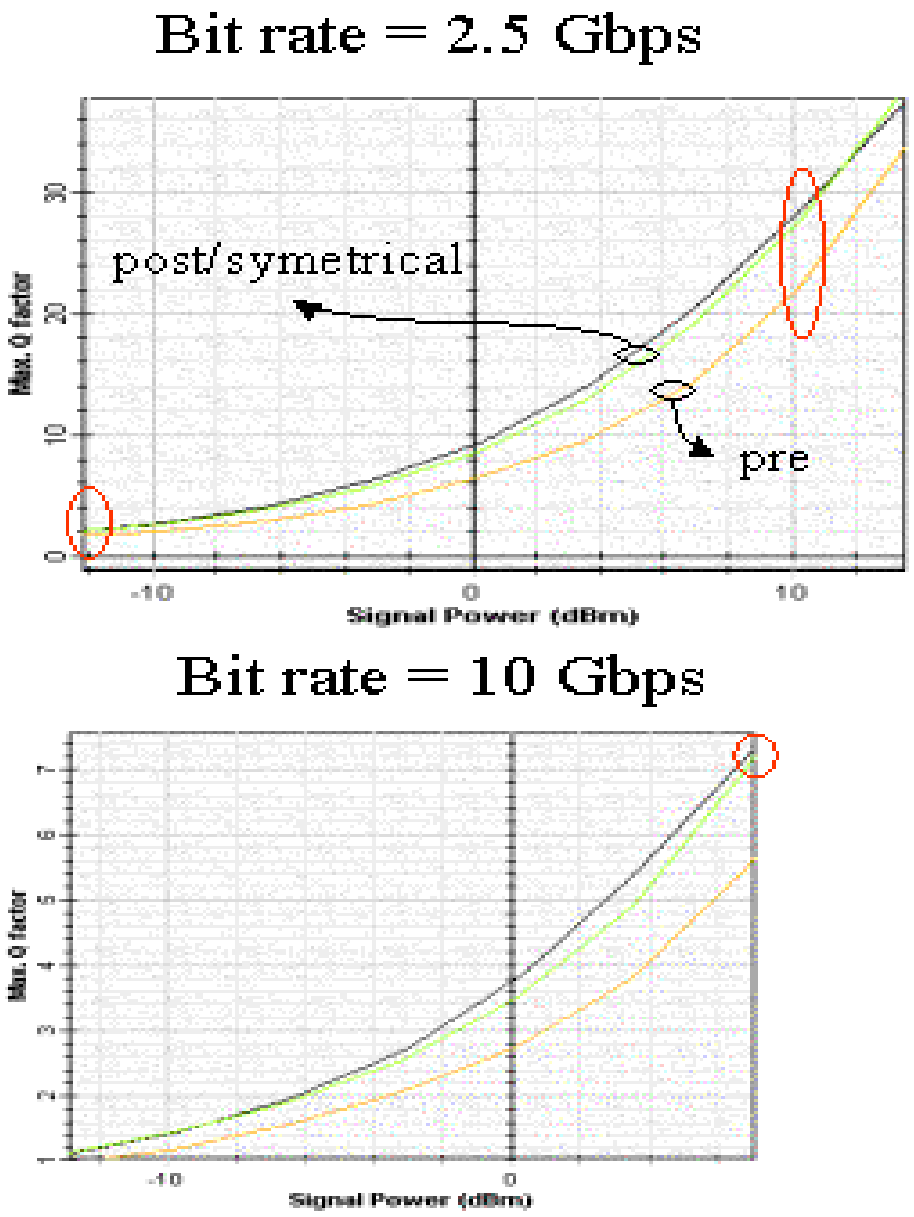

Fig. 2: Q factor verses signal power at 2.5 and 10 Gb/s bit rates for pre-, post-, and symmetrical dispersion compensations

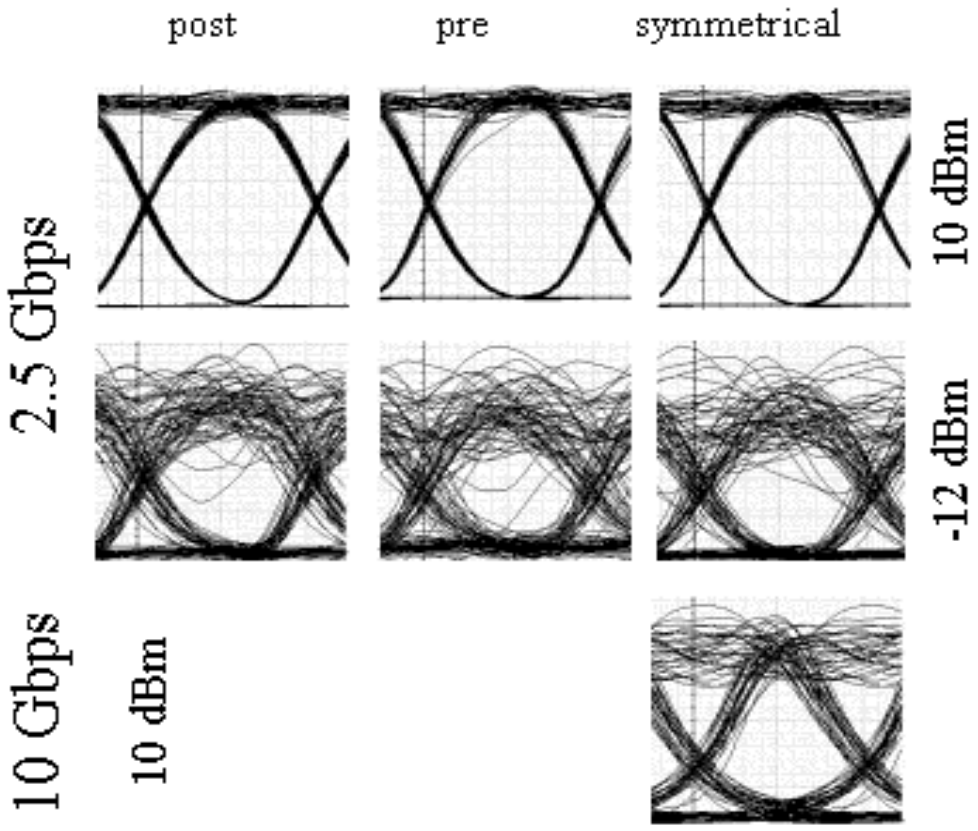

Fig. 3: System performance at 2.5 and 10 Gb/s bit rates for pre-, post-, and symmetrical dispersion compensations. The eye diagrams for these cases have been shown for –12 and 10 dBm signal powers, respectively.

References:

1. G. P. Agrawal, Fiber Optic Communication Systems, Wiley-Interscience, 1997.
2. R. Ramaswami and K. N. Sivarajan, Optical Networks: A practical Perspective, Morgan Kaufmann, 1998.
3. M. I. Hayee and A. E. Willner, “Pre- and post-compensation of dispersion and nonlinearities in 10-Gb/s WDM systems”, IEEE Poton. Tech. Lett. 9, pp. 1271, 1997.

Example: Precompensation Technique using SOA

Amplifier- induced chirp SLA compression.**osd**

Compression of weak picosecond pulses by using gain saturation effects in SOA

The gain saturation induced self-phase modulation in SOA affects in the formation of positive chirp of the pulse in the process of amplification. From the theory of propagation of phase modulated optical signals in dispersive medium [1] we know that depending on the signs of the chirp of signal and the chirp of the dispersive medium, different scenarios are possible. For equal signs of chirps the dispersion effect is amplified. On other hand, in the case of different signs of the chirps the effect of pulse dispersion can be reduced which effectively leads to pulse compression.

If we would like to use the positive chirp created in the process of pulse amplification in SOA for compression we have to propagate this pulse with dispersive media that creates negative chirp. Such media could be standard single mode fiber used for wavelengths larger than the zero dispersion wavelength or in other words in the region of anomalous group velocity dispersion. This idea has been proposed and realized in [2]. In this project, using SOA component we will try to interpret results obtained in [2].

Following parameters of SOA have been used in [2]: Unsaturated single pass gain G_0 = 30 dB; linewidth enhancement factor α = 5; saturation energy E_{sat} ~ 6 pJ. Ratio E_{in} / E_{sat} has been varied over the range 0.01 to 0.2. Typical values for the carrier lifetime are given as 200-300 ps. Pulses for which the condition T_0 / T_{sat} << 1 is valid have been considered

We use following global parameters: bit rate B = 40 Gb/s $\Rightarrow$ T_B = 25 ps **(Table 1)**.

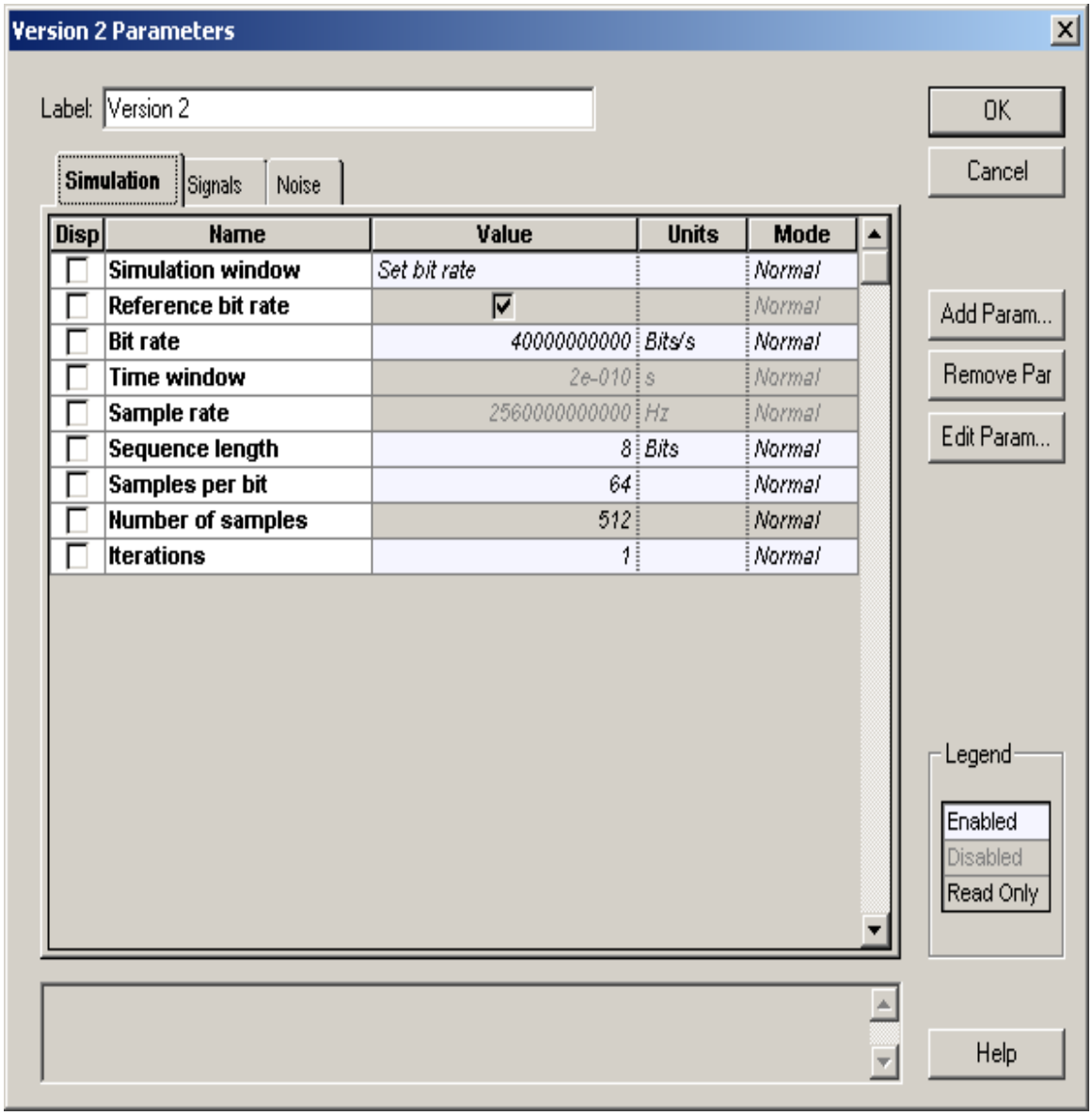

Table 1: Simulation parameters

We also consider pulses with T_{FWHM} =25 ps $\Rightarrow$ T_0 ~ 15 ps. The other optical Gaussian pulse generator parameters are shown in **Table 2**.

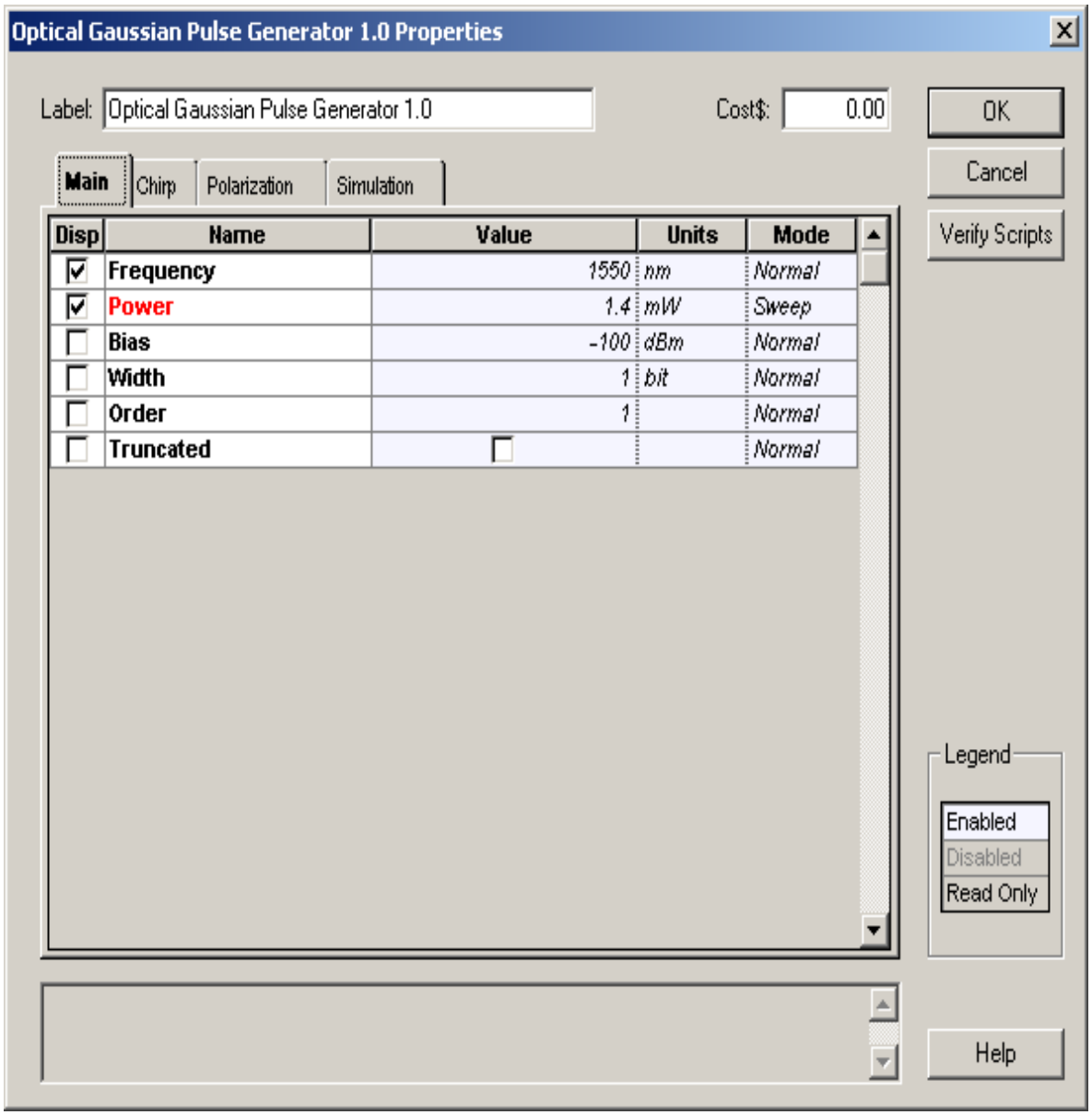

Table 2:Optical Gaussian pulse generator (Main)

The semiconductor optical amplifier parameters are shown in **Table 3**.

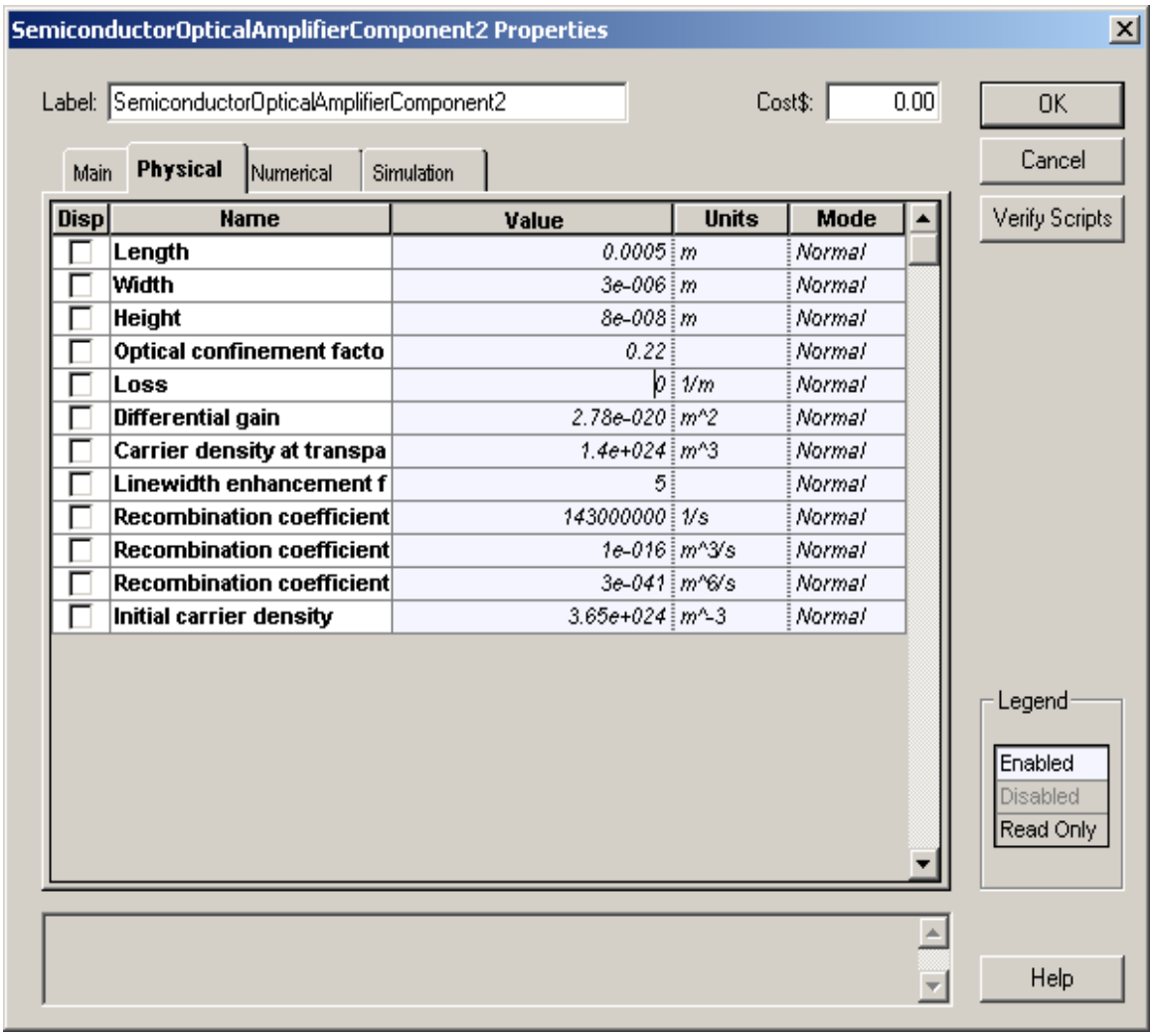

Table 3: Semiconductor optical amplifier component (Physical parameters)

The default values of the SOA component, i.e., the carrier lifetime and the saturation energy are τ_C ~ 1.4 ns and E_{sat} ~ 5 pJ, respectively.

To satisfy the conditions $T_0 / T_{sat} << 1$ and E_{in} / E_{sat} ~ 0.01 to 0.2 we can use the Gaussian pulse with T_0 ~ 15 ps for which T_0 / T_{sat} ~0.011 and initial peak pulse powers as 3 mW, 30 mW and 60 mW (which correspond to E_{in} / E_{sat} = 0.01, 0.1 and 0.2 respectively).

Dispersion length L_D in standard single mode fiber (D ~16 ps /nm.km) for pulse with T_0 ~ 15 ps will be L_D ~ 11 km. The other fiber parameters are shown in **Tables 4,5, and 6**, respectively.

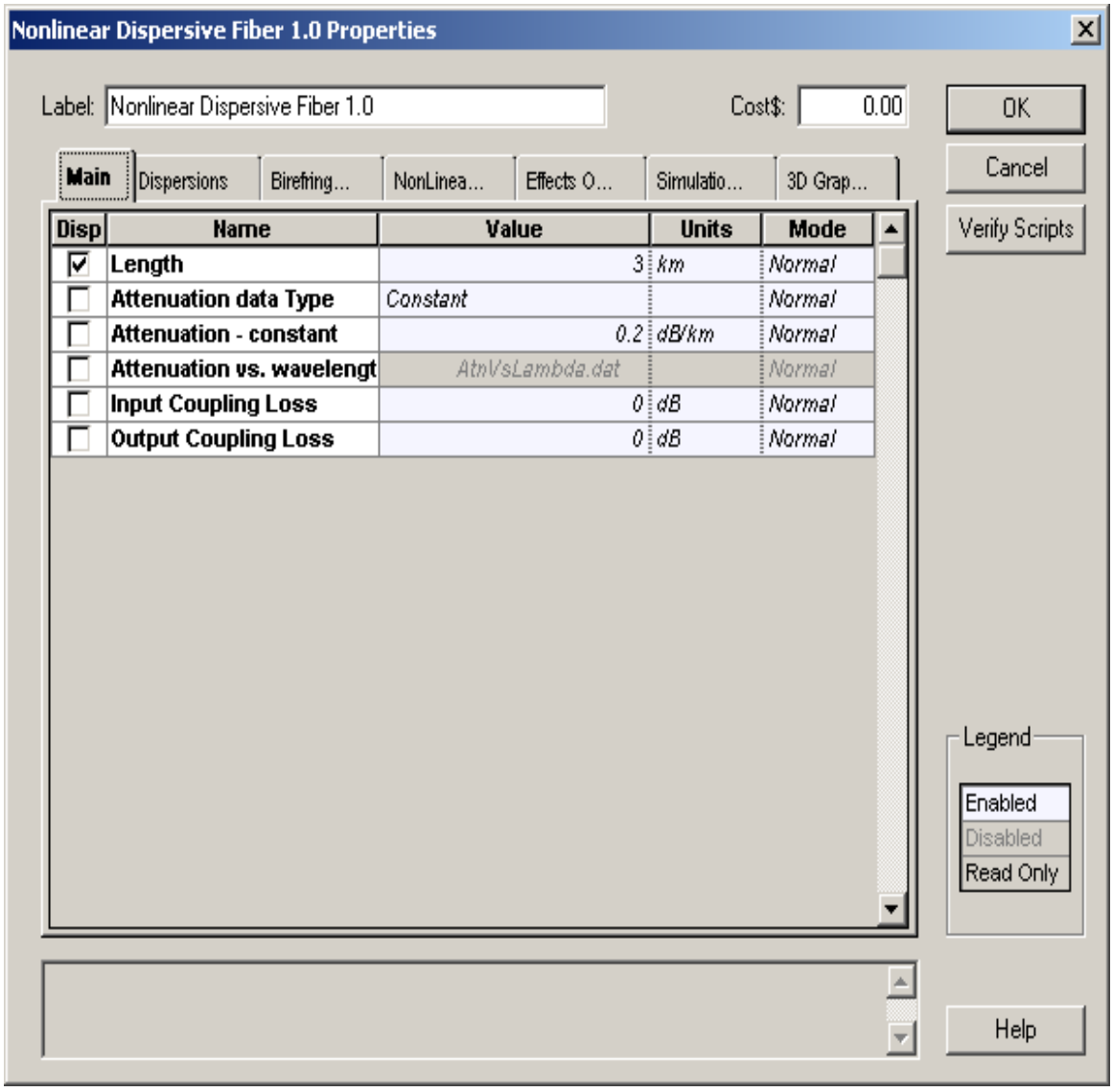

Table 4: Fiber parameters (Main)

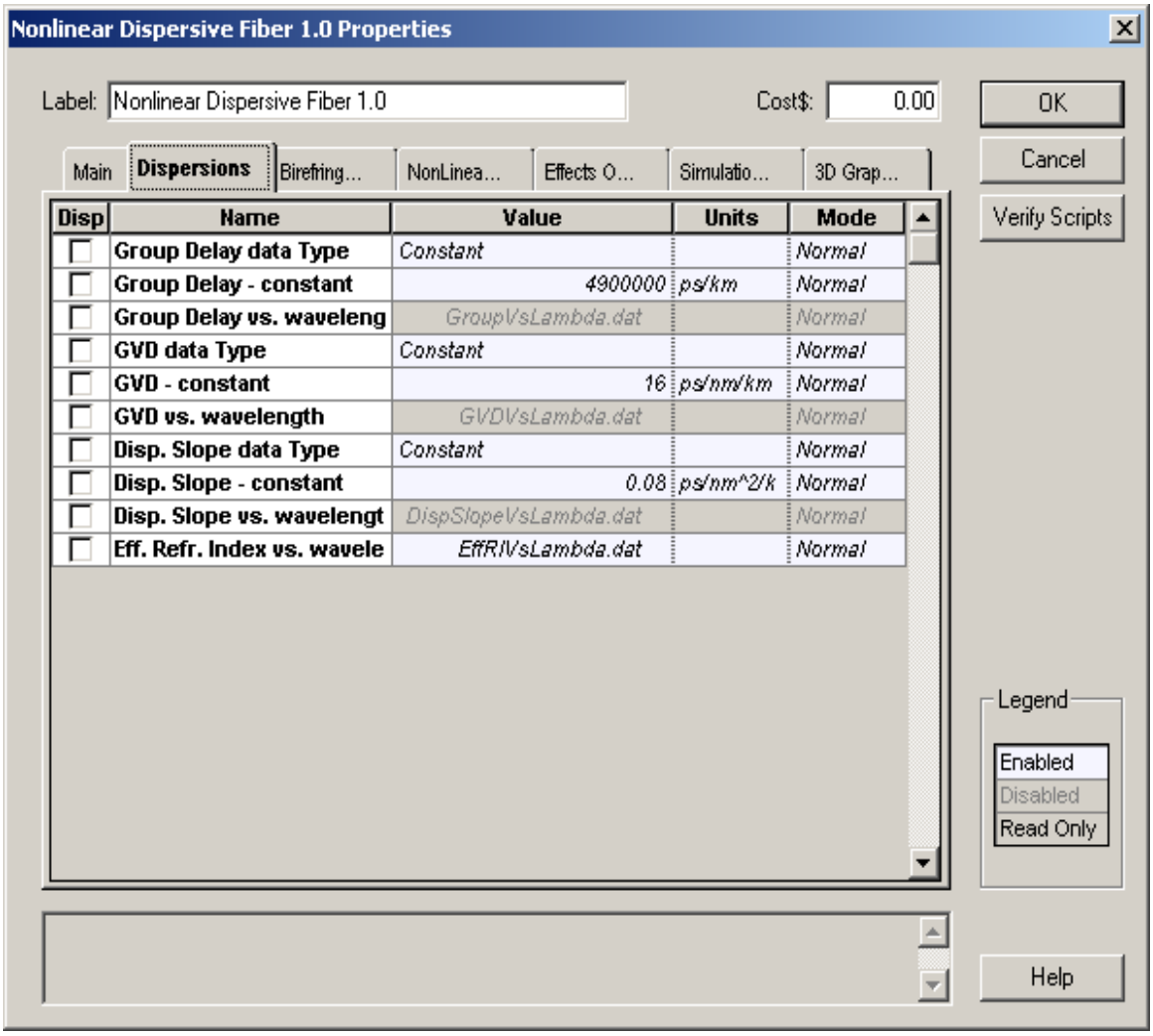

Table 5: Fiber parameters (Dispersion)

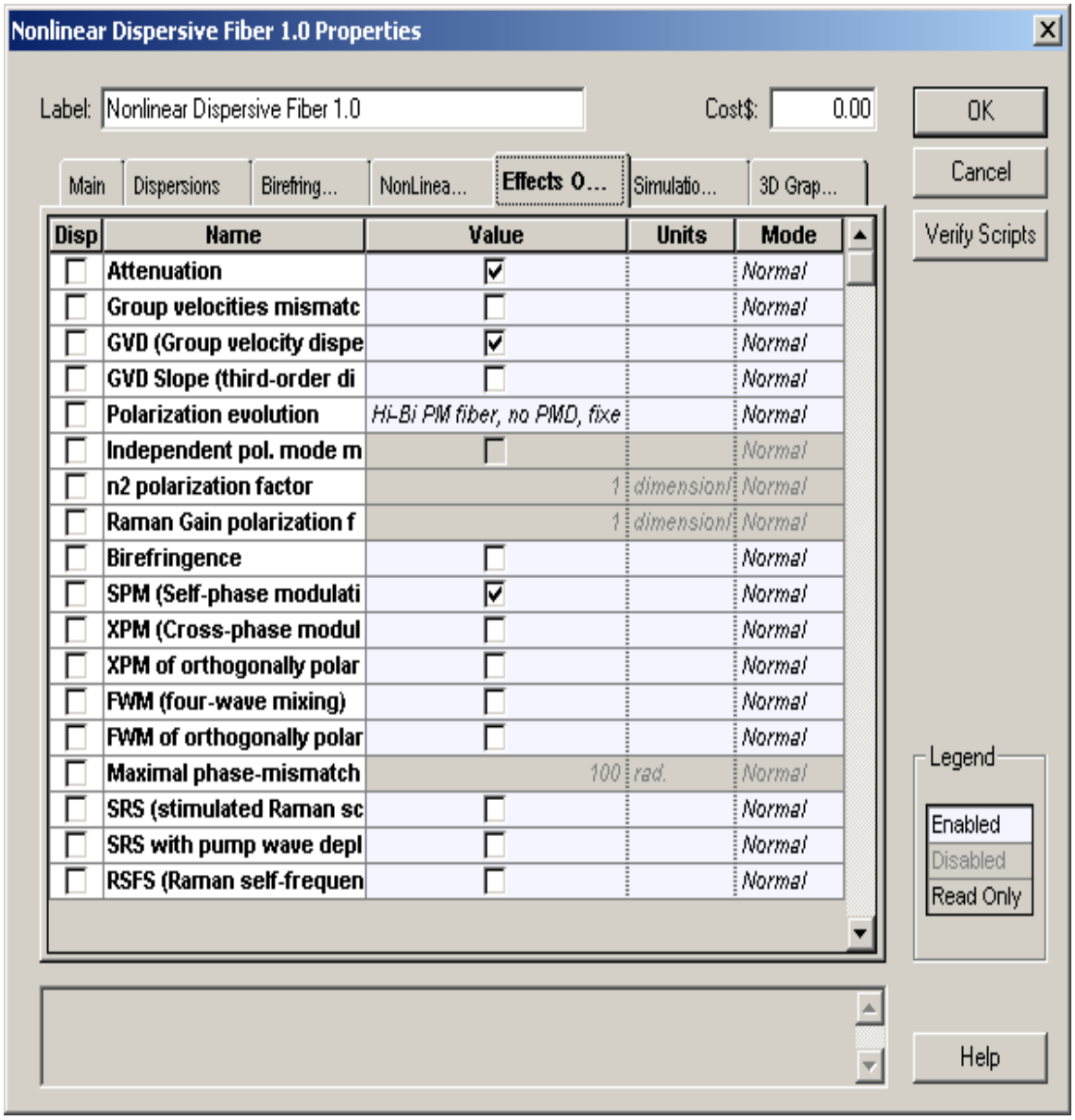

Table 6: Fiber parameters (Effects on/off)

To satisfy the condition L_C / L_D ~ 0.3 given in [1], where L_C is the length of the fiber used for compression, the value of L_C ~ 3.3 km has been used. The layout for the project is shown in Fig. 4.

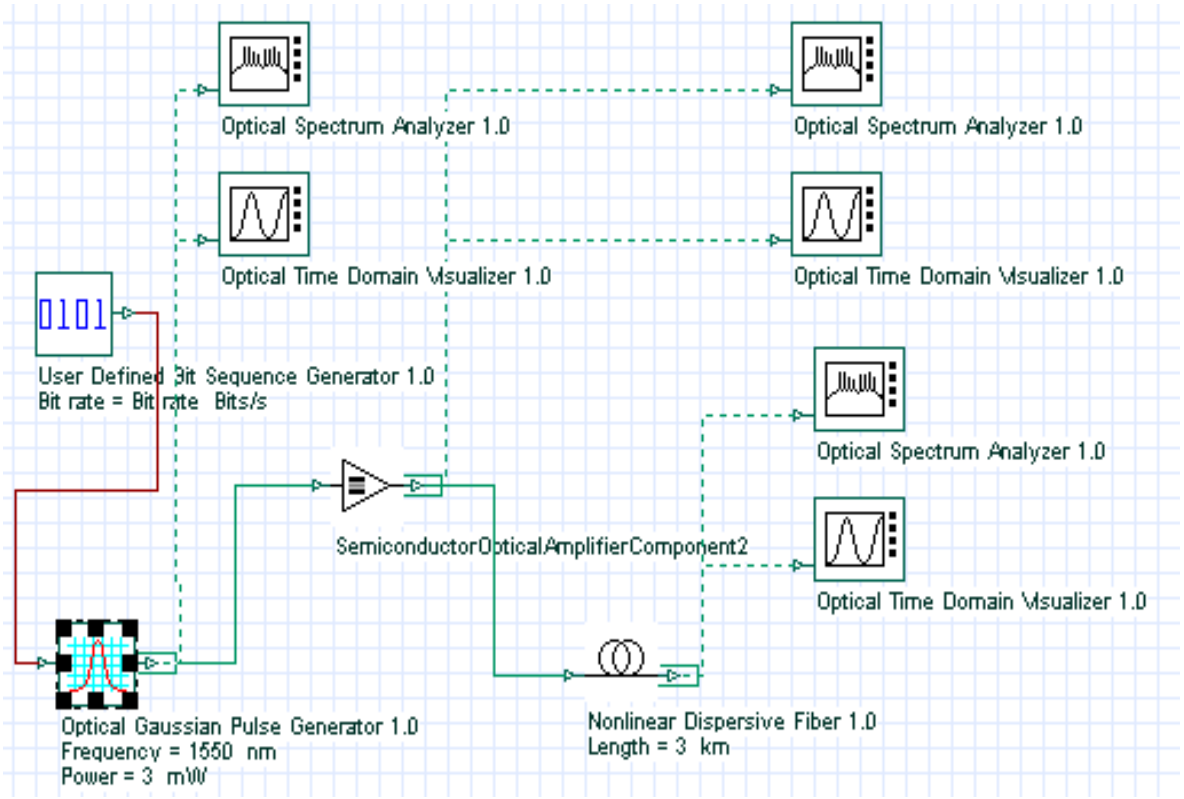

Fig. 4: Layout: Amplifier- induced chirp SLA compression

Initial shape and pulse spectrum with T_{FWHM} =25 ps and initial peak pulse powers = 3 mW have been shown in **Figs. 5 and 6**, respectively.

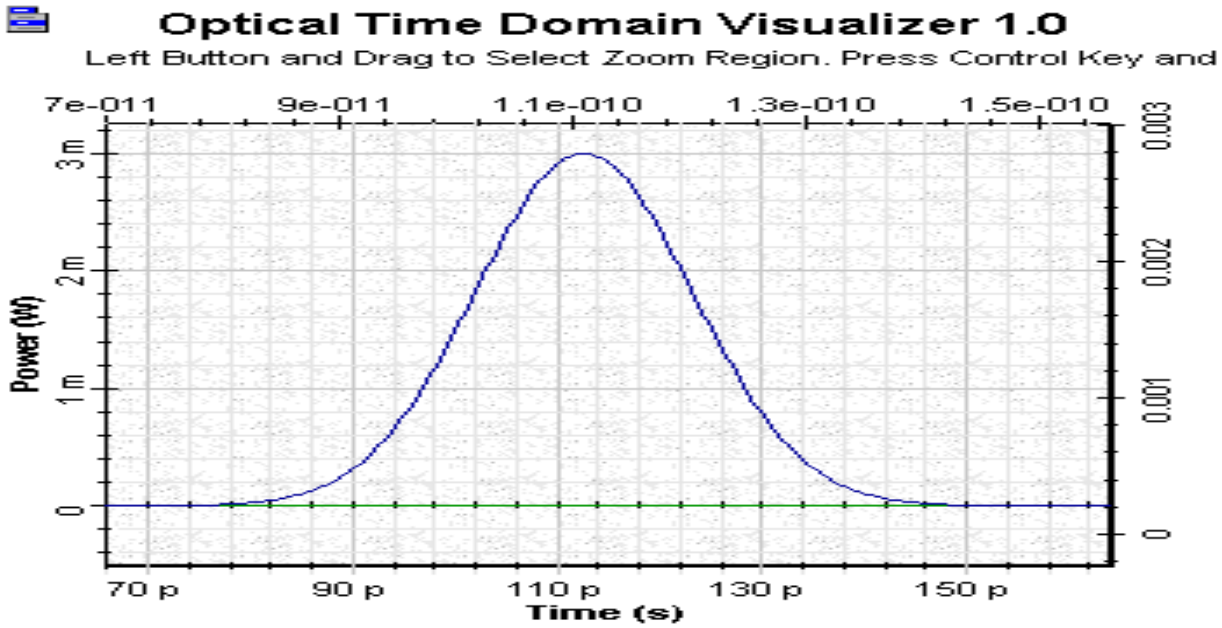

Fig. 5: Initial shape of pulse

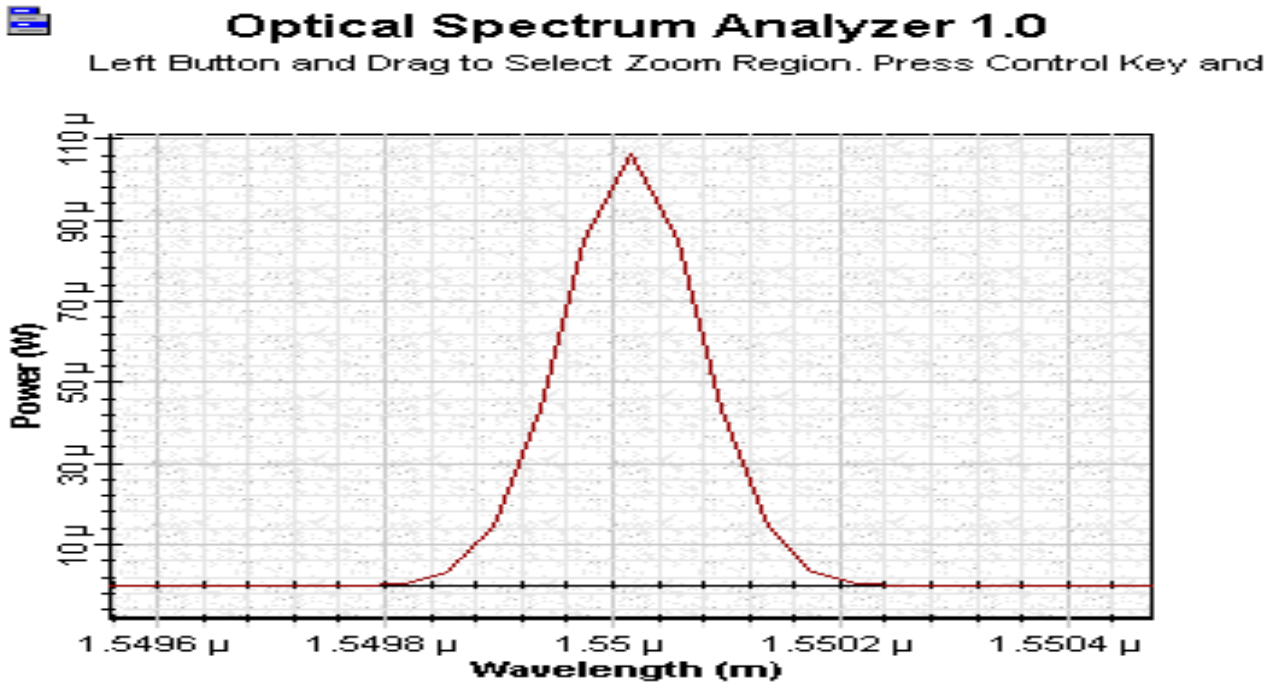

Fig.6: Initial pulse spectrum

Figs. 7 and 8 show the shape (with corresponding positive induced chirp) and spectra after amplification with SOA (G_0 = 30 dB and linewidth enhancement factor α = 5).

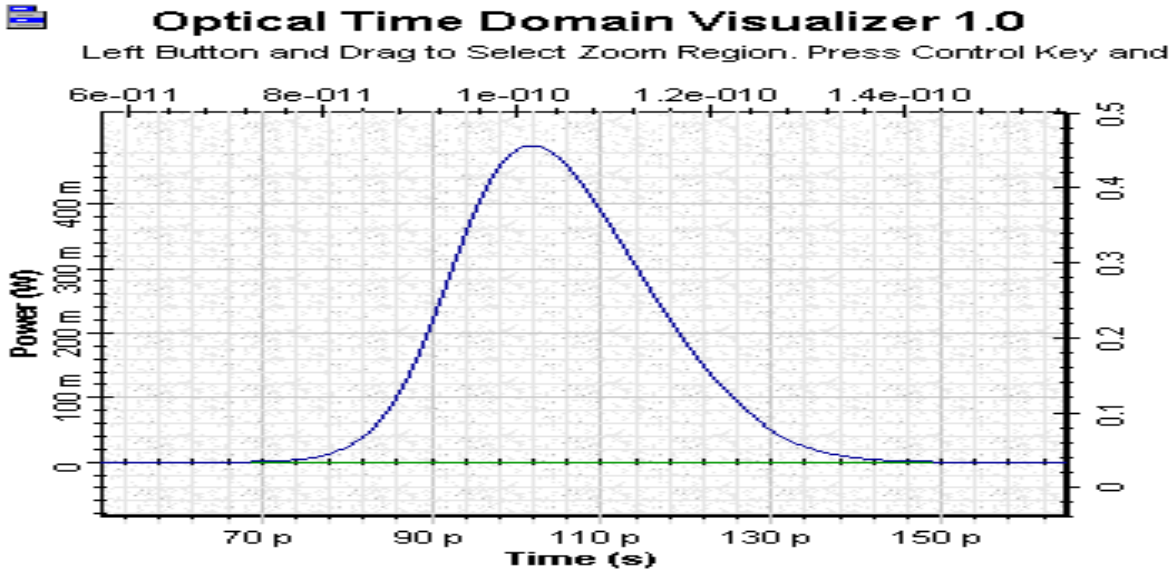

Fig. 7: Shape after amplification with SOA

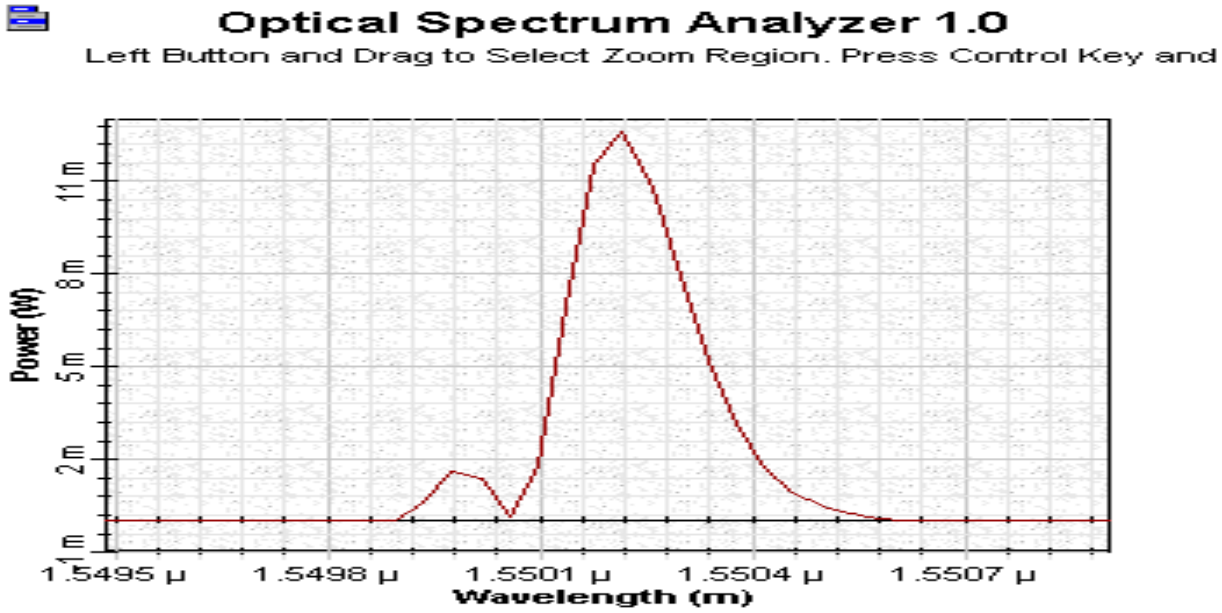

Fig. 8: Spectrum after amplification with SOA

Figs. 9 and 10 show, the shape and spectra of the amplified pulse after passing through 3 km standard single mode fiber (SMF).

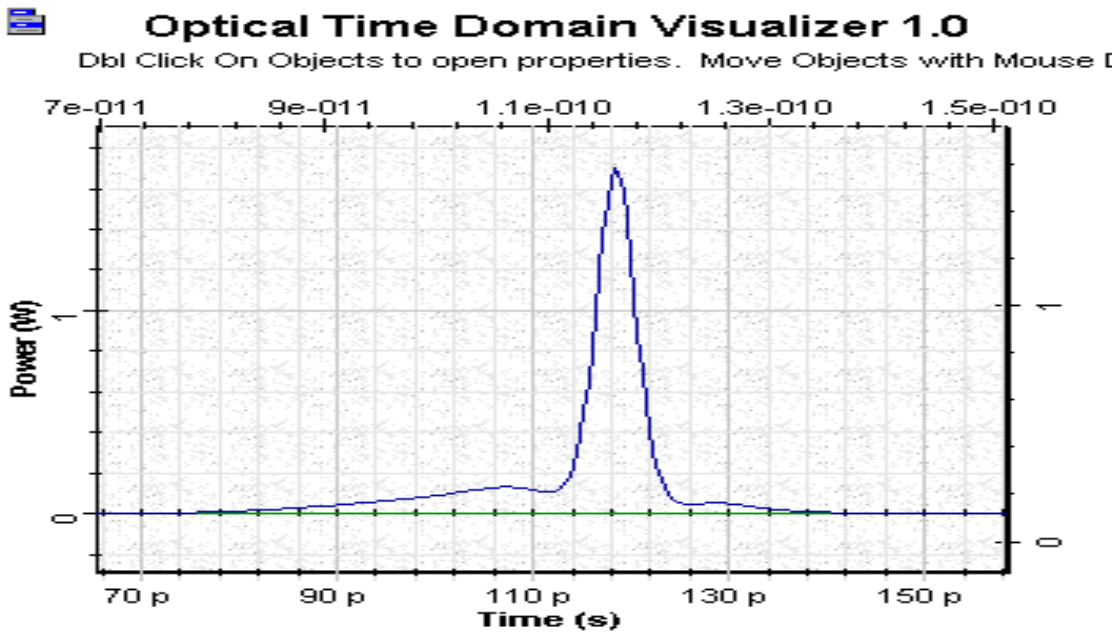

Fig. 9: Shape of the amplified pulse after passing through SMF

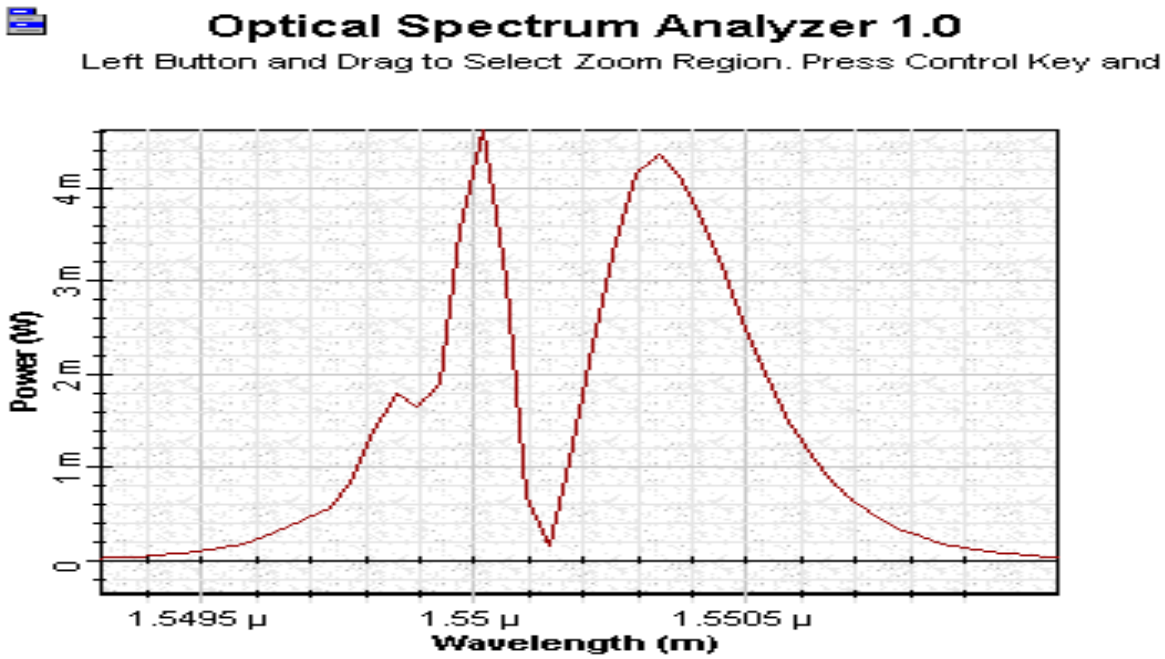

Fig. 10: Spectra of the amplified pulse after passing through SMF

The comparison of the width of the pulse after fiber shows a compression factor of about 7 times with peak power enhanced by a factor of several hundreds. Two important physical facts should be mentioned in the Fig. 9. First, this is a broad pedestal on the leading side of the pulse that leads to increased dispersion of this part of the pulse. The second point is connected with the shift of the pulse towards later time. This fact is due to the red shift of central frequency of the amplified pulse that in anomalous group velocity dispersion leads to time delay of the pulse.

As is mentioned in [2] the compression factor depends on several input parameters, such as the pulse energy, the pulse width, the amplifier gain, and the compressor length. For non optimal parameters another type of phenomena can appear as for example pulse breaking which is demonstrated in Figs. 11 and 12, where the shapes and spectra of pulses with initial peak powers 3, 30 and 60 mW are presented.

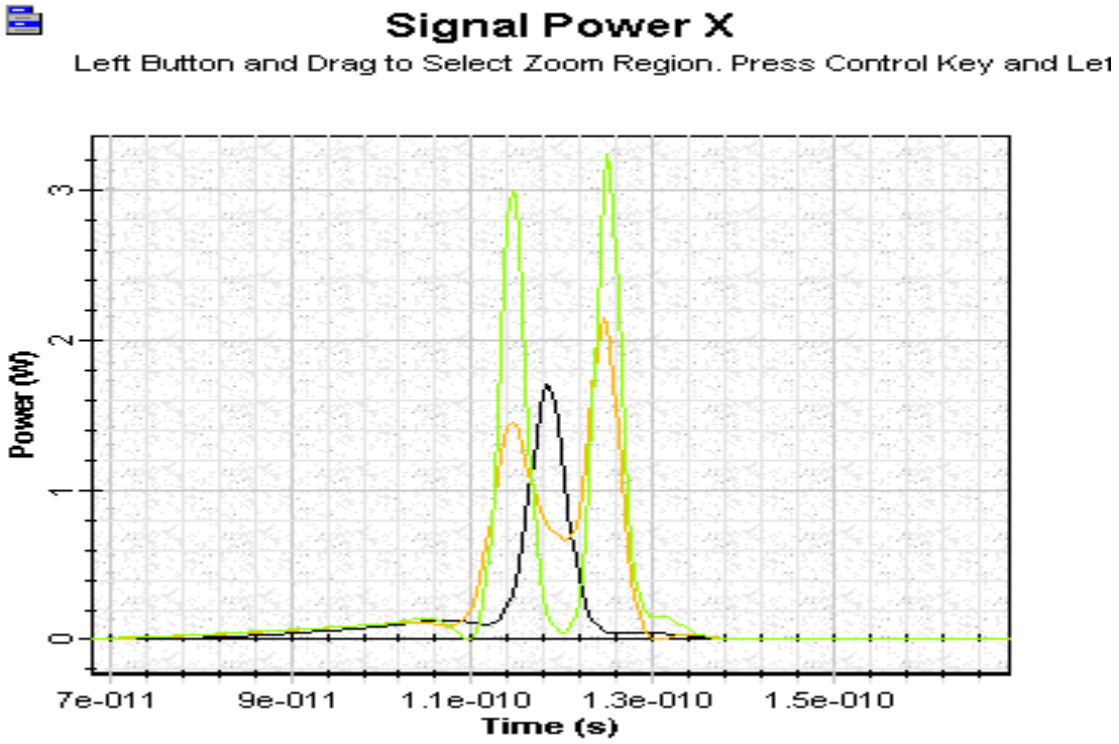

Fig. 11: Shape of the pulse for non optimal parameters

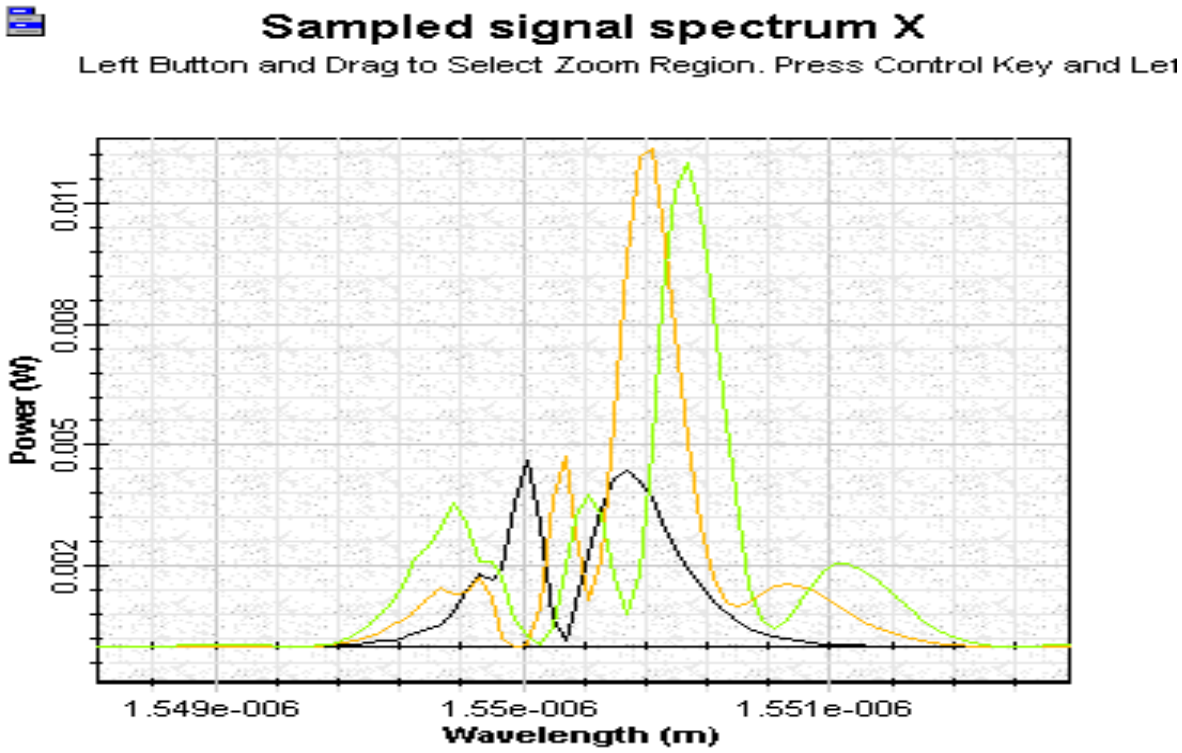

Fig. 12: Spectra of the pulse for non optimal parameters

As we see from Fig. 11, larger input peak power can lead to pulse breaking phenomena with connected complicated spectra structure.

We have demonstrated pulse compression of weak pulses (peak energy smaller than pJ) based on the use of the gain saturation induced self-phase modulation effect in SOA.

References:

[1] G.P. Agrawal, “Nonlinear fiber optics”, third edition, Academic press, 2001.

[2] G.P. Agrawal and N.A. Olsson, “Amplification and compression of weak picosecond optical pulses by using semiconductor laser amplifier”, Optics Letters, vol.14, pp. 500-502, 1989.

Examples: 40 Gbps

High-dispersion fibers 40 Gbps in SMF NRZ.**osd**
High-dispersion fibers 40 Gbps in SMF RZ pre.**osd**
High-dispersion fibers 40 Gbps in SMF RZ.**osd**

40 Gb/s single channel transmission in standard mode fibers (SMF)

The fundamental limitation to high- speed communication systems over the embedded standard single mode-mode fiber at 1.55 μm is the linear chromatic dispersion. Typical value of β_2 = - 20 ps^2/ km at 1.55 μm for SMF leads to D = 16 ps/(nm . km). For bit rate B = 40 Gb/s, the slot duration will be T_B = 25 ps. For duty cycle 0.5 $\Rightarrow$ T_{FWHM} = 12.5 ps $\Rightarrow$ T_0 = 7.5 ps. Therefore the corresponding dispersion length will be approximately L_D ~ 2.8 km. The aims of this project are as follows:

a) to compare RZ versus NRZ- modulation format transmission in SMF at 40 Gb/s taking into account: group velocity dispersion, self-phase modulation due to the Kerr nonlinearity, linear losses and periodical amplification with ASE noise. The large group velocity dispersion is compensated with post- dispersion compensation scheme.

b) to analyze influence of accumulated amplifier noise and self-phase modulation for RZ -modulation format transmission in SMF at 40 Gb/s.

c) to compare post- and pre- dispersion compensation schemes for RZ - modulation format transmission in SMF at 40 Gb/s.

Figs. 13 (a) and 13 (b) show the layouts for RZ and NRZ modulation formats.

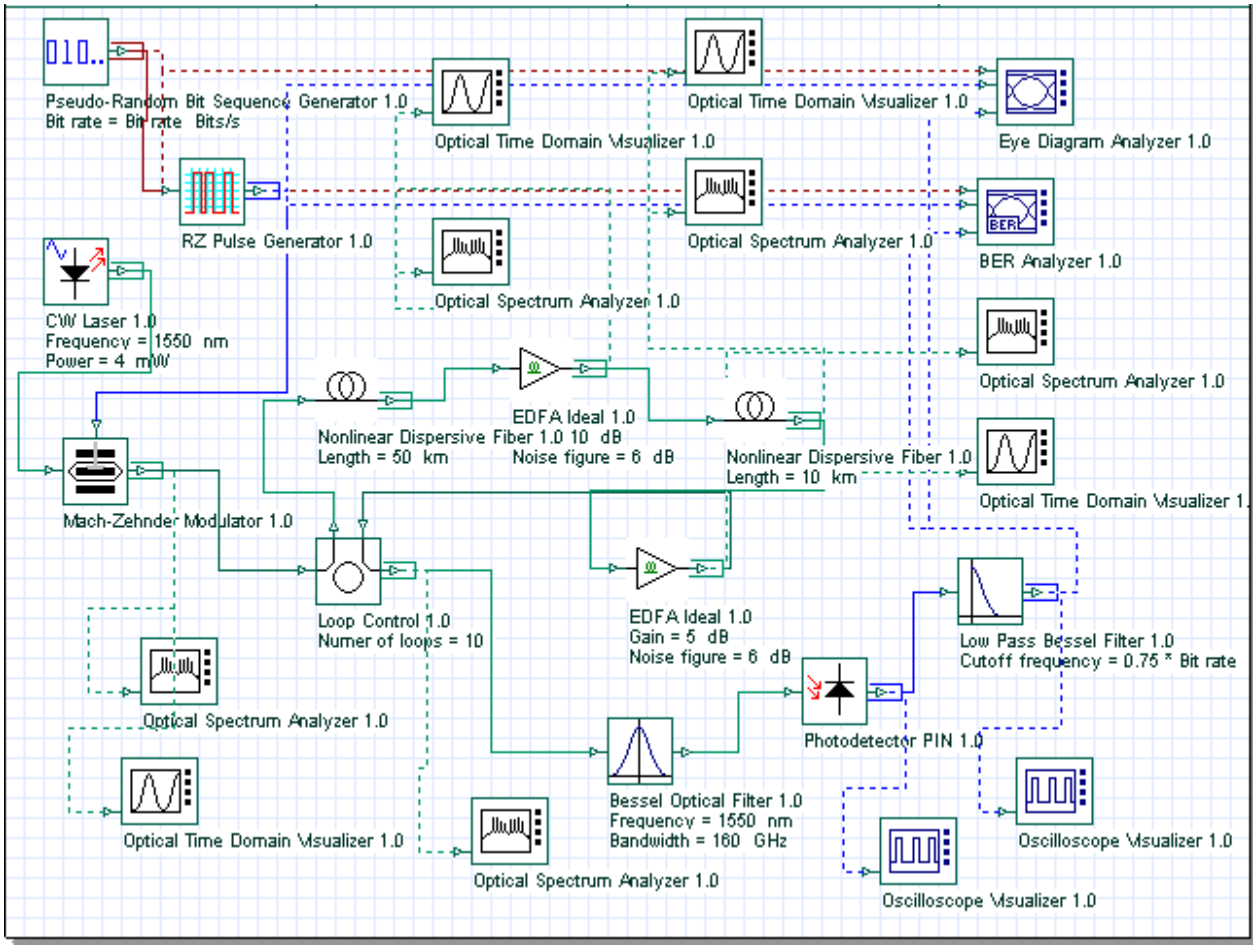

Fig. 13 (a): Layout: RZ format

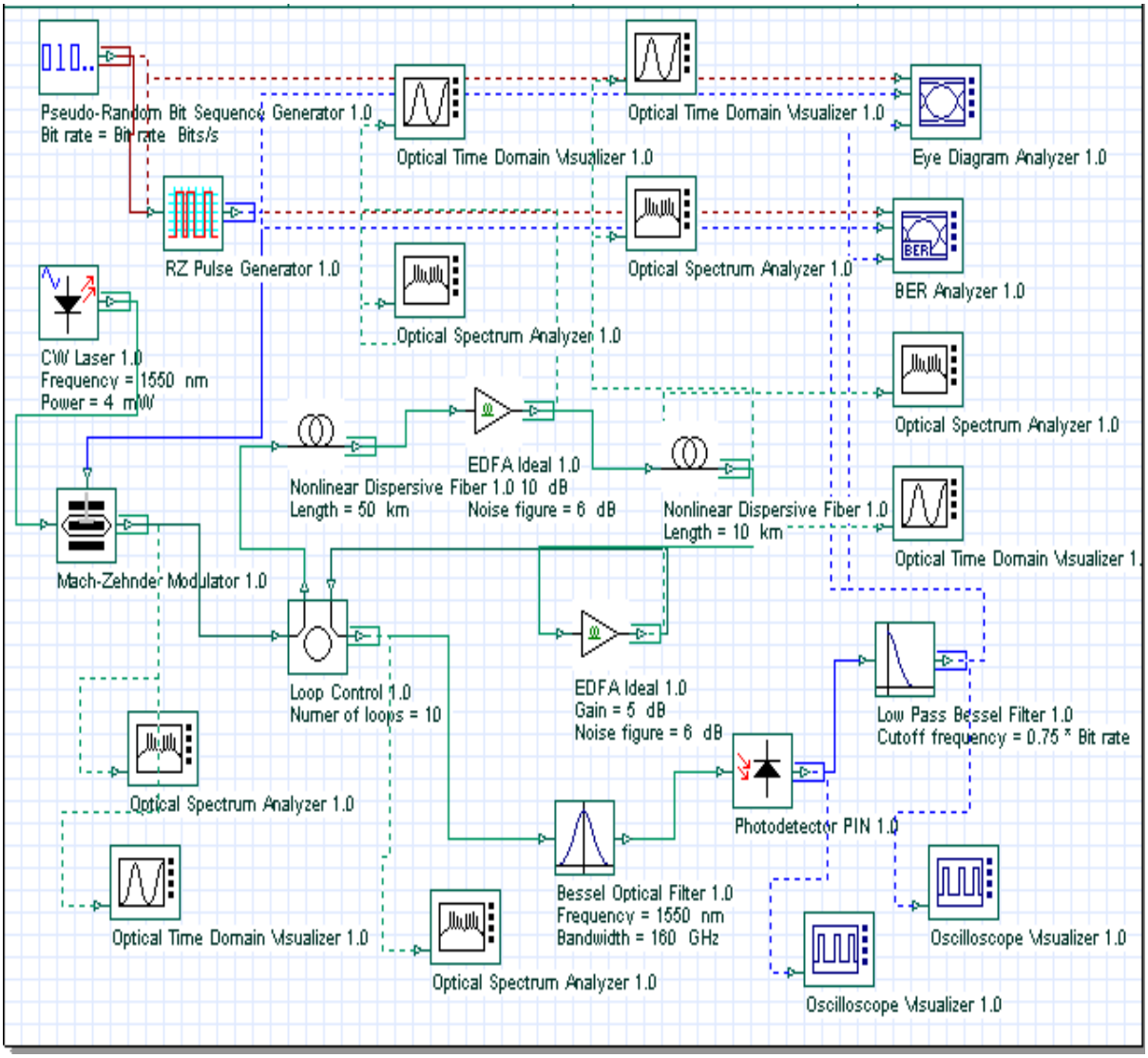

Fig. 13 (b): Layout: NRZ format

Global parameters used for this project are: Bit rate = 40 Gb/s, Sequence length = 128 Bits and Samples per bit = 128. Therefore Number of samples = Sequence length * Samples per bit= 16384; Time window= Sequence length*Bit slot = 3.2 ns; Sampling interval= Time window / Number of samples = 0.195 ps; Sample rate= 1 / sampling interval= 5.12 THz.

RZ- generator has following properties: rectangle shape: Gaussian; duty cycle= 0.5 bit; rise time= 0.15 bit; fall time = 0.25 bit.

As an optical source an externally modulated CW Laser with carrier wavelength λ=1550 nm and linewidth = 0.1 MHz is used.

The standard single mode optical fiber used has dispersion coefficient $D=17\left[\frac{ps}{nm.km}\right]$, the slope $\frac{\partial D}{\partial \lambda}=0.08\left[\frac{ps}{nm^2\ km}\right]$, the nonlinear coefficient $\gamma=1.31\left[\frac{1}{km\ W}\right]$, linear losses α = 0.2 dB/ km and fiber length L_{SMF} = 50 km.

After each segment from SMF an amplifier compensates the linear losses. Dispersion compensation fiber has dispersion coefficient $D=-80\left[\frac{ps}{nm.km}\right]$, slope $\frac{\partial D}{\partial \lambda}=0.08\left[\frac{ps}{nm^2\ km}\right]$, nonlinear coefficient $\gamma=5.24\left[\frac{1}{km\ W}\right]$, linear losses α = 0.5 dB/ km and fiber length L_{DCF} = 10 km. After each segment from SMF an amplifier compensates the linear losses.

Properties of Bessel optical filter used are: carrier wavelength λ=1550 nm and bandwidth = 4 $\times$ Bit rate.

The cutoff frequency of the low pass Bessel electrical filter used is 0.75 × Bit rate.

Ideal periodical amplification is performed with the help of ideal EDFA component of OptiSystem that also takes ASE noise into account. The amplifier used after SMF has a gain of 10 dB and noise figure of 6 dB and the amplifier used after DCF has a gain of 5 dB with the same noise figure value.

Some of above parameters are chosen in accordance with [1], which allows comparison of results.

Part I: Comparison of RZ and NRZ formats

In the project High-dispersion fibers 40 Gbps in SMF RZ**. Osd,** (Fig.13(a)) the transmission over a distance of 500 km SMF (10 loops × 50 km) with periodical amplification after every 50 km of fiber has been considered. The result for the dependence of the max Q with the input power is shown in Fig.14. The Fig.15 shows the eye diagram for the optimal point at input power ~ 4 mW (cf. Fig. 14).

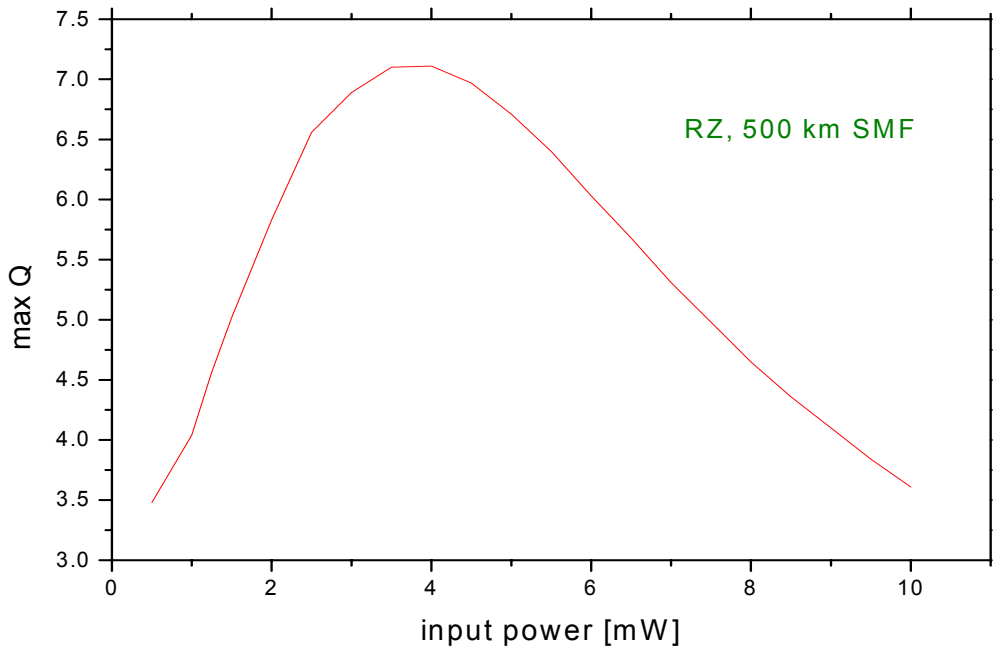

Fig.14: Max Q vs. input power (RZ modulation)

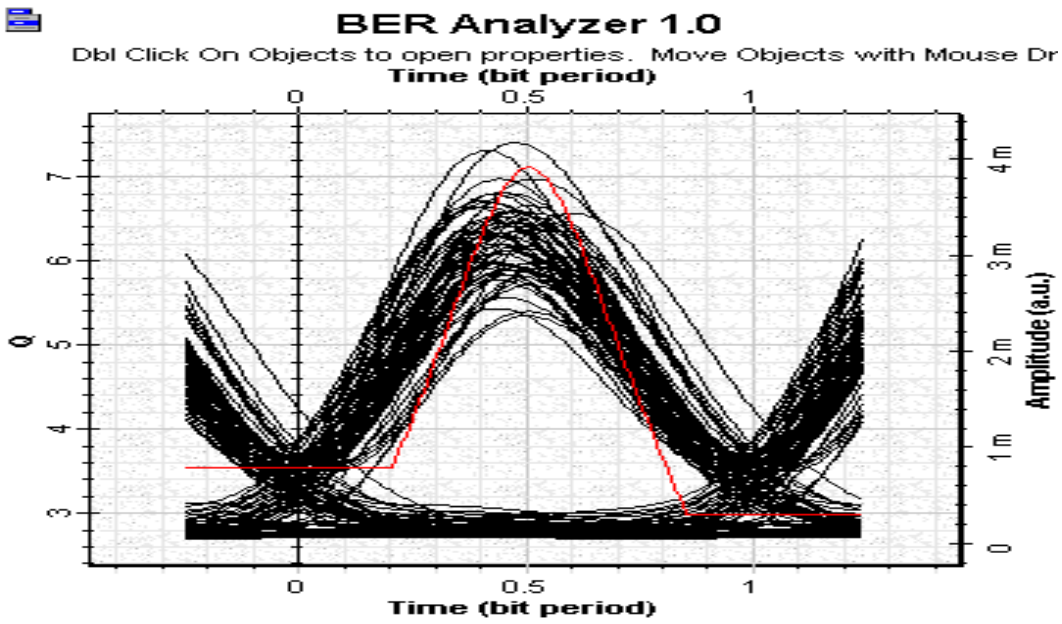

Fig. 15: Eye diagram at input power ~ 4 mW (cf. Fig. 14)

Well-expressed maximum in Fig.14 could be identified. (Note that we have not performed any fitting to this curve.) At distances larger than 500 km max Q becomes smaller than 6, therefore this is the maximum distance with good Q performance.

In the project High-dispersion fibers 40 Gbps in SMF NRZ**. osd** , (Fig.13(b))**,** the transmission at a distance of 250 km SMF (5 loops × 50 km) with a periodical amplification after every 50 km has been considered. The result of the dependence of the max Q vs. input power is shown in Fig.16. Fig.17 shows the eye diagram for the optimal point at input power ~ 1.25 mW (cf. Fig. 16).

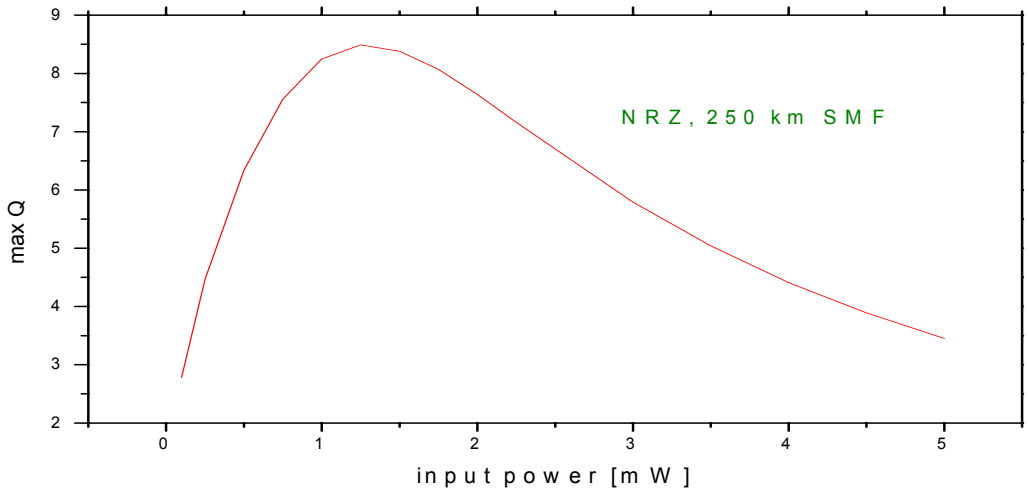

Fig.16: Max Q vs. input power (NRZ modulation)

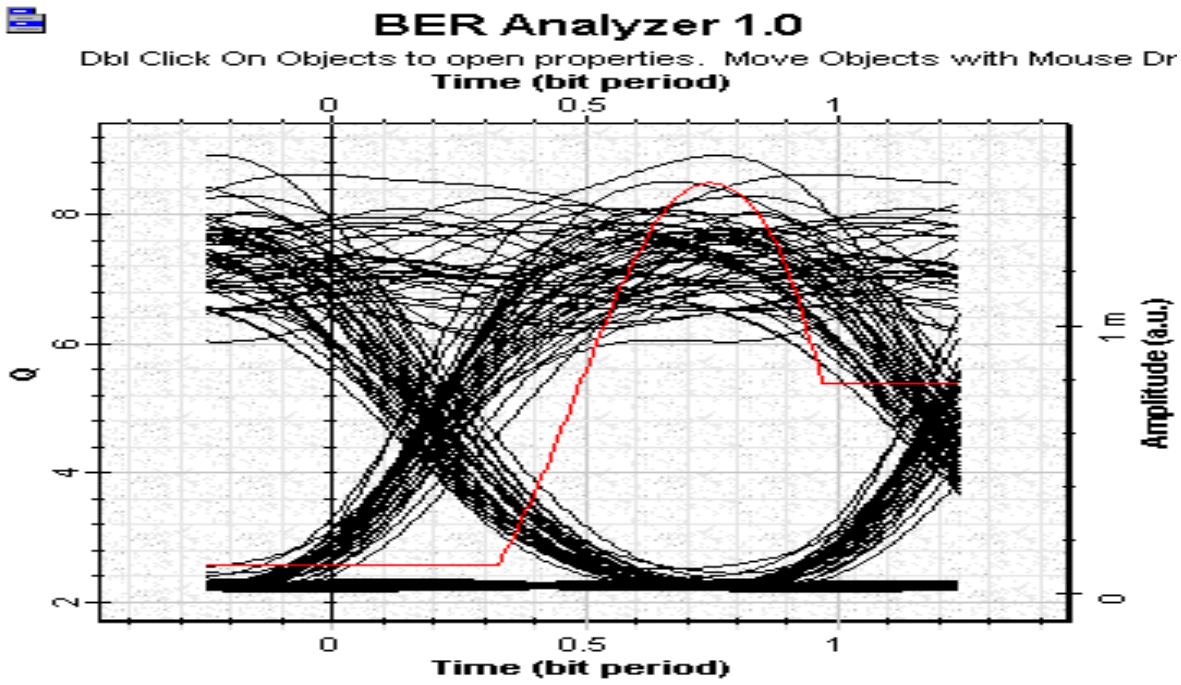

Fig. 17: Eye diagram at input power ~ 1.25 mW (cf. Fig. 16)

Well-expressed maximum in Fig.16 could also be identified. (no fitting of this curve was performed). At distances larger than 250 km max Q becomes smaller than 6, therefore this is the maximum available distance with good Q performance.

Comparing positions of the maximums of both the curves we can clearly see the shift toward larger input powers for the RZ format. Obtained results show that the RZ-modulation format duty cycle = 0.5 is superior compared to conventional NRZ- modulation format.

Part II: Influence of accumulated amplifier noise and self-phase modulation on the RZ-modulation transmission

In this project we have considered two different situations. In first situation, the self-phase modulation was assumed zero, and in another one the noise figure was not taken into account. Obtained results are presented in Fig. 18.

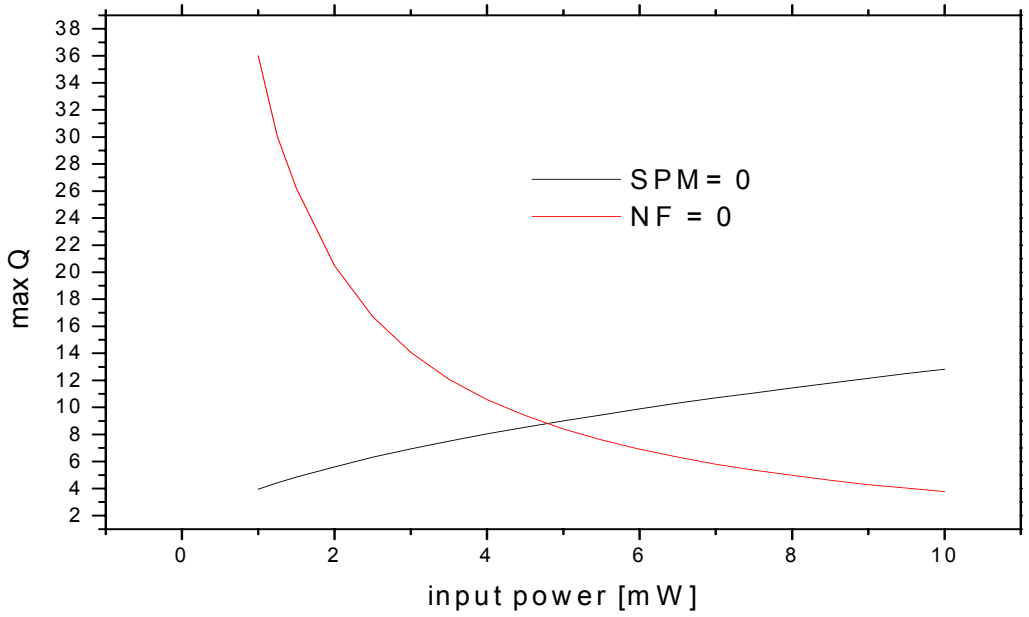

Fig.18: Max Q vs. input power for two separate cases (Case I: SPM = 0, Case II: Noise figure = 0)

As we see at low power levels, the performance is mainly hampered by the accumulated amplifier noise. At high input power levels, the transmission distance is significantly reduced due to the self-phase modulation. As we see just these effects determine the well expressed maximum in the Q curve in Fig.16.

In the project, High-dispersion fibers 40 Gbps in SMF RZ _pre**. osd** (Fig.19)**,** two schemes of dispersion compensation are studied, i.e., post- and pre-compensation.

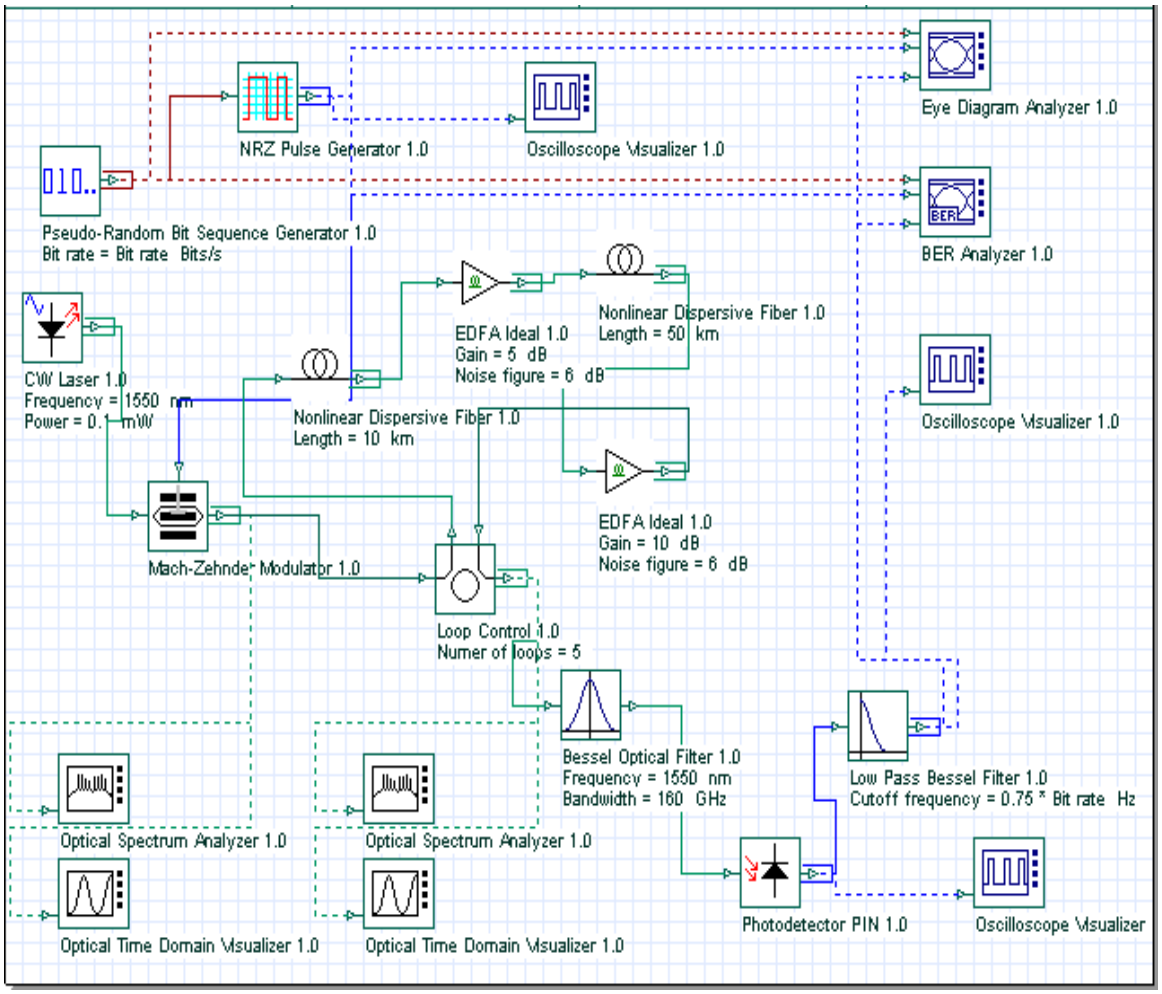

Fig.19: Layout: High-dispersion fibers 40 Gbps in SMF RZ _pre

The corresponding results for the RZ-modulation transmission in SMF at 40 Gb/s are shown in Fig.20.

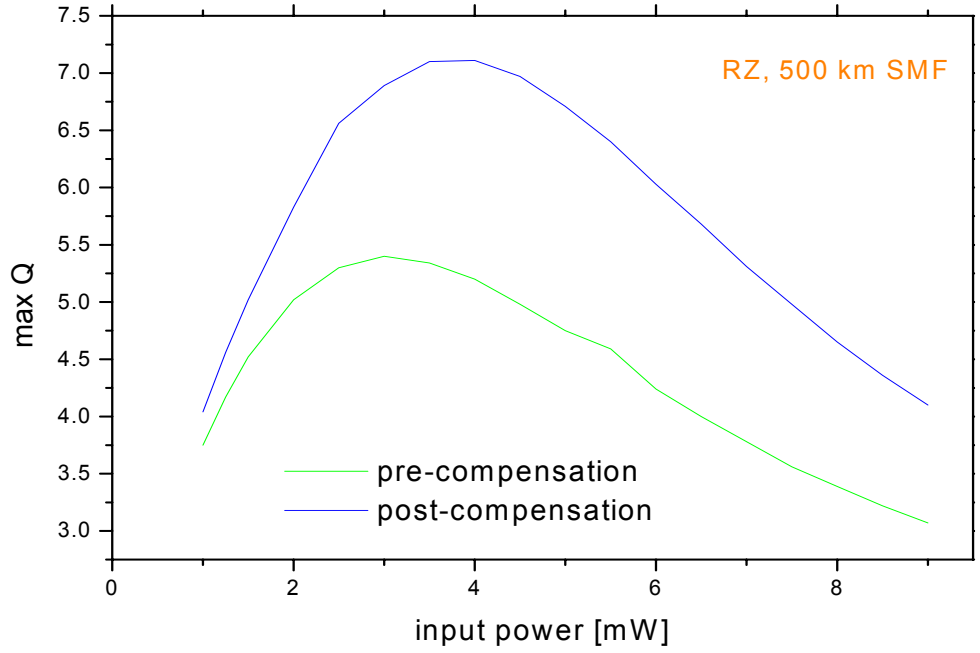

Fig. 20: RZ modulation format transmission at 40 Gb/s over 500 km in SMF

Results indicate that post-compensation scheme is superior compared to pre-compensation one in dispersion compensated systems at 40 Gb/s in SMF.

We have thus shown that for upgrading the existing standard fiber network at 1.55 μm with 40 Gb/s:

a) Dispersion compensation is necessary
b) RZ is superior compared to conventional NRZ – modulation format
c) At low power levels, the performance is mainly hampered by the accumulated amplification and at higher input powers, the transmission distance is significantly reduced by nonlinear self-phase modulation
d) Post compensation scheme is superior compared to pre-compensation scheme.

The obtained results agree well with those of [1-3].

References:

[1] D. Breuer and K. Petermann, "Comparison of NRZ and RZ- modulation format for 40 Gbit/s TDM standard-fiber system", IEEE Photon. Technol. Lett., vol. 9, pp.398-400, 1997.
[2] M.I. Hayee and A.E. Willner, "NRZ Versus RZ in 10-40 Gb/s Dispersion – Managed WDM Transmission systems", IEEE Photon. Technol. Lett., vol. 11, pp.991-993, 1999.
[3] C.M. Weinert, R. Ludvig, W. Papier, H.G. Weber, D. Breuer, K. Petermann and F. Kuppers, "40 Gbit/s Comparison and 4 × 40 Gbit/s TDM/WDM Standard Fiber Transmission", Journal of Lightwave Technology, vol. 17, pp.2276-2284, 1999.

Example: Uniform - Period Gratings

Dispersion compensation_post with FBG.**osd**

Project "Dispersion compensation_post with FBG**.osd**" (Fig.21) shows the dispersion compensation by using fiber Bragg grating. It shows how the amount of compensating dispersion affects the system performance.

In the project we prefer post-compensation scheme because of its simplicity comparing to symmetrical compensation scheme. It's performance is as good as symmetrical compensation scheme.

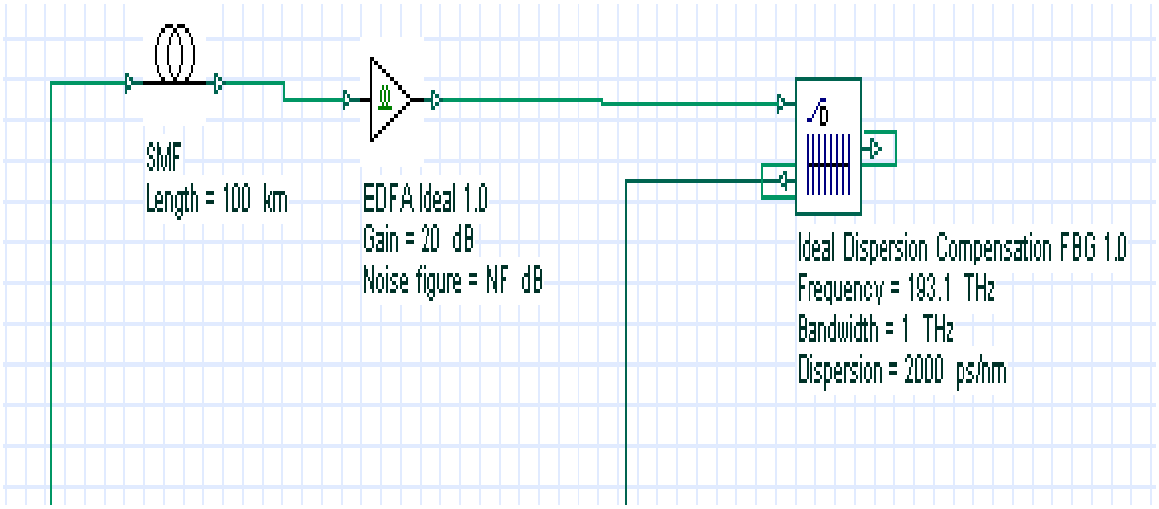

Fig. 21: Layout: Dispersion compensation_post with FBG

In this case, the total accumulated dispersion of the SMF is 16×100 = 1600 ps/nm. We swept the total dispersion of FBG from 0 to -2000 ps/nm. In this simulation, we just want to see the dispersion-limited performance of the system.

Therefore we keep the power at 0 dBm. This is needed to avoid triggering of any fiber nonlinearity. Effects of residual dispersion to nonlinear effects will be considered in other examples. Fig. 22 shows the eye diagrams at the receiver end for several total compensation dispersion values. This simulation shows that, in the linear regime (low power), compensating fiber dispersion completely gives the best result. Over compensation degrades the system performance.

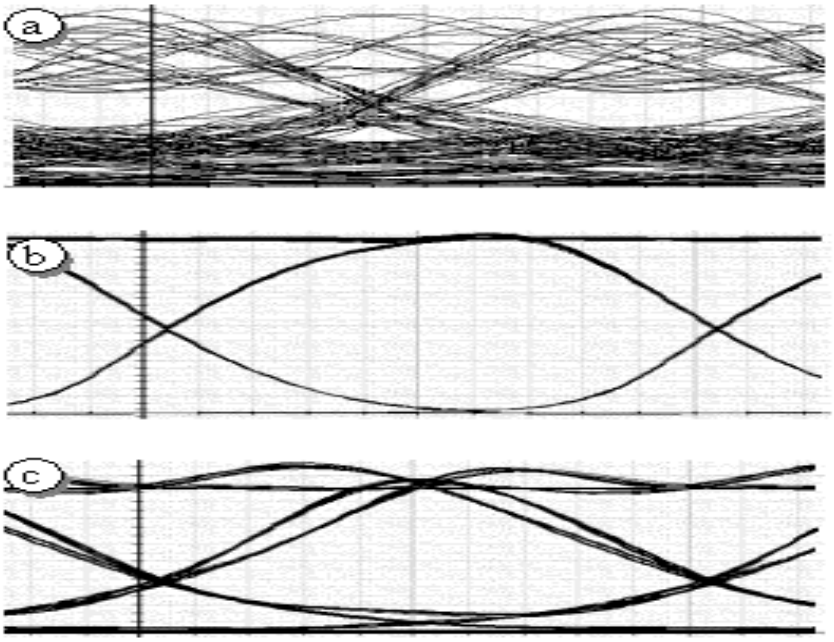

Fig. 22: Eye diagrams at the receiver end when the total compensation dispersion is a) 0, b) 1600, and c) 2000 ps/nm

Example: Fiber Nonlinearities and Dispersion

Fiber nonlinearities and dispersion_single channel.**osd**

Fiber nonlinearities and dispersion_multi channel.**osd**

Fiber nonlinearities and dispersion_multi channel Tagal.**osd**

As long as the optical power within an optical fiber is small, the fiber can be treated as linear medium. However, when the power level is high, we have to consider the impact of nonlinear effects. They can be classified into two categories. Some of them occur in multi channel WDM systems where interaction of signals at different wavelengths is possible. These categories and nonlinear effects in single channel and multi-channel systems are shown in Table 7.

	Single channel	Multi channel
Refractive index related	Self phase modulation (SPM)	Cross phase modulation (XPM) Four wave mixing (FWM)
Scattering related	Stimulated Brillouin scattering (SBS)	Stimulated Raman scattering (SRS)

Table 7: Nonlinear effects in the fiber

SPM and XPM affect the phase of signals and cause spectral broadening, which in turn, leads to increase in dispersion penalties. SBS and SRS provide gains to some channels at the expense of depleting power from other channels. The nonlinear interaction depends on transmission length and effective area of the fiber. Since loss in the fiber decreases the signal power, we use an effective instead of physical length. In practice, SPM can be a significant consideration in designing 10 Gbps systems, and restricts to maximum power channel below a few dBm. XPM becomes an important consideration when the channel spacing is of the order of a few tens of GHz. FWM efficiency depends on signal power and dispersion, as well as channel separation in WDM systems. If the channel is close to zero dispersion wavelength of the fiber, considerably high power can be transferred to FWM components. Using unequal channel spacing can also reduce effect of FWM.

Dispersion plays a key role in reducing the effects of nonlinearities. However, dispersion itself cause to inter-symbol interference. Fortunately, the good thing is that we can engineer systems with zero total dispersion but with a certain amount of local dispersion along the link.

Fiber nonlinearities and dispersion single channel

In this section we will consider effects of dispersion compensation to system performance in high power regime where nonlinearities are active. Let us first consider a dispersion post-compensated system with single channel. The project is given in Fiber nonlinearities and dispersion_single channel**.osd** file. In this file, we have two different versions of same project. In the first version, system residual dispersion is 0, whereas it is 800 ps/nm in the second version. Transmission link contains 5 spans and bit rate is 10 Gbps. Dispersion of 100 km SMF is 16 ps/nm-km and its effective area is 72 micron-square. Dispersion of 20 km DCF is – 80 ps/nm-km for the first version, and –72 ps/nm-km for the second one. Effective area of DCF is 30 micron-square. SMF and DCF losses are compensated by an EDFA with 35 dB gain. Noise figure of the EDFA is set to zero, because the purpose of this example is to deal with nonlinear and dispersion effects. If we only consider the SMF and also include the effect of amplification (5 times), we can estimate the threshold power for SPM [1,2]. If we do so, we find that after about 10 dBm average power, SPM becomes a limiting effect. However, we need to investigate if that is the case then how the residual system dispersion affects it. Fig.23 shows the eye diagrams for two different residual dispersion values and three different signal powers.

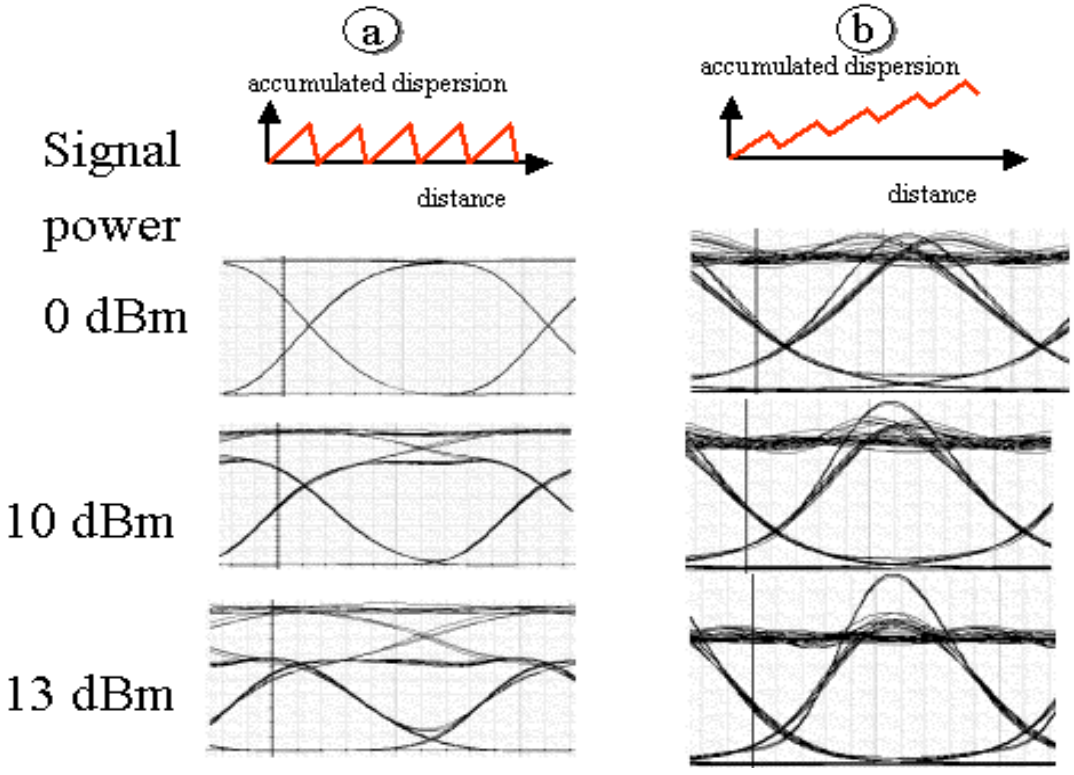

Fig. 23: Eye diagrams of the received signal for several signal powers when system residual dispersion is a) 0, b) 800 ps/nm. Inset on the top shows the dispersion map for each case.

This simulation shows that the effect of SPM can be reduced by not completely compensating the dispersion, but leaving some residual dispersion in the system. Notice how power increase results in eye closure in zero residual dispersion case.

Fiber nonlinearities and dispersion multi channel (Equal channel spacing)

Let us now consider a multi-channel system with 8 channels. The first channel is at 193.1 THz and they are separated with 100 GHz. SMF and DCF parameters are same as above. Even though the dispersion of fiber depends on wavelength, we set both fibers' dispersion to constant values. This will not affect the basic idea that we want to show here. We again have two versions of the design. The project is given in Fiber nonlinearities and dispersion_multi channel**.osd** file. In this file, we have three different versions of same project. In the first version, fiber dispersions are set to zero. Therefore, residual and local dispersion is zero. In the second version, system residual dispersion is 0, whereas it is 800 ps/nm in the third one. In Fig.24**,** simulation results are given for these three cases with several channel powers.

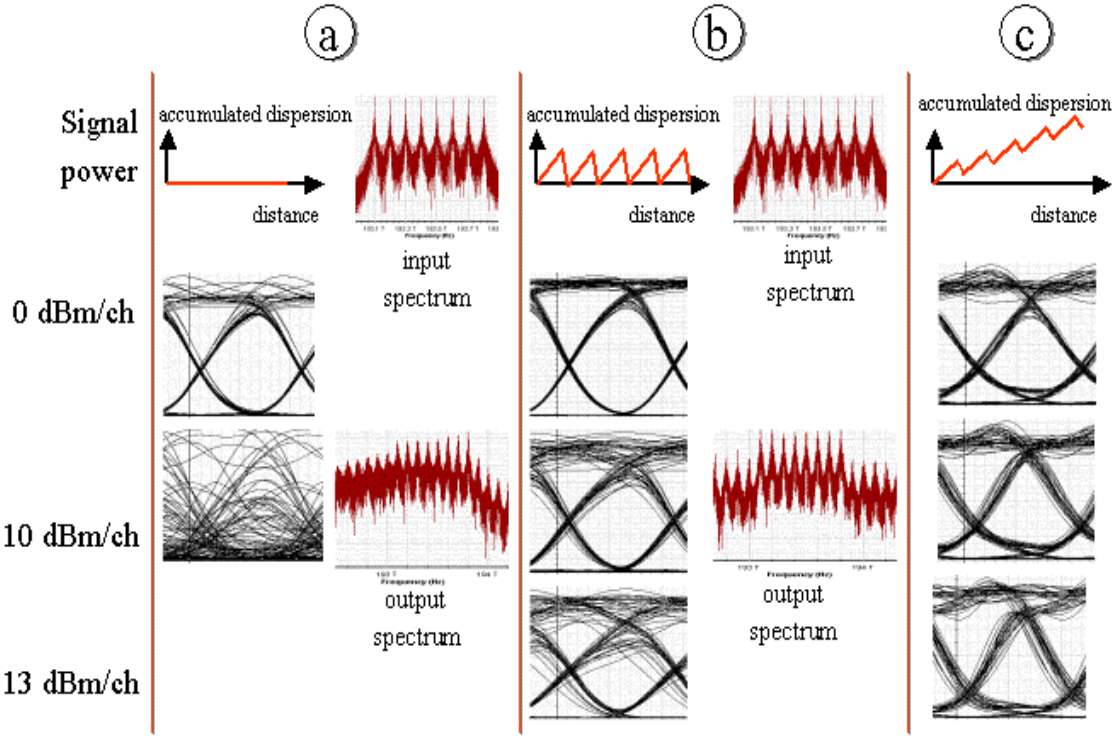

Fig. 24: Eye diagrams of the received signal for several signal powers when a) fiber dispersion is 0; b) and c) when system residual dispersion is 0 and 800 ps/nm, respectively. Insets show the power spectrums and dispersion maps for each case.

For an eight-channel system, the threshold power is about 10 dBm per channel. Simulation results justify this finding. In this simulation, both SPM and XPM affect the system performance. This simulation shows that nonlinear effects can be reduced by local dispersion. Better performance is obtained with nonzero residual dispersion [3].

Fiber nonlinearities and dispersion multi channel (Unequally spaced channels)

We will now show another example with 4 unequally spaced channels. Channels are at 1553.5, 1555.5, 1558.0, and 1560 nm. Bit rate is 10 Gb/s. In this case, we used wavelength dependent dispersion profile. Dispersion profiles are provided in two files, DSF1Taga.dat and DSF2Taga.dat. In this example we have used the values from Taga's experiment [4]. Project is given in Fiber nonlinearities and dispersion_multi channe Tagal**.osd.** As in the experiment, we have used two types of DSFs. Dispersion of third channel is totally compensated whereas channel four is over-compensated. Total power is 11 dBm (5 dBm per channel). Baseline power spectrum and power spectrum after 1500 km of transmission is shown in Fig.25.

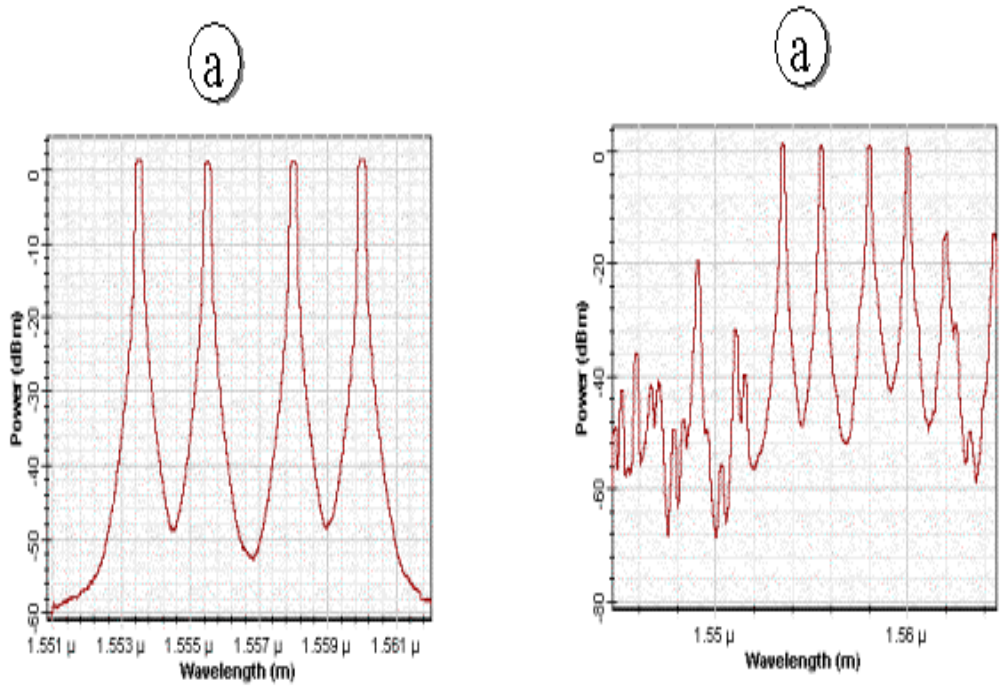

Fig. 25: a) Baseline power spectrum and b) Power spectrum after 1500 km of transmission

In this spectrum note the FWM spectrum components. Since they do not overlap with channels, FWM effect is decreased. Fig. 26 shows the eye diagrams and Q factors for each channel. Simulation is in perfect agreement with the experiment.

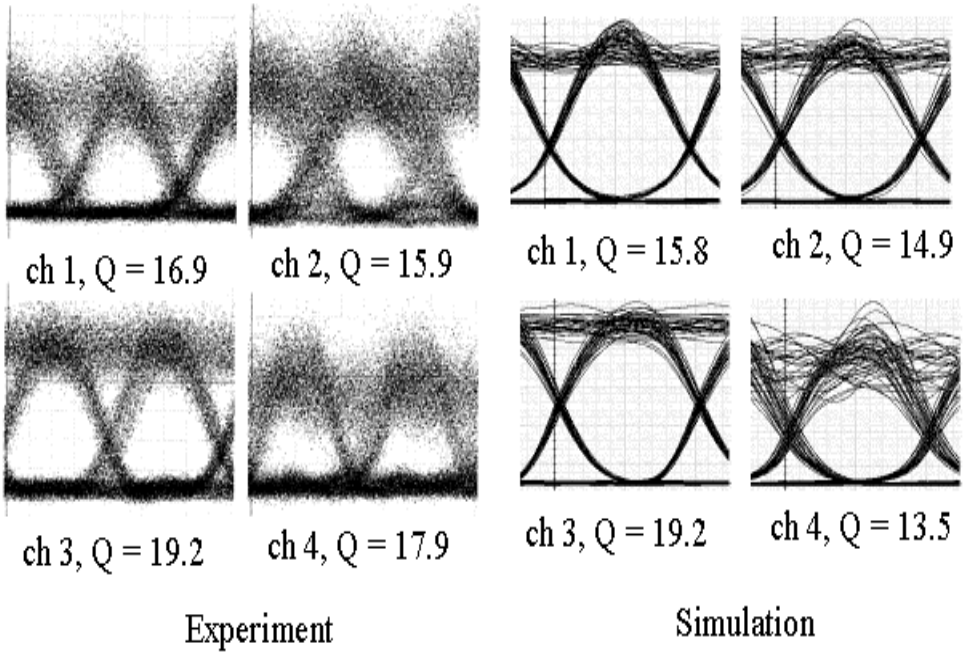

Figure 26: Eye diagram of channels as obtained from the experiment [4] and simulation

References:

1. G. P. Agrawal, Fiber Optic Communication Systems, Wiley-Interscience, 1997.
2. R. Ramaswami and K. N. Sivarajan, Optical Networks: A practical Perspective, Morgan Kaufmann, 1998.
3. G. Bellotti et. al., “Dependence of self-phase modulation impairments on residual dispersion in 10 Gb/s based terrestrial transmission using standard fiber”, IEEE Poton Tech. Lett. 11, pp. 824, 1999.
4. H. Taga, “Long distance transmission experiments using the WDM technology”, J. Lightwave Tech. 14, pp. 1287, 1996.

Example: Negative Dispersion Fiber and Applications for Metro Networks

Negative dispersion fiber and applications for metro networks**.osd**

Project file "Negative dispersion fiber and applications for metro networks.**osd**" compares two types of fibers namely Corning's MetroCor and SMF-28 Fibers. MetroCor Fiber has a negative dispersion parameter whereas SMF-28 has a positive dispersion parameter in the EDFA band where we run our simulations. We also consider effects of source chirp on the network performance. For metro applications, directly modulated sources are preferred because of their low cost, but they result in more chirp, and more penalty due to dispersion when classic positive dispersion SMF is used. One option to overcome this effect is to use a fiber with negative dispersion. This example shows that, with the same amount of accumulated dispersion, MetroCor fiber performs better when a directly modulated source is used

In the project, directly modulated laser sources are used with bit rate equal to 2.5 Gb/s. Three channels at 191.9 THz, 192.3 THz, and 192.5 THz are multiplexed and propagated on a span, which consists either MetroCor or SMF-28 fiber followed by an amplifier. The chirp on the pulse at the source is shown in Fig.27.

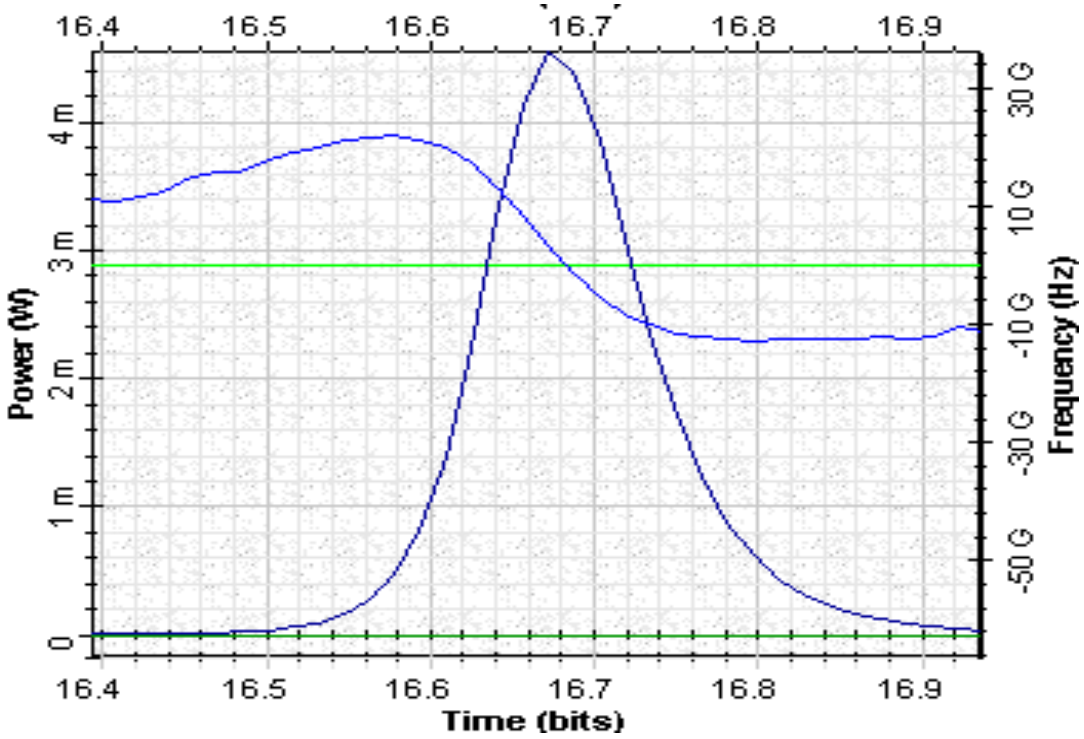

Fig. 27: Pulse shape and the chirp at the output of directly modulated laser

It is known that the line width of the source affects the broadening factor [3]. It is given as

$$\frac{\sigma}{\sigma_0}=\left[\left(1+\frac{C\beta_2 z}{2\sigma_0^{\,2}}\right)^2+\left(1+\left[2\sigma_\omega\sigma_0\right]^2\right)\left(\frac{\beta_2 z}{2\sigma_0^{\,2}}\right)\right]$$

where σ_ω is the rms width of the Gaussian source spectrum. Directly modulated sources have broader spectrums and this contributes more in the broadening of the pulse. It can even dominates the broadening originated from the group velocity dispersion (GVD) itself when $\left(2\sigma_\omega\sigma_0\right)^2 >> 1$.

Fig. 28 shows eye diagram of Channel 1 at 192.5 THz (1557.36 nm) after 170 km (2 spans) of propagation in SMF-28 where total accumulated dispersion is about 3000 ps/nm.

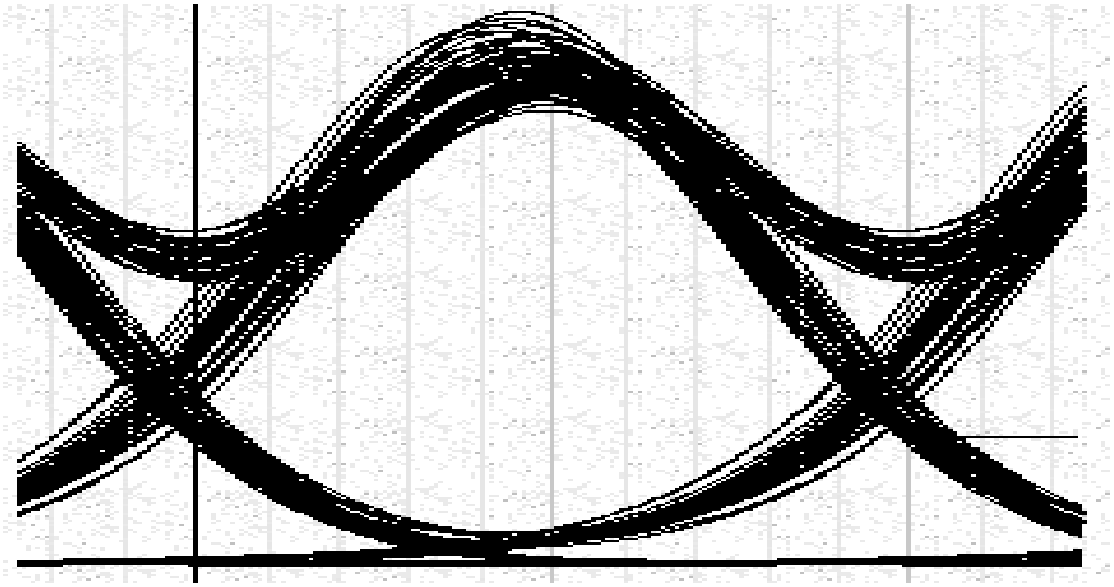

Fig. 28: Eye diagram of channel 1 after 170 km of propagation in a SMF

Fig.29, on the other hand, shows the eye diagram of the same channel after 425 km (5 spans) of propagation in MetroCor where total accumulated dispersion is again about 3000 ps/nm.

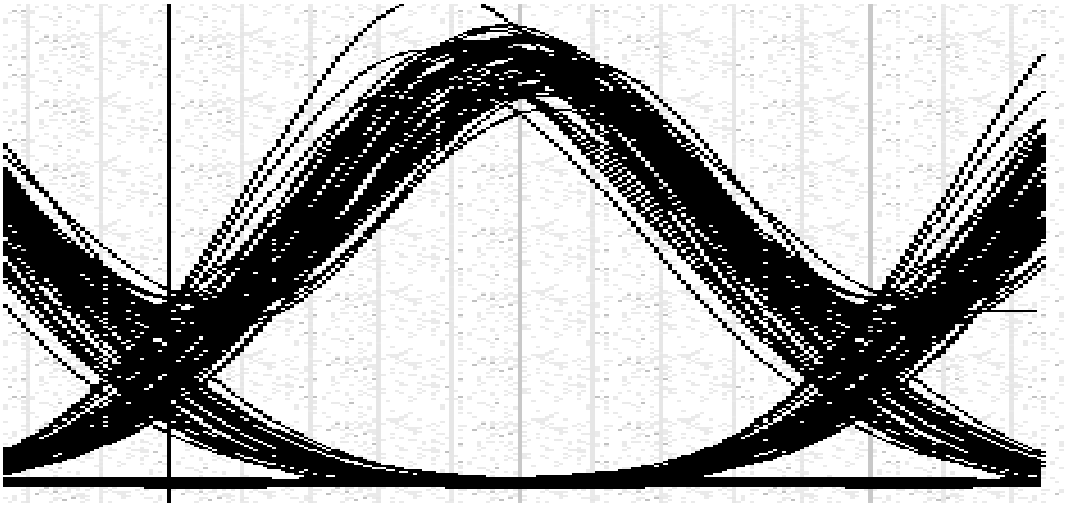

Fig. 29: Eye diagram of channel 1 after 425 km of propagation in a MetroCor fiber

Even though the accumulated dispersion is same for both tested links, we have more clear eye in the case of MetroCor fiber link. This is contributed with the interplay between the positive chirp of the directly modulated laser and the opposite chirp introduced by the negative dispersion parameter for the case of MetroCor fiber. Note that in the transmission band, the dispersion parameter of MetroCor is negative whereas that of SMF is positive. One should also note that MetroCor link contains 5 EDFA that brings more noise (OSNR at the receiver end is about 15 dB), whereas SMF-28 link has 2 EDFA (OSNR at the receiver end is about 19 dB).

These results show that with the same amount of accumulated dispersion, MetroCor fiber performs better when a directly modulated source is used. Moreover, we can conclude that use of negative dispersion fiber also increases transmission distance.

References:

1. Chris Kennedy et. al., “The performance of negative dispersion fiber at 10 GBps and significance of externally and directly modulated lasers”, NFOEC’01, 2001.
2. David Culverhouse et. al., “Corning MetroCore Fiber and its Application in Metropolitan Networks”, Corning’s White Paper WP5078.
3. G. P. Agrawal, Nonlinear Fiber Optics, Second Edition, Academic Press, 1995.

Example: Migrating to 10 Gb/s Metro System and Dispersion Limited Transmission

Migrating to 10 Gb/s_no dispersion compensation.**osd**

Migrating to 10 Gb/s_dispersion compensation at each node.**osd**

Migrating to 10 Gb/s_lumped dispersion compensation.**osd**

In project files "Migrating to 10 Gb/s_no dispersion compensation.**osd**", "Migrating to 10 Gb/s_dispersion compensation at each node.**osd**", and "Migrating to 10 Gb/s_lumped dispersion compensation.**osd**", we investigate the issues at high data bit rate, particularly 10 Gb/s (OC-192) systems in metro area ring networks. In higher bit rates, in addition to loss compensation, we also need to consider the chromatic dispersion compensation. Two possibilities, namely "lumped" and "at each node" dispersion compensation schemes are shown and they are compared for metro applications.

For this case, the receiver sensitivity is –16 dBm which reduces the allowable loss to $L_{allowable} = 3-(-16) = 13\ dB$. Assuming again a power of 3 dBm per channel, the amount of amplification needed in the ring is $G_{required} = -\left(3-4\times 0.25\times 50-4\times 3.8-(-16)-3\right) = 49.2\ dB$. We can again use unity gain segment approach for power compensation. This example shows that migration is easily done in terms of power budgeting since the total loss is not changed, even though the allowable loss is changed

Let us now look at the criteria for dispersion and try to see if it is a real issue for metro networks.

GVD-limited transmission distance

In the case of directly modulated DFB lasers, limiting transmission distance is [1,2]

$$L < \frac{1}{4B|D|\sigma_\lambda}$$

where σ_λ is root-mean-square spectral width, with a typical value around 0.15 nm, for D=16 ps/(km-nm) and 2.5 Gbps $L \approx 42\ km$.

For externally modulated sources, limiting transmission distance is

$$L < \frac{2\pi c}{16|D|\lambda^2 B^2}$$

Again for D=16 ps/(km-nm) and 2.5 Gbps, $L \approx 500\ km$. Therefore Group Velocity Dispersion (GVD) is not a limiting effect in the above example for a 2.5 Gb/s communication network.

No dispersion compensation

At high bit rates, GVD may become a limiting parameter for the transmission distance. When the bit rate increased to 10 Gb/s, GVD-limited transmission distance drops to 30 km. Fig. 30 shows the eye diagram when the bit rate is 10 Gb/s and transmitter power is 3 dBm/channel. In this example, we have used unity gain segment approach, which means for loss in each fiber span a node is compensated immediately at the following node. This project is given in Migrating to 10 Gb/s_no dispersion compensation**.osd** file.

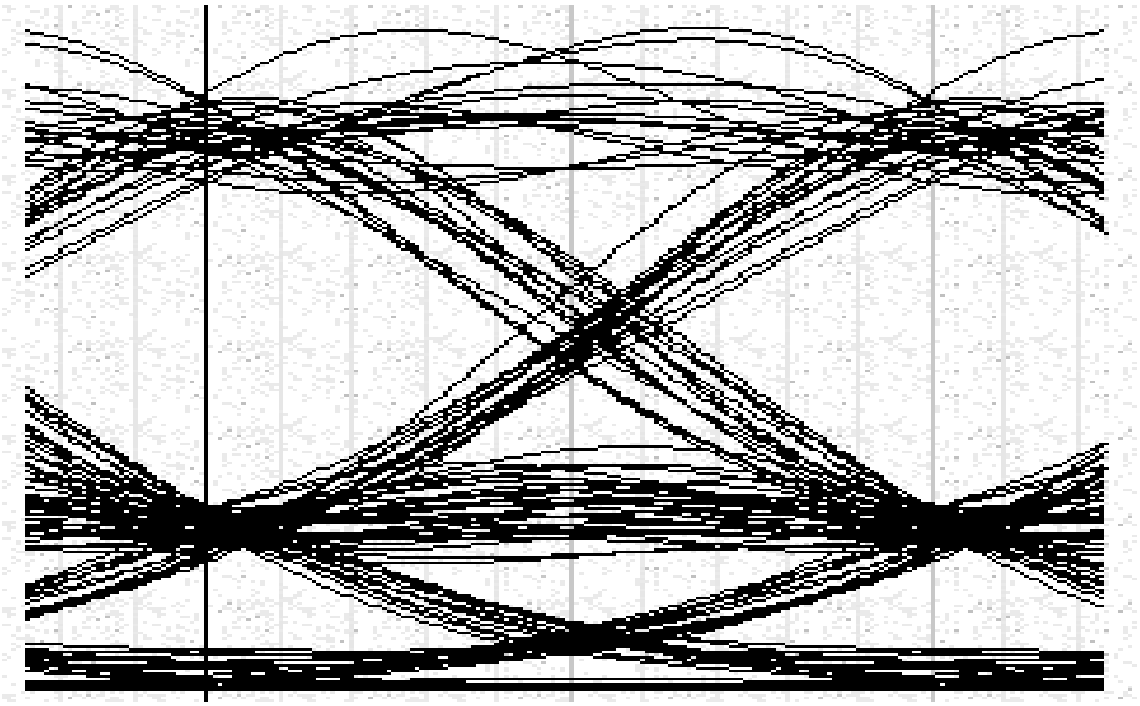

Fig. 30: Eye diagram of channel 1 at node 4 when the transmitter power is 3 dBm and bit rate is 10 Gb/s

Therefore, at this rate one has to consider dispersion management. Total dispersion per 50 km span is around $16 \times 50 = 800\ ps/nm$. This will require 10 km of dispersion compensating fiber (DCF) with $D = -80\ ps/nm/km$ for each fiber span. We can again follow several avenues to compensate the accumulated dispersion.

"Per span" dispersion compensation

For example, DCF can be used after each span or total accumulated dispersion can be compensated at a certain point. Again for the scalability of the network and considering the dynamic structure of the metro traffic, it seems to be the best choice to distribute the dispersion compensation to every node. This will also

make sure that dispersion experienced by dynamically routed signals will be compensated properly. For this case, you also need to compensate the power loss of DCFs. For that purpose 5 dB more gain added to each amplifier. The simulation project is given in Migrating to 10 Gb/s_dispersion compensation at each node.**osd** file. Fig. 31 shows the network layout when unity gain approach and per node dispersion compensation is used.

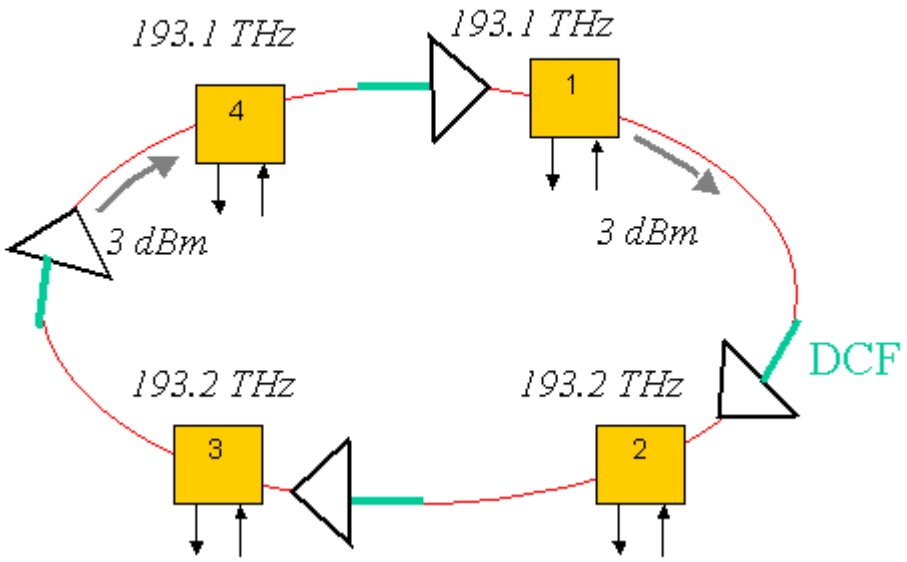

Fig. 31: Ring network layout when unity gain approach and per span dispersion compensation is used

Fig.32 shows the eye diagram at the receiving end when per span dispersion compensation is used.

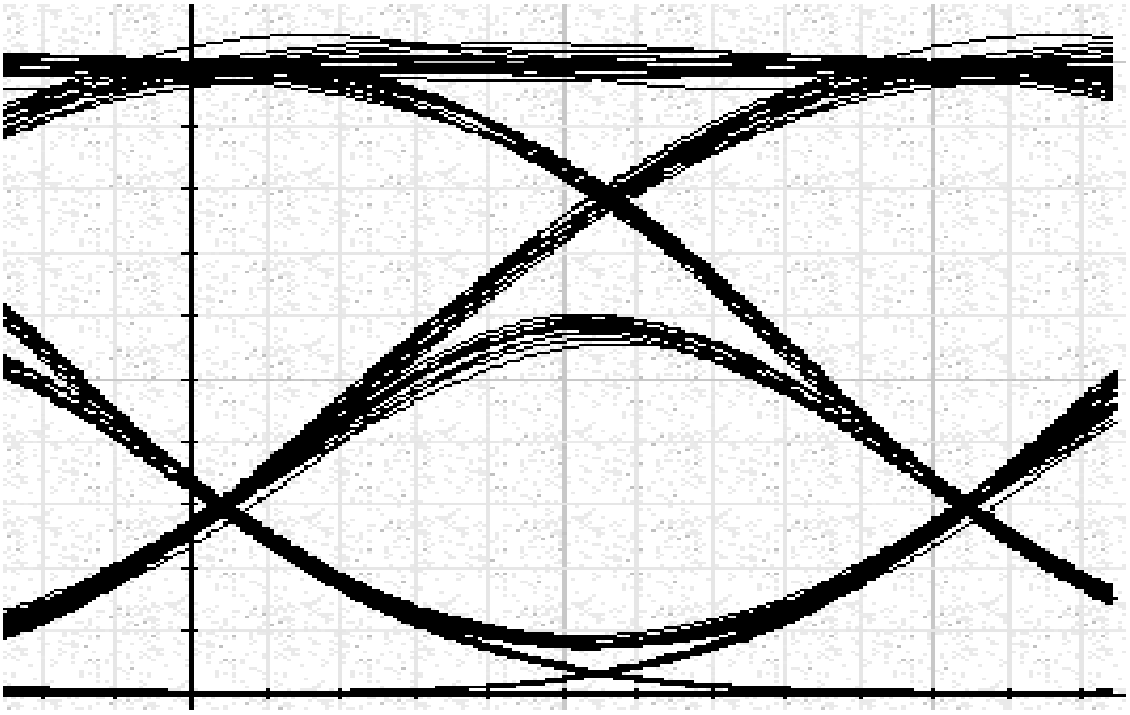

Fig. 32: Eye diagram at node 4 when per span dispersion compensation is used

"Lumped" dispersion compensation

Now consider the "lumped" dispersion compensation case. In this case, one DCF and extra amplifier is inserted just before node 2 to compensate the total dispersion and extra loss of DCF. This project is given in Migrating to 10 Gbps_lumped dispersion compensation**.osd** file. Fig. 33 shows the eye diagram at node 4 for this configuration. As can be seen from the eye diagram, this configuration definitely improves the network performance for the considered channel comparing with the uncompensated case, but worst than the case with distributed compensation. Moreover, "lumped" dispersion compensation is not suitable for metro networks in which the wavelength routing path cannot be estimated.

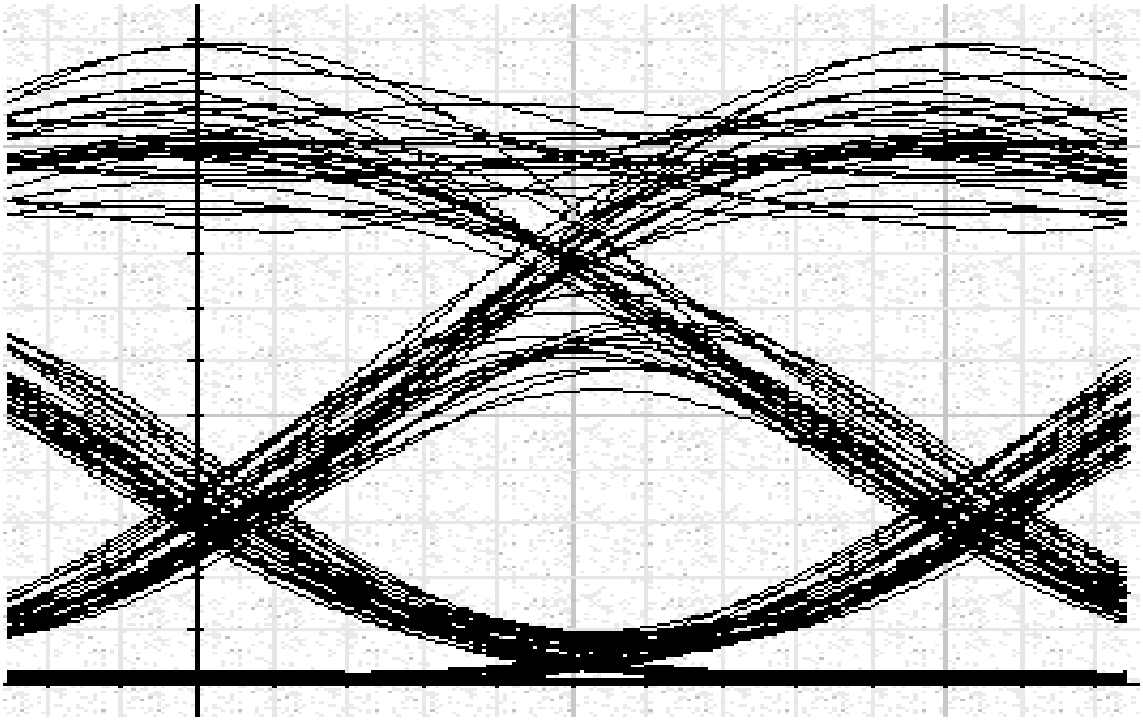

Fig. 33: Eye diagram at node 4 when "lumped" dispersion compensation is used

References:

1. G. P. Agrawal, Fiber-Optic Communication Systems, Wiley-Interscience, 1997.
2. R. Ramaswami and K. N. Sivarajan, Optical Networks: A practical Perspective, Morgan Kaufmann, 1998.

Chapter 8 - Multichannel Systems

Example: WDM Ring Network

WDM ring with WISE_directly modulated source_RZ**.osd**
WDM ring with WISE_directly modulated source_NRZ**.osd**
WDM ring with WISE_externally modulated source_RZ**.osd**
WDM ring with WISE_externally modulated source_NRZ**.osd**

Project files for this example are "WDM ring with WISE_directly modulated source_RZ**.osd**", "WDM ring with WISE_directly modulated source_NRZ**.osd**", "WDM ring with WISE_externally modulated source_RZ**.osd**", and "WDM ring with WISE_externally modulated source_NRZ**.osd**".

In this example, we will show realization of a WDM ring network using wavelength independent subscriber equipment to share bandwidth [1,2]. We will also investigate the effects of source type and bit rate to network performance.

The metro-ring network we modeled operates with 2 wavelength carriers as shown in Fig. 1. In this configuration, several subscribers share the bandwidth. For illustration purpose, the network contains one Network Node (NN) and one Access Node (AN). By using a packet format, multiple users can share a single wavelength. All wavelengths are sourced at the NN whose output wavelengths are multiplexed on the ring fiber. NN also contains an associated set of WDM. The resulting architecture can simultaneously support cost-shared virtual rings (the distribution ring network connected to AN, single wavelength goes around this sub-rings), distribution stars with a dedicated wavelength per user (every End Station (ES) uses a different wavelength), or a combination.

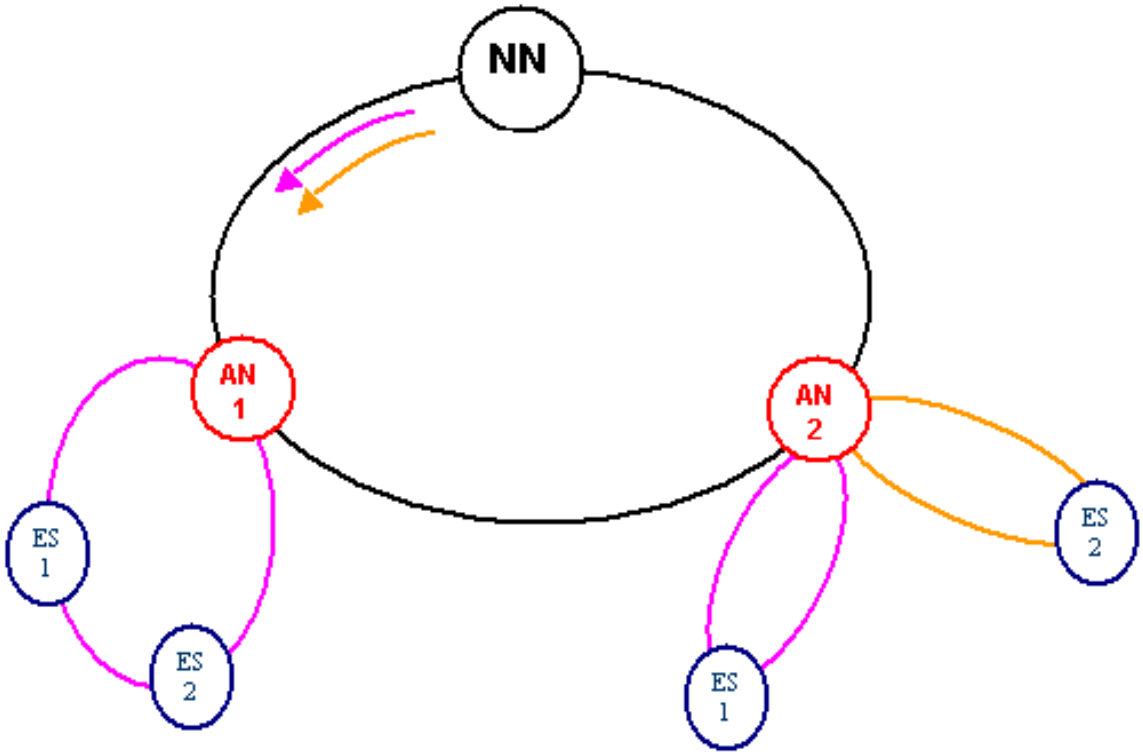

Fig. 1: A ring network with 4 end stations (subscribers) and 2 access nodes

We simulate the case when we have one NN and one AN (AN 1). In this configuration two end stations (ES1 and ES 2) share the same wavelength λ_1. In a real application, end users via a packet protocol as shown in Fig. 2 share this wavelength. Incoming packet data is directed to user's receiver via a 3-dB splitter. Each outgoing packet is created by modulating an incoming "optical chalkboard", which consists of a string of all ones' sourced at the NN. Here, for illustration purpose, we modulated the optical carrier at NN and assumed that the modulation and packet organization takes place at another sub-ring or star (at any ES who wants to communicate with ES 1 or/and ES 2).

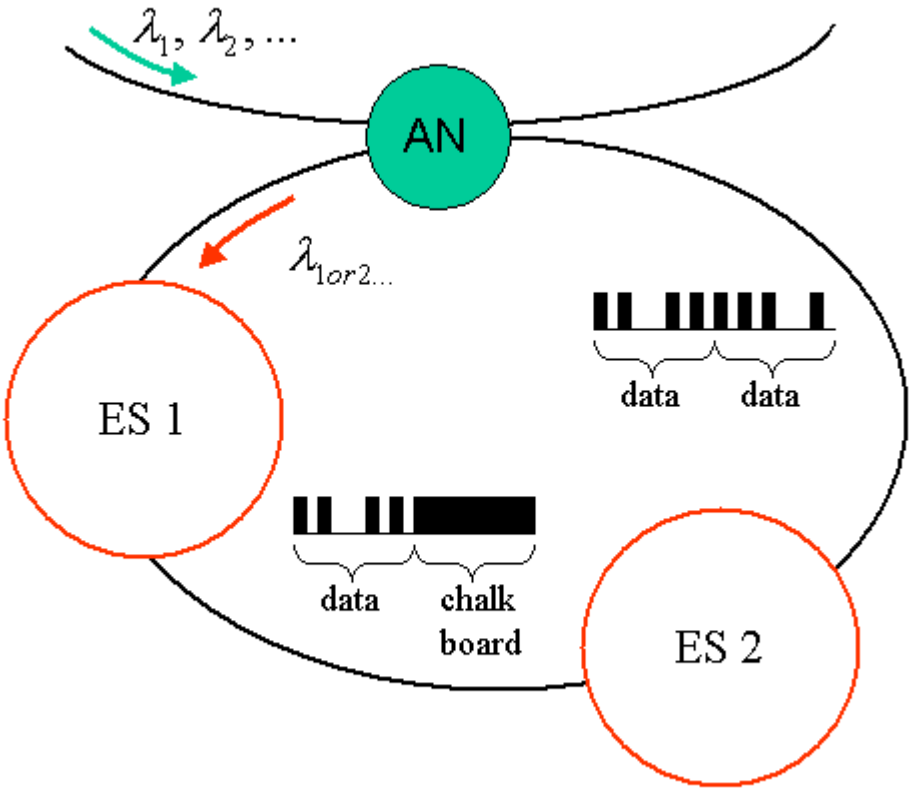

Fig. 2: Details of end stations and writing data on a "chalk board

We simulate the system by using two different types of sources, namely directly modulated and externally modulated sources to examine the effect of the transmitter type to network performance. It is known that the line width of the source affects the broadening factor [3]. It is given as:

$$\frac{\sigma}{\sigma_0} = \left[\left(1 + \frac{C\beta_2 z}{2\sigma_0^{\,2}} \right)^2 + \left(1 + \left[2\sigma_\omega \sigma_0 \right]^2 \right) \left(\frac{\beta_2 z}{2\sigma_0^{\,2}} \right) \right] \qquad (1)$$

where σ_ω is the rmsa width of the Gaussian source spectrum. Directly modulated sources have broader spectrums and this contributes more in the broadening of the pulse. It can even dominate the broadening originated from the group velocity dispersion (GVD) itself when $\left(2\sigma_\omega\sigma_0\right)^2 >> 1$.

Directly modulated sources

Power spectrum after the multiplexer is given in Fig. 3 when a directly modulated source and RZ modulation is used. The project for this case is given in WDM ring with WISE_directly modulated source_RZ**.osd**. In this case, bit rate is 2.5 Gb/s and laser power is 6 dBm. As eye diagram (Fig. 4) shows, at 2.5 Gb/s one can get a reasonable performance from the directly modulated source at this power level. System does not work properly at 10 Gb/s bit rate for a power of 6 dBm/channel at the transmitter. Eye diagram for this case has been shown in Fig. 5. If we further increase the transmitter power to 15 dBm/channel we see that the eye opens (Fig. 6), but further increase of the power does not help since the transmission is dispersion limited and dispersion compensation is required at this bit rate. Externally modulated transmitter shows a better performance as shown in the eye diagrams (Figs. 8 and 9).

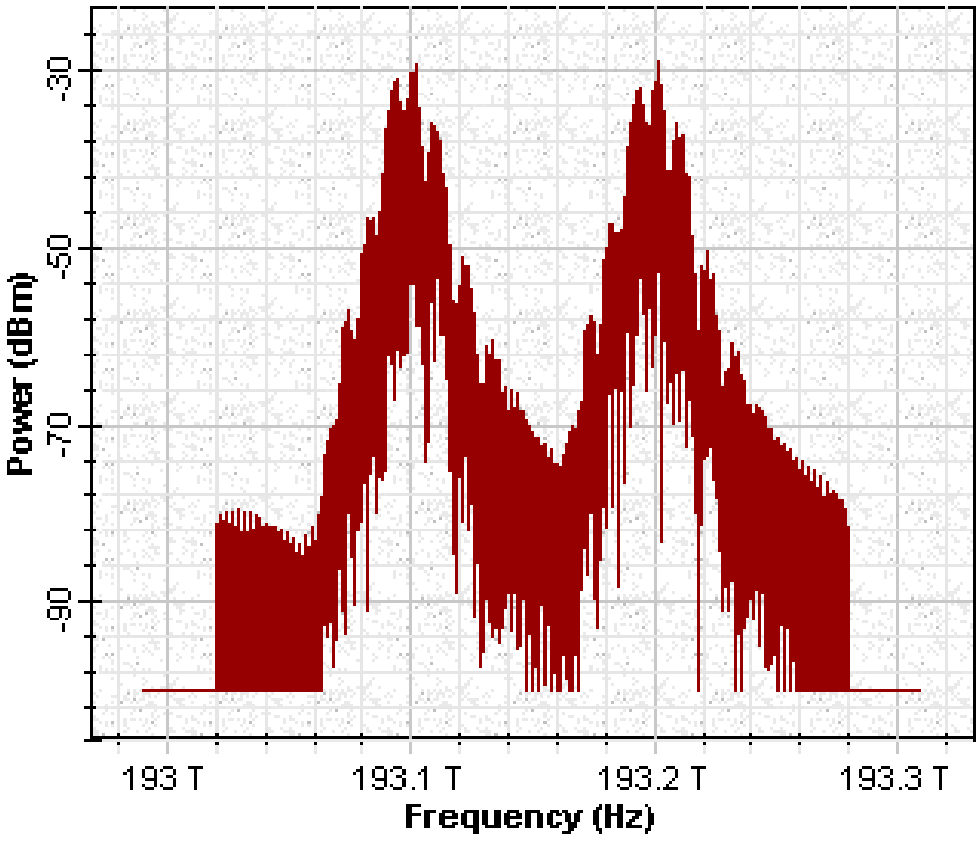

Fig. 3: Power spectrum after the multiplexer, when directly modulated sources are used.

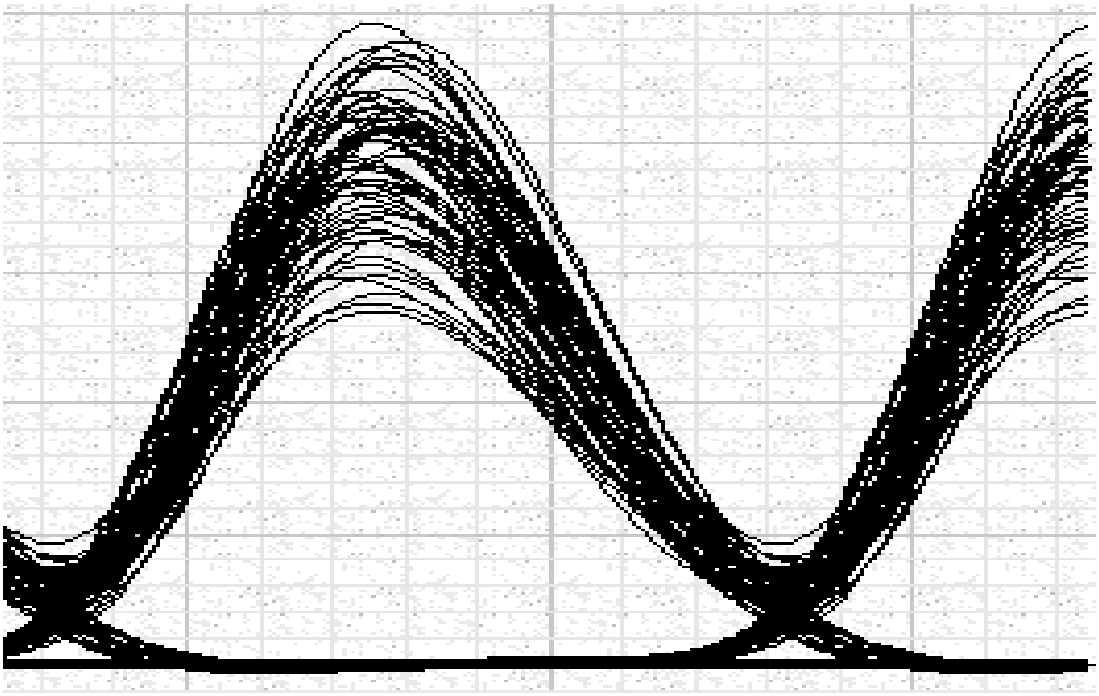

Fig. 4: Eye diagram at ES 2 when directly modulated sources are used and bit rate is 2.5 Gbps

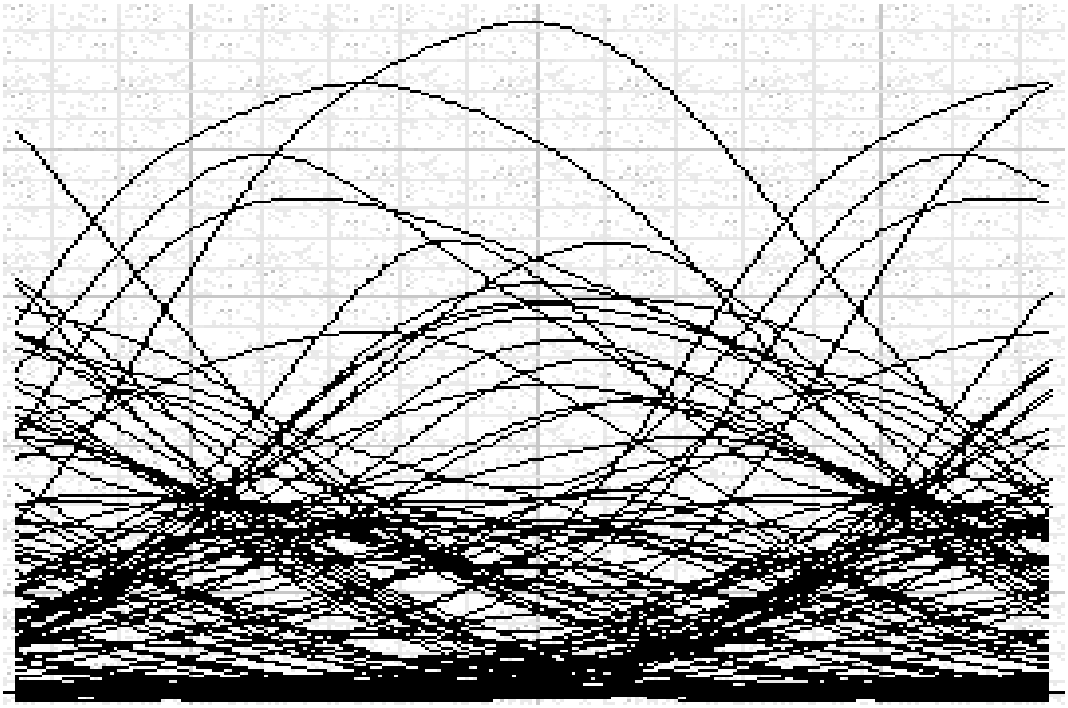

Fig. 5: Eye diagram at ES 2 when directly modulated sources (6 dBm/channel) are used and bit rate is 10 Gbps

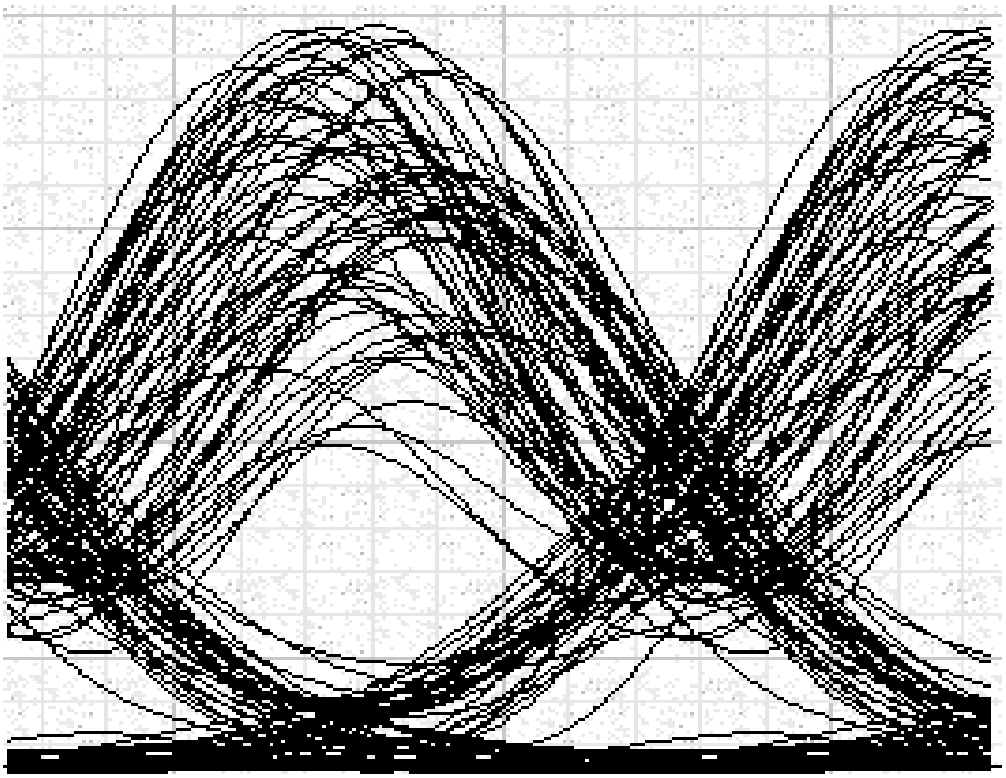

Fig. 6: Eye diagram at ES 2 when directly modulated sources (15 dBm/channel) are used and bit rate is 10 Gbps

Externally modulated sources

The project for this case is given in WDM ring with WISE_externally modulated source_RZ**.osd**. As shown in Fig. 7, power spectrum after the multiplexer is narrower than that of directly modulated case and as shown in Fig. 8 and Fig. 9, the performance is much better for both 2.5 Gb/s and 10 Gb/s cases.

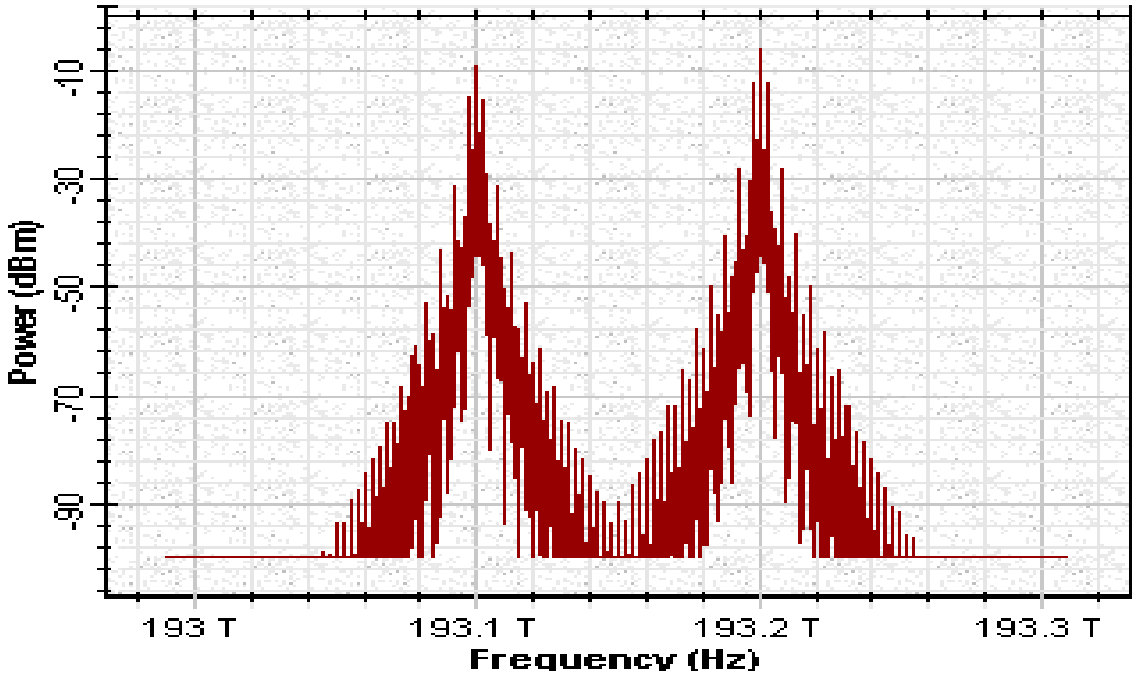

Fig. 7: Power spectrum after the multiplexer, when externally modulated sources are used.

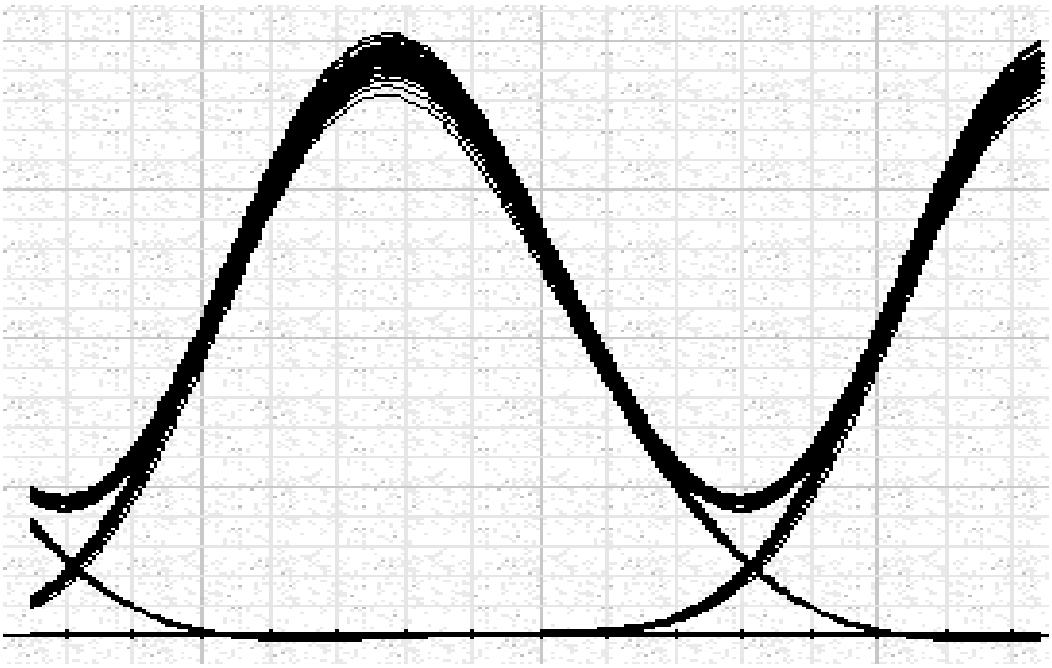

Fig. 8: Eye diagram at ES 2 when externally modulated sources (6 dBm/channel) are used, and bit rate is 2.5 Gbps.

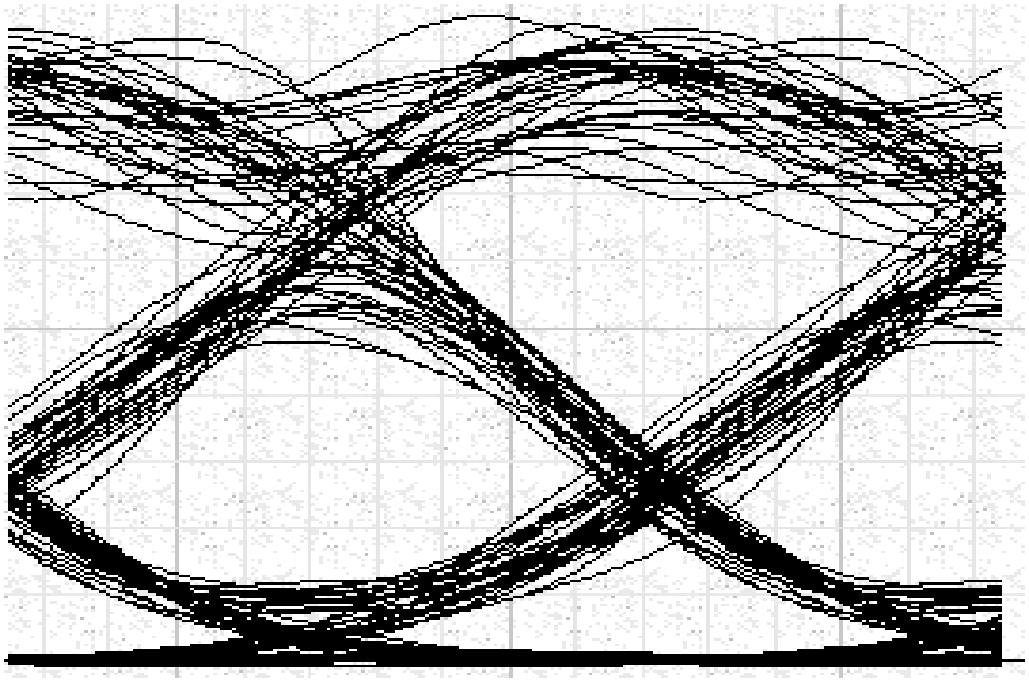

Fig. 9: Eye diagram at ES 2 when externally modulated sources (6 dBm/channel) are used and bit rate is 10 Gbps.

Fig. 10 shows the eye diagram when NRZ modulation format is used. The project for this simulation is given in WDM ring with WISE_externally modulated source_NRZ**.osd**

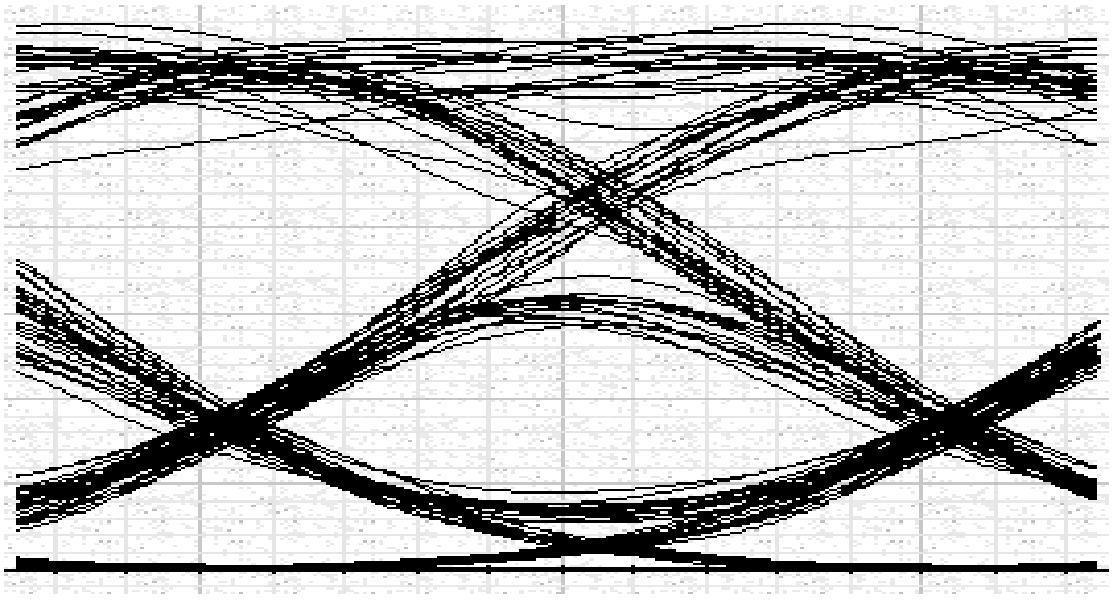

Fig. 10: Eye diagram at ES 2 when externally modulated sources (6 dBm/channel) and NRZ formats are used and bit rate is 10 Gbps.

Fig. 11 shows the eye diagram when direct modulation NRZ format is used. The project for this simulation is given in WDM ring with WISE_directly modulated source_NRZ**.osd**

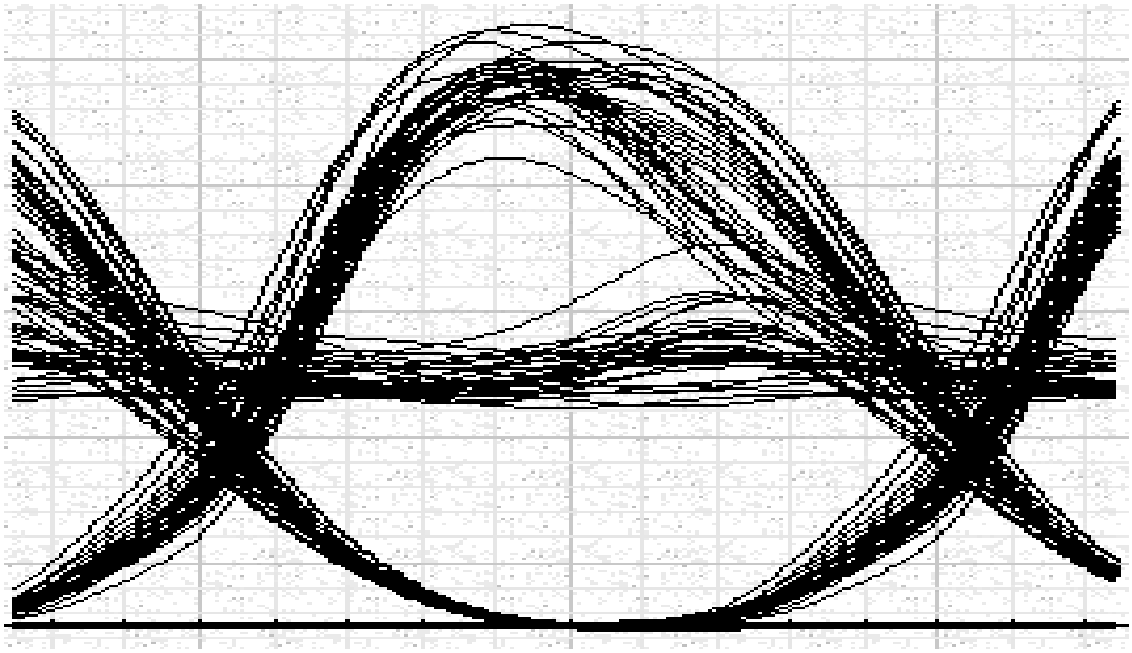

Fig. 11: Eye diagram at ES 2 when directly modulated sources (6 dBm/channel) and NRZ format are used and bit rate is 2.5 Gbps

As can be seen from these simulations, the best performance is obtained with external modulation. Directly modulated source seems to work better when RZ modulation is used at 2.5 Gb/s bit rate. We have also shown here a WDM ring network where wavelengths are shared by subscribers.

References:

1. P. P. Iannone et. al., “A flexible metro WDM ring using wavelength-independent subscriber equipment to share bandwidth”, OFC’00, paper PD38, 2000.
2. P. P. Iannone et. al., “A transparent WDM network featuring shared virtual rings”, J. Lightwave Tech., vol. 18, pp 1955, 2000.
3. G. P. Agrawal, Nonlinear Fiber Optics, Second Edition, Academic Press, 1995.

Example: Dual Fiber Protected Ring Architecture

Dual fiber protected ring architecture**.osd**

Project file "Dual fiber protected ring architecture**.osd**" shows the design of a dual fiber protected ring architecture. It also shows how a "lumped' dispersion compensation behaves for a dynamic network. This architecture consists of two fiber rings where the signal flow is opposite to each other. In this topology, primary and secondary (protection) rings are used for signal transmission at normal condition. In this way, the transmission rate is doubled. If there is a fiber cut, secondary ring is used as a protection link. Details of this example are given below.

Dual fiber protected ring architecture

As the requested bit rate increases, the network architecture must be modified to accommodate this demand. To do so we also need to keep in mind the cost of this modification. In this example, we will show design of dual fiber protected ring architecture [1]. We will also show how a "lumped' dispersion compensation behaves for a dynamic network. This architecture consists of two fiber rings where the signal flow is opposite to each other. In this topology, primary and secondary (protection) rings are used for signal transmission at normal condition. In this way, we can double the transmission rate. The topology layout is shown in Fig. 12. If there is a fiber cut, secondary ring is used as a protection link as shown in Fig. 13. Fiber cut is modeled by using the switch subsystems. This protection path makes it feasible and cost effective to provide up to 20 Gbps of bandwidth when both rings are in normal operation. This requires some extra devices at the nodes.

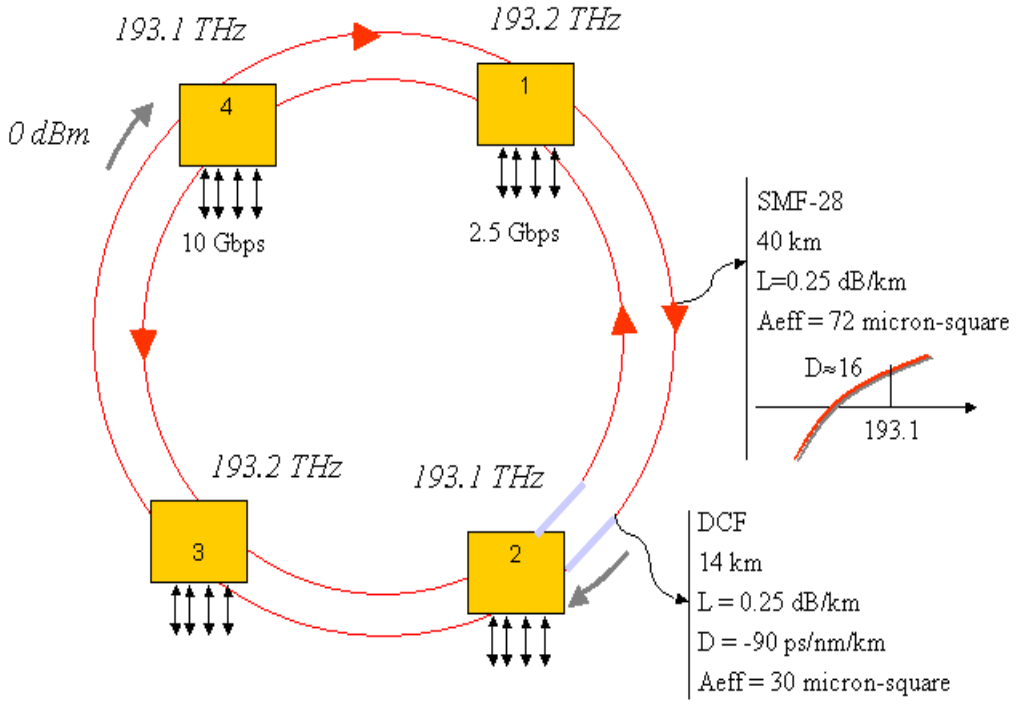

Fig. 12: Dual fiber protected ring architecture

We have inserted two dispersion compensating fibers before and after node 2 to compensate the accumulated dispersion over the ring. Fiber parameters are given in the figure. Project file is Dual fiber protected ring architecture**.osd.** Switches are modeled by using subsystems. Each of these subsystems contain four digital optical switches and loop control elements. To demonstrate, different bit rates in the same simulation, we “pumped” the network with two different bit rates. Node 2 communicates with node 4 at 10 Gb/s bit rate and node 1 communicates with node 3 at 2.5 Gb/s bit rate. If there is a fiber cut, communication speed is reduced to 10 Gb/s.

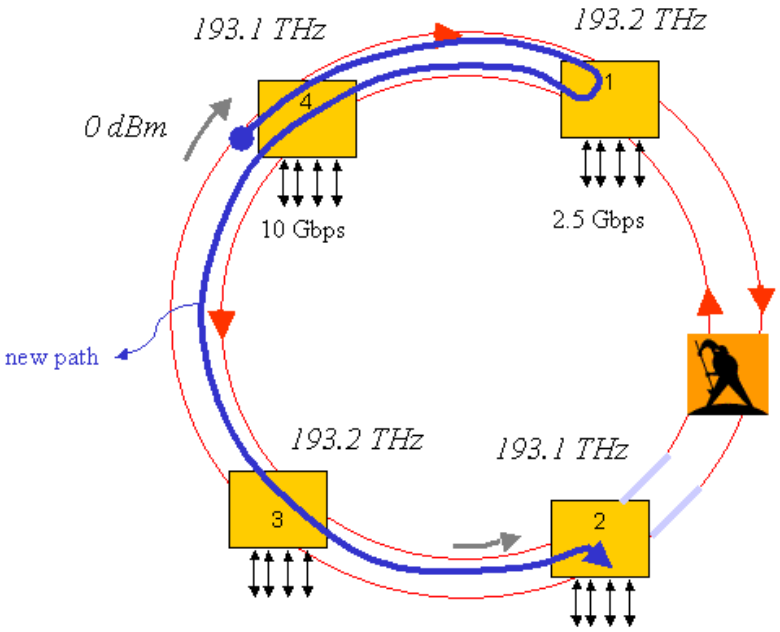

Fig. 13: Dual fiber protected ring with a fiber cut between nodes 1 and 2

Fig. 14 shows the simulation results for normal and protected operations. In normal operation, ch 1 on secondary path does not pass over DCF. The eye is more closed than the ch 1 on primary path that includes a DCF. As can be seen from Fig. 14, if there is a fiber cut, channel one has to follow a new path, which does not contain a DCF. In this case the eye closes. This simulation shows that we have to use a more intelligent dispersion compensation plan. For example, we can use “per span” dispersion compensation instead of “lumped” dispersion compensation.

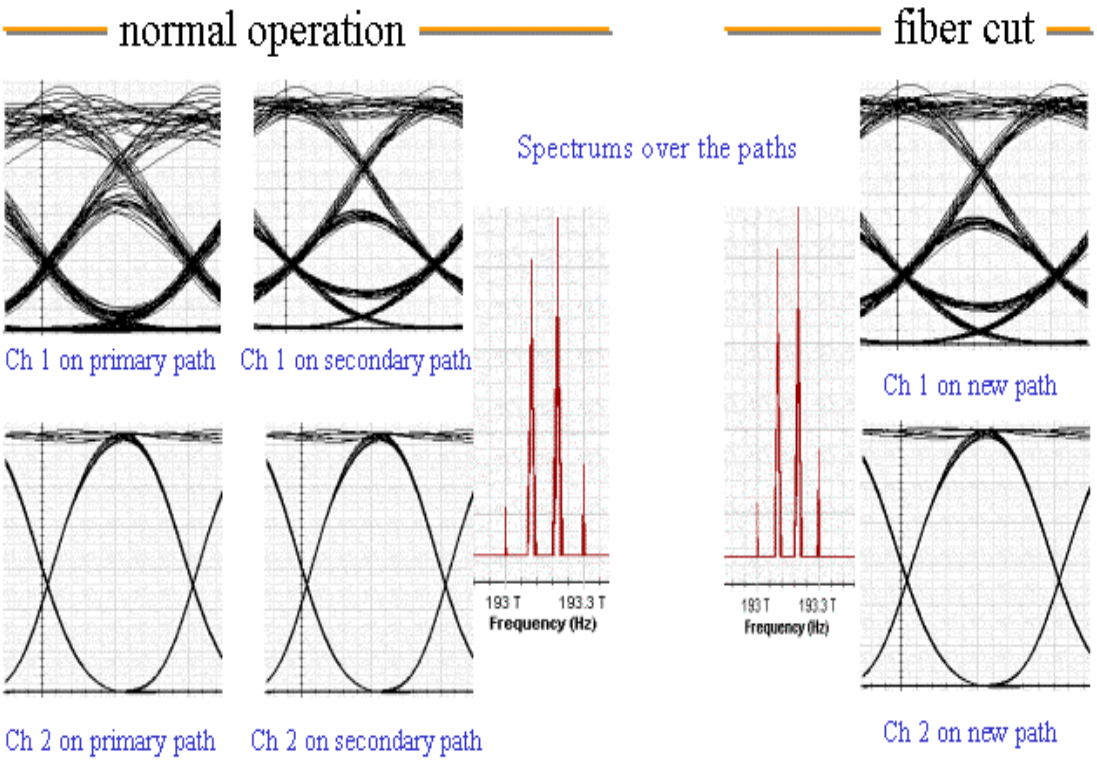

Fig. 14: Simulation results for dual fiber protected ring network

Reference:

1. Peeya Iwagoshi, “High-speed ethernet optical architecture for metropolitan area networks”, NFOEC’2001, 2001.

Example: Fabry-Perot Filter

Fabry-Perot filter**.osd**

The project “Fabry-Perot filter**.osd**“ (Fig.15) shows the transmission of a Fabry-Perot filter used as a tunable optical filter. The frequency spacing between two successive transmission peaks is known as free spectral range (Fig.16)**.**

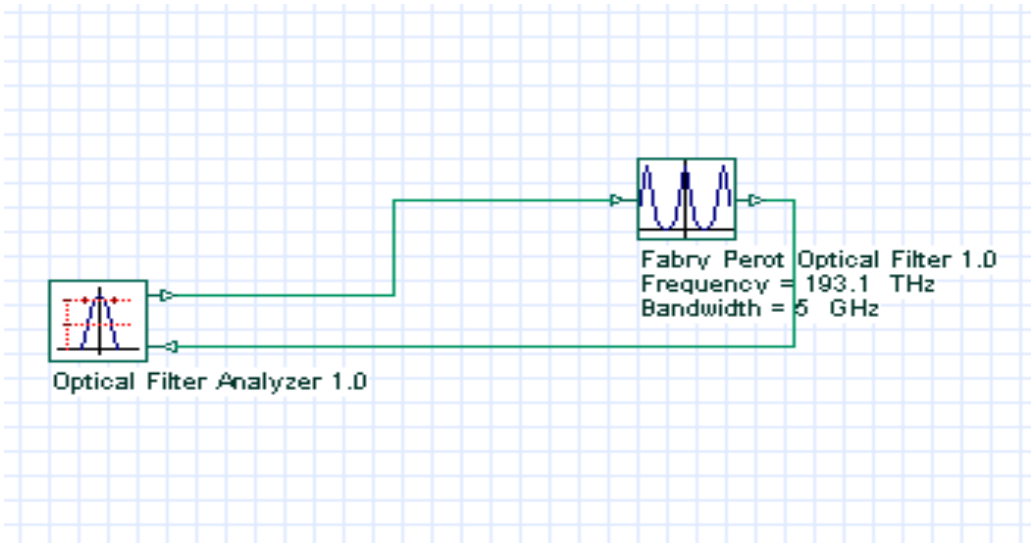

Fig.15: Layout: Fabry-Perot filter

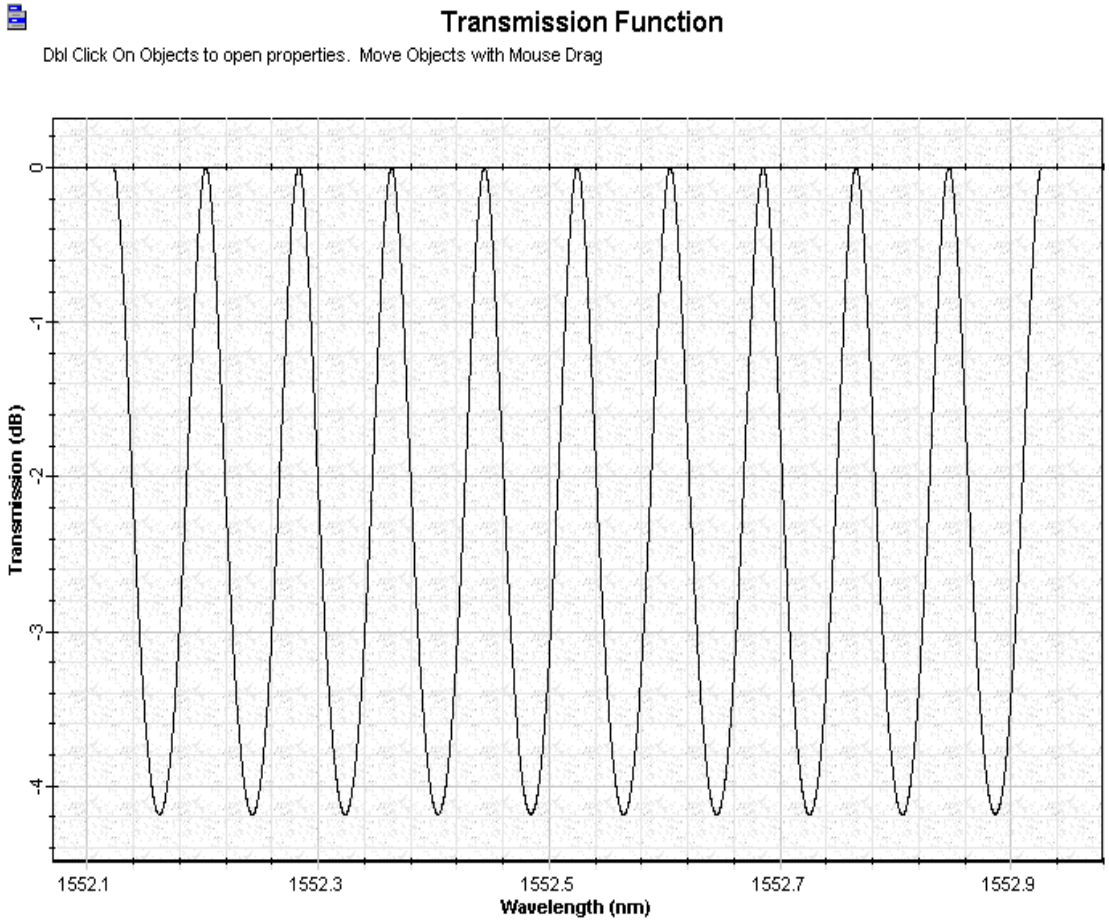

Fig.16: Fabry-Perot filter transmission

Example: Uniform FBG Filter

FBG filter transmission.**osd**

A separate class of optical filters makes use of the wavelength selectivity provided by a Bragg grating. The project "FBG filter transmission.**osd**" (Fig.17) shows the transmission of a uniform FBG filter (Fig.18).

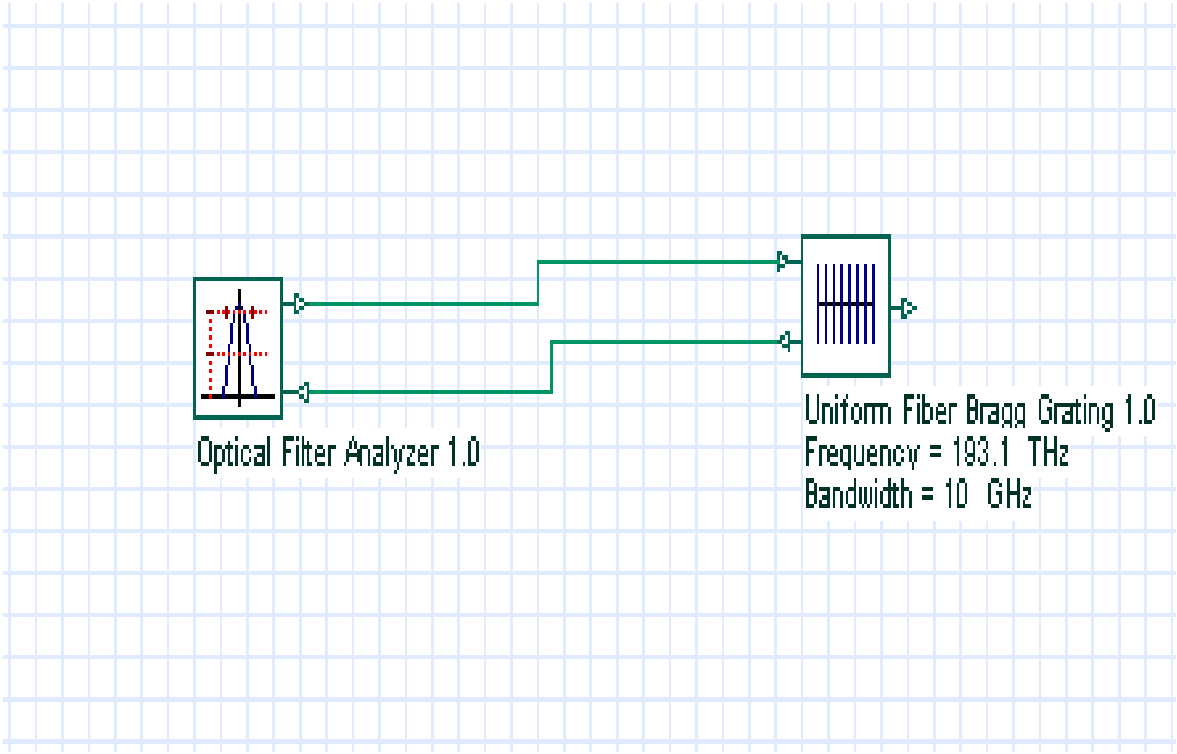

Fig.17: Layout: FBG filter transmission

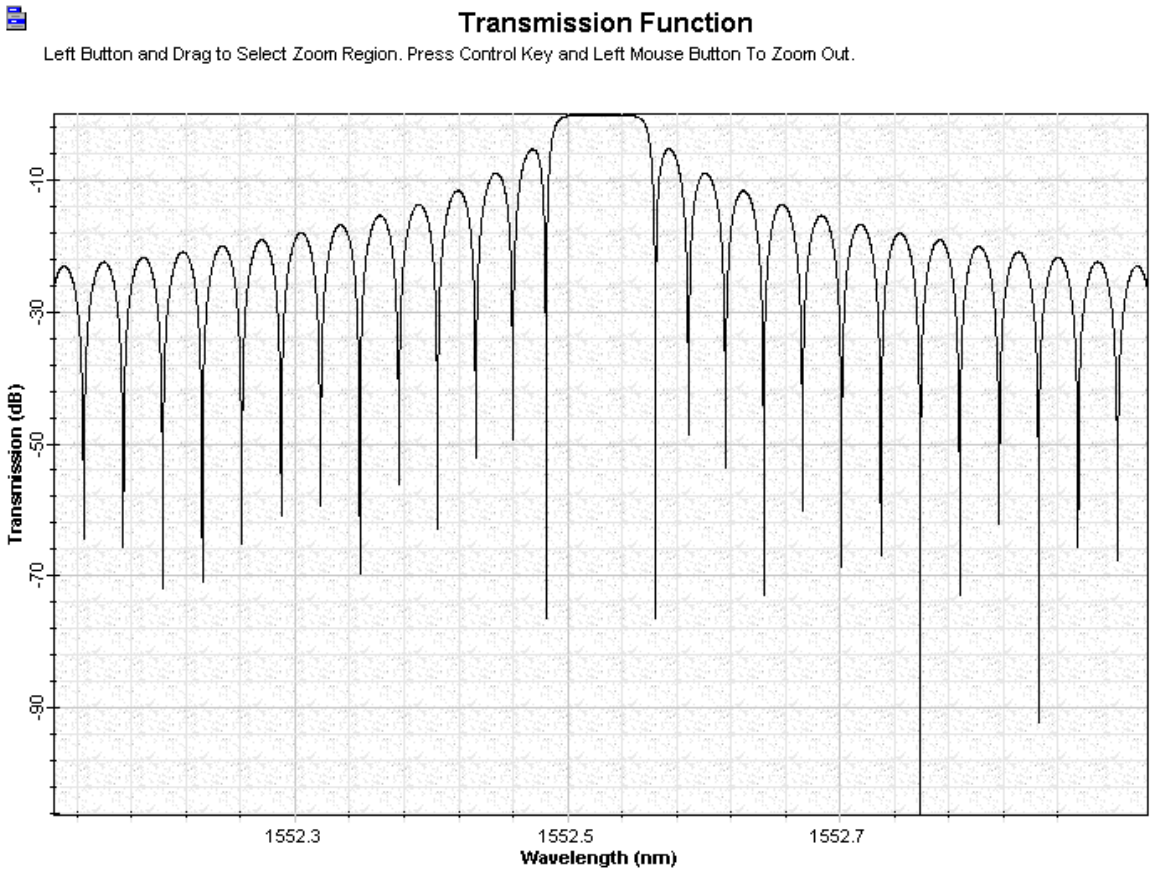

Fig.18: FBG filter transmission

Example: AWG Demultiplexer

AWG demultiplexer.**osd**

Fiber Bragg gratings can be used for making all fiber demultiplexers. The project "AWG demultiplexer.**osd**" (Fig. 19) shows an Array waveguide grating (AWG) demultiplexer.

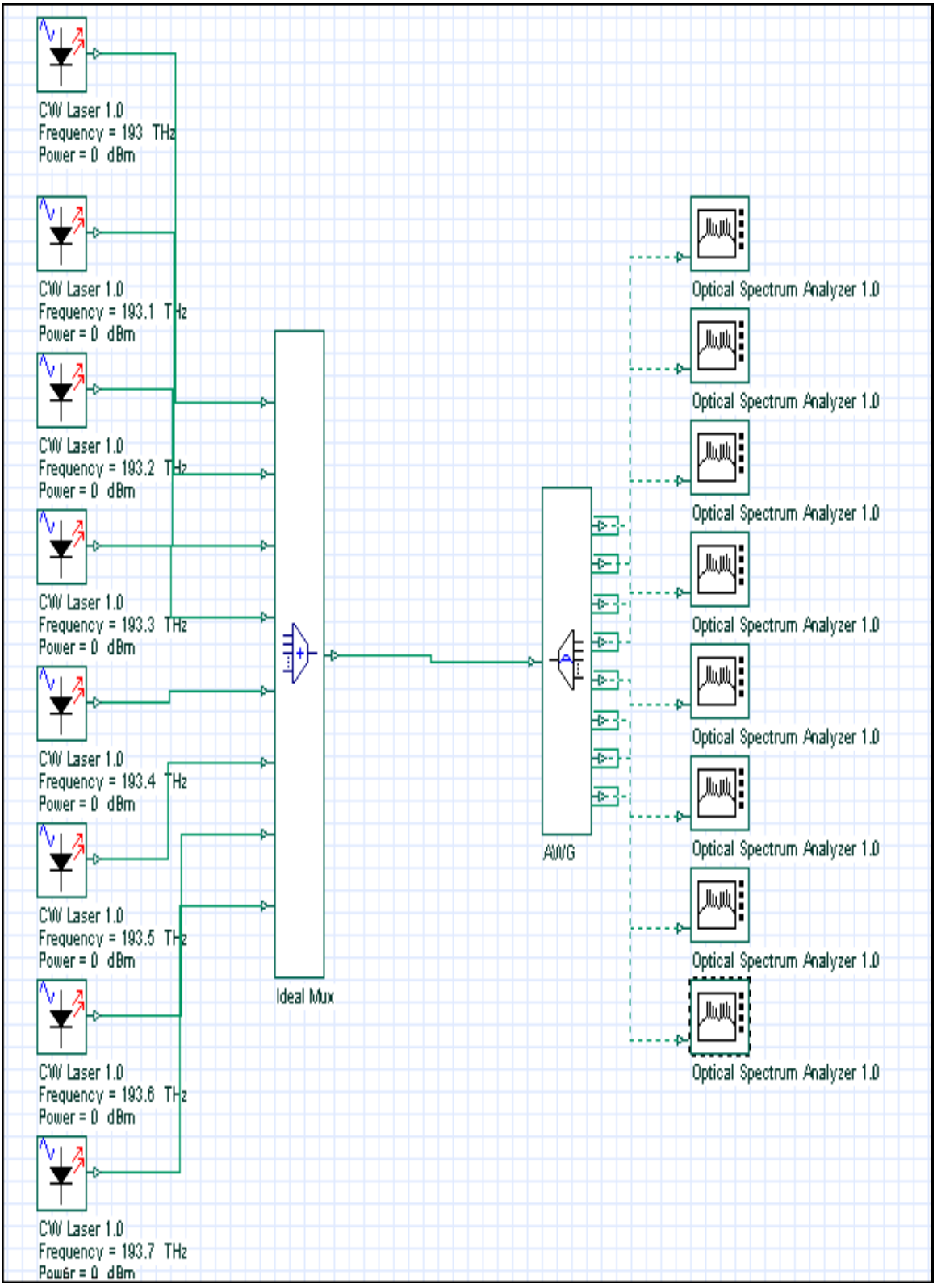

Fig.19: Layout: AWG demultiplexer

The OSA at the AWG output shows the selected WDM channel. For the first channel, the AWG input has been shown in Fig. 20.

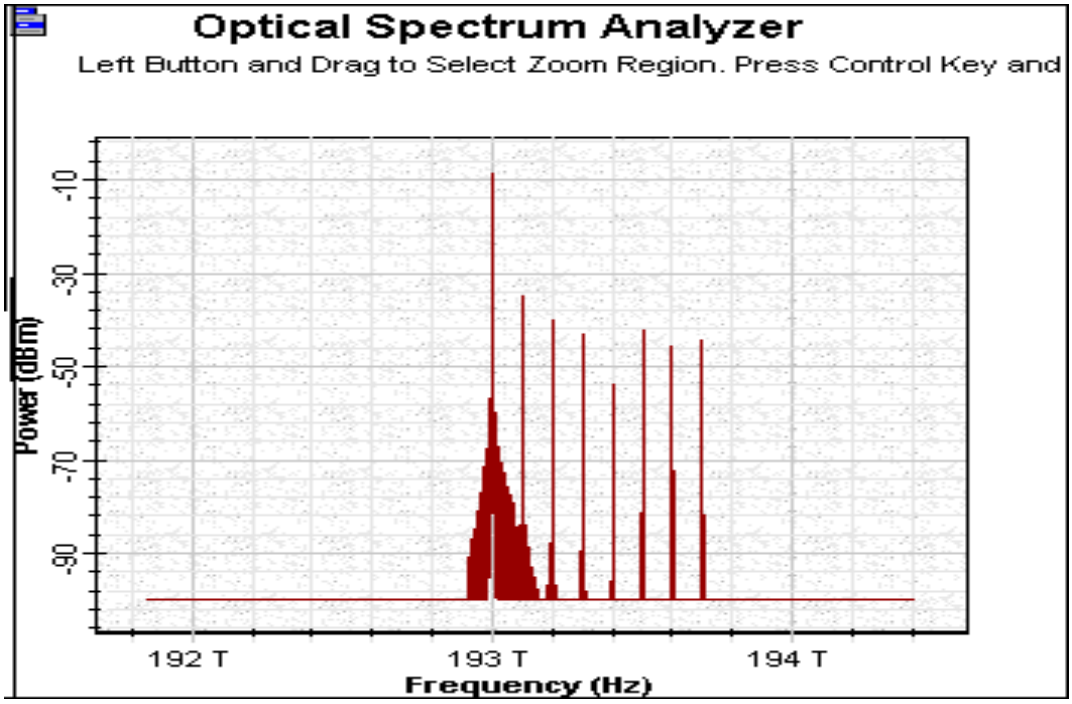

Fig.20: AWG input

The AWG transmission is shown in Fig. 21.

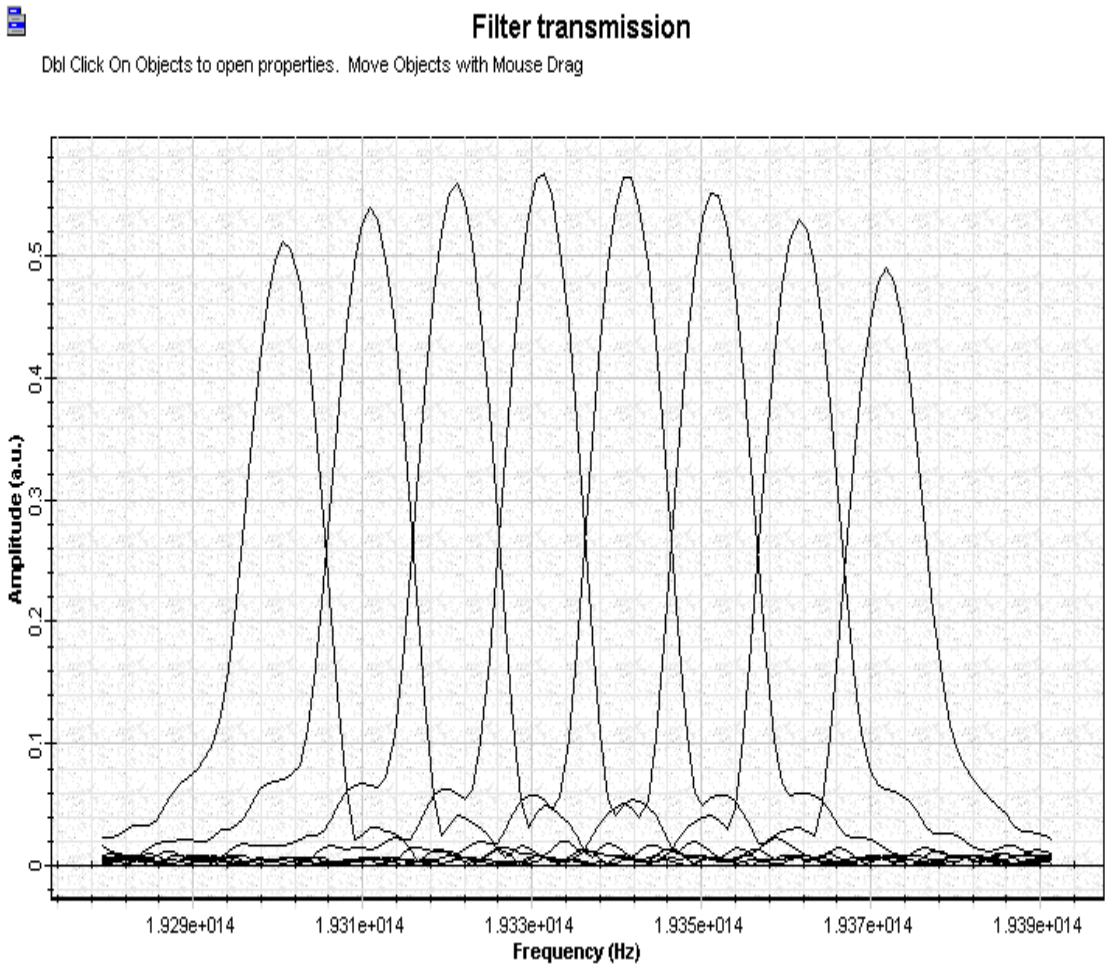

Fig.21: AWG transmission

Example: Star Coupler

Star couplers**.osd**

The role of a star coupler is to combine the optical signals entering its multiple input ports and divide them equally amongst its output ports. The project "Star couplers**.osd**" (Fig. 22) shows a star coupler with 8 input ports, each port has a transmitter working at different wavelengths.

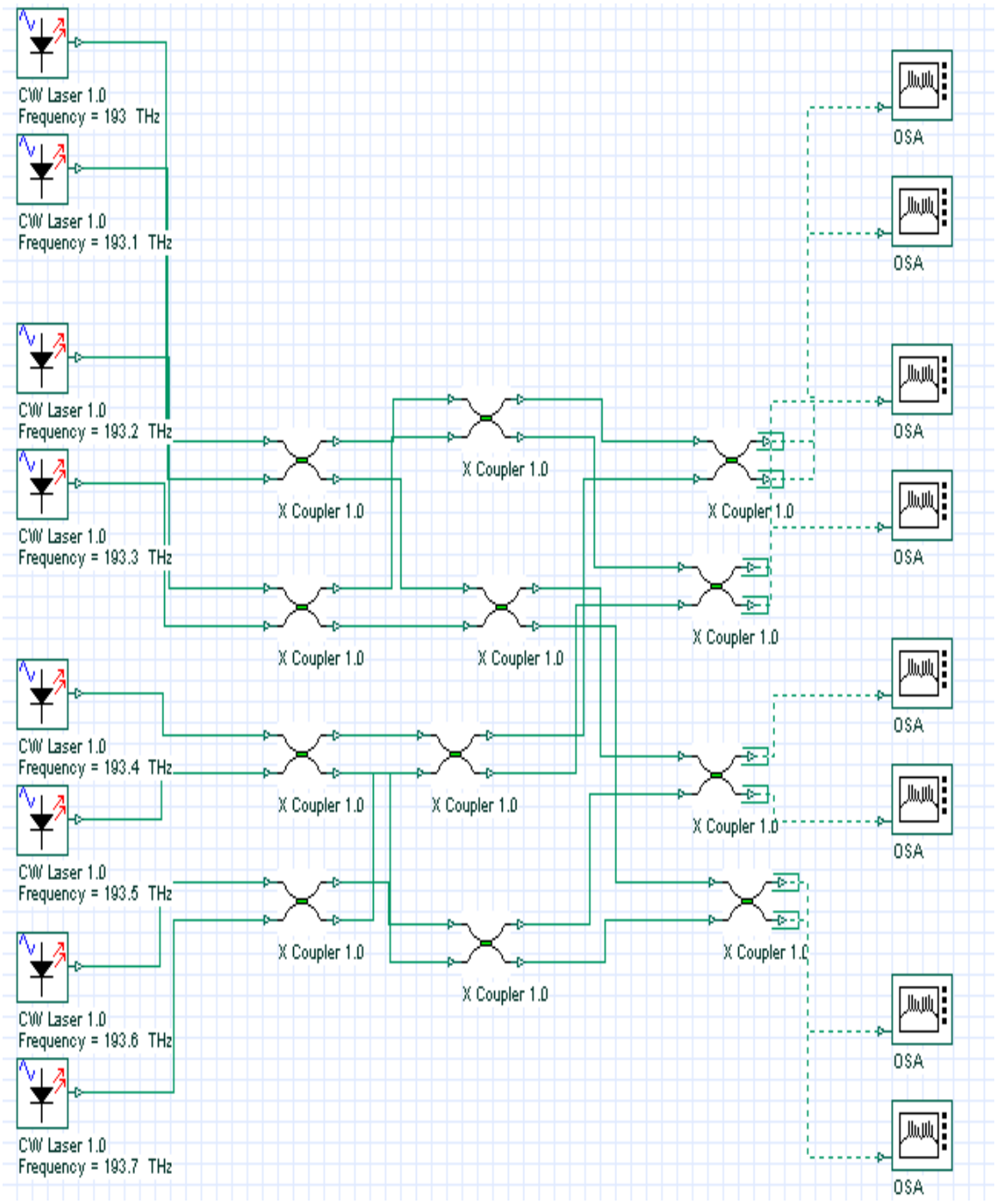

Fig.22: Layout: Star couplers

The output of the star coupler can be visualized by attaching an OSA at any of the output ports (Fig. 23).

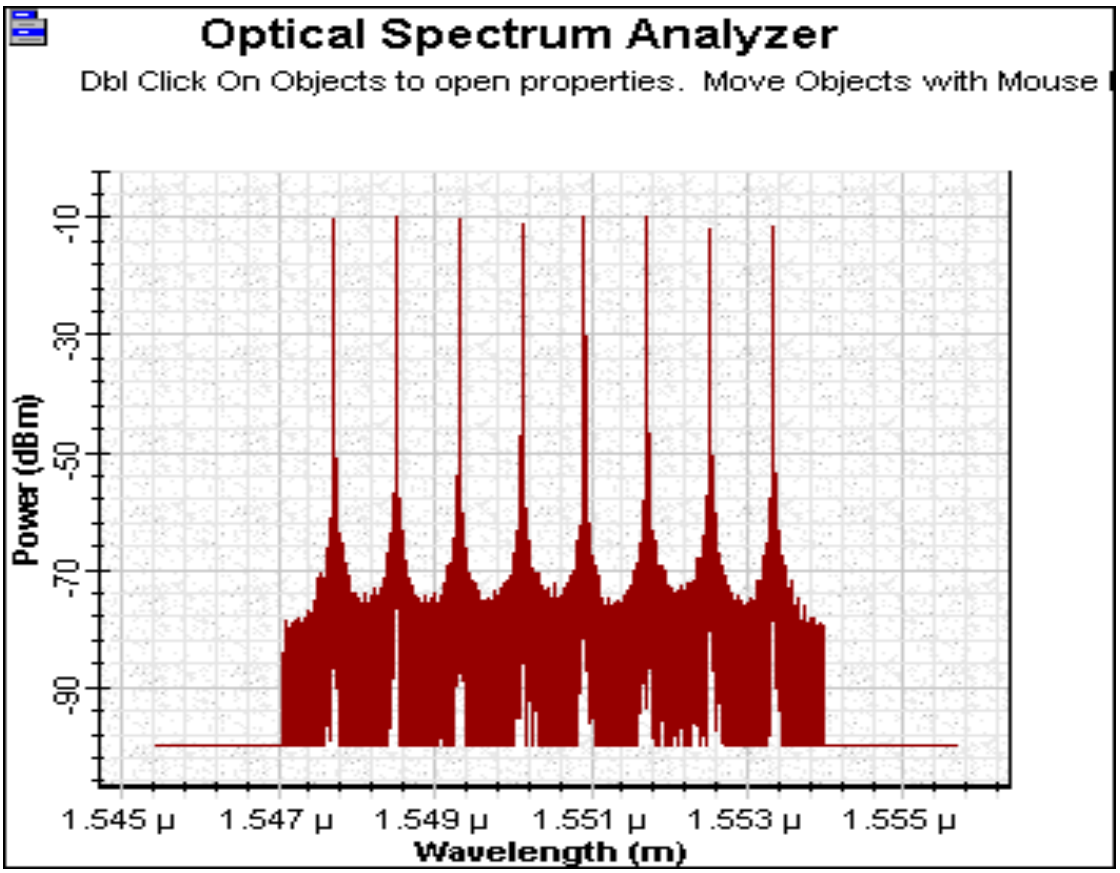

Fig.23: Output spectrum

Example: 8 by 8 Star Coupler

8 by 8 Star coupler**.osd**

Project file "8 by 8 Star coupler**.osd**" generates a basic 8x8 star coupler. This coupler is formed by using passive X- Coupler components. The function of this coupler can be seen by looking at the output spectrums. You can experiment with the project file by changing the powers and frequencies.

Example: Optical Cross-Connects

OXC project**.osd**

The development of wide-area WDM networks requires wavelength routing that can be reconfigure the network while maintaining its transparent nature. Project

"OXC project**.osd**" (Fig. 24) shows an optical cross connect with 2 input and 2 outputs, each port accommodates 4 wavelengths:

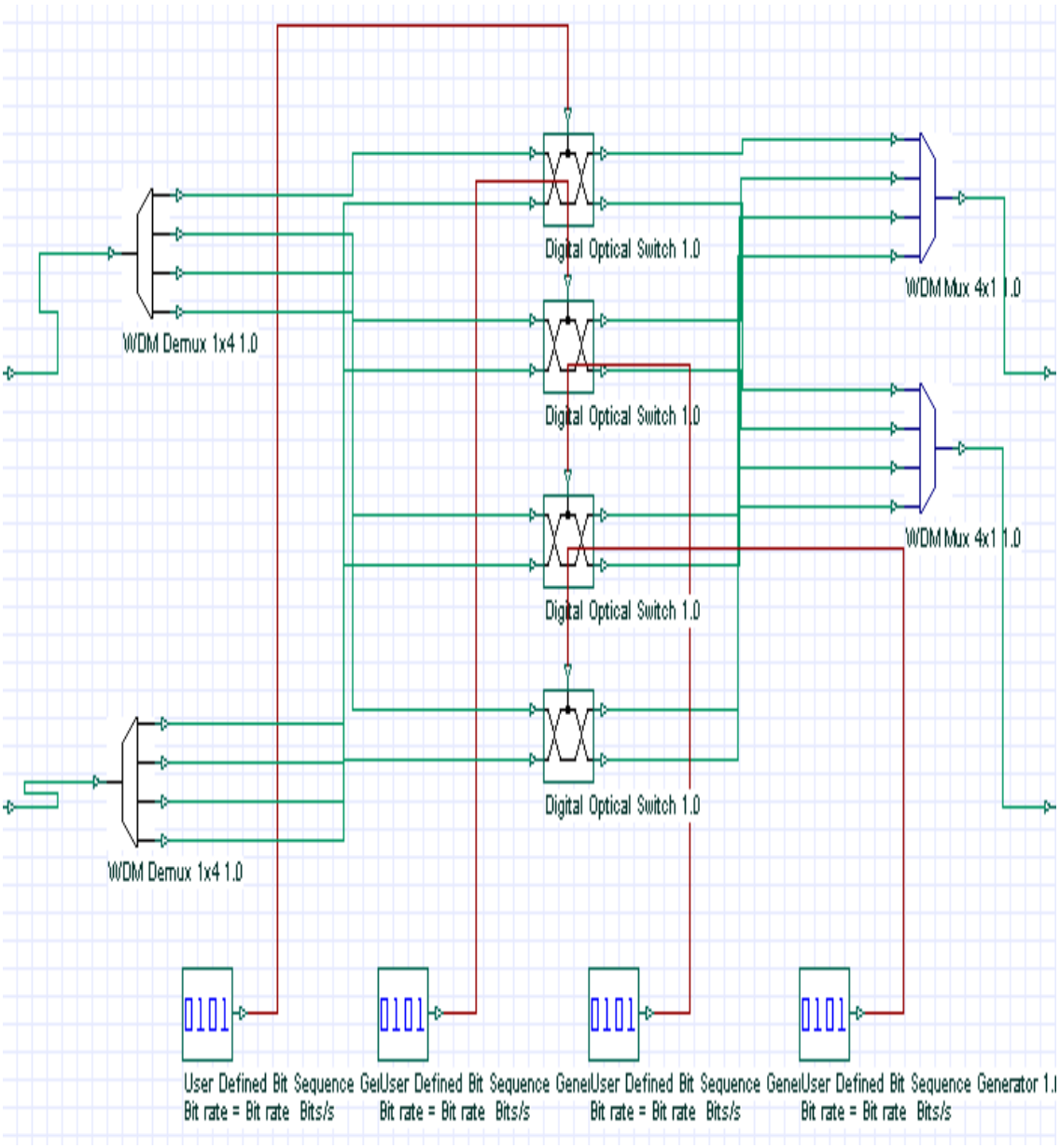

Fig.24: Layout: OXC project

Example: Wavelength Converters SLA and FWM

Wavelength converters SLA and FWM**.osd**

The aim of this project is to demonstrate the application of traveling wave SOA as wavelength converter using the four-wave mixing effect.

Four-wave mixing is a non-linear effect that takes place when two waves (signal and pump) at different wavelengths are injected into an SOA. A third optical field is generated at the device output, with frequency $\omega_c = 2\ \omega_p - \omega_s = \omega_p - \Omega$, where ω_p and ω_s are the frequencies of the pump and signal field respectively and $\Omega = \omega_s - \omega_p$ is detuning between signal and pump.

Several physical phenomena can generate FWM in SOA. When detuning is of the order of several GHz, the main mechanism is the carrier density pulsation induced by the signal-pump beating. The carrier density pulsation appears because of the stimulated emission. Our SOA component can handle just this mechanism of generation of FWM. For higher values of detuning, carrier pulsation is no more effective and FWM is created from the two fast intraband relaxation processes, i.e., spectral hole burning and carrier heating. As their characteristic times are of the order of hundreds of femtoseconds they become important for values of detuning larger than 1THz [2,3].

The main advantage of the frequency conversion based on FWM is independent of the modulation format and the bit rate. Additional advantage of this technique is the inversion of the signal spectrum and therefore the reversal of the frequency chirp. This property can be used to achieve dispersion compensation. The main disadvantage of the FWM converter is its low conversion efficiency [2,3].

To realize this idea, two CW signals are multiplexed and then launched into SOA as shown in **Fig. 25**.

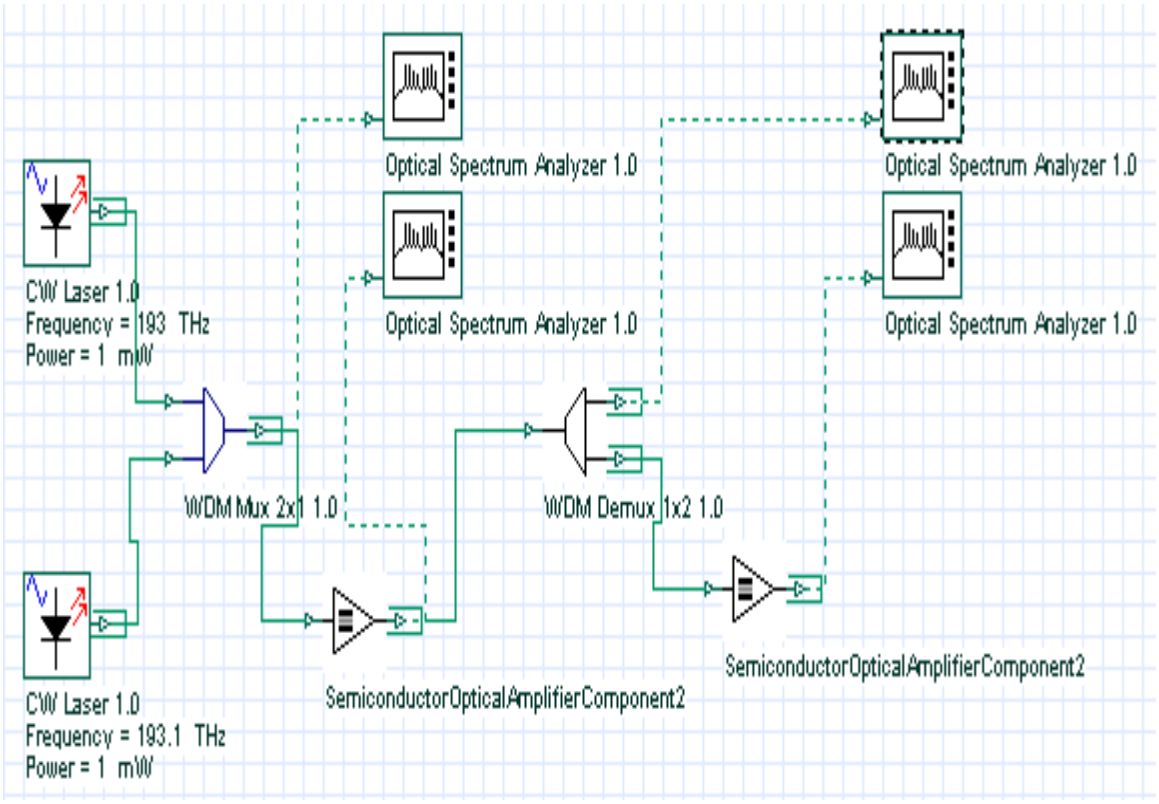

Fig.25: Layout: Wavelength converters SLA and FWM

In this project, we would like to demonstrate the principle of carrier density pulsation induced FWM in SOA. To demonstrate this two CW signals with carrier frequencies 193 and 193.1 THz and powers 1 mW (without linewidths, initial phases and polarizations) are multiplexed with the help of WDM Mux 2×1 and launched in SOA. The parameters of WDM Multiplexer and SOA are shown in **Table 1**, **Table 2**, and **Table 3**, respectively.

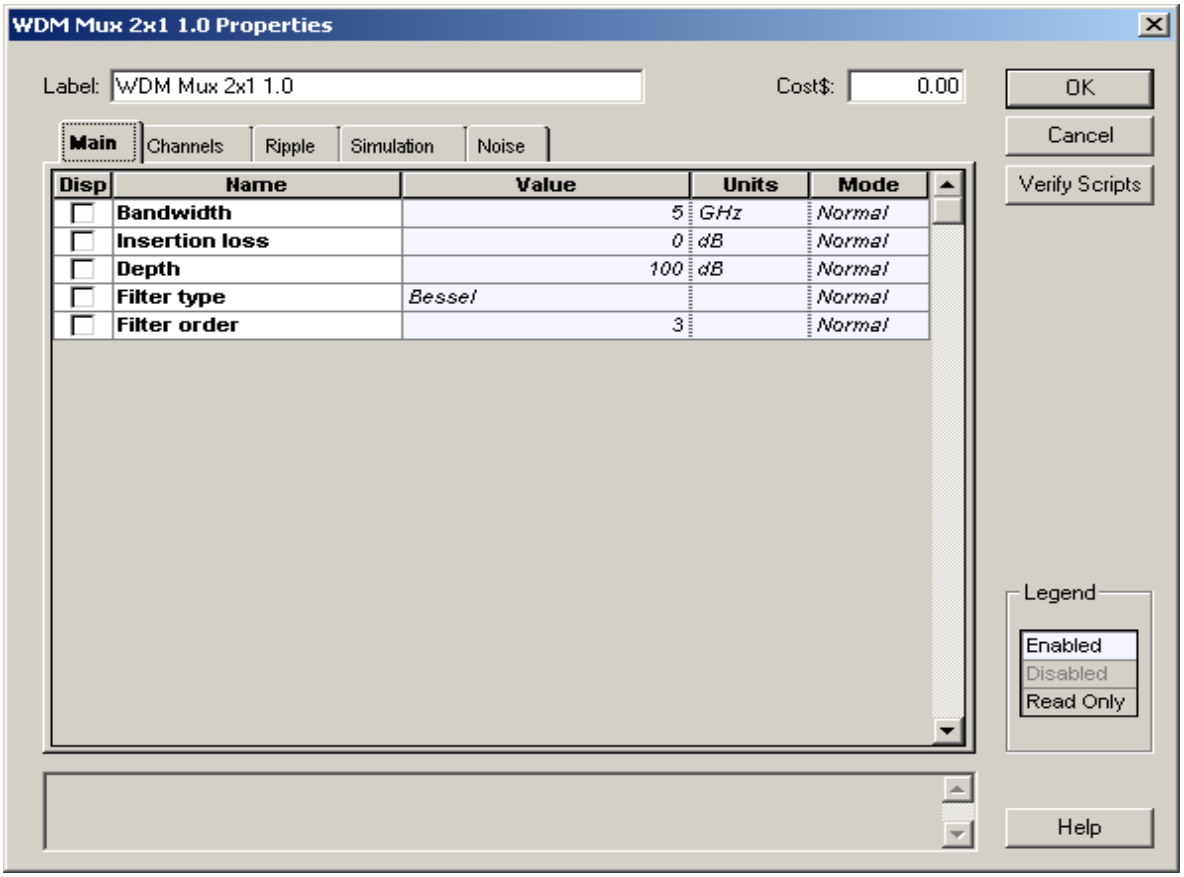

Table 1: WDM Multiplexer parameters (Main)

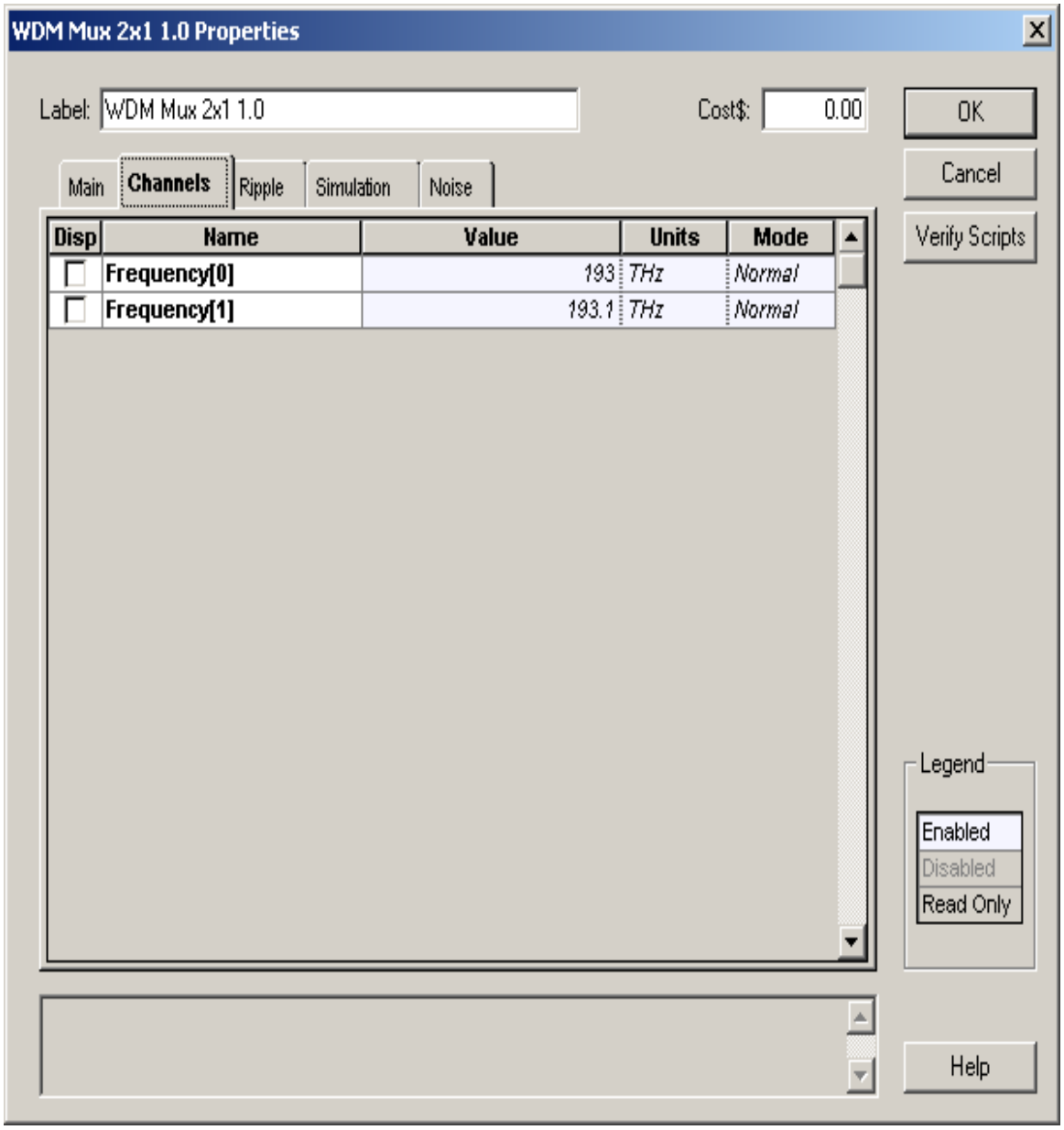

Table 2: WDM Multiplexer parameters (Channels)

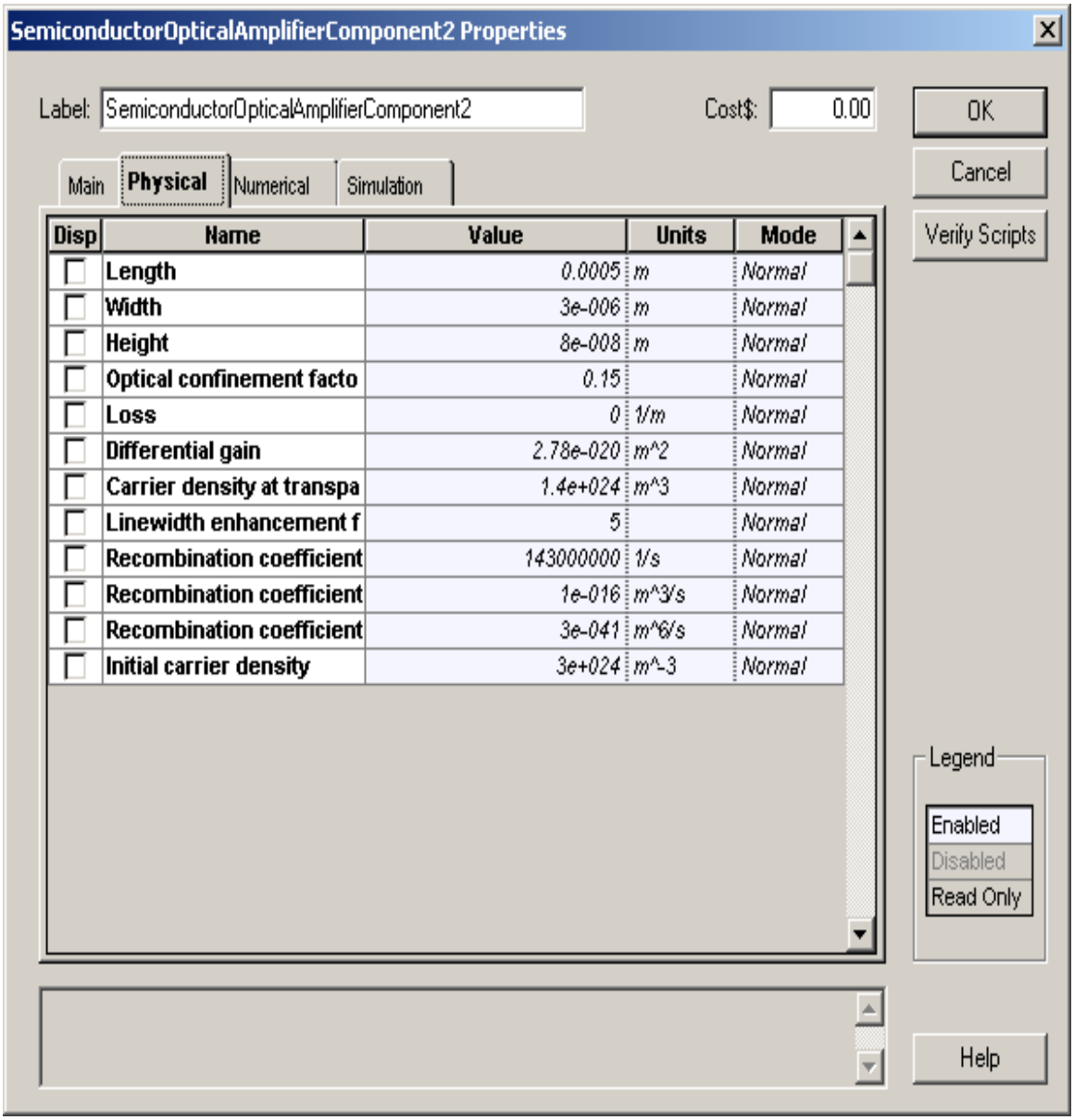

Table 3: SOA parameters (Physical)

The signal power after WDM Mux 2×1 is shown in Fig. 26.

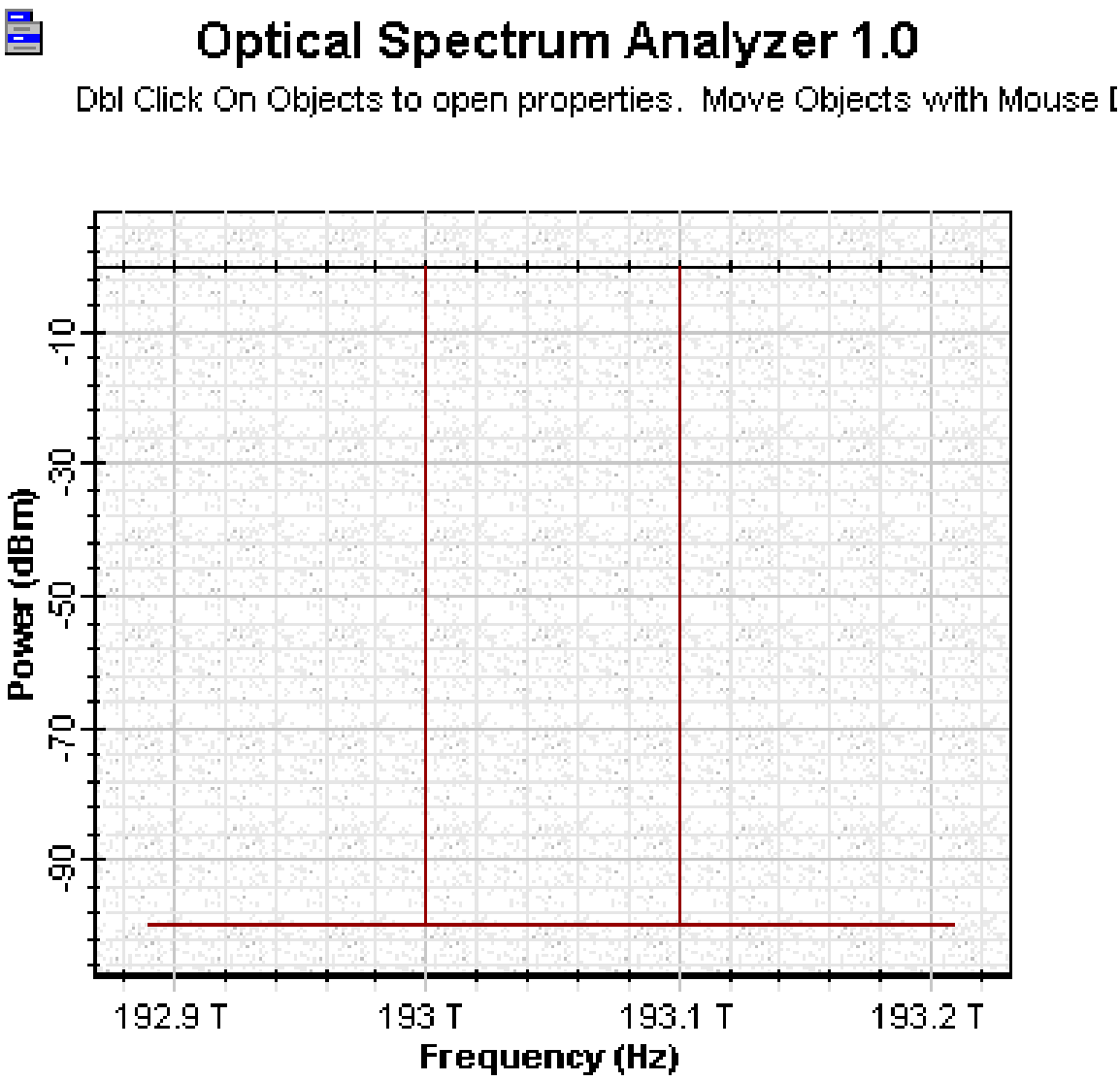

Fig.26: Signal power after WDM multiplexer

The signal power after first SOA is shown in the **Fig. 27**.

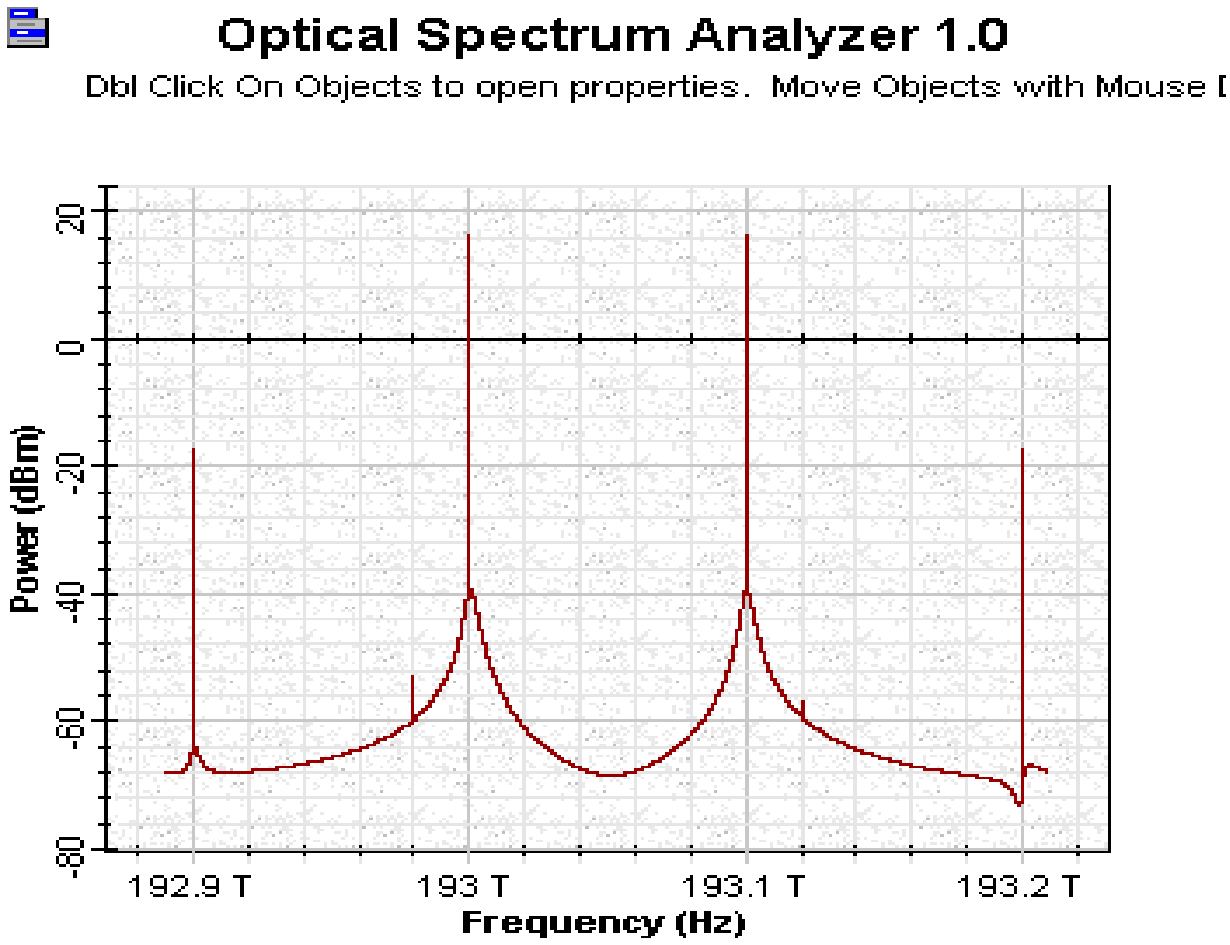

Fig.27: Signal power after first SOA

Fig. 27 shows the generated power from new FWM frequencies at 192.9 and 193.2 THz, respectively. With the following demultiplexer we separate the frequencies into 193.1 and 193.2 THz. To make this feasible, the channel parameters of the demultiplexer have been changed as shown in Table 4.

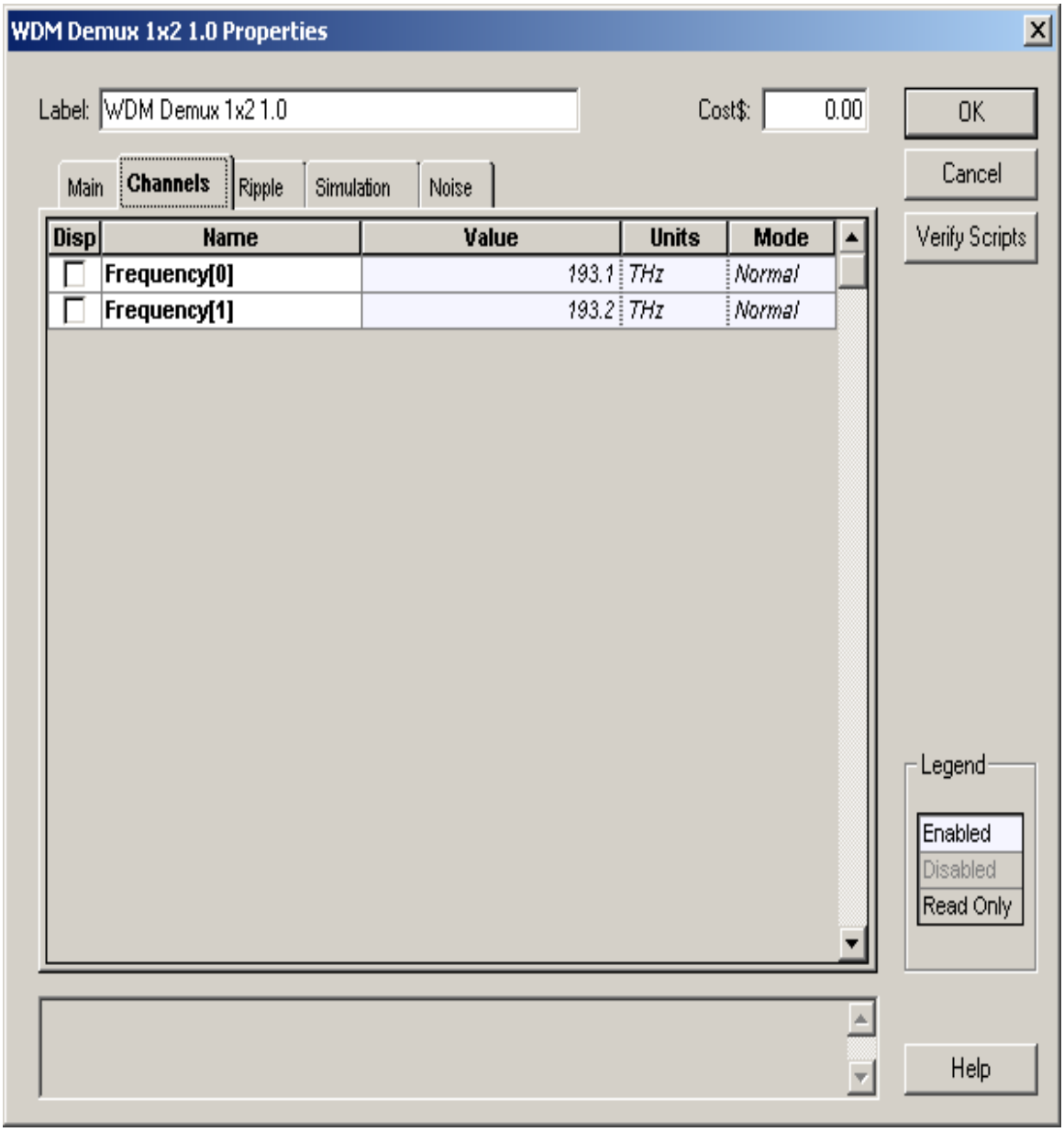

Table 4:WDM demultiplexer parameters (Channels)

The spectrum of the channel at 193.1 THz after Demux is shown in Fig. 28.

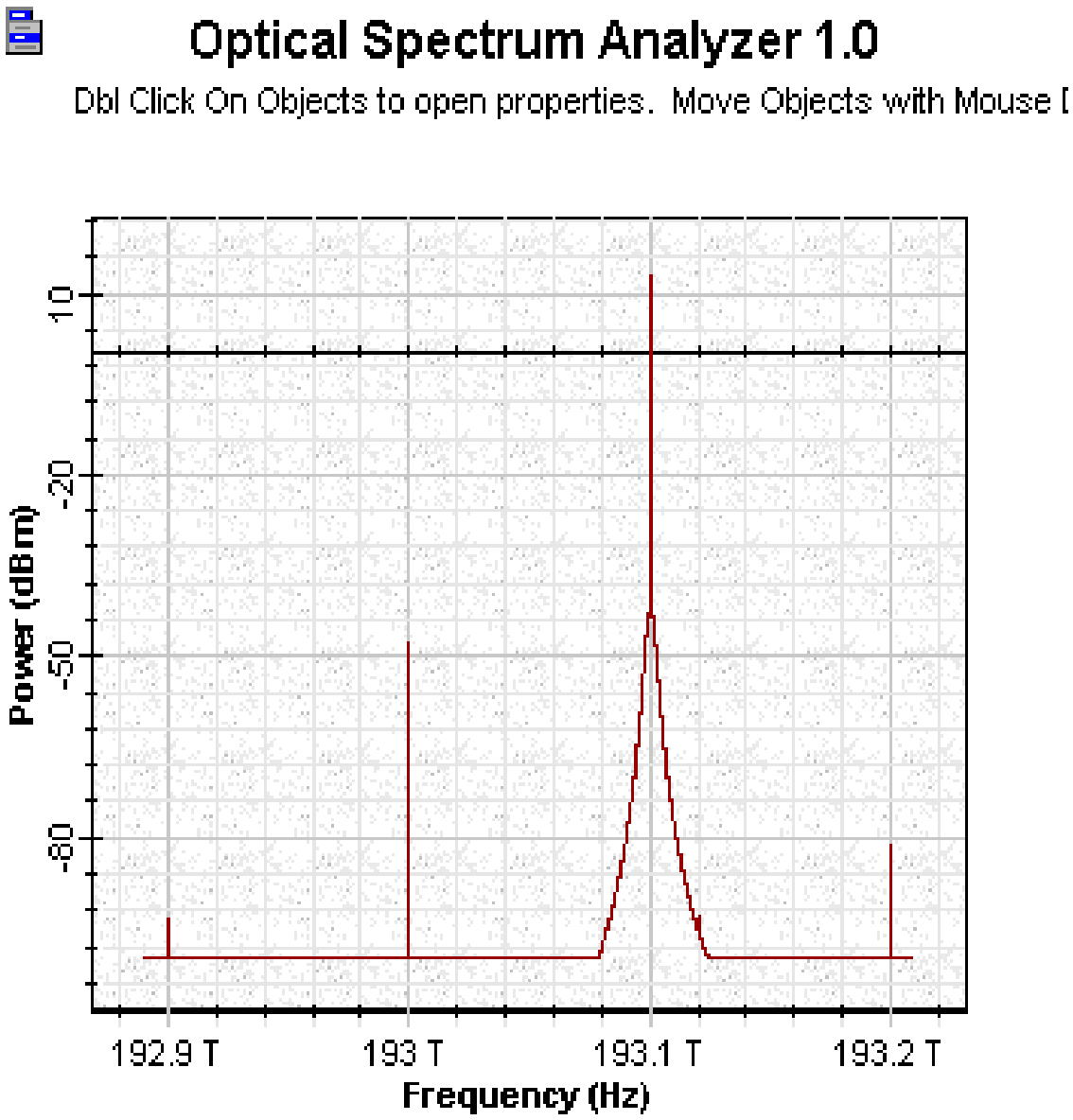

Fig.28: Channel spectra at 193.1 THz after demultiplexing

To obtain a better signal from the FWM at 193.2 THz after Demux we amplify this signal with the second SOA with the same properties as the first one. Resulting spectra are shown in Fig. 29.

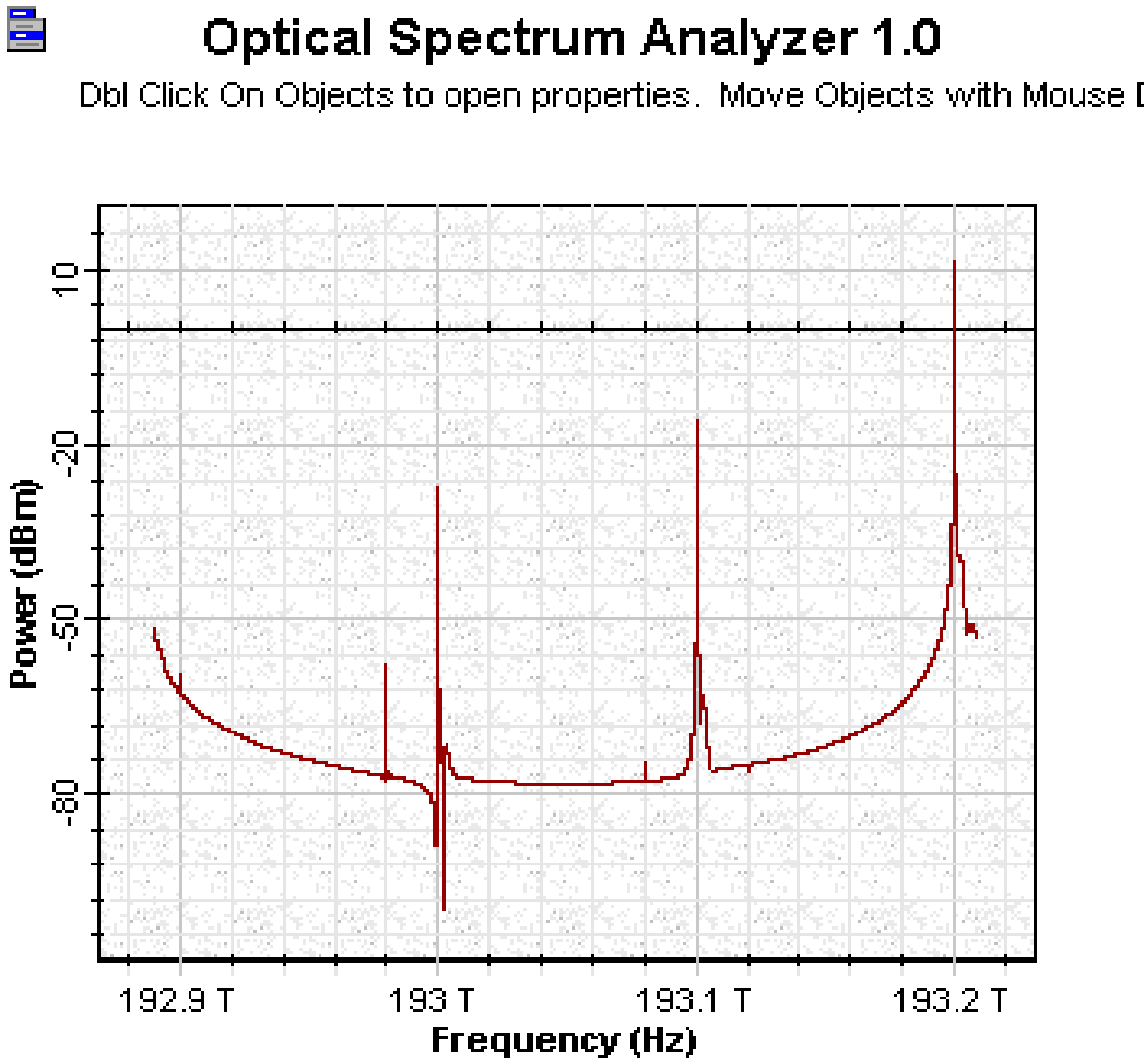

Fig.29: Signal from the FWM at 193.2 THz after demultiplexing

The second FWM signal at 193.2 THz with the power comparable with the initial CW signal at 193.1 THz is obtained.

References:

1. Terji Durhuus, Benny Mikkelsen, Carsten Joergensen, Soergen Danielsen, Kristian Stunkjaer, “All- optical wavelength conversion by semiconductor optical amplifier”, J. Lightwave Technology, vol.14, pp.942-954,1996.
2. G.P. Agrawal, “Fiber Optic Communication Systems”, second edition , John Wiley @ Sons, Inc., 1997.
3. R.Sabella and P.Ludgi, “High speed optical communications”, Kluwer Academic Publishers, 1999.

Example: Wavelength Converters SLA and XGM

Wavelength converters SLA and XGM**.osd**

The aim of this project is to demonstrate the application of traveling wave SOA as wavelength converter using cross-gain saturation effect.

The principle use of the cross-gain modulation in SOA is to modulate the gain of an intensity-modulated input signal via gain saturation effect. With this phenomenon, a continuous wave signal at the desired output wavelength is modulated by the gain variation. After the SOA, the continuous wave signal carries the same information as the intensity modulated signal. The input signal and the CW signal can be launched either co-directionally or counter-directionally into the SOA. We consider a co-propagation here.

To realize this idea the intensity-modulated input signal and a CW signal are multiplexed and then launched into SOA as shown in Fig. 30.

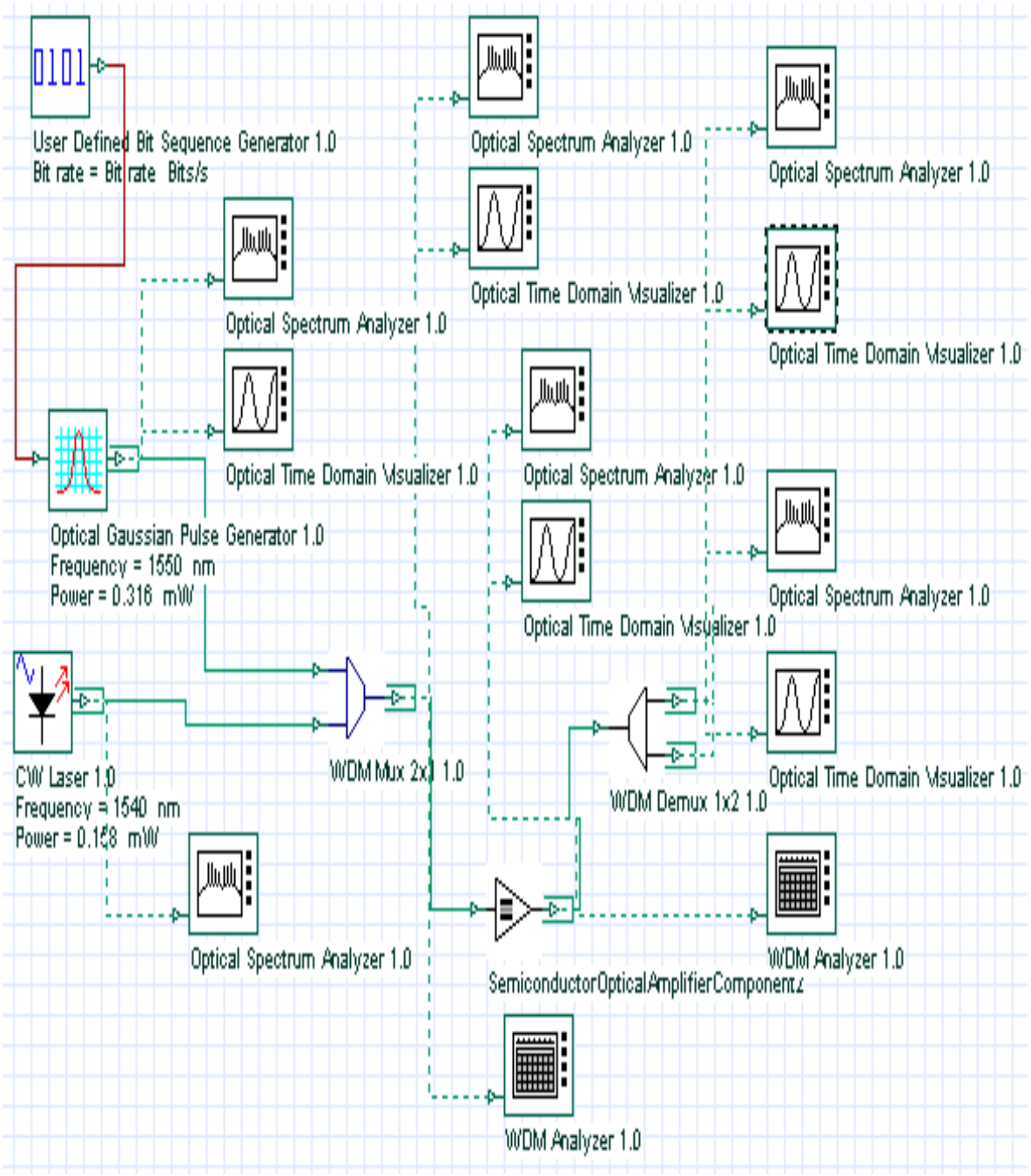

Fig.30: Layout: Wavelength converters SLA and XGM

We demonstrate the conversion at 10 Gb/s. The corresponding simulation parameters are given in **Table 5**.

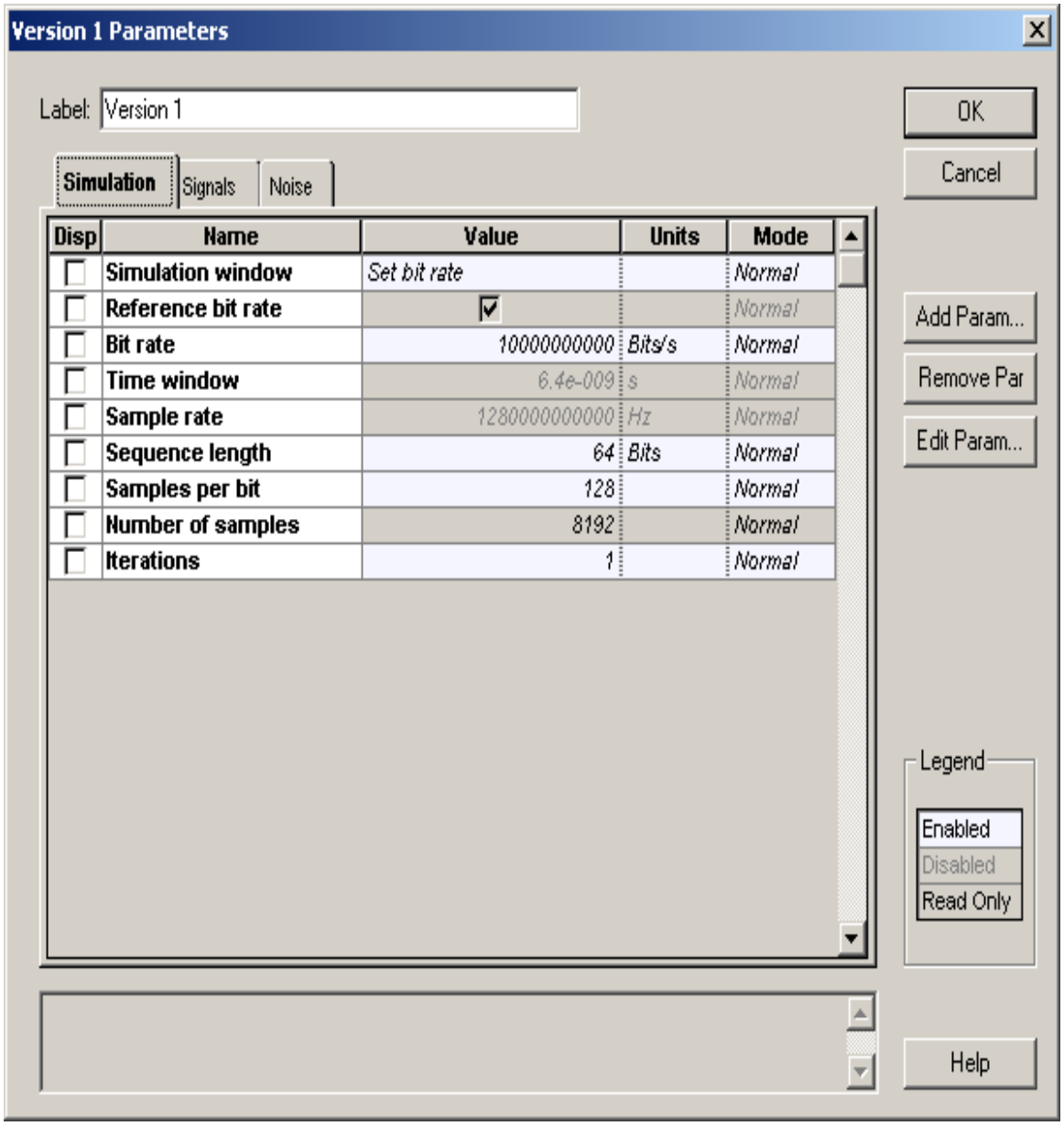

Table 5:Simulation parameters

The intensity-modulated input signal and a CW signal have carrier wavelengths 1550 and 1540 nm (or frequency separation from 1.25 GHz) and powers 0.316 mW and 0.158 mW (without linewidths, initial phases, and polarizations), respectively. The signals are multiplexed with the help of WDM Mux 2×1 and launched in SOA. The parameters of the optical Gaussian pulse generator are shown in **Table 6**.

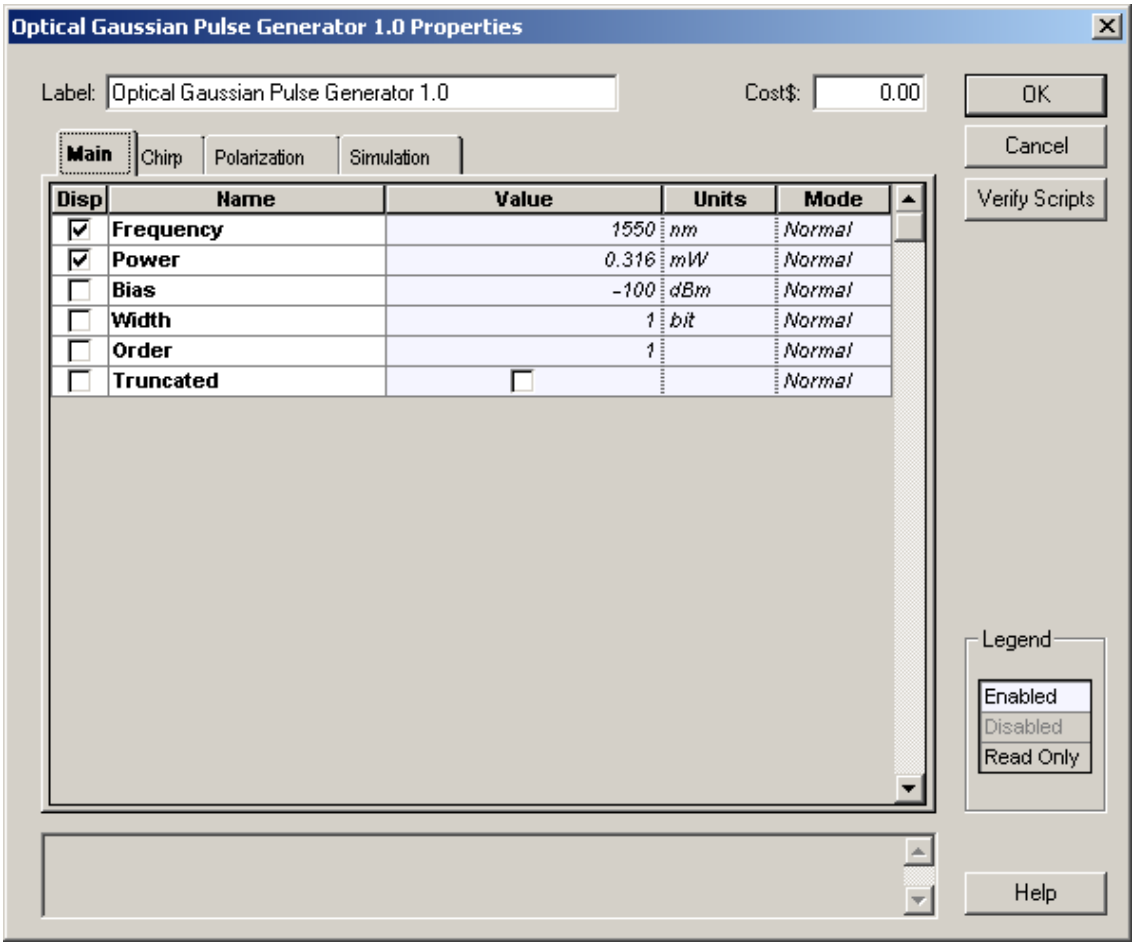

Table 6:Optical Gaussian pulse generator parameters (Main)

The shape and spectra of the intensity modulated signal have been shown in Fig. 31 and Fig. 32, respectively.

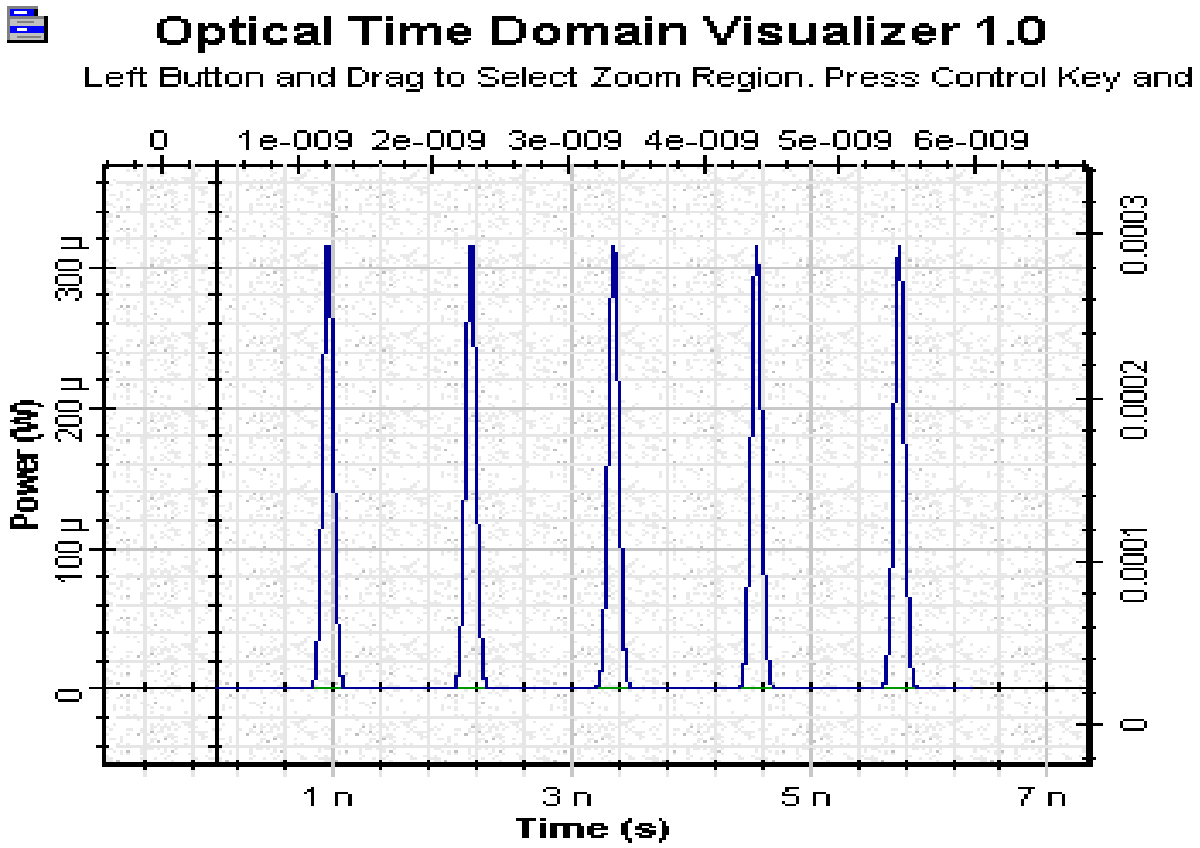

Fig. 31: Shape of the intensity modulated signal

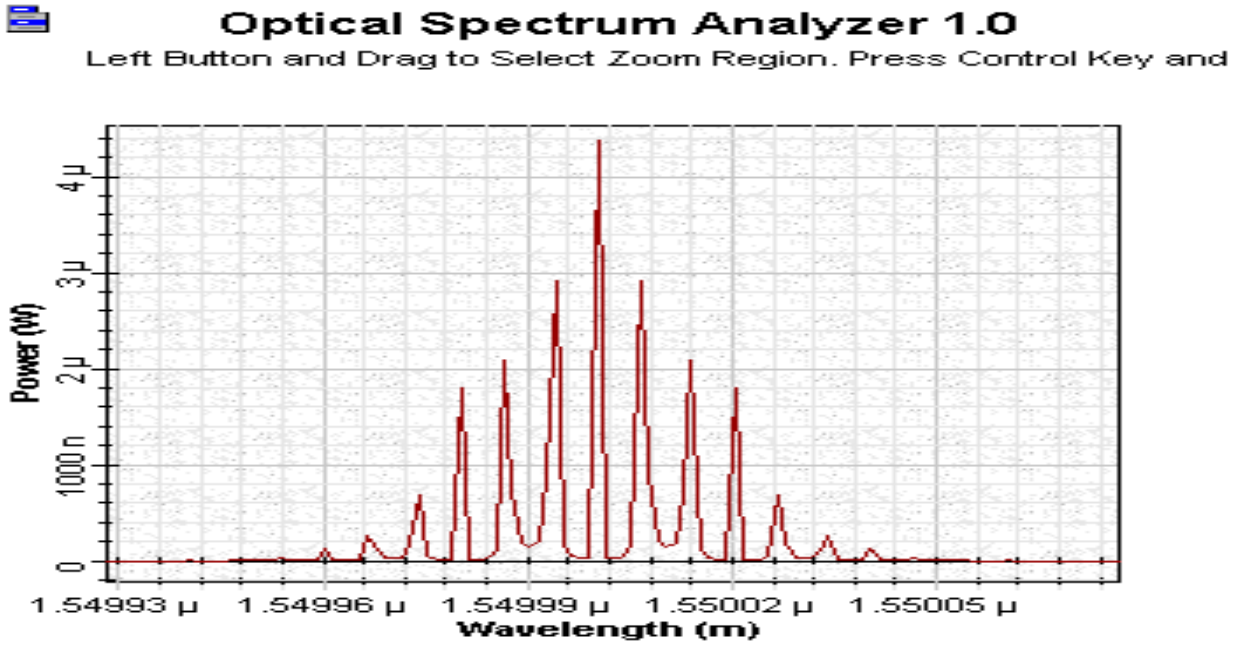

Fig. 32: Spectrum of the intensity modulated signal

The multiplexer parameters (Main and Channels) are shown in Table 7 and Table 8, respectively.

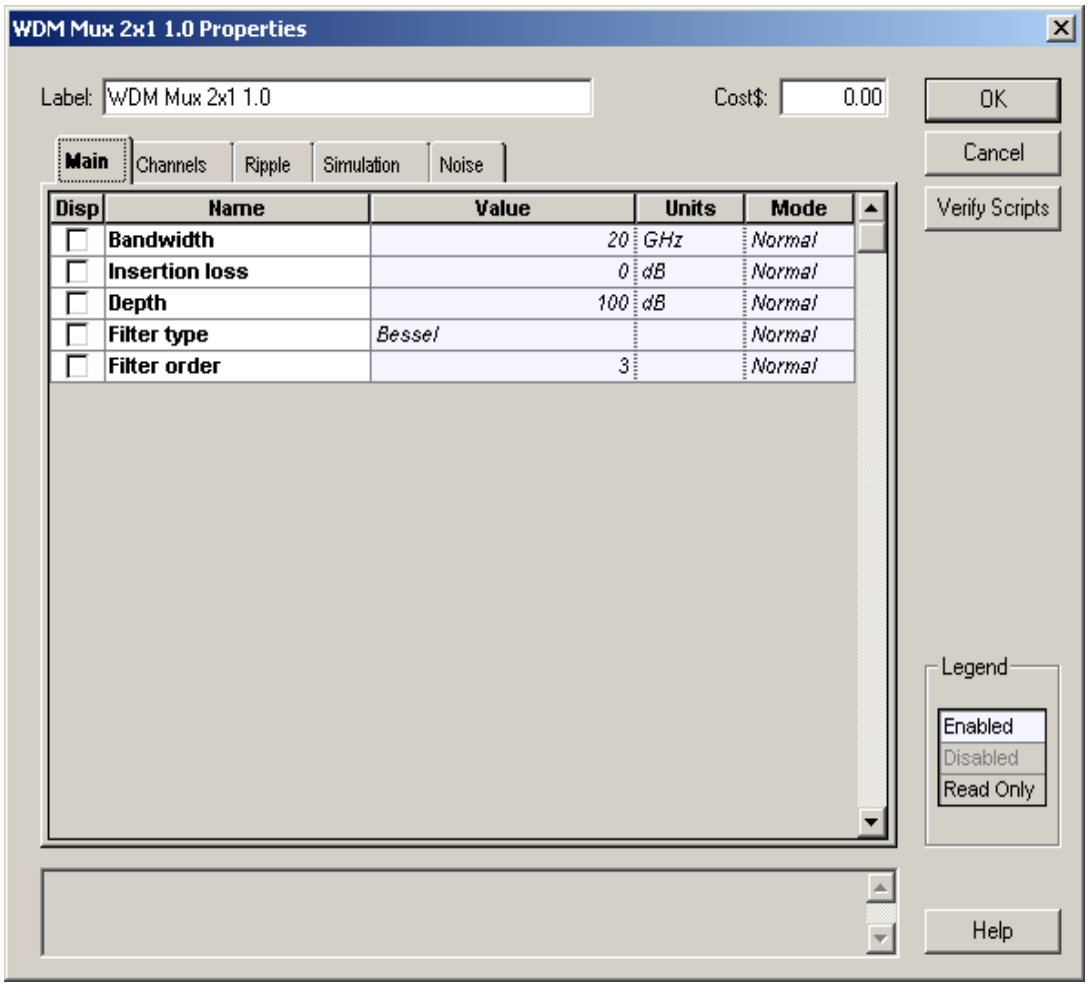

Table 7:WDM multiplexer parameters (Main)

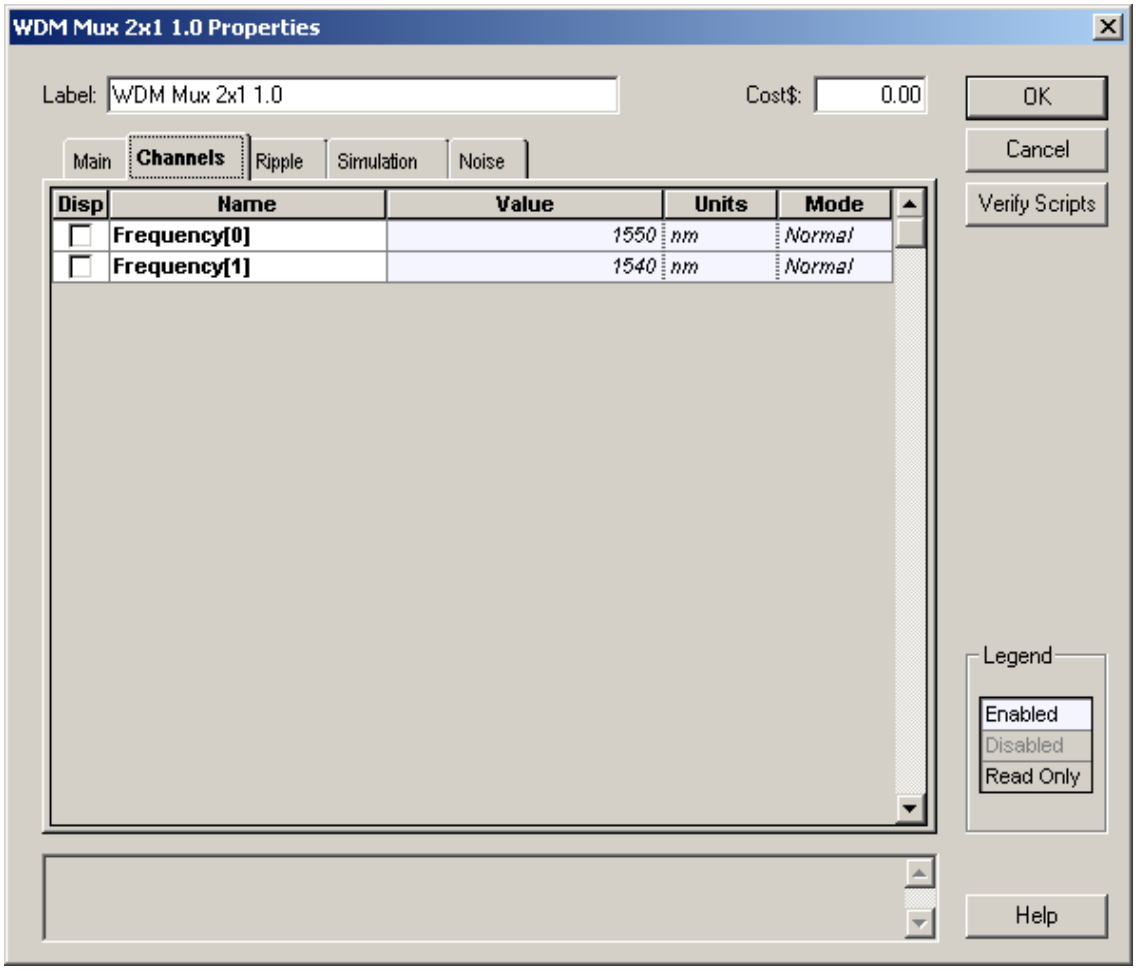

Table 8:WDM multiplexer parameters (Channels)

Fig. 33 shows the shape of the signal after multiplexing.

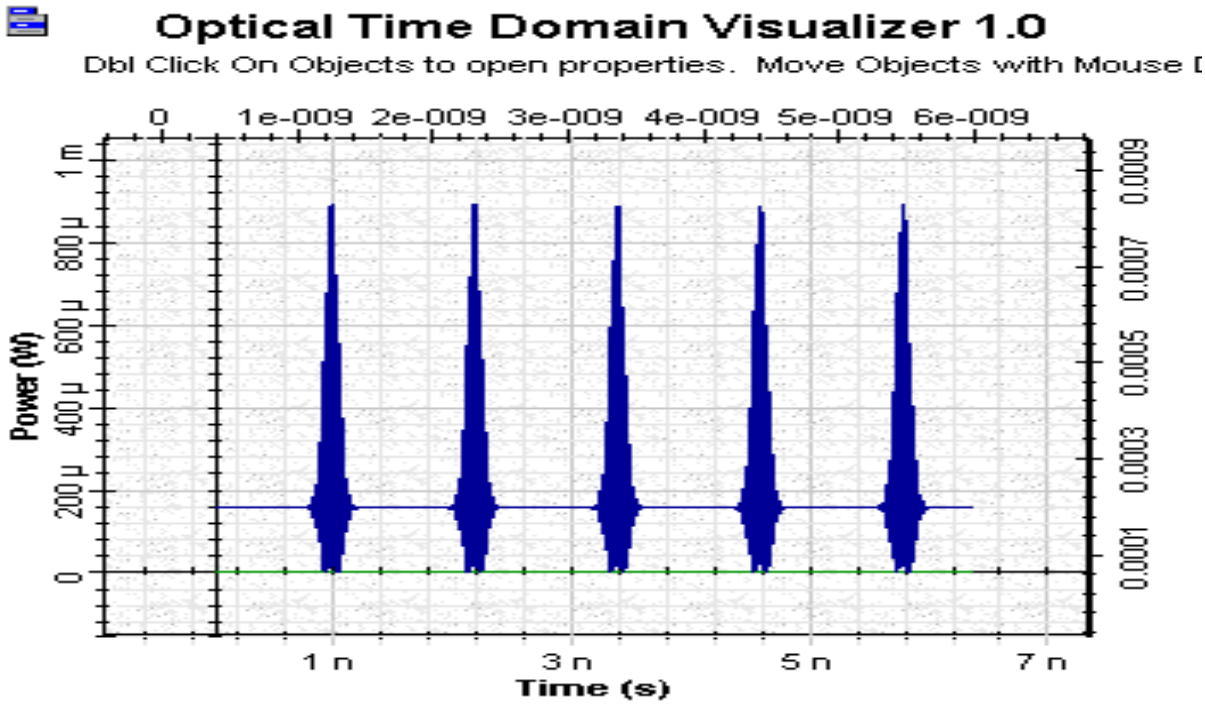

Fig. 33: Shape of the signal after multiplexing

SOA parameters (Main and Physical) are shown in Table 9 and Table 10, respectively.

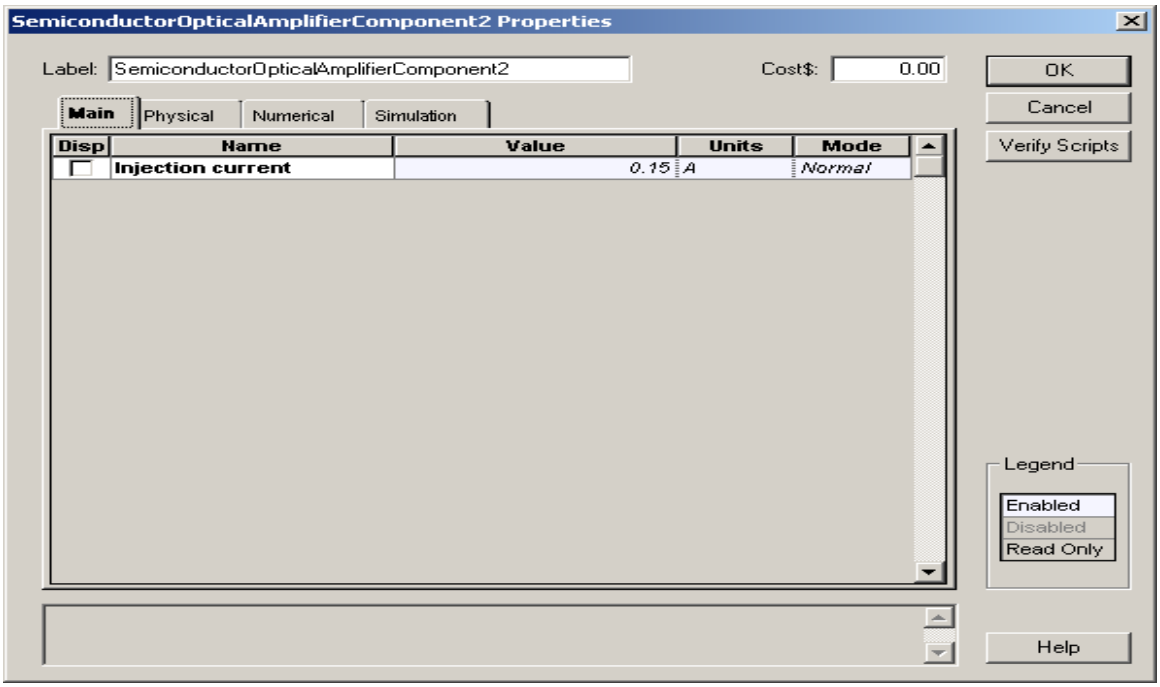

Table 9: SOA parameters (Main)

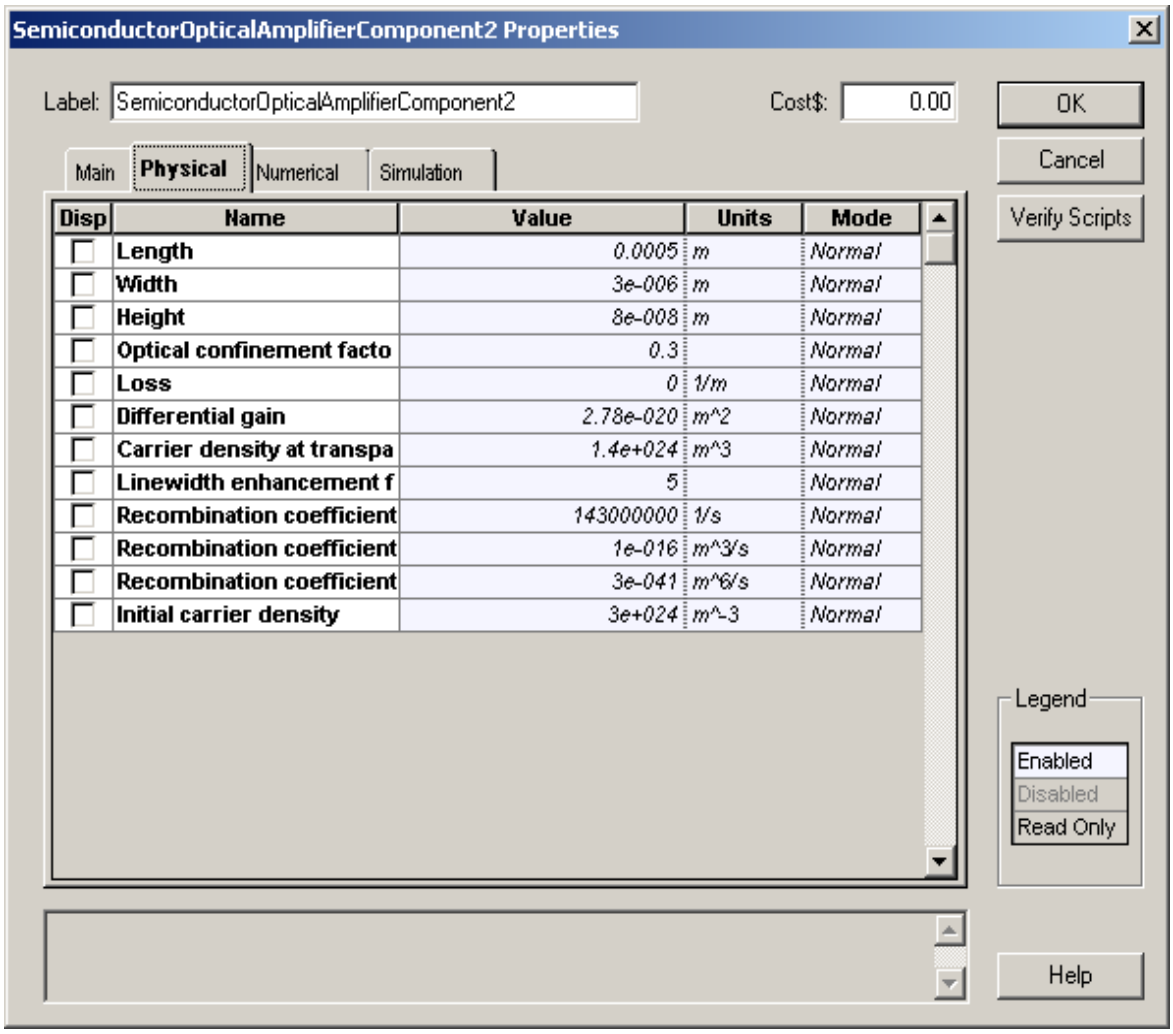

Table 10: SOA parameters (Physical)

These parameters of the amplifier gives unsaturated single pass gain G_0 ~ 29 dB. Fig. 34 shows the amplified signal.

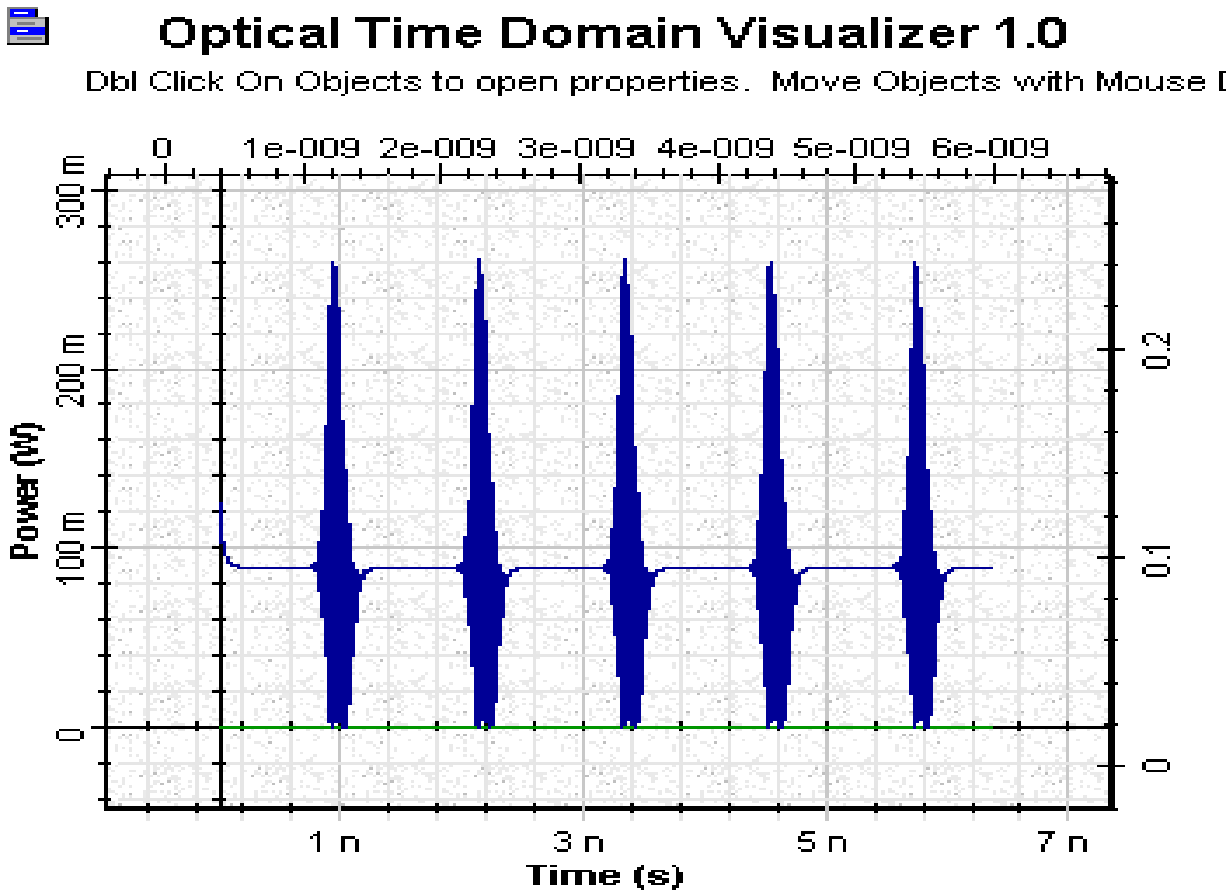

Fig.34: Amplified signal

The amplified signal passed through demultiplexer, which has similar properties of the multiplexer. Figs. 35 and 36 show the signal shape and spectrum at λ =1550 nm after the demultiplexer.

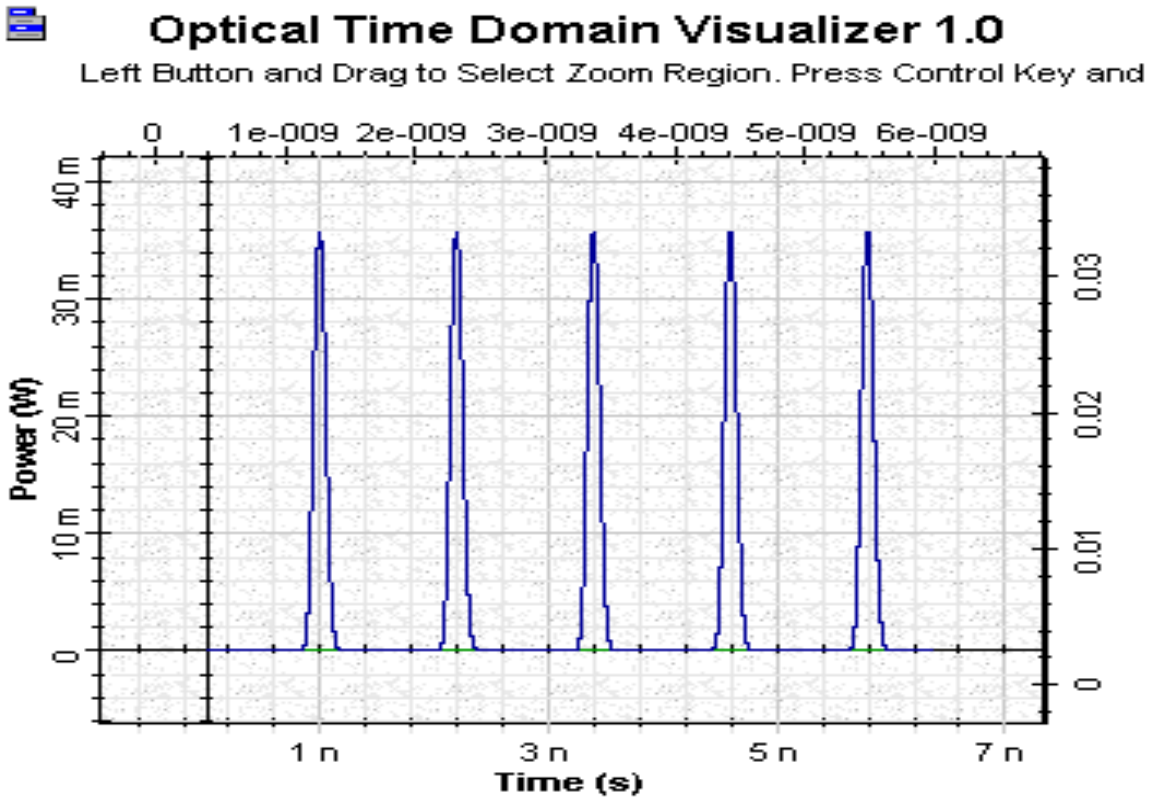

Fig.35: Shape of the signal at λ =1550 nm

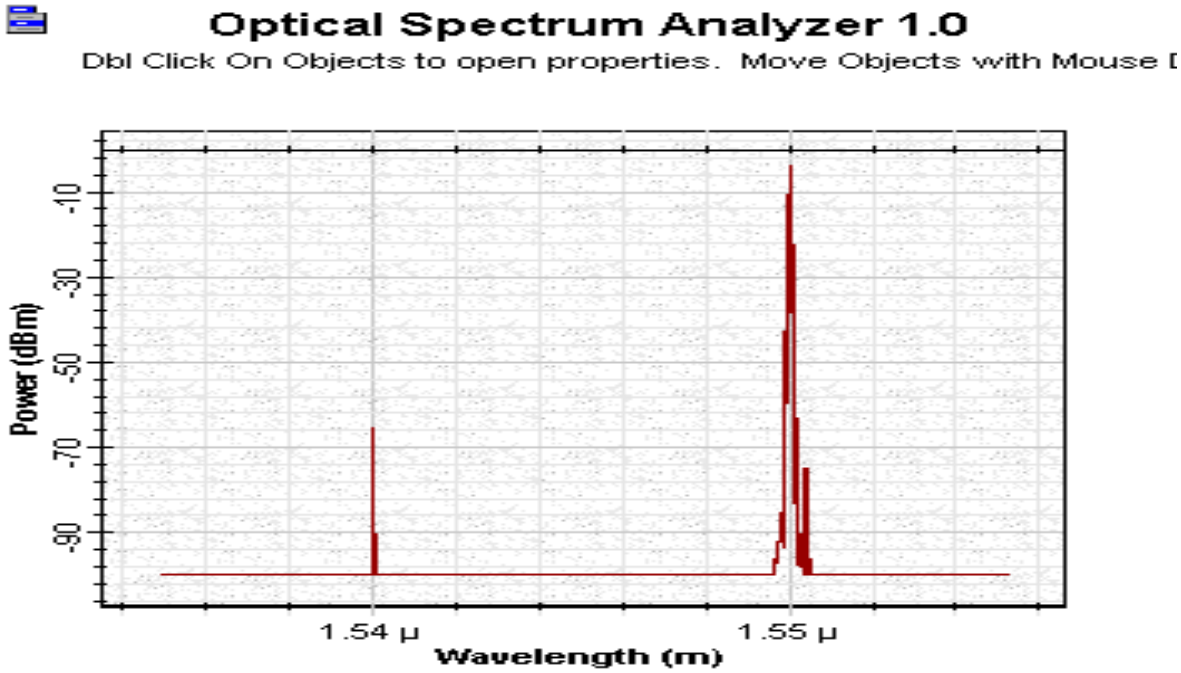

Fig.36: Spectum of the signal at λ =1550 nm

Figs. 37 and 38 show the shape and spectra of signal at λ =1540 nm after demultiplexing.

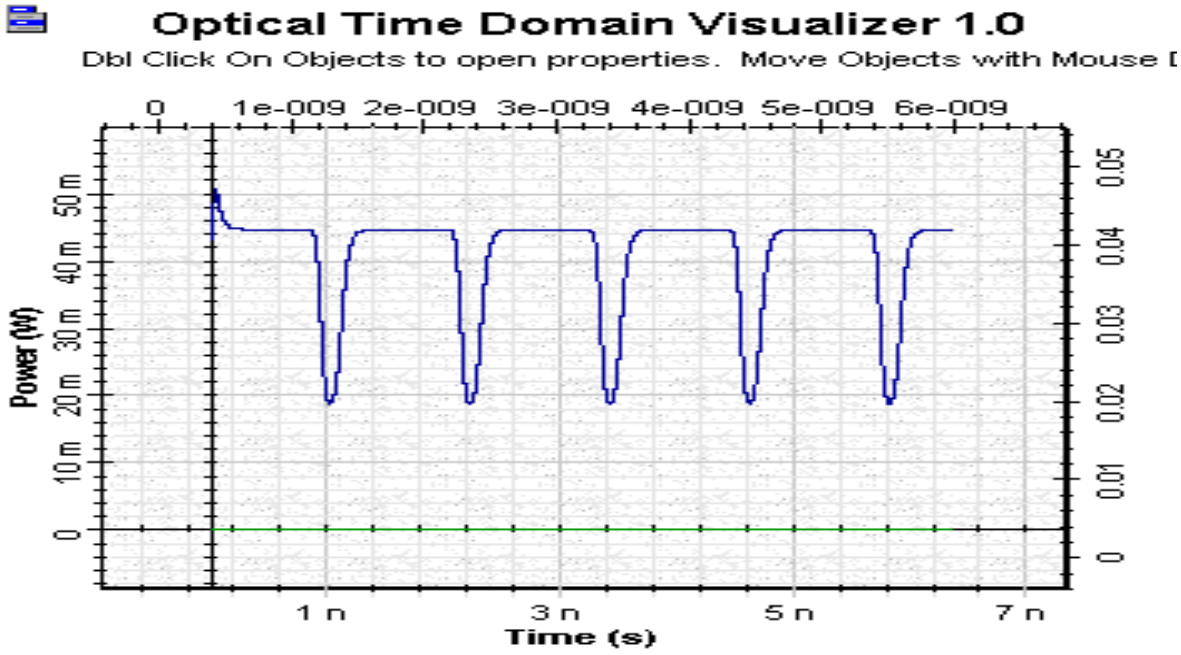

Fig. 37: Shape of the signal at λ =1540 nm

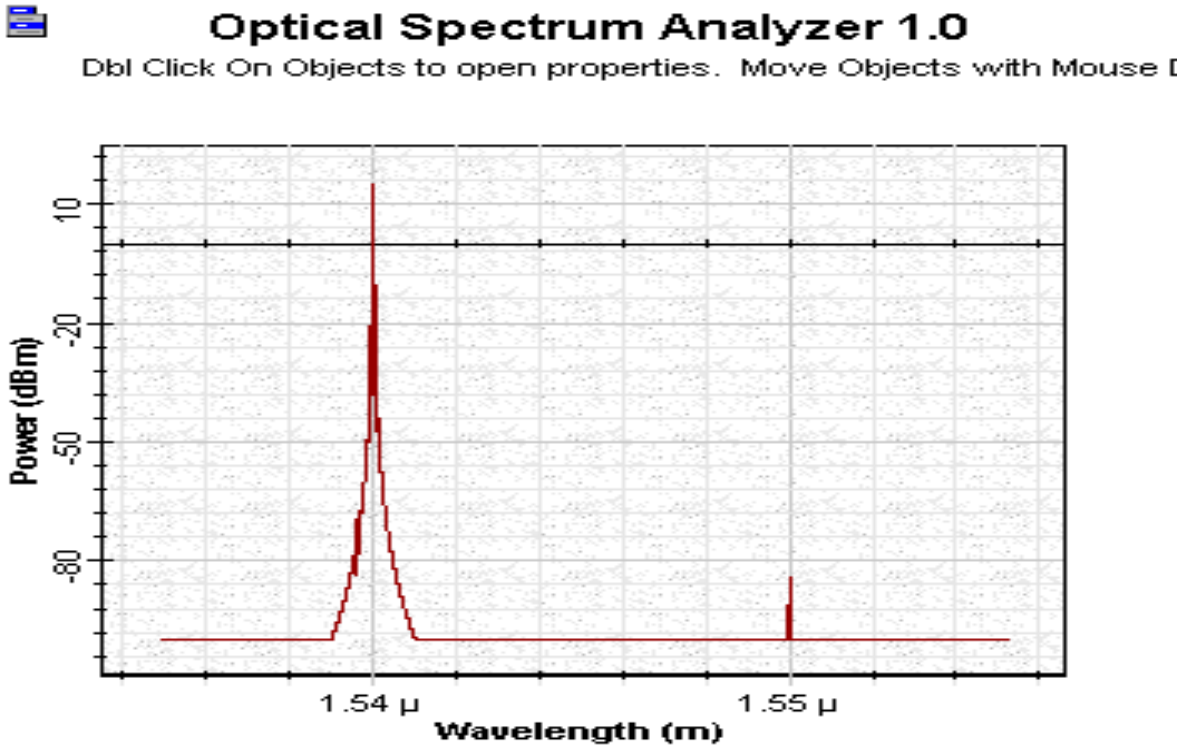

Fig. 38: Shape of the signal at λ =1540 nm

The inversion of the signal can be clearly seen.

References:

1. Terji Durhuus, Benny Mikkelsen, Carsten Joergensen, Soergen Danielsen, Kristian Stunkjaer, “All- optical wavelength conversion by semiconductor optical amplifier”, J. Lightwave Technology, vol.14, pp.942-954,1996.
2. G.P. Agrawal, “Fiber Optic Communication Systems”, second edition , John Wiley @ Sons, Inc., 1997.
3. R.Sabella and P.Ludgi, “High speed optical communications”, Kluwer Academic Publishers, 1999.

Example: Channel Multiplexing

OTDM multiplexer**.osd**

In optical time-division multiplexing (OTDM) systems, several optical signals modulated at the bit rate *B* using the same carrier frequency, are multiplexed optically to form a composite optical signal at a bit rate *NB*, where *N* is the number of multiplexed optical channels. This has been shown in the project “OTDM multiplexer.osd” (Fig. 39)**.**

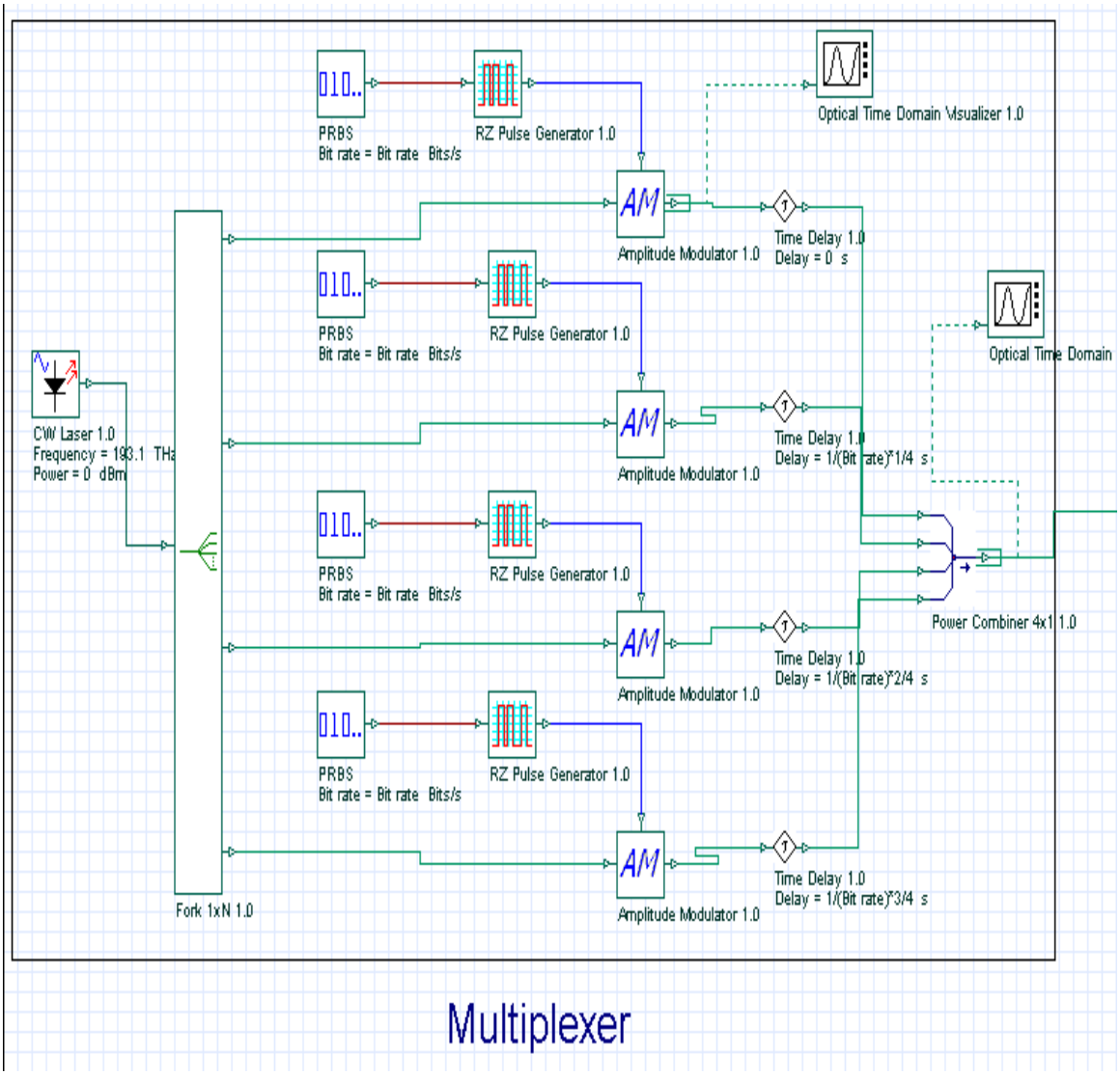

Fig. 39: Layout: OTDM multiplexer

Each modulator generates short pulses with 10 Gb/s bit rate, the pulse 3 dB pulse width is 0.05 bit period (Fig. 40).

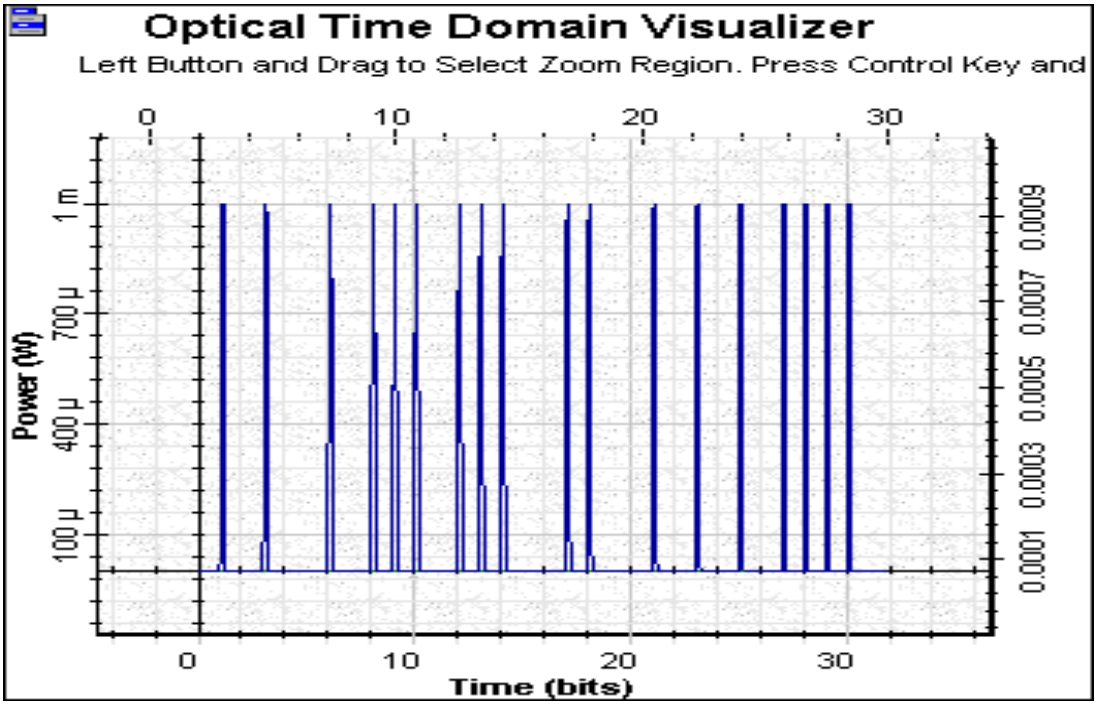

Fig. 40: Pulses after modulator

The signals are combined in order to generate a 40 Gb/s bit rate at the multiplexer output (Fig. 41).

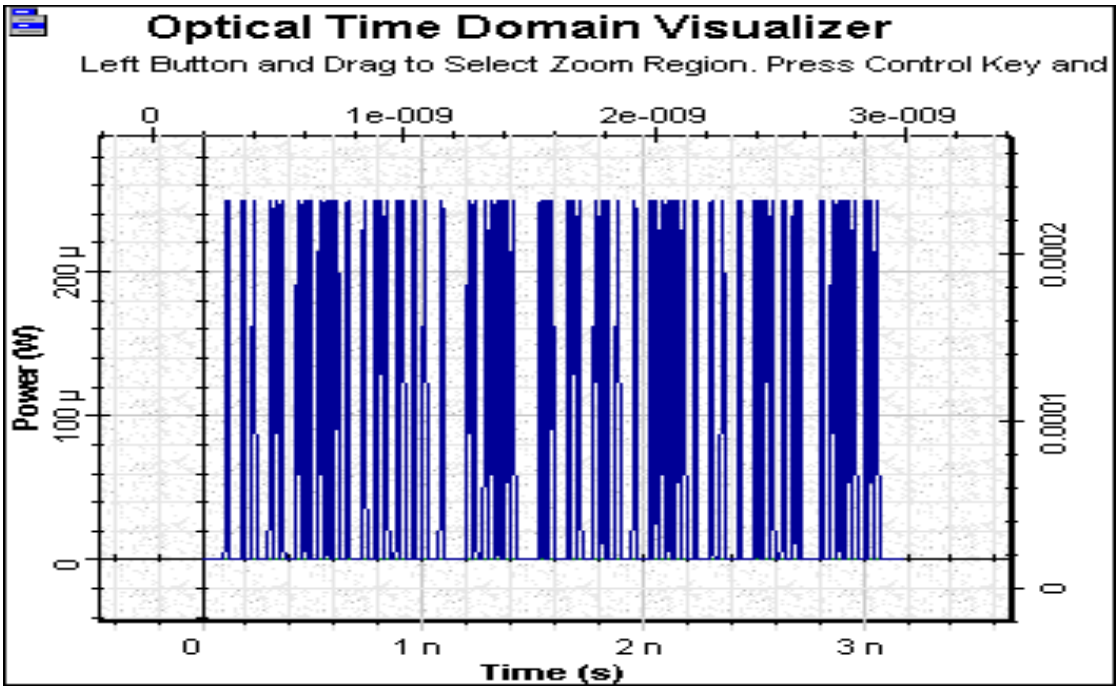

Fig. 41: Pulses after multiplexer

The demultiplexer stage uses a modulator working at 10 Gb/s clock. In this example the output signal is the first channel (Fig.42).

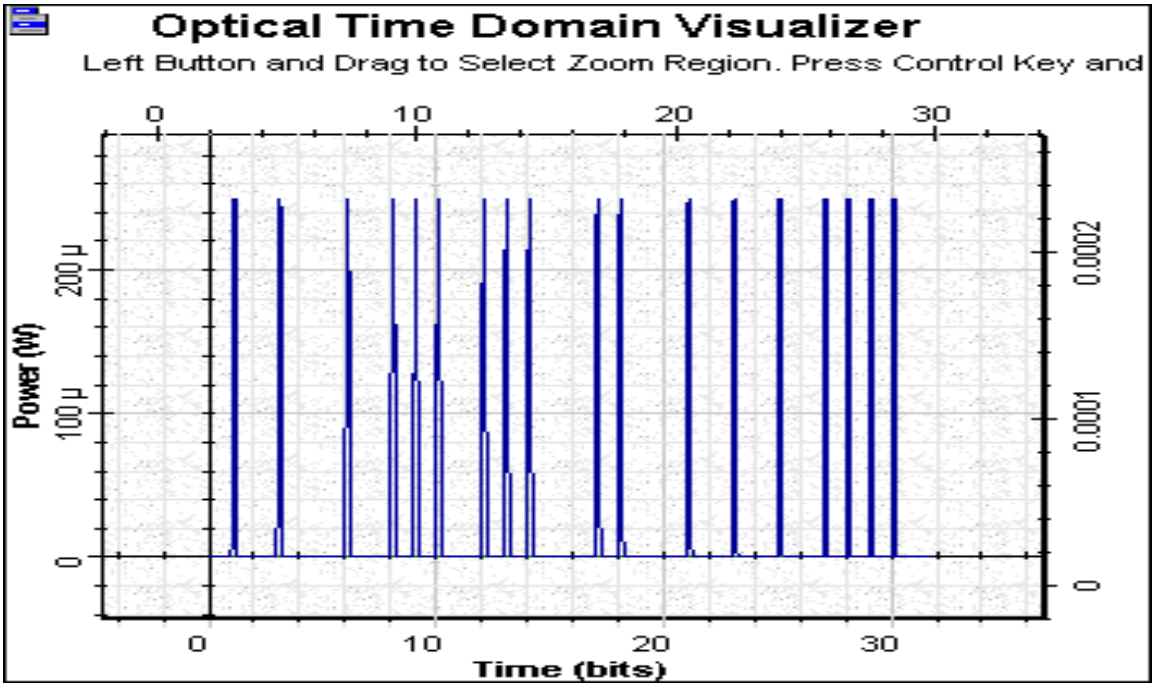

Fig.42: Pulse after demultiplexer

Example: Channel Demultiplexing

DeMUX by FWM**.osd**

Project file "DeMUX by FWM**.osd"** generates a demultiplexing scheme that makes use of FWM in nonlinear fiber. In this configuration, the optical TDM signal at 1550 *nm* is launched together with the clock signal at a different frequency of 1552 *nm* into fiber. The clock signal acts as a pump for the FWM process. A new pulse train is generated at a third frequency, $2\times1552-1550=1554\ nm$, that is an exact replica of the channel that needs to be demultiplexed. An optical band-pass filter centered at 1554 nm is used to separate the demultiplexed channel from the optical TDM and clock signal. In the given example, the second channel is demultiplexed. How could you demultiplex the first channel? Try yourself.

Example: Linear Crosstalk

Interchannel crosstalk at ADM in a ring network.**osd**

Project file "Interchannel crosstalk at ADM in a ring network**.osd**" generates the effect of linear interchannel crosstalk in a ring network to system performance. The ring network in this example contains four nodes. One can see the crosstalk effect by looking at the eye diagram in OSA. Crosstalk is originated from the filters in ADMs.

Inter-channel cross-talk can arise from a variety of sources. One example to this is an optical filter or ADM that selects one channel (drop) and passes others over the network. Another example is an optical switch, switching different wavelengths where cross-talk arises owing to imperfect isolation between the switch ports. Other cross-talk types can be mentioned such as amplifier induced, router induces, XPM induced etc. [1]. A particular signal can accumulate cross-talk from different elements and channels over the network. Cross-talk can be reduced by using several techniques such as wavelength dilation and filter cascading. In this example, we will investigate the effect of inter-channel cross-talk at ADM to a ring network. The project is given in Interchannel crosstalk at ADM in a ring network**.osd.** This network contains 4 nodes and these nodes communicate over two channels at 193 THz and 193.1 THz as shown in **(Fig. 43)**. We have considered the bit rate of 10 Gb/s. ADMs at each node is modeled by using WDM add and WDM drop components. WDM add and drop components are created by using 4^{th} order Bessel filters. The ring is ended with a ring control component that can circulate the signals around ring for a given number of times. The distance between the nodes is 12.5 km and we inserted an ideal amplifier just before node 2 to compensate the fiber loss.

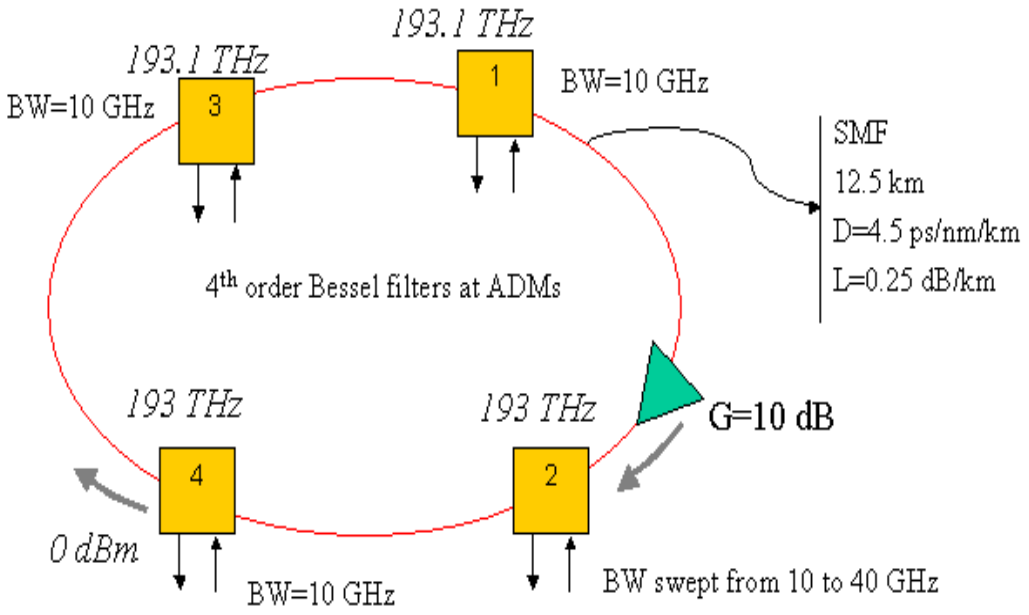

Figure 43: A basic ring network with 4 nodes

To show the effect of inter-channel cross-talk, we have swept the bandwidth of the filters in ADM of node 2 from 10 to 40 GHz. The eye diagrams and power spectrums at node 2 for several bandwidths are given in Fig. 44. Fig. 45 shows the cross--talk [1-3] verses filter bandwidth. Of course this type of characteristic of the ADM at node 2 will also affect the received signals at other nodes and other channel performances. For example, Fig. 46 shows the eye diagram at node 1 which communicates on channel 1 at 193.1 THz.

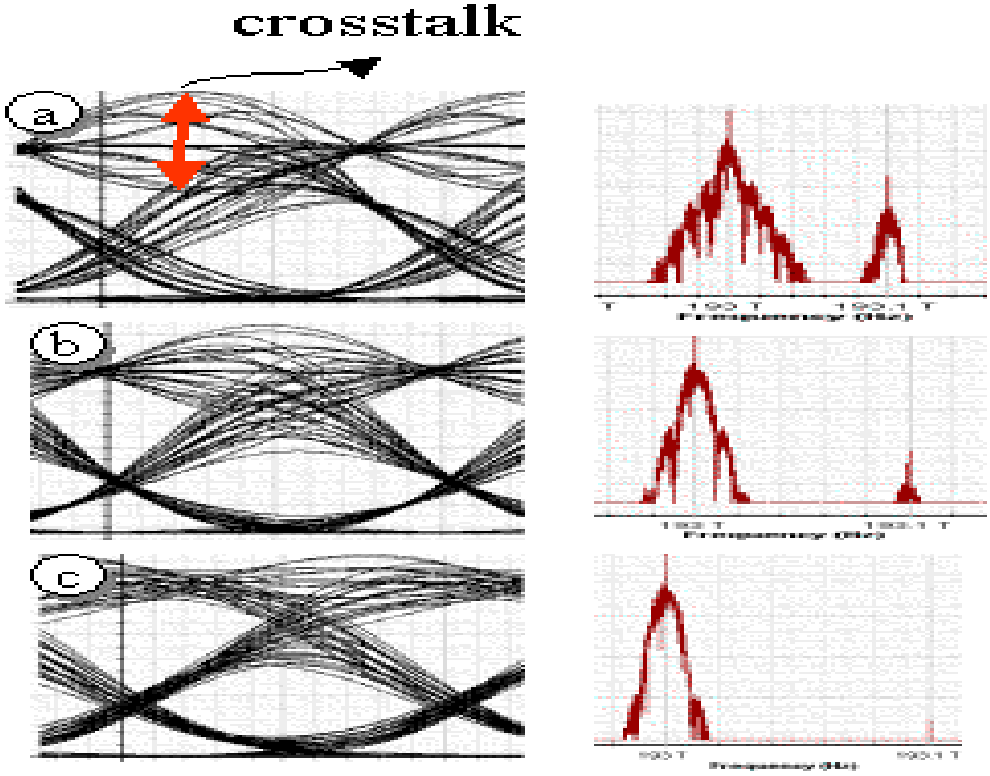

Figure 44: Eye diagrams and power spectrums at node 2 when bandwidth of the filters in ADM of node 2 is a) 40 GHz, b) 17.5 GHz, and c) 10 GHz.

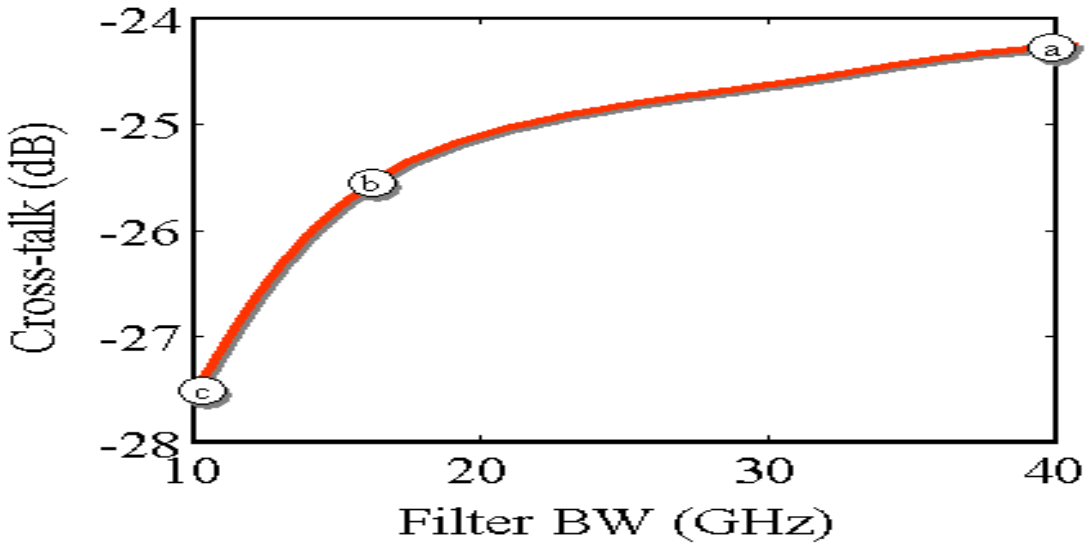

Figure 45: Cross-talk as a function of filter bandwidth of the ADM at node 2

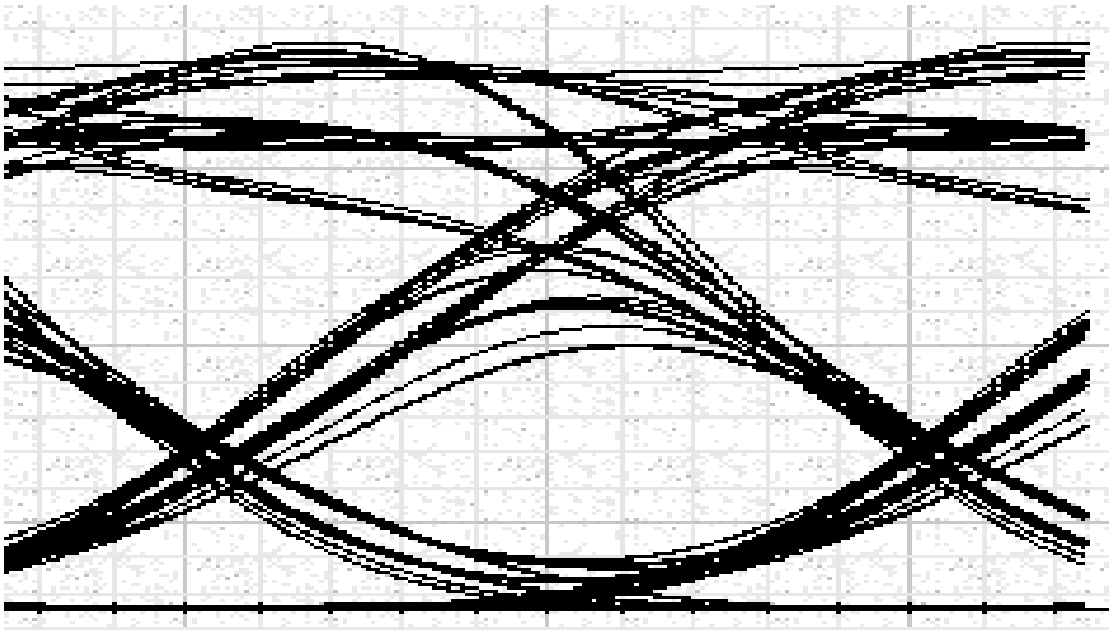

Figure 46: Eye diagram at node 1 that communicates on channel 1 at 193.1 THz.

References:

1. G. P. Agrawal, Fiber Optic Communication Systems, Wiley-Interscience, 1997.
2. Tim Gyselings et. al, “Crosstalk analysis of multi-wavelength optical cross connects”, J. Light. Tech. 17, pp. 1273, 1999.
3. R. Ramaswami and K. N. Sivarajan, Optical Networks: A practical Perspective, Morgan Kaufmann, 1998.

Example: Subcarrier Multiplexing

Subcarrier multiplexing**.osd**

Project file "Subcarrier multiplexing**.osd**" generates an analog SCM lightwave system designed with a single optical carrier at 193.1 THz. Three sinusoidal signals ($0.5+0.5*\sin(W_0*t)$) with frequencies of 56 MHz, 116 Mhz, and 176 MHz are first combined in electronic domain. This signal modulates the amplitude of optical carrier. Light is sent to fiber and at the receiver end, subcarriers are separated by filters.

Different parameters can be changed in this example, where the new results compared with the previous one. Different filter bandwidths, optical carrier wavelengths, and fiber parameters can be considered to perform additional simulations.

Chapter 9 – Soliton Systems

Example: Fundamental and Higher-Order Solitons

Fundamental and higher-order solitons**.osd**

The aim of this example is to present numerical results for fundamental and higher- order solitons in SMF at 1.55 μm.

The basic parameter N is defined by $N^2 = \gamma P_0 L_D$, where $\gamma = \frac{2\pi n_2}{\lambda A_{eff}}$ is nonlinear coefficient, $L_D = \frac{T_0^2}{|\beta_2|}$ is the dispersion length, P_0 is the peak power, n_2 is the nonlinear refractive index, A_{eff} is the effective core area, $T_0 = T_{FWHM}/1.763$ and $\beta_2 = \frac{\partial^2 \beta}{\partial \omega^2}$ at w_0 where β is the propagation constant. The basic parameter N represents a dimensionless combination of the pulse and fiber parameters.

The optical pulse which corresponds to N=1 is called fundamental soliton. Pulses with N=2, and 3 are called second and third-order solitons. The layout for generation of the solitons is shown in Fig.1.

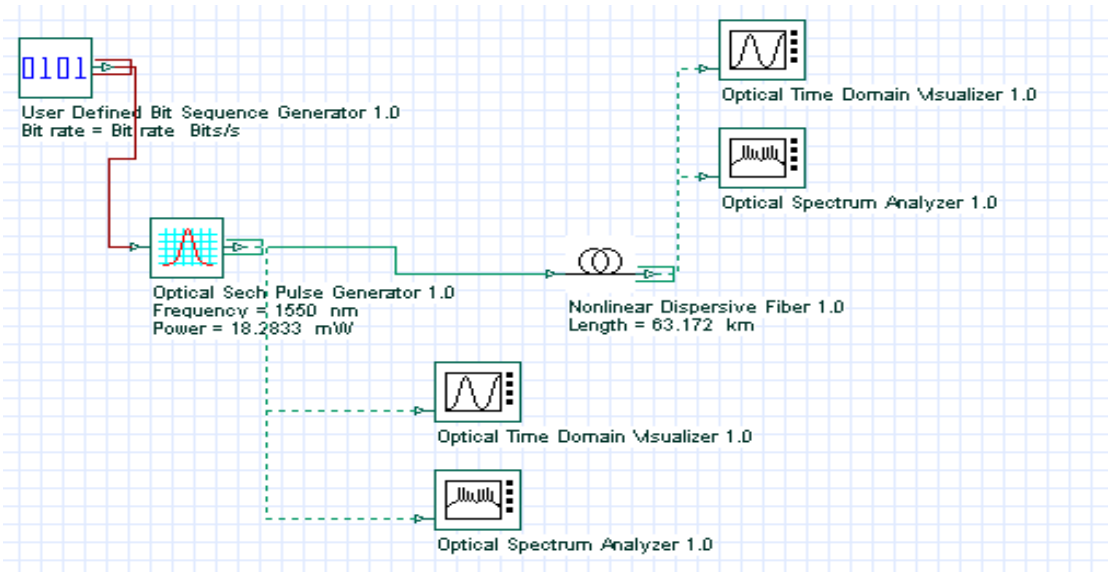

Fig.1: Layout: For generation of solitons

As an optical source an optical sech pulse generator has been chosen.

A 10 Gb/s transmission at 1.55 μm in SMF (β_2 = - 20 ps^2/ km or to D = 16 ps/(nm . km)) is considered. We consider, T_B =100 ps, T_{FWHM}= 50 ps (duty cycle = 0.5) $\Rightarrow$ L_D = 40.2166 km and γ = 1.36 (1/km.W) $\Rightarrow$ the peak power of the fundamental soliton P_0 ~ 18.28335 mW. The powers required for obtaining of second- and third-order solitons are 73.1334 and 164.5501 mW, respectively.

Distance at which the three types of solitons were propagated is equal to so-called soliton period ($z_0 = \frac{\pi}{2} L_D$). In our case z_0 = 63.172 km. The evaluation of fundamental, second order and third order solitons is shown in **Figs. 2,3, and 4**.

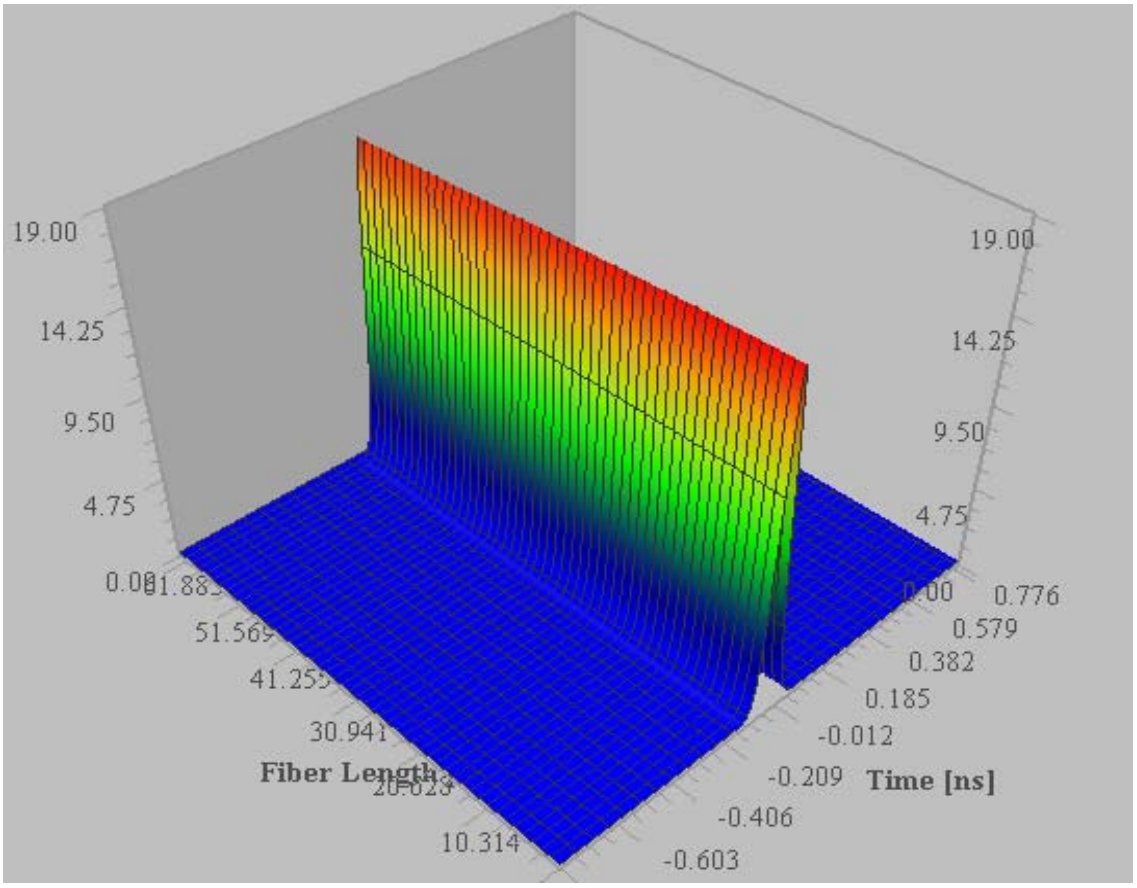

Fig. 2: Evolution of the fundamental soliton over one soliton period

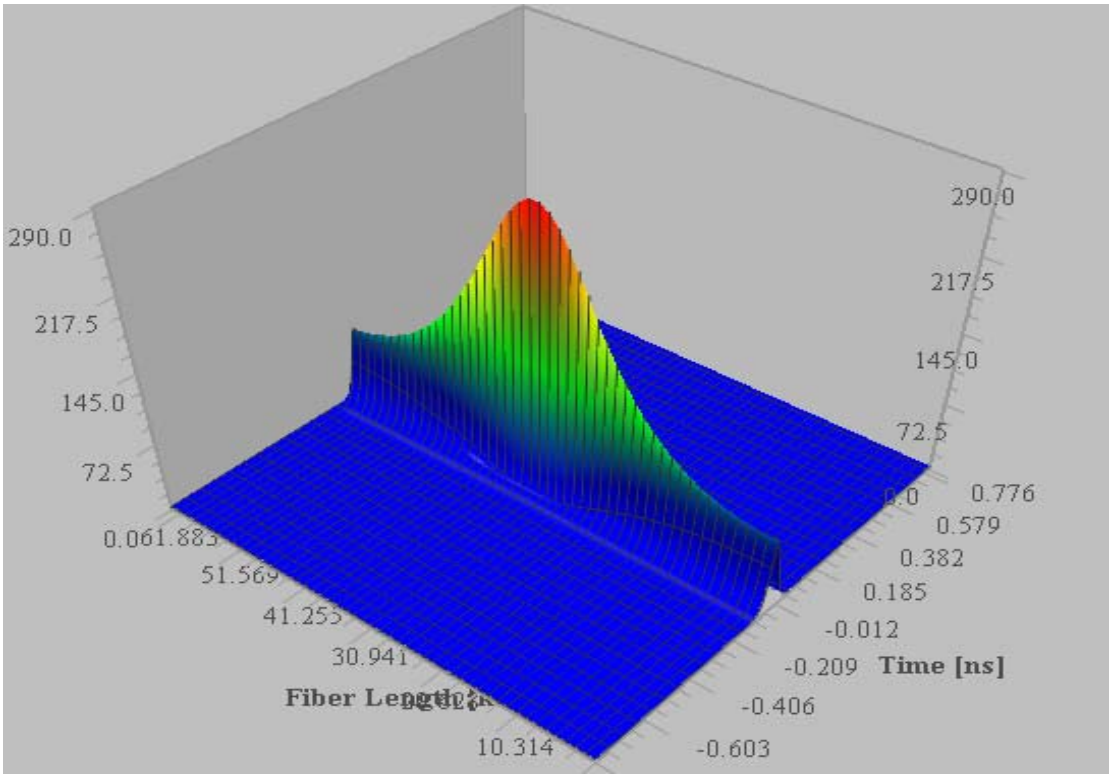

Fig. 3: Evolution of the second-order soliton over one soliton period

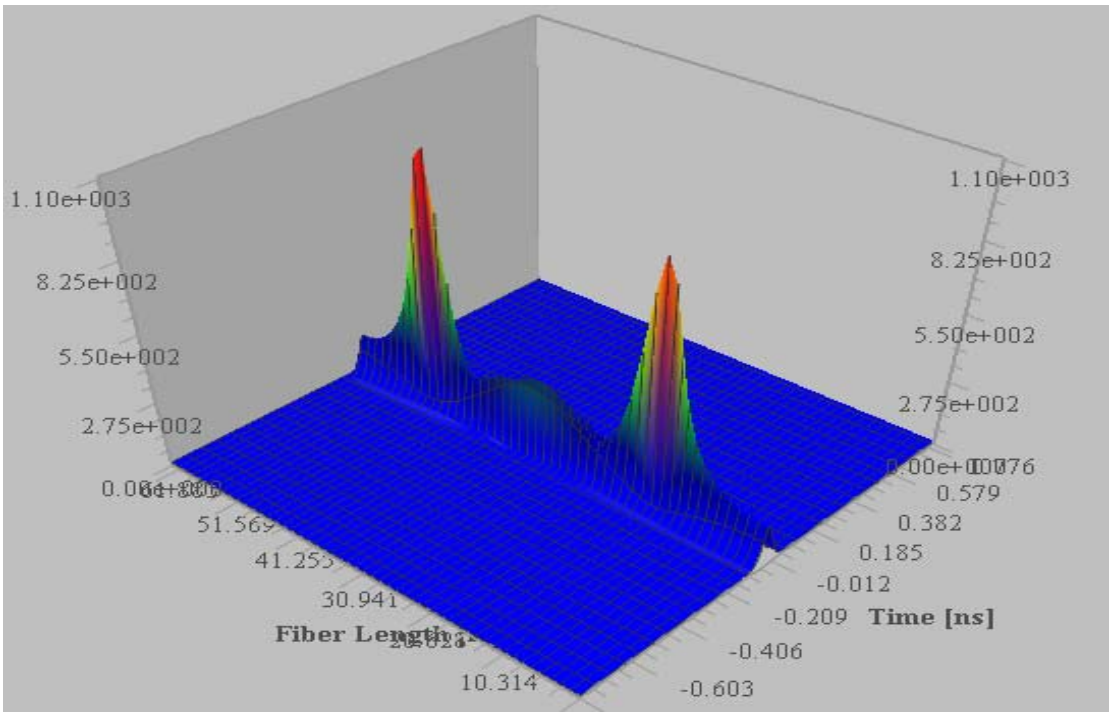

Fig.4: Evolution of the third - order soliton over one soliton period

References:

1. G.P.Agrawal, "Nonlinear Fiber optics", third edition, Academic Press, 2001.
2. G.P.Agrawal, Fiber optics communication Systems", John Wiley & Sons, INC, 1997.

Example: Dark Solitons

Dark solitons**.osd**

Project file "Dark solitons**.osd**" shows propagation of a black soliton pair in a single mode fiber. The required power and phase profile is generated by using the Measured Optical Pulse Sequence component. These profiles are loaded to component from "Input Pulses .txt" file. Optical attenuator is used to adjust the background power. You can calculate the bright background power that is needed to support black solitons. This can be done satisfying the condition of $N^2 = \gamma P_0 T_0^2 L_D = 1$ for a fundamental black soliton. The current set of parameters satisfy this condition. You can see that the power and phase profile is preserved during propagation in nonlinear fiber. You can see the evaluation of the pulse inside the fiber by looking at "Fiber 3D Graph" in Graphs tab. Change the background power by adjusting the attenuation and see the formation of new dark soliton pairs when N > 1. Moreover, see how the black pulse evolves when N < 1. You can also try to see the effect of phase profile by preparing a new input pulse data file and loading it to Measured Optical Pulse Sequence component.

Example: Information Transmission with Solitons

Interaction of a pair of fundamental solitons**.osd**

Project file "Interaction of a pair of fundamental solitons**.osd**" demonstrates the interaction of two adjacent solitons. If the solitons are not well separated in time, depending on their phases either they periodically collide or repeal from each other. In this example, two in phase solitonic pulses are launched into a nonlinear dispersive fiber. They periodically collide inside the fiber. The collision period depends on the input time shift between pulses. Estimate the collision point and verify your estimation by looking at the evaluation of the pulses inside fiber. You can see the evaluation of the pulses inside the fiber by looking at "Fiber 3D Graph" in Graphs tab. You can change the signal power or fiber parameters to see how solitonic pulses behave.

Example: Average Soliton Regime

Average -soliton regime**.osd**

The aim of this example is to demonstrate the average soliton regime at 10 Gb/s transmission over a 500 km optical link consisting of SMF. The corresponding layout has been shown below **(Fig.5).**

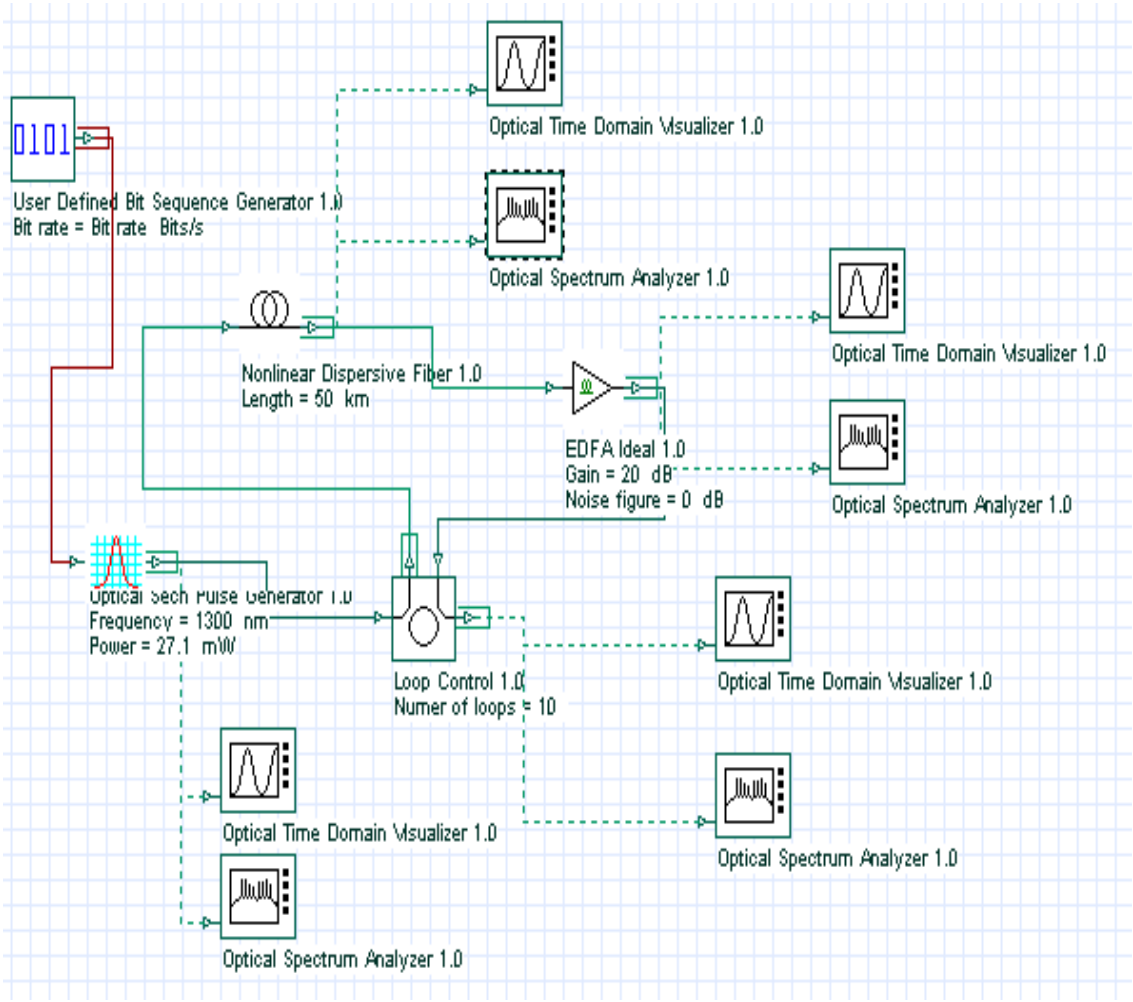

Fig. 5: Layout: Average soliton regime

The following global **(Table (1a))** and pulse parameters **(Table (1b))** have been used to get transmission at 10 Gb/s.

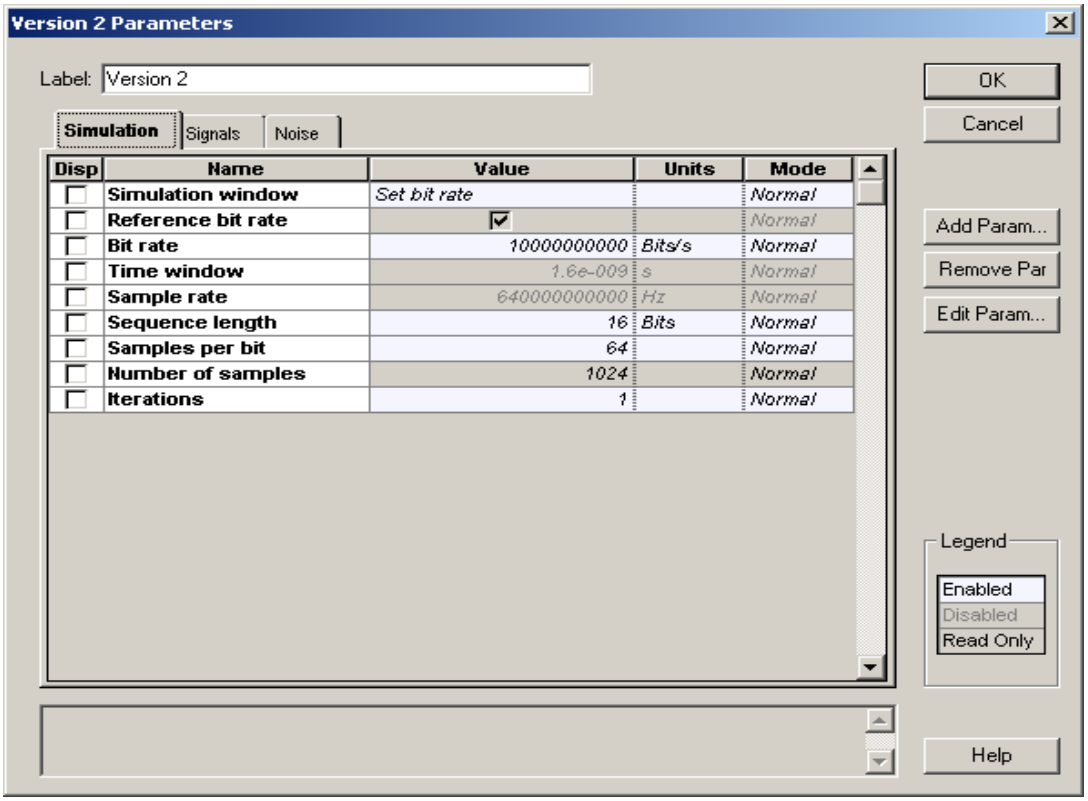

Table 1(a): Global parameters

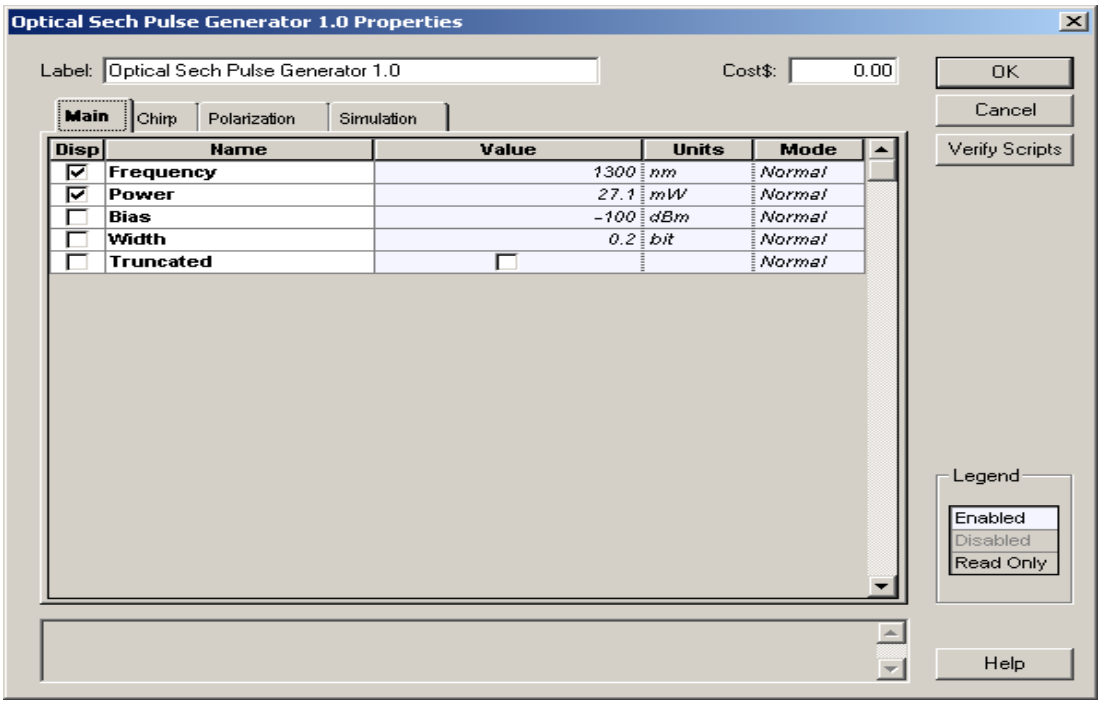

Table 1(b): Pulse parameters

We fixed B= 10 Gb/s $\Rightarrow$ T_B = 100 ps. The sequence length is 16 bit. The carrier wavelength of the pulse is λ ~1300 nm. T_{FWHM} = 20 ps $\Rightarrow$ $T_0 = 0.567\ T_{FWHM}$ ~ 11.34 ps. The input peak power is 21.7 mW. Let us now fix the fiber parameters as given in **(Tables 2(a) and 2(b))**.

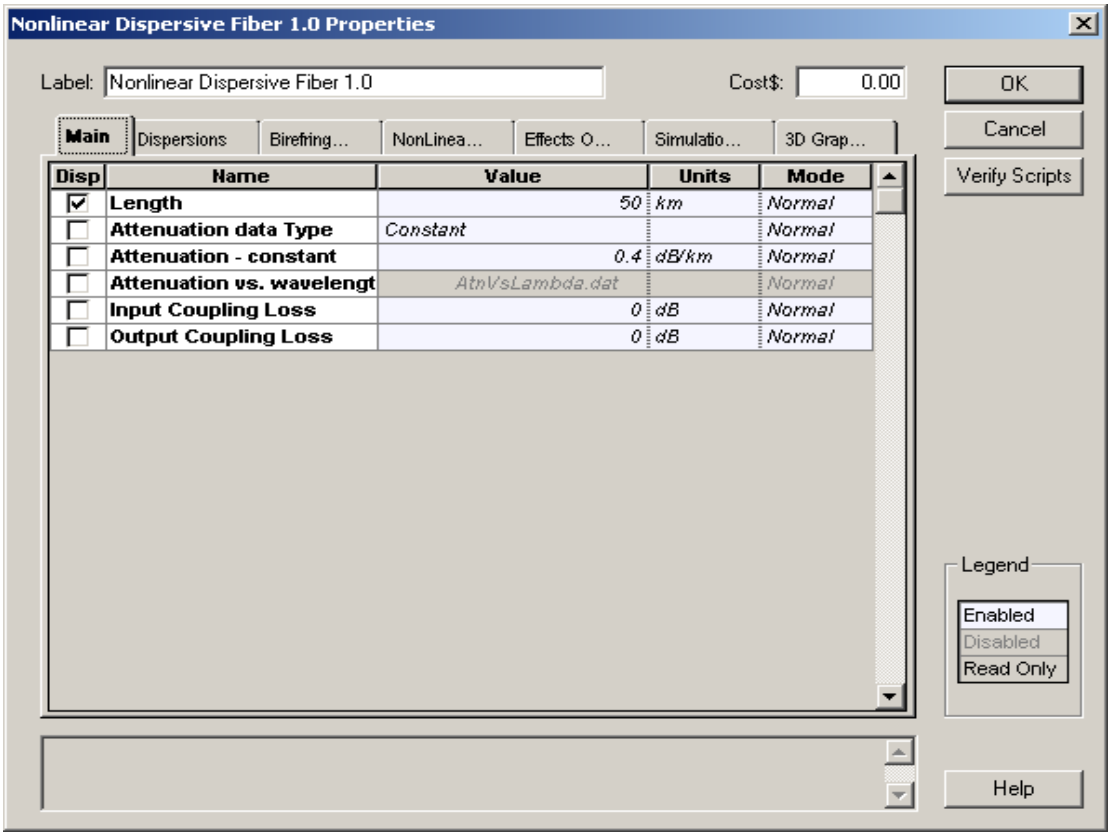

Table 2(a): Fiber parameters (Main)

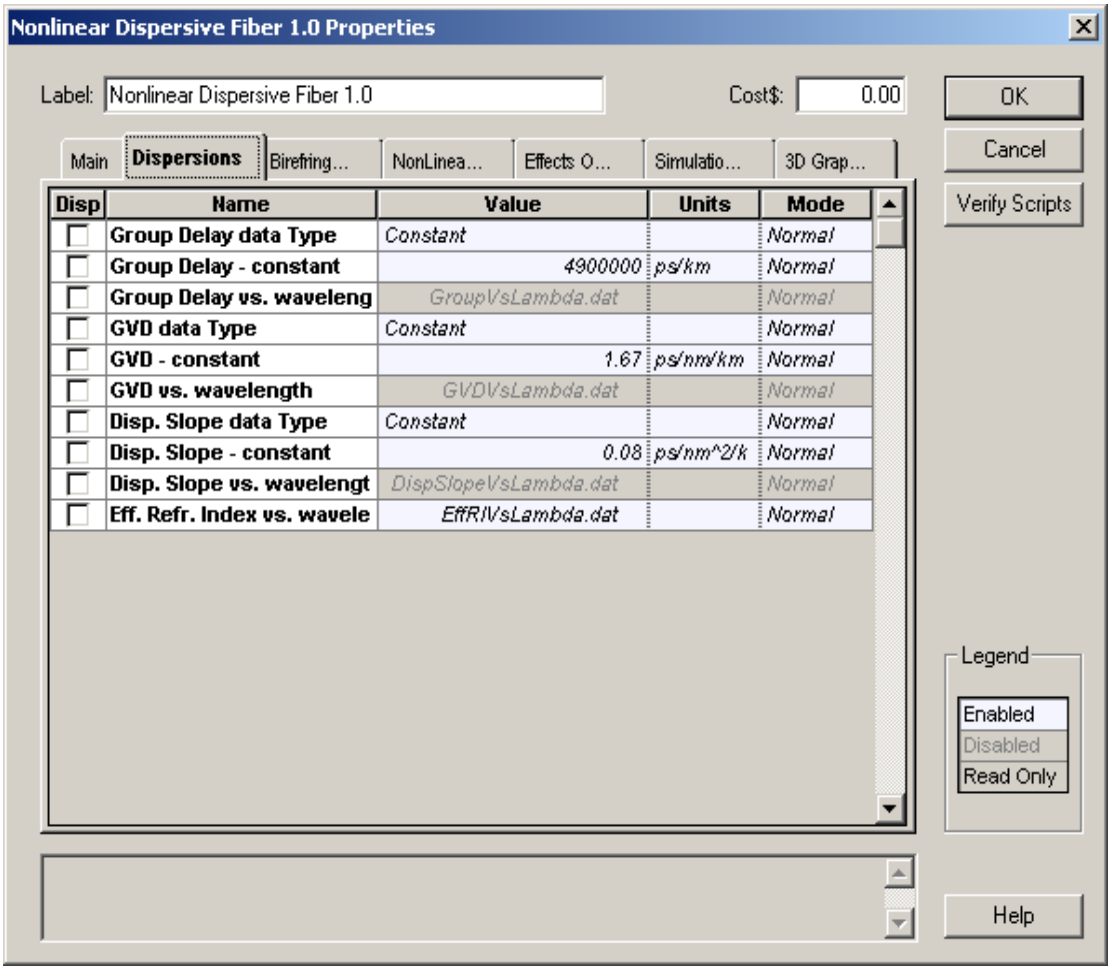

Table 2(b): Fiber parameters (Dispersion)

We have considered SMF with length 50 km and losses 0.4 dB/km. For k_2 (= $-\lambda^2 D/(2\pi c)$) ~ -1.5 (ps^2/km) $\Rightarrow$ D ~1.67 (ps/nm.km)$\Rightarrow$ L_D (= $T_0^2/|k_2|$) ~ 85 km. *(The effects of group delay and third order of dispersion are not taken into account)*. After each fiber the signal will be amplified with SOA, therefore L_A ~ 50 km. Note that the condition $L_A < L_D$ is satisfied.

The value of Kerr nonlinearity coefficient γ (= $n_2\ \omega_0$ / c A_{eff}) can be calculated from the **Table 3** where the fixed value of nonlinear refractive index n_2 has been taken as 2.6 10^{-20} [m^2/W] with ω_0 / c = 2 π / λ = 2 π /1.3 10^{-6} [m^{-1}] and A_{eff} = 62.8 [μm^2]. The value of γ comes out to be 2 [1/km.W].

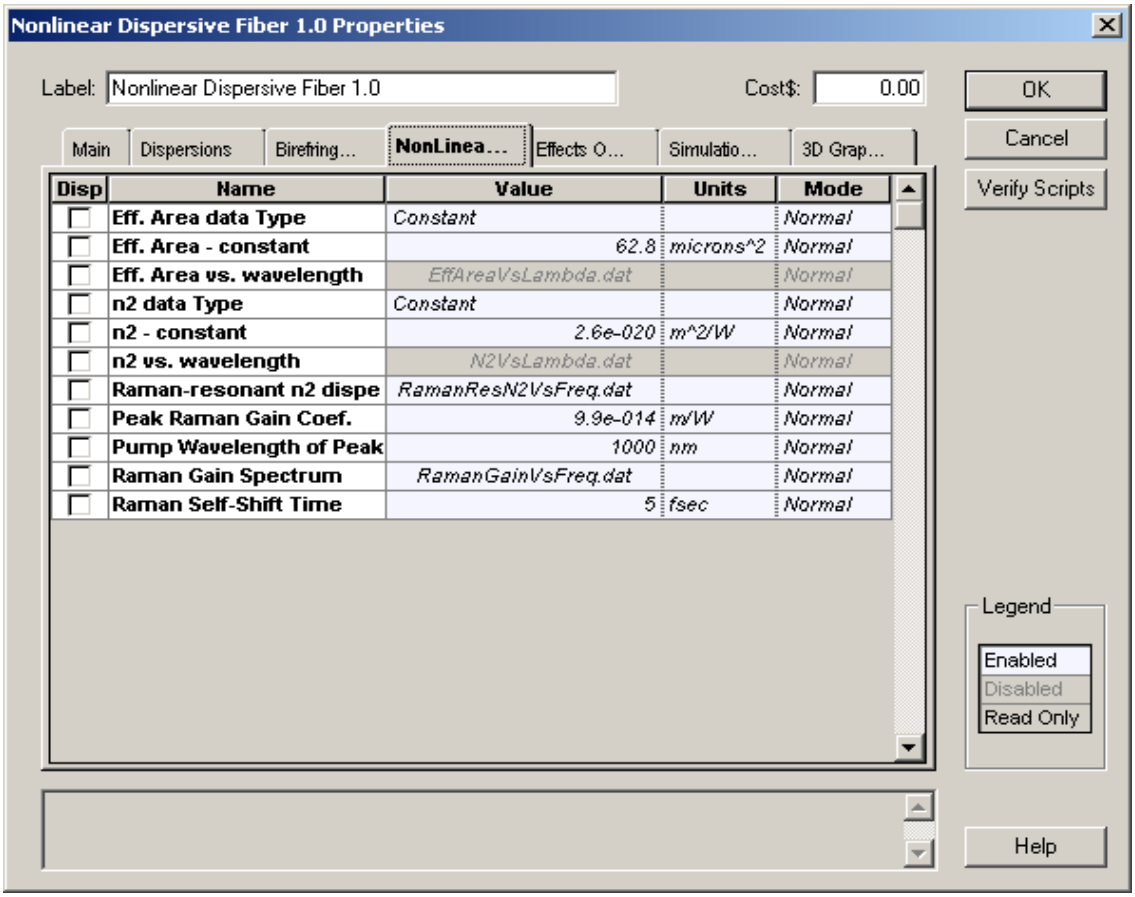

Table 3: Fiber parameters (Nonlinear)

The linear losses for 50 km SMF are 20 dB. The losses are periodically compensated with ideal EDFA with 20 dB gain.

Soliton peak power for this fiber is 5.8 mW. The input power of the average soliton is 27.1 mW. To demonstrate the importance of the input power of the average soliton we will consider soliton propagation in a 500 km SMF with two different input powers: 5.8 mW – usual soliton peak power (Version insufficient power) and 27.1mW – modified soliton peak power which takes into account the periodical amplification (Version average soliton), respectively. Each version includes sweeps on the number of loops 0,4,7 and 10 which represent the propagation distances 0, 200, 350 and 500 km in SMF.

Figs. 6(a), 6(b), 6(c) and 6(d), show the initial pattern of pulses and the pattern of pulses after 200, 350 and 500 km transmission in SMF, respectively. The periodic amplification has been done with EDFA at every 50 km of distance with the 27.1mW – modified soliton peak power.

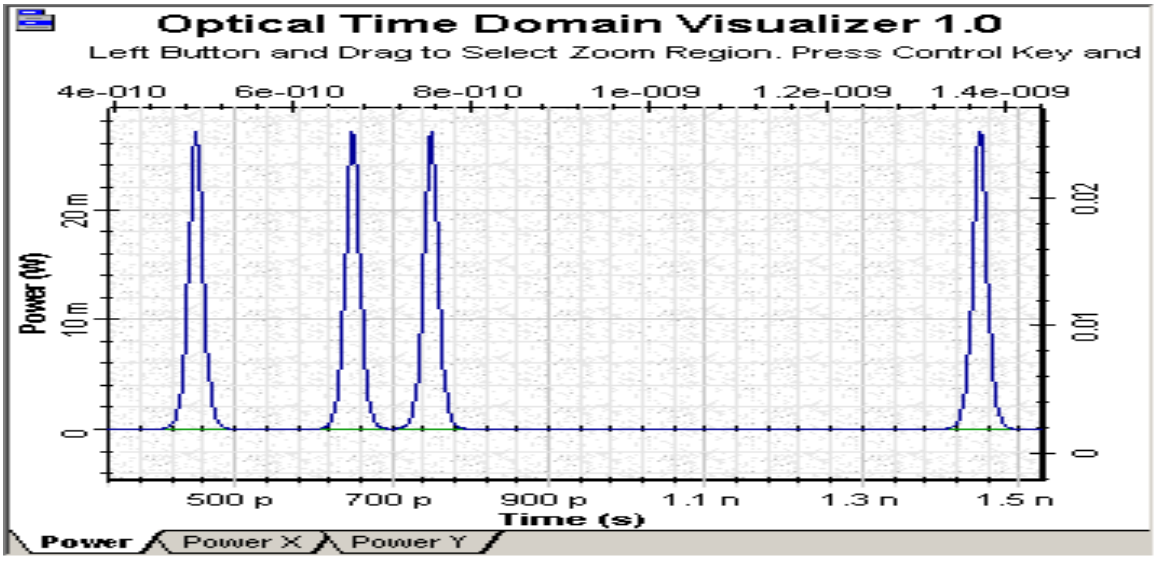

Fig. 6(a): Initial pulse pattern

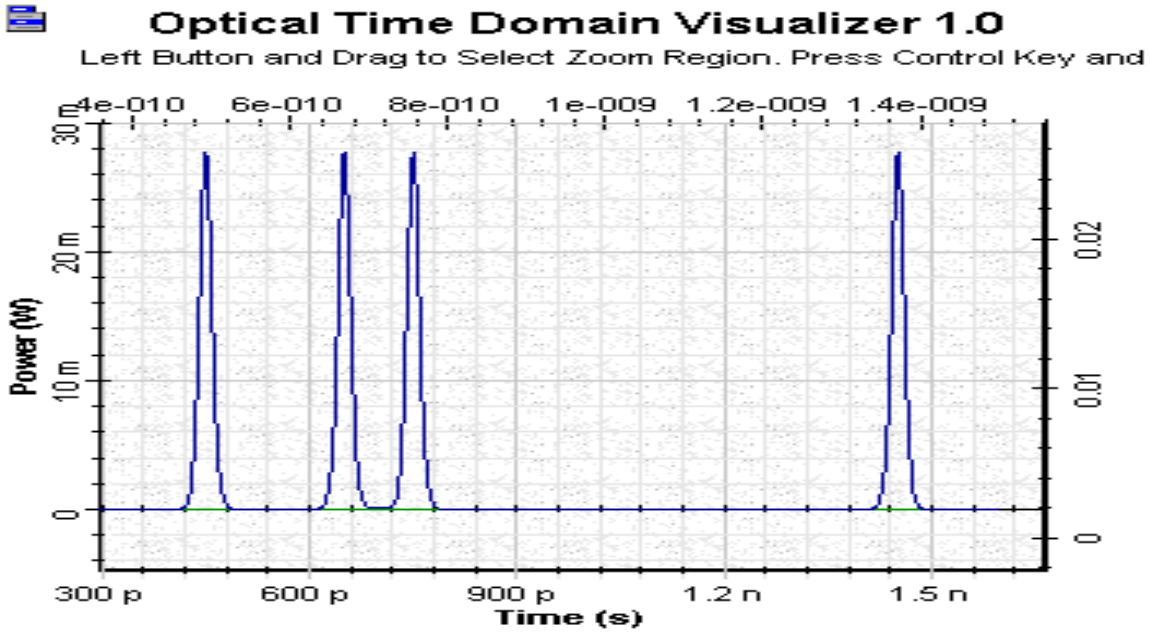

Fig. 6(b):Pulse pattern after 200 km SMF

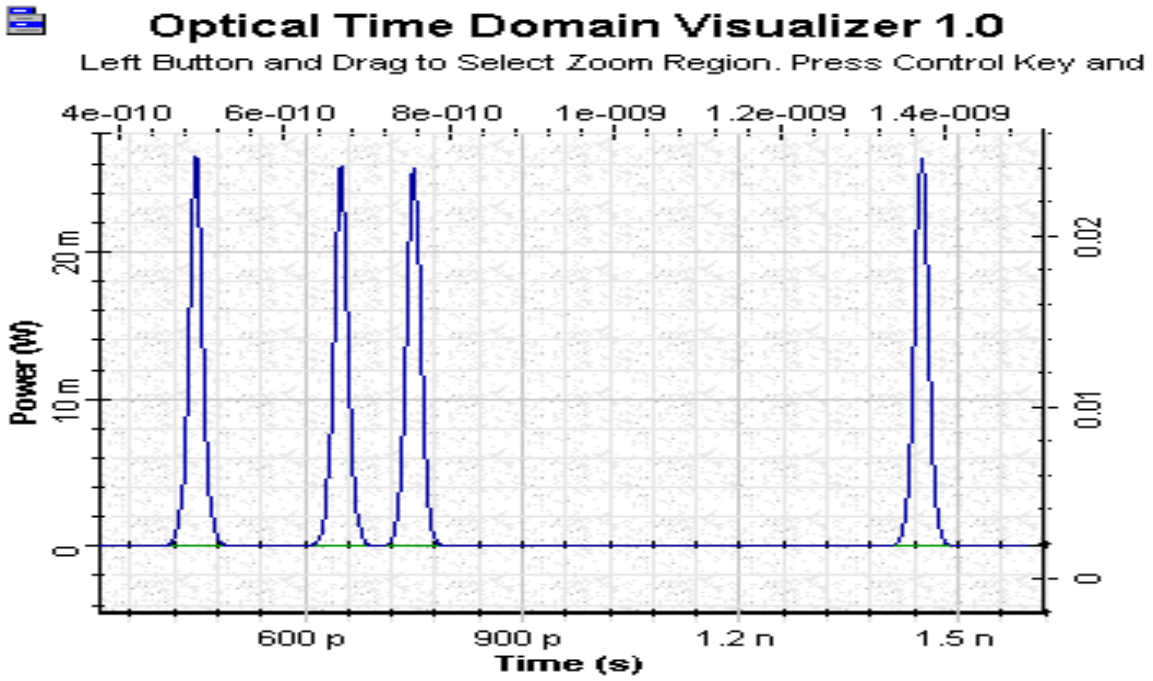

Fig. 6(c): Pulse pattern after 350 km SMF

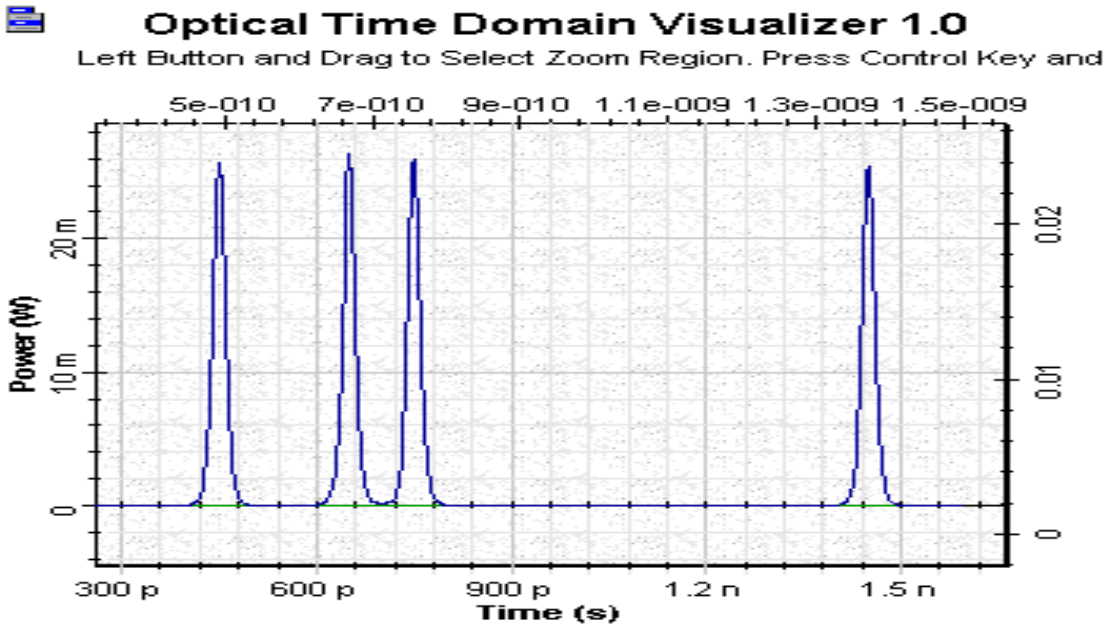

Fig. 6(d): Pulse pattern after 500 km SMF

As can be seen, the pattern of pulses is well-preserved. The average soliton concept is valid for these pulse, fiber, and amplification parameters.

Figs. 7(a), 7(b), 7(c) and 7(d) show the initial pattern of pulses and the pattern of pulses after 200, 350 and 500 km transmission in SMF, respectively. The periodic amplification has been done with EDFA at every 50 km of distance with the 5.8 mW – modified soliton peak power.

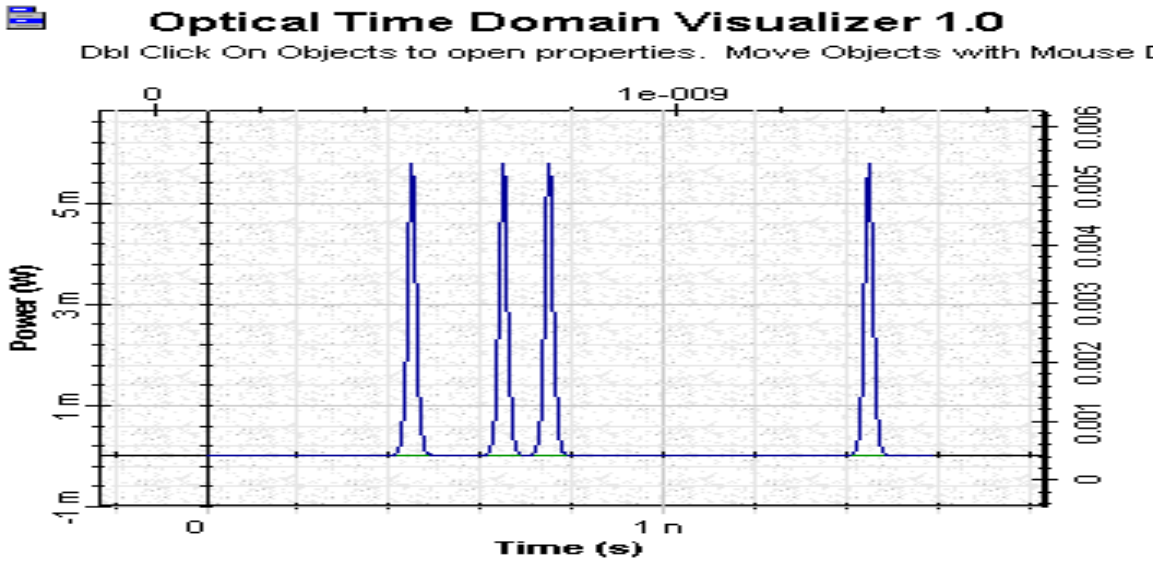

Fig. 7(a): Initial pulse pattern

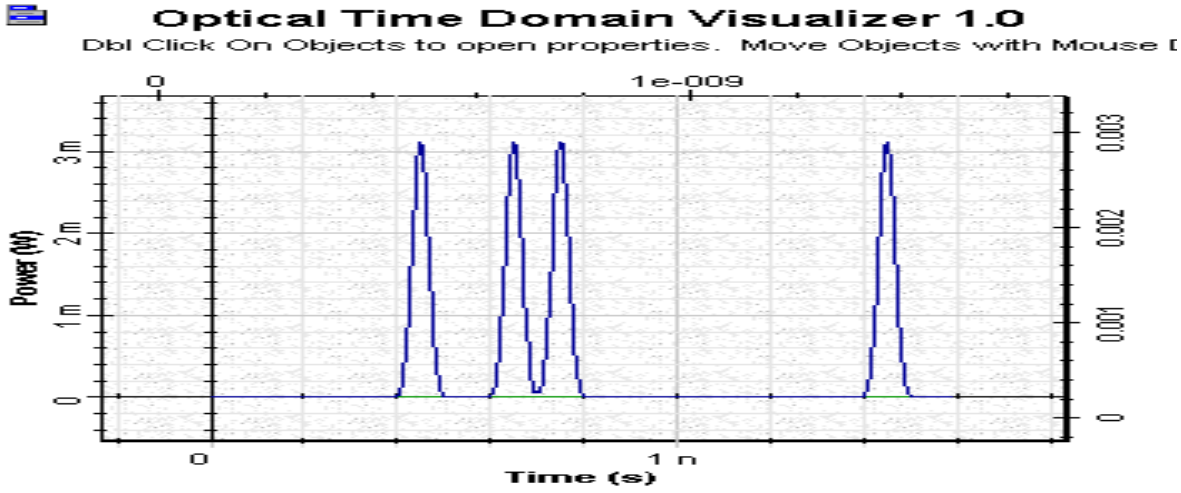

Fig. 7(b): Pulse pattern after 200 km SMF

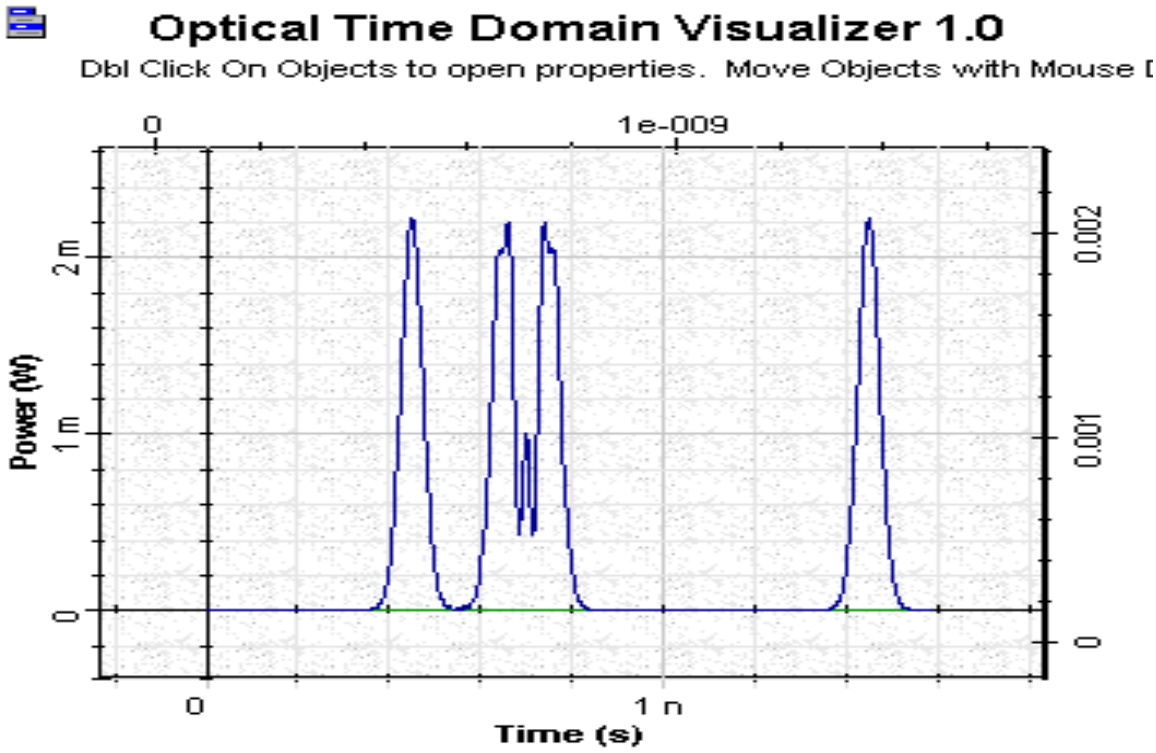

Fig. 7(c): Pulse pattern after 350 km SMF

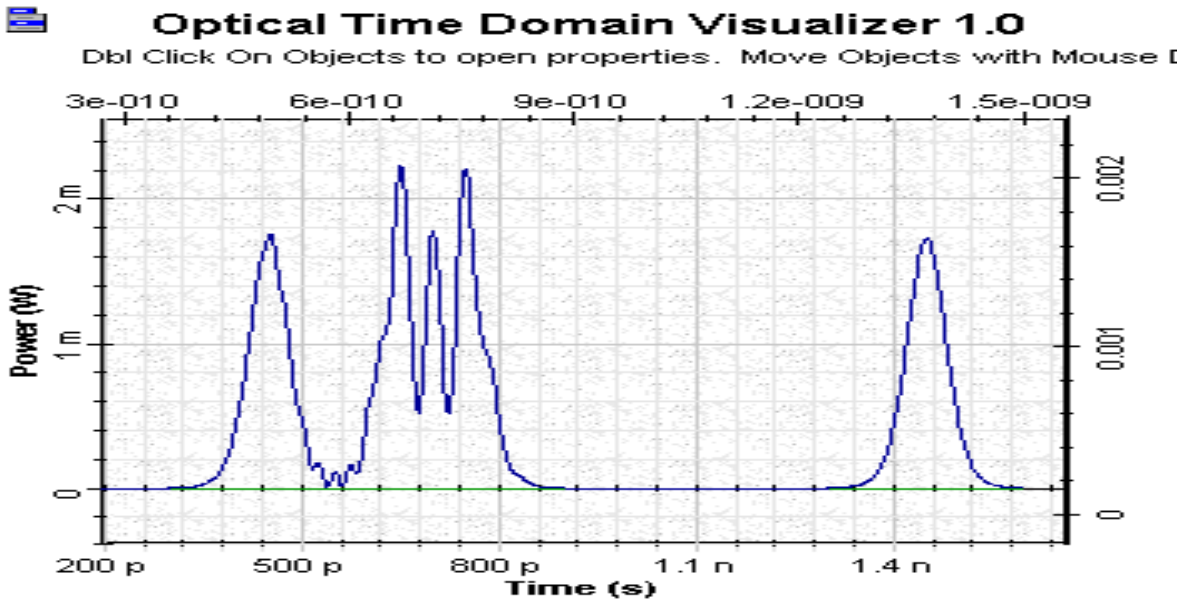

Fig. 7(d): Pulse pattern after 500 km SMF

Because of the improper pulse power used, the pulses in the pattern do not preserve their forms. As a result, pulses broaden and complicated structures appear.

References:

1. G.P. Agrawal, “Applications of nonlinear fiber optics”, Academic Press, 2001.
2. G.P. Agrawal, “Fiber Optic Communication Systems”, second edition, John Wiley @ Sons, Inc., 1997.

Example: Soliton Collisions

Interaction of a multicolor solitons**.osd**

Project file “Interaction of a multicolor solitons**.osd**” demonstrates a 2 channel soliton communication system. First version shows interaction of two isolated pulses each one of which carried on two different carrier frequencies. In this case, power of each channel must be adjusted according to the value of dispersion at that specific wavelength to satisfy the soliton condition for each soliton pulse from different channels. In the second version, each channel contains two soliton pulses; they interact among themselves and with the pulses in other channels.